UNIVERSITÀ DEGLI STUDI DI TRIESTE
e
UNIVERSITÀ CA' FOSCARI DI VENEZIA

XXXI CICLO DEL DOTTORATO DI RICERCA IN CHIMICA

PALLADIUM ORGANOMETALLIC COMPOUNDS BEARING *N*-HETEROCYCLIC CARBENE LIGANDS AS PROMISING ANTICANCER AGENTS

Settore scientifico-disciplinare: **CHIM/03**

DOTTORANDO
THOMAS SCATTOLIN

COORDINATORE
PROF. BARBARA MILANI

SUPERVISORE DI TESI
PROF. FABIANO VISENTIN

CO-SUPERVISORE DI TESI
PROF. LUCIANO CANOVESE

ANNO ACCADEMICO 2017/2018

Table of Contents

Abstract 9

List of abbreviations 13

1. GENERAL INTRODUCTION

1.1. GENERAL ASPECTS ABOUT CANCER 18

1.1.1. What is cancer? 18

1.1.2. Incidence, mortality and risk factors 19

1.1.3. Carcinogenesis 22

1.1.4. An in-depth analysis of the cell cycle 24

1.1.5. Apoptosis 25

1.1.6. Ovarian cancer 26

1.2. CANCER THERAPY 28

1.2.1. Surgery 28

1.2.2. Radiotherapy 29

1.2.3. Photodynamic therapy (PDT) 29

1.2.4. Immunotherapy 30

1.2.5. Chemotherapy 31

1.3. AN OVERVIEW OF ANTICANCER COMPOUNDS 33

1.3.1. Origin and modern organic anticancer research 33

1.3.2. Metal-based anticancer compounds 34

1.3.3. Target for organometallic anticancer compounds 37

1.3.4. Platinum: from cisplatin to the next generation drugs 38

1.3.5. Ruthenium and gold complexes with antitumor activity 43

1.3.6. Palladium compounds: recent investigations of promising anticancer agents 45

1.4. *N*-HETEROCYCLIC CARBENES AS ANCILLARY LIGANDS 50

1.5. PHOSPHINES, ARSINES AND ISOCYANIDES AS SPECTATOR LIGANDS 54

1.6. ORGANOMETALLIC FRAGMENTS 55

1.6.1. η^3-allyl-Pd(II) fragment 55

1.6.2. Palladacyclopentadienyl fragment 58

1.6.3. η^2-olefin-Pd(0) fragment 60

1.7. REFERENCES 62

2. AIM OF THE PROJECT 69

3. PURINE-BASED NHC COMPLEXES

3.1. INTRODUCTION 72

3.2. SYNTHESIS OF FUNCTIONALIZED XANTHINES 75

3.3. PURINE-BASED IMIDAZOLIUM SALTS 77

3.4. SILVER (I) PURINE-BASED NHC COMPLEXES 82

3.5. PALLADIUM η^3-ALLYL COMPLEXES BEARING PURINE-BASED NHCs 89

3.5.1. Mixed NHC/PPh_3 η^3-allyl complexes 89

3.5.2. Mixed NHC/TPPTS and NHC/PTA η^3-allyl complexes 93

3.5.3. Mixed NHC/DIC η^3-allyl complexes 98

3.5.4. Bis(NHC) η^3-allyl complexes 101

3.6. PALLADACYCLOPENTADIENYL COMPLEXES BEARING PURINE-BASED NHCs 103

3.6.1. Mixed NHC/PPh_3 palladacyclopentadienyl complexes 103

3.6.2. Mixed NHC/PTA palladacyclopentadienyl complexes 106

3.6.3. Mixed NHC/DIC palladacyclopentadienyl complexes 108

3.6.4. Bis(NHC) palladacyclopentadienyl complexes 110

3.7. PALLADIUM (0) η^2-OLEFIN COMPLEXES BEARING PURINE-BASED NHCs 113

3.7.1. Mixed NHC/PPh_3 and NHC/$AsPh_3$ complexes 116

3.7.2. Bis(NHC) complexes 122

3.7.3. Bis(PTA) complexes 125

3.8. ANTIPROLIFERATIVE AND PROAPOPTOTIC ANALYSIS 129

3.8.1. Activity of Pd(II) η^3-allyl complexes bearing purine-based NHCs toward ovarian cancer cell lines 129

3.8.2. Activity of palladacyclopentadienyl complexes bearing purine-based NHCs toward ovarian cancer cell lines 136

3.8.3. Activity of Pd(0) olefin complexes bearing purine-based NHCs toward ovarian cancer cell lines 140

3.9. CONCLUSIONS 144

3.10. REFERENCES 145

4. PALLADIUM COMPLEXES WITH "CLASSICAL" NHCs AND BRIDGED BISNHCs

4.1. INTRODUCTION 148

4.2. SYNTHESIS OF THE IMIDAZOLIUM AND BISIMIDAZOLIUM SALTS 150

4.3. SYNTHESIS OF THE SILVER-NHC COMPLEXES 152

4.4. SYNTHESIS OF PALLADACYCLOPENTADIENYL COMPLEXES 154

4.4.1. Palladacyclopentadienyl complexes bearing bidentate bisNHCs 155

4.4.2. Palladacyclopentadienyl complexes bearing two monodentate NHCs 162

4.4.3. Palladacyclopentadienyl complexes with chelating NHC-thioether or NHC-pyridine ligands 166

4.4.4. Mixed NHC/PPh_3 palladacyclopentadienyl complexes 171

4.4.5. Mixed NHC/DIC palladacyclopentadienyl complexes 176

4.4.6. Palladacyclopentadienyl complexes bearing chelating N-S and N-P ligands 180

4.5. ANTIPROLIFERATIVE ACTIVITY AND BIOLOGIAL ASSAYS ON PALLADACYCLOPENTADIENYL COMPLEXES 181

4.5.1. Antiproliferative activity of palladacyclopentadienyl compounds on different cancer cell lines and fibroblasts 182

4.5.2. Reactivity of complexes with reduced L-glutathione (GSH) 186

4.5.3. Uptake analysis 188

4.5.4. Biological tests for the determination of the biological target 188

4.6. SYNTHESIS OF η^3-ALLYL PALLADIUM COMPLEXES 193

4.6.1. η^3-allyl palladium complexes bearing bidentate bisNHCs 194

4.6.1.1. Complexes with R= methyl or benzyl 195

4.6.1.2. Complexes with R= mesityl 196

4.6.2. η^3-allyl palladium complexes bearing two monodentate NHCs 204

4.6.3. η^3-allyl palladium complexes bearing chelating NHC-thioether or NHC-pyridine ligands 207

4.6.4. Mixed NHC/PPh_3, NHC/PTA, NHC/DIC and PPh_3/DIC η^3-allyl palladium complexes 210

4.6.4.1. Mixed NHC/PPh_3 complexes 210

4.6.4.2. Mixed NHC/PTA complexes 213

4.6.4.3. Mixed NHC/DIC and PPh_3/DIC complexes 215

4.6.5. η^3-allyl palladium complexes bearing chelating phosphino-carbene ligands 216
4.6.6. η^3-allyl palladium complexes bearing chelating N-P and N-S ligands 217
4.7. ANTIPROLIFERATIVE ACTIVITY OF ALLYL PALLADIUM COMPLEXES 218
4.8. CONCLUSIONS 220
4.9. REFERENCES 221

5. CARBOHYDRATE BASED NHC COMPLEXES

5.1. INTRODUCTION 226
5.1.1. Carbohydrates: general aspects 226
5.1.2. Anomeric effect and anomerization 228
5.1.2.1. Mutarotation 229
5.1.2.2. Anomerization 230
5.1.3. Metal-based compounds with glycosidic groups and Warburg effect 231
5.2. SYNTHESIS OF 2,3,4,6-TETRA-O-ACETYL-α-D-GLUCOPYRANOSYL BROMIDE 234
5.3. SYNTHESIS OF 1-(2,3,4,6-TETRA-O-ACETYL-β-D-GLUCOPYRANOSYL) IMIDAZOLE 236
5.4. SYNTHESIS OF IMIDAZOLIUM SALTS 237
5.5. SYNTHESIS OF SILVER(I) COMPLEXES 242
5.6. SYNTHESIS OF η^3-ALLYL PALLADIUM COMPLEXES 244
5.6.1. Neutral η^3-allyl Pd(II) complexes 244
5.6.2. Mixed NHC/PPh_3 η^3-allyl Pd(II) complexes 250
5.7. MIXED NHC/PPh_3 PALLADACYCLOPENTADIENYL COMPLEXES 253
5.8. ANTIPROLIFERATIVE ACTIVITY: PRELIMINARY RESULTS 256
5.9. CONCLUSIONS 256
5.10. REFERENCES 257

6. Pd(II) COMPLEXES BEARING *N*-TRIFLUOROMETHYL NHCs

6.1. INTRODUCTION 260
6.1.1. Trifluoromethyl and polyfluorinated groups in medicinal chemistry 260
6.1.2. Synthetic methodologies for the introduction of the trifluoromethyl group 262
6.1.3. N-Trifluoromethyl NHC ligands 265
6.2. N-TRIFLUOROMETHYL BENZIMIDAZOLIUM SALTS 268
6.3. Pd (II) η^3-ALLYL COMPLEXES BEARING *N*-TRIFLUOROMETHYL NHCs 271
6.3.1. Mixed NHC/PPh_3 complexes 272
6.3.2. Mixed NHC/PTA complexes 275
6.4. ANTIPROLIFERATIVE ACTIVITY AND BIOLOGIAL ASSAYS 278
6.5. CONCLUSIONS 282
6.6. REFERENCES 283

7. CONCLUSIONS AND FUTURE PERSPECTIVES 285

8. PUBLICATIONS AND COMUNICATIONS AT CONFERENCES 289

9. EXPERIMENTAL SECTION 293

10. SUPPLEMENTARY MATERIALS 399

Abstract

Since the discovery of the antitumor properties of cisplatin and its approval by the FDA in 1978 (40 years ago), inorganic compounds have been considered for the first time as anticancer agents. Cisplatin, however, has some limitations due to side effects on kidneys, liver and brain and the resistance, intrinsic or acquired over time, by some types of neoplasia.

Despite the appearance in the market of platinum compounds with minor side effects (i.e. carboplatin and oxaliplatin), they did not solve the ineffectiveness on some types of tumors, having the same mechanism of action proposed for cisplatin (DNA platination).

For this reason, many research groups have focused their attention on the synthesis and determination of the anticancer properties of compounds with metals different from platinum.

Among the most investigated metals there are certainly ruthenium and gold and, only recently, palladium.

The latter, despite belonging to the same group of platinum, has some rather different features:

- Better water solubility of its complexes.
- Structure-activity relationships and mechanisms of action generally different from platinum compounds.

However, the fast dissociation pattern of palladium complexes compared to platinum represents a problem since the speciation, which heavily affects the biological activity and the pharmacokinetic properties, could be increased. To remedy this contraindication the most direct option is the introduction of ligands firmly anchored to the metal such as *N*-Heterocylic Carbenes (NHCs), which are known to give strong σ-bonds with most of the transition metals.

Moreover, several NHC-palladium complexes have already exhibited an interesting cytotoxic activity *in vitro* and tumour growth suppression even *in vivo*.

In this PhD thesis, the synthesis and characterization of new palladium compounds stabilized by different types of *N*-Heterocyclic Carbenes and important organometallic fragments such as η^3-allyl-Pd(II), palladacyclopentadienyl and η^2-olefin-Pd(0) will be exposed (see Fig. A.1).

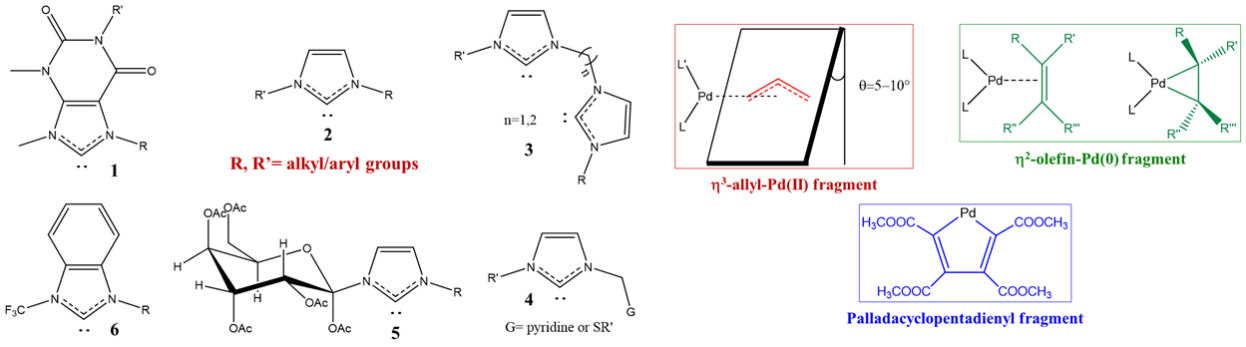

Fig. A1

The reactivity and the importance in many catalytic processes of the fragments reported in Fig. A1 are well known, on the contrary, their biological activity is almost unexplored.

Starting from these premises, it was decided to test the synthesized compounds toward different tumor lines, particularly on ovarian carcinoma, and human fibroblasts (healthy cells).

From the antiproliferative activity data collected for about one hundred compounds, emerges that, regardless of the nature of the selected carbene ligand, the most active compounds bear the allyl fragment.

The allyl derivatives are generally much more active than cisplatin in the tumor lines taken into consideration (IC_{50} <1 μM) and some of these, reported in Figure A2, are poorly cytotoxic on healthy cells (selective cytotoxic activity).

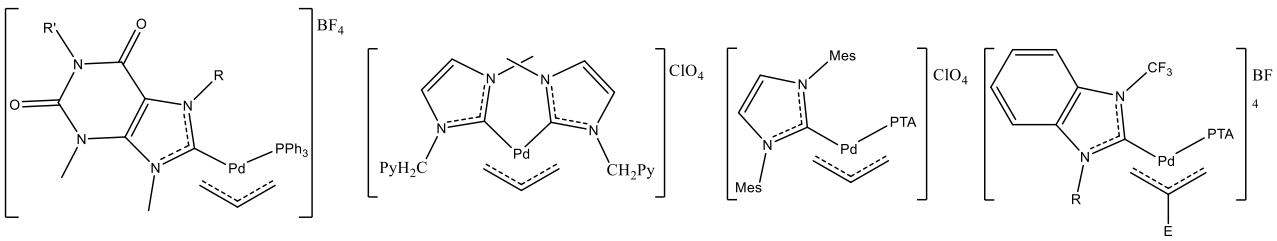

Fig. A2

For these species the evaluation of their activity *in vivo* and experiments aimed at identify the primary biological target, in order to propose the possible mechanism of action, are planned.

A class of compounds generally slightly less active than that containing the allyl residue is represented by the palladacyclopentadienyl complexes and their derivatives. Nevertheless, for some of the synthesized compounds (see Fig. A3), an excellent antiproliferative and proapoptotic activity has been shown on ovarian cancer cell lines (CisPt sensitive and CisPt resistance), accompanied by a poor activity against normal cells.

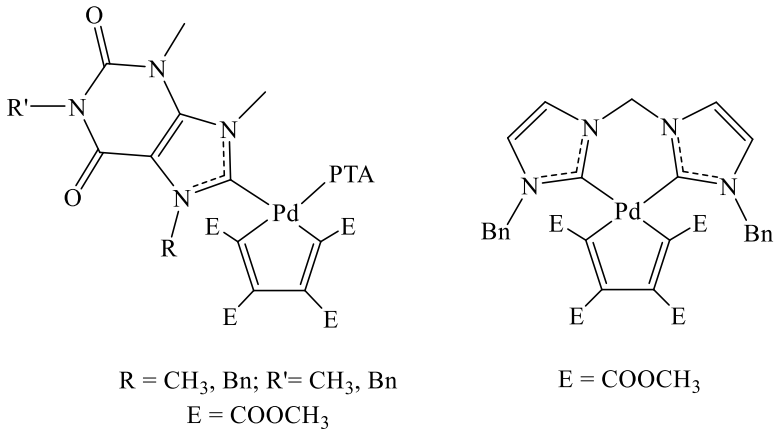

Fig. A3

For the compound **40a** a thorough investigation on the main biological target, which was found to be DNA, and on the degree of uptake in tumor cells was also carried out.

Due to the high stability imparted by the palladaciclopentadienyl fragment and the chelatig biscarbene ligand, this compound does not undergo substitution reactions when reacted with reduced glutathione (GSH), which is a potential coordinating species present in abundance in the biological environment. It is therefore reasonable to suppose that the interaction with the DNA occurs through non-covalent interactions with the polynucleotide chain.

Finally, the class of compounds decidedly less active than those described so far is represented by the Pd (0) derivatives stabilized by olefinic ligands. For these complexes the antiproliferative and proapoptotic activity was evaluated only in ovarian carcinoma lines, observing only in very few cases IC_{50} values comparable to those of cisplatin. For instance, the unpublished complex bearing two PTA ligands, shown in figure A4, is characterized by IC_{50} values of 3 and 5 μM on the CisPt-sensitive and CisPt-resistant line, respectively.

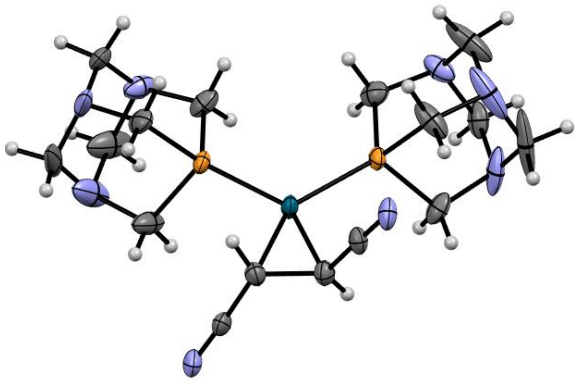

*Fig. A4 Ellipsoid representation of **26** crystal ASU contents (50% probability)*

List of abbreviations

Bn	Benzyl group
Bpy	2,2'-Bipyridine
CDK	Cyclin-dependent-kinase
COD	Cyclooctadiene
COSY	Correlation Spectroscopy
CytC	Cytochrome C
δ	Chemical shift (NMR)
DAPI	2-(4-Amidinophenyl)-1*H*-indole-6-carboxamidine
Dba	E,E-dibenzylideneacetone
DCE	Dichloroethane
DFT	Density Functional Theory
DIC	2,6-dimethylphenyl isocyanide
DMA	Dimethylacetylenedicarboxylate
DMF	Dimethylformamide
Dmfu	Dimethylfumarate
Dmso	Dimethyl sulfoxide
DNA	Deoxyribonucleic acid
DPPQ	8-Diphenylphosphinoquinoline
EGFR	Epidermal growth factor receptor
EPR	Enhanced Permeability and Retention
ESI-MS	Electrospray Ionisation Mass Spectrometry
FAD	Flavin Adenine dinucleotide
FDA	Food and Drug Administration
Fn	Fumaronitrile
GSH	Reduced glutathione
η	Hapticity in ligands with contiguous donor atoms
H2AX	Type of histone protein from the H2A family
HMBC	Heteronuclear Multiple Bond Correlation
HMQC	Heteronuclear Multiple-Quantum Correlation
HSQC	Heteronuclear Single-Quantum Correlation
IARC	International Agency for Research on Cancer
IC_{50}	Half maximal inhibitory concentration

ICP-MS	Inductively coupled plasma mass spectrometry
IR	Infrared
J	Coupling constant
JC-1	5,5′,6,6′-tetrachloro-1,1′,3,3′-tetraethyl-imidacarbocyanine iodide
L	Generalized ligand, most often a 2e ligand
M	Metal
μ	Descriptor for bridging with a superscript for the number of metals bridged
Ma	Maleic anhydride
Me	Methyl group
Mes	Mesityl group
MMR	Mismatch Repair
NAD	Nicotine Adenine dinucleotide
NAMI-A	New Anticancer Metastasis Inhibitor-A
NER	Nucleotides Excision Repair
NHC	*N*-Heterocyclic Carbene
NMP	*N*-Methyl-2-pyrrolidone
NMR	Nuclear Magnetic Resonance
NOESY	Nuclear Overhauser effect spectroscopy
Nq	Naphthoquinone
Me-PyCH$_2$SPh	2-methyl-6-((phenylthio)methyl)pyridine
PDT	Photodynamic Therapy
PET	Positron emission tomography
Ph	Phenyl group
Phen	1,10-Phenantroline
PTA	1,3,5-triaza-7-phosphoadamantane
Py	Pyridine
RAPTA	Ruthenium Arene PTA complexes
ROS	Reactive Organic Species
RT	Room temperature
Ser139	Monoclonal Antibody for studying H2AX
t-BuOK	Potassium tertbutoxide
TEP	Tolman electronic parameter

THF	Tetrahydrofuran
Tmetc	Tetramethyl ethene-1,1,2,2-tetracarboxylate
TMQ	8-Thiomethylquinoline
TMQ-Me	2-methyl-8-methylthioquinoline
TPPTS	Sodium 3,3’,3’’-phosphinetriylbenzenesulfonate
Trx	Thioredoxin reductase (Trx)
TTBQ	8-Tertbutylthioquinoline

1

General Introduction

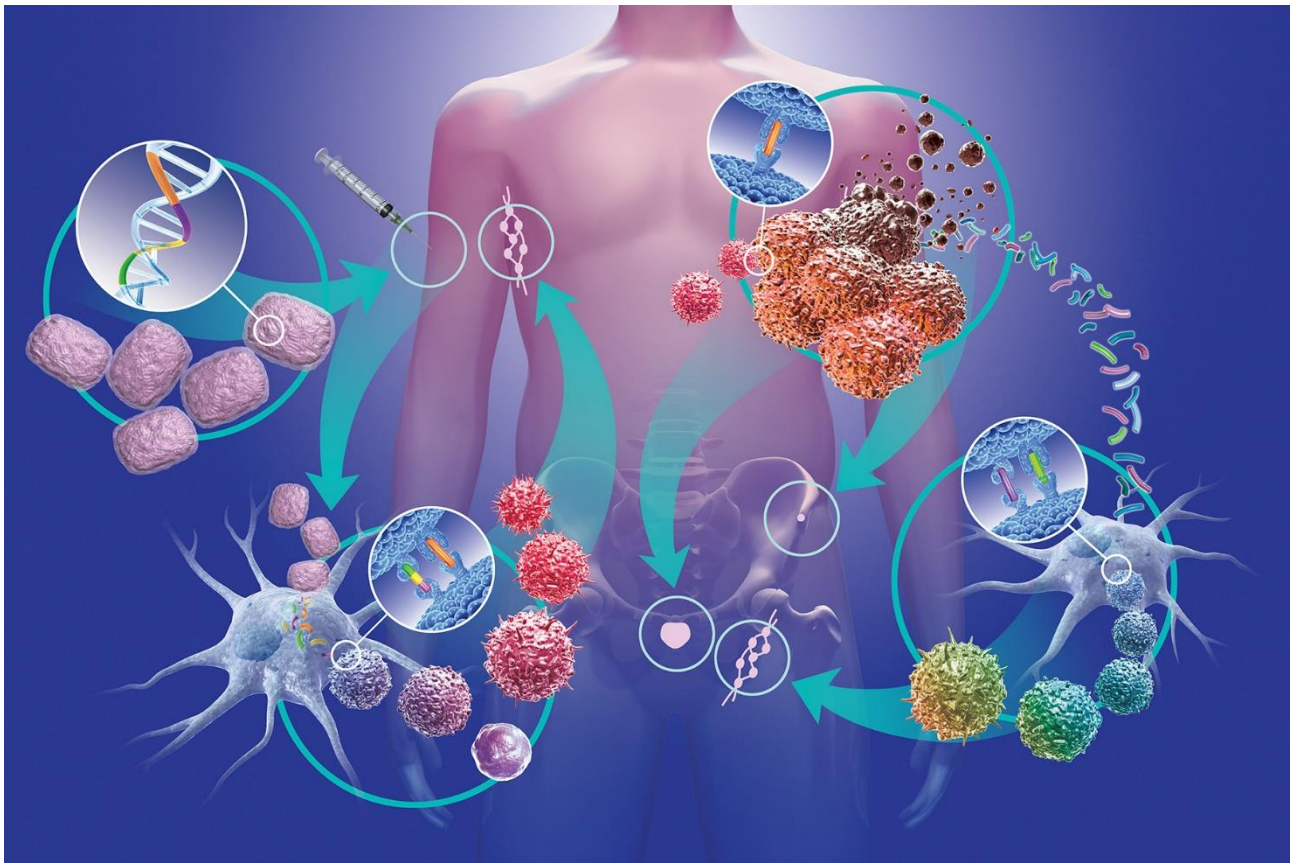

This introductory chapter will illustrate the basic concepts about cancer. The main types of neoplasia, the incidence, the risk factors and the carcinogenesis process will be expounded. A deepening on the ovarian cancer, which represents the type of tumour most taken into consideration in this work will be developed.

The core of this introduction will be dedicated to the cancer therapy and particular emphasis will be devoted on the metallodrugs as anticancer agents. Owing to the complexity of the subject, a brief overview of the coordination and organometallic compounds of platinum, ruthenium, gold and palladium will be presented.

Finally, the stereoelectronic properties of the *N*-Heterocyclic Carbene ligands and the organometallic fragments used in this work will be discussed.

The figure proposed at the beginning of the chapter is related to this source: http://epicstudios.com/?p=4877

1.1. General aspects about cancer

1.1.1. What is cancer?

Cancer represents an extensive and heterogeneous class of pathologies caused by an uncontrolled cells reproduction with consequent formation of solid masses called tumours.

The process that transforms a healthy cell into a cancerous one occurs in several stages and is often generated by an accumulation of genetic anomalies affecting the genes responsible for the control of DNA repair, death and cell division processes.

The tumour in its initial stage is called primary tumour. Often it become dangerous for the life of the ill person since obstructs organs and/or blood vessels. In the case of malignancy, death is most commonly caused by the spread of the primary neoplasia to vital organs, in a process known as metastasis. This diffusion process occurs through the lymphatic system or the bloodstream.

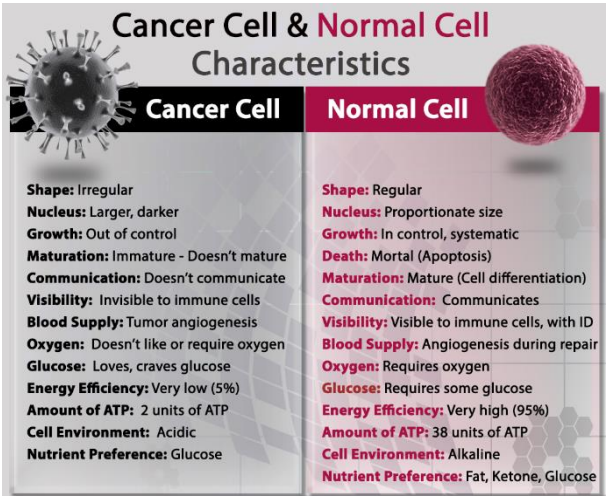

Fig. 1.1 Main differences between tumour and healthy cells [1].

Surgery is not very effective in the case of metastasis and therefore the pharmacological approach remains the main treatment.

The classification of the disease based on the target organ or on the type of cancer cells, includes more than 200 categories of tumours [2]. However, it is noteworthy that this approach is simplistic, since many different tumours afflict the same organ, respond to the treatments differently and with different rates of progression.

However, in the sake of simplification a very rough classification divides the tumours into six large classes (Tab. 1.1) [2].

Principal type of cancer	Origin of the tumour	Frequency (estimation)	Localisation
Adenocarcinoma	Epithelium (surface tissue of many glands)	85% of all cancers	Breast, liver, kidney, prostate, pancreas, ovary, thyroid, colon, stomach, salivary glands, lungs.
Squamous-cell carcinoma	Squamous epithelial cells (epidermis)		Skin, gastrointestinal tract, lung, uterus, pancreas
Sarcoma	Connective tissues (bones, muscles)	2-4% of all cancers	Bone, cartilage, lungs, fat tissue, blood vessels
Hodgkin's Lymphoma	B and T lymphocyte (large atypical cells)	5-7% of all cancers	Lymph nodes, spleen
Non-Hodgkin's Lymphoma	B and T lymphocyte		Lymph nodes, gastrointestinal tract, skin, brain, bones, reproductive organs, lungs
Leukaemia	Bone marrow cells (blast)	4-6% of all cancers	Blood
Myeloma	Bone marrow cells (plasmocyte)		Bone marrow

Tab. 1.1 Classification by type of cancer [2].

The table shows that carcinoma constitutes about 85% of human tumours and affects the epithelium of internal organs, glands and cavities. This pathology is common in the breast, colon, lungs, prostate and ovaries.

Despite chemotherapy and other focoused therapies, the cancer remains a pathology (or a set of pathologies) difficult to treat. This is essentially due to the enormous diversity between the various tumors, their resistance to pharmacologic therapy and the side effects of different treatments. For these reasons, the cancer remains the crucial challenge in the medical field of the 21st century.

1.1.2. Incidence, mortality and risk factors

Because of the long period that often occurs between exposure to a carcinogen and the diagnosis of the neoplasia (up to 20-30 years), the current incidence data reflect the environmental conditions and lifestyles of a few decades ago. In the USA, the *American Cancer Society* estimated that in 2015 about 166,000 new cases of cancer were diagnosed [3]. The data on the diagnosed tumours, classified according to area of the body in which they are localised, are reported in Figure 1.2 and show that the reproductive tract cancers constitute the most recurring cases, regardless of the individual gender.

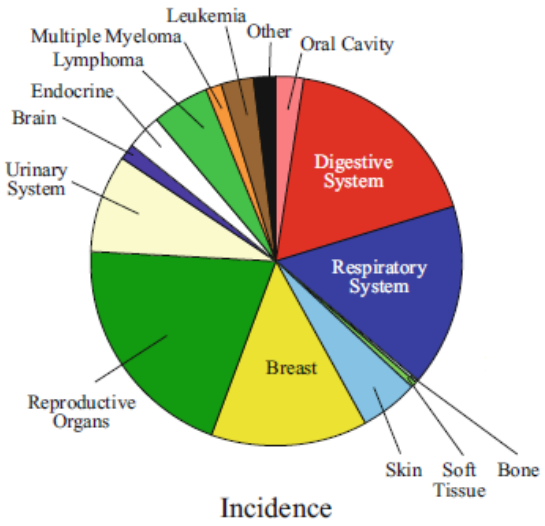

Fig. 1.2 Incidence of the main types of cancer in the USA in 2015 [3].

The same study found that the number of deaths attributable to cancer was about 590,000 (53% men and 47% women), and the tumors that produced the highest number of deaths are those related to the digestive and respiratory systems.

Very similar results can be found in the investigations conducted by the IARC (*International Agency for Research on Cancer*) [3] (Fig. 1.3), which estimated about 13 million the number of new cancers diagnosed worldwide in 2008 whereas, the RTI (*Registro Tumori Italiani*), indicates about 365,000 new cases diagnosed in Italy in the 2016 [4].

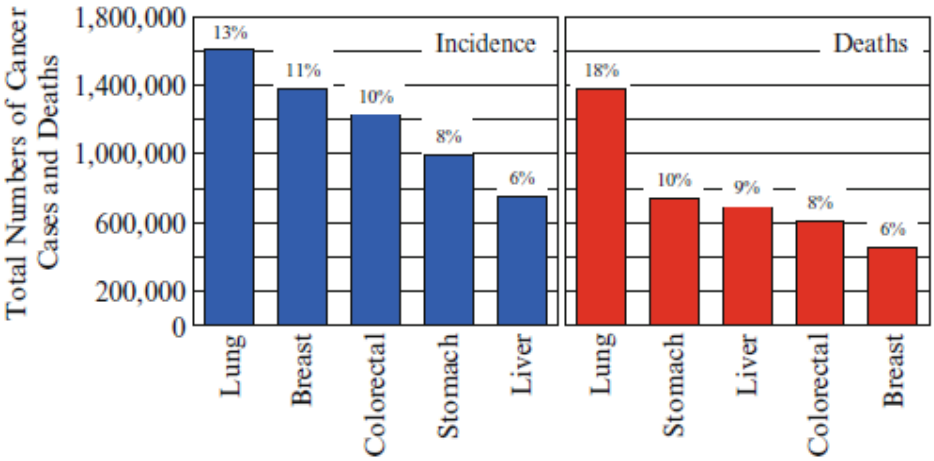

Fig. 1.3 Percentage rates of incidence and mortality worldwide related to the main types of cancer [3].

Generally, in the older people, an increase in the probability of the disease, mainly due to the decrease in the efficiency of the immune system and the greater probability of presenting genetic mutations, is observed [5]. Exceptions include breast cancer, which mainly affects younger women (40-65 years), specific types of leukemia and the childhood cancers.

Although in the last 50 years there has been a steady progress in prevention, treatment and improvement of the lifestyle of the population, from the data of the *Center for Disease Control and Prevention* emerges that cancer is still the second cause of death of the American population after cardiovascular diseases. However, a comforting fact is that since 2003 the number of deaths due to cancer has decreased compared to 1930, despite the increase in population and average life expectancy [2]. This result is due to the effectiveness of the therapies, a better strategy of prevention and the change of bad habits regarding exercise and diet.

Among the risk factors for cancer onset there are:

- ethnicity;
- exposure to carcinogens (environmental risk);
- type of diet;
- exposure to the sun;
- exposure or intake of hormones.

Figure 1.4 shows how environmental parameters have the greatest influence on the birth and evolution of cancer [6].

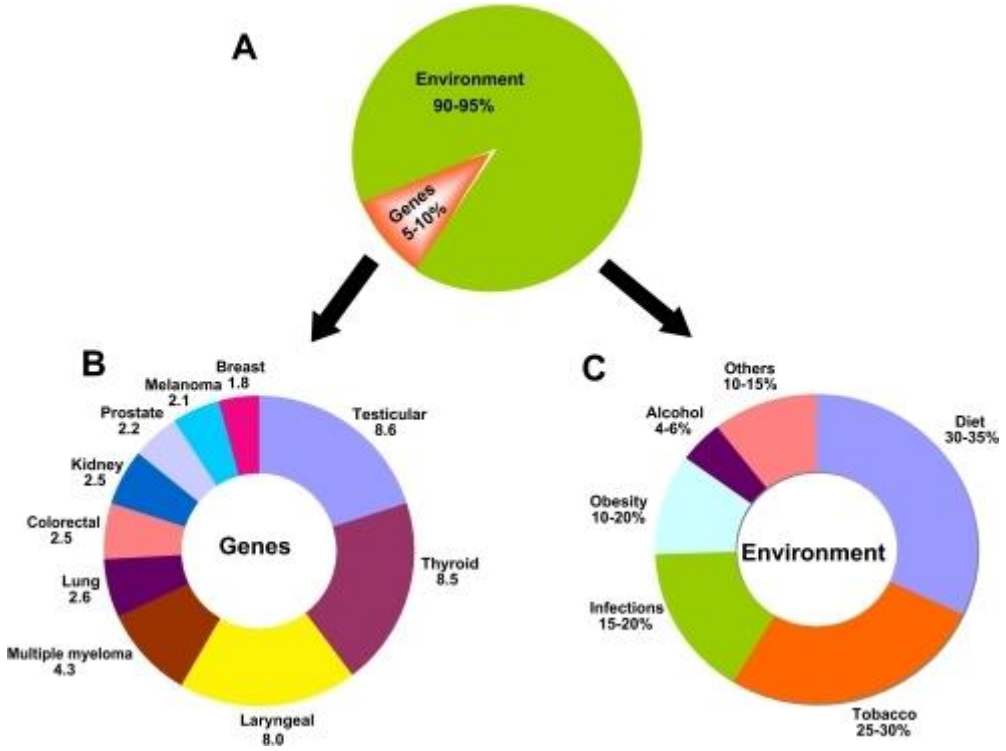

Fig. 1.4 The role of genes and environmental in the development of cancer [6].

1.1.3. Carcinogenesis

Robert A. Weinberg [7] contributed in reinforcing the idea that many cancer cells are the result of important changes in the cell physiology, eventually leading to the proliferation of malignant tumours. According to his studies, all tumors have some common features that distinguish them from other diseases:

- self-sufficiency in growth signals;
- intensification of growth inhibition signals;
- lack or reduction of programmed cell death (apoptosis);
- limited potential for reproduction;
- pronounced angiogenesis;
- tissue invasion and metastasis.

The genetic changes that induce the appearance of cancer occur at different levels and with different mechanisms. The most common are mutations, involving changes in the sequence of DNA nucleotides. These mutations, which alter the expression of some genes, can be caused by five main factors:

1. Inheritance: some people inherit the predisposition for cancer development from their family members. One or more genes therefore have mutations already from birth.
2. Viruses: if a virus infects a cell, it introduces genetic material that can sometimes contain oncogenes. Furthermore, they can deactivate some genes or activate cell proliferation genes.
3. Mutagenic factors: some molecules present in the environment, in addition to UV, X-rays and in general all ionizing radiations, can produce DNA alterations.
4. Copying errors: during the cell division, unrecognized errors in the copy of the DNA can generate carcinogenic mutations.
5. Epigenetic: small molecules (i.e. methylating agents) can bind to a gene. The enzyme responsible for DNA reading, sometimes is not able to read the entire gene and therefore the presence of an altered gene.

The transformation of a normal cell into a tumour cell occurs according to a series of chain processes caused by an error occured in the initial phase. These processes can be summarized in the following steps [2]:

1. A healthy cell can regulate its division via *proliferation gene* or decide to have a rest via an *antiproliferation gene*. In the presence of appropriate signals, it can also undertake the programmed death via the *apoptosis gene*.

2. During cell division the DNA is duplicated and the daughter cell receives a copy from the mother cell, while the *DNA repair gene* continuously checks that the copy received is identical to the original one.
3. If an error occurs in the phase described above, the *proliferative gene* is mutated at variance with the *antiproliferative gene* which fortunately remains intact. In this case the growth slowing or induction of programmed cell death via apoptosis can occur.
4. When the *proliferative gene* undergoes mutation, such cell no longer responds to the signals of end proliferation or apoptosis: the cell becomes cancerous and therefore refuses to die and duplicates in an uncontrolled way.
5. The protection systems collapse one after the other, the *DNA repair genes* are damaged and the cell accumulates over time many errors in the DNA.

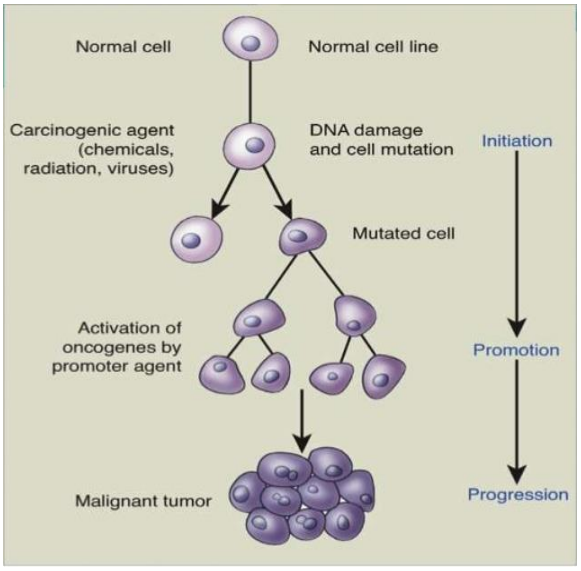

Fig. 1.5 Stages of the carcinogenesis process [8].

The cancer cells are therefore grouped into solid clusters called tumours and some of these may undergo further mutations that allow them to enter inside the blood vessels. These cells can be easily fed by the glucose present in the blood vessels and transported to the rest of the body via bloodstream. Through this metastasis process they can affect other organs and tissues, creating new tumour masses.

1.1.4. An in-depth analysis of the cell cycle

The cell cycle can be subdivided into four phases: G_1, S, G_2 and M. In particular, the S and M phases represent the main steps of the whole process. The duplication of the genetic patrimony of the cell takes places during the S phase, whereas in the M phase mitosis occurs, with the consequent segregation of the chromosomes and cytokinesis (division of the cell into two daughter cells).
Clearly, besides DNA replication, it is important that the cell could increase its size and double its protein and organelle mass. For this reason, the gap phases G_1 and G_2 appear within the cell cycle. The gap phases allow the cell to have the necessary time to grow and control the internal and external environment, verifying that the conditions for the progress of the cell cycle are suitable and that all the preparatory steps before the S and M phases are completed. If the extracellular conditions are unfavorable, the cells may delay the G_1 process and enter in a state of rest (G_0), in which they can spend few hours or many years as well, before resuming proliferation [9].
A complex network of regulatory proteins (control system) works inside the cell, monitoring the cycle progression and postponing the following event until the completion of the previous one. Moreover, the control system intervenes in the stimulation or blocking proliferation as a consequence of the signals arriving from outside the cell itself [9].
Therefore, there are *control points* that authorize the progress or the blocking of the cycle:

- Restriction point: located in late G_1, corresponds to the point where the cell is allowed to enter in the cell cycle and duplicate the chromosomes.
- G_2/M: located between phase G_2 and M, corresponds to the point where the *control system* triggers early mitotic events.
- Metaphase-anaphase transition: a point in which the *control system* stimulates the completion of mitosis and cytokinesis.

If the *control system* detects problems inside or outside the cell, the progression of the cell cycle will be blocked in one of these points until new favorable conditions.

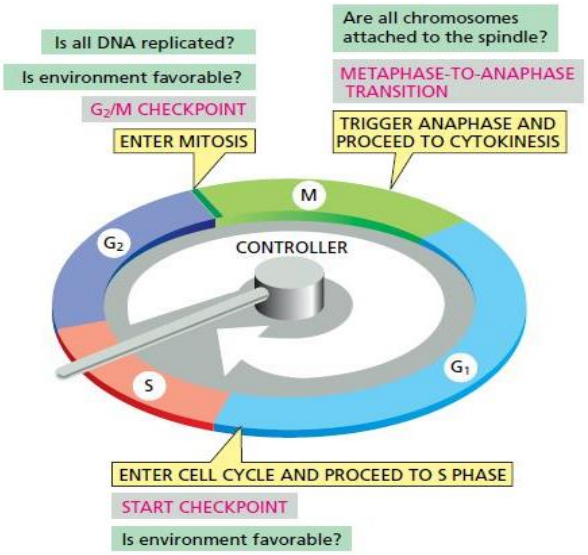

Fig. 1.6 Cell cycle control [9].

Many human cells present a restricted number of replication processes and in their absence, the cell cycle is permanently stopped and no replication processes are allowed anymore. This phenomenon is known as senescence and is related to the progressive consumption of chromosomal ends (or telomere). Over time, the telomeres become shorter and the proteic structures protecting them progressively deteriorate (the cell cycle arrest is similar to that caused by other types of alterations). However, cancer cells regain the ability to produce telomerase, the enzyme that intervenes in the replication processes of telomeres and promotes the synthesis of proteic structures to protect these sequences, and therefore are able to preserve the function of telomeres during proliferation and bypass the process of senescence [9].

1.1.5. Apoptosis

Apoptosis is a process programming the cell death. The cell die in a controlled manner and is quickly eliminated without inflammatory responses [2]. The cell that undergoes this mechanism shows characteristic morphological changes *i.e.* it reduces and condenses its size, the cytoskeleton collapses, the chromatin condenses and breaks up. The cell surface often produces vesicles and it is divided into fragments enclosed within membranes called apoptotic bodies. Moreover, during the process, the plasma membrane undergoes chemical alterations. For example, the phosphatidylserine (a negatively charged phospholipid that normally is contained in the cytoplasm) is expelled from the cell. The expulsion of this protein triggers the phagocytosis of the cell by macrophages.

An important role in the apoptotic process is played by the caspases which are proteolytic enzymes containing one cysteine in their active site. Caspases are able to cut on specific points a series of

intracellular proteins (target proteins) promoting the cell death. Caspases can be distinguished in initiator and effector; usually they are present as inactive precursors called procaspases. Once activated, the initiator caspases, through a proteolytic cut, give the effector caspases that acting on specific cytosolic proteins and nuclear laminae, lead the cell to a controlled death in accord with a chain mechanism called proteolytic cascade.
Often, many cancerous cells regulate abnormally the apoptotic process, stimulating the expression of factors able to inhibit its function or alter the coding mechanism of the p53 protein, which is responsible for the activation of the protective mechanisms and promotes apoptosis in the case of DNA alterations. Mutations in the p53 gene are in fact observed in about 50% of tumors [9].

1.1.6. Ovarian cancer

Ovarian cancer, which is the most investigated type of cancer in this work, is a malignant tumor that develops in the tissues of the ovaries, the woman reproductive organs in which the ova are formed and where the female hormones are produced.
Depending on the cell type from which the neoplasia originates, it is possible to identify three categories of ovarian cancer [10]:

- Epithelial cancer: originates from epithelial cells that superficially cover the ovaries.
- Germine tumor: originates from germ cells (those secerning the ova).
- Stromal tumor: originates from the gonadal stroma (ovary support tissue).

Most of the malignant tumors affecting the ovaries are epithelial and represent a total of about 90% of the recorded cases [11]. Based on the new knowledge acquired over time, a new classification has been introduced [12], in which the ovarian carcinoma is subdivided into two different classes of tumors, according to its morphological and genetic-molecular characteristics:

- Type I tumors: these tumors are confined on the ovary and are characterized by slow growth and rarely show mutation of the p53 gene. They are generally associated with mutations in specific genes.
- Type II tumor: these tumors, usually detected in advanced stage, are aggressive and show a high frequency of mutation of the p53 gene and are genetically unstable.

The 5-year overall survival of patients with malignant epithelial tumors of the ovary is around 50% and an important role, able to significantly affect life expectancy, is played by the stage in which the carcinoma is identified. Unfortunately, the non-specific and late symptomatology of the disease and

the lack of diagnostic procedures of adequate sensitivity and specificity, often allows the identification of the disease when it has reached advanced stages (stages III and IV, Fig. 1.7) [13].

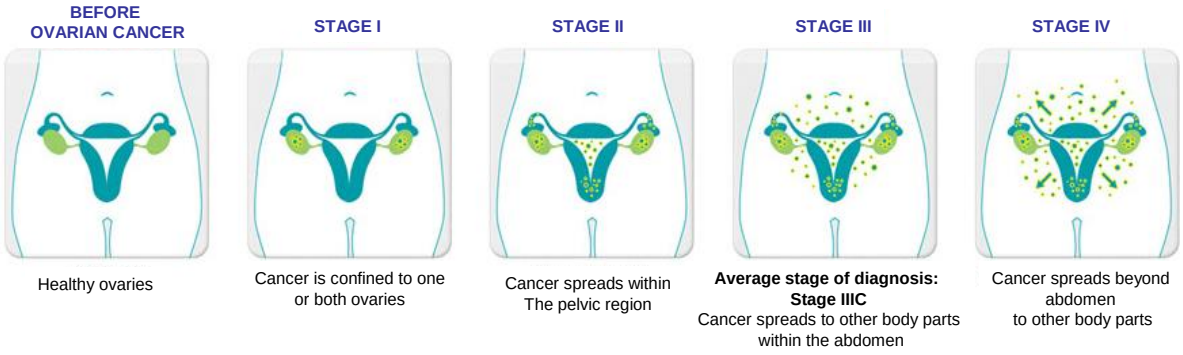

Fig. 1.7 Stages of ovarian cancer [14].

Generally, the used tools for the diagnosis of epithelial tumors are the pelvic ultrasound and the determination of CA125, which is a protein produced by the uterus or by the Fallopian tubes. CA125 is found in small quantities in the blood because of damage or inflammation of the tissues of the cited organs, but the effectiveness of these investigations is insufficient. Recently, another marker called HE4, which appears to be more specific and sensitive in diagnosis than CA125, has been individuated [15]. With respect to the treatment of the pathology, the initial surgical approach plays an important role both for diagnostic and therapeutic purposes, since it allows the histopathological assessment of the nature of the mass and the stage of the tumor. If the tumor is present at an initial stage, a radical surgery can be decisive and when necessary, the surgical remotion can be enforced by an adjuvant chemotherapy. If the disease is at an advanced stage, the surgeon tries to remove as much as possible the mass of the tumor, which will be subsequently treated chemotherapeutically [2, 13].

The chemotherapy cycles are calibrated according to the stage of the tumor and the general clinical situation. Usually a combined therapy (multiple drugs) is used in order to minimize the possibility of resistance phenomena. The commonly used chemotherapeutic agents are compounds based on platinum (cisplatin or carboplatin) and taxanes, such as paclitaxel or docetaxel. In the last twenty years, no chemotherapy regimen has proved to be more effective than standard carboplatin/paclitaxel treatment.

After this primary treatment, it is possible to activate secondary treatments with the aim of preventing or combating recurrence [2, 13]. In fact, about 70-80% of people with advanced ovarian malignancy have recurrence of the disease within the first two years from the initial treatment. At this point, a second line therapy has mainly palliative purposes, since it results curative in a narrow minority of patients.

1.2. Cancer therapy

The choice of the appropriate treatment after the diagnosis of a tumor, is probably one of the most critical problems. There are numerous factors that contributing to the choice of the best treatment i.e.: the type of cancer, its stage, the presence of metastasis, the age and the health conditions of the patient. The five traditional methods are surgery, radiotherapy, photodynamic therapy, immunotherapy and chemotherapy. Surgery, radiotherapy and photodynamic therapy are often used for the treatment of locally confined tumors, whereas chemotherapy and immunotherapy are systemic methods. A combination of these strategies is often possible.

1.2.1. Surgery

Surgery is a generally used approach in the case of tumor confined in a specific region. Such method may provide good chances of recovery especially in absence of metastasis. The amount of tissue that can be surgically removed depends on the size of the tumor and the presence of metastasis.

If a person presents a predisposition to a specific form of cancer, it is possible to intervene in a preventive manner. For example, a genetic alteration of the BRACA/1 and BRACA/2 genes predisposes to the onset of ovarian carcinoma and therefore the removal of the ovaries represents a precautionary measure [2]. During diagnostic or staging surgery, tissue samples can also be removed to identify the benign or malignant nature of the tumor by biopsy.

If it is not possible to remove the whole tumor, the first objective of the intervention is to remove as much tumor as possible, in order to make radio- or chemo-therapy treatments (adjuvant therapy) more effective. In some cases, it can also be used a reverse approach (neoadjuvant therapy).

1.2.2. Radiotherapy

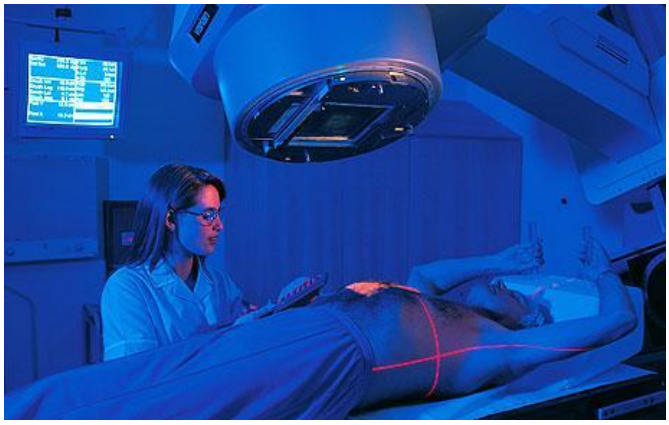

Radiotherapy uses ionizing radiation, usually X-rays, to destroy cancer cells by irradiating the mass of the cancerous tissue. The radiations used can be emitted by radioactive substances such as iodine or cobalt (^{131}I or ^{60}Co) or produced by specific devices (linear accelerators) [2]. Thanks to the high energy and the ability to cross cancer cells, X-rays can heavily damage the DNA. The goal of radiotherapy is the induction of severe alterations in the DNA of the cell, which will die since its functionality is compromised. During the therapy, some healthy cells can be affected by the radiation. However, since such cells are not affected by anomalies in repair mechanisms of the DNA or apoptosis, they have a better resistance toward any suffered damage. The duration and overall dose of treatment depend on the type, size and location of the tumour in the body. Once the appropriate overall therapeutic dose has been determined, the planning of the therapeutic treatment (through a single or repetitive fractions) will be established.

1.2.3. Photodynamic therapy (PDT)

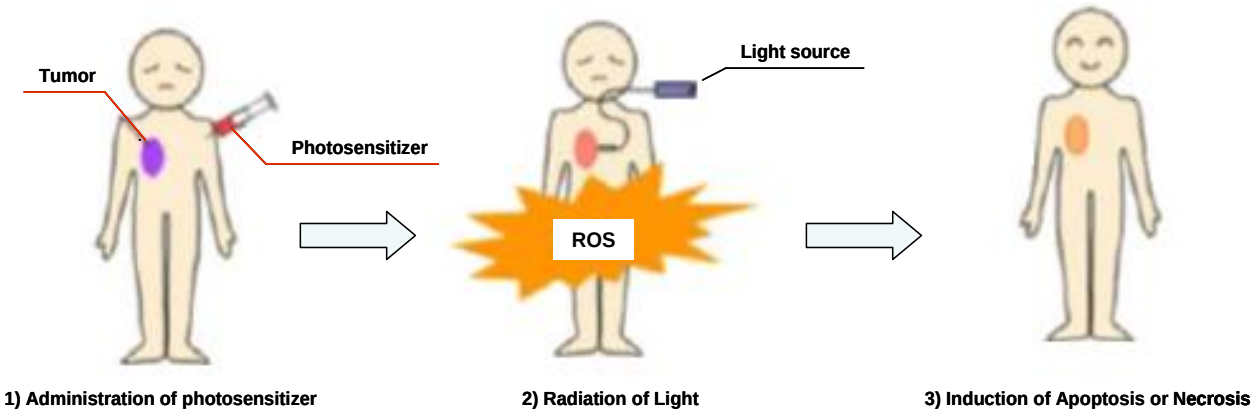

Photodynamic therapy (PDT) has been used since the 1990s and utilize light irradiation to contrast the skin, lung, bladder, prostate, urinary tract, esophagus and ophthalmic neoplasms in the case of localized and not deep-rooted tumours [16]. The PDT utilizes photo-sensitizers, or molecules capable

of absorbing visible light at an appropriate wavelength interval, to produce the cytotoxic ROS (*Reactive Organic Species*) which eventually lead the death of tumour cells by apoptosis and necrosis. This technique allows a precise spatio-temporal control of the treatment, which can also be repeated. The photo-sensitizer is activated only in the irradiated areas and theoretically induces the destruction of the diseased tissue without causing serious damage to healthy one. This technique also allows the treatment of the not surgically operable areas.

The first FDA approved photosensitizer was Photofrin, consisting of a mixture of dimers and oligomers of porphyrin type units. Thereafter, a second and third generation compounds were developed and coupled with a variety of biological targeting vectors [16]. In the case of porphyrins, it is possible to exploit their fluorescent and phosphorescent emissions, to define the limit between the diseased and the healthy tissues. This technique is also useful for the tumor imaging and the so-called "guided surgery".

The biomedical research are now looking for a possible therapeutic use of the photochemistry mediated by metal complexes on the basis of two different points of view. In one case, starting from a coordinated saturated complex one or more coordination sites will be made vacant allowing the interaction of the metal centre with biomolecules. Alternatively, the biologically active fragment will be constituted by the released ligand. In any case, the irradiation with light will cause the transformation of the pro-drug (stable in the dark) in the active species [16].

1.2.4. Immunotherapy

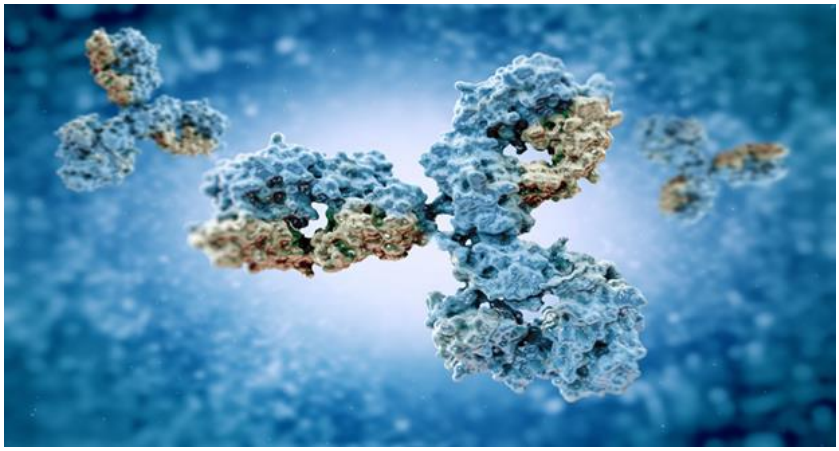

The goal of the biological therapy or immunotherapy is the increase of the body's ability to identify and destroy cancer cells and repair the cells damaged during the treatment [2].

For this purpose, the following techniques are used:

- Interferons and cytokines: molecules used by the cells of the immune system to communicate each other. Their use can stimulate in some types of cells their immune system and increase their activity level.
- Monoclonal antibodies: proteins produced by some white blood cells that assist the immune system in identifying microbes or malignant cells and then destroying them. Several monoclonal antibodies could selectively bind some proteins present on the surface of tumor cells, marking them as foreign and making them easily identifiable and therefore attackable by the immune system.
- Gene therapy: introduction into the cells of DNA fragments containing genes encoding specific functions. This introduction can be done for example in the cells of the immune system so that proteins can be coded to increase their performance or within the cancer cells for their identification and destruction.

1.2.5. Chemotherapy

Technically, chemotherapy defines any therapeutic treatment perpetrated by means the use of chemicals, but usually the term is associated with the use of drugs for the treatment of cancer [2]. Chemotherapy, unlike surgery or radiotherapy, is a systemic form of treatment because the drugs used can spread in the body, allowing the neutralization of cancer cells also not under the form of solid tumour (i.e. leukaemia or lymphoma) or metastatic repetitions.

In the best of cases, chemotherapy can be used to eliminate all the cancer cells in the body, but it can also be used to minimize, after surgery, the possibility of regrowth of a tumour or to inhibit the future development of metastasis. If a cure for the disease is not available, you can resort to chemotherapy for palliative purposes or to extend the duration and quality of the life of a person.

The anticancer drugs can be distinguished on the basis of their biological action in:

- Antimetabolites: they intervene by blocking a particular metabolic pathway or interfering with the functionality of specific enzymes.
- Alkylating and coordinating agents: they modify the structure of the DNA bases by alkylating (or coordinating) them. After this kind of modification some important functions of the cell can be alterated and cause:
    - An excessive DNA fragmentation promoted by the enzymes responsible for the repair of the alterations caused by the alkylating (or coordinating) agent.
    - Incorrect coupling of DNA bases.
    - Formation of permanent cross-links between the two DNA strands preventing their separation in the replication process.
- Inhibitors of topoisomerases: are a class of enzymes important for the regulation of DNA metabolism.
- Mitotic inhibitors.

1.3. An overview of anticancer compounds

1.3.1. Origin and modern organic anticancer research

In the modern age, the study of organic compounds as anticancer agents can be traced back to the observation of the drastic reduction of the somatic cells proliferation, particularly the lymph nodes, showed by the victims of chemical weapons (i.e. mustard gas).

As a consequence of that observation, the pharmacologists Philips, Goodman and Gilman treated mice affected by lymphomas with analogues of mustard gas, observing the suppression of the tumour. Subsequently they treated a human patient with mustine (a derivative of mustard gas), noting the reduction of the tumour mass already from the first day of treatment [17].

In the 1950s, Sydney Farber observed that folic acid (vitamin B9) stimulated the proliferation of acute lymphoblastic leukaemia. Treating these cells with folic acid antagonists, such as aminopterin and amethopterin, he observed tumour regression [18]. For this reason, Farber can be considered the "father of the anticancer chemotherapy" (Fig. 1.8).

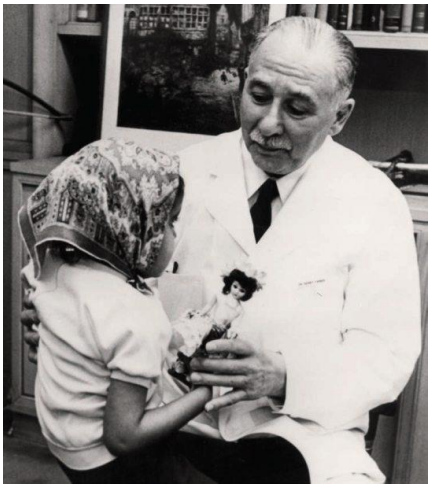

Fig. 1.8 Sidney Farber father of the modern anticancer chemotherapy and founder of the pediatric pathology [19].

Following his work, many natural organic metabolites and molecules were studied for their possible anticancer activity. For example, in 1954 important studies of the antitumor properties of 6-mercaptopurine and 5-fluorouracil were reported [20, 21].

In 1966, Dara Richardson synthesized for the first time the tamoxifen (an estrogen receptor antagonist) that was studied against breast cancer and subsequently approved by the FDA [22, 23].

In the second half of the 20th century, people began to think about the so-called “targeted therapy”, where the drug interacted selectively with the vital processes of the cancer cells. For example, in the 1990s, studies of the AbI-Bcr oncogene showed that it produced analogues of tyrosine kinase proteins

within the tumours. The selective inhibition of this protein was tested by screening a large number of molecules synthesised on the basis of a rational drug design. The use of some organic compounds as agents against different types of chronic leukaemia and other neoplasms represents the consequent extension of the previous described results. Figure 1.9 shows a selection of organic molecules with marked anti-tumour activity.

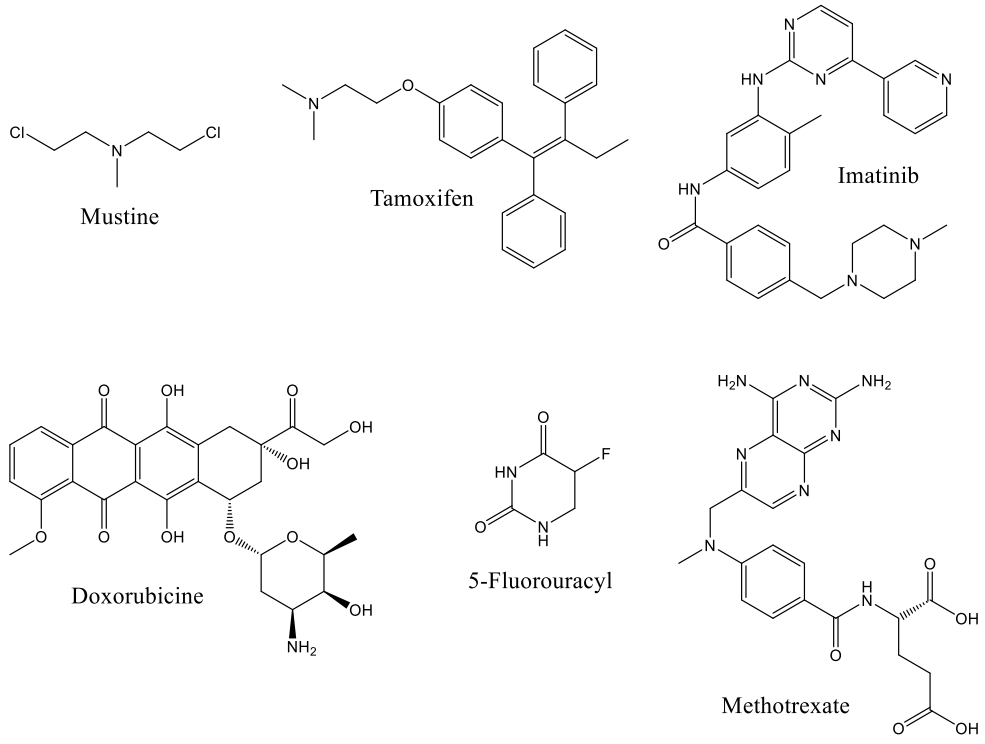

Fig. 1.9 Important organic anticancer compounds.

1.3.2. Metal-based anticancer compounds

For many decades, the research was aimed at discovering anticancer drugs able to block the essential functions of cells. The interactions of the drugs with the physiological environment are numerous *i.e.* they can interfere with microtubules (Taxol) [24], modify the DNA (cisplatin) [25], influence the synthesis of metabolites (Methotrexate) [26] or have effects on chromosome topology (Rinotecan) [27]. Some exceptions are represented by the estrogen receptor modulators in anti-hormonal therapy (i.e. Tamoxifen) [28] and epidermal growth factor receptor tyrosine kinase inhibitors (i.e. Gefitinib) [29]. Among all of these, cisplatin [25] is one of the most important compounds in chemotherapy and was widely used against malignant solid tumors for more than 30 years. At the really beginning of chemotherapy the compounds containing metals were not considered as possible drugs because their toxicity and the well known poor stability.

From the serendipitous discovery of the anticancer properties of cisplatin, which was approved by the FDA in 1978, researchers began to consider as candidate drugs against cancer also metal-based

compounds and in particular the organometallic compounds, which by definition present at least one metal-carbon bond. This type of bond is generally strong and contributes to the stability of the corresponding complexes. This quality is extremely useful since does not allow the presence in physiological environment of the free metal, which causes a general toxicity.

The first organometallic compound whose antiproliferative activity was reported is ferrocene (Cp_2Fe) [30], which was followed by ruthenium and osmium derivatives.

Moving from the coenzyme B_{12} (natural organometallic compound discovered in 1961 [31]) to titanocene dichloride (the first non-platinum organometallic compound), which underwent clinical trials in 1998 [32]), the bioorganometallic chemistry developed very rapidly (Fig. 1.10).

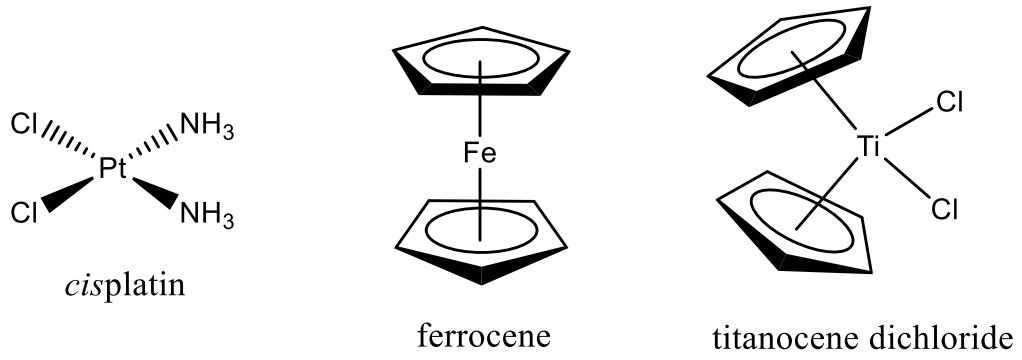

*cis*platin ferrocene titanocene dichloride

Fig. 1.10 Historically important metal complexes in the development of anticancer drugs.

The basic research in the field of organometallic chemistry, concerning the synthesis of new compounds, the study of their reactivity, accompanied by mechanistic studies also supported by DFT calculations, certainly allowed an easiest investigation on their possible applications as chemotherapeutics [33, 34]. As described in the following paragraphs, cisplatin and analogues are used in about 70% of the chemotherapeutic regimens concerning solid tumors. Their collateral toxicity, their ineffectiveness against some types of tumors and drug resistance, which is sometimes developed by the treated cells [35-37], are the main reasons leading many research groups to look for new metal-based compounds that could solve, or partially solve, the problems related to platinum compounds.

The great structural variability of the organometallic derivatives, due to the different stereoelectronic characteristics of the ligands available, represents an advantage with respect to the organic compounds. For example, several half-sandwich ruthenium (II) complexes may act as bio-catalysts [38], DNA modifiers [39] or protein kinase inhibitors [40], simply by varying the type of chelating N-N ligand.

The anticancer compounds can be classified according to their mechanism of action, in function of the damage they cause to DNA, the type of cellular process with which they interfere or the source from which they derive.

Drugs containing metals can be divided into five broad categories [41]:

- Functional compounds (pro-drugs): their main action mechanism is based on the direct coordination of the metal to one or more target biomolecules. Therefore, they must possess at least one free coordination site that is made available by the *in vivo* dissociation of labile ligands. Secondary non-coordinating interactions such as hydrogen bonds and hydrophobic interactions can also be important. In the case of total dissociation of the initial ligands, the "naked" metal could also replace an essential metal by interfering with the metabolism. The activation of the functional species is triggered by the chemical-physical environmental conditions of the diseased tissue (i.e. hypoxia and low pH) or is induced by external stimuli.
- Structural compounds can perform their function keeping intact their initial form, interacting with target biomolecules through purely supramolecular interactions (among them we find the "intercalators" of DNA). These complexes must therefore have high kinetic and thermodynamic stability; therefore, they often contain multidentate chelating ligands and/or organometallic fragments.
- Compounds in which the metal behaves as carrier toward the active ligand, possibly protecting it before the delivery.
- Compounds in which the metal is a catalyst aimed at accelerating a process, for example the formation of ROS (*Reactive Oxygen Species*).
- Compounds containing a photoactive metal that acts as a photosensitizer (with subsequent applications in the photodynamic therapy).

In any case, a very important feature for a chemotherapeutic agent is the selectivity or the preferential absorption of the compound by the tissue/organ that has to be treated.

In particular, the main mechanism of passive selectivity is represented by the Enhanced Permeability and Retention (EPR), which is based on the greater permeability of the blood vessels of the solid tumors toward macromolecules or nanoparticles and on their greater retention, due to deficiencies in drainage owing to the poor efficiency of their lymphatic system.

The induced or active selectivity, is obtained by the functionalization of the active principle (or of the nanoparticle surface) with appropriate targeting vectors able to selectively recognize the overexpressed proteins on the tumor surface and thus guide the accumulation of the drug in the diseased tissues [16].

1.3.3. Target for organometallic anticancer compounds

The three most common targets for organometallic antitumor compounds are DNA, proteins and redox systems. In this section the three categories will be discussed in detail.

1. DNA

   Organometallic compounds acting on DNA are rather promising since they often act differently from cisplatin, showing in some cases a significant reduction of the general toxicity and side effects. For example, some organometallic derivatives of ruthenium and osmium have as main target topoisomerase (Fig. 1.11, complex A) [42], special DNA sequences [43] or G-quadruplex (Fig. 1.11, complex B) [44].

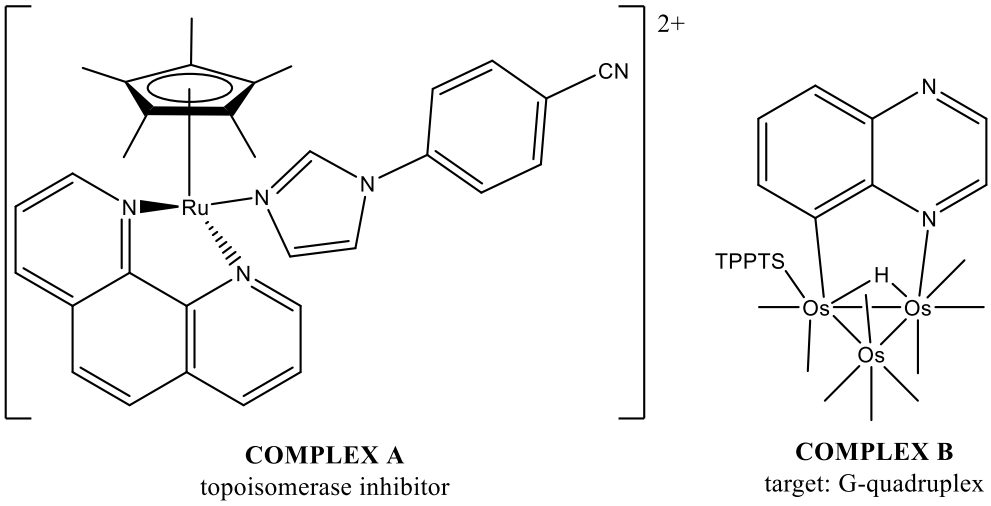

COMPLEX A
topoisomerase inhibitor

COMPLEX B
target: G-quadruplex

Fig. 1.11 Example of organometallic complexes acting on DNA.

2. Essential proteins for proliferation

   Several types of promising protein targeting agents for the treatment of neoplasms have recently been studied. These include aurora-kinase inhibitors, epidermal growth factor receptor (EGFR) inhibitors and cyclin-dependent-kinase (CDK) inhibitors. For example, the ferrocene carboxaldehyde exhibits good anticancer activity *in vitro* and has been shown to be an EGFR inhibitor [45].

   Ruthenium (II) arene RAPTA derivatives undergo hydrolysis of the two chloride ligands and hence they interact with the DNA [46]. However, studies carried out by Messori demonstrate that these compounds simultaneously inhibit two enzymes such as cathepsin B and thioredoxin reductase (Trx) [47]. Some research groups have adopted as their strategy the synthesis of organometallic compounds that have the shape and chemical characteristics capable of interact with certain proteins involved in the proliferation of tumor cells [48].

Although this idea is valid, it is not easy to prepare a complex that shows selectivity for a given protein without a concomitant interaction with other bio-targets.

3. Redox systems

   Within the cells, the redox hierarchy can be expressed by the following order on going from the most reducing to the most oxidizing environment: mitochondria > nucleus > cytoplasm > endoplasmic reticulum > extracellular space [49]. Thus, the oxidizing species can preferentially damage the mitochondria membrane, altering the level of thiols such as glutathione (GSH).

   As a matter of fact, the amount of glutathione in tumour tissues is one of the factors influencing resistance to chemotherapy in certain neoplasms [50]. In addition to the thiol/disulphide pair, another important redox pair is NADH/NAD^+. Some ruthenium arene complexes are able to selectively reduce NAD^+ to NADH under physiological conditions [51]. In any case, the redox activity and the correlation of redox activity/antitumor activity are certainly less clear and explored than that of compounds acting on DNA and/or on some proteins overexpressed in tumour tissues.

1.3.4. Platinum: from cisplatin to the next generation drugs

Cisplatin [(*cis*-diamino-dichloroplatin (II)], which is a yellow solid with a square planar geometry, was the first inorganic drug to be used in the clinical setting, individually or in combination with other drugs, for the treatment of various neoplasms including those of the lungs, ovaries, testicles, prostate and neck. However, despite the appearance of second and third generation analogues that have overtime replaced its use, it remains a standard compound with which to compare new potentials inorganic antitumor species [52]. Despite its effectiveness, especially for testicular cancer, where success of the cure spans between 90 and 100%, its clinical use is limited by dose-dependent side effects on the brain, liver and kidneys and by intrinsic or acquired resistance by malignant cells [53]. Cisplatin is administered intravenously into the bloodstream and due to the high concentration of chlorides present (about 100 mM), remains in the neutral form without giving rise to ligands dissociation. When the complex permeates the cell membrane, the lower concentration of chlorides (about 4-20 mM) promotes the slow release of one or both of the coordinated chlorides, with consequent formation of mono- and di-aqua cationic species. The entry into the cell occurs mainly by passive transport because of the neutral nature of the complex. Once inside the cellular environment, the aquaction process and the consequent formation of cationic species, prevents the expulsion of the drug. Unfortunately, a similar mechanism probably contributes to the high cytotoxicity of the compound.

On the other hand, it has been discovered that cellular uptake can also occur according to active transport mechanisms. The trans-membrane protein CRT1 and in general the proteins involved in copper transport seem to play an important role in controlling the accumulation and the expulsion of substances from the cell [16, 53]. The cationic mono- and di-aquo species formed inside the cell are very electrophilic and can react with the numerous biological ligands present in the cellular environment. The soft nature of Pt (II) allows the interaction of its complexes mainly with the -SH groups present in metallothioneins and cysteines, although their primary target seems to be DNA. The nucleophilicity of N7 nitrogen of adenine and guanine present in the DNA, form with cisplatin monoadducts or bifunctional adducts, mainly by intrastrand bonds with two contiguous guanines, a guanine and an adjacent adenine or with two guanines spaced from a third intermediate base. Remarkably, these interactions are not possible with transplatin for geometric reasons. In addition, interstrand bonds are possible with two bases belonging to different filaments and between DNA and proteins (Fig. 1.12).

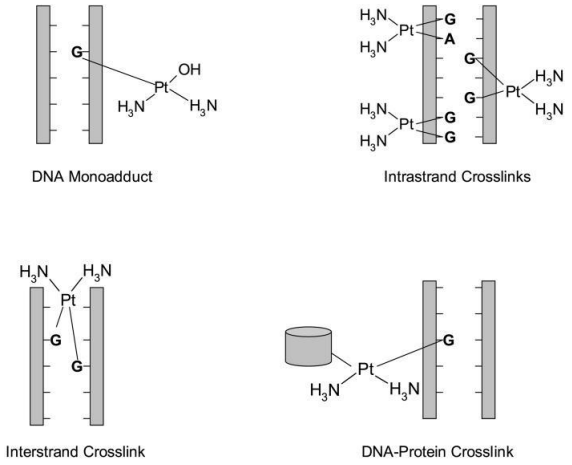

Fig. 1.12 Adducts between DNA and platinated agents.

The DNA platination, in the case of the formation of the bifunctional adduct between the two adjacent guanine, induces a distortion of the dihedral angle between the two bases, a bending and a partial unwinding of the double helix near the involved sites [16]. Conformational modifications can be recognized by specific proteins capable of triggering a series of events aimed at repairing the damage or, hopefully promoting the cell death. As mentioned earlier, an important limitation in the use of cisplatin is the intrinsic or acquired resistance manifested by the malignant cells.

A series of mechanisms responsible for this characteristic have been identified [16, 54]:

- Decreased cisplatin level within the cell caused by a minor uptake and a greater efflux of the complex which is regulated by the trans-membrane proteins and by the specific proteins related to copper leakage (ATP7A and ATP7B).

- Increased concentration of glutathione (GSH) and metallothioneins with consequent increase their competitiveness toward DNA. The electrophilic character of the cationic complexes formed by the cisplatin inside the cell and the soft nature of Pt (II), promote an interaction between the metal and the thiol groups of these species. Specific pumps are then able to expel the complexes formed.
- Increased DNA repair capacity, which is mainly due the efficiency of the NER (*Nucleotides Excision Repair*), a system able to recognize, cut, remove and synthesize the altered site. An inefficient NER system is thought to cause the effectiveness of cisplatin in the treatment of testicular tumours.
- Increased tolerance of damaged DNA due to deficiencies in the MMR (*Mismatch Repair*), which is a system involving various proteins and enzymes responsible for DNA damage repair.
- Bypass of apoptotic responses through changes in signal chains and activation of survival pathways.

Probably is a combination of these mechanisms that reduces the therapeutic efficacy of the drug [16, 54].

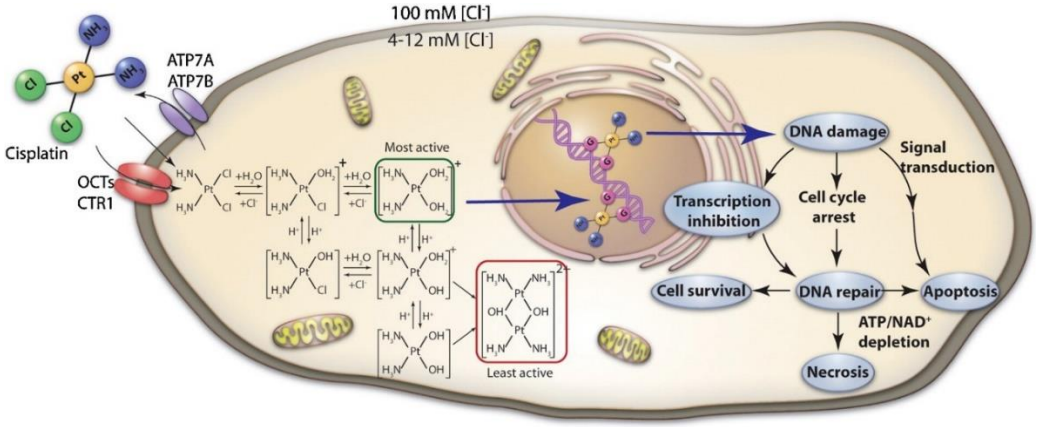

Fig. 1.13 Cisplatin mechanism of action [55].

Over the years, numerous platinum-based compounds have been synthesized, with the aim of obtaining new therapeutic agents characterized by less toxicity and less resistance developed by malignant cells. Despite the efforts, only carboplatin and oxaliplatin are currently used in the therapeutic field for the treatment of different types of cancer all over the world. However, it is noteworthy that nedaplatin and lobaplatin have been approved for clinical use in Japan, China and Korea, respectively [56].

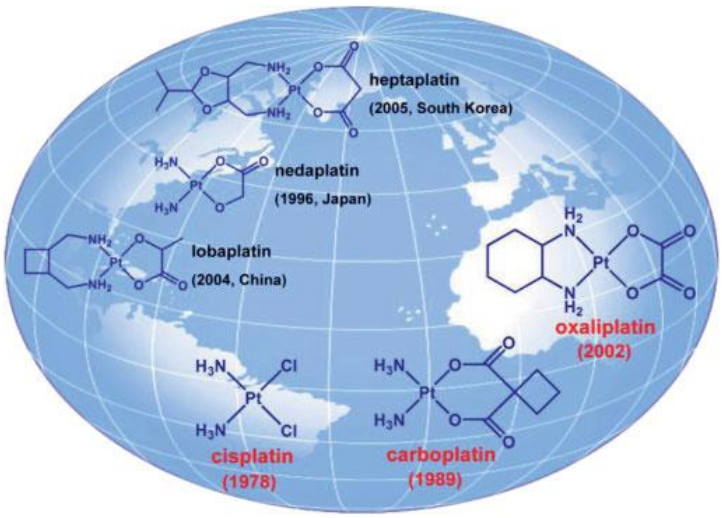

Fig. 1.14 Cisplatin and commercial analogues [16].

Carboplatin differs from cisplatin for the presence of the 1,1-cyclobutandicarboxylate group, which is hydrolyzed more slowly than chlorides. It is used against the same type of neoplasia treated with cisplatin but, owing to its reduced cytotoxicity, it requires a higher dosage (about four times higher) [16, 57].

Oxaliplatin has the oxalate as the displaceable group and the 1R,2R-diaminocyclohexane (DACH) as spectator ligand. This compound forms adducts with DNA analogous to those observed in the case of cisplatin and carboplatin, but the presence of a non-labile ligand more bulky and hydrophobic than ammonia, contrasts the action of the proteins involved in the repair of DNA and the altered site. These considerations confirm the hypothesis that structural modifications of the inert ligand may affect the activity of the compound [16].

Pt (IV) octahedral complexes have also been tested. These complexes show some advantages compared to square planar Pt (II) derivatives since they are inert toward substitution reactions therefore allowing the minimization of the collateral interactions with biological agents before reaching DNA [16]. The activation of these complexes inside the cell occurs as a consequence of the reduction of Pt (IV) to Pt (II) by reducing agents such as glutathione. Moreover, the presence of two further coordination sites renders more easy the modulation of their reactivity and activity, intervening on properties such as redox potential, kinetic stability, lipophilicity and selectivity toward specific sites.

In this respect, Dyson and coworkers have proposed that the intracellular reduction of the pro-drug of Pt (IV), leads to the formation of cisplatin and promotes the release of two equivalents of ethacrynic acid, an inhibitor of glutathione S-transferase, enzyme responsible for drug resistance in some cancers (Figure 1.15) [41, 58].

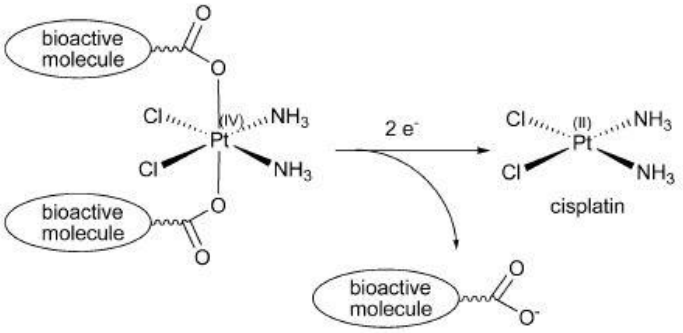

Fig. 1.15 Schematic approach of target delivery [41].

The numerous derivatives of Pt (II) and Pt (IV) tested over the years as possible anti-tumour agents, allowed the identification of correlations between the structure of the complexes and their activity [16]:

- The square planar complexes of Pt (II) must exchange only some of their ligands and the activation occurs as a result of the hydrolysis of the anionic leaving groups. The leaving groups must also be *cis* each other, since the *trans* isomers are in fact generally inactive.
- The rate of hydrolysis must be moderate, to avoid the indiscriminate interaction of the complex with the biological components before reaching the tumour cells. However, the rate of hydrolysis cannot be too low otherwise the complex will be inert and therefore almost ineffective.
- The ligand *trans* to the leaving groups must be firmly coordinated to the metal. The presence of hydrogen atoms in these groups can promote the formation of hydrogen bonds with the target molecule and influence the nature of the adducts between the complex and the DNA.
- The complexes, although the active form may be charged as a consequence of the solvolysis, should initially be neutral.
- In the case of Pt (IV) complexes, the two additional ligands in axial position may confer particular properties to the compound or act as targeting ligands once released as a consequence of the reduction of the metal.

As previously reported, cisplatin and its currently used analogues present a series of limitations in their clinical utilization owing to their toxicity and the intrinsic or induced mechanisms of resistance of some tumour cells. Furthermore, the applicability of a limited type of tumours and the cytotoxicity extended to healthy cells, encuoraged the researchers to turn their attention also toward metal derivatives different from those of platinum. Their different nature and reactivity might open new and interesting perspectives in the therapeutic field.

1.3.5. Ruthenium and gold complexes with antitumor activity

The first investigated ruthenium compounds were the octahedral Ru (III) chloro-complexes which were activated *in vivo* by reduction to Ru (II) and subsequent dissociation of chlorides [16].

At the end of the 1980s the [ImH][*trans*-$RuCl_4$(dmso-S)(Im)], known as NAMI-A, a water-soluble imidazolium salt, was investigated (Fig. 16).

Experimental evidence indicates that the NAMI-A binds less effectively DNA, which apparently does not represent the main target. At variance, NAMI-A interacts very quickly with some plasma proteins, such as albumin and transferrin, which may also have an active role in its transport within the tumor tissue, explaining the marked antimetastatic activity shown in preliminary *in vivo* tests.

However, despite the high expectations, this compound did not overcome the clinical phase 2 because of its side effects and other problems related to its use [52].

In the same period, the complex Na[trans-$RuCl_4(Ind)_2$] ((N)KP1339) was also tested. Its high cytotoxicity toward a cisplatin-resistant colorectal tumor type suggests a totally different mechanism of action, probably involving an alteration of the mitochondrial function (Fig. 1.16).

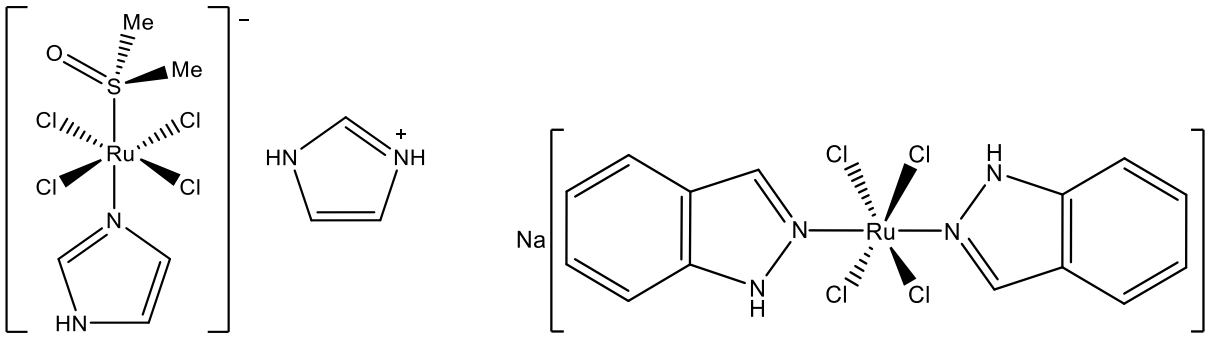

Fig. 1.16 NAMI-A and (N)KP1339 structures

Recently, some researchers have been focused their attention on Ru (II) half-sandwich complexes. As a matteter of fact the presence of the arene, firmly bound to the metal center, confers a lipophilic character to the molecule and furthermore favors its intercalation toward the DNA [16 and Refs. therein]. By varying the type of ligands on the other three available sites, a number of complexes have been synthesized; one of the most representative is RM175 reported in Fig. 1.17.

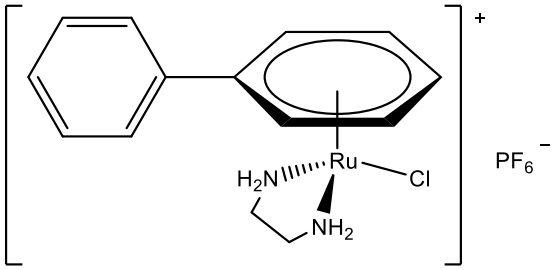

Fig. 1.17 RM175 structure

In RM175 there is only one labile ligand (Cl^-) whose dissociation allows the formation of monofunctional adducts with DNA, which are stabilized by hydrogen interactions promoted by the ethylenediamine. The coordination of the PTA (1,3,5-triaza-7-phosphoadamantane), confers to the neutral RAPTA (*Ruthenium Arene PTA*) complexes a water-soluble character. There are some evidences that seem to identify the proteins of chromatin histones as the target of this type of compounds (Fig. 1.18).

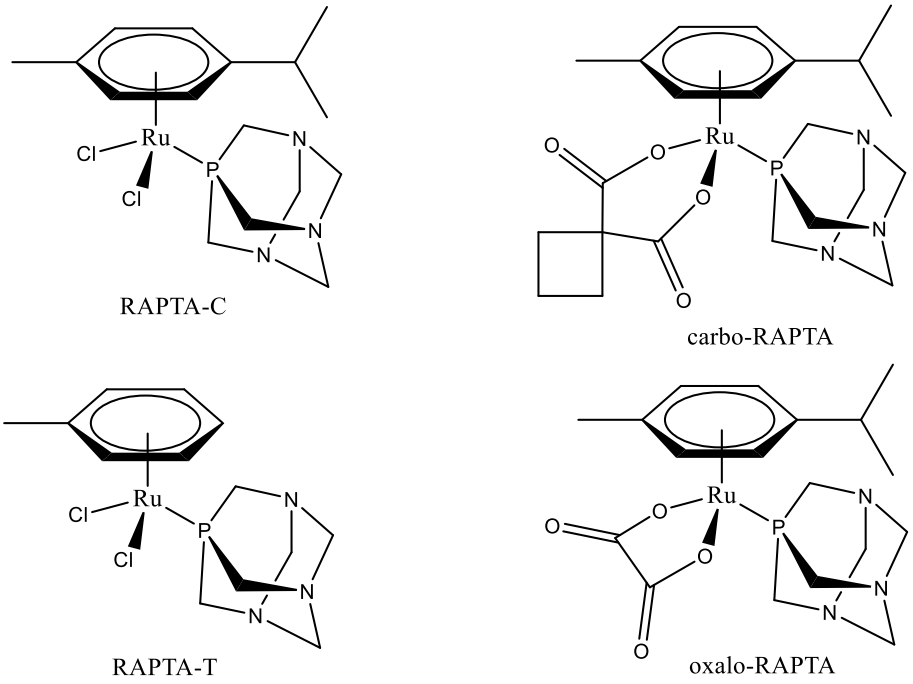

Fig. 1.18 Examples of RAPTA complexes.

Since the end of the last century it has been considered the possibility of using Au (I) compounds in the biomedical field and in particular in the preparation of drugs against arthritis, antibacterial and finally of chemotherapeutic agents in substitution or coupled with cisplatin or organic compounds (i.e. Taxol).

For the treatment of rheumatoid arthritis, the most active compounds were Aurothiomalate, Aurothioglucose and above all Auranofin [59]. The latter has been approved by the FDA and is commonly used successfully with these types of arthritis.

In 1985 prof. Mirabelli and collaborators studied the antitumor properties of Auranofin [60], opening the way to the synthesis of gold compounds as possible chemotherapeutic agents. Although the mechanisms of action are still debated, the main target seems to be Thioredoxine reductase (Trx), a key enzyme overexpressed by tumor cells. The Au (I) complexes selectively and covalently bind selenium present in selenocysteine inhibiting such an enzyme [61].

Since 2008, interesting studies have been reported on Au (I) complexes stabilized by NHC ligands [62]. *In vitro* and *in vivo* studies on Au (I) complexes, and recently on Au (III) derivatives (i.e. Au (III) porphyrins and Au (III) dithiocarbamates), are of great interest in the case of different types of tumors and leukemia (Fig. 1.19).

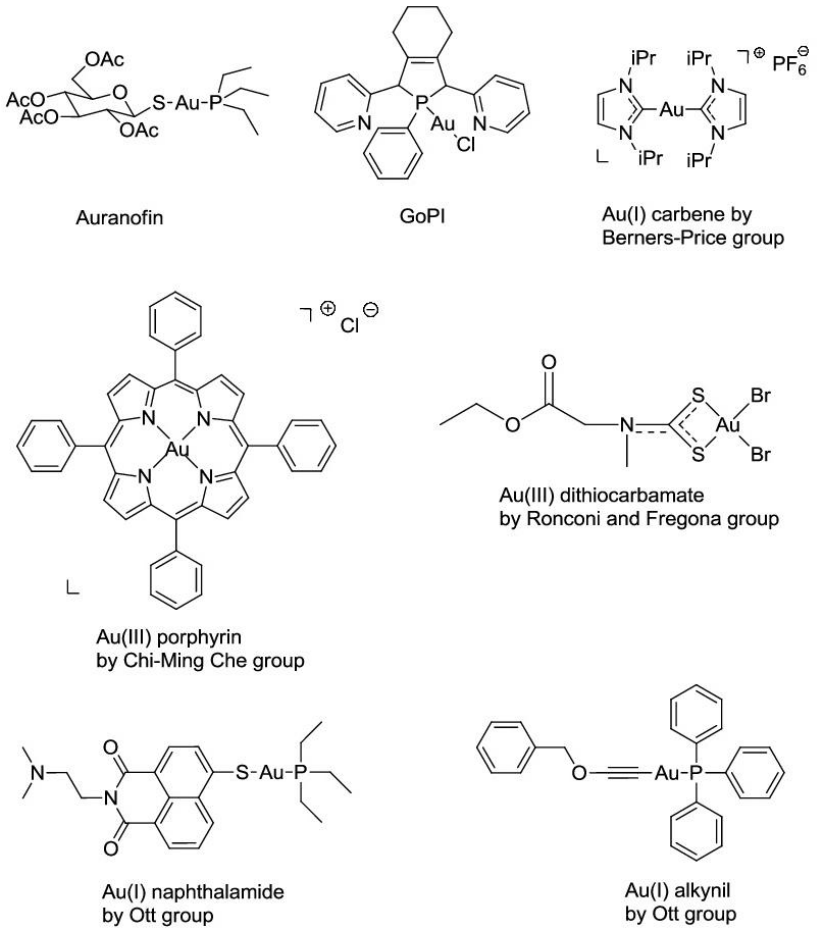

Fig. 1.19 Gold complexes with anticancer activity [62].

1.3.6. Palladium compounds: recent investigations of promising anticancer agents

On the basis of the chemical similarities with platinum, palladium has recently awaked remarkable interest as anticancer agents. This metal, whose catalytic activity is well known and widely exploited [63], has been marginally explored for biological purposes especially if compared with platinum.
Thus, recently interesting studies have been carried out and some palladium complexes have shown promising cytotoxic activity *in vitro* and *in vivo* for different types of tumor lines [64, 65].
Curiously, at variance with platinum, palladium *trans* isomers with the generic formula L_2PdCl_2 show an high cytotoxic activity [66]. Thus, many Pd (II) compounds of this class were prepared and their electronic properties, solubility and selective uptake capacity were carefully modulated by the introduction of suitable ligands including substituted pyridines [67], water-soluble phosphines and

glucopyranosidic groups [68]. In some cases, encouraging results in *in vitro* tests for several tumor lines have been obtained (Fig. 1.20).

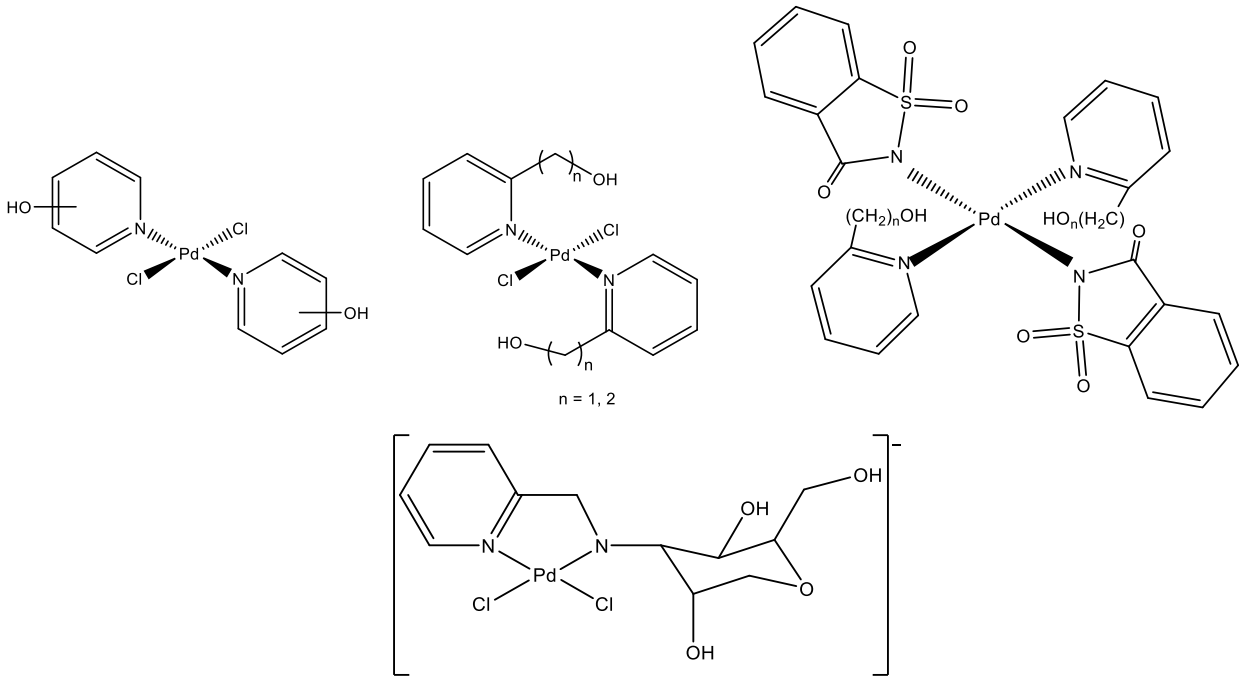

Fig. 1.20 Pd(II) complexes of which is known the in vitro anticancer activity.

For example, Pd (II) complexes containing PTA ligands (Fig. 1.21) show IC_{50} value comparable to that of cisplatin in the case of A2780 tumour cells (sensitive cisplatin ovarian carcinoma) and, at the same time, a high cytotoxicity toward the A2780-R line (cisplatin resistant) [69].

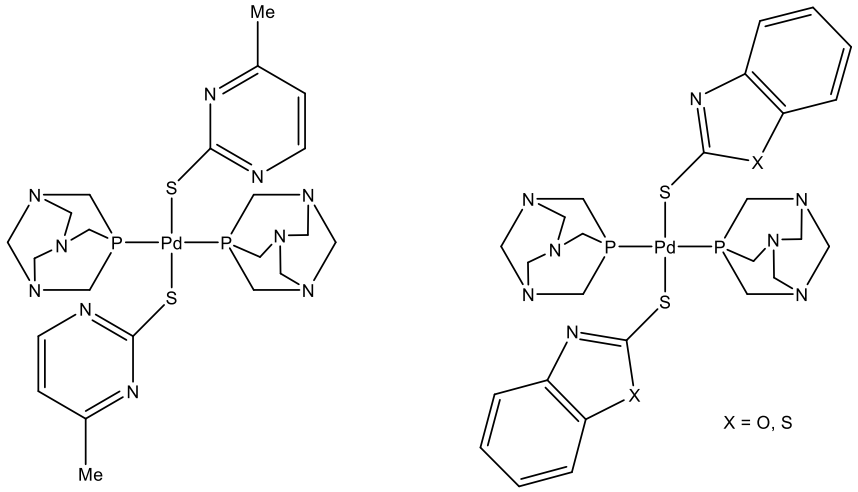

Fig. 1.21 Example of complexes containing PTA and tested in A2780 and A2780-R cell lines.

Despite the similar electronic and structural characteristics, the Pd (II) complexes, when compared with their Pt (II) homologues, show a better water solubility and generally a greater reactivity in the substitution reactions (10^4-10^5 times higher) [65, 70].

The greater lability of the coordinated ligands renders the hydrolysis processes easy in biological environment. Sometimes the sequestration of the metal by numerous soft bio-ligands, principally proteins, is also observed. This sort of reactivity reduces the possibility for the palladium compound to reach selectively the bio-target thereby increasing its general toxicity [71]. It should be emphasized that the bio-target may be not DNA; it has been experimentally demonstrated in fact, that some Pd (II) compounds stabilized by organic phosphines interact with the thiols present in proteins of the mitochondrial membrane [72].

All these critical points suggest that a careful choice of the ligands coordinating the metal play a key role in the design of Pd (II) complexes to be tested as chemotherapeutics. In particular, the most promising strategy seems to be to use polydentate ligands and/or organometallic structures in which the strong carbon-palladium bond prevents or slows down the hydrolysis processes.

Recently, numerous mono- and poli-nuclear cyclopalladates containing strong σ Pd-N, Pd-C, Pd-S and Pd-P bonds have been synthesized, using ligands such as bipyridine, phenanthroline, modified ethylenediamines, dithiocarbamates and diphosphines (Fig. 1.22) [73].

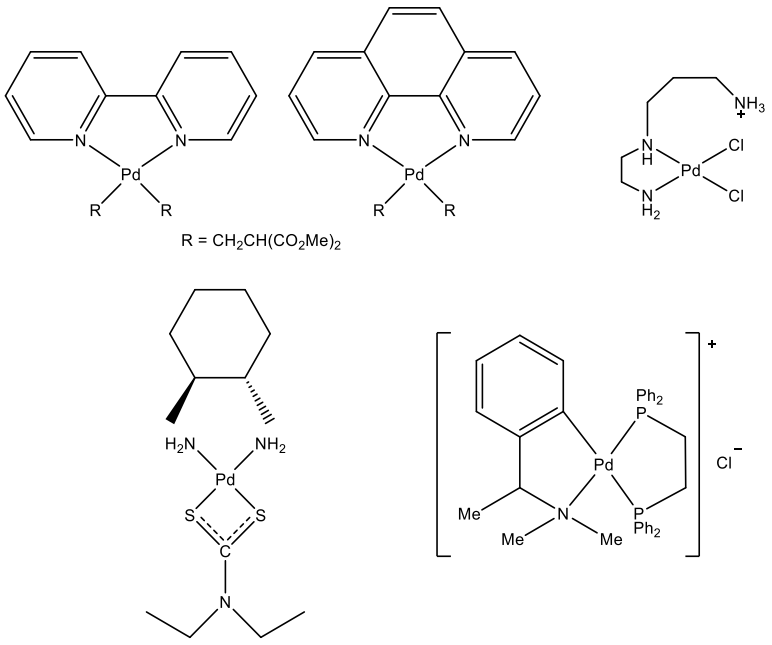

Fig. 1.22 Example of mononuclear cyclopalladated complexes containing σ Pd-N, Pd-C, Pd-S e Pd-P bonds.

Another class of strong and generally bulky ligands recently employed in biomedical field are the *N*-Heterocyclic Carbenes (NHCs), which have been coordinated to metal centres of Au, Ru, Ag, Cu, Pt, Ni and Pd [74] (Fig. 1.23). A recent study has shown that complexes of the type [(NHC)Pd(pyridine)Cl_2] and [$(NHC)_2PdCl_2$], reported in Figure 1.23, show a good anti-tumour activity and are able to trigger apoptotic processes in cancer cells [75].

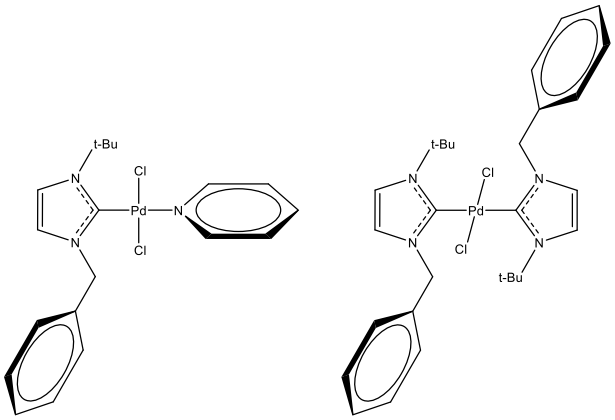

Fig. 1.23 Examples of tested Pd (II) complexes containing N-Heterocyclic Carbene ligands.

In another work, some cyclometallated Pd (II) complexes bearing NHC ligands (Fig. 1.24) have been shown a high stability in the presence of biological thiols such as glutathione and a considerable cytotoxic activity toward different tumor lines, combined with a less invasiveness toward healthy cells (fibroblasts).

These compounds seem to induce alterations at the mitochondrial level (inhibition of the respiratory chain) leading to death of cells by apoptosis. These promising results *in vitro* have also been preliminarily confirmed *in vivo* [76].

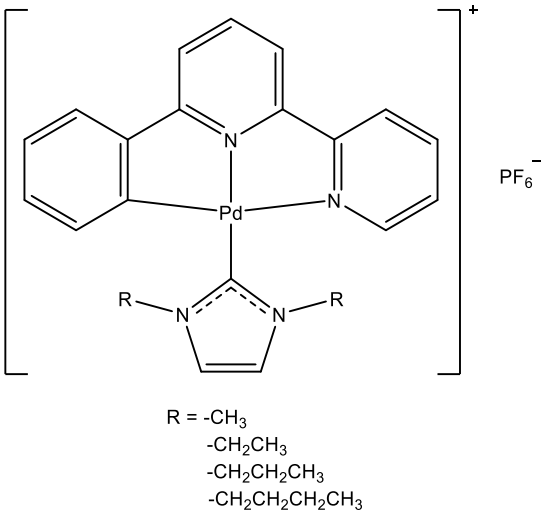

Fig. 1.24 Examples of cyclopalladated complexes with high stability in the presence of bio-thiols.

On the contrary, the cytotoxic activity of the Pd (0) complexes is poorly investigated and one of the few examples so far reported in the literature, concerns the complex $[Pd_2(dba)_3]\cdot CHCl_3$ (dba = E,E-dibenzylideneacetone). For this derivative (Fig. 1.25), two isomers are known. The main isomer presents three s-*cis*, s-*trans* bridged dba molecules, whereas the minor isomer shows one dba molecule in s-*trans*, s-*trans* configuration [77].

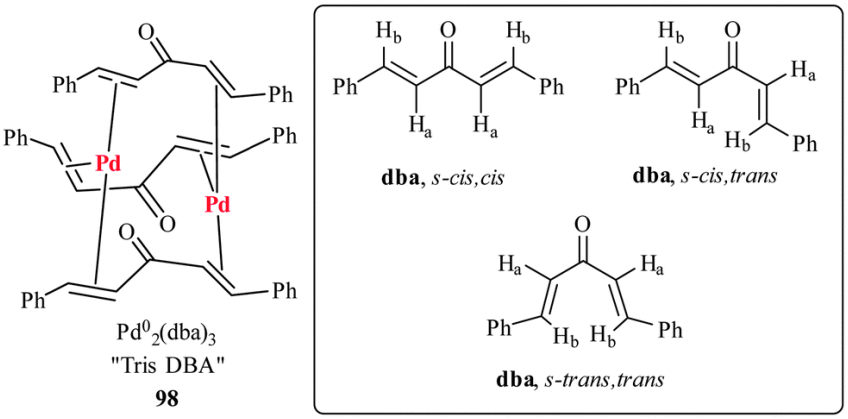

Fig. 1.25 $[Pd_2(dba)_3]\cdot CHCl_3$ structure and dba configurations [64]

The compound proved to be active against murine and human melanoma cells and was able to inhibit numerous *pathways* necessary for carcinogenesis [64, 78]. Its use in the treatment of pancreatic carcinoma and its ability to induce apoptosis in cells of chronic lymphocytic leukaemia seems also promising [79, 80].

1.4. *N*-Heterocyclic Carbenes as ancillary ligands

In the last 20 years, *N*-Heterocyclic Carbenes have become one of the most important ligands in organometallic chemistry and in catalysis [81, 82]. In most cases, they are characterized by the presence of an imidazole ring bearing two nitrogen atoms adjacent to the carbenic carbon (Fig. 1.26).

Fig. 1.26 General structure of NHCs derived from imidazole ring.

The first stable carbene of this type was isolated by Arduengo and co-workers in 1991 [83]. These ligands represent a subcategory of the Fisher carbenes that, showing a strong σ-donor capability, have in some cases replaced the classic aminic and phosphinic ligands.

The presence in the alpha position of two nitrogen atoms is a key factor for the stability of these ligands for the following two reasons:

1. Inductive effect: this effect is due to the difference in electronegativity between nitrogen and carbon rending the nitrogen σ-acceptor.
2. Mesomeric effect: this effect is due to the presence in the nitrogen atoms of filled orbitals and empty orbitals of the same symmetry of those of the carbenic carbon. In this case, the nitrogen atoms act as excellent π-donors.

The combination of these two factors allows the stabilization of the σ orbital of the carbene (increases its s-character) and the increasing of the energy of the unoccupied p_π orbital. The σ-p_π gap is then increased and the singlet state is by far the favored one (Fig. 1.27).

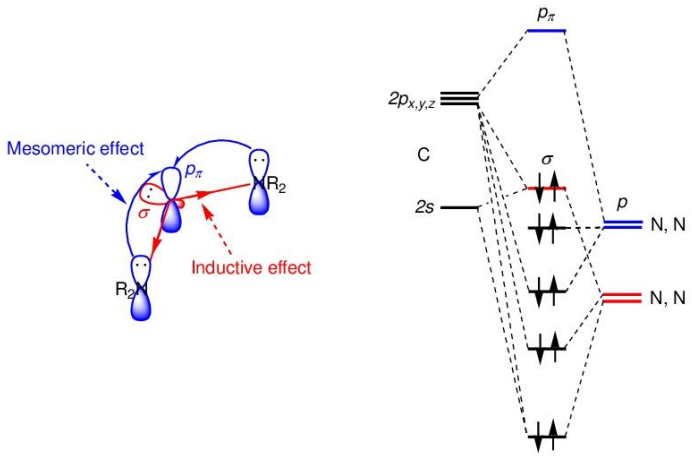

Fig. 1.27 Representation of the mesomeric and inductive effect stabilizing NHCs (left); qualitative MO diagram of the N-C-N fragment (right).

It is also possible to obtain more stable complexes using polydentate *N*-Heterocyclic Carbene ligands (polyNHCs). In this case, there is an increase in the σ-donation to the metal center (the metal itself is more electron-rich and polarizable) and an increased stability toward decomposition due to the chelating effect [84]. Moreover, NHCs ligands can be easily functionalizated and this possibility permits to modulate their stereo-electronic features. NHCs porperties depends by:

- Nature of the nitrogenous heterocyclic ring: in addition to imidazole, the pyrazole, triazole, tetrazole and benzimidazole derivatives can be considered as potential precursors of NHCs. There are also examples of NHCs based on six- and seven-membered rings (Fig. 1.28) [84].

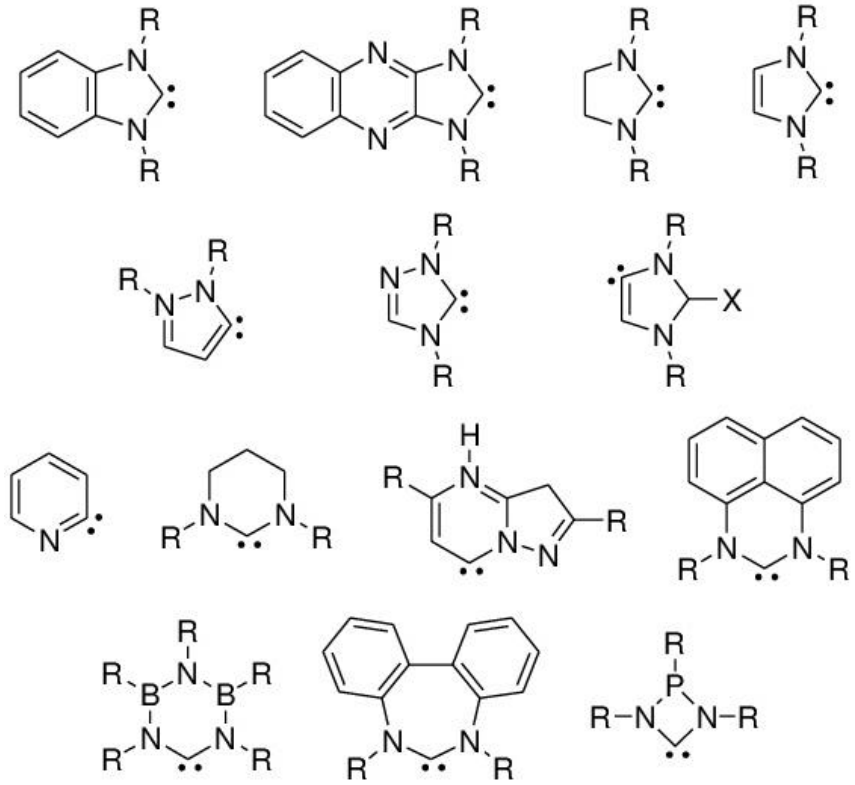

Fig. 1.28 NHCs based on different heterocycles.

- Nature of the groups linked to the nitrogens adjacent to the carbenic carbon: these groups may be more or less bulky and present a further donor atom allowing to obtain chelating or bridging ligands.

Typically, the *N*-Heterocyclic Carbenes synthetic protocol involves the deprotonation of the corresponding imidazolium salts by a strong base (i.e. t-BuOK). This strategy is not applicable if other functional groups susceptible of modification are present [83].

In some cases, it is possible to bypass the problem using silver oxide, which allows the deprotonation of the starting imidazolium salt and, at the same time, the stabilization of the resulting carbene as

silver derivative [85]. This protocol allows the synthesis of several complexes by transmetallation in which the carbenic fragment is transferred to other metals. The precipitation of the silver halide represent the driving force of the whole process (Scheme 1.1).

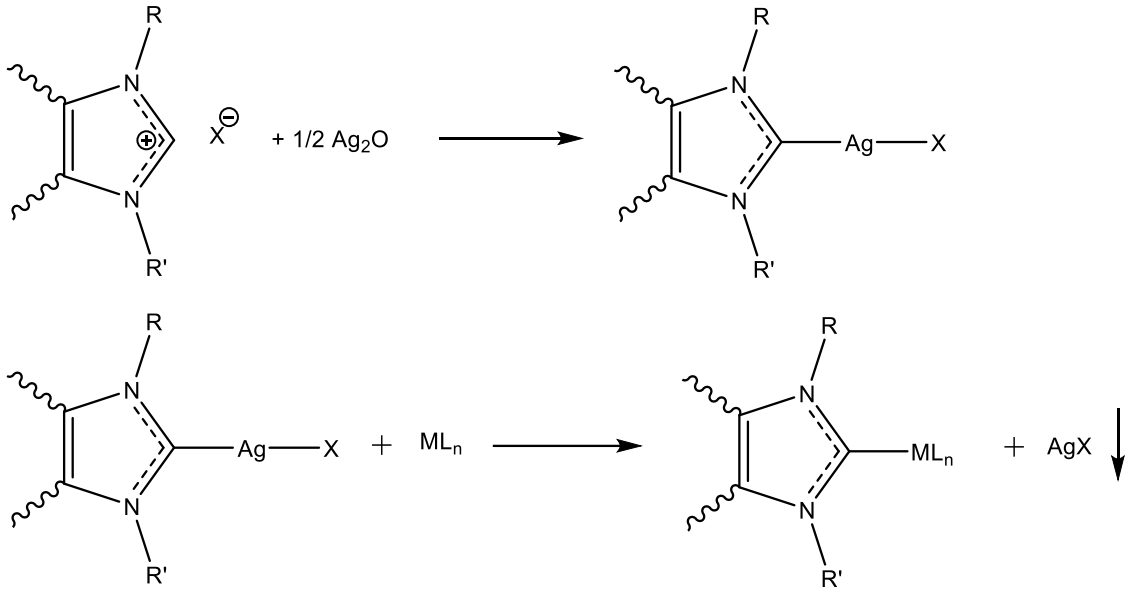

Scheme 1.1 Deprotonation of the imidazolium salt and the transmetallation process.

The advantages in the use of NHCs in homogeneous catalysis are the following:

- High thermal stability toward hydrolysis owing to the exceptional strength of the M-C bond.
- Their synthesis are generally easy and with high yields.
- At variance with phosphines is not necessary to use an excess of the ligand.

The best-known example of the application of NHCs is represented by the second-generation catalysts for olefinic metathesis processes described by Grubbs [86].

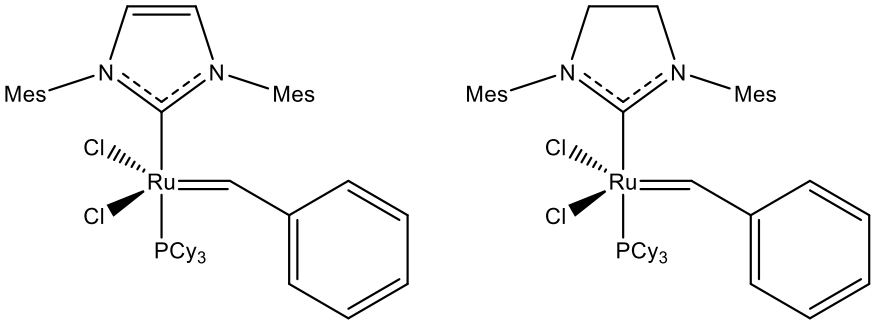

Fig. 1.29 Second generation Grubb's Catalysts.

Another very important example is given by the highly performing catalysts (Fig. 1.30) empolyed in Heck cross-coupling reactions [87].

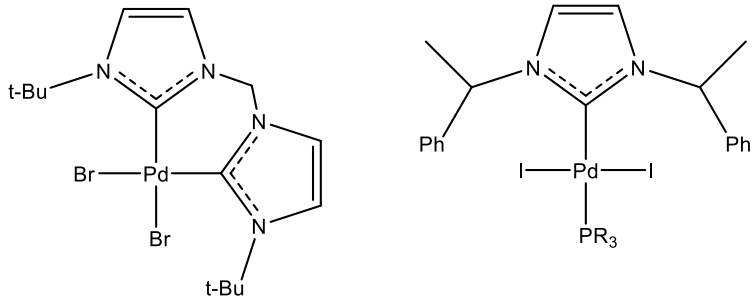

Fig. 1.30 Pd(II) NHCs catalysts for Heck type reactions.

The high stability of the NHC complexes and the possibility of a fine tuning of their stereo-electronic properties, allow their applications not only in catalysis but also in the biomedical field, in supramolecular chemistry and in materials science.

In the biomedical field there are examples of Ag (I) carbene complexes with excellent antimicrobial properties due to the gradual release of Ag^+ ions [88].

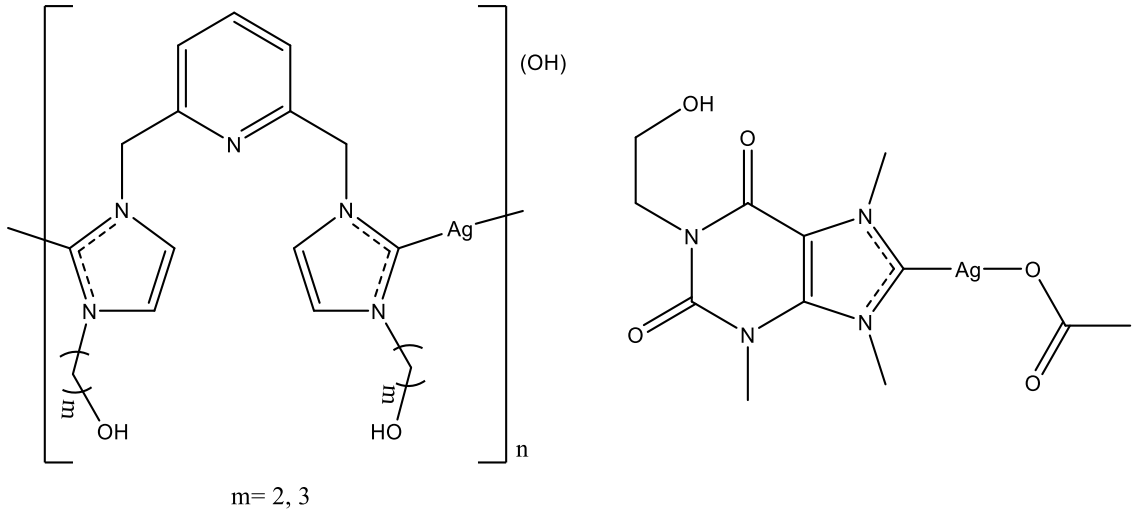

Fig. 1.31 Examples of Ag(I) NHC complexes as antimicrobial agents.

Furthermore, as previously reported, the anticancer activity carried out by metal complexes containing *N*-Heterocyclic Carbene ligands has recently been studied [89, 90]. Some of these have shown a comparable or even better activity than cisplatin, in several cancer lines.

1.5. Phosphines, arsines and isocyanide as spectator ligands

In organometallic chemistry the spectator ligands are very important since, although they do not undergo modifications and do not play an active role in the reactions involving the complex, are able to influence significantly the course of the processes, modulating the properties of the metal centre. Tertiary phosphines (PR_3) represent an important and extremely versatile class of ancillary ligands since an appropriate variation of the substituents R directly bound to the phosphorus allows the modification of their electronic and steric properties [91], promoting their use in many applications in the fields of organometallic chemistry and homogeneous catalysis [92].

Alkyl phosphines are strong σ-donor, whereas the introduction of aryl, dialkylamino or alkoxide substituents implies an increasing π-acidity, which can even be compared to that of CO in the case of PF_3 owing to the π-backdonation of the metal electrons to the σ* orbitals of PR [91].

The phosphines used in this work were triphenylphosphine, TPPTS (sodium 3,3′,3″-phosphinetriyltribenzenesulfonate) and PTA (1,3,5-triaza-7-phosphoadamantane).

The solubility in water of such compounds (TPPTS and PTA) is generally transferred to the complexes with different metal centres, facilitating their use in the biological environment (Fig. 1.32).

Arsines are ligands similar to phosphines but show a reduced σ-donation for the increased s-character of the lone pair of the arsenic and the consequent decrease of the bond overlapping. The minor electronegativity of the arsenic as acceptor atom and its wide orbitals, also contribute in reducing the metal backdonation [93].

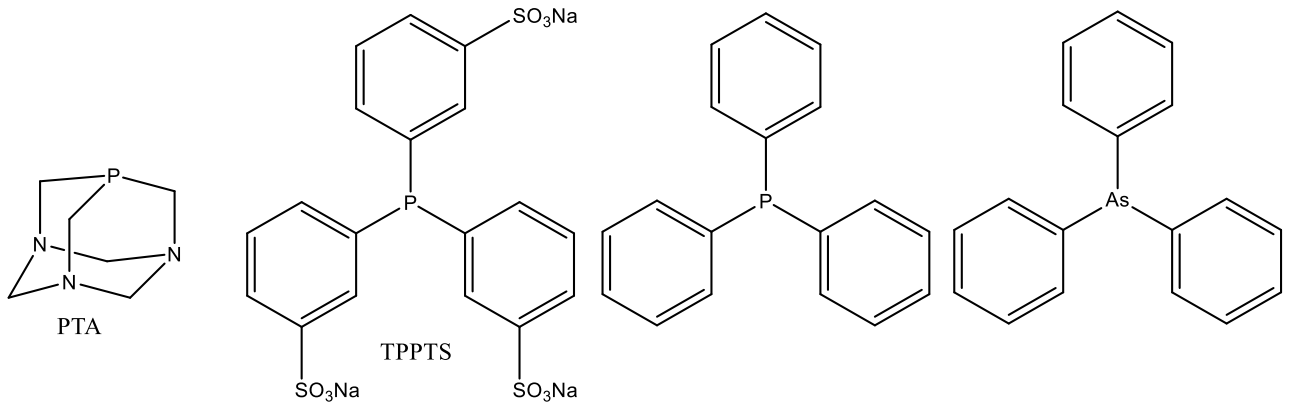

Fig. 1.32 Chemical structures of PTA, PPh_3 and $AsPh_3$.

Another type of common ancillary ligands are the isocyanides (CN-R), whose structure is exhaustively described by the two resonance formulas reported in Scheme 1.2.

Scheme 1.2 Resonance structures of a general isocyanide.

Isocyanides are isoelectronic with CO and hence they show an electron-withdrawing character as a consequence of π-backdonation prevailing on their σ-donation nature. However, this feature can be modulated to some extent by a focused selection of the substituent R [91].

1.6. Organometallic fragments

As mentioned previously (Section 1.3.6.), one of the problems of palladium compounds is their rapid hydrolysis if compared to platinum homologues. This feature might permit the coordination of many potential ligands present in the biological environment (i.e. glutathione) and/or the formation of palladium nanoparticles, enhancing its collateral toxicity.

To overcome this contoindication, a posssible option is prepare complexes with ligands firmly tethered to the metal. Among them, organometallic palladium derivatives could be particularly suibtable because of the strength of the Pd-C bond.

In this chapter we will give a brief description of the organometallic fragment used in this work.

1.6.1. η^3-allyl-Pd(II) fragment

The synthesis, the properties and the applications of complexes containing this organometallic fragment have been studied since the 1960s. The allyl group in homogeneous catalysis represents a reactive actor ligand and as demonstrated in numerous studies, usually undergoes nucleophilic attack [94]. Among the best-known processes there is the Tsuji-Trost reaction [91, 95], involving the use of an allyl acetate as starting reagent and, through the cycle shown below, yields the introduction of a group at the terminal allylic position. The rate-determining step is often represented by the nucleophilic attack at the intermediate allyl complex (Fig. 1.33).

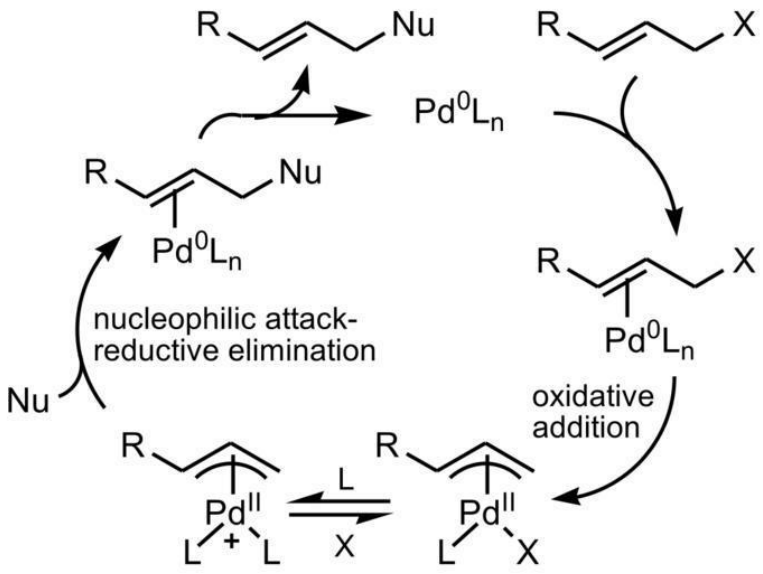

Fig. 1.33 Tsuji-Trost allylation mechanism (X = OAc).

In the original procedure, proposed by Tsuji in 1965, the nucleophile (Nu) was diethyl malonate, whereas amines, carbanions, isocyanates and carbamates were subsequently used [96].
The allyl fragment coordinates in two different ways:

- η^3 hapticity: the allyl fragment acts as a bidentate ligand. Such a coordination mode represents by far the most observed one.
- η^1 hapticity: the allyl fragment acts as a monodentate ligand. The related complexes are rare but they are observed mainly when no two free coordination sites are available [97].

The first example of η^3-allyl-palladium complex was reported by Smidt and Hafner in 1959 [98]. They prepared the dimeric complex $[Pd(\mu\text{-}Cl)(\eta^3\text{-}C_3H_5)]_2$ starting from $PdCl_2$ and allyl alcohol.
The labile bridge formed by the chloride ligands allows the easily introduction of a monodentate ligand or, after dehalogenation, the introduction of two monodentate or one chelating ligand (Scheme 1.3).

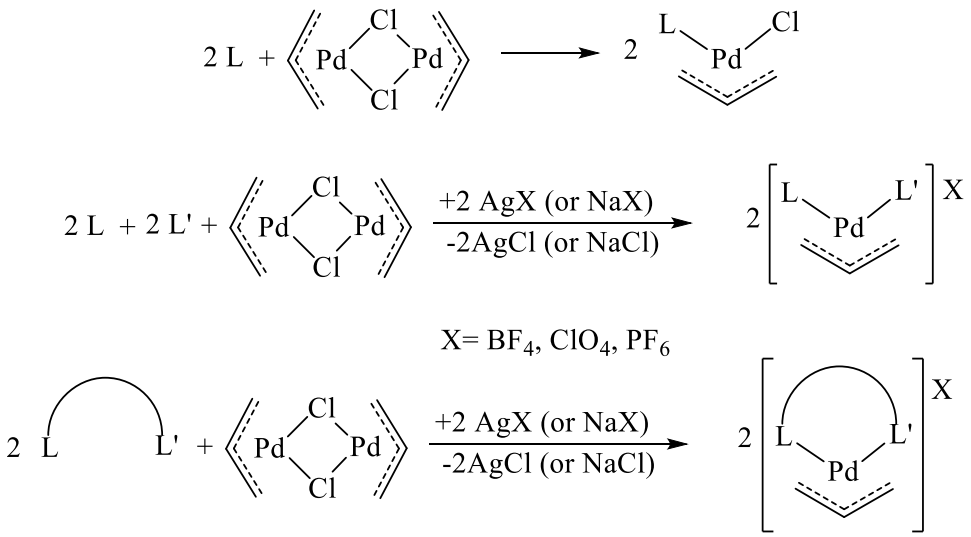

Scheme 1.3 General synthesis of Pd(II) η^3-allyl complexes with mono- and bidentate ancillary ligands.

The following two resonance forms (Scheme 1.4) are used for describing the structure of η^3-allyl-palladium bond:

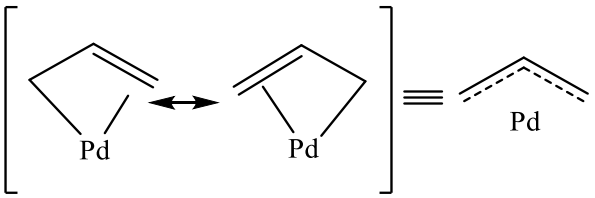

Scheme 1.4

In this configuration, the allyl group is symmetrical, with C-C bond lengths of about 1,35 Å and oriented side-on with respect to the metal. The plane identified by the three carbon atoms, is slightly inclined with an angle Θ = 5-10° with respect to the perpendicular at the main coordination plane of the complex [91, 99]. This inclination allows a better overlapping between the orbital $d\pi_{x,z}$ of the metal and the π_n of the allyl (Fig. 1.34).

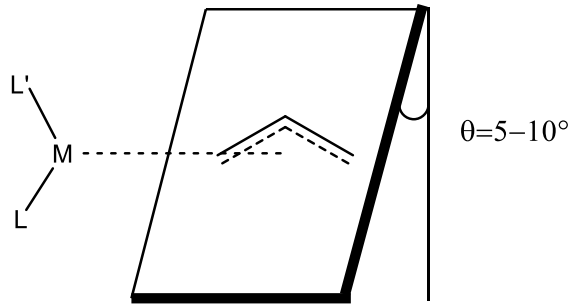

Fig. 1.34

The four allyl protons are called *syn* and *anti*, on the basis of their position toward the *central* allyl proton. They do not lie perfectly in the plane defined by the three carbon atoms due to a slight rotation of the CH_2 groups around the C-C axis. H-*syns* are therefore found to be significantly closer to the metal than H-*antis* (Fig. 1.35).

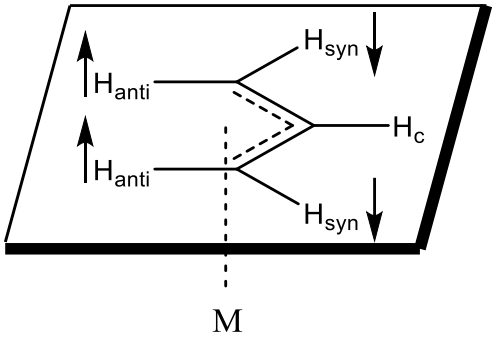

Fig. 1.35

H-*syns* and H-*antis* can sometimes exchange positions for example through η^3-η^1-η^3 rearrangements in solution. A possible mechanism for this process is illustrated in the following diagram (Scheme 1.5).

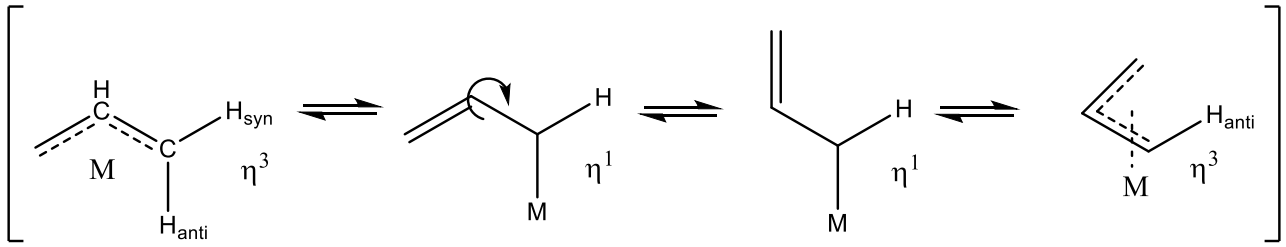

Scheme 1.5

Our research group has published many works on the synthesis and reactivity of allyl palladium complexes [100].

1.6.2. Palladacyclopentadienyl fragment

The first example of palladacyclopentadienyl polymeric compound $[PdC_4(COOCH_3)_4]_n$ was described by Maitlis in the 1970s by oxidative coupling between $Pd_2(dba)_3 \cdot CHCl_3$ (dba = dibenzylideneacetone) and dimethylacetylenedicarboxylate (DMA), carried out in different solvents [101]. Subsequently, it was noted that the lability of the bridges between the monomeric units could be exploited to synthesize a wide range of palladium mononuclear complexes by reaction of the Maitlis polymer with mono- or bi-dentate ligands (Scheme 1.6).

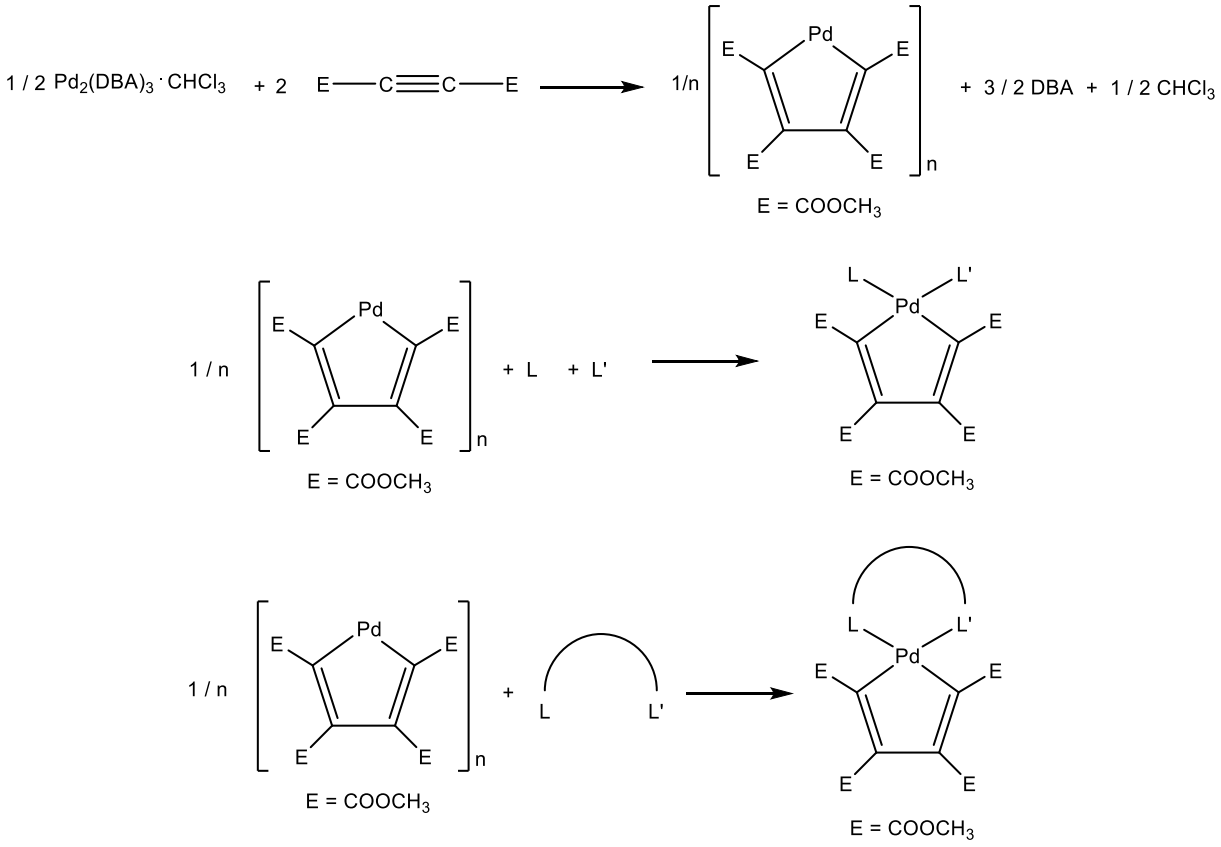

Scheme 1.6 Synthesis of the $[PdC_4(COOCH_3)_4]_n$ precursor and reactions with mono- or bi-dentate ligands.

Subsequent studies have shown that the $PdC_4(COOCH_3)_4$ unit may behave as an actor ligand and to be attacked by halogens or alkyl/aryl halides to give the corresponding Pd(II) butadienyl complexes, in a process consisting in an oxidative addition and subsequent stereospecific reductive elimination, yielding the Z/Z geometry isomer. The butadienyl fragment can then be released from the metal centre by a further oxidative addition and consecutive reductive elimination (Scheme 1.7) [102].

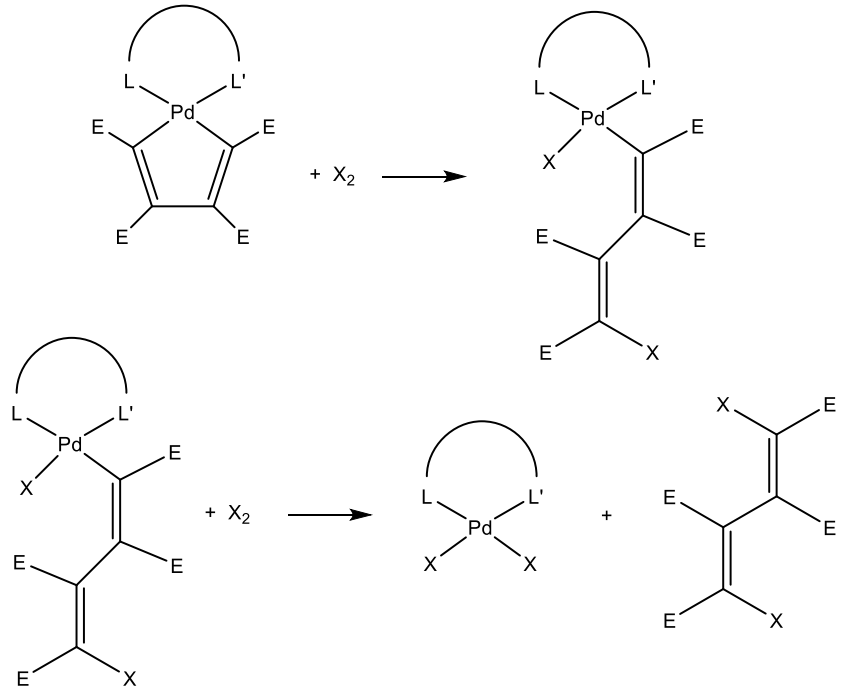

Scheme 1.7 Addition of halogens to palladacyclopentadienyl complexes (E = $COOCH_3$).

The group with I worked as PhD student has recently studied the reactivity of the palladacyclopentadienyl complexes stabilized by a wide range of spectator ligands, including *N*-Heterocyclic Carbenes. The achievement of different types of products, some of which definitely unusual, have been obtained [103].

1.6.3. η^2-olefin-Pd(0) fragment

The first example of a η^2-olefin complex was obtained by William Zeise in 1827, by reacting K_2PtCl_4 with EtOH, but only in the 50s of the last century the real nature of this product was understood. The complex can be described by the formula $K_2[PtCl_3(\eta^2\text{-}C_2H_4)]\cdot H_2O$, suggesting that the ethanol dehydration yields ethylene which eventually acts as a π-ligand [91].

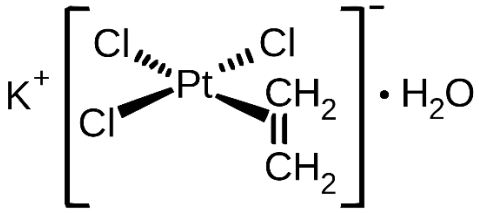

Fig.1.36 Chemical structure of the Zeise's salt.

Generally, the metal-olefin bond is described by means of two limit models, respectively known as the Dewar-Chatt-Duncanson and the metal-cyclopropane models, described below (Fig. 1.37).

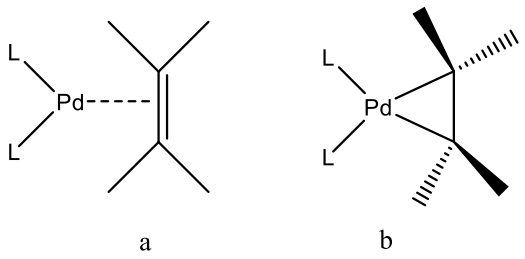

Fig. 1.37 a) Dewar-Chatt-Duncanson model b) Metal-cyclopropane model.

The metal-olefin bond involves the donation of C=C electrons to an empty orbital of the metal and the back-donation of two d-electrons of the metal to the C=C π* anti-bonding orbital of the alkene (Fig. 1.38).

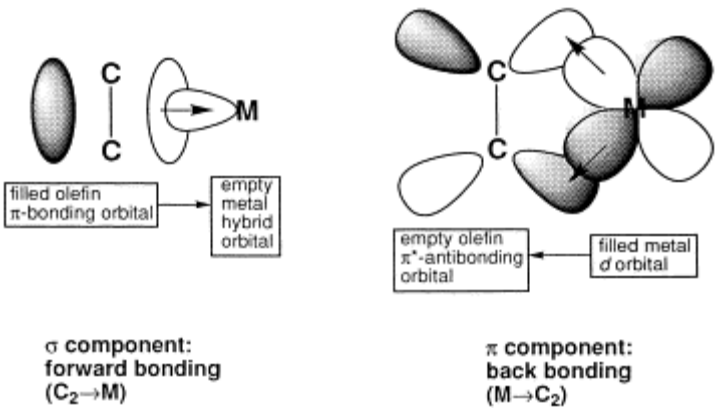

Fig. 1.38 Representation of the metal-olefin bond [104].

It has been possible to demonstrate that an adequate π-backdonation from the metal makes the bond and therefore also the complex stable. On the contrary, in the case of poor π-backdonation, the bond becomes labile and the release/substitution of the olefin is facilitated. In order to favor π-backdonation it is convenient to choose spectator ligands with good σ-donating capability, so that the electronic density on the metal increases, and olefins with electron-withdrawing substituents [91].
Numerous studies have been carried out on olefinic exchange reactions in Pd complexes of the type $L_2Pd(\eta^2\text{-olefin})$, which allowed to define the following order of stability for the metal-alkene bond, valid independently of the type of spectator ligands L [105]:

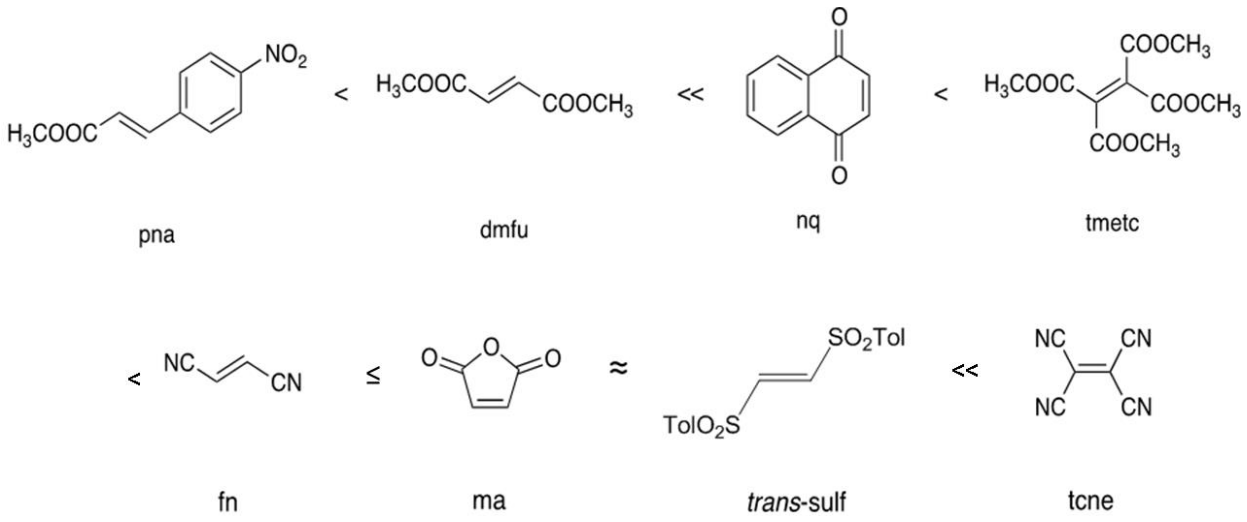

Fig. 1.38 Stability order of the Pd-alkene bond, related to the equilibrium constant in a process of olefin exchange $[(L\text{-}L)Pd(\eta^2\text{-}olefin_1)] + olefin_2 \rightleftharpoons [(L\text{-}L)Pd(\eta^2\text{-}olefin_2)] + olefin_1$.

The synthesis of Pd(0) and Pt(0) η^2-olefin complexes and the study of their reactivity, particularly with respect to oxidative addition and olefinic exchange processes, have been widely studied by our research group [106].

1.7. References

[1] http://drjockers.com/the-difference-between-normal-and-cancer-cells/#lightbox/1

[2] C.A. Almeida, S.A. Barry, *Cancer: Basic Science and Clinical Aspects*, Wiley-Blackwell, 2010.

[3] W.B. Coleman, G.J. Tsongalis, *The Molecular Basis of Human Cancer*, Humana Press, 2017.

[4] AIOM (Associazione Italiana di Oncologia Medica), *I numeri del cancro in Italia*, 2016.

[5] (a) G.R. Newell, M.R. Spitz, J.G. Sider, *Semin. Oncol.*, 1989, **16**, 3; (b) R.A. Miller, *Cancer.*, 1991, **68**, 2496.

[6] P. Anand, A. Kunnumakara, C. Sundaram, K. Harikumar, S. Tharakan, O. Lai, B. Sung, B. Aggarwal, *Pharmaceut. Res.*, 2008, **25**, 2097.

[7] D. Hanahan, R. A. Weinberg, *Cell*, 2000, **100**, 57.

[8] http://cisncancer.org

[9] B. Alberts, A. Johnson, J. Lewis, M. Raff, K. Roberts, P. Walter, New York: Garland Science, 2008.

[10] V.W. Chen, B. Ruiz, J.L. Killeen, T.R. Coté, X. Wu, C.N. Correa, *Cancer*, 2003, **97** (S10), 2631.

[11] U.A. Matulonis, A.K. Sood, L. Fallowfield, B.E. Howitt, J. Sehouli, B.Y. Karlan, *Nat. Rev. Dis. Primer*, 2016, **2** (16061), 1.

[12] R.J. Kurman, I.M. Shih, *Hum. Pathol.*, 2011, **42** (7), 918.

[13] AIOM (Associazione Italiana di Oncologia Medica), *I numeri del cancro in Italia*. Il Pensiero Scientifico Editore, 2017.

[14] http://ovarian.org/about-ovarian-cancer/what-is-ovarian-cancer/types-a-stages

[15] AIOM (Associazione Italiana di Oncologia Medica), *Linee guida tumori dell'ovaio*, 2015.

[16] (a) E. Alessio, *Bioinorganic Medicinal Chemistry*, Wiley-VCH, 2011; (b) E. Alessio, Teaching material for the "Metals in medicine" course offered by the Venice-Trieste inter-university doctorate school, 2016.

[17] L.S. Goodman, M.W. Wintrobe, W. Dameshek, M.J. Goodman, A. Gilman, *Journal of American Medicinal Association*, 1984, **251**, 2255.

[18] S. Farber, L.K. Diamond, R.D. Mercer, R.S. Sylvester, J. Wolff, *N. Engl. J. Med.*, 1948, **238**, 787.

[19] https://alchetron.com/Sidney-Farber

[20] J. H. Burchenal, R.R. Ellison, M.L. Murphy, D.A. Karnofsky, M.P. Sykes, C. Tan, A.C. Mermann, M. Yuceoglu, W.P.L. Myers, I. Krakoff, N. Alberstadt, *Annals New York Academy of Sciences*, 1954, 359.

[21] D.B. Longley, D.P. Harkin, P.G. Johnston, *Nat. Rev. Cancer*, 2003, **3**, 330.

[22] V.C. Jordan, *Nat. Rev. Drug Discov.*, 2003, **2**, 205.

[23] J. Lao Romera, T.J. Puertolas Hernández, I. Peláez Fernández, T. Sampedro Gimeno, R. Fernández Martínez, I. Fernández Pérez, V. Iranzo González Cruz, J.J. Illarramendi Manas, J.S. Garcera, G.E.M. Ciruelos, *Adv. Ther.*, 2011, **28**, 1.

[24] P.B. Schiff, J. Fant, B. Horwitz, *Nature*, 1979, **277**, 665.

[25] E.R. Jamieson, S.J. Lippard, *Chem. Rev.*, 1999, **99**, 2467.

[26] A.M. Murad, F.F. Santiago, A. Petroianu, P.R.S. Rocha, M.A.G. Rodrigues, M. Rausch, *Cancer*, 1993, **72**, 37.

[27] D. Cunningham, Y. Humblet, S. Siena, D. Khayat, H. Bleiberg, A. Santoro, D. Bets, M. Mueser, A. Harstrick, C. Verslype, I. Chau, E. Van Cutsem, *N. Engl. J. Med.*, 2004, **351**, 337.

[28] The Arimidex, Tamoxifen, Alone or in Combination (ATAC) Trialists' Group, *Lancet Oncol.*, 2008, **9**, 45.

[29] J. G. Paez, P.A. Jänne, J.C. Lee, S. Tracy, H. Greulich, S. Gabriel, P. Herman, F.J. Kaye, N. Lindeman, T.J. Boggon, K. Naoki, H. Sasaki, Y. Fujii, M.J. Eck, W.R. Sellers, B.E. Johnson, M. Meyerson, *Science*, 2004, **304**, 1497.

[30] P. Köpf-Maier, H. Köpf, E.W. Neuse, *Angew. Chem. Int. Ed.*, 1984, **23**, 456.

[31] P.G. Lenhert, D.C. Hodgkin, *Nature*, 1961, **192**, 937.

[32] A. Korfel, M.E. Scheulen, H.J. Schmoll, O. Grundel, A. Harstrick, M. Knoche, L.M. Fels, M. Skorzec, F. Bach, J. Baumgart, G. Sass, S. Seeber, E. Thiel, W. E. Berdel, *Clin. Cancer Res.*, 1998, **9**, 2701.

[33] C.G. Hartinger, P.J. Dyson, *Chem. Soc. Rev*., 2009, **38**, 391.

[34] J. Halpern, *Pure Appl. Chem*., 2001, **73**, 209.

[35] D.B. Zamble, S.J. Lippard, *Trends Biochem. Sci.*, 1995, **20**, 435.

[36] K. Ishibiki, K. Kumai, S. Kodaira, O. Abe, K. Yamamoto, T. Oouchi, Y. Fukaya, K. Kimura, K. Takamatsu, E. Ootsuka, *Gan to Kagaku Ryoho*, 1989, **16**, 3185.

[37] G. Chu, *J. Biol. Chem.*, 1994, **269**, 787.

[38] S.J. Dougan, A. Habtemariam, S.E. McHale, S. Parsons, P.J. Sadler, *Proc. Natl. Acad. Sci. U. S. A.*, 2008, **105**, 11628.

[39] H. Chen, J.A. Parkinson, S. Parsons, R.A. Coxall, R.O. Gould, P. J. Sadler, *J. Am. Chem. Soc*., 2002, **124**, 3064.

[40] K.S. Smalley, R. Contractor, N.K. Haass, A.N. Kulp, G.E. Atilla-Gokcumen, D.S. Williams, H. Bregman, K.T. Flaherty, M.S. Soengas, E. Meggers, M. Herlyn, *Cancer Res.*, 2007, **67**, 209.

[41] T. Gianferrara, I. Bratsos, E. Alessio, *Dalton Trans.*, 2009, **37**, 7588.

[42] S.K. Singh, S. Joshi, A.R. Singh, J.K. Saxena, D.S. Pandey, *Inorg. Chem.*, 2007, **46**, 10869.

[43] J. Malina, M.J. Hannon, V. Brabec, *Chem. Eur. J.*, 2008, **14**, 10408.

[44] L. Xu, D. Zhang, J. Huang, M. Deng, M. Zhang, X. Zhou, *Chem. Commun.*, 2010, **46**, 743.

[45] J. Spencer, A.P. Mendham, A.K. Kotha, S.C. Richardson, E.A. Hillard, G. Jaouen, L. Male, M.B. Hursthouse, *Dalton Trans.*, 2009, 918.

[46] C. Scolaro, A. Bergamo, L. Brescacin, R. Delfino, M. Cocchietto, G. Laurenczy, T.J. Geldbach, G. Sava, P.J. Dyson, *J. Med. Chem.*, 2005, **48**, 4161.

[47] A. Casini, C. Gabbiani, F. Sorrentino, M.P. Rigobello, A. Bindoli, T.J. Geldbach, A. Marrone, C.G. Hartinger, P.J. Dyson, L. Messori, *J. Med. Chem.*, 2008, **51**, 6773.

[48] E. Meggers, *Chem. Commun.*, 2009, 1001.

[49] J.M. Hansen, Y.M. Go, D.P. Jones, *Annu. Rev. Pharmacol. Toxicol.*, 2006, **46**, 215.

[50] C.P. Schroder, A.K. Godwin, P.J. O'Dwyer, K.D. Tew, T.C. Hamilton, R.F. Ozols, *Cancer Invest.*, 1996, **14**, 158.

[51] Y. Yan, M. Melchart, A. Habtemariam, A. Peacock, P.J. Sadler, *J. Biol. Inorg. Chem.*, 2006, **11**, 483.

[52] J.C. Dabrowiak, *Metals in medicine*, Wiley, 2009.

[53] Y. Jung, S.J. Lippard, *Chem. Rev.*, 2007, **107** (5), 1387.

[54] C.A. Rabik, M.E. Dolan, *Cancer Treat. Rev.*, 2007, **33** (1), 9.

[55] P. Ma, H. Xiao, C. Li, Y. Dai, Z. Cheng, Z. Hou, J. Lin, *Mater. Today*, 2015, **18** (10), 554.

[56] N. Muhammad, Z. Guo, *Curr. Opin. Chem. Biol.*, 2014, **19**, 144.

[57] S. Dasari, P. Bernard Tchounwou, *Eur. J. Pharmacol.*, 2014, **740**, 364.

[58] W.H. Ang, C.S. Allardyce, L. Juillerat-Jeanneret, P.J. Dyson, *J. Am. Chem. Soc.*, 2005, **127** (5), 1382.

[59] W.O. Foye, T.L. Lemke, D.A. Williams, *Foye's principles of medicinal chemistry*, Lippincott Williams & Wilkins, 6th edn, 2008, 989.

[60] C.K. Mirabelli, R.K. Johnson, C.M. Sung, L. Faucette, K. Muirhead, S.T. Crooke, *Cancer Research*, 1985, **30**, 32.

[61] (a) A.G. Cox, K.K. Brown, E.S.J. Arner, M.B. Hampton, *Biochemical Pharmacology*, 2008, **76**, 1097; (b) K. Becker, S. Gromer, R.H. Schirmer, S. Müller, *European Journal of Biochemistry*, 2000, **267**, 6118; (c) T. Sandalova, L. Zhong, Y. Lindqvist, A. Holmgren, G. Schneider, *Proceedings of the National Academy of Sciences U.S.A.*, 2001, **98**, 9533; (d) A. Bindoli, M. P. Rigobello, G. Scutari, C. Gabbiani, A. Casini, L. Messori, *Coord. Chem. Rev.*, 2009, **253**, 1692; (e) A. Casini, C. Gabbiani, F. Sorrentino, M. P. Rigobello, A. Bindoli, T. J. Geldbach, A. Marrone, N. Re, C. G. Hartinger, P. J. Dyson, L. Messori, *J. Med. Chem.*, 2008, **51**, 6773; (f) A. Casini, L. Messori, *Current Topics in Medicinal Chemistry*, 2011, **11**, 2647;

(g) C. Gabbiani, G. Mastrobuoni, F. Sorrentino, B. Dani, M.P. Rigobello, A. Bindoli, M.A. Cinellu, G. Pieraccini, L. Messori, A. Casini, *Med. Chem. Comm.*, 2011, **2**, 50.

[62] (a) L. Ray, V. Katiyar, S. Barman, M.J. Raihan, H. Nanavati, M.M. Shaikh, P. Ghosh, *J. Organomet. Chem.*, 2007, **692**, 4259; (b) J. Lemke, A. Pinto, P. Niehoff, V. Vasylyeva, N. Metzler-Nolte, *Dalton Trans.*, 2009, **35**, 7063; (c) M.V. Baker, P.J. Barnard, S.J. Berners-Price, S.K. Brayshaw, J.L. Hickey, B.W. Skelton, A.H. White, *Dalton Trans.*, 2006, **30**, 3708; (d) J.L. Hickey, R.A. Ruhayel, P.J. Barnard, M.V. Baker, S.J. Berners-Price, A. Filipovska, *J. Am. Chem. Soc.*, 2008, **130**, 12570.

[63] J. Hartwig, *Organotransition Metal Chemistry: from Bonding to Catalysis*, University Science Books, 2010.

[64] A.R. Kapdi, I.J.S. Fairlamb, *Chem. Soc. Rev.*, 2014, **43**, 4751.

[65] M.D. Coskun, F. Ari, A.Y. Oral, M. Sarimahmut, H.M. Kutlu, V.T. Yilmaz, E. Ulukaya, *Bioorg. Med. Chem.*, 2013, **21**, 4698.

[66] (a) A.S. Abu-Surrah, H.H. Al-Sadoni, M.Y. Abdalla, *Cancer Ther.*, 2008, **6**, 1; (b) M. Navarro, N.P. Pena, I. Colmenares, T. Gonzalez, M. Arsenak, P. Taylor, *J. Inorg. Biochem.*, 2006, **100**, 152; (c) E. Budzisz, U. Krajewska, M. Rozalski, A. Szulawska, M. Czyz, B. Nawrot, *Eur J. Pharm.*, 2004, **502**, 59.

[67] (a) R.S. Srivastava, F.R. Fronczek, R.S. Perkins, T. Fukuyama, W. Xu, *Int. J. Oncol.*, 2010, **36**, 1591; (b) T.S. Kamatchi, N. Chitrapriya, H. Lee, C.K. Fronczek, K. Natarajan, *Dalton Trans.*, 2012, **41**, 2066; (c) B.N. Chaudhari, P.S. Gide, R.S. Kankate, Z.J. Jain, R.D. Kakad, *Int. J. Pharm. Chem.*, 2012, **2**, 27; (d) L. Maiore, M.A. Cinellu, S. Nobili, I. Landini, E. Mini, C. Gabbiani, L. Messori, *J. Inorg. Biochem.*, 2012, **108**, 123; (e) M. Gras, B. Therrien, G. Suss-Fink, A. Casini, F. Edafe, P.J. Dyson, *J. Organomet. Chem.*, 2010, **695**, 1119; (f) F. Huq, H. Tayyem, P. Beale, J.Q. Yu, *J. Inorg. Biochem.*, 2007, **101**, 30.

[68] M. Tanaka, H. Kataoka, S. Yano, H. Ohi, K. Kawamoto, T. Shibahara, T. Mizoshita, Y. Mori, S. Tanida, T. Kamiya, T. Joh, *BMC Cancer*, 2013, **13**, 1.

[69] (a) E. Guerrero, S. Miranda, S. Luttenberg, N. Frohlich, J.M. Koenen, F. Mohr, E. Cerrada, M. Laguna, A. Mendia, *Inorg. Chem.*, 2013, **52**, 6635; (b) M. Carreira, R. Calvo-Sanjuaı`n, M. Sanauı`, I. Marzo, M. Contel, *Organometallics*, 2012, **31**, 5772.

[70] M.M. Shoukry, A.A. Shoukry, M.N. Hafez, *J. Coord. Chem.*, 2010, **63**, 652.

[71] A.S. Abu-Surrah, M. Kettunen, *Curr. Med. Chem.*, 2006, **13**, 1337.

[72] H. Nawaz, A. Waseem, Z. Rehman, M. Nafees, M. N. Arshad, U. Rashid, *Appl. Organomet. Chem.*, 2017.

[73] (a) Z.D. Matovic, E. Mrkalic, G. Bogdanovic, V. Kojic, A. Meetsma, R. Jelic, *J. Inorg. Biochem.*, 2013, **121**, 134; (b) E.S. Koumousi, M. Zampakou, C.P. Raptopoulou, V. Psycharis,

C.M. Beavers, S.J. Teat, G. Psomas, T.C. Stamatatos, *Inorg. Chem.*, 2012, **51**, 7699; (c) J. Albert, J. Granell, J.A. Durán, A. Lozano, A. Luque, A. Mate, J. Quirante, M.K. Khosa, C. Calvis, R. Messeguer, L. Baldomà, J. Badia, *J. Organomet. Chem.*, 2017, **839**, 116.

[74] (a) W. Li, R. Gust, *Chem. Soc. Rev.*, 2013, **42**, 755; (b) I. Ott, *Medicinal Chemistry of Metal N-Heterocyclic Carbene Complexes* (book chapter of *Inorganic and Organometallic Transition Metal Complexes with Biological Molecules and Living Cells*), 2017, 147.

[75] S. Ray, R. Mohan, J.K. Singh, M.K. Samantay, M.M. Shaikh, D. Panda, P. Gosh, *J. Am. Chem. Soc.*, 2007, **129**, 15042.

[76] T.T. Fong, C. Lock, C.Y. Chung, Y.E. Fung, P. Chow, P. Wan, C. Che, *Angew. Chem. Int. Ed.*, 2016, **55**, 11935.

[77] A.R. Kapdi, A.C. Whitwood, D.C. Williamson, J.M. Lynam, M.J. Burns, T.J. Williams, A.J. Reay, J. Holmes, *J. Am. Chem. Soc.*, 2013, **135** (22), 8388.

[78] S.S. Bhandarkar, J. Bromberg, C. Carrillo, P. Selvakumar, R.K. Sharma, B.N. Perry, B. Govindarajan, L. Fried, A. Sohn, K. Reddy, J.L. Arbiser, *Clin. Cancer Res.*, 2008, **14** (18), 5743.

[79] B. Díaz, K.T. Ostapoff, J.E. Toombs, J. Lo, M.Y. Bonner, A. Curatolo, V. Adsay, R.A. Brekken, J.L. Arbiser, *Oncotarget*, 2016, **7** (32), 51569.

[80] N.E. Kay, T. Sassoon, C. Secreto, S. Sinha, T.D. Shanafelt, A.K. Ghosh, J. Arbiser, *Leuk. Lymphoma*, 2016, **57** (10), 2409.

[81] (a) F.E. Hahn, M.C. Jahnke, *Angew. Chem. Int. Ed.*, 2008, **47**, 3122; (b) W. A. Herrmann, *Angew. Chem. Int. Ed.*, 2002, **41**, 1290.

[82] (a) D.J. Nelson, S.P. Nolan, *Chem. Soc. Rev.*, 2013, **42**, 6723; (b) S.P. Nolan, *N-Heterocyclic Carbenes in Synthesis*, Wiley-VCH, 2006.

[83] A.J. Arduengo, R.L. Harlow, M. Kline, *J. Am. Chem. Soc.*, 1991, **113**, 361.

[84] M. Poyatos, J.A. Mata, E. Peris, *Chem. Rev.*, 2009, **109**, 3677.

[85] I.J.B. Lin, C. S. Vasam, *Coord. Chem. Rev.*, 2007, **251**, 642.

[86] (a) M. Scholl, T.M. Trnka, J.P. Morgan, R.H. Grubbs, *Tetrahedron Lett.* **1999**, *40*, 2247; (b) J. Huang, H.Z. Schanz, E.D. Stevensen, S.P. Nolan, *Organometallics* **1999**, *18*, 5375.

[87] (a) W.A. Hermann, M. Elison, J. Fischer, C. Köcher, G.R.J. Artus, *Angew Chem.*, 1995, **107**, 2602; (b) W.A. Hermann, M. Elison, J. Fischer, C. Köcher, G.R.J. Artus, *Angew. Chem. Int. Ed. Engl.*, **1995**, *34*, 2371.

[88] K.M. Hindi, M.J. Panzner, C.A. Tessier, C.L. Cannon, W.J. Youngs, *Chem. Rev.*, 2009, **109** (8), 3859.

[89] M.L. Teyssot, A.S. Jarrousse, M. Manin, A. Chevry, S. Roche, F. Norre, C. Beaudoin, L. Morel, D. Boyer, R. Mahiou, A. Gautier, *Dalton Trans.*, 2009, 6894.

[90] (a) M.Z. Ghdhayeb, R.A. Haque, S. Budagumpi, M.B.K. Ahamed, A.M.S.A. Majid, *Polyhedron*, 2017, **121**, 222; (b) M.Z. Ghdhayeb, R.A. Haque, S. Budagumpi, M.B.K. Ahamed, A.M.S.A. Majid, *Inorg. Chem. Commun.*, 2017, **75**, 41.

[91] R.H. Crabtree, *The Organometallic Chemistry of the Transition Metals*, Wiley-Interscience, 4th edn, 2005.

[92] P.C.J. Kamer, P.W.N.M. Van Leeuwen, *Phosphorus(III) Ligands in Homogeneous Catalysis: Design and Synthesis*, Wiley-VCH, 2012.

[93] E. Constable, *Comprehensive Coordination Chemistry II: From Biology to Nanotechnology*. Newnes, 2003.

[94] B. M. Trost, *Acct. Chem. Res.*, 2002, **35**, 695.

[95] J. Tsuji, *Palladium reagent and catalysts*, John Wiley and sons, 1995, 5.

[96] A. Heumann, *Transition metals for organic synthesis*, Wiley-VCH, 2004, vol. 1, chap. 2.14.

[97] (a) L. Canovese, F. Visentin, C. Santo, V. Bertolasi, *Organometallics*, 2014, **33**, 1700; (b) L. Canovese, F. Visentin, C. Santo, C. Levi, *Organometallics*, 2009, **28**, 6762.

[98] J. Smidt, W. Hafner, *Angew. Chem.*, 1959, **71,** 284.

[99] (a) L. Canovese, F. Visentin, C. Levi, C. Santo, V. Bertolasi, *J. Organomet. Chem.*, 2013, **732**, 27; (b) L. Canovese, F. Visentin, T. Scattolin, C. Santo, V. Bertolasi, *Polyhedron*, 2016, **119**, 377.

[100] (a) L. Canovese, G. Chessa, F. Visentin, *Inorganica Chim. Acta*, 2010, **363**, 3426; (b) L. Canovese, F. Visentin, C. Santo, G. Chessa, V. Bertolasi, *Organometallics*, 2010, **29**, 3027; (c) L. Canovese, F. Visentin, C. Levi, A. Dolmella, *Dalton Trans.*, 2011, **40**, 966; (d) L. Canovese, F. Visentin, C. Levi, C. Santo, V. Bertolasi, *Inorganica Chim. Acta*, 2011, **378**, 239; (e) L. Canovese, F. Visentin, C. Levi, C. Santo, V. Bertolasi, *J. Organomet. Chem.*, 2013, **732**, 27.

[101] K. Moseley, P.M. Maitlis, *J. Chem. Soc. Dalton Trans.*, 1974, 169.

[102] R. Van Belzen, C.J. Elsevier, A. Didieu, N. Veldman, A.L. Speck, *Organometallics*, 2003**,** **22**, 722.

[103] (a) L. Canovese, F. Visentin, T. Scattolin, C. Santo, V. Bertolasi, J. *Organomet. Chem.*, 2016, **808**, 48; (b) L. Canovese, F. Visentin, T. Scattolin, C. Santo, V. Bertolasi, *Polyhedron*, 2016, **113**, 25; (c) T. Scattolin, F. Visentin, C. Santo, V. Bertolasi, L. Canovese, *Dalton Trans.*, 2016, **45**, 11560; (d) L. Canovese, F. Visentin, T. Scattolin, C. Santo, V. Bertolasi, *Dalton Trans.*, 2015, **44**, 15049; (e) L. Canovese, C. Santo, T. Scattolin, F. Visentin, V. Bertolasi, J. *Organomet. Chem.*, 2015, **794**, 288; (f) F. Visentin, C. Santo, T. Scattolin, N. Demitri, L. Canovese, *Dalton Trans.*, 2017, **46**,10399.

[104] R. B. King, *J. Organomet. Chem.*, 2001, **635**, 75.

[105] L. Canovese, F. Visentin, *Inorganica Chim. Acta*, 2010, **363**, 2375.

[106] (a) L. Canovese, F. Visentin, T. Scattolin, C. Santo, V. Bertolasi, *Polyhedron*, 2018, **144**, 131*;* (b) L. Canovese, F. Visentin, T. Scattolin, C. Santo, V. Bertolasi, *Polyhedron*, 2017, **129**, 229*;* (c) L. Canovese, T. Scattolin, F. Visentin, C. Santo, *J. Organomet. Chem.*, 2017, **834**, 10*;* (d) T. Scattolin, F. Visentin, C. Santo, V. Bertolasi, L. Canovese, *Dalton Trans.*, 2017, **46**, 5210*;* (e) L. Canovese, F. Visentin, C. Santo, Inorganica Chim. Acta, 2014, **421**, 326*;* (f) L. Canovese, F. Visentin, C. Santo, V. Bertolasi, *J. Organomet. Chem.*, 2014, **749**, 379*;* (g) L. Canovese, F. Visentin, C. Biz; T. Scattolin, C. Santo, V. Bertolasi, *Polyhedron*, 2015, **102**, 94*;* (h) L. Canovese, F. Visentin, C. Biz, T. Scattolin, C. Santo, V. Bertolasi, *J. Organomet. Chem*, 2015, **786**, 21; (i) L. Canovese, F. Visentin, G. Chessa, P. Uguagliati, C. Levi, A. Dolmella, *Organometallics*, 2005, **24**, 5537; (j) L. Canovese, F. Visentin, C. Levi, C. Santo, *J. Organomet. Chem.*, 2008, **693**, 3324; (k) L. Canovese, C. Santo, F. Visentin, *Organometallics*, 2008, **27**, 3577*;* (l) L. Canovese, F. Visentin, C. Santo, A. Dolmella, *J. Organomet. Chem.*, 2009, **694**, 411; (m) V. Lucchini, G. Borsato, L. Canovese, C. Santo, F. Visentin, A. Zambon, *Inorganica Chim. Acta*, 2009, **362**, 2715; (n) L. Canovese, F. Visentin, C. Levi, C. Santo, V. Bertolasi, *Inorganica Chim. Acta*, 2012, **390**, 105.

2

Aim of the project

The primary goal of this thesis is the synthesis and characterization of new organometallic palladium complexes bearing *N*-Heterocyclic Carbenes as spectator ligands.

In this respect, the six types of NHC ligands which have been taken into consideration are (Fig. 2.1):

1. Carbenes deriving from functionalized purine bases.
2. Alkyl and/or aryl imidazole derivatives.
3. Chelating biscarbenes with a methylene or ethylene bridge.
4. Bidentate carbenes derived from imidazoles having a linked pyridine or thioether group.
5. Carbenes with a glucopyranosidic group.
6. Carbenes derived from trifluoromethylbenzimidazole.

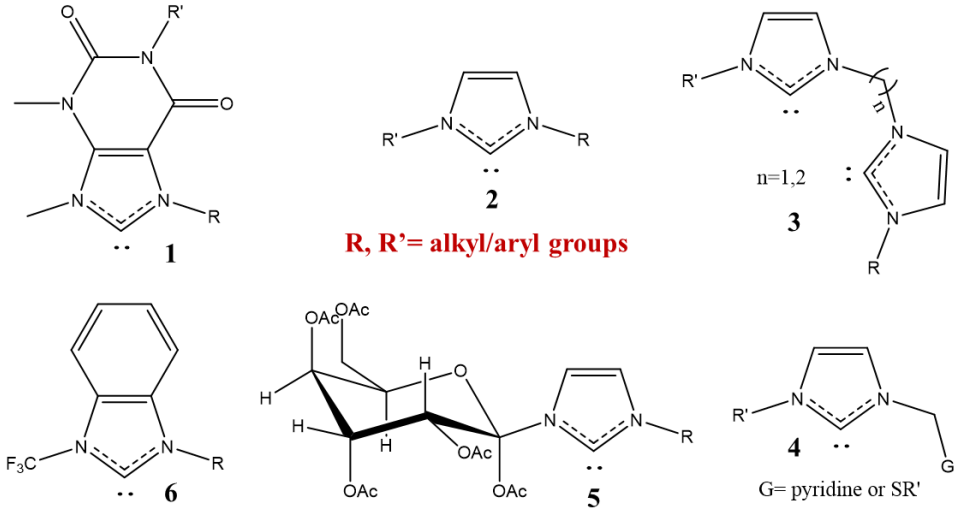

Fig. 2.1

The figure proposed at the beginning of the chapter is related to this source: https://www.marketingbinder.com

As mentioned in the introductory section, the novelty of this work is represented by the first attempt to study the anticancer activity of palladium compounds stabilized by organometallic fragments (η^3-allyl-Pd(II), palladacyclopentadienyl and η^2-olefin-Pd(0)) and NHCs (spectator ligands). Remarkably, the application in catalysis and the reactivity of these species have been widely studied, whereas their biological activity is substantially unexplored.

The use of organometallic fragments (Fig. 2.2), combined with the presence of carbene ligands should render our compounds more resistant to hydrolysis *in vivo* and thus reduce the general problem of collateral toxicity.

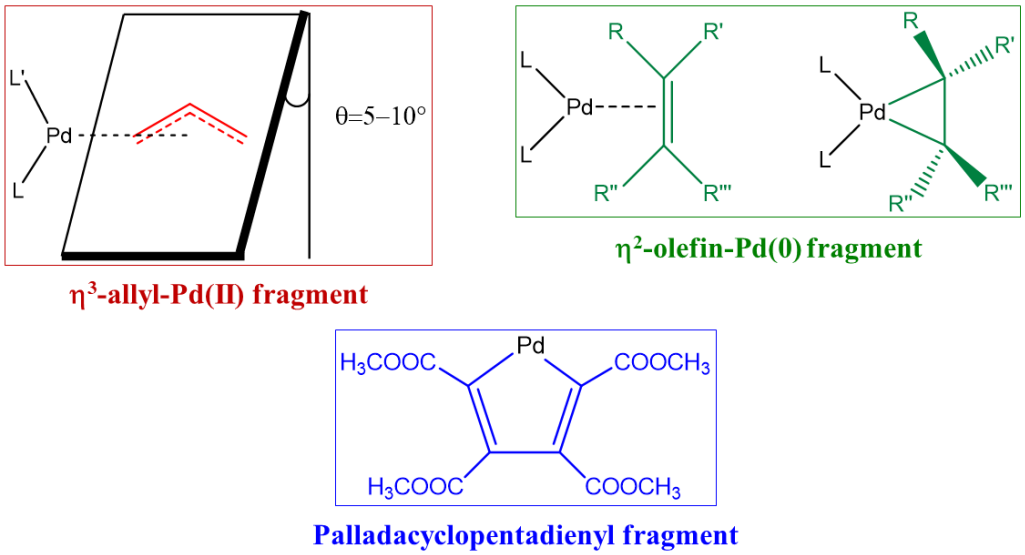

Fig. 2.2

A systematic study of their biological activity as potential antitumor agents against ovarian carcinoma and other tumor lines (colon and lung cancer and malignant melanoma), will be proposed. For a small class of compounds, a study on their toxicity toward healthy cells (fibroblasts) will also be presented and, by means of cellular uptake analyses, stability studies and specific biological tests, some hypotheses about their possible mechanism of action will be advanced.

3

Purine-based NHC complexes

The first class of compounds, whose cytotoxic activity was evaluated, is represented by the palladium complexes stabilized by *N*-Heterocyclic Carbene ligands derived from the functionalization of natural purine bases. Such a choice was based on the hope that the natural origin of these molecules could render the final complexes more compatible with the biological matrix. This kind of strategy has already given interesting results and, in the most favourable cases, the ligand has represented a real targeting vector for its metal derivatives [1].

In this chapter the synthesis of palladium η^3-allyl, palladacyclopentadienyl and palladium (0) η^2-olefin complexes stabilized by these carbenes will be illustrated in detail.

In order to modulate the stereoelectronic features of the examined complexes, it will also be presented cases where the carbenic ligand is combined with an other different spectator ligand such as phosphines (PPh_3, TPPTS and PTA) and isocyanides (i.e. DIC). In the final part of the following chapter the results of the antiproliferative and proapoptotic activity of these compounds versus cisplatin-sensitive and cisplatin-resistant ovarian cancer lines will be highlighted.

The figure proposed at the beginning of the chapter is related to this source: H. Valdes et al., *J. Organomet. Chem.*, 2018, **867**, 51.

3.1. Introduction

Purine bases are a class of organic compounds whose chemical structure derives from purine, a molecule consisting in a condensed pyrimidine and imidazole ring.

Many purine derivatives, especially those of adenine, are involved in several metabolic processes [2]. For example, the 5-triphosphate adenosine (ATP) is an important energy resource for the body, while NAD (nicotinamide adenine dinucleotide) and FAD (flavin adenine dinucleotide) are coenzymes involved in redox cellular processes. Together with pyrimidines, purines are important building blocks of DNA and RNA [3].

In nature the purine bases can be distinguished in two main categories (Fig. 3.1):

- Purine bases of nucleic acids (adenine and guanine).
- Purine bases deriving from xanthine (caffeine, theobromine and theophylline).

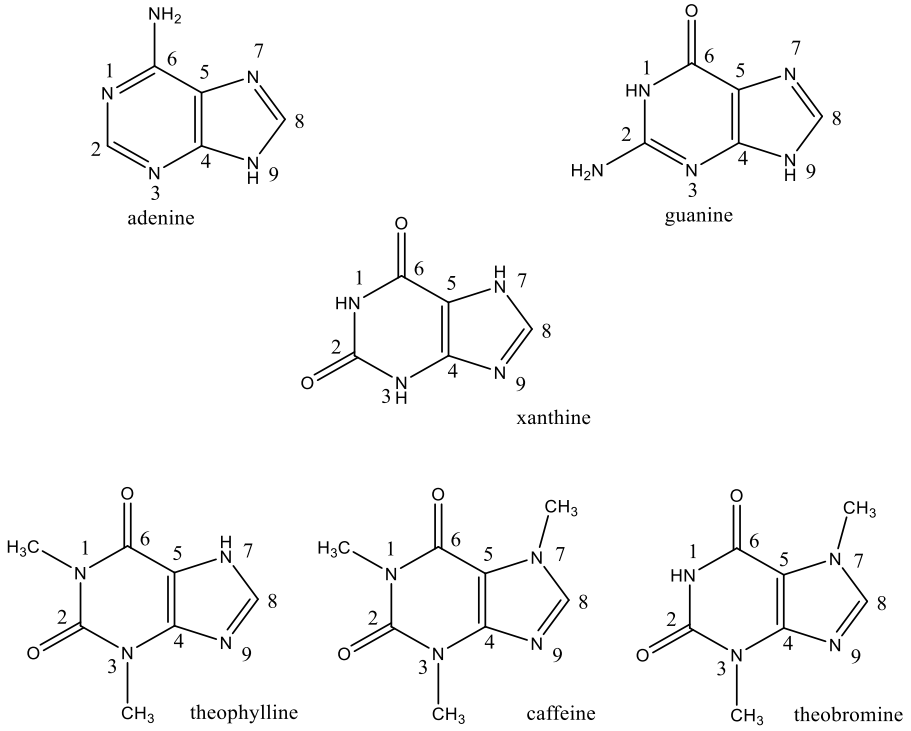

Fig. 3.1 Chemical structure of the most important purine bases.

Xanthine bases are commercial compounds of natural origin extracted respectively from the seeds of Coffee Arabica (caffeine), the leaves of Sinensis Thea (theophylline) and the seeds of Cacao (theobromine). Caffeine and theobromine have stimulating properties [4] while theophylline is an antiasthmatic [5].

Generally, the synthetic derivatives of xanthine are prepared starting from theophylline or theobromine, which have an NH group in position 7 and 1, respectively. Such a group can be easily functionalized by generic alkylating agents (R-X), in the presence of a base [6] (Scheme 3.1).

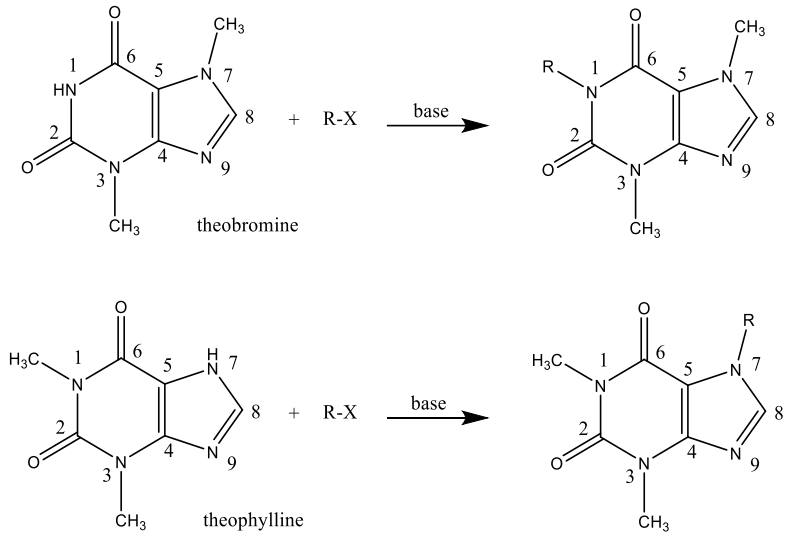

Scheme 3.1 Theophylline and Theobromine functionalization-

The functionalization of N-9 is unfortunately limited to the introduction of methyl [7], ethyl [8] or benzyl [9] groups. Furthermore, this process requires drastic experimental conditions with unsatisfactory yields as reported in Scheme 3.2, in the case of some alkylation reactions of the caffeine.

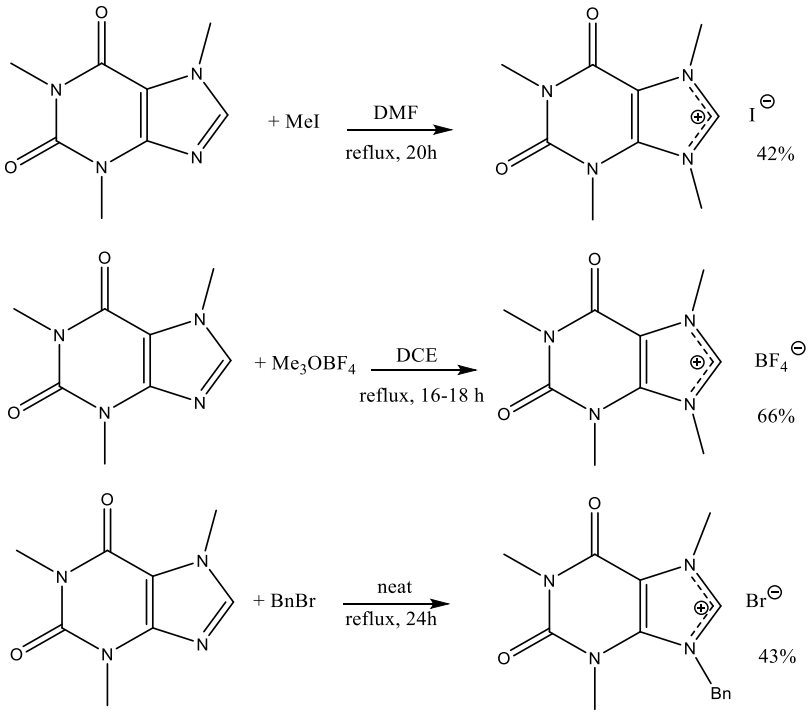

Scheme 3.2 Experimental conditions for the caffeine functionalization.

The imidazolium salts obtained by the exhaustive functionalization can be considered precursors of the *N*-Heterocyclic Carbene ligands.

As a matter of fact, many examples of complexes of Ir [10], Rh [10, 11], Ru [12], Ag [13, 14], Cu [15], Pt [16] and Au [17] have been synthesized and in some cases their antiproliferative activity has been studied (Fig. 3.2).

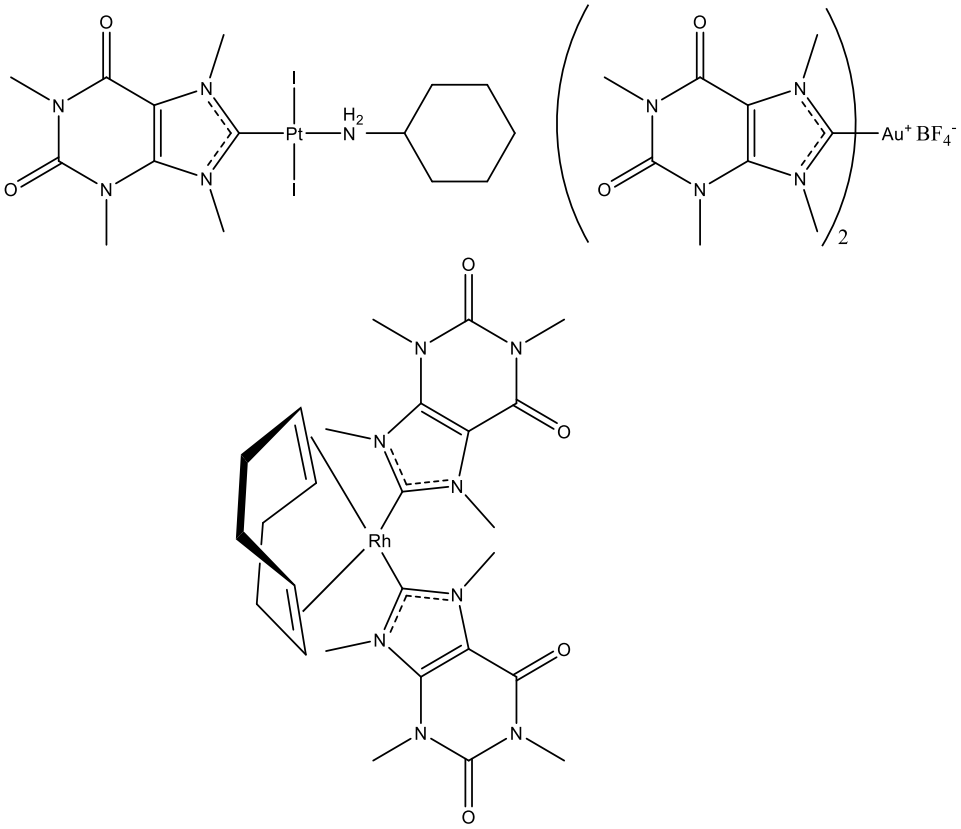

Fig. 3.2 Examples of late transition metal complexes bearing purine based-NHC.

As for palladium, despite of the number of derivatives described in the literature, there are very few examples of complexes with purine-based NHCs and their antiproliferative activity is not reported (Fig. 3.3) [9, 17].

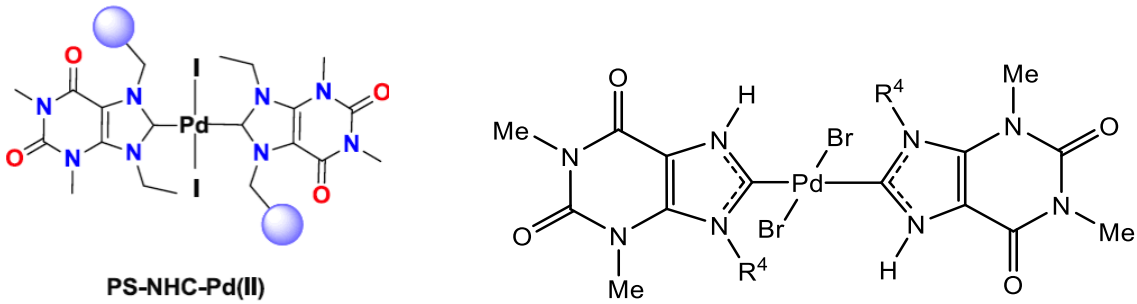

Fig. 3.3 Examples of Pd(II) complexes with purine-based NHC ligands.

3.2. Synthesis of Functionalized Xanthines

A number of theophylline and theobromine derivatives can be quite easily prepared by alkylation, under mild conditions, of the NH groups in positions 7 and 1, respectively. In this work we have synthesized, and used in subsequent synthetic steps, the benzyl and phenylpropargyl derivatives of theophylline and theobromine (Scheme 3.3).

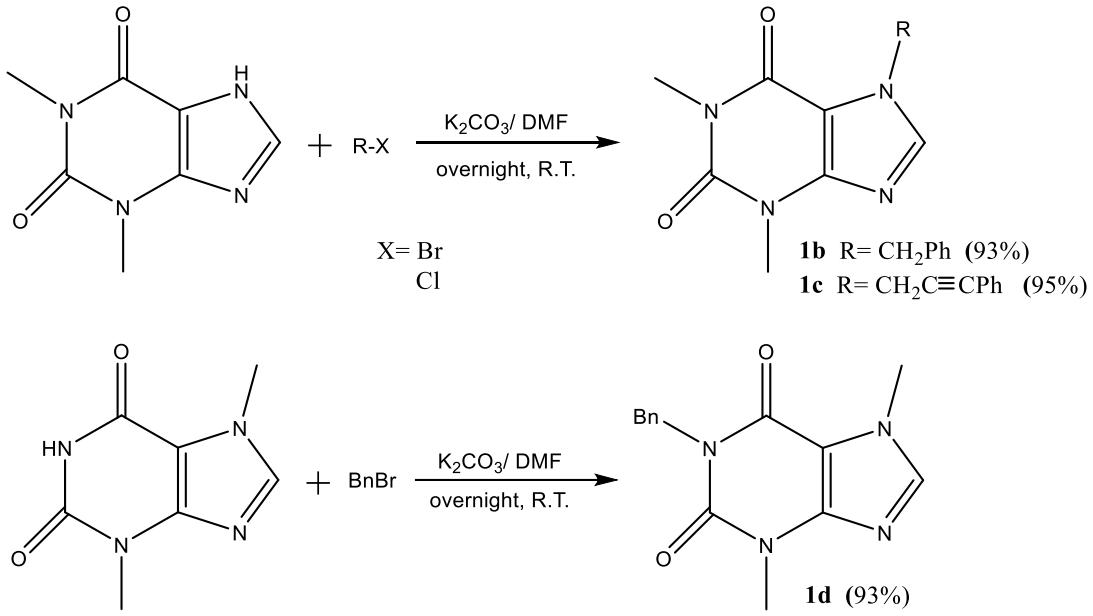

*Scheme 3.3 Synthesis of functionalized xanthines **1b-d.***

Preliminary tests have demonstrated that benzyl and phenylpropargyl substituents were the most suitable alkylating agent owing the good yields and purity of the obtained derivatives. As reported in the above scheme, theophylline and theobromine were reacted in DMF at RT overnight, with benzyl bromide or phenylpropargyl chloride, in the presence of K_2CO_3 as base. This process represents a slightly modified version of the methodology reported by Groundwater and co-workers in 2012 [6]. The final products were easily precipitate by addition of water to the final reaction mixture. The success of the process is proved by ^{1}H-NMR spectra, in which the disappearance of the peak related to the NH group (broad signal within 11-13 ppm) and the simultaneous appearance of the signals of the benzyl or phenylpropargyl group (NCH_2 protons resonate as a singlet within 5-6 ppm and the aromatic ones within 7.2-7.6 ppm) are observed. The slight shift related to the other signals (NCH_3 and NCHN groups) with respect to that of the starting purines is also apparent (Fig. 3.4).

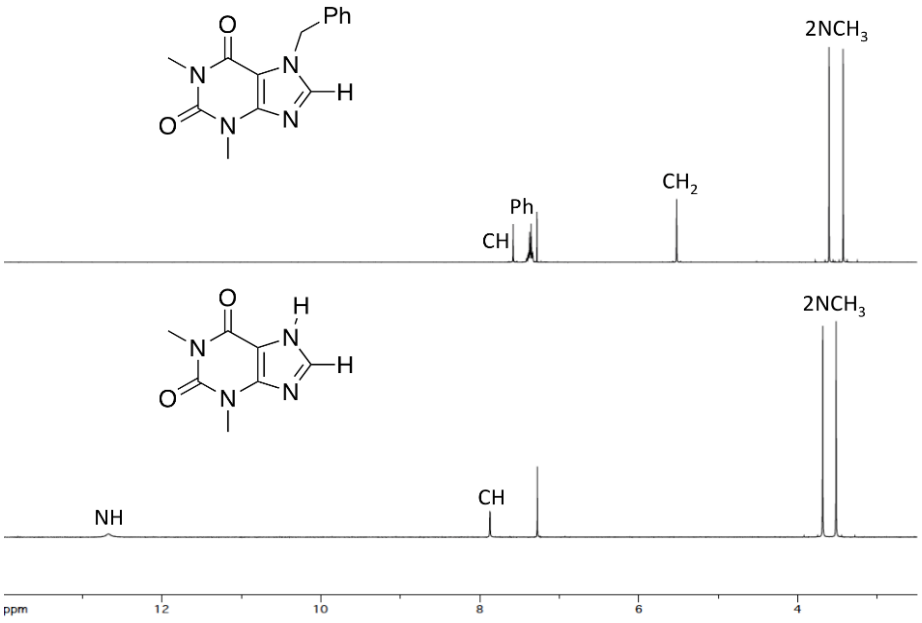

*Fig. 3.4 ^{1}H-NMR spectra of theophylline and **1b** derivative (T=298K, $CDCl_3$).*

The $^{13}C\{^{1}H\}$-NMR spectra (Fig. 3.5) show the following signals:

- NCH_3 and NCH_2 in the 28 - 50 ppm interval.
- Alkyne carbons (for the compound **1c**) within 80 and 88 ppm.
- C^5 and C^4 at about 107 and 149 ppm, respectively.
- Aromatic carbons within 121-137 ppm.
- Imidazole carbon (NCHN) at about 141 ppm.
- Two carbonyl carbons within 151-156 ppm.

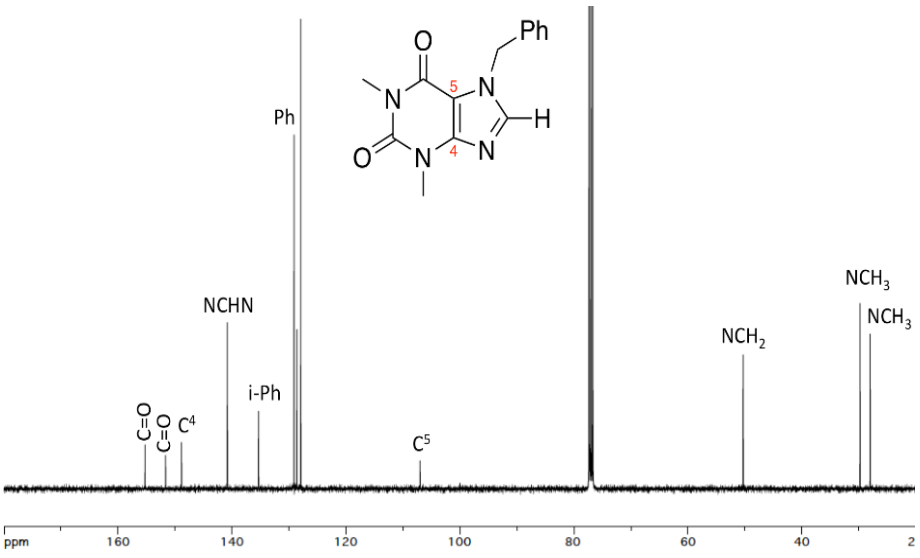

*Fig. 3.5 $^{13}C\{^{1}H\}$-NMR spectrum of **1b** (T=298K, $CDCl_3$).*

3.3. Purine-based imidazolium salts

The previously described xanthine derivatives (**1b-d)** and the commercially available caffeine (**1a**) contain a sp^2 nitrogen in position 9 that must be functionalized in order to obtain the corresponding imidazolium salts. This functionalization, as already stated, is restricted to the introduction of methyl [7], ethyl [8] or benzyl [9] substituents under very drastic conditions and often with low yields. In the present work the methylation of the alkylated xanthines **1** was obtained by a new protocol based on the modified conditions proposed by Hermann [7b] and Casini [16]. Such a protocol implies the reaction in acetonitrile at RT of a slight excess of Me_3OF_4 as methylating agent (Meerwein's salt), in the presence of sodium carbonate as inorganic base (Scheme 3.4).

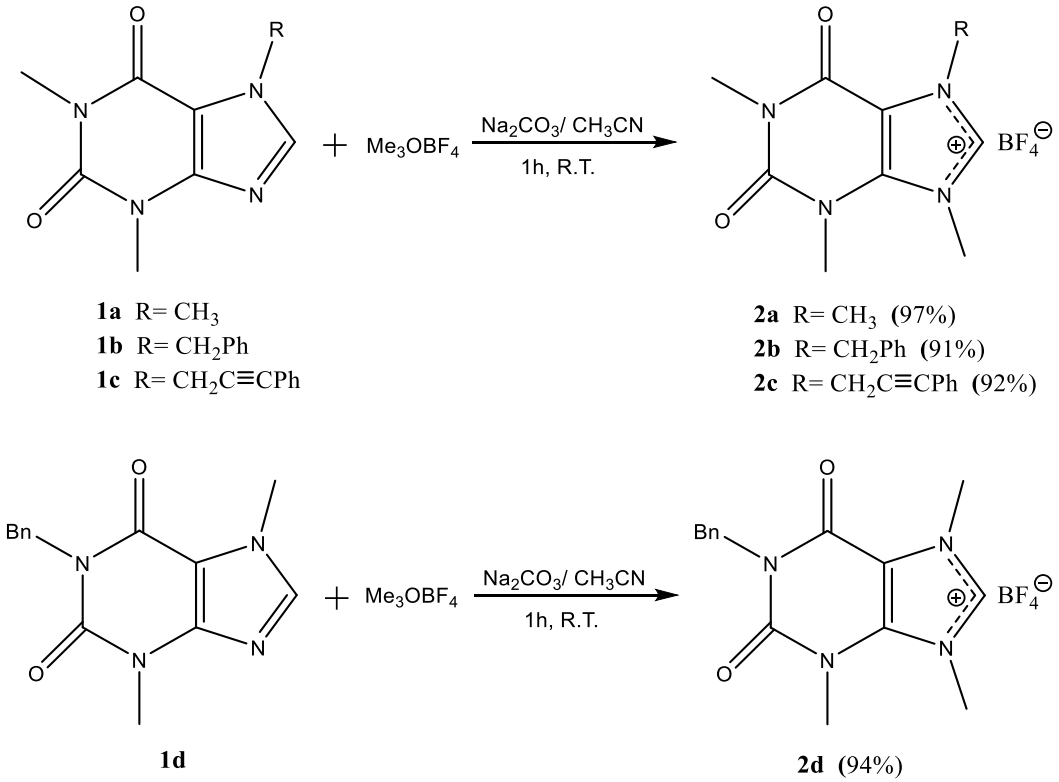

Scheme 3.4

In particular, the advantages of this protocol are:

- Me_3OBF_4 is easier to handle and a less dangerous methylating agent if compared to methyl iodide or dimethylsulfate. Moreover, its use in slight excess reduces the problems of the waste dispersion in the environment.
- The use of a polar solvent such as acetonitrile renders the rate of the nucleophilic substitution higher than that promoted by the chlorinated solvents.
- The reaction is carried out at RT, in the air and with very short reaction times.

- The use of the easily removable by filtration inorganic base Na_2CO_3, contributes to the achievement in an almost quantitative yields (>90%) of the wanted fully alkylated species. As a matter of fact, the sodium carbonate deprotonates the by-product formed in the reaction of the starting xanthines **1** with HBF_4, which is produced in small quantities when Me_3OBF_4 reacts with traces of H_2O. Therefore, the restored species **1** can undergo an exhaustive methylation (Scheme 3.5).

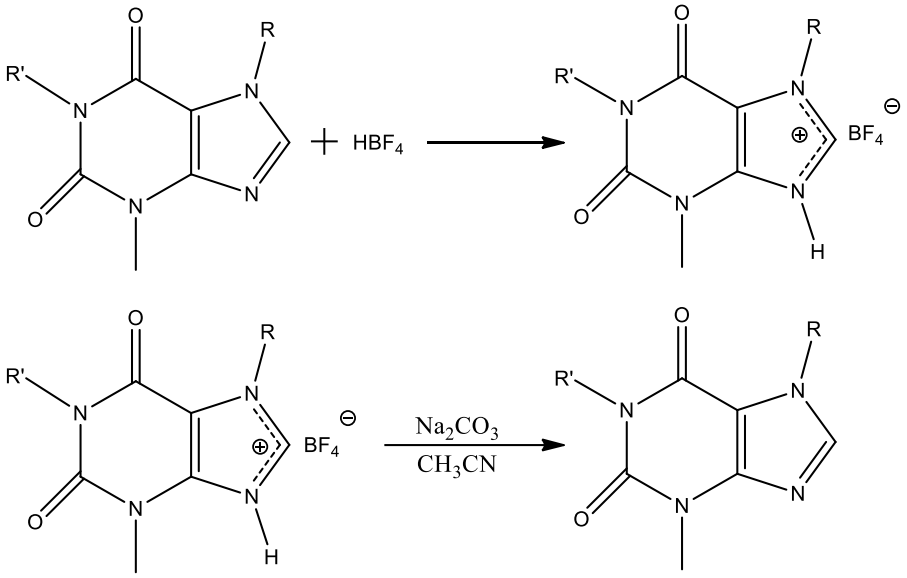

Scheme 3.5

The successful result of the methylation is evident from the analysis of ^{1}H-NMR spectra. The reaction products show the signal of the N-CH_3 group at lower fields if compared to the other pre-existing methyl groups. Moreover, the imidazolic proton (NCHN) of the methylated species shifts at lower field (ca. 1 ppm) than that of the compounds **1** (Fig. 3.6).

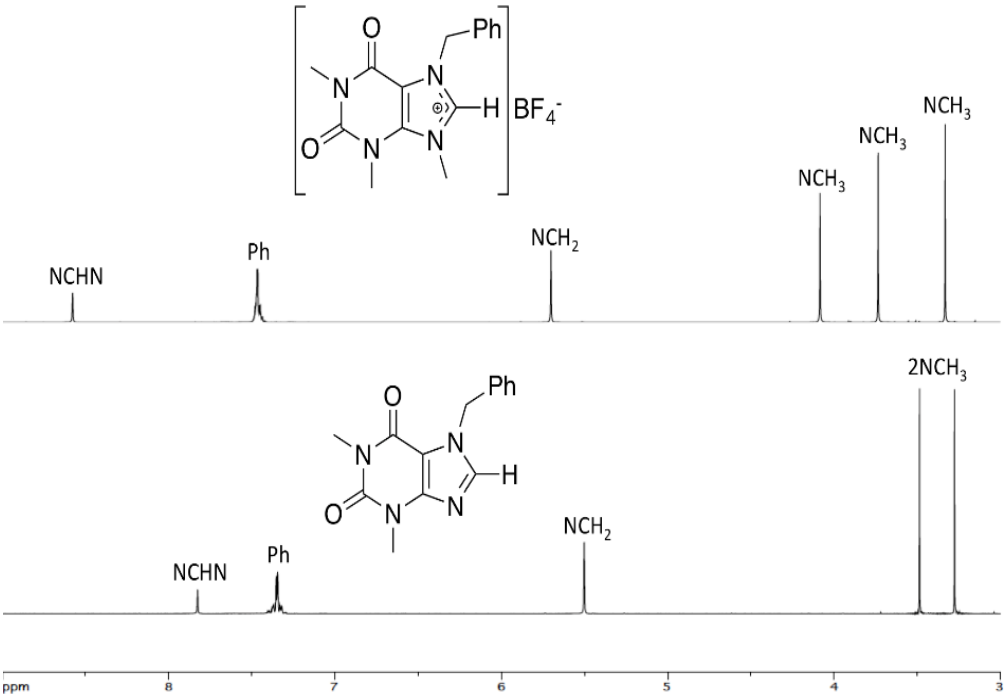

*Fig. 3.6 ^{1}H-NMR spectra of **1b** and **2b** (T = 298K, CD_3CN).*

The $^{13}C\{^{1}H\}$-NMR (Fig. 3.7) and ESI-MS spectra confirm the structure of the obtained products.

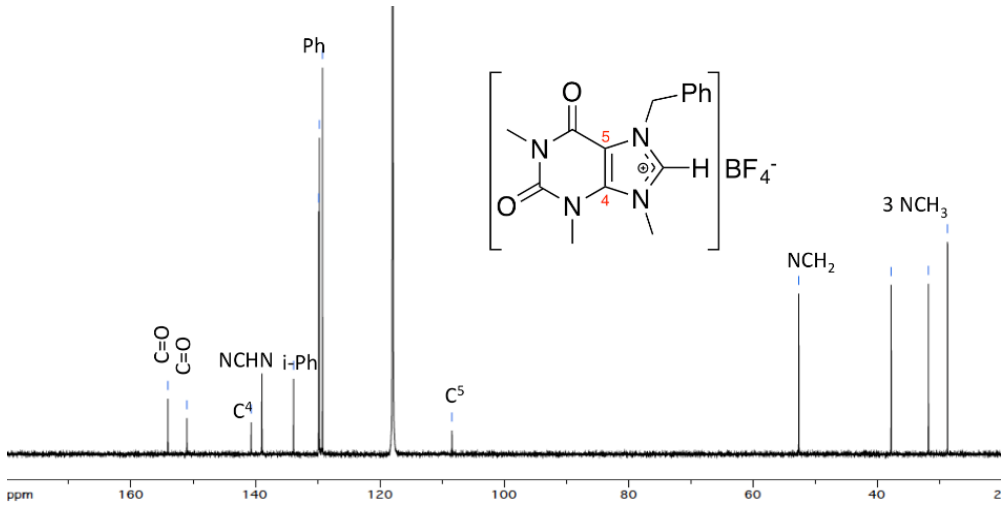

*Fig. 3.7 $^{13}C\{^{1}H\}$-NMR spectrum of **2b** (T = 298K, CD_3CN).*

The synthesis of Pd (0) and some Pd (II) complexes is easily feasible when Ag (I) carbene precursors obtained from imidazolium hydrochlorides are used as starting compounds. Thus, the imidazolium hydrochlorides have been synthesized in water by reacting the imidazolium tetrafluoroborates with $AsPh_4Cl$ (Scheme 3.6) [18]. Any traces of arsenic salts are completely removed in the subsequent steps, exploiting their different solubility with respect to the Ag (I) intermediate compounds and to the final palladium complexes.

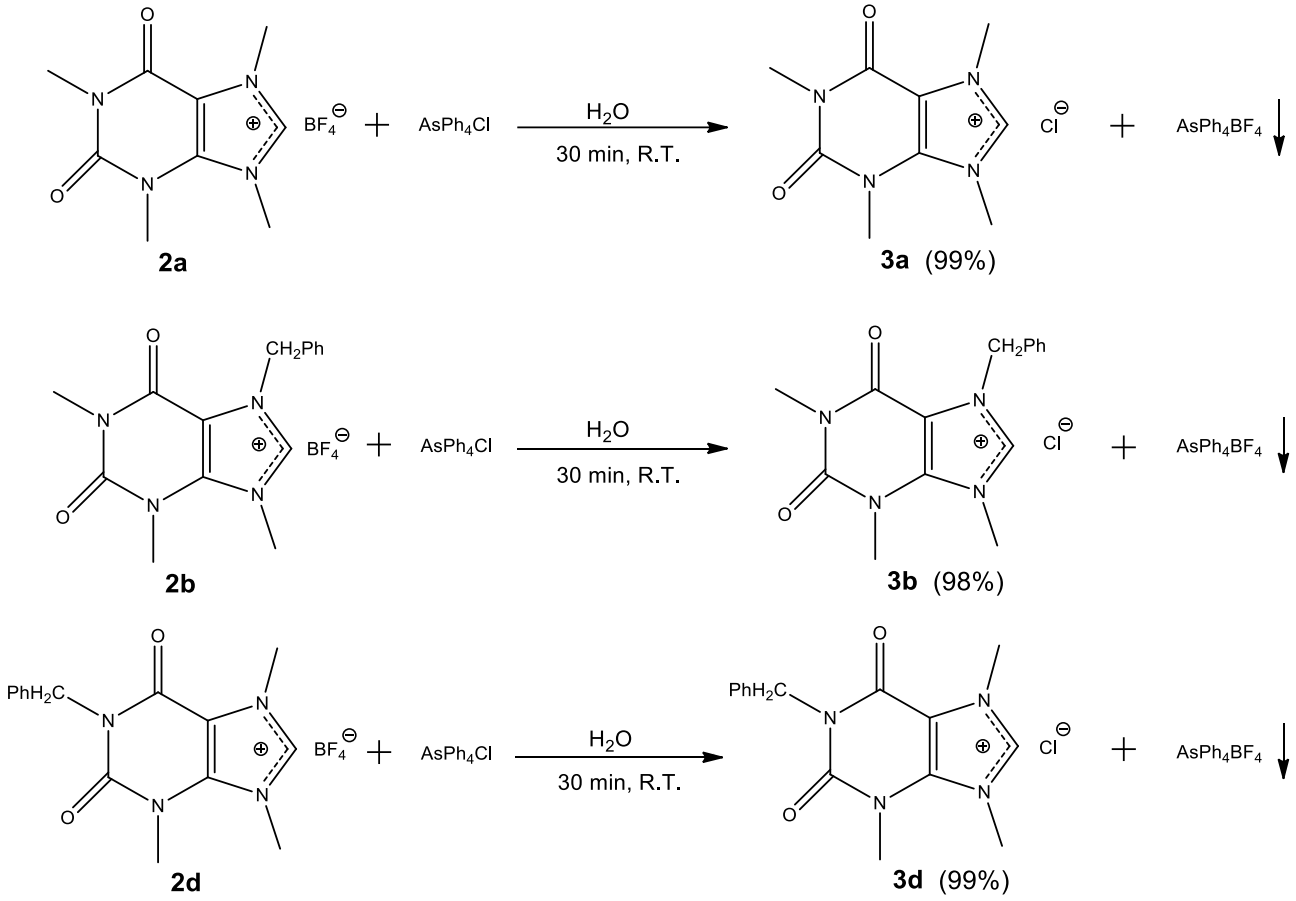

*Scheme 3.6 Synthesis of the imidazolium salts **3a-c.***

Another efficient method, although less rapid, is based on the exchanging anions by treating in methanol the imidazolium salts **2a,b** and **2d** for 24 hours with the ion exchange resin DOWEX-21KCl. Regardless of the chosen synthetic path, it is possible to verify the nature of the obtained product by NMR, ESI-MS and elemental analysis.

From the comparison of the ^{1}H-NMR spectrum of the imidazolium salt **3a** with that of **2a** (Fig. 3.8), it is possible to see how the substitution of the initial BF_4^- counterion with Cl^- slightly affects the chemical shifts of the related protons. This influence is particularly remarkable in the case of the methyl groups of the imidazole system resonating between 3.4 and 4.2 ppm, since the splitting of two peaks that previously appeared overlapped becomes apparent. Moreover, although the position of the signal of the imidazole proton is not particularly diagnostic owing to its acidity, in the case of the hydrochloride derivative a significant downfield shift ($\Delta\delta \approx 1.5$ ppm) is observed.

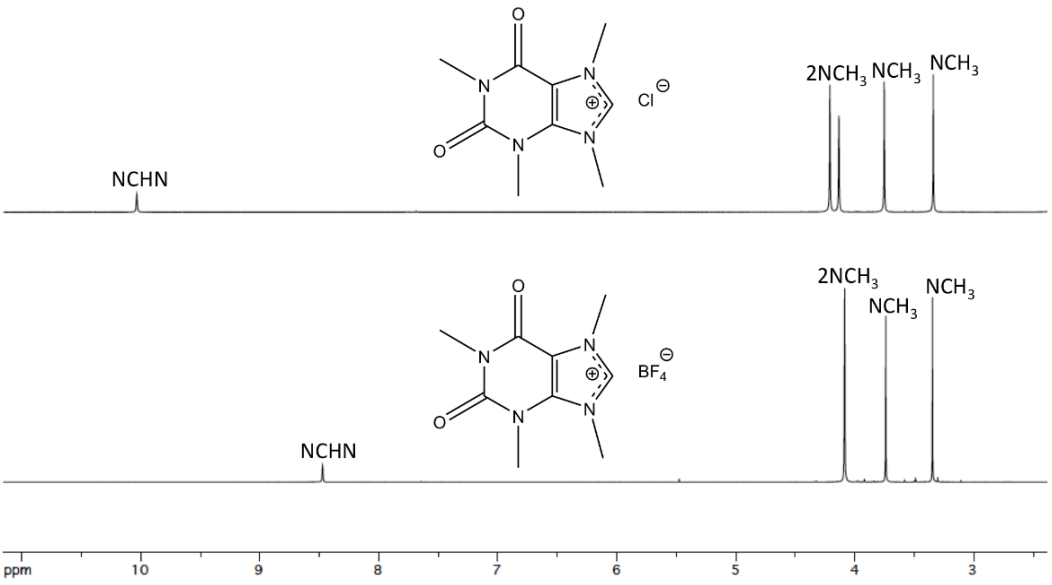

*Fig. 3.8 ^{1}H-NMR spectra of **3a** and **2a** (T = 298K, CD_3CN).*

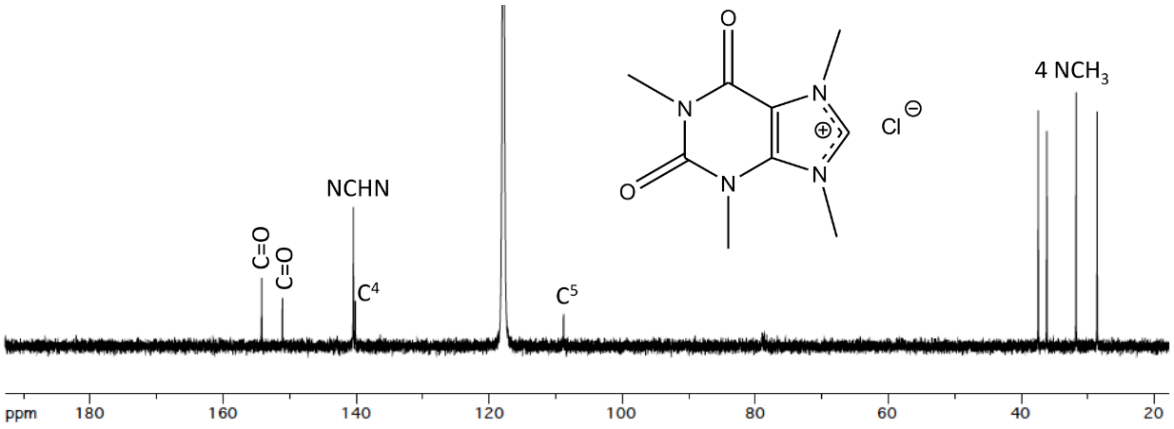

*Fig. 3.9 $^{13}C\{^{1}H\}$-NMR spectrum of **3a** (T = 298K, CD_3CN).*

Considerations similar to those made for product **3a** can be extended to compounds **3b** and **3d**.
In the case of compound **3c**, traces of decomposition can be detected in the NMR spectra and for this reason, such a compound was not used in the synthesis of Pd (0) and Pd (II) neutral complexes.

3.4. Silver (I) purine-based NHC complexes

The synthesis of the Ag (I) complexes was carried out by reacting the imidazolium salts **2-3** with 0.5 equivalents of silver oxide. Starting from the imidazolium salts **2a-d**, the addition of Ag_2O, carried out in acetonitrile for 28 hours, led to the formation of equimolar mixtures of the biscarbene complexes **4a-d** and $AgBF_4$ (Scheme 3.7).

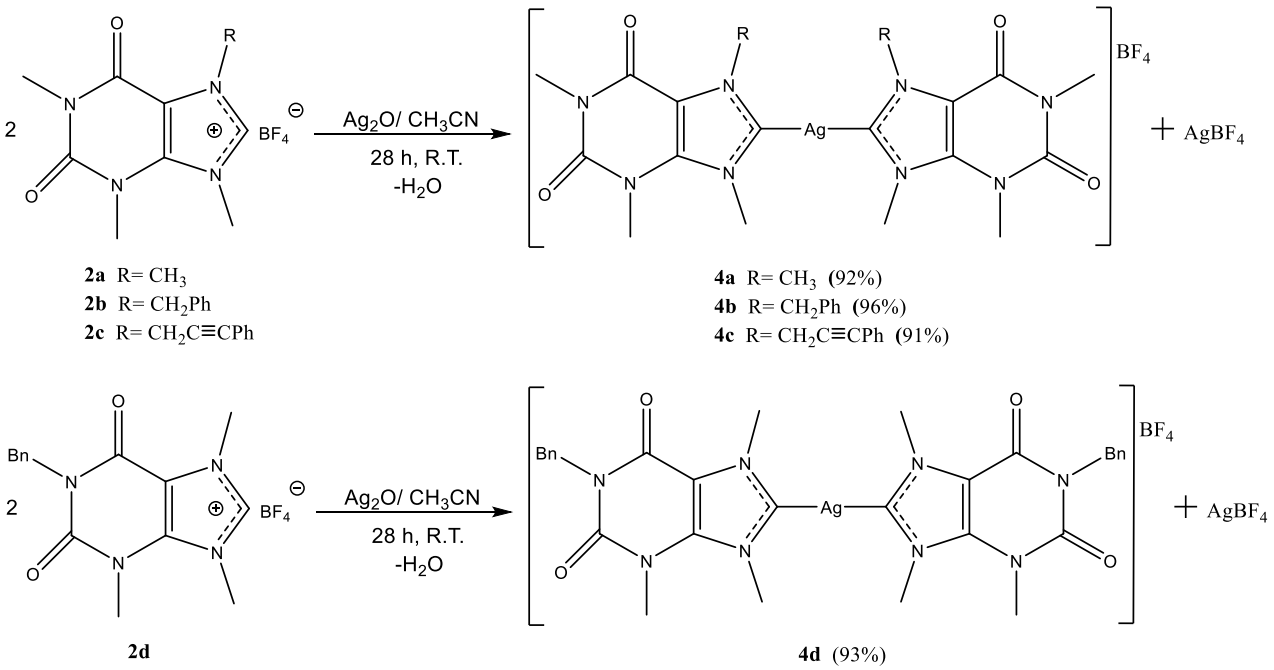

*Scheme 3.7 Synthesis of the **4a-d**/$AgBF_4$ mixtures.*

This result is confirmed by NMR, ESI-MS (Fig. 3.10), elemental analysis and, in the case of complex **4b,** by the solid state structure obtained by single crystal X-ray diffraction (Fig. 3.11).

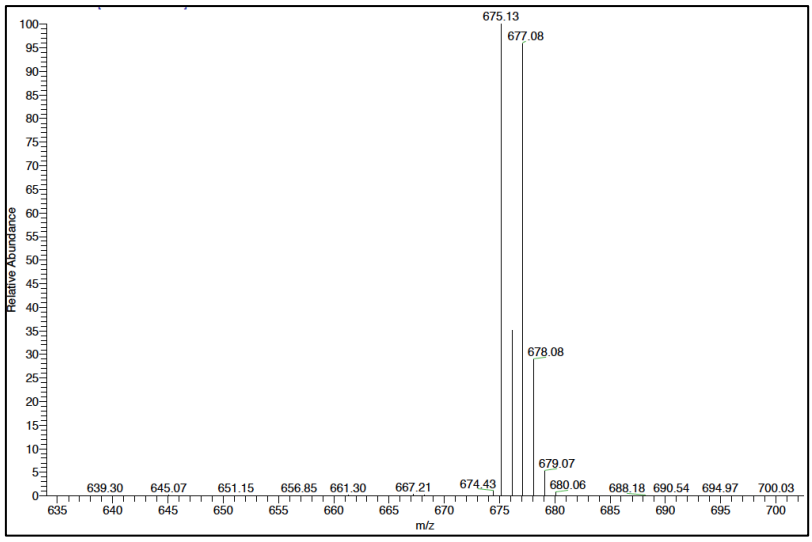

*Fig. 3.10 ESI-MS spectrum of **4b**/$AgBF_4$ ($[NHC\text{-}Ag\text{-}NHC]^+$ as molecular ion peak).*

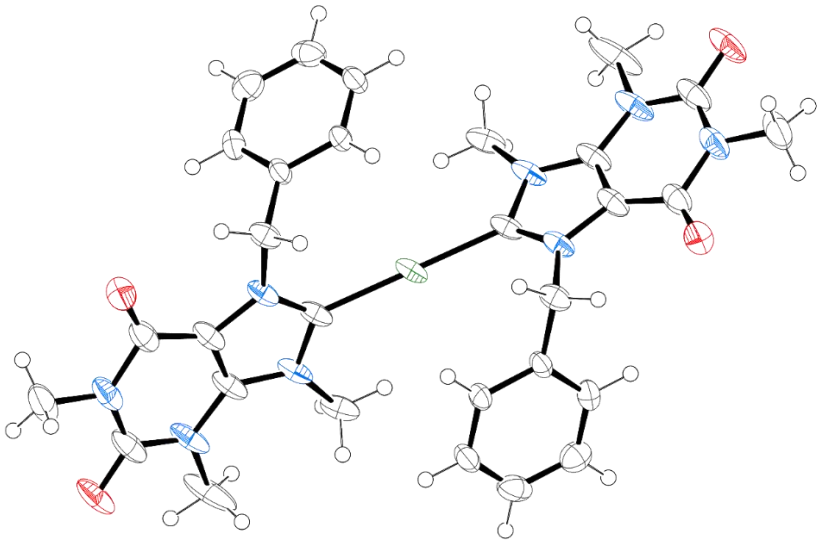

*Fig. 3.11 Ellipsoid representation of **4b** crystal ASU contents (50% probability).*

The ^{1}H-NMR spectra are characterized by the slight displacement of the signals with respect to those of the starting imidazolium salts and by the absence of the peak of the imidazole proton NCHN (Fig. 3.12).

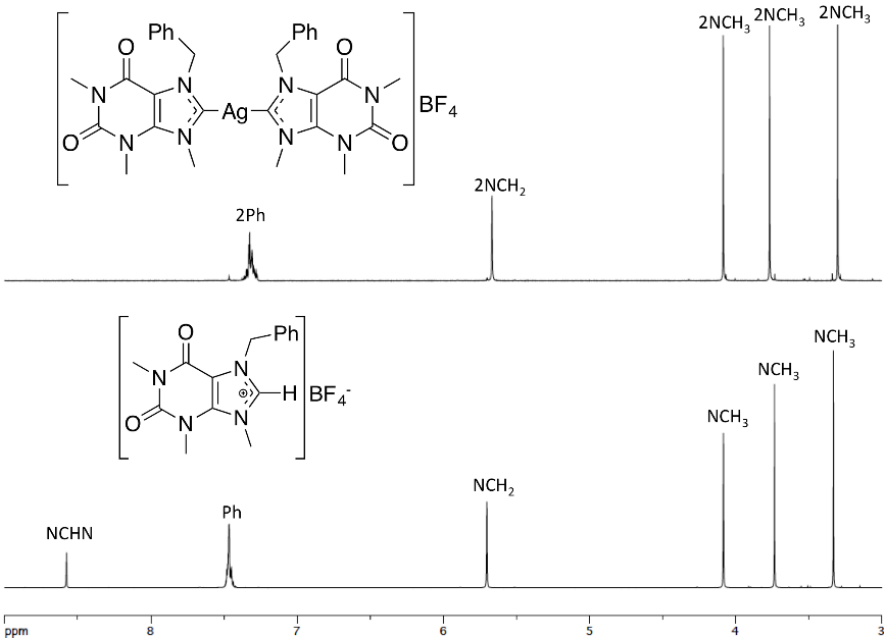

*Fig. 3.12 ^{1}H-NMR spectra of **2b** and **4b** (400 MHz, T=298K, CD_3CN).*

The marked downfield shift of the imidazole carbon NCN in the $^{13}C\{^{1}H\}$-NMR spectra from about 140 ppm of the starting compound to 180-190 ppm, which is the typical resonance of the coordinated carbenic carbon, represents a further evidence confirming the coordination process (Fig. 3.13).

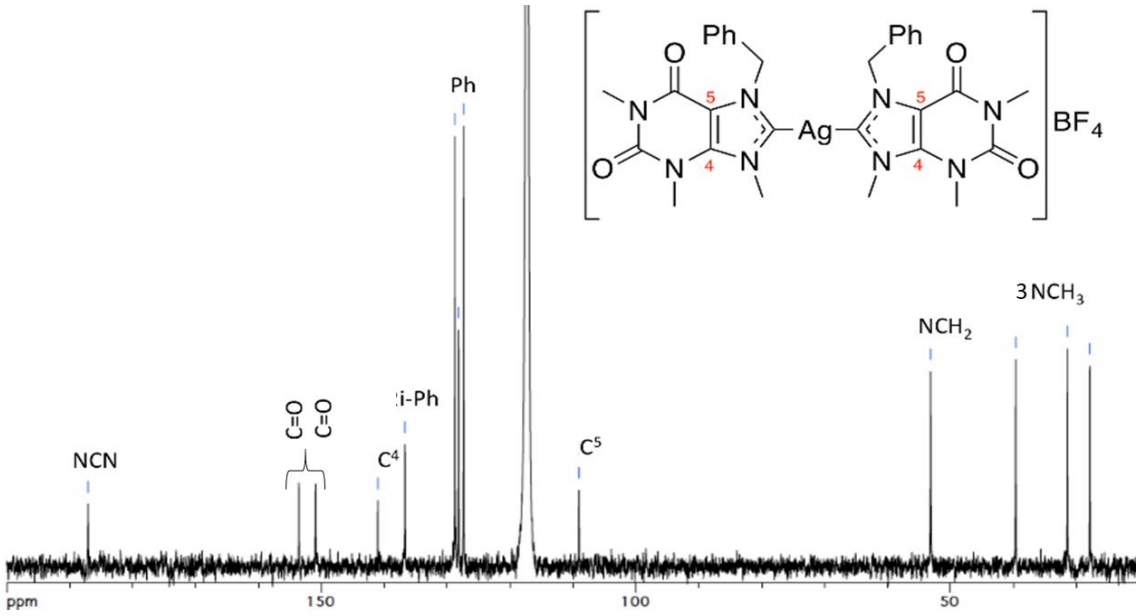

*Fig. 3.13 $^{13}C\{^{1}H\}$-NMR spectrum of **4b** (T=298K, CD_3CN).*

The attribution of the proton and carbon signals was carried out by bidimensional HMQC and HMBC spectra (Figs. 3.14 and 3.15).

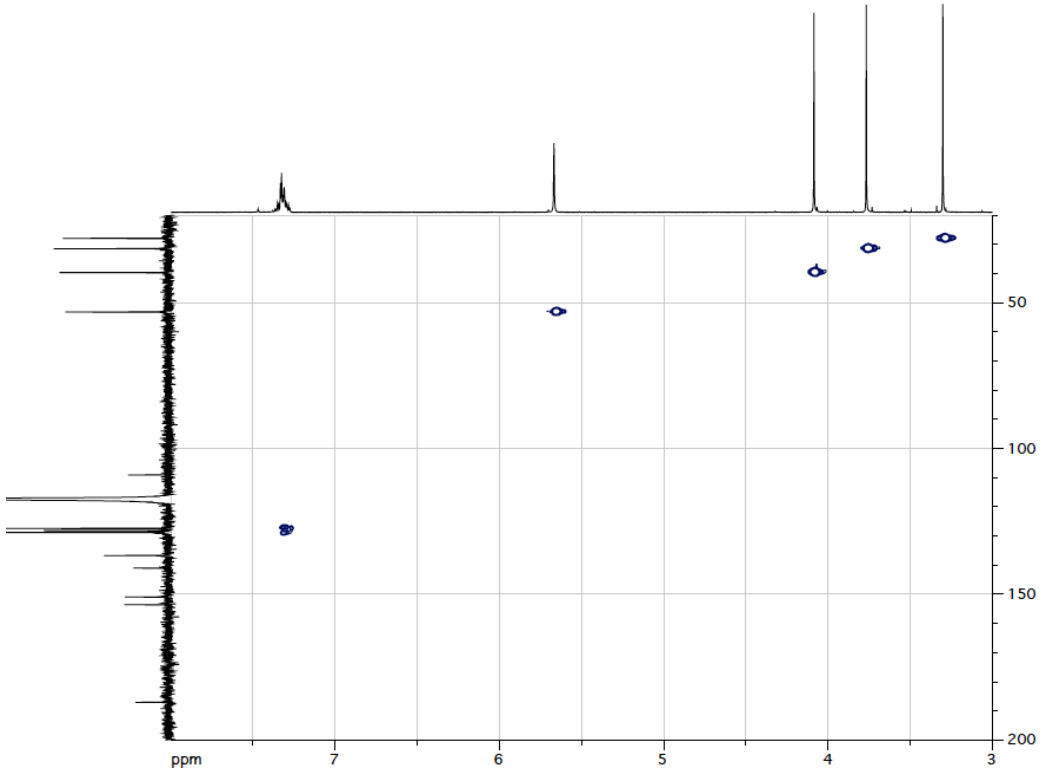

*Fig. 3.14 HMQC spectrum of **4b** (T=298K, CD_3CN).*

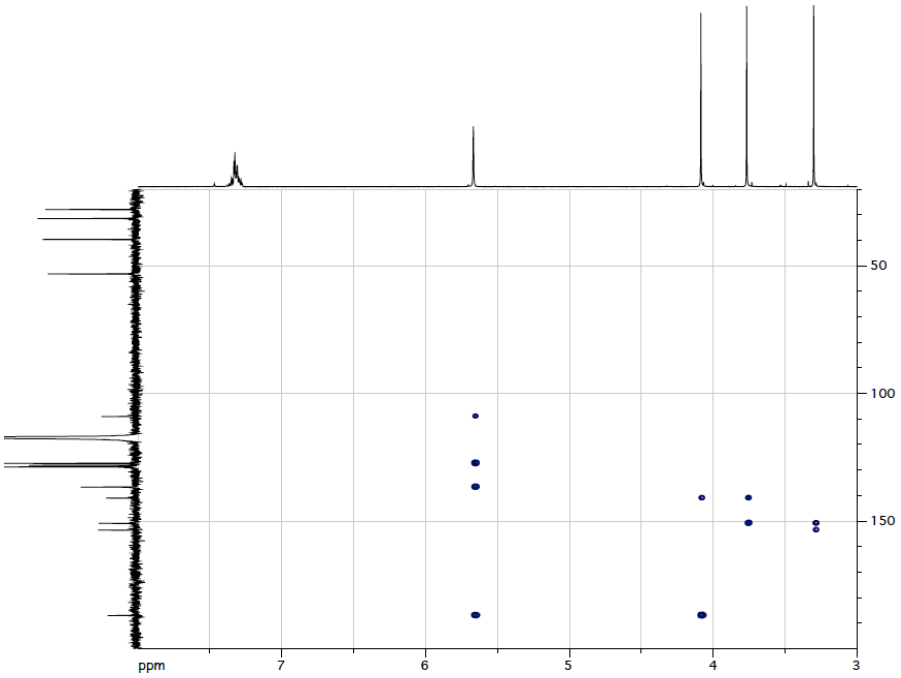

*Fig. 3.15 HMBC spectrum of **4b** (T=298K, CD_3CN).*

Beside the formation of the complex [NHC-Ag-NHC]BF_4, the presence of $AgBF_4$ in a 1:1 ratio is noticed as suggested by the darkening of the precipitate within 1-2 days. However, as will be seen later, the presence of $AgBF_4$ does not represent a problem for the transmetallation process but rather an advantage.

Similar approach has been used in the synthesis of type **5** complexes, which were obtained from the reaction between the imidazolium salts **3** and silver oxide.

The reactions were carried out in acetonitrile, where the progressive dissolution of the silver oxide and the simultaneous precipitation of the products as white solids were observed. The final complexes were separated by filtration, subsequently dissolved in dichloromethane and finally filtered off on millipore apparatus in order to eliminate the residual Ag_2O. From the resulting solutions, the products **5a-b** and **5d** were obtained in pure form by precipitation with diethylether (Scheme 3.8).

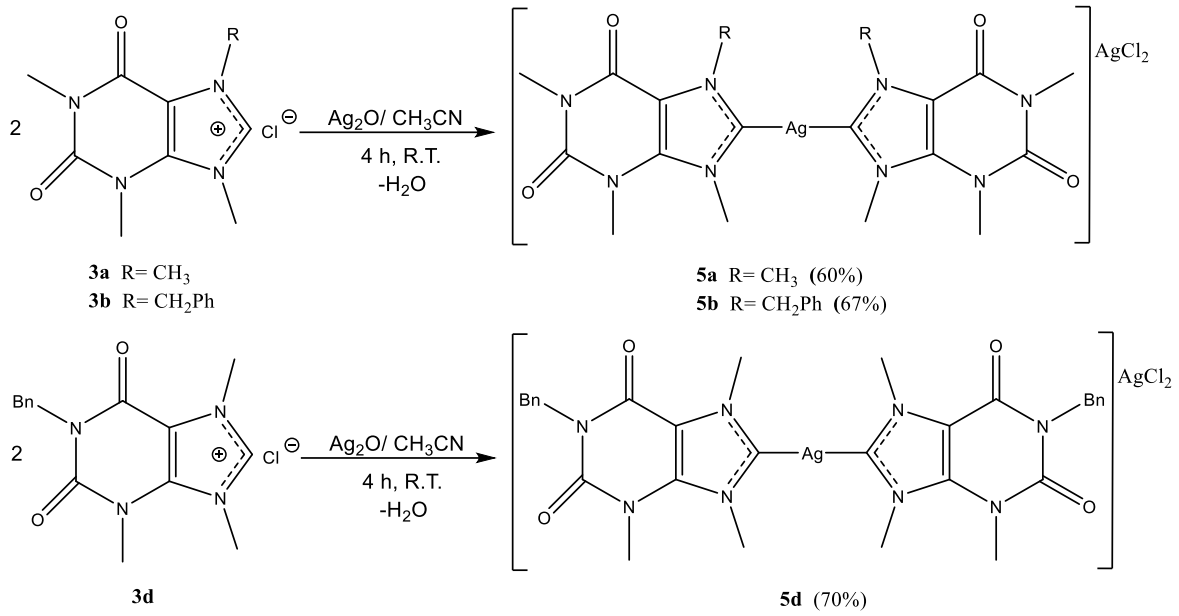

*Scheme 3.8 Synthesis of **5a-b** and **5d.***

As an example, the ^{1}H-NMR spectra of complex **5b** shows the signals of the alkyl and aryl groups slightly displaced with respect to those of the corresponding imidazolium salt **3b** as a consequence of the coordination of the metal (Fig. 3.16). The disappearance, in the ^{1}H-NMR spectrum of the complex **5b,** of the signal related to the imidazole proton NCHN is also particularly diagnostic.

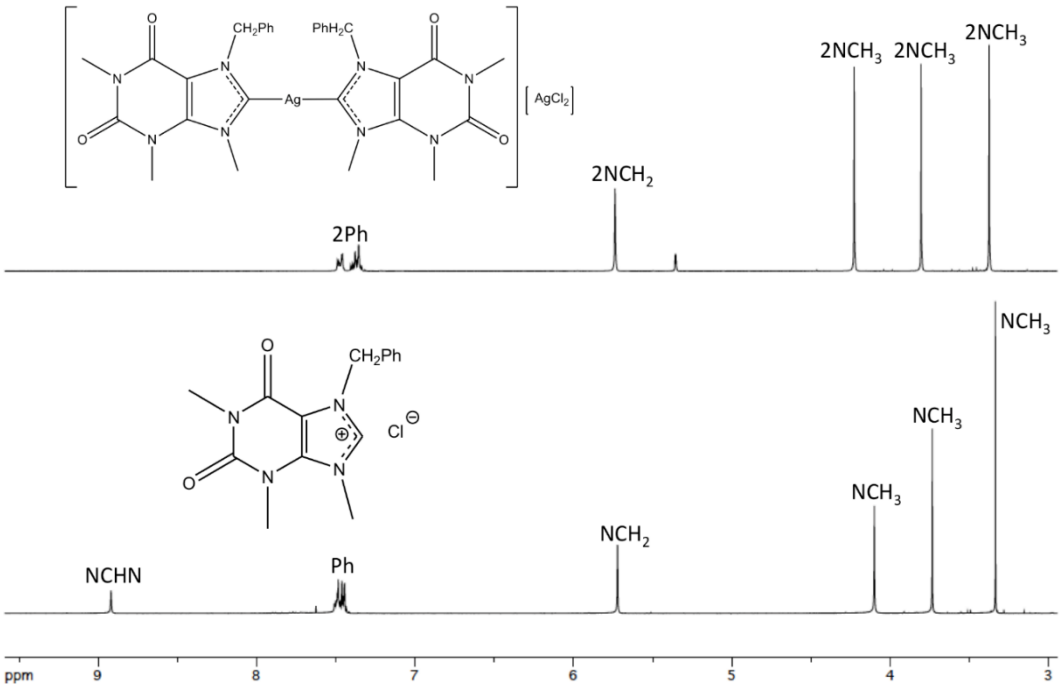

*Fig. 3.16 ^{1}H-NMR spectra of **3b** e **5b** (T = 298K, CD_2Cl_2 and CD_3CN).*

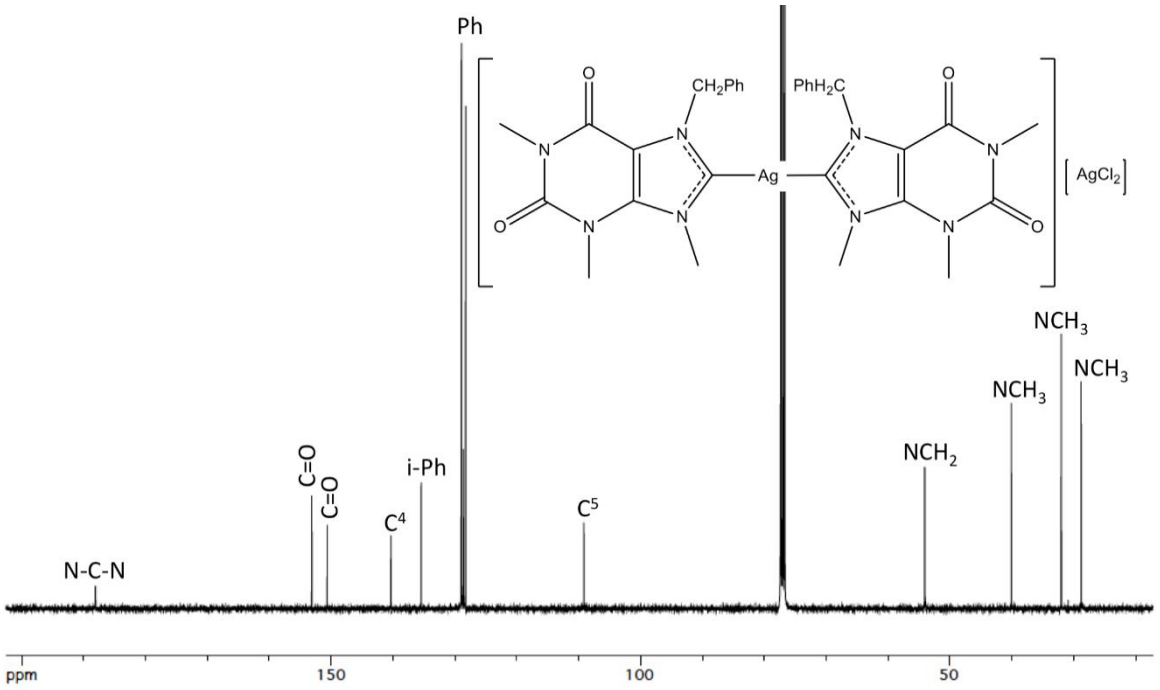

*Fig. 3.17 ^{13}C {^{1}H}-NMR spectrum of **5b** (T = 298K, $CDCl_3$).*

The simple formula [(NHC)-Ag-Cl] was initially hypothesized for the Ag (I) complexes prepared. However, the ESI-MS spectrum (Fig. 3.18), indicates the presence of the molecular ion $[NHC\text{-}Ag\text{-}NHC]^+$, therefore we propose a structure of the type $[NHC\text{-}Ag\text{-}NHC][AgCl_2]$.

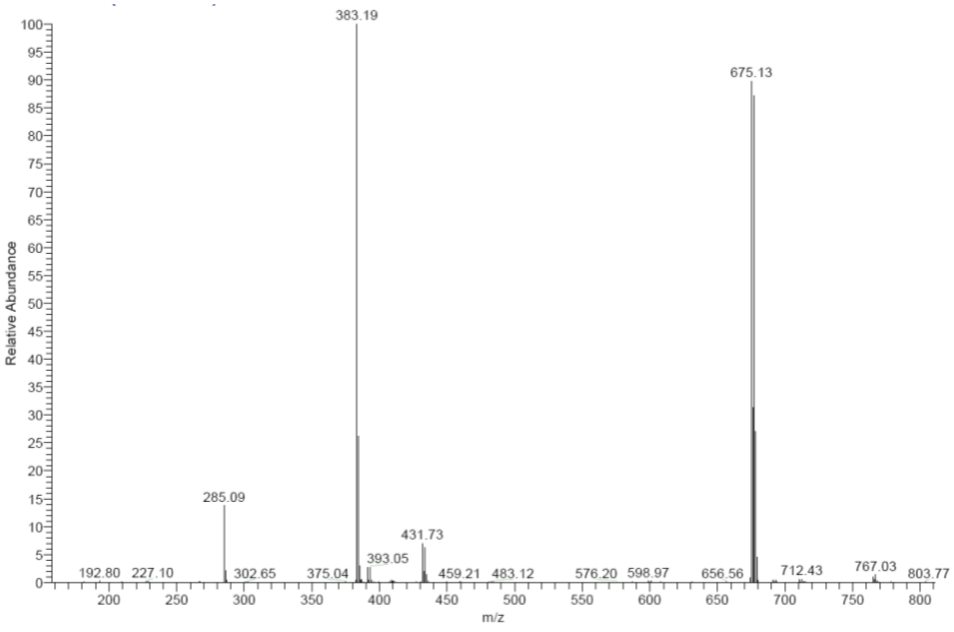

*Fig. 3.18 ESI-MS spectrum of **5b.***

This assumption is supported by literature data describing cationic complexes of Ag (I) containing the species $[AgCl_2]^-$ as a counterion (Fig. 3.19) [19, 20].

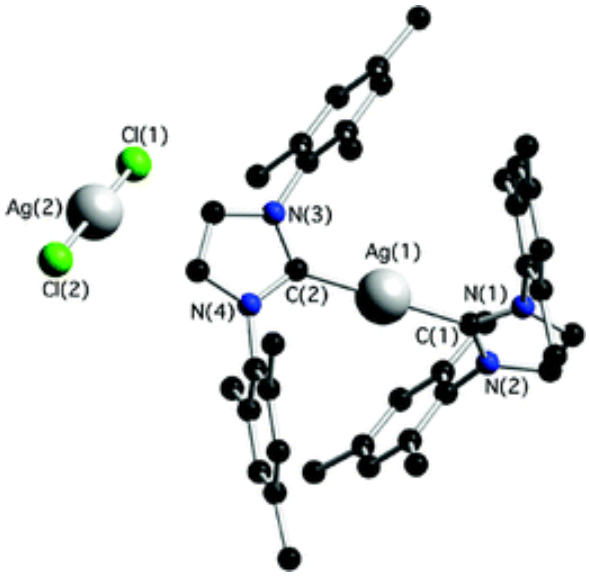

Fig. 3.19 Structure of the complex $[(IMes)_2Ag][AgCl_2]$ (ball and stick model) [19]

3.5. Palladium (II) η^3-allyl complexes bearing purine-based NHCs

The synthesis of cationic Pd(II) η^3-allyl complexes, (see section 1.6.1.), is generally carried out by reacting the dimeric precursor $[Pd(\mu\text{-}Cl)(\eta^3\text{-allyl})]_2$, with two monodentate or one bidentate ligands (Scheme 3.9).

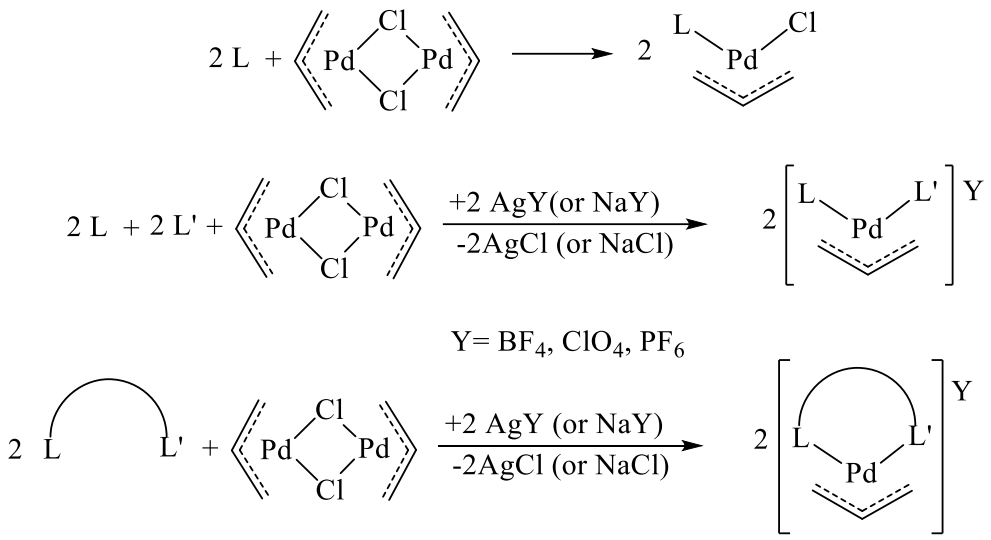

Scheme 3.9 General synthesis of Pd(II) η^3-allyl complexes with mono- and bidentate ancillary ligands.

A dechlorinating agent (i.e. $NaClO_4$ or $AgBF_4$) is often necessary to ensure the coordination of both the spectator ligands since in aprotic solvent a competitive coordination between the ligands and the free chloride might established. In this paragraph the synthesis of η^3-allyl complexes bearing two purine-based carbene ligands (biscarbene compounds) and complexes bearing one purine-based carbene and one different ligand such as a phosphine or an isocyanide (mixed NHC/L complexes), will be discussed. The presence of a different spectator ligand was taken into consideration since it allows the modulation of the stereoelectronic characteristics and the solubility of the mixed complexes. In our case, the dechlorinating agent is not necessary since the $AgBF_4$ present as companion of the Ag (I) carbene precursors reacts with the free chloride to give the insoluble AgCl which can be easily removed by filtration.

3.5.1. Mixed NHC/PPh_3 η^3-allyl complexes (6)

The first class of η^3-allyl compounds we have synthesized was stabilized by one purine-based carbene and one triphenylphosphine as spectator ligands. These compounds were obtained by addition of the Ag (I) carbene complex (**4a-d**/$AgBF_4$ mixtures) and a stoichiometric amount of triphenylphosphine,

dissolved in acetonitrile, to an acetonitrile solution of the dimeric precursor $[Pd(\mu\text{-}Cl)(\eta^3\text{-allyl})]_2$ (Scheme 3.10).

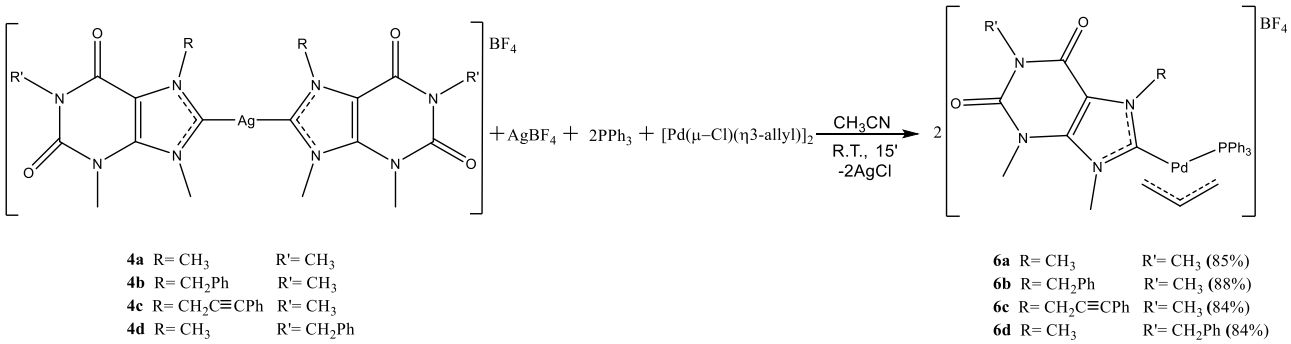

*Scheme 3.10 Synthesis of complexes **6a-d.***

The precipitation of AgCl, which is subsequently removed by filtration on millipore (or Celite), is a clear indication of the reaction progress. The products were isolated by precipitation induced by addition of diethylether to the concentrated solution. The reactions lead in all cases to the exclusive formation of the mixed NHC/PPh_3 derivatives, whereas the presence of the species with two carbene ligands (biscarbenes) and two phosphinic ligands was never observed. The selective formation of mixed derivatives will be discussed in detail in paragraph 4.6.4.

The mixed NHC/PPh_3 complexes **6a-d** were characterized by IR, NMR and elemental analysis.

The NMR spectra of the products **6a-d** confirm their nature and suggest some important structural characteristics:

1. Since the involved carbene ligands are not symmetric and their rotation around the Pd-C bond is prevented, the ensuing complexes are present in solution as a pair of atropoisomers according to the different position of the allyl fragment with respect to the carbene fragment (Fig. 3.20).

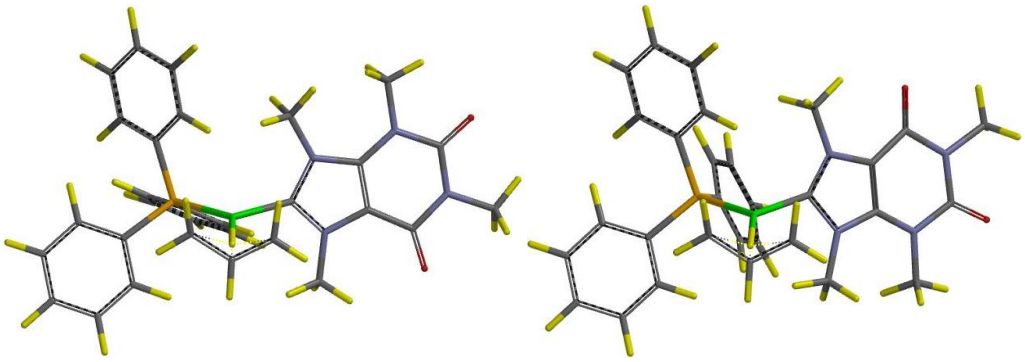

*Fig. 3.20 Representation of the two atropoisomers for the complex **6a** (DFT calculations).*

This fact is confirmed by the doubling of all signals in the ^{1}H-NMR, ^{31}P{^{1}H}-NMR and ^{13}C{^{1}H}-NMR spectra. As expected, the concentration of the two isomers is practically equal.

2. The presence of the coordinated phosphine is attested by the position of the ^{31}P{^{1}H}-NMR signals at about 25-26 ppm ($\Delta\delta \approx 30$ ppm compared to the free triphenylphosphine).

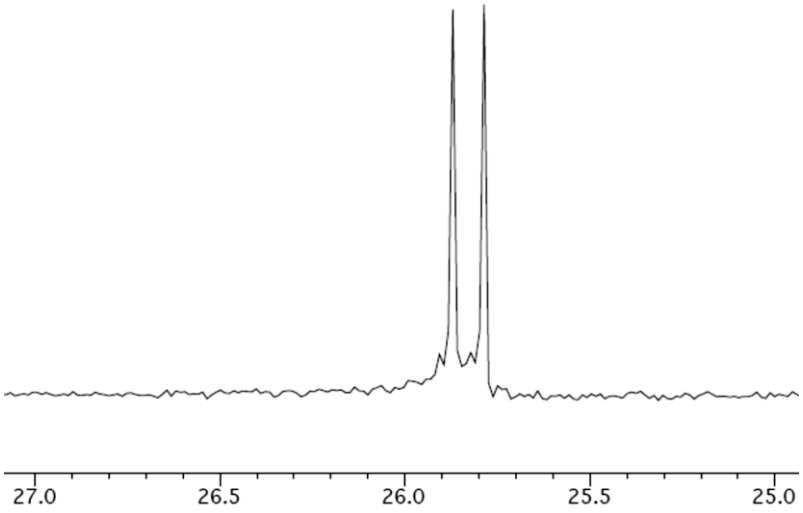

*Fig. 3.20 $^{31}P\{H^{1}\}$ NMR spectrum of complex **6a** in $CDCl_3$ at 298K.*

3. The five different signals for each isomer traceable back to the allyl protons are listed below and indicate the coordination of both phosphine and carbene with the consequent induced dissymmetry of the allyl fragment:
   a) H *anti*, *trans* to carbene; doublet with J = 13-14 Hz at 2.9-3.3 ppm.
   b) H *anti*, *trans* to PPh_3; multiplet between 2.4 and 3.8 ppm.
   c) H *syn*, *trans* to carbene; doublet with J = 6-8 Hz at 4.0-4.3 ppm.
   d) H *syn*, *trans* to PPh_3; multiplet or doublet of doublet ($J_{H-H} = J_{H-P}$ = 6-8 Hz) between 3.6 and 4.7 ppm.
   e) H *central*; multiplet between 5 and 6 ppm.

   Owing to the well differentiated resonances of the four terminal allyl protons, no fluxionality of the allyl systems (syn-syn/anti-anti, or η^3-η^1 isomerization) was detected by ^{1}H NMR experiment at RT.

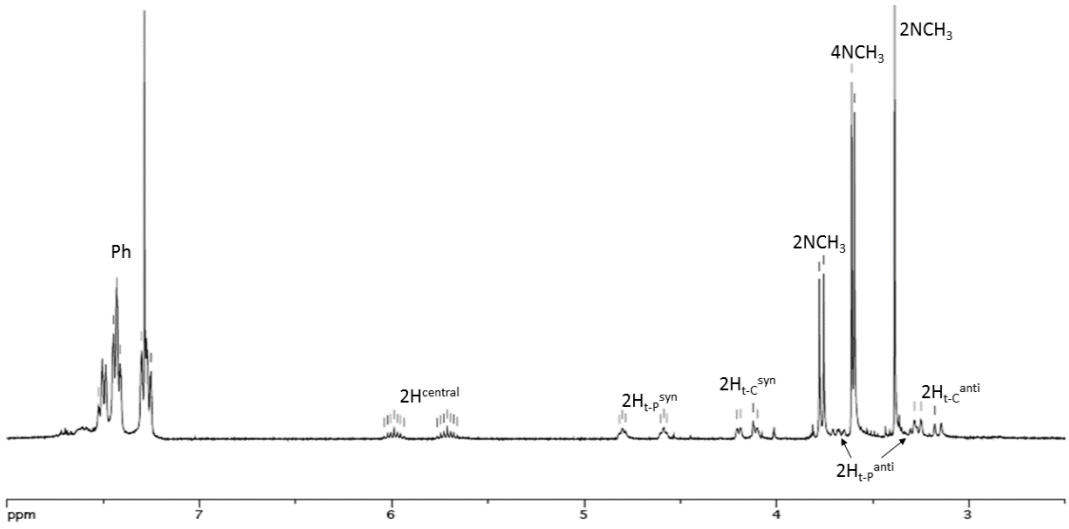

*Fig 3.21 ^{1}H NMR spectrum of complex **6a** in $CDCl_3$ at 298K.*

4. In the $^{13}C\{^{1}H\}$-NMR spectra, the chemical shifts of the two terminal allyl carbons are very close (at about 70 ppm), confirming that the *trans*-influence of carbene ligands and triphenylphosphine is comparable. Both carbons resonate as a doublet due to the coupling with phosphorus (J = 27-28 Hz for the carbon *trans* to phosphine and J = 1-2 Hz for that *trans* to carbene). The doublets (J_{C-P} = 18-20 Hz) related to the carbene carbons are detected between 186 and 188 ppm.

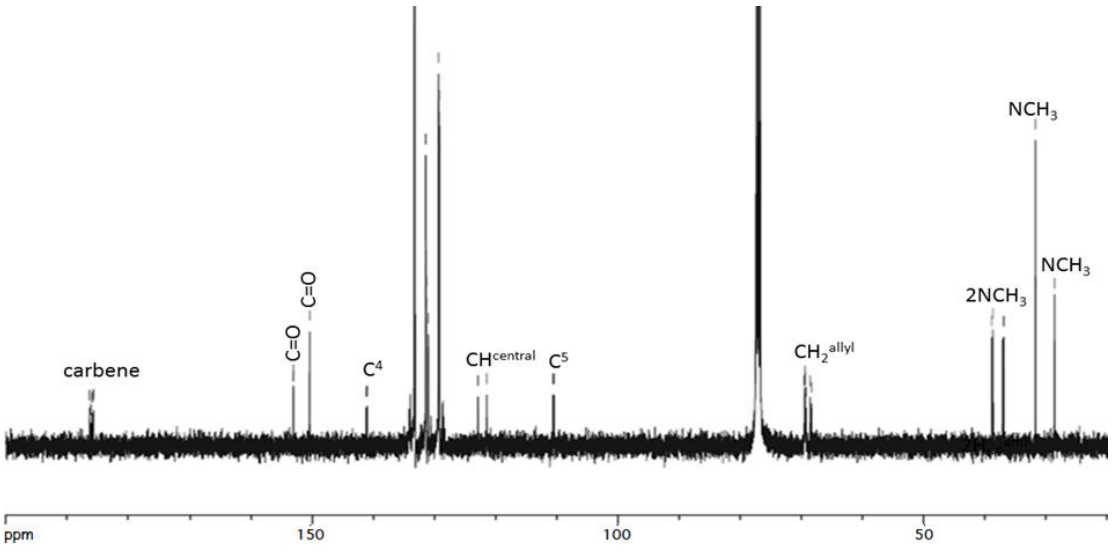

*Fig 3.22 $^{13}C\{H^{1}\}$ NMR spectrum of complex **6a** in $CDCl_3$ at 298K.*

5. The presence of the carbene ligand is also confirmed by the signals detected in both the ^{1}H-NMR and $^{13}C\{^{1}H\}$-NMR, traceable back to the NCH_3 present in the purine structure and, for compounds **6b-d**, by the resonances of the benzyl or phenylpropargyl groups. In the case of

the ^{1}H-NMR spectra of the complexes **6b** and **6d**, the $\underline{CH_2}$Ph protons are observed as an AB system (one for each isomer, J = 14-18 Hz) due to the diastereotopicity induced by the hindered rotation.

The IR spectra show the presence of the characteristic stretching of BF_4^- ($\tilde{\nu}_{B-F}$ = 1055 cm^{-1}) and signals related to the C=O groups ($\tilde{\nu}_{C=O}$ = 1660-1710 cm^{-1}). The solid state structure of complex **6a** was resolved by X-ray single crystal diffraction (Figure 3.23).

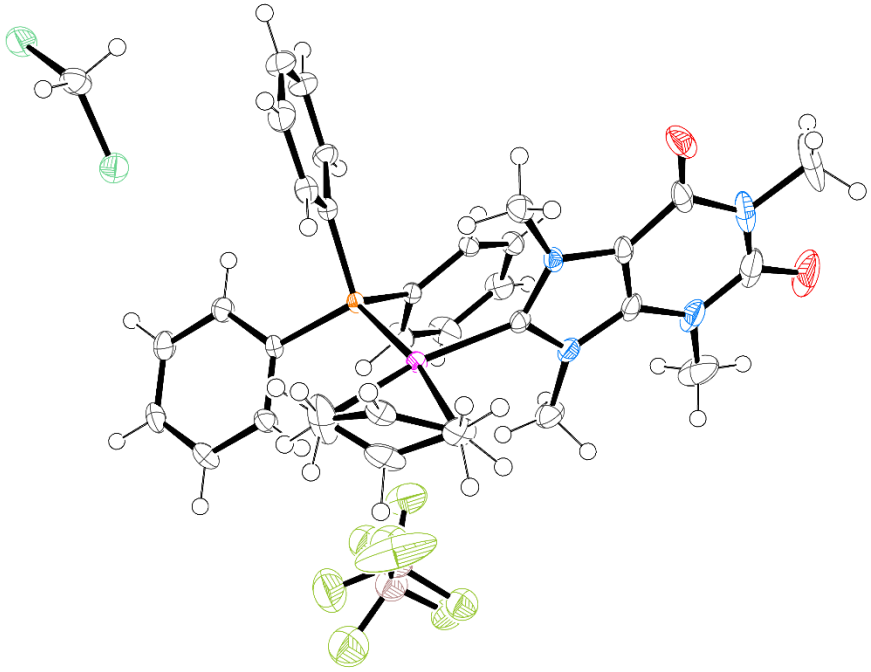

*Figure 3.23 Ellipsoid representation of **6a** crystal ASU contents (50% probability).*

3.5.2. Mixed NHC/TPPTS and NHC/PTA η^3-allyl complexes (7-8)

In order to evaluate whether water-soluble complexes might have comparable or different activity than that of the previously discussed species, it was decided to synthesize mixed complexes bearing the phosphines TPPTS and PTA. As a matter of fact, the water-soluble PTA ensures good solubility in both polar and less polar solvents to its derivatives and has been widely used for the synthesis of complexes with antitumor properties (See in paragraph 1.3.5 of the introductory part the characteristics of the ruthenium compounds RAPTA).

Therefore, we have synthesized the complexes **7** and **8** by reacting the precursor [Pd(μ-Cl)(η^3-allyl)]$_2$, the water-soluble phosphine (PTA or TPPTS) and the mixture of the silver precursors **4** and $AgBF_4$, in stoichiometric amount (Scheme 3.11).

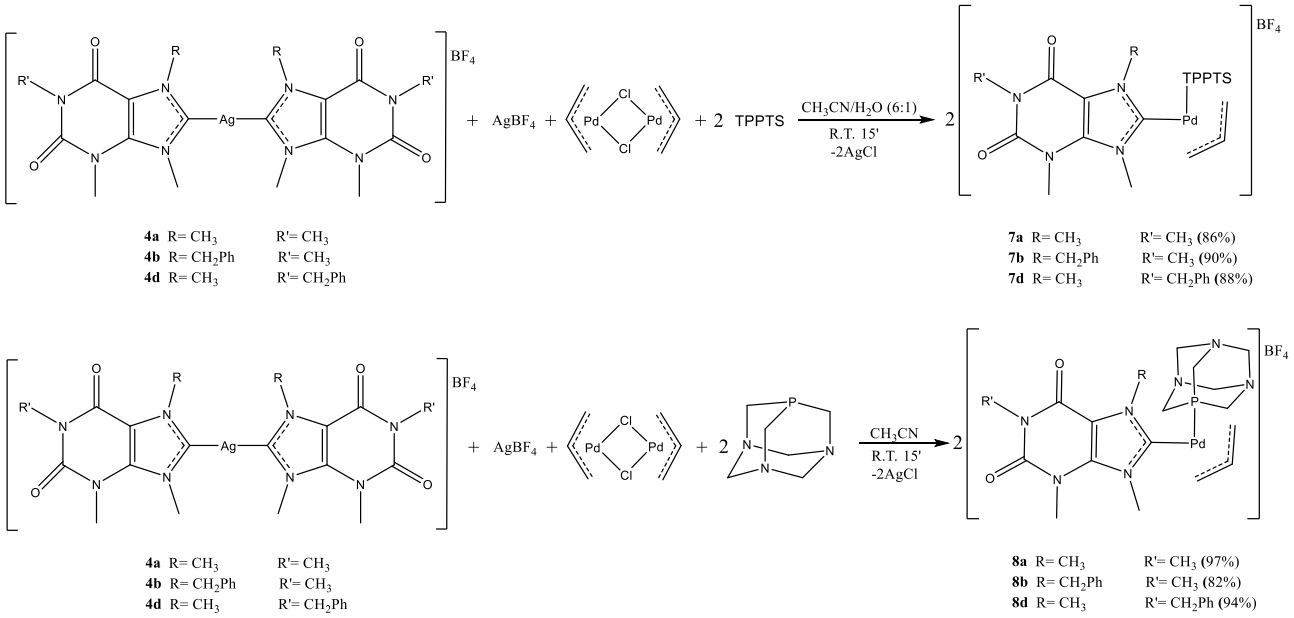

*Scheme 3.11 Synthesis of complexes **7** and **8.***

The reactions were carried out at room temperature for 15' in CH_3CN in the case of the PTA complexes **8** or in CH_3CN : H_2O (6 : 1 vv) for the TPPTS derivatives **7**. As usual, the almost instantaneous precipitation of AgCl testified the reaction progress.

From the NMR spectra it is possible to state that:

1. All the reported complexes (**7**-**8**) were present in solution as a pair of atropoisomers. This fact is confirmed by the two peaks (different or coincident) present in the $^{31}P\{^1H\}$-NMR spectra and by the doubling of all the signals in the ^1H-NMR and $^{13}C\{^1H\}$-NMR spectra.
2. The TPPTS coordination is confirm by the marked downfield shift of the signals in the $^{31}P\{^1H\}$-NMR (Fig. 3.24) compared to those of the uncoordinated TPPTS ($\Delta\delta \approx 34$ ppm).

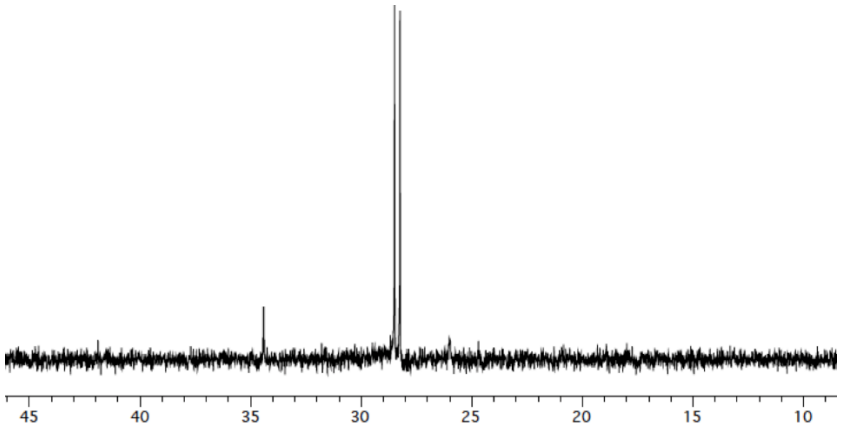

*Fig. 3.24 $^{31}P\{^1H\}$-NMR spectrum of **7a** ($T=298K$, D_2O).*

3. The five different signals of the allyl protons, present for each isomer, are listed below:
   a) H *anti*, *trans* to carbene; doublet with J = 13-14 Hz at 3-3.4 ppm.
   b) H *anti*, *trans* to TPPTS; multiplet at about 3.5 ppm.
   c) H *syn*, *trans* to carbene; doublet with J = 7-8 Hz at 4.3-4.5 ppm.
   d) H *syn*, *trans* to TPPTS; multiplet at about 4.6 ppm.
   e) H *central*, multiplet at 5.7-5.9 ppm.

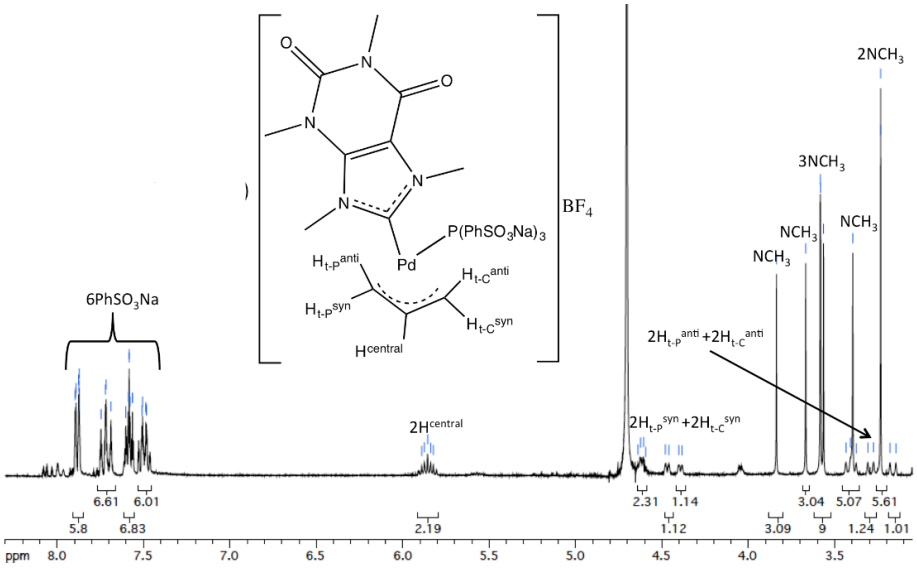

*Fig. 3.25 ^{1}H-NMR spectrum of **7a** (T=298K, D_2O).*

4. Owing to the comparable *trans*-influence of the carbene and TPPTS, in the $^{13}C\{^{1}H\}$-NMR spectra (Fig. 3.26) the two terminal ally carbons resonate at ca. 69 ppm. The signal of the carbon *trans* to the phosphine (present as doublet due to the phosphorus coupling) resonates to a slightly higher field ($\Delta\delta \approx 1$ ppm) than that *trans* to carbene.

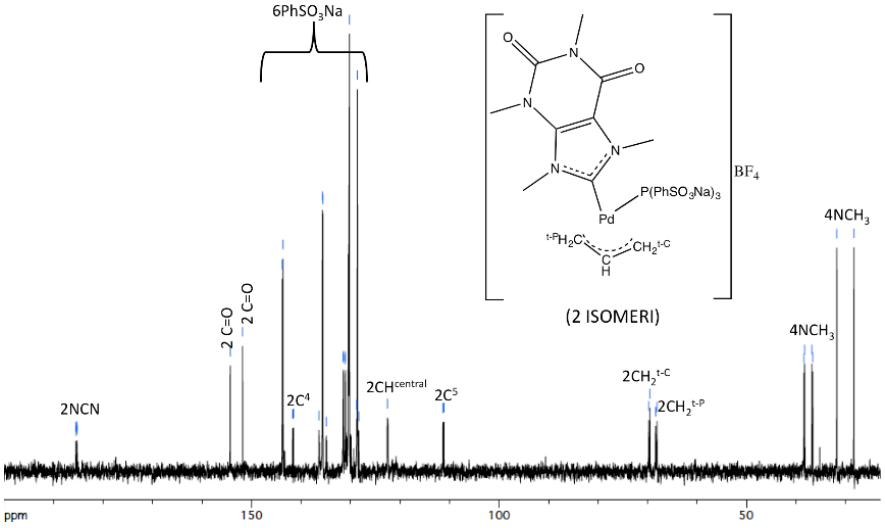

*Fig. 3.26 $^{13}C\{^{1}H\}$-NMR spectrum of **7a** (T=298K, D_2O).*

5. The signals of the carbene carbons are detected between 185 and 187 ppm as doublets owing to the J^2 coupling with the TPPTS phosphorus (J_{C-P} = 19-20 Hz).

6. The presence of the carbene ligand is also confirmed by high-field signals, in both the ^{1}H- and $^{13}C\{^1H\}$-NMR spectra, of the NCH_3 groups of the purine structure and, in the case of compounds **7b** and **7d**, by the resonance of the benzyl substituent ($-CH_2Ph$). In these last two cases, the $-\underline{CH_2}Ph$ protons are observed in ^{1}H-NMR spectra as AB system (one for each isomer) due to the diastereotopicity induced by the hindered rotation (Fig. 3.27).

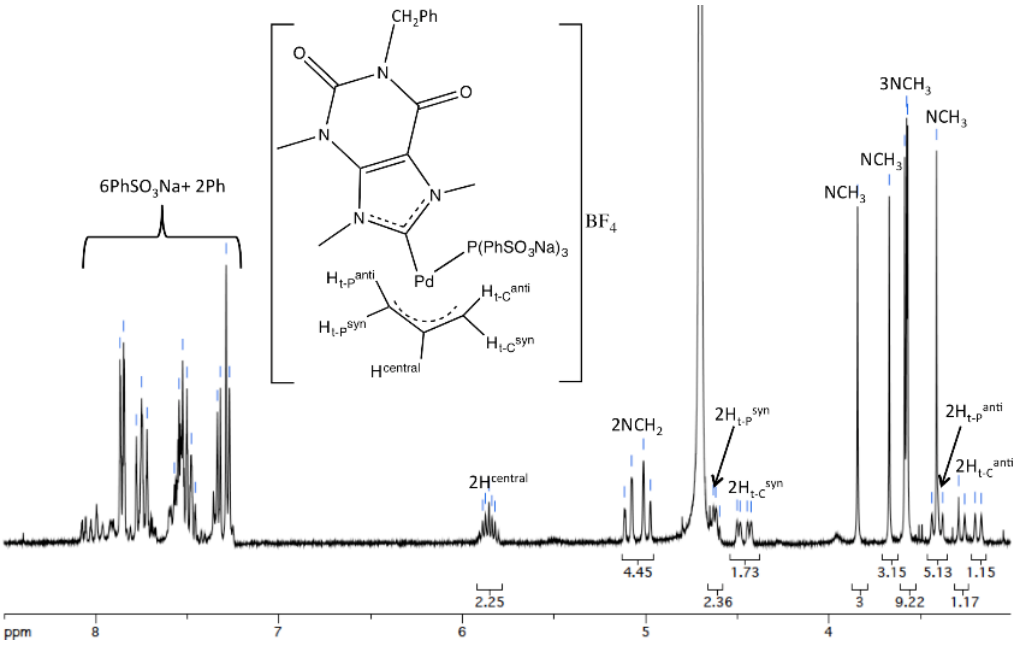

*Fig. 3.27 ^{1}H-NMR spectrum of **7d** (T=298K, D_2O).*

As for the mixed NHC/PTA complexes, it is possible to observe for each atropoisomer that:

1. the presence of the coordinated PTA is indicated by the position of the signals in the $^{31}P\{^1H\}$-NMR spectra at fields significantly lower than those of the free ligand ($\Delta\delta \approx 45$ ppm).

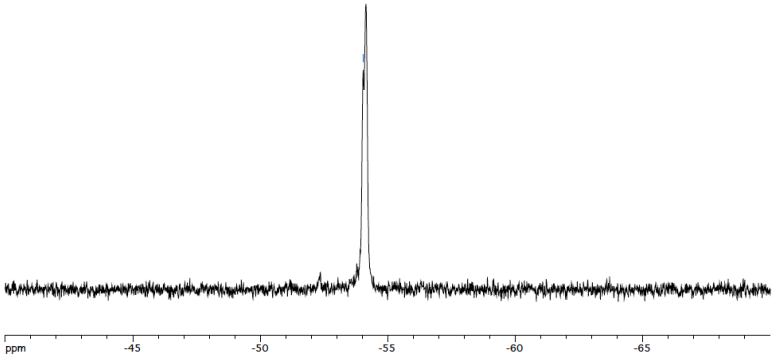

*Fig. 3.28 $^{31}P\{^1H\}$-NMR spectrum of **8b** (T=298K, D_2O).*

In the ^{1}H-NMR spectra, the NCH_2P protons are present as two singlets (one for each isomer) practically coincident at about 4.2 ppm whereas the NCH_2N protons are detected as a multiplet at about 4.5 ppm.

In the $^{13}C\{^{1}H\}$-NMR spectra, the NCH_2N systems are found as singlets at about 70-71 ppm and the NCH_2Ps as doublets (with J = 13-14 Hz) at about 50-51 ppm.

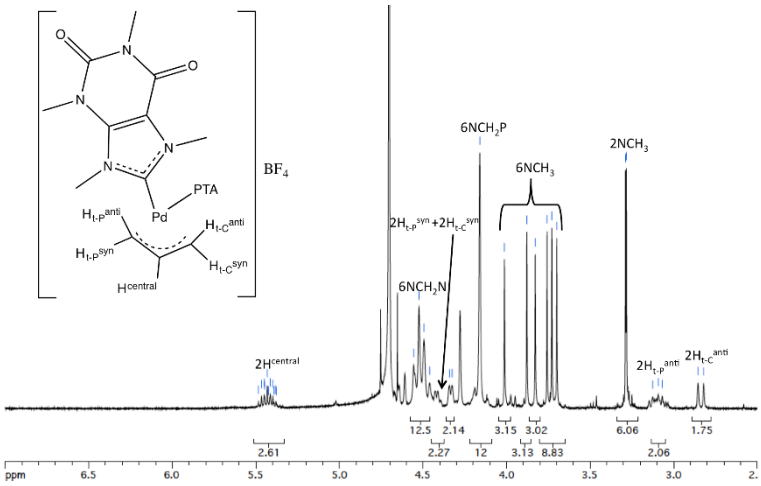

*Fig. 3.29 ^{1}H-NMR spectrum of **8a** (T=298K, D_2O).*

2. The coordination of the allyl fragment is confirmed by the presence in the ^{1}H-NMR spectra of five different signals:
   a) H *anti*, *trans* to carbene; doublet with J = 13-14 Hz at about 2.7 ppm.
   b) H *anti*, *trans* to the PTA; a multiplet at about 3 ppm.
   c) H *syn*, *trans* to carbene; a doublet with J = 6-7 Hz at about 2.7 ppm.
   d) H *syn*, *trans* to the PTA; multiplet at about 4.4 ppm.
   e) *H central*, multiplet at about 5.4 ppm.

3. In the $^{13}C\{^{1}H\}$-NMR spectra the two terminal allyls carbons resonate at quite different chemical shifts (at about 63 ppm for that *trans* to carbene and at 69 ppm for that *trans* to PTA).

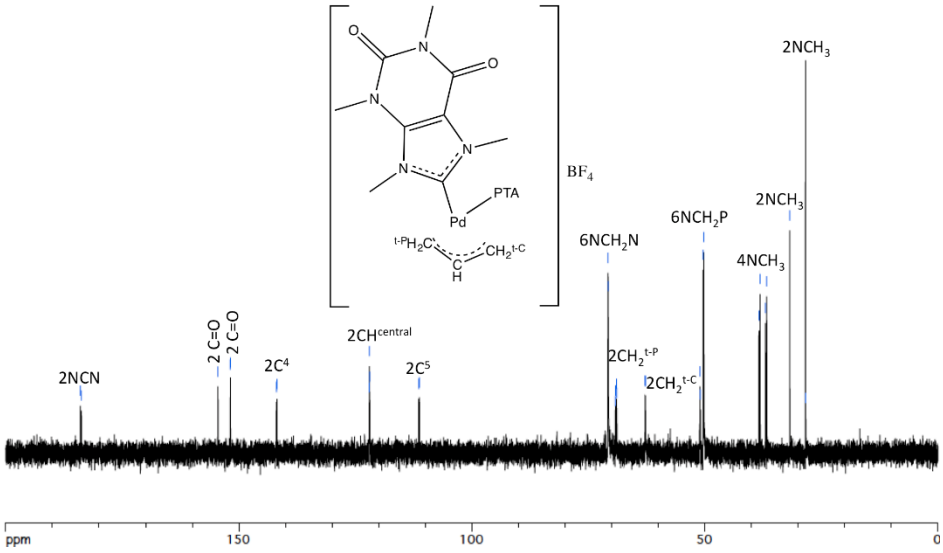

*Fig. 3.30 $^{13}C\{^1H\}$-NMR spectrum of **8a** (T=298K, D_2O).*

Owing to the coupling with the PTA phosphorus, the signals ascribable to carbene carbons are observed between 184 and 186 ppm as doublets (J_{C-P} = 19-20 Hz).

3.5.3. Mixed NHC/DIC η^3-allyl complexes (9)

After the synthesis of the mixed NHC/phosphine complexes **6**, **7** and **8**, we taken in account the possibility of isolate novel mixed NHC/isocyanide complexes. Due to their π-acid character, isocyanides impart to their complexes remarkable differences with respect to that observed in alkyl or aryl phosphines derivatives. In our case the best synthetic results were obtained with the 2,6-dimethylphenyl isocyanide (DIC). The NHC/DIC complexes were synthesized according to the following Scheme 3.12.

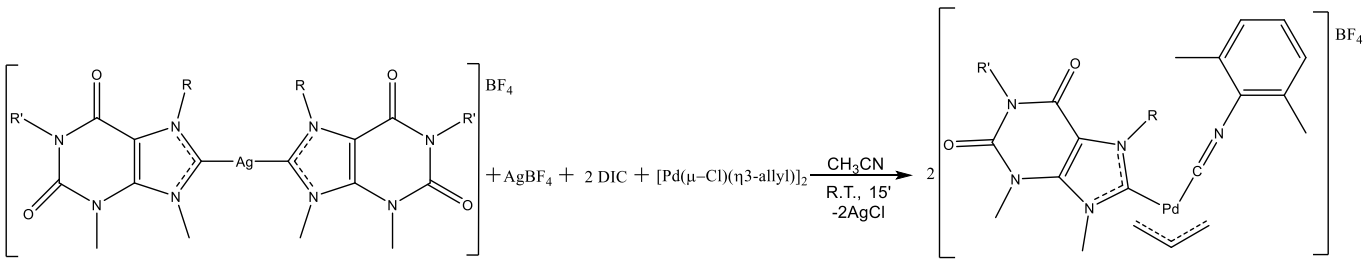

4a R= CH_3 R'= CH_3
4b R= CH_2Ph R'= CH_3
4d R= CH_3 R'= CH_2Ph

6a R= CH_3 R'= CH_3 (88%)
6b R= CH_2Ph R'= CH_3 (88%)
6d R= CH_3 R'= CH_2Ph (92%)

*Scheme 3.12 Synthesis of complexes **9a-d.***

From the NMR spectra of the final products **9** it is possible to infer some important structural features:

1. At variance with the NHC/phosphine complexes described so far, the presence of atropoisomeric species is not observed at 298 K.

2. The presence of the coordinated isocyanide is deduced from the downfield shift of the signals related to the methyl substituents (at about 2.3 ppm).

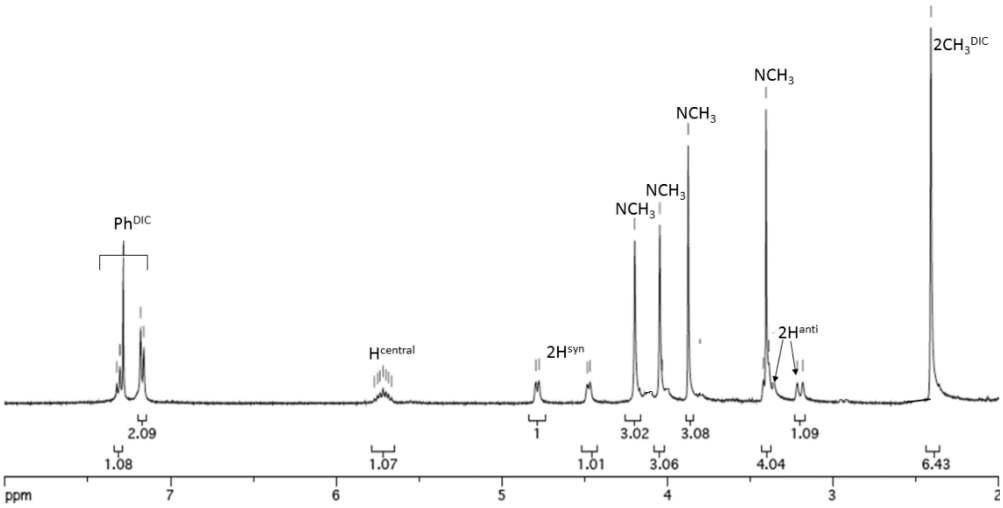

*Fig. 3.31 ^{1}H-NMR spectrum of **9a** in $CDCl_3$ at 298K.*

In the $^{13}C\{^{1}H\}$-NMR spectra the DIC methyl groups are observed as singlets at ca. 19 ppm and the CN carbon as a broad signal at ca. 151 ppm.

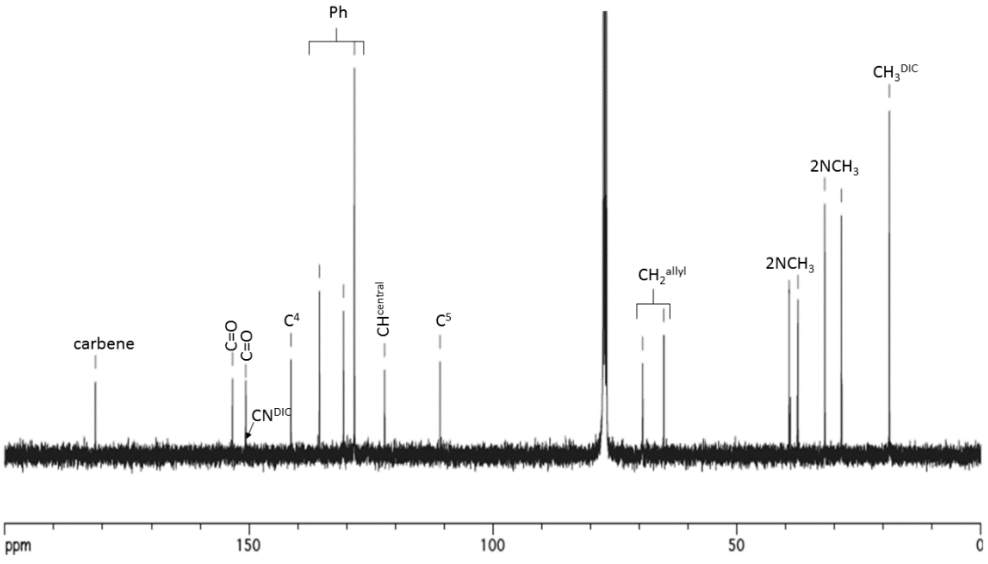

*Fig. 3.32 $^{13}C\{^{1}H\}$-NMR spectrum of **9a** in $CDCl_3$ at 298K.*

3. The coordination of the allyl fragment is confirmed by the presence in the ^{1}H-NMR spectra of complexes **9** of five different signals:
   a) H *anti*, *trans* to carbene; doublet with J = 13.5 Hz between 3.2 and 3.5 ppm.
   b) H *anti*, *trans* to isocyanide; doublet with J = 12.5 Hz between 3.4 and 3.5 ppm.
   c) H *syn*, *trans* to carbene; doublet with J = 6-7 Hz between 4.2 and 4.5 ppm.
   d) H *syn*, *trans* to isocyanide; doublet with J = c.a. 7.5 Hz between 4.6 and 4.8 ppm.
   e) H *central*; multiplet at about 5.7 ppm.

4. In the ^{13}C{^{1}H}-NMR spectra the two terminal allyl carbons are observed within 65 and 69 ppm, whereas the chemical shift of the central carbon resonates at ca. 122 ppm.

5. The signal ascribable to the carbene carbon is detected as a singlet within 181 and 183 ppm.

The IR spectra show the ν_{CN} stretching of the coordinated isocyanide at about 2175 cm^{-1}, the BF_4^- peak ($\nu_{B\text{-}F}$ = ca. 1055 cm^{-1}) and those of the carbonyl groups ($\nu_{C=O}$ = 1660-1710 cm^{-1}).

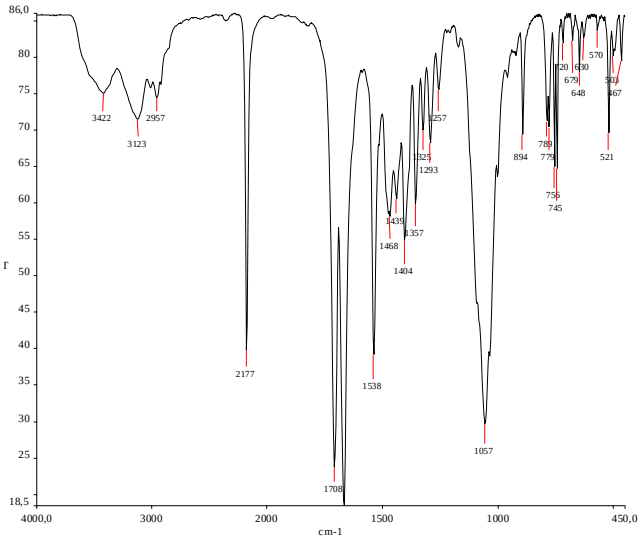

*Fig. 3.33 IR spectrum of complex **9a** in KBr.*

3.5.4. Bis(NHC) η^3-allyl complexes

The Pd(II) η^3-allyl complexes bearing two purine-based NHCs as spectator ligands were synthesized by reacting the stoichiometric mixture of the silver precursors **4** and $AgBF_4$ with the palladium allyl dimer, in the presence of KI. The addition of potassium iodide is necessary to remove all the silver from the reaction mixture (Scheme 3.13).

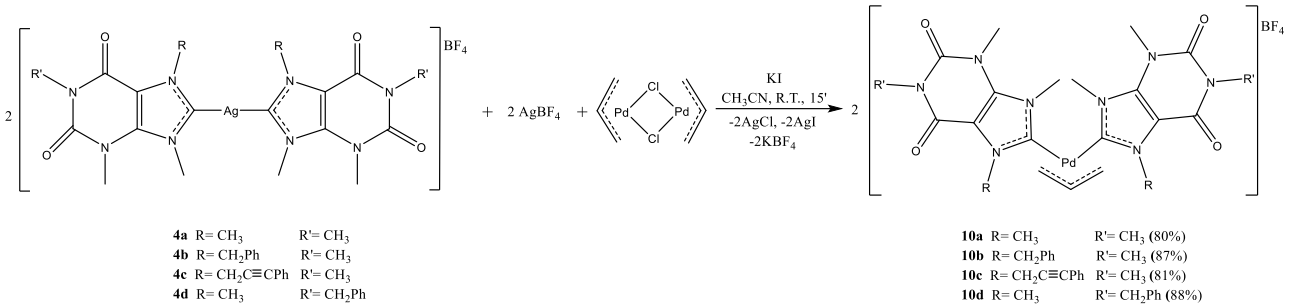

*Scheme 3.13 Synthesis of complexes **10a-d.***

The **10a-d** biscarbene complexes were characterized by IR, NMR and elemental analysis.

The most significant conclusion that can be immediately noticed by NMR spectra of complexes **10** is the presence, of an only set of signals. This observation suggests that there is free rotation of the two *N*-Heterocyclic Carbene ligands about the Pd-C bond.

The ^{1}H-NMR spectra show three different signals for the allyl protons indicating the coordination of two equal carbene ligands. In particular:

a) H *anti*; doublet with J = 13-14 Hz at about 3 ppm.
b) H *syn*; doublet with J = 7-8 Hz at 4 ppm.
c) H *central*; as multiplet between 5.5 and 6 ppm.

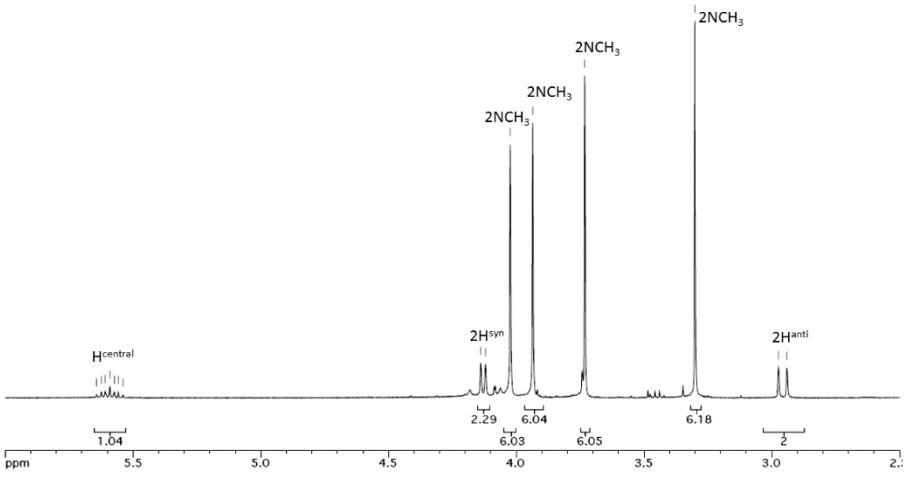

*Fig. 3.34 ^{1}H NMR spectrum of complex **10a** in CD_3CN at 298K.*

In the $^{13}C\{^{1}H\}$-NMR spectra, the two terminal allyl carbons resonate between 60 and 65 ppm, unlike the central allyl carbon which resonates at 120-122 ppm. The signal of carbene carbons are detected at ca. 185 ppm.

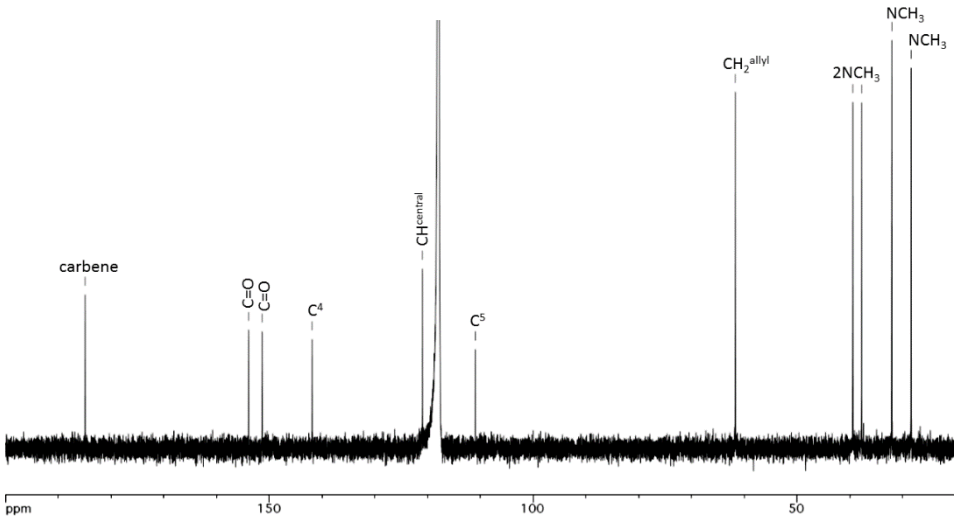

*Fig. 3.35 $^{13}C\{H^{1}\}$ NMR spectra of complex **10a** in CD_3CN at 298K.*

In the case of the complex **10d** it was possible to resolve its solid state structure by X-ray single crystal diffraction (Figure 3.36).

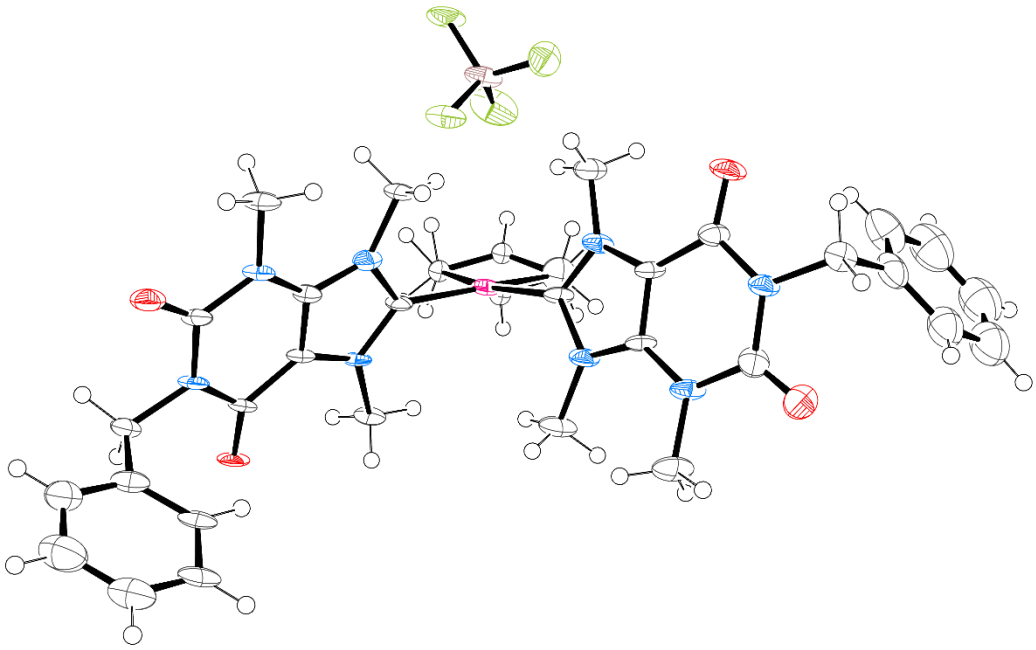

*Fig. 3.36 Ellipsoid representation of **10d** crystal ASU contents (50% probability).*

3.6. Palladacyclopentadienyl complexes bearing purine-based NHCs

$[PdC_4(COOCH_3)_4]_n$ was used for the synthesis of the palladacyclopentadienyl complexes. This precursor can be obtained by oxidative coupling of $Pd_2(DBA)_3 \cdot CHCl_3$ with dimethylacetylene dicarboxylate (DMA) (Scheme 3.14).

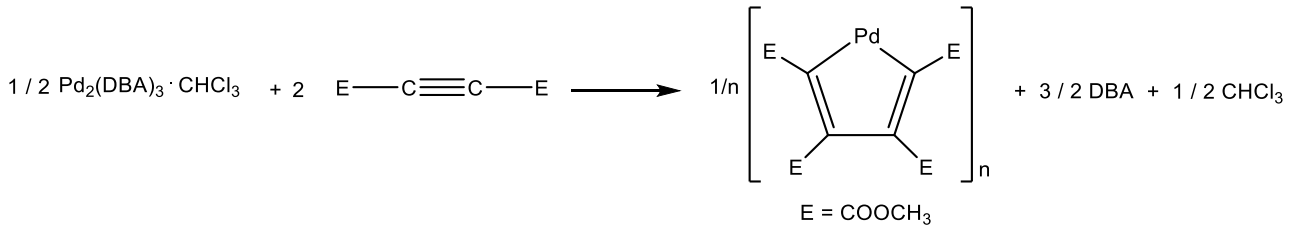

Scheme 3.14 Synthesis of the polymeric precursor $[PdC_4(COOCH_3)_4]_n$

This polymer is an ideal precursor for the synthesis of our complexes since the presence of oxygen-labile bridges allows an easy introduction of two monodentate spectator ligands or a bidentate one.

3.6.1. Mixed NHC/PPh_3 palladacyclopentadienyl complexes

The palladacyclopentadienyl complexes containing a purine-based NHC and a triphenylphosphine (compounds **11a-b** and **11d**) were synthesized in good yields. The synthesis of these compounds was carried out by adding to a CH_2Cl_2 solution of the $[PdC_4(COOCH_3)_4]_n$ precursor, a mixture of the silver carbene complex (**5a-b** or **5d**) and triphenylphosphine. The process is relatively fast and takes about an hour to be complete (Scheme 3.15).

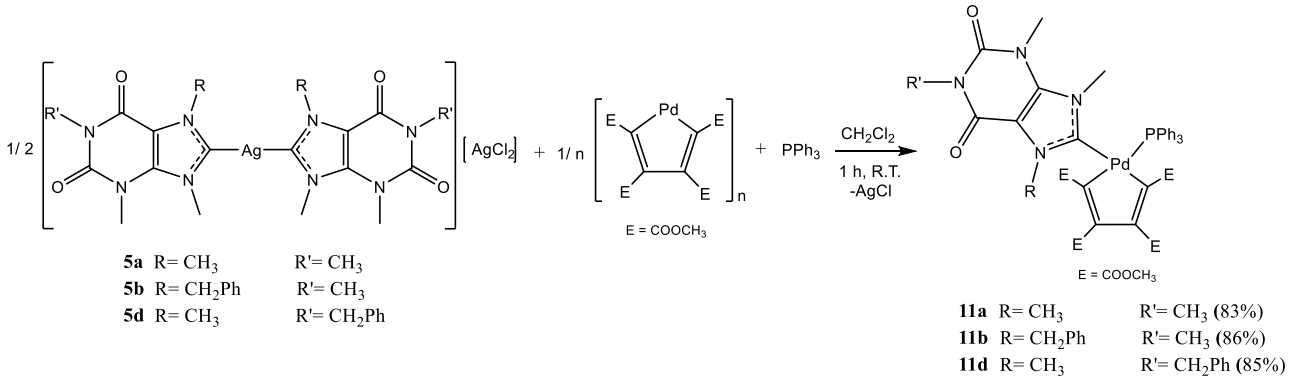

*Scheme 3.15 Synthesis of the mixed NHC/PPh_3 complexes **11a-b** and **11d.***

The final products were isolated, after separation of AgCl by filtration on millipore membrane and reduction of the solvent to small volume, by precipitation with diethylether.

Complexes **11a-b** and **11d** were characterized by NMR and IR spectroscopy. The formation of a single species is inferred from the presence of a single peak at about 25-26 ppm in the $^{31}P\{^{1}H\}$-NMR spectra ($\Delta\delta \approx 30$ ppm compared to the uncoordinated PPh_3).

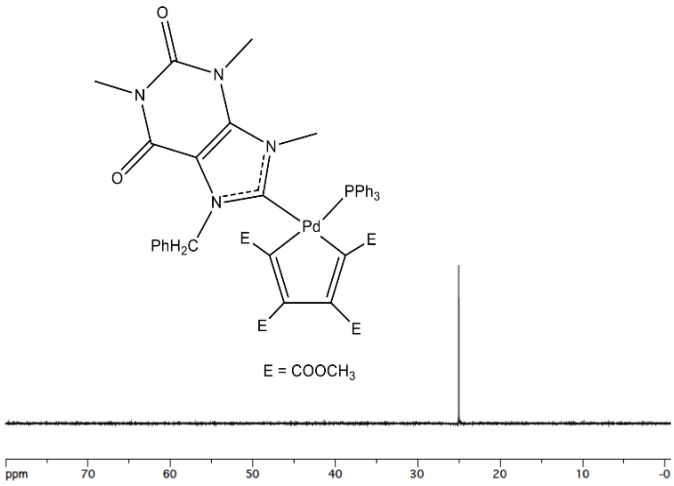

*Fig. 3.37 $^{31}P\{^{1}H\}$-NMR spectrum of the complex **11b** (T = 298K, $CDCl_3$).*

The nature of the obtained products was deduced on the basis of the ^{1}H- and $^{13}C\{^{1}H\}$-NMR spectra. In fact, owing to the presence of two different spectator ligands, four signals corresponding to the four magnetically non-equivalent ester groups ($COOCH_3$) are observed. As for the carbene ligand, in addition to the signals of the NCH_3 groups, for the compounds **11b** and **11d** it is possible to observe the signals due to two methylene protons NCH_2 resonating as an AB system. In this case the magnetic non-equivalence is again due to the prevented rotation of the carbene ligand about the Pd-C bond (Fig. 3.38).

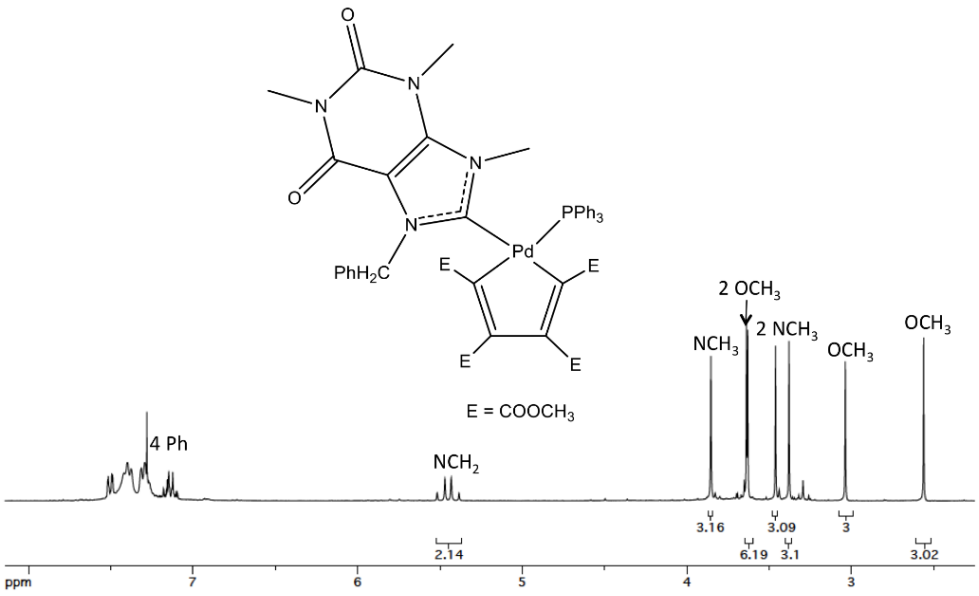

*Fig. 3.38 ^{1}H-NMR spectrum of the complex **11b** (T = 298K, $CDCl_3$).*

In the $^{13}C\{^1H\}$-NMR spectra (Fig. 3.39), the most important signal, for all the synthesized compounds, is detected at about 190 ppm and is ascribable to the doublet ($J_{C\text{-}P} \approx 16$ Hz) due to the coupling with the phosphorus of triphenylphosphine of the carbenic carbon.

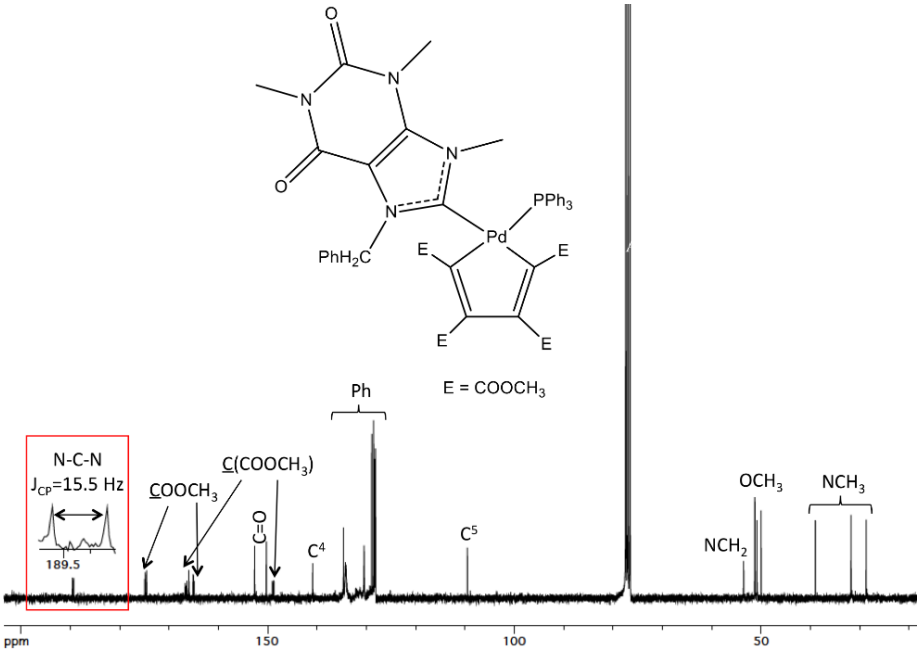

*Fig. 3.39 $^{13}C\{^1H\}$-NMR spectrum of the complex **11b** ($T = 298K$, $CDCl_3$).*

As a further and definitive confirmation of the conclusions obtained by IR and NMR techniques, we report, for complex **11b**, the solid state structure obtained by X-ray diffraction (Fig. 3.40).

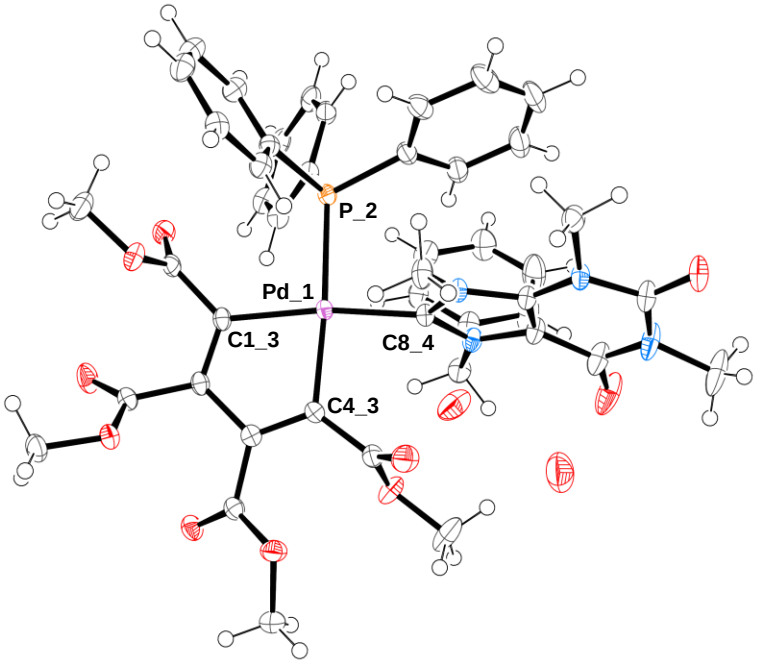

*Fig. 3.40 Ellipsoid representation of **11b** crystal ASU contents (50% probability).*

3.6.2. Mixed NHC/PTA palladacyclopentadienyl complexes

The synthesis of the mixed NHC/PTA palladacyclopentadienyl complexes was carried out similarly to that previously described, in agreement with the scheme proposed below (Scheme 3.16).

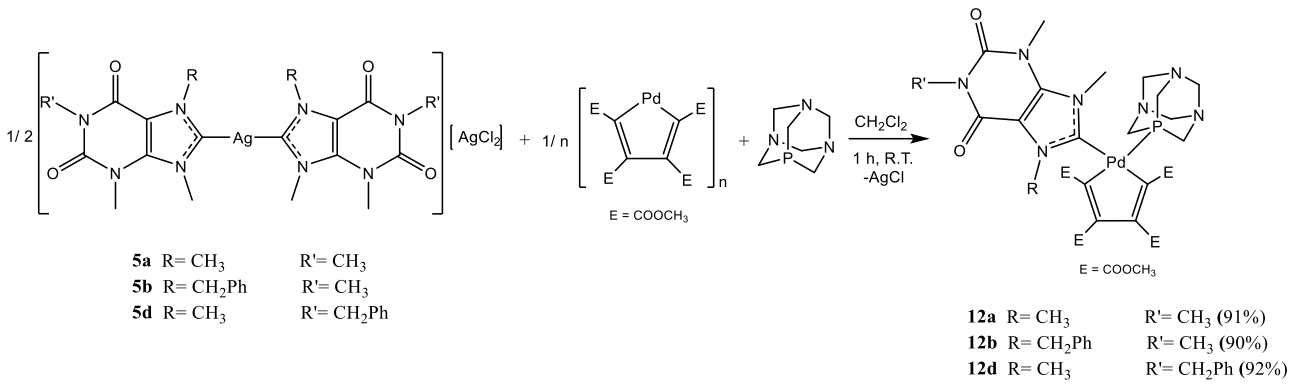

*Scheme 3.16 Synthesis of the mixed NHC/PTA complexes **12a-b** and **12d.***

The exclusive obtainment of the mixed derivatives is unequivocally confirmed by the ^{1}H-NMR spectra (Figs 3.41 and 3.42), in which the signals related to the NCH_3 (singlets) and NCH_2 (AB systems within 5.3-6.2 ppm) groups of the carbene ligand, the four different ester groups of the palladacycle, the methylene protons of the coordinated PTA (NCH_2N; AB system within 4.3-4.5 ppm and NCH_2P; doublet, $J_{H-P} \approx 2$ Hz, within 3.5 and 4 ppm) can be observed.

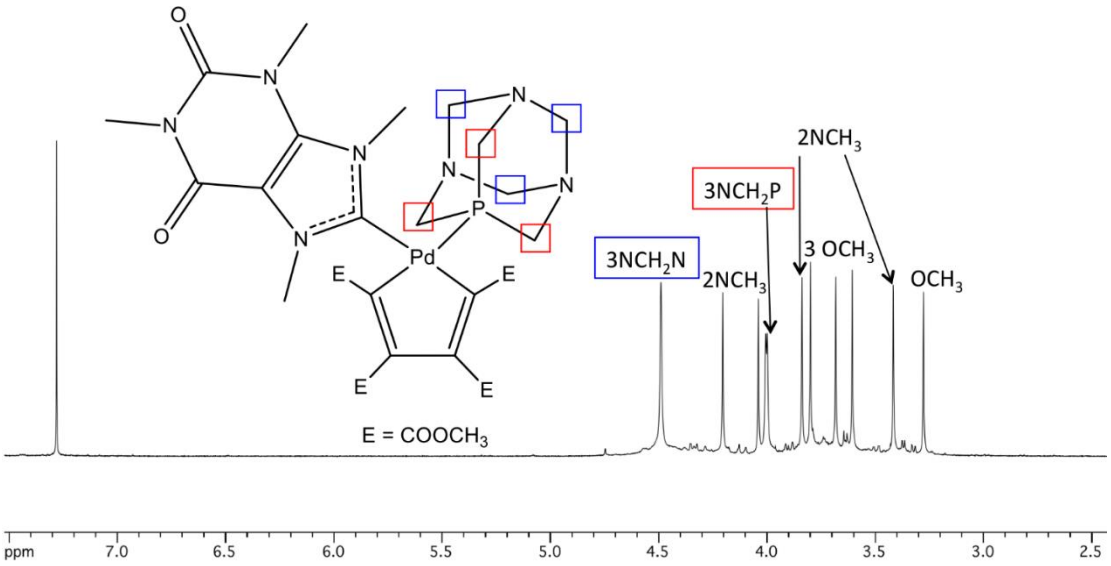

*Fig. 3.41 ^{1}H-NMR spectrum of the complex **12a.***

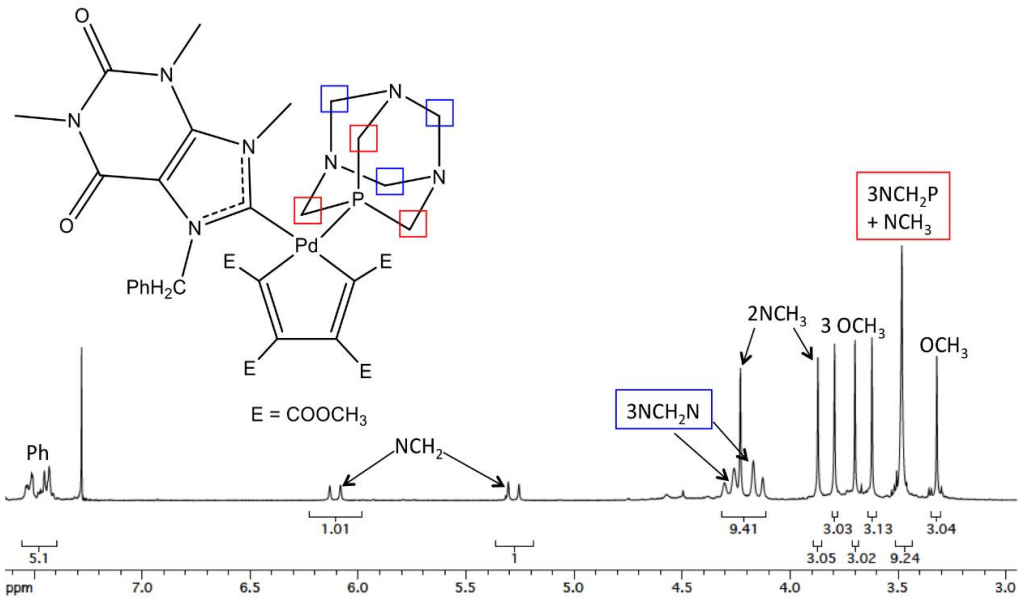

*Fig. 3.42 ^{1}H-NMR spectrum of the complex **12b** (T = 298K, $CDCl_3$).*

In the $^{13}C\{^{1}H\}$-NMR spectra (Fig. 3.43) it is possible to observe at 180-190 ppm the signal of the carbene carbon which resonates as a doublet ($J_{C\text{-}P} \approx 17\text{-}18$ Hz). As for the coordinated PTA, the peaks of the NCH_2P and NCH_2N methylene carbons at about 50 ppm (doublet with $J_{C\text{-}P} \approx 10$ Hz) and 73 ppm (doublet with $J_{C\text{-}P} \approx 6$ Hz) can be detected.

These signals, together with all the others related to the spectator ligands and to the cyclometallated fragment, have been attributed on the basis of the interpretation of the bidimensional HSQC and HMBC spectra.

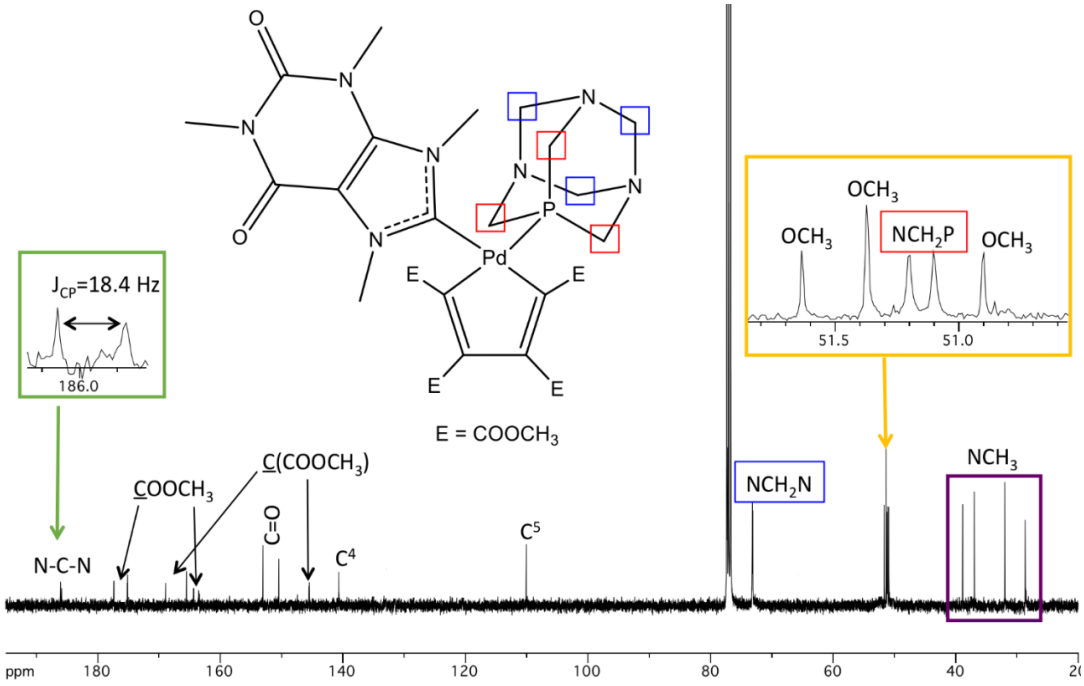

*Fig. 3.43 $^{13}C\{^{1}H\}$-NMR spectrum of the complex **12a** (T = 298K, $CDCl_3$).*

Finally, the $^{31}P\{^{1}H\}$-NMR spectra show the presence of a single peak. Its position at chemical shift higher than that of the free ligand ($\Delta\delta \approx 45$ ppm), confirms the coordination of the PTA.

3.6.3. Mixed NHC/DIC, palladacyclopentadienyl complexes

The success of the reactions with PTA and triphenylphosphine prompted us to use the same synthetic approach to obtain cyclometallated complexes with a purine-based NHC and an isocyanide (i.e. DIC) as spectator ligands. The synthesis of this class of compounds requires much longer times than that necessary in the case of mixed NHC/phosphines complexes. As a matter of fact, the addition of the DIC isocyanide and the silver carbene complex to the solution of the palladacyclic precursor, yields in few minutes a mixture containing the mixed product and the two bis-DIC and bis-NHC palladacyclopentadienyl species. However, in around 48 hours at room temperature it is possible to observe the progressive transformation of the two bis-DIC and bis-NHC palladacyclopentadienyl species into the mixed derivative.

Therefore, it was possible to synthesize with good yields the compounds **13a-b** and **13d**, adopting the conditions shown in Scheme 3.17.

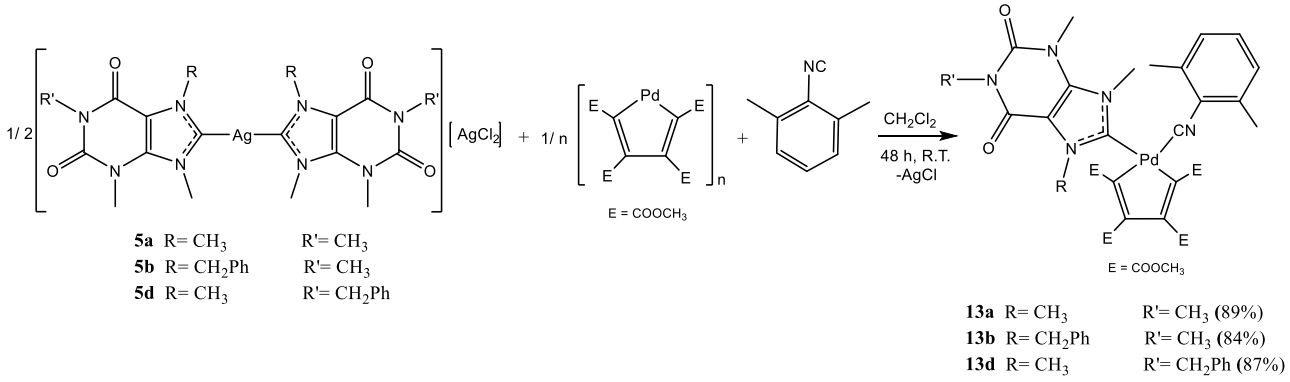

*Scheme 3.17 Synthesis of the mixed NHC/DIC complexes **13a-b** and **13d.***

In the ^{1}H-NMR spectra (Fig. 3.44), the signals of the two different spectator ligands (isocyanide and carbene) can be easily identified. The presence of the palladacyclic fragment is evidenced by the four different peaks that can be assigned to the OCH_3 groups together to the singlet observed between 2 and 2.5 ppm, which is attributable to the two methyl groups of the coordinated isocyanide.

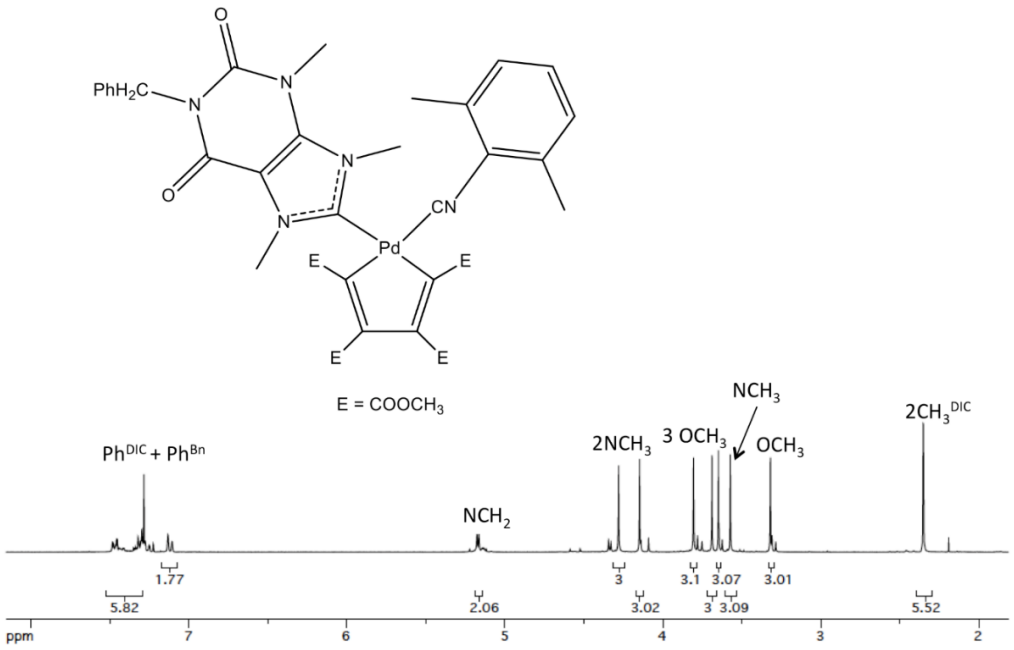

*Fig. 3.44 ^{1}H-NMR spectrum of the complex **13d** (T = 298K, $CDCl_3$).*

In the $^{13}C\{^{1}H\}$-NMR spectra (Fig. 3.45), the weak signals ascribable to the CN group (149 ppm) and the coordinated carbenic carbon (180-190 ppm) are also identified.

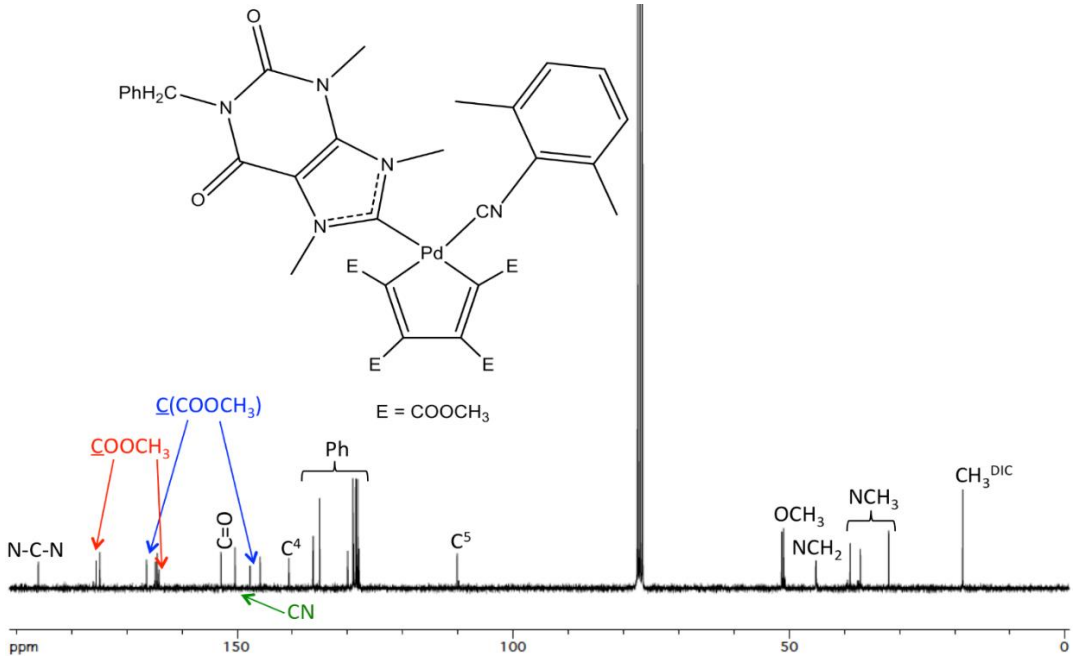

*Fig. 3.45 $^{13}C\{^{1}H\}$-NMR spectrum of the complex **13d** (T = 298K, $CDCl_3$).*

Finally, in the IR spectra (Fig. 3.46) a medium intensity and the strong bands at 2175-2180 cm^{-1} and between 1670 and 1710 cm^{-1} have been assigned to the ν_{CN} of the coordinated isocyanide and to the ν_{CO}, respectively.

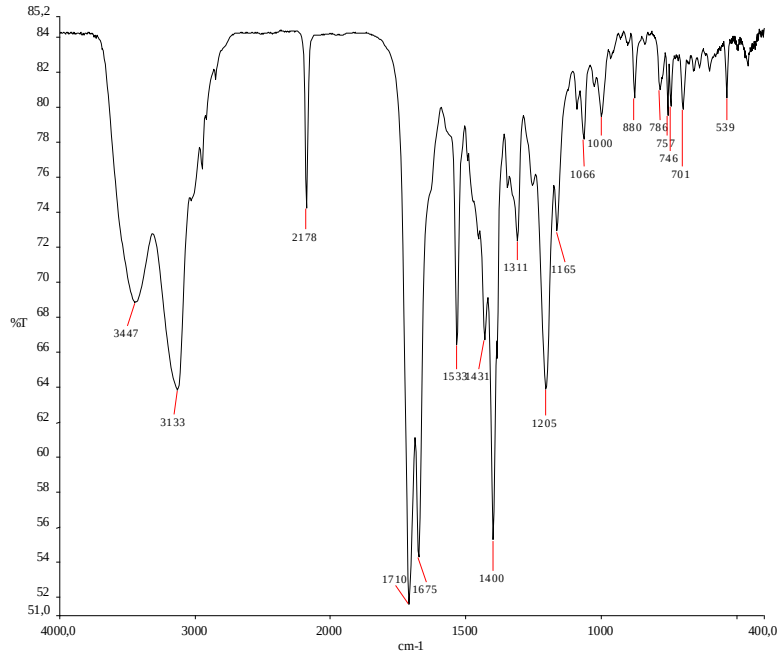

*Fig. 3.46 IR spectrum (in KBr) of the complex **13d.***

3.6.4. Bis(NHC) palladacyclopentadienyl complexes

The synthesis of the palladacyclopentadienyl complexes with two purine-based NHC ligands was successfully performed according to the following scheme (Scheme 3.18).

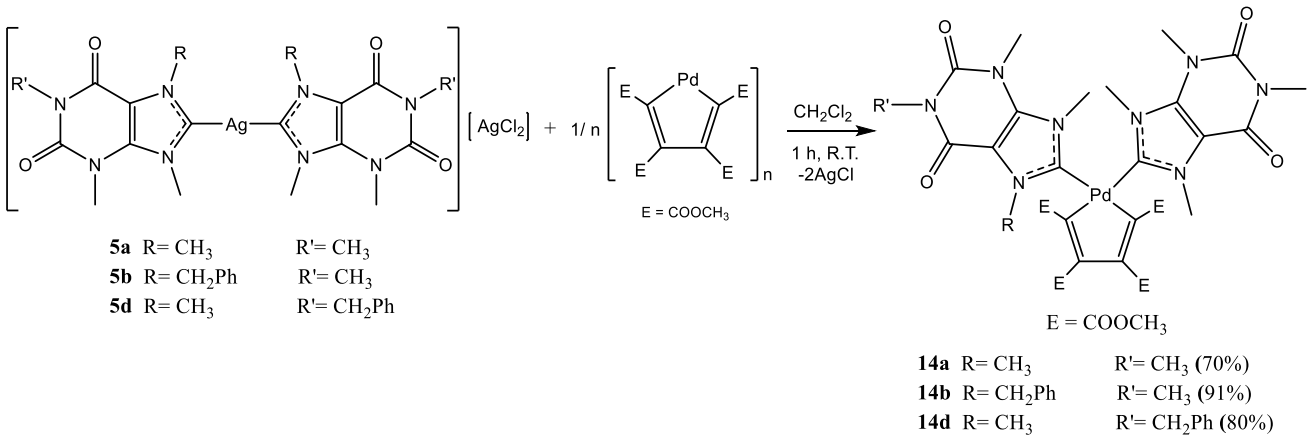

*Scheme 3.18 Synthesis of the bisNHCs palladacyclopentadienyl complexes **14a-b** and **14d.***

All recorded spectra show the presence of two atropoisomeric species due to the asymmetry of the carbene ligand and the hindered rotation about the Pd-C bond (Fig. 3.47).

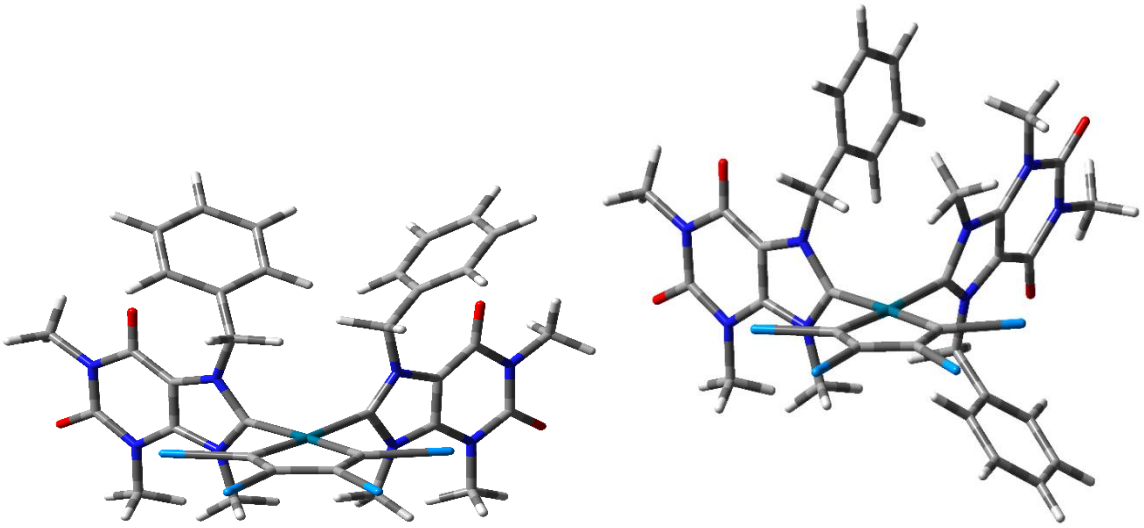

*Fig. 3.47 Representation of the two atropoisomers related to the complex **14b**, obtained by DFT calculations (with E = CN instead of $COOCH_3$).*

As can be seen in Figure 3.47, in the case of compound **14b** the nature of the atropoisomers is determined by the mutual position of the two benzyl substituents with respect to the main coordination plane. The ^{1}H-NMR spectra of the atropoisomers (Figs. 3.48 and 3.49) are characterized by:

- The presence of the signals relating to the NCH_3 groups of the purine base resonating at different chemical shifts with respect to those of the starting silver complex.
- The presence of two signals ascribable to the two distinct pairs of OCH_3 groups.
- The presence, in the case of compounds **14b** and **14d** (Fig. 3.49), of an AB system related to the methylene protons of the benzyl groups, at about 5-6 ppm.

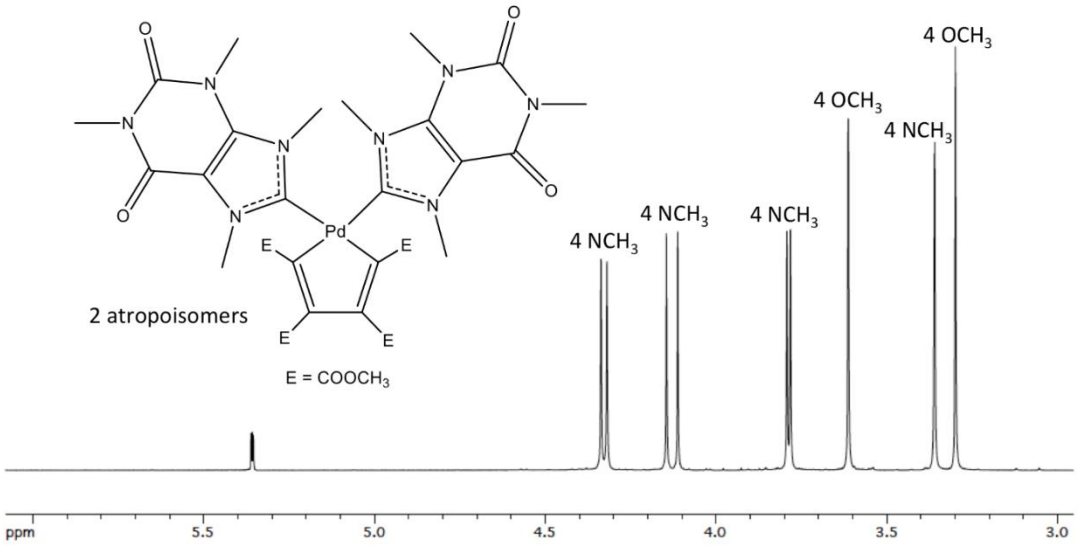

*Fig. 3.48 ^{1}H-NMR spectrum of the complex **14a** (T = 298K, CD_2Cl_2).*

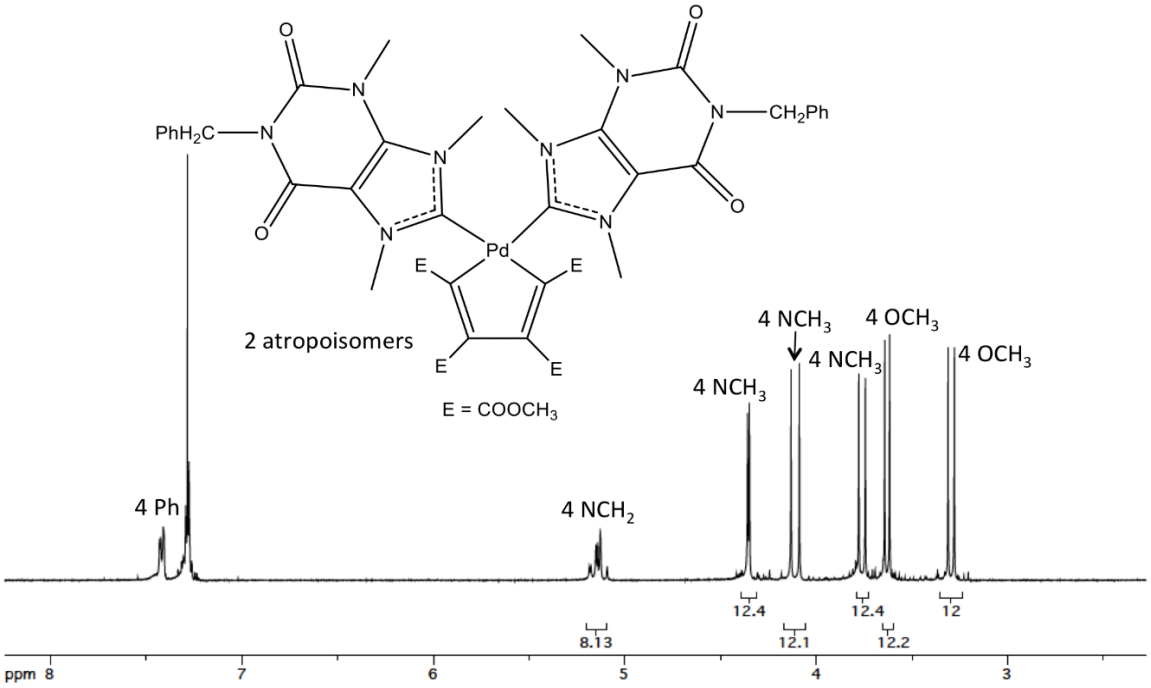

*Fig. 3.49 ^{1}H-NMR spectrum of the complex **14d** (T = 298K, $CDCl_3$).*

The ^{13}C{1H}-NMR spectra (Fig. 3.50) of the atropoisomers show the signals ascribable to the different pairs of the $COOCH_3$ and $\underline{C}(COOCH_3)$ groups and those of the coordinated carbenic carbon at about 188 ppm.

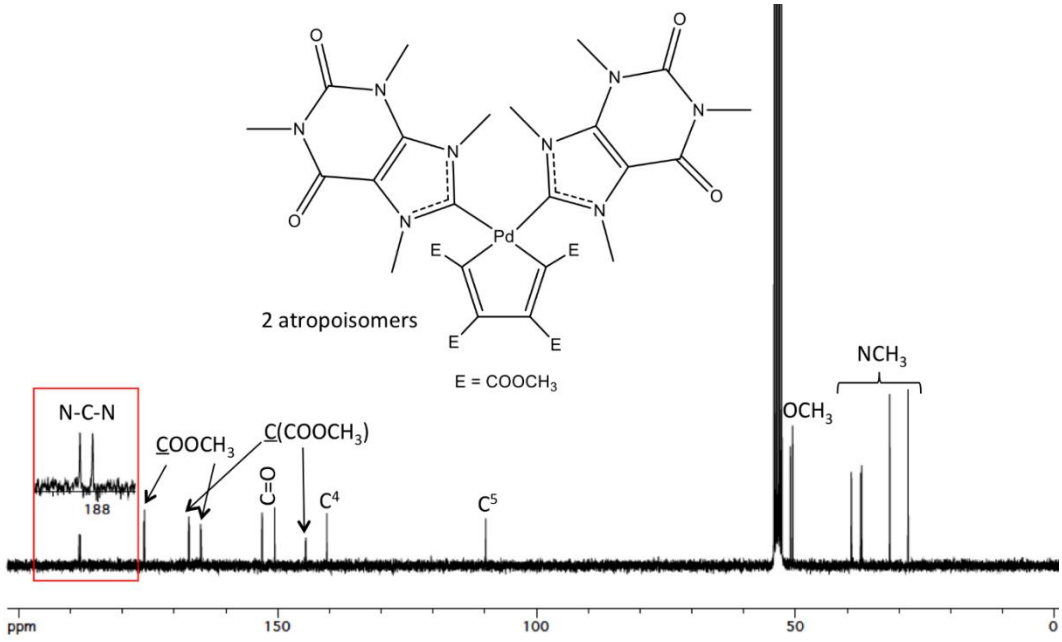

*Fig. 3.50 $^{13}C\{^{1}H\}$-NMR spectrum of the complex **14a** (T = 298K, CD_2Cl_2).*

3.7. Palladium (0) η^2-olefin complexes bearing purine-based NHCs

As already stated (section 1.3.6), the cytotoxic activity of the Pd(0) complexes is almost unexplored. In this section, the synthesis and characterization of unpublished Pd(0) olefin complexes stabilized by xanthine-based NHC ligands will be dealt with. The adopted synthetic approach is based on a previous work published by our research group [21]. This approach is based on the preliminary synthesis of Pd (0) olefin complexes stabilized by bidentate N-S ligands (2-methyl-6-(methylthiophenyl)pyridine (Me-PyCH$_2$SPh) and 2-methyl-8-methyltoquinoline (TMQ-Me)), using the complex $Pd_2(dba)_3 \cdot CHCl_3$ as precursor. Instead of N-S, the ligands COD (cyclooctadiene) or t-BuDAB (1,4-diterbutyl-1,4-diaza-1,3-butadiene) were used by other authors [22], but in these cases they were able to obtain only complexes stabilized by the strongly deactivated olefin maleic anhydride.

At variance with the former derivatives, the complexes containing the Me-PyCH$_2$SPh and TMQ-Me ligands show a remarkable versatility as precursors since their stabilization and consequent easily manipulation is obtained with a number of different olefins [23]. Although not commercially available, the N-S ligands can be easily synthesized [24] and the corresponding pallada-olefin complexes suddenly obtained by reacting simultaneously the $Pd_2(dba)_3 \cdot CHCl_3$, the Me-PyCH$_2$SPh (or TMQ-Me) ligand and the wanted olefin (Scheme 3.19).

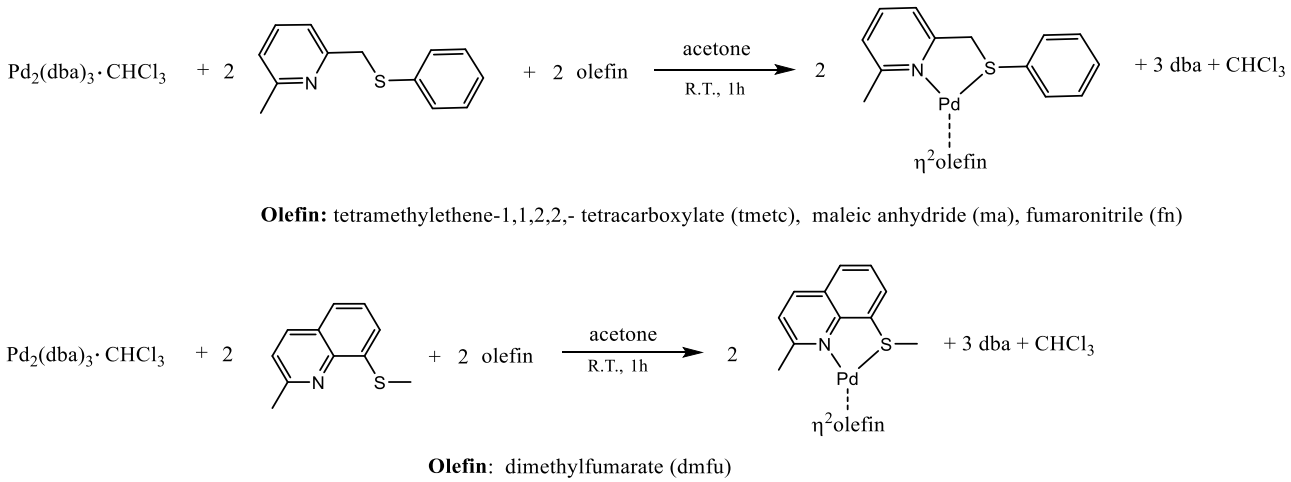

Scheme 3.19 Synthesis of the Pd(0) olefin precursors.

The distortion of the chelated ring induced by the steric interference of the methyl substituent in the pyridine or quinolinic moiety [21], renders these ligands labile and consequently their derivatives good starting complexes for successive synthesis. Among the olefins taken into consideration, only dimethylfumarate (dmfu) is unable to stabilize the complexes with the Me-PyCH$_2$SPh ligand. Dmfu

is indeed the most labile among the olefins used (Fig. 3.51) and therefore the potentially most able in promoting oxidative additions [25].

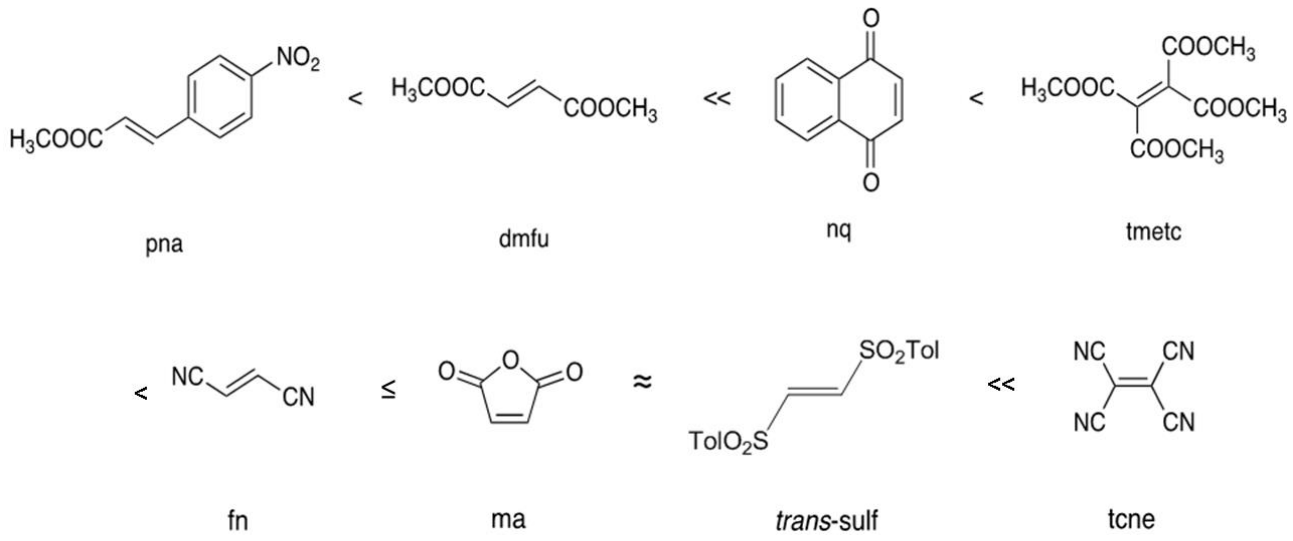

Fig. 3.51 Stability order of the Pd-alkene bond related to the equilibrium constant in a process of olefin exchange [(L-L)Pd(η^2-olefin$_1$)]+olefin$_2$ ⇌ [(L-L)Pd(η^2-olefin$_2$)] + olefin$_1$.

The starting complex bearing dmfu as stabilizing olefin was therefore synthesized using TMQ-Me as ancillary ligand, since its ensuing derivative is stable.

A further synthetic step can be obtained by the displacement of the labile N-S ligand from the (Me-PyCH$_2$SPh)Pd(η^2-olefin) or (TMQ-Me)Pd(η^2-dmfu) complexes by one bidentate or two monodentate ligands (Scheme 3.20).

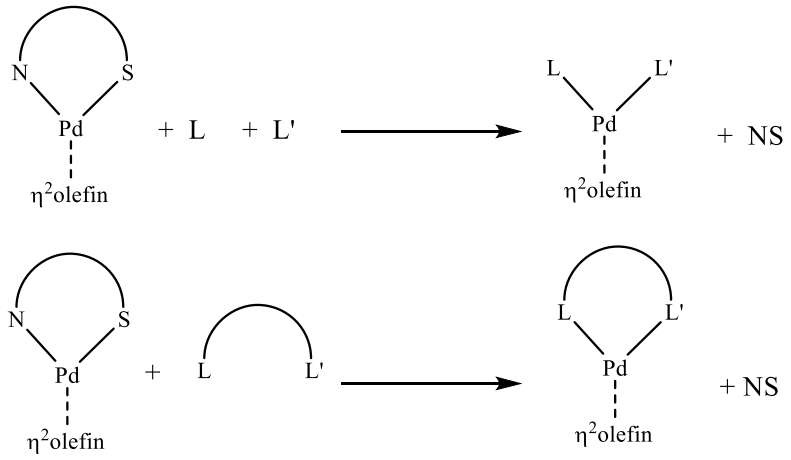

Scheme 3.20 Reactions of (NS)Pd(η^2-olefin) precursors with mono- or bi-dentate ligands.

By means of the described synthetic approach, a number of biscarbene and mixed NHC/L (L = PPh$_3$ or AsPh$_3$) complexes have been isolated. Preliminary tests have shown that is not possible to obtain

selectively the mixed NHC/DIC and NHC/PTA derivatives. In fact, a mixture of the wanted product and of the two species bis-DIC or bis-PTA is obtained. In Figure 3.52, one test carried out with PTA, among all those preliminarily explored, is reported as an example.

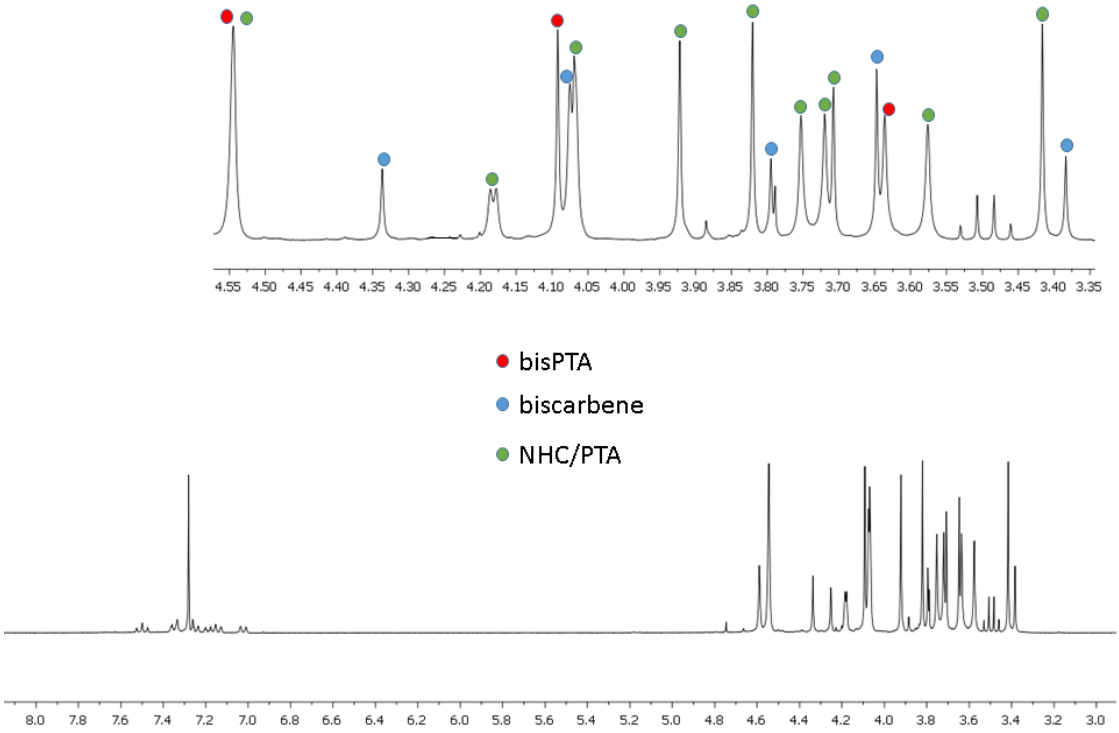

Figure 3.52 ^{1}H-NMR spectrum of the reaction between the silver complex ***5a****, PTA and the Pd(Me-PyCH$_2$SPh)(η^2-tmetc) precursor.*

It was decided to synthesize complexes bearing different spectator ligands and olefins in order to verify whether the cytotoxicity might be somehow traceable back to the Pd-olefin bond strength according to the coordinative capability trend reported in Figure 3.51.

3.7.1. Mixed NHC/PPh_3 and NHC/$AsPh_3$ complexes

The mixed NHC/PPh_3 and NHC/$AsPh_3$ complexes were synthesized by adding a mixture containing triphenylphosphine (or triphenylarsine) and the silver carbene complex (**5a-b** or **5d**) to a dichloromethane solution of the olefinic precursor of interest (Scheme 3.21). The reaction proceeds for about one hour and is characterized by the progressive precipitation of AgCl. After the filtration of the reaction mixture by a Millipore apparatus, the products were isolated by precipitation from a dichloromethane/diethylether mixture (**16a**, **17a, 18a, 20a, 21a** and **22a**) or obtained by the removal of the solvent (**15a-b, 15d, 19a-b** and **19d**).

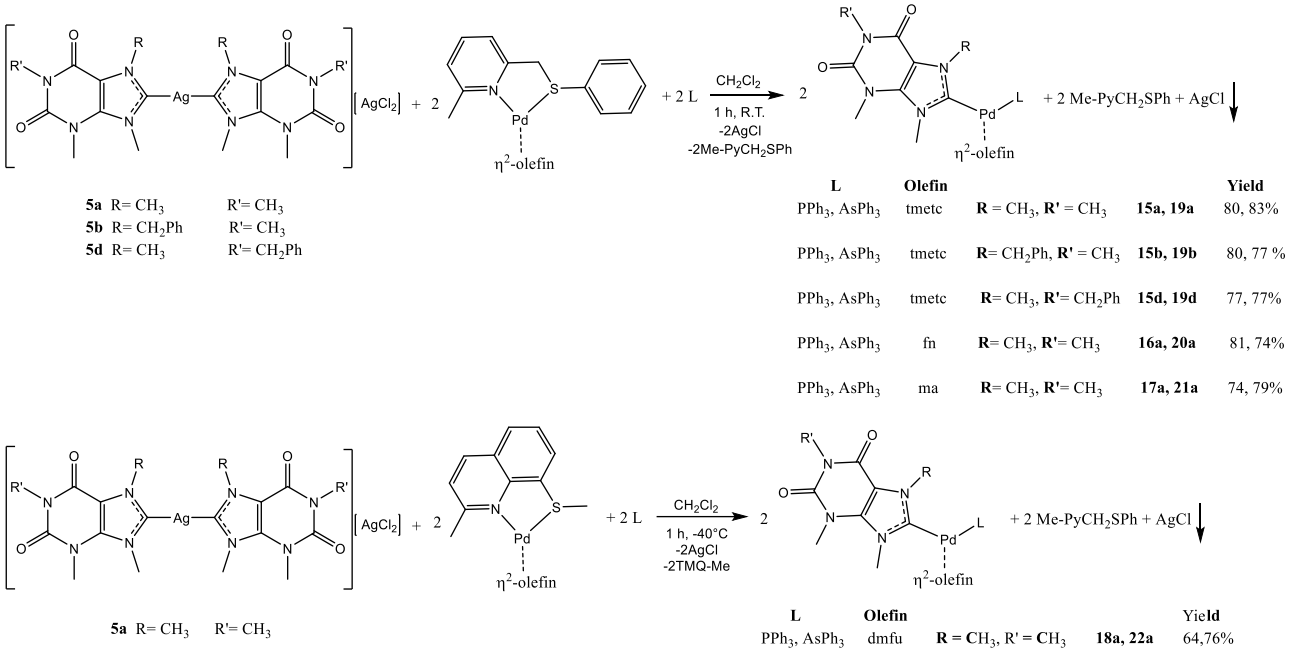

*Scheme 3.21 Synthesis of the mixed NHC/PPh_3 and NHC/$AsPh_3$ complexes **15-22.***

The obtained complexes were characterized by NMR and IR spectroscopy and the relevant responses are reported below.

All the ^{1}H-NMR spectra show the presence of the signals ascribable to the NCH_3 (singlets at 3-4 ppm) and NCH_2 groups (AB systems or singlets at 5-6 ppm) of the carbene moiety.

The same groups resonate in the ^{13}C-NMR between 25 and 50 ppm, whereas the signal of the coordinated carbenic carbon is observed as a singlet for the mixed NHC/$AsPh_3$ complexes and as a doublet, due to the coupling with phosphorus ($J_{C\text{-}P} \approx 15$ Hz), for the mixed NHC/PPh_3 complexes, between 195 and 200 ppm.

Moreover, for complexes containing PPh_3, it is possible to observe a single peak at 25-30 ppm in the ^{31}P-NMR spectra (Fig. 3.53), shifted downfield of about 30-35 ppm with respect to the uncoordinated triphenylphosphine.

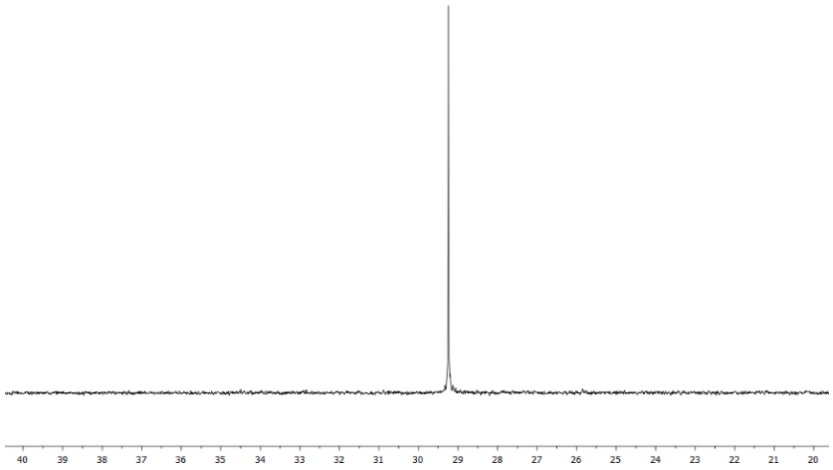

*Fig. 3.53 $^{31}P\{^{1}H\}$-NMR spectrum of the complex **15d** (T = 298K, $CDCl_3$).*

Complexes with tmetc

In the ^{1}H-NMR spectra of the complexes **15a-b** and **15d** (Fig. 3.54) it is possible to observe four signals ascribable to the OCH_3 groups of the coordinated tmetc between 3.1 and 3.7 ppm. This differentiation is due to the presence of two different ancillary ligands and to the hindered rotation of the asymmetric carbene about the C-Pd bond.

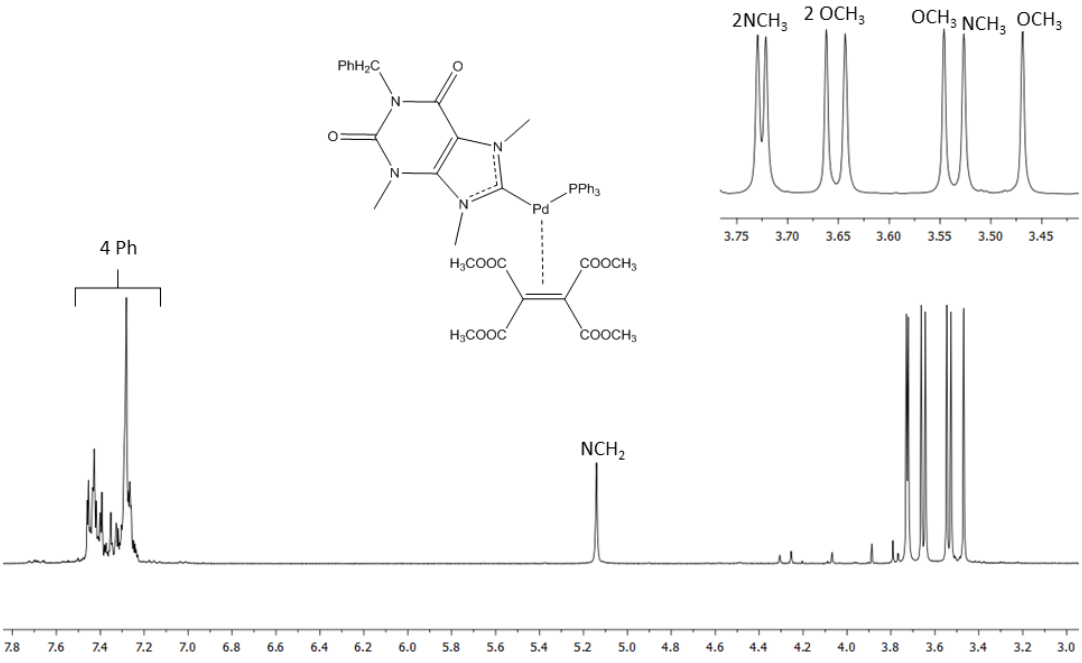

*Fig. 3.54 ^{1}H-NMR spectrum of the complex **15d** (T = 298K, $CDCl_3$).*

Moreover, in the $^{13}C\{^{1}H\}$-NMR spectra (Fig. 3.55) of the complexes **15a-b** and **15d** it is possible to observe the signals ascribable to the OCH_3 groups between 51 and 53 ppm and those related to the olefinic carbons between 60 and 65 ppm. These latter resonate as singlets in the case of NHC/$AsPh_3$ complexes and as doublets ($J_{C\text{-}P} \approx 38$ Hz) in the case of the NHC/PPh_3 derivatives. The highfield shift

of the olefinic carbons with respect to the uncoordinated olefin ($\Delta\delta \approx 80$ ppm), is a direct consequence of its coordination on the palladium center and of the high degree of back-donation, particularly marked in the presence of strongly electron-withdrawing olefins.

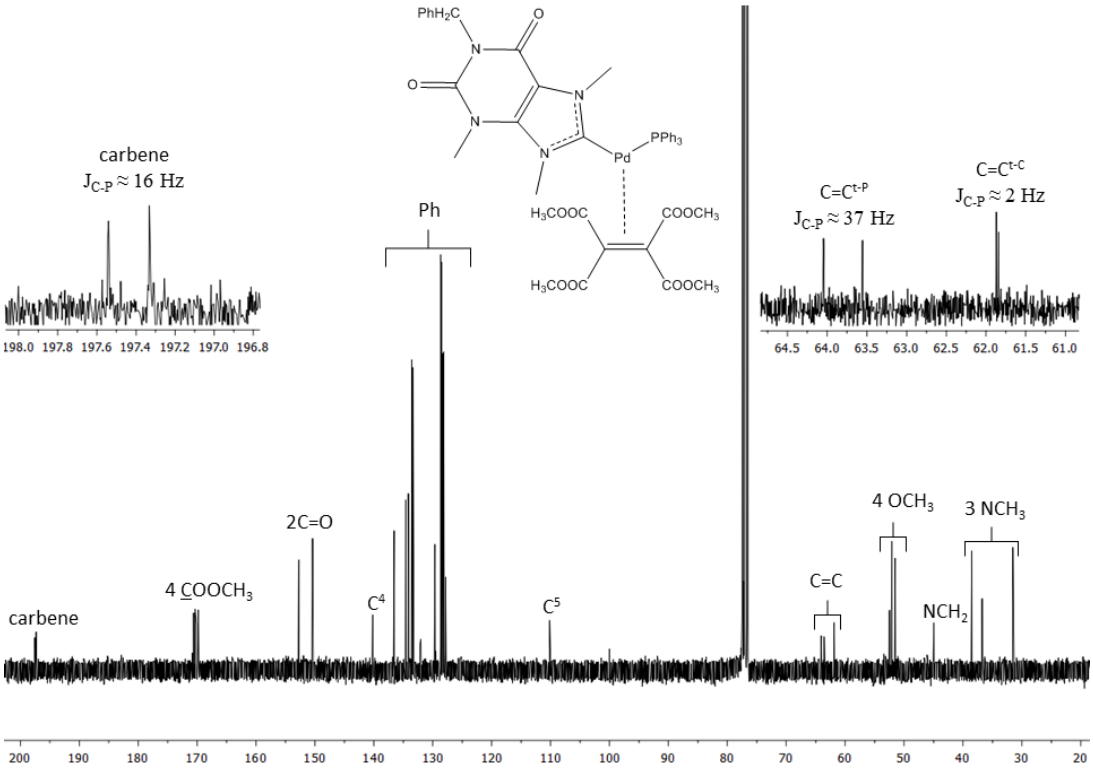

*Fig. 3.55 $^{13}C\{^1H\}$-NMR spectrum of the complex **15d** ($T = 298K$, $CDCl_3$).*

Complexes with fumaronitrile

The ^{1}H-NMR spectra (Fig. 3.56) of complexes **16a** and **20a** are characterized by the following signals:

- one doublet of doublets ascribable to the olefin proton pseudo-*trans* to the phosphine (J_{H-H} = 9.4 Hz and J_{H-P} = 3.4 Hz) at about 2.9 ppm and one doublet ascribable to the olefin proton pseudo-*trans* to the carbene (J_{H-H} = 9.4 Hz) at about 3 ppm, in the case of complex **16a**.
- Two doublets related to the different olefin protons between 2.8 and 3.2 ppm, for complex **20a**.

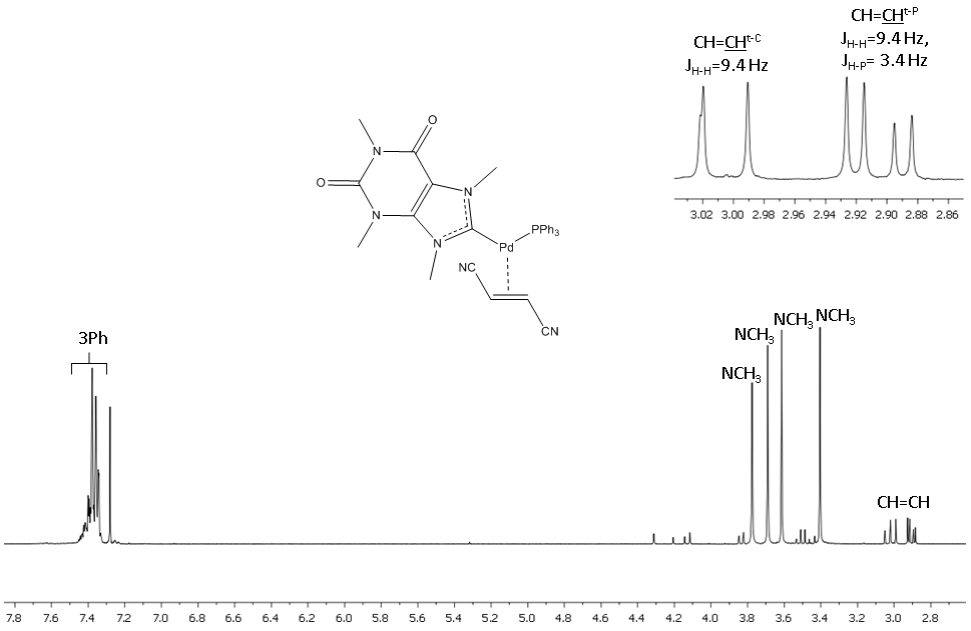

*Fig. 3.56 ^{1}H-NMR spectrum of the complex **16a** (T = 298K, $CDCl_3$).*

The $^{13}C\{^{1}H\}$-NMR spectra (Fig. 3.57) of complexes **16a** and **20a** are characterized by the following signals:

- One doublet ascribable to the olefin carbon pseudo-*trans* to the carbene (J_{C-P} = 3 Hz) at about 22.5 ppm and a doublet ascribable to the olefin carbon pseudo-*trans* to the phosphine (J_{C-P} = 38 Hz) at 22.9 ppm, for complex **16a**.
- The signals of the coordinated olefin at about 38 ppm in the case of complex **20a**.
- The signals of the CN carbons at about 123 ppm.

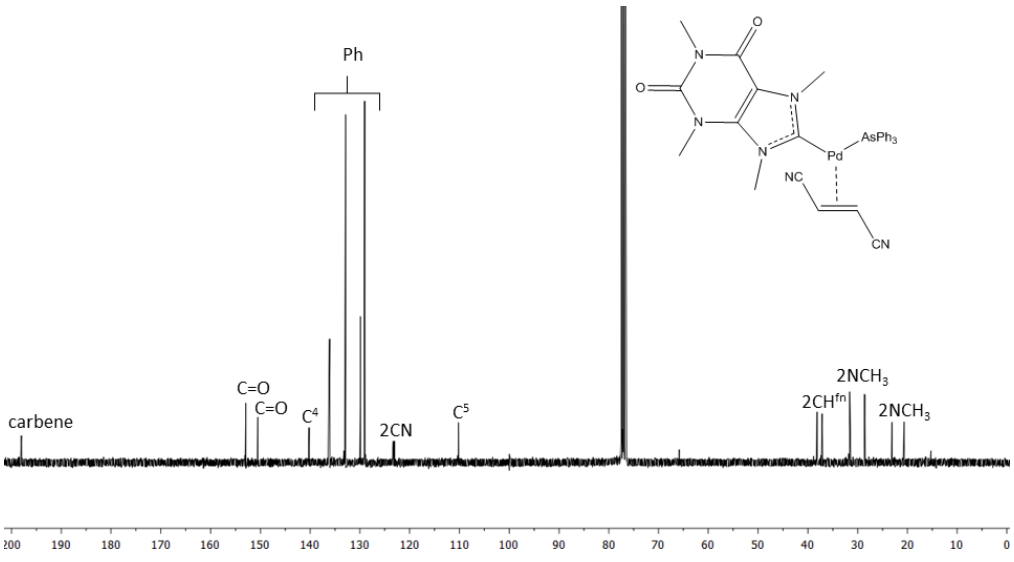

*Fig. 3.57 $^{13}C\{^{1}H\}$-NMR spectrum of the complex **20a** (T = 298K, $CDCl_3$).*

The IR spectra show the typical band of the coordinated fumaronitrile at 2191 cm^{-1} and the signals of the carbonyl groups within 1665 and 1710 cm^{-1}.

Complexes with maleic anhydride

The ^{1}H-NMR spectra (Fig. 3.58) of complexes **17a** and **21a** are characterized by the following signals:

- One doublet of doublets ascribable to the olefin proton pseudo-*trans* to the carbene at about 4 ppm (J_{H-H} = 3.9 Hz and J_{H-P} = 2.9 Hz) and one doublet of doublets related to those pseudo-*trans* to the phosphine at about 4.2 ppm (J_{H-H} = 3.9 Hz and J_{H-P} = 9.8 Hz), for complex **17a**.
- Two doublets related to the coordinated olefin protons between 3.5 and 4.6 ppm, in the case of complex **21a**.

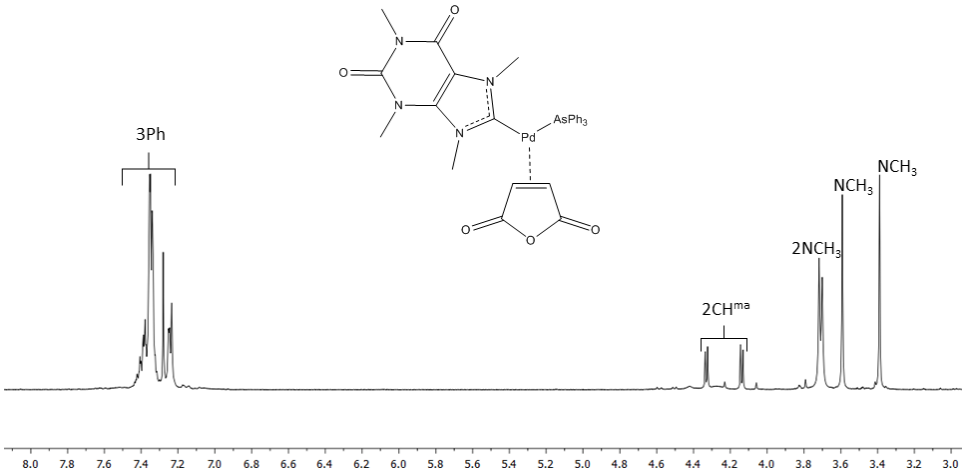

*Fig. 3.58 ^{1}H-NMR spectrum of the complex **21a** (T = 298K, $CDCl_3$).*

The ^{13}C{^{1}H}-NMR spectra (Fig. 3.59) show the following signals:

- One singlet ascribable to the olefin carbon pseudo-*trans* to the carbene at 45.6 ppm and one doublet related to the olefin carbon pseudo-*trans* to the phosphine (J_{C-P} = 27.8 Hz) at about 47.5 ppm, for complex **17a**.
- The signals of the coordinated olefin carbons between 43 and 47 ppm, for complex **21a**.
- A doublet ascribable to the carbonyl carbon of maleic anhydride pseudo-*trans* to the carbene (J_{C-P} = 2 Hz) and a doublet ascribable to those pseudo-*trans* to the phosphine (J_{C-P} = 6 Hz) at about 172 ppm, for complex **17a**.
- The signals of the carbonyl carbons at about 173 ppm, for complex **21a**.

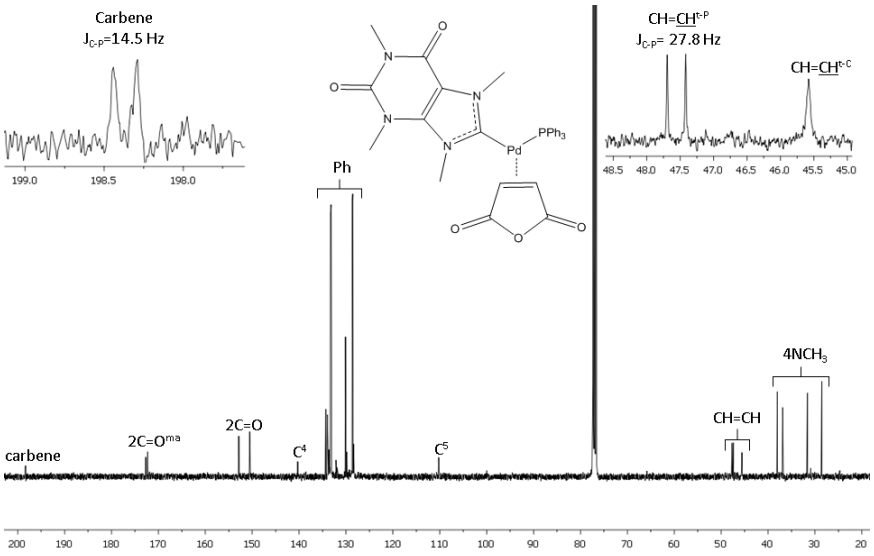

*Fig. 3.59 $^{13}C\{^1H\}$-NMR spectrum of the complex **17a** (T = 298K, $CDCl_3$).*

Complexes with dimethylfumarate

The ^{1}H-NMR spectra (Fig. 3.60) of the complexes **18a** and **22a** show the following signals:

- One broad singlet and two singlets ascribable to the OCH_3 groups of the coordinated dimethyl fumarate (3.2-3.6 ppm) for complexes **18a** and **22a**, respectively.
- One doublet of doublets ascribable to the olefin proton pseudo-*trans* to the carbene at about 4.1 ppm ($J_{H\text{-}H}$ = 9.5 Hz) and one doublet of doublets for those pseudo-*trans* to the phosphine at about 4 ppm ($J_{H\text{-}H}$ = 9.5 Hz and $J_{H\text{-}P}$ = 2.6 Hz), for complex **18a**.
- Two singlets between 4 and 4.2 ppm related to the olefinic protons in the case of complex **22a**.

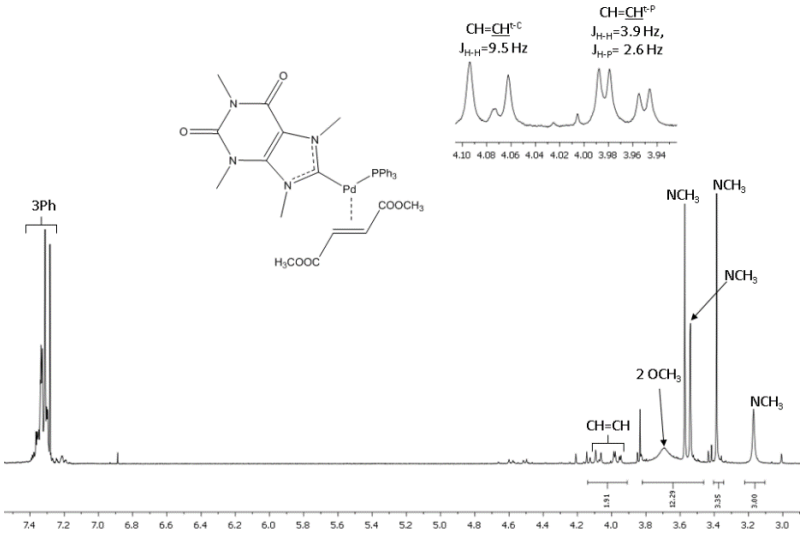

*Fig. 3.60 ^{1}H-NMR spectrum of the complex **18a** (T = 298K, $CDCl_3$).*

The $^{13}C\{^{1}H\}$-NMR spectra show two peaks at about 38 ppm ascribable to the OCH_3 groups and the signals of the olefinic carbons between 45 and 48 ppm.

3.7.2. Bis(NHC) complexes

The Pd (0) biscarbene compounds were obtained by transmetallation between the Ag (I) complexes **5a-b** or **5d** and the [(Me-PyCH$_2$SPh)Pd(η^2-olefin)] precursor, according to the Scheme 3.22.

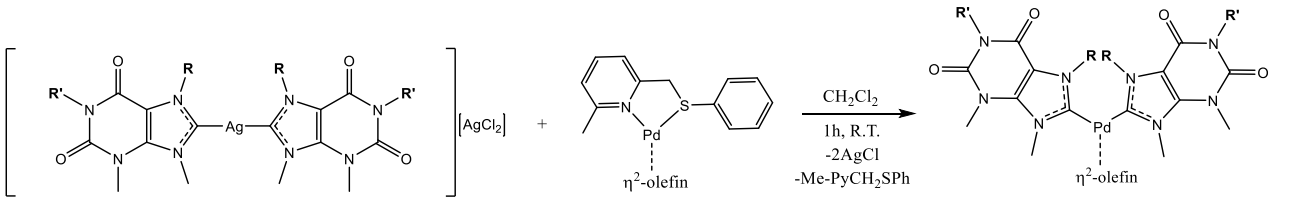

5a R= CH_3 R'= CH_3
5b R= CH_2Ph R'= CH_3
5d R= CH_3 R'= CH_2Ph

Olefin:				**Yield:**
tmetc	**R** = CH_3	**R'** = CH_3	**23a**	99%
tmetc	**R**= CH_2Ph	**R'** = CH_3	**23b**	86%
tmetc	**R**= CH_3	**R'**= CH_2Ph	**23d**	95%
fn	**R**= CH_3	**R'**= CH_3	**24a**	86%

*Scheme 3.22 Synthesis of the biscarbene complexes **23-24.***

It was possible to obtain in good yields and purity the complexes with tetramethylethene-1,1,2,2-tetracarboxylate (tmetc) (**23a-b** and **23d**) and fumaronitrile (fn) (**24a**), only. The preliminary tests carried out with the maleic anhydride and dimethylfumarate have highlighted the formation of mixtures of products of difficult identification.

All the ^{1}H-NMR spectra show the presence of the signals ascribable to the NCH_3 (singlets at 3-4 ppm) and NCH_2 (singlets at 5-6 ppm) groups of the carbene moiety.

The signals related to these groups are observed in the ^{13}C-NMR between 25 and 50 ppm, whereas the signal of the coordinated carbenic carbon resonates as a singlet between 195 and 200 ppm.

Complexes with tmetc

The ^{1}H-NMR spectra (Fig. 3.61) of the complexes **23a-b** and **23d** show a singlet ascribable to the OCH_3 groups of the coordinated olefin at about 3.6 ppm.

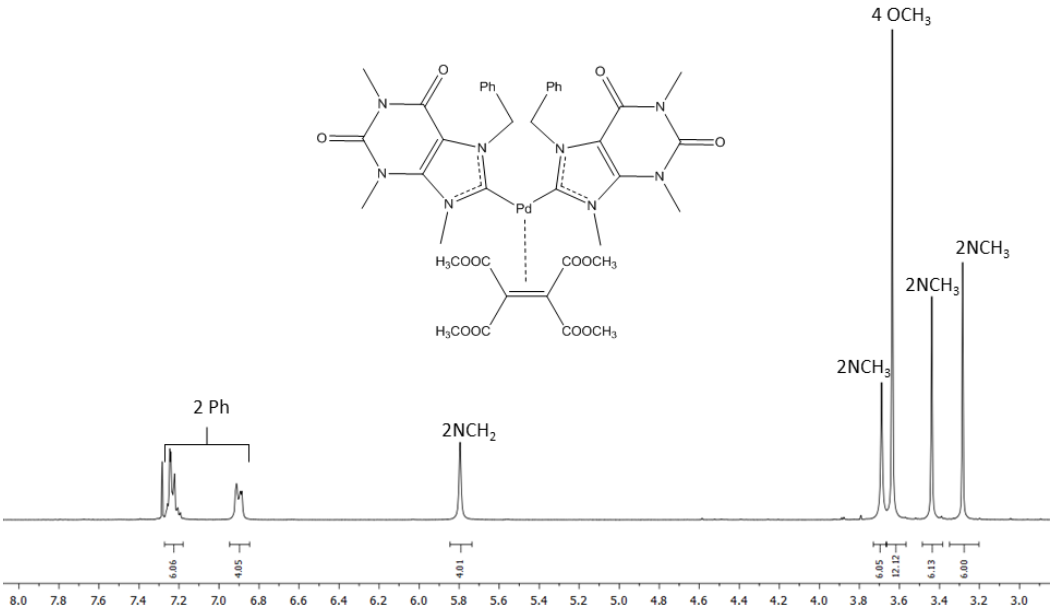

*Fig. 3.61 ^{1}H-NMR spectrum of the complex **23b** (T = 298K, $CDCl_3$).*

The $^{13}C\{^{1}H\}$-NMR spectra (Fig. 3.62) of the complexes **23a-b** and **23d** show:

- Signals related to the coordinated olefinic carbons at about 58 ppm.
- Signals of the four OCH_3 groups of the coordinated tmetc at about 52 ppm.
- Signals ascribable to the carbonyl carbons at about 171 ppm.

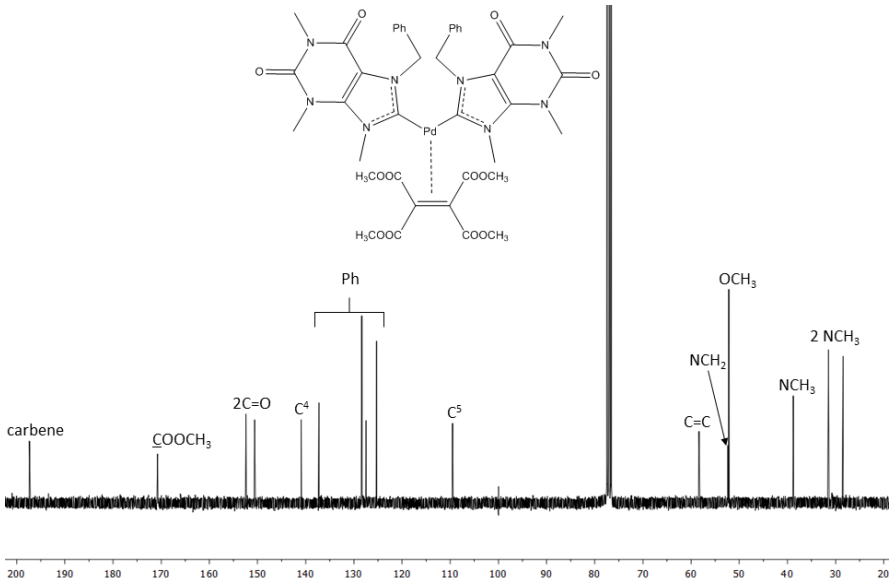

*Fig. 3.62 $^{13}C\{^{1}H\}$-NMR spectrum of the complex **23b** (T = 298K, $CDCl_3$).*

Complex with fumaronitrile

The ^{1}H-NMR spectrum of complex **24a** (Fig. 3.63) shows a singlet ascribable to the olefinic protons of the coordinated fumaronitrile at about 2.6 ppm.

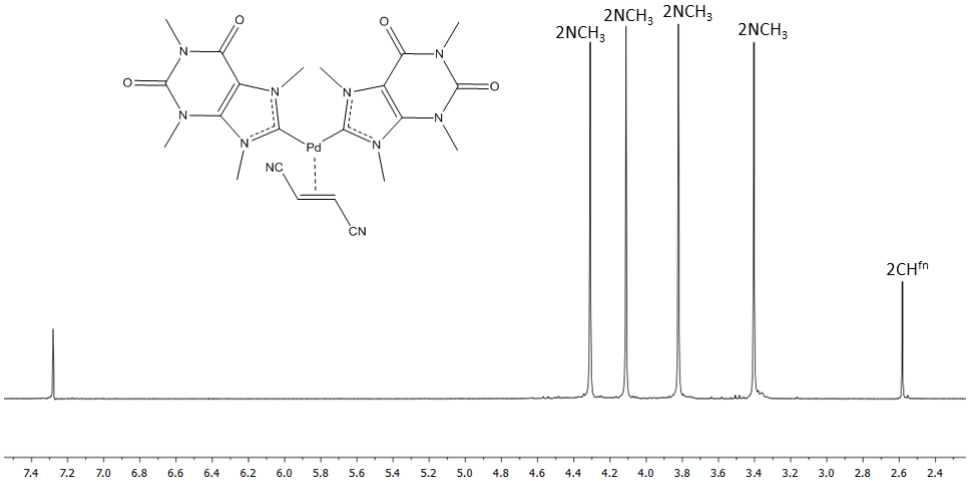

*Fig. 3.63 ^{1}H-NMR spectrum of the complex **24a** (T = 298K, $CDCl_3$).*

The ^{13}C{^{1}H}-NMR spectrum of complex **24a** (Fig. 3.64) shows the signals related to the olefinic carbons and to the CN groups at 16 and 125 ppm, respectively.

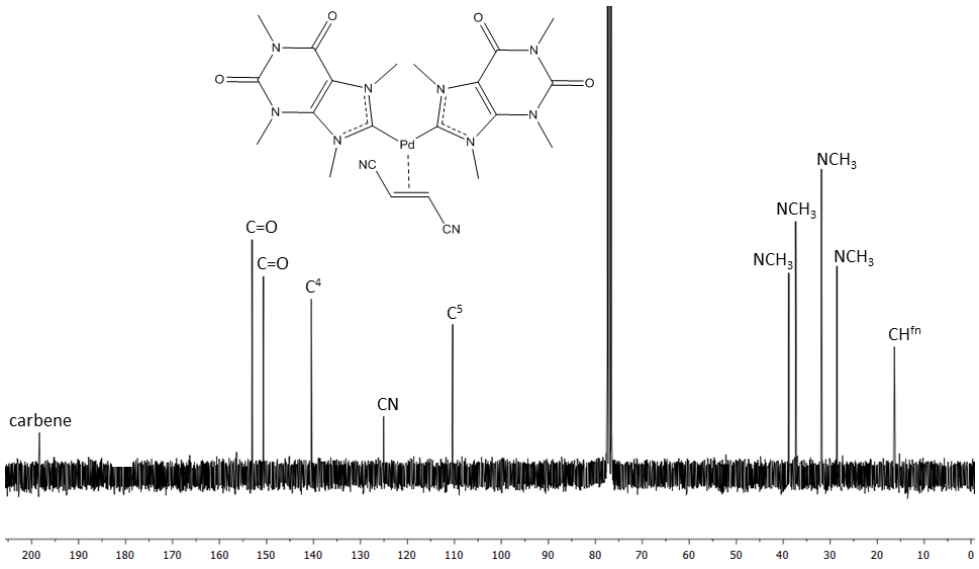

*Fig. 3.64 ^{13}C{^{1}H}-NMR spectrum of the complex **24a** (T = 298K, $CDCl_3$).*

3.7.3. Bis(PTA) complexes

Due to the capability of PTA of increasing the solubility in water of its complexes and the cytoxicity of many its derivatives toward several tumor lines [26], we decided to synthesize compounds containing two PTA fragments. This choice was also supported by the fact that in the literature no Pd(0) olefin complexes bearing this spectator ligand are reported.

The synthesis of the bis-PTA complexes (Scheme 3.23) was carried out in dichloromethane by reacting the olefinic precursor [Pd(Me-PyCH$_2$SPh)(η^2-olefin)] (olefin = maleic anhydride, fumaronitrile, tetracarboxymethylethylene) or [Pd (TMQ-Me)(η^2-dmfu)] and two equivalents of PTA.

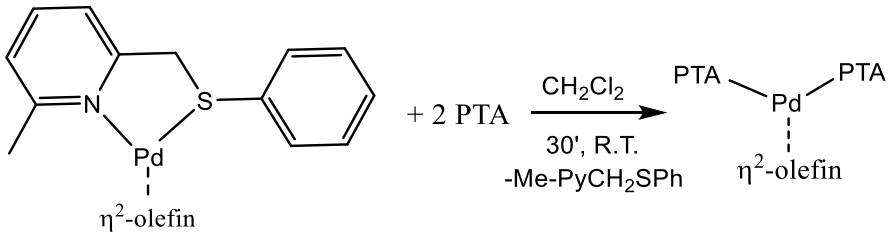

Olefin:		**Yield:**
tmetc	**25**	91%
fn	**26**	98%
ma	**27**	93%

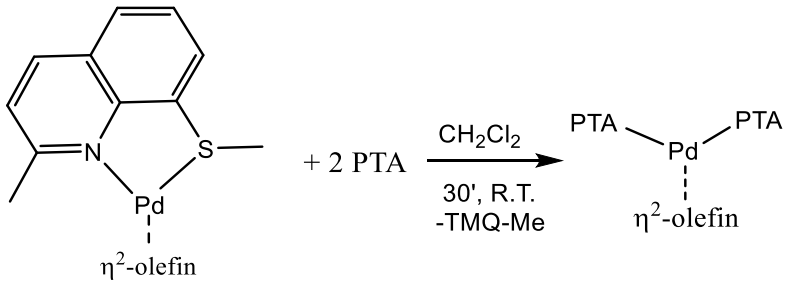

Olefin:		**Yield:**
dmfu	**28**	90%

*Scheme 3.23 Synthesis of the bis(PTA) complexes **25-28.***

The compounds were precipitated by addition of diethyl ether to the concentrated solutions and characterized by NMR and IR spectroscopy.

The ^{1}H-NMR spectra show for the PTA ligand the following signals:

- One AB system (J = 10-15 Hz) ascribable to the NCH$_2$P protons at about 4.1 ppm.
- One AB system (J = 13-20 Hz) ascribable to the NCH$_2$N protons at about 4.5 ppm.

The signals of the olefinic protons are reported below:

- Tmetc: one singlet for the OCH_3 groups at about 3.6 ppm.
- Maleic anhydride: one singlet at about 4.2 ppm.
- Fumaronitrile: one singlet at about 3 ppm.
- Dimethylfumarate: one singlet related to the OCH_3 protons at about 3.6 ppm.

The ^{1}H-NMR spectrum of compound **25** is reported in the following figure.

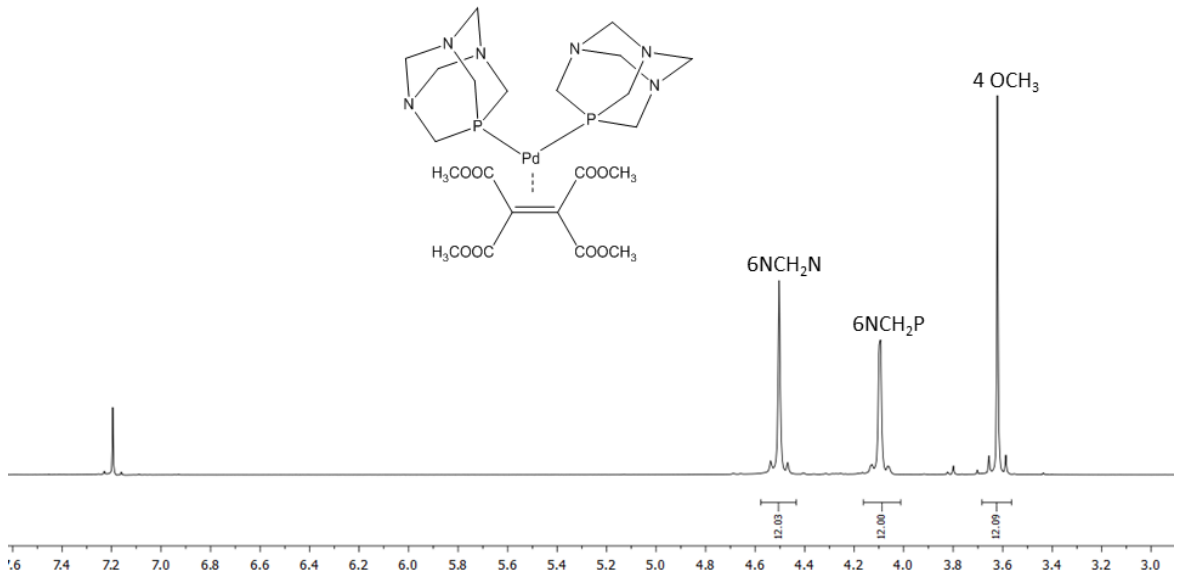

*Fig. 3.65 ^{1}H-NMR spectrum of the complex **25** (T = 298K, $CDCl_3$).*

Depending on the coordinated olefin, the $^{31}P\{^1H\}$-NMR spectra (Fig. 3.66) show one singlet between -61 and -64 ppm ($\Delta\delta \approx 50$ ppm downfield of the uncoordinated PTA).

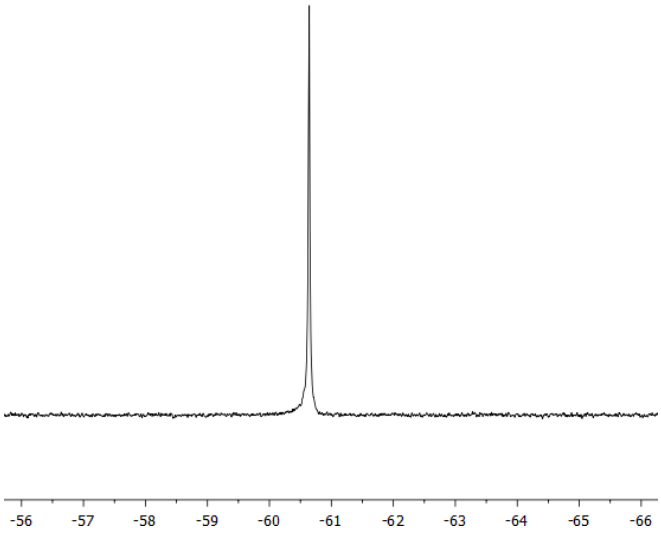

*Figure 3.66 $^{31}P\{^1H\}$-NMR spectrum of the complex **25** (T = 298K, $CDCl_3$).*

The $^{13}C\{^{1}H\}$-NMR spectra show for the PTA ligand one doublet ascribable to the NCH_2P system at 53-54 ppm (J_{C-P} = 8-9 Hz) and one doublet related to the NCH_2N system at 73-74 ppm (J_{C-P} = 6-7 Hz).

The signals of the olefin carbons are listed below:

- Tmetc: one singlet for the OCH_3 groups at 52 ppm, the signal of the olefinic carbons at 67 ppm and that of the carbonyl carbons at 168 ppm.
- Maleic anhydride: the signal of the olefin and carbonyl carbons at 51 and 171 ppm, respectively.
- Fumaronitrile: the signal of the olefinic carbons and of the CN groups at 27 and 121 ppm, respectively.
- Dimethylfumarate: signals of the olefinic carbons and of the carbonyl groups at 52 and 173 ppm, respectively.

As an example, the $^{13}C\{^{1}H\}$-NMR spectrum of compound **25** is shown in the following figure.

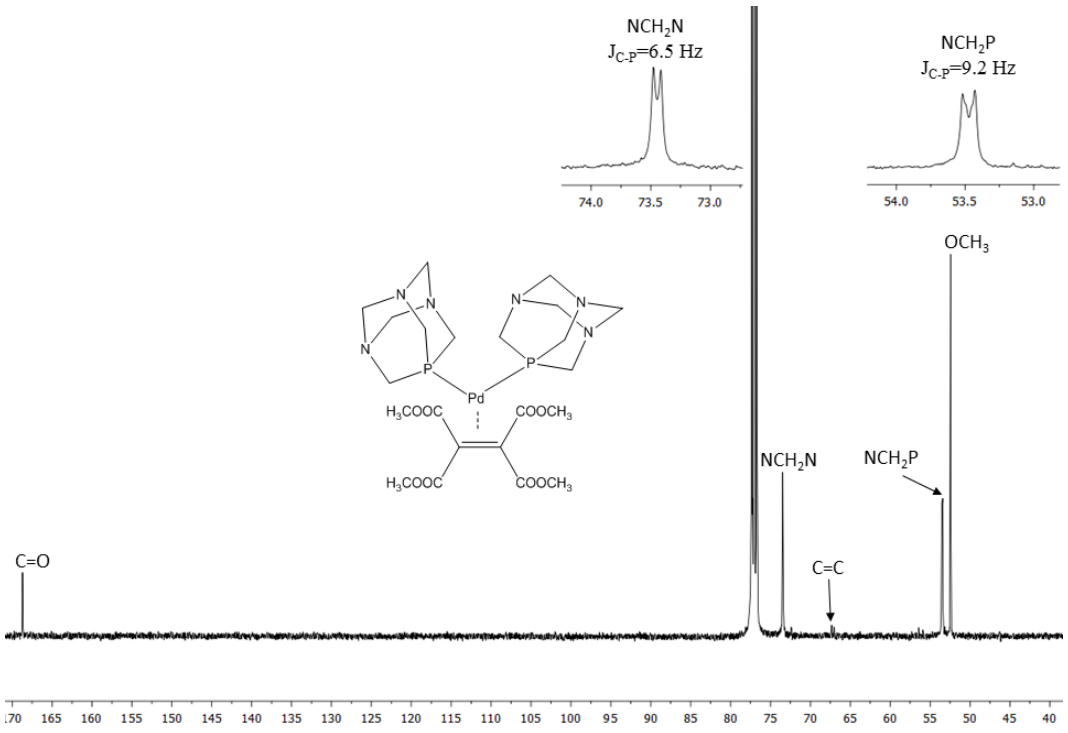

*Fig. 3.67 $^{13}C\{^{1}H\}$-NMR spectrum of the complex **25** (T = 298K, $CDCl_3$).*

In the case of the complex **26** it was possible to solve the crystal structure by means of the X-ray diffraction of the single crystal (Figure 3.68).

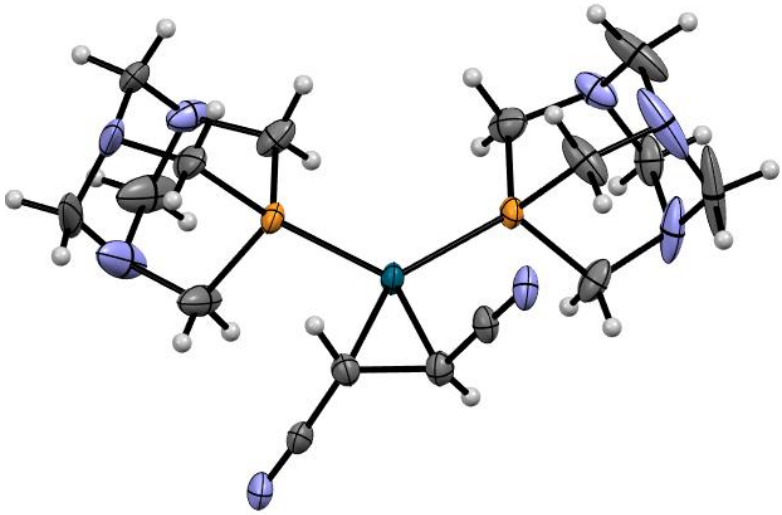

*Fig. 3.68 Ellipsoid representation of **26** crystal ASU contents (50% probability).*

3.8. Antiproliferative and proapoptotic analysis

The cytotoxic activity of the Pd (0) and Pd (II) complexes containing purine-based NHC ligands toward human ovarian cancer cell lines, in collaboration with the molecular biology group of the University of Ferrara (coordinator: Prof. Roberto Gambari), has been evaluated.
In particular, the following tumour lines were examined:

- A2780
- A2780-R
- SKOV-3

A2780 cells derive from a patient who has not undergone any therapy. These cells grow in adhesion to form a monolayer and from which, through chronic exposure to increasing amounts of cisplatin, the A2780-R line were obtained. A2780-R cells show also resistance to irradiation, melphalan (alkylating agent) and adriamycin (antineoplastic antibiotic) [27].
SKOV-3 line represents ovarian carcinoma cells growing in adhesion, extracted from the ascitic fluid of a 64-year-old Caucasian patient [27].
The results of the antiproliferative and proapoptotic activity will be presented below, considering the different class of organometallic compounds.

3.8.1. Activity of Pd (II) η^3-allyl complexes bearing purine-based NHCs toward ovarian cancer cell lines

With regard to the η^3-allyl complexes (compounds **6-10**), the antiproliferative activity was tested on A2780 (cisplatin-sensitive) and SKOV-3 (cisplatin-resistant) tumor lines. Stock solutions of each compound (25-50 mM) were prepared in DMSO; the working solutions were produced by diluition of the stock solution with water.
Preliminarily, the stability of our complexes was checked in 1:1 dmso-d6/D_2O solution (**6**, **9** and **10**) or D_2O (**7** and **8**): after 48 hours at room temperature no degradation and no ligand replacement was observed.
In addition to the complexes of interest, also the antiproliferative activities of the $[Pd(\mu\text{-}Cl)(\eta^3\text{-allyl})]_2$ precursor, the imidazolium salts **2a-d** and cisplatin were evaluated. The latter is nowadays used as a reference both to detect any anomalies in the analysis protocols (positive control) and to compare the activity of the tested compounds. The antiproliferative activity data are reported in Table 3.1 expressed as IC_{50} (concentration of the complex that leads to the death of 50% of the cells inserted in the culture medium), with the exception of imidazolium salts **2a-d** which were substantially inactive in both the lines (IC_{50}> 100 μM).

COMPLEX	IC_{50} (μM)	
	A2780	**SKOV-3**
Cisplatin	1.5 ± 0.2	5.94 ± 0.08
$[Pd(\mu\text{-}Cl)(\eta^3\text{-}C_3H_5)]_2$	7.8 ± 0.2	10 ± 4
6a	5 ± 2	5 ± 1
6b	4 ± 2	3 ± 1
6c	0.09 ± 0.02	4.02 ± 0.09
6d	0.81 ± 0.08	1.7 ± 0.9
7a	82 ± 9	66 ± 13
7b	7 ± 1	40 ± 2
7d	9.2 ± 0.8	57 ± 8
8a	7 ± 2	5.20 ± 0.08
8b	7.60 ± 0.07	6.5 ± 0.7
8d	0.9 ± 0.2	50.5 ± 0.5
9a	5 ± 2	4.0 ± 0.7
9b	3.72 ± 0.06	5 ± 1
9d	5 ± 1	3 ± 1
10a	7 ± 2	7.7 ± 0.4
10b	4 ± 1	61 ± 7
10c	3.8 ± 0.5	60 ± 6
10d	6.4 ± 0.7	39 ± 6

Table 3.1 Effects of the Pd(II) allyl complexes on the proliferation of A2780 and SKOV-3 cells (72h). The inhibition of cell growth is represented as IC_{50}.

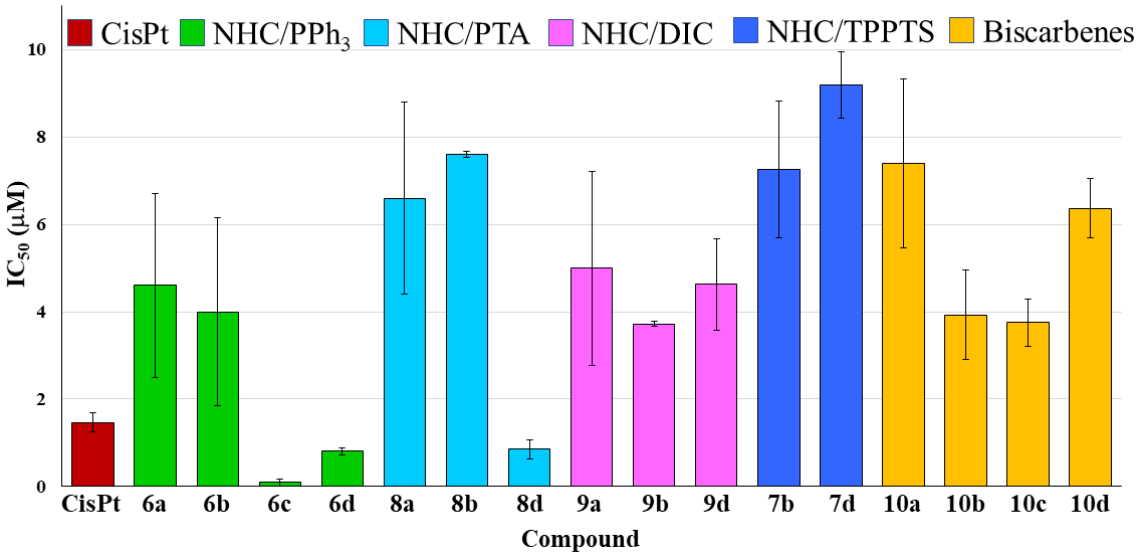

Fig. 3.77 Pd(II) allyl complexes with IC_{50}<10 μM on A2780 cell line.

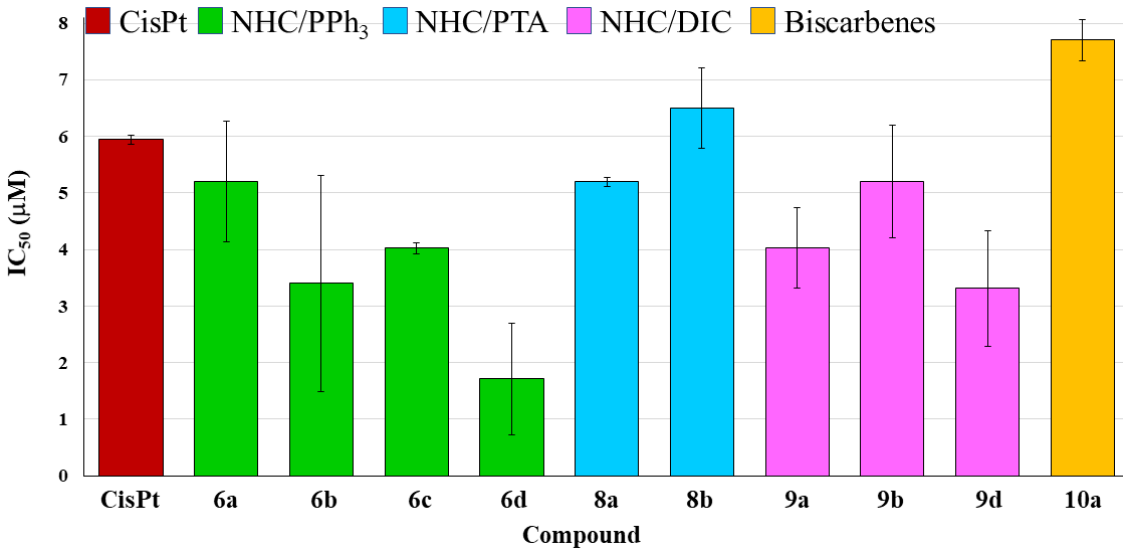

Fig. 3.78 Pd(II) allyl complexes with IC_{50}<8 μM on SKOV-3 cell line.

All of the assayed complexes, except for **7a**, showed good antiproliferative activity on the cisplatin-sensitive A2780 cell line. Compounds **6c-d** (mixed NHC/PPh_3) and **8d** (mixed NHC/PTA) are more active than cisplatin showing 0.09 ± 0.02, 0.81 ± 0.08 and 0.9 ± 0.2 μM IC_{50} values, respectively.

As for the cisplatin-resistance SKOV-3 cells, the IC_{50} values are comparable to cisplatin one (IC_{50} = 5.94 ± 0.08 μM) or higher, as in the case of complexes **7a**, **7b**, **7d**, **8d**, **10b**, **10c** and **10d** which have average values between 38 and 66 μM. The mixed NHC/PPh_3 complexes **6a-d** are the most performing also in this tumour line, with average IC_{50} values ranging from 1.7 to 5 μM (similar or better than cisplatin).

Biscarbene **(10a-d)** and mixed NHC/TPPTS (**7a-b** and **7d)** complexes are instead the species less active.

To test the selectivity of Pd-compounds *versus* cancer cells, normal human fibroblasts (MRC-5) were treated with four different complexes (**6d**, **8d**, **9b** and **10a**) representative of different subclasses with high activity on cancer cells. As shown in Table 3.2, the compounds are almost inactive on fibroblasts, suggesting a preferential activity on cancer cells. In particular, the compound **6d** is more active than **8d**, **9b** and **10a** on A2780 and SKOV-3 cancer cell lines but with an $IC_{50} > 100$ μM on fibroblasts.

Complex	**IC_{50} (μM)**
Cisplatin	14 ± 1
6d	>100
8d	22 ± 6
9b	17 ± 1
10a	>100

Table 3.2 Effects of the Pd(II) allyl complexes on the proliferation of MRC-5 cells (72h). The inhibition of cell growth is represented as IC_{50}.

Pro-apoptotic effect

To verify if the antiproliferative activity exerted by our complexes is associated with an apoptotic process, the proapoptotic effect was assessed for both the cell lines (A2780 and SKOV-3), using the Muse cytometer (Merck Millipore, Billerica, MA, USA) and the Muse® Annexin V and Dead Cell Assay Kit.

The marker used is the Annexin V-PE, which allows to exploit on the one hand the ability of Annexin to bind to phosphatidylserine (a phospholipid exposed outside the cell membrane during apoptosis) and on the other the luminescent properties of PE (phycoerythrin) to identify cells. The use of Annexin V-PE in combination with the 7AAD cell death marker (7 aminoactinomycin D) allows to distinguish cells in early or late apoptosis from those dead by necrosis.

The two concentrations used for each complex were close to the previously determined IC_{50} value.

In Table 3.3, the percentage of total apoptosis was reported and each data was compared to the analysis of untreated cells (negative control, C-), in which the observed total apoptosis was less than 5%.

Complex	Total apoptosis (%)	Dead cells (%)	Total apoptosis (%)	Dead cells (%)
	A2780	A2780	SKOV-3	SKOV-3
C-	2.61	1.96	5.30	0.50
Cisplatin	38.25 (2.5 μM)	3.30 (2.5 μM)	13.33 (5 μM)	1.17 (5 μM)
$[Pd(\mu\text{-}Cl)(\eta^3\text{-}C_3H_5)]_2$	8.15 (1 μM) 29.40 (10 μM)	2.00 (1 μM) 1.00 (10 μM)	6.55 (1 μM) 7.10 (10 μM)	0.55 (1 μM) 2.20 (10 μM)
6a	3.80 (1 μM) 12.35 (10 μM)	0.30 (1 μM) 0.25 (10 μM)	6.35 (1 μM) 12.71 (10 μM)	5.35 (1 μM) 4.86 (10 μM)
6b	8.35 (1 μM) 10.66 (10 μM)	0.50 (1 μM) 0.33 (10 μM)	7.25 (1 μM) 44.31 (10 μM)	8.05 (1 μM) 1.12 (10 μM)
6c	54.04 (0.1 μM) 98.35 (1 μM)	0.25 (0.1 μM) 0.24 (1 μM)	43.78 (1 μM) 84.04 (10 μM)	15.83 (0.1 μM) 3.16 (1 μM)
6d	2.25 (1 μM) 21.00 (10 μM)	7.62 (1 μM) 1.45 (10 μM)	6.50 (0.5 μM) 52.35 (5 μM)	3.70 (1 μM) 0.57 (10 μM)
7a	3.20 (50 μM) 2.21 (100 μM)	2.10 (50 μM) 1.31 (100 μM)	12.55 (50 μM) 44.96 (100 μM)	0.36 (50 μM) 0.29 (100 μM)
7b	2.66 (1 μM) 1.60 (10 μM)	2.26 (1 μM) 1.30 (10 μM)	11.25 (25 μM) 53.01 (50 μM)	0.15 (1 μM) 0.25 (10 μM)
7d	2.97 (1 μM) 5.65 (10 μM)	0.86 (1 μM) 0.96 (10 μM)	8.73 (50 μM) 36.37 (100 μM)	0.51 (1 μM) 0.34 (10 μM)
8a	3.00 (1 μM) 15.25 (10 μM)	0.30 (1 μM) 0.00 (10 μM)	2.45 (1 μM) 3.10 (10 μM)	0.10 (1 μM) 0.65 (10 μM)
8b	4.25 (1 μM) 7.05 (10 μM)	0.80 (1 μM) 0.15 (10 μM)	3.00 (1 μM) 3.65 (10 μM)	0.45 (1 μM) 0.65 (10 μM)
8d	5.49 (1 μM) 5.76 (10 μM)	2.32 (1 μM) 1.43 (10 μM)	9.82 (50 μM) 27.49 (100 μM)	3.06 (1 μM) 1.71 (10 μM)
9a	9.50 (1 μM) 9.20 (10 μM)	0.60 (1 μM) 0.15 (10 μM)	15.05 (1 μM) 34.55 (10 μM)	0.60 (1 μM) 0.15 (10 μM)
9b	26.52 (1 μM) 61.18 (10 μM)	0.59 (1 μM) 0.18 (10 μM)	6.26 (1 μM) 69.10 (10 μM)	0.59 (1 μM) 0.18 (10 μM)
9d	1.40 (1 μM) 79.45 (10 μM)	8.92 (1 μM) 0.34 (10 μM)	3.45 (1 μM) 52.95 (10 μM)	0.90 (1 μM) 0.15 (10 μM)
10a	2.65 (1 μM) 3.50 (10 μM)	0.20 (1 μM) 0.25 (10 μM)	3.65 (1 μM) 30.89 (10 μM)	0.35 (1 μM) 0.46 (10 μM)
10b	5.69 (1 μM) 43.03 (10 μM)	1.86 (1 μM) 0.34 (10 μM)	6.32 (50 μM) 56.60 (100 μM)	0.41 (1 μM) 0.44 (10 μM)
10c	1.39 (1 μM) 23.66 (10 μM)	7.28 (1 μM) 3.09 (10 μM)	7.84 (50 μM) 52.01 (100 μM)	0.39 (1 μM) 0.38 (10 μM)
10d	5.90 (1 μM) 61.17 (10 μM)	0.56 (1 μM) 0.00 (10 μM)	12.74 (25 μM) 79.32 (50 μM)	1.29 (1 μM) 3.18 (10 μM)

Table 3.3 Pro-apoptotic effects of the Pd-complexes on A2780 and SKOV-3 cell lines detected at two different concentrations. (C-: untreated cells).

The compounds that showed the highest pro-apoptotic activity on the A2780 cell line are **6c-d**, **9b**, **9d** and **10b-d**, with a total pro-apoptotic effect between 21% (**6d**) and 98% (**6c**). Furthermore, compound **6c** shows the greatest total pro-apoptotic activity even with the lowest tested concentration (0.1 μM, total apoptosis = 54%). The remaining compounds are moderately active in inducing the apoptosis process.

With regard to the SKOV-3 line (CisPt resistant), compounds **6b-d**, **7a-b**, **7d**, **8d**, **9a-b**, **9d** and **10a-d** were found to be particularly active, with a total pro-apoptotic effect between 28% (**8d**) and 84% (**6c**). As for the A2780 line, compound **6c** is very active even at the lowest tested concentration (1 μM, total apoptosis = 44%).

The proportion of dead cells, also reported in Table 3.3, suggest that apoptotic effects and antiproliferative activity are not associated with major cytotoxicity.

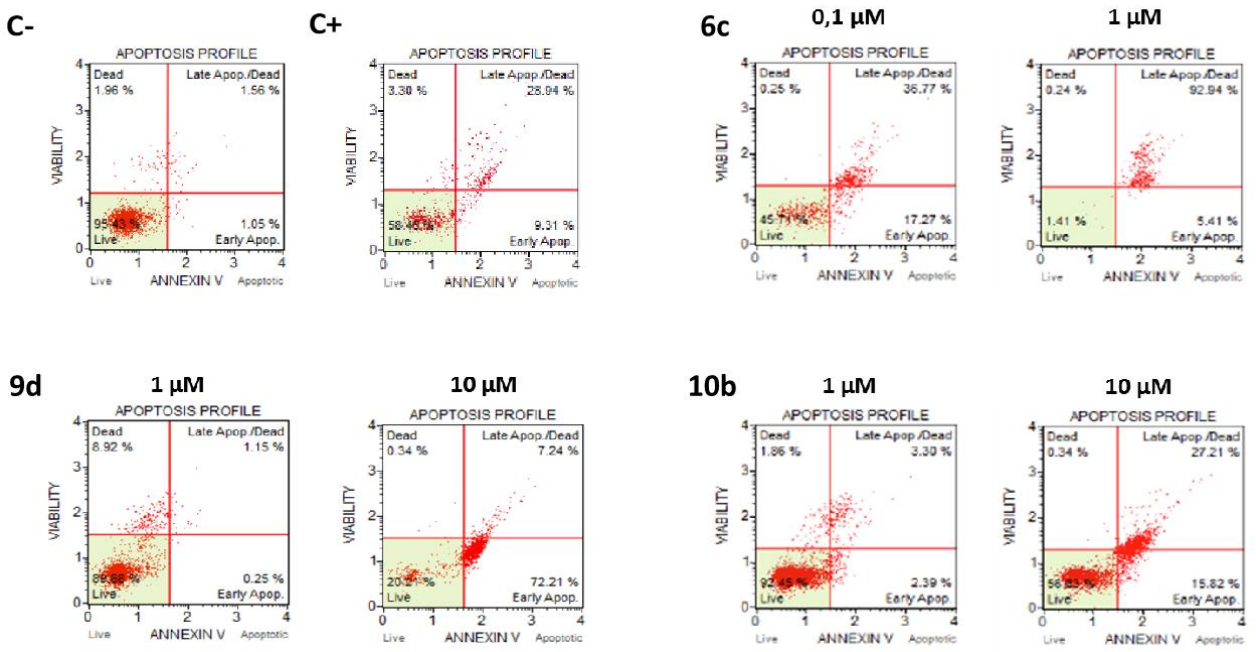

*Fig. 3.79 Representative apoptosis profile of A280 cells untreated (**C-**), treated with cisplatin (**C+**) and with complexes **6c**, **9d** and **10b** (1-10 μM) for 72 h.*

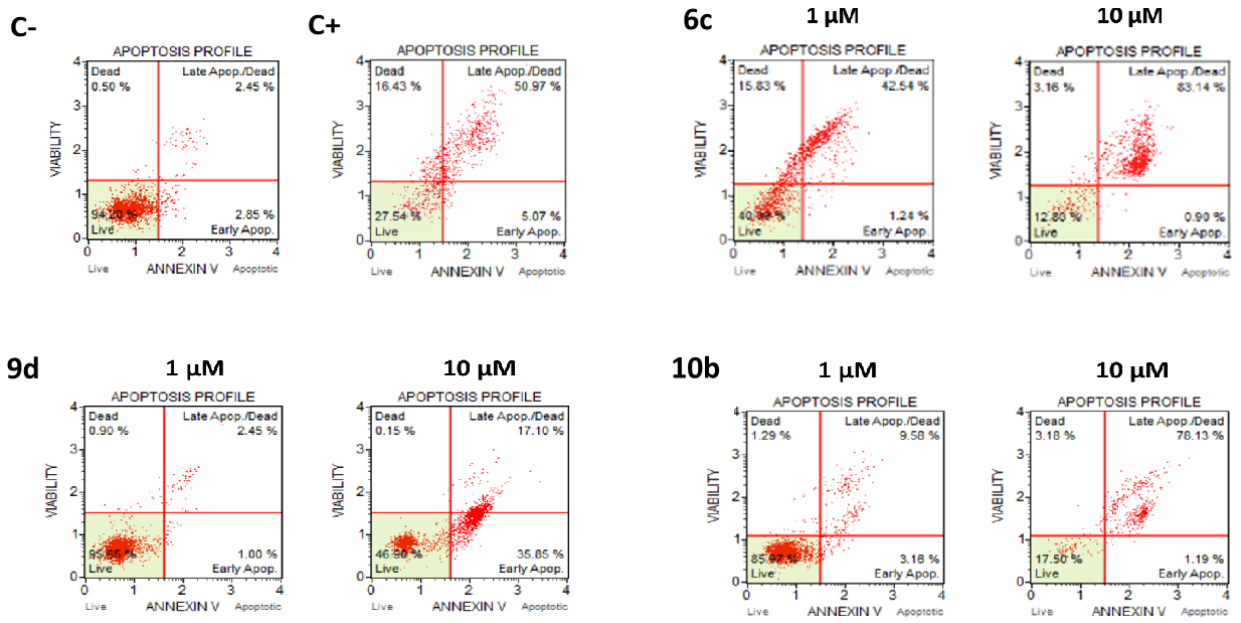

*Fig. 3.80 Representative apoptosis profile of SKOV-3 cells untreated (**C-**), treated with cisplatin (**C+**) and with complexes **6c**, **9d** and **10b** (1-10 µM) for 72 h.*

From the analysis of antiproliferative data, we can therefore conclude that the η^3-allyl complexes display a good activity against A2780 and SKOV-3 ovarian cancer cell lines. In particular, the species coordinating a purine-based NHC ligand and PPh_3 (mixed NHC/PPh_3 complexes) are the most active. Moreover the most active compounds on cancer cells are almost inactive on normal cells, suggesting a marked cancer selectivity.

Finally, it was proved that the antiproliferative activity of many of the synthesized complexes is associated with induction of apoptosis.

3.8.2. Activity of palladacyclopentadienyl complexes bearing purine-based NHCs toward ovarian cancer cell lines

The antiproliferative activity of the palladacyclopentadienyl complexes (compounds **11-14**) was tested on A2780 (cisplatin-sensitive) and A2780-R (cisplatin-resistant) tumour lines. A stock solution in DMSO (50 mM) was prepared for each compound and the working solutions were obtained by diluting the stock solution with ethanol. All complexes are stable for at least 48 hours at room temperature in dmso-d6. The antiproliferative activity data are reported in Table 3.4 , in which is also apparent the low activity of the $[PdC_4(COOCH_3)_4]_n$ precursor in both the lines (IC_{50} > 100 μM).

COMPLEX	**IC_{50} (μM)**	
	A2780	**A2780-R**
Cisplatin	0.6 ± 0.1	6 ± 1
$[PdC_4(COOCH_3)_4]_n$	>100	>100
11a	5.3 ± 0.7	6.7 ± 0.8
11b	5.0 ± 0.2	5.25 ± 0.05
11d	6.66 ± 0.03	16 ± 1
12a	4.3 ± 0.7	0.6 ± 0.2
12b	0.9 ± 0.1	1.0 ± 0.3
12d	0.56 ± 0.08	0.64 ± 0.07
13a	3.3 ± 0.6	2.1 ± 0.4
13b	1.6 ± 0.3	1.8 ± 0.9
13d	0.70 ± 0.05	0.87 ± 0.09
14a	9.0 ± 0.7	9.0 ± 0.7
14b	6.5 ± 0.5	6.5 ± 0.5
14d	81 ± 4	81 ± 4

Table 3.4 Effects of the palladacyclopentadienyl complexes on the proliferation of A2780 and A2780-R cells (72h). The inhibition of cell growth is represented as IC_{50}.

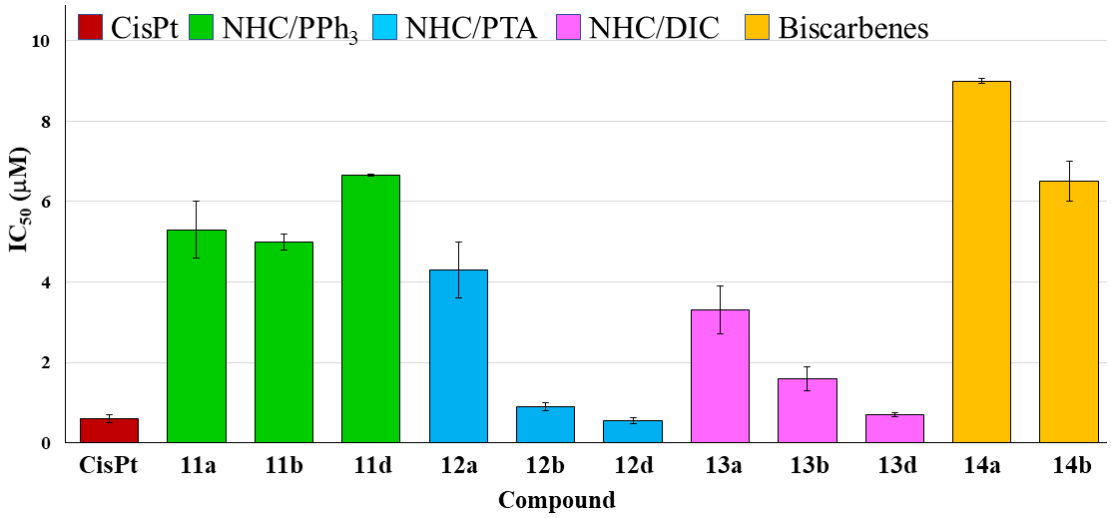

Fig. 3.81 Palladacyclopentadienyl complexes with IC_{50}<10 μM on A2780 cell line.

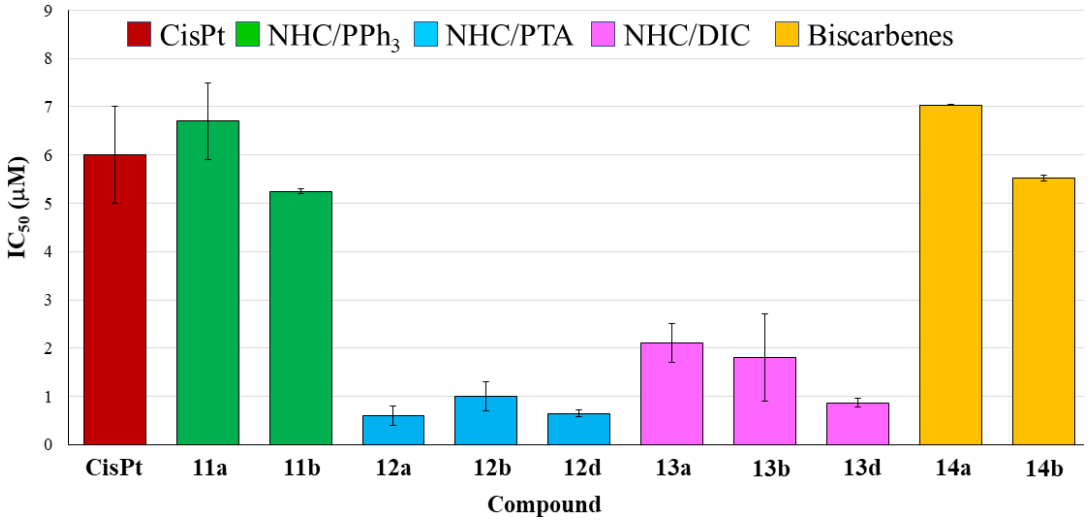

Fig. 3.82 Palladacyclopentadienyl complexes with IC_{50}<8 μM on A2780-R cell line.

To test the selectivity of the palladacyclopentadienyl complexes *versus* cancer cells, normal human fibroblasts (MRC-5) were treated with two different complexes (**11b** and **12d**). As shown in Table 3.5, the compounds are poorly active (**11b**) or inactive (**12d**) on fibroblasts, suggesting a preferential activity on cancer cells.

Complex	**IC_{50} (μM)**
*Cis*platin	14 ± 1
11b	30 ± 15
12d	>100

Table 3.5 Effects of the palladacyclopentadienyl complexes on the proliferation of MRC-5 cells.

With regard to the proapoptotic effect for some representative compounds (**11b**, **12d**, **13d** and **14b**) the percentage of total apoptosis was reported in Table 3.6.

COMPLEX	Total apoptosis (%)	
	A2780	A2780-R
C-	6.0	11.3
Cisplatin	19.5 (0.6 μM) 16.9 (1.2 μM)	48.1 (6 μM) 68.0 (12 μM)
11b	97.3 (5 μM) 95.8 (7.5 μM)	91.0 (5 μM) 92.0 (8 μM)
12d	53.2 (0.6 μM) 87.2 (0.8 μM)	34.8 (0.6 μM) 52.3 (0.9 μM)
13d	8.8 (0.7 μM) 19.25 (1 μM)	17.4 (0.9 μM) 15.4 (1.3 μM)
14b	96.0 (6.5 μM) 95.8 (9 μM)	14.6 (5.5 μM) 23.7 (8.5 μM)

Table 3.6 Pro-apoptotic effects of palladacyclopentadienyl complexes (C-: untreated cells).

The analysis of data shows that compounds **11b**, **12d** and **14b** have an excellent pro-apoptotic activity at concentrations between 0.8 and 6.5 μM on the A2780 line. In particular, the total apoptosis (early and late) stands at between 87 and 97%. Furthermore, compound **12d** shows the greatest total pro-apoptotic activity even with the lowest tested concentration (0.6 μM, total apoptosis = 53%).
In the case of the A2780-R cell line, complexes **11b** and **12d** are those with the greater percentages of total apoptosis; however, the value between 52 and 92% is smaller than that found for the cisplatin-sensitive line.
On the basis of the above results the following considerations can be proposed:

1. The compounds with the best antiproliferative activity are the mixed NHC/DIC and NHC/PTA complexes. The latter compounds are particularly interesting since the only soluble in water among those texted. The less active complexes are the biscarbene derivatives. In detail, it was possible to observe the following activity trend:

   $$\text{NHC/PTA, NHC/DIC} > \text{NHC/PPh}_3 > \text{Bis(NHC)}$$

2. For the same spectator ligand (PPh_3, DIC or PTA), there is no general trend that correlates antiproliferative activity with the type of N-substituents present in the carbenic fragment.

3. For the same compound, the IC_{50} values regarding the two different cell lines are in many cases comparable. This fact seems to indicate that the mechanism of action of the palladacyclopentadienyl complexes might be different from that proposed for cisplatin.

4. With regard to the cisplatin-sensitive A2780 cell line, compounds **12b** and **12d** (NHC/PTA) and **13d** (NHC/DIC) have IC_{50} values comparable to cisplatin.

5. As for the cisplatin-resistance A2780-R line, there are four compounds (**11a-b** and **14a-b**) that have activity comparable to cisplatin and six (**12a-b**, **12d**, **13a-b** and **13d**) which are more active. These values are very interesting if compared with the most active Pd complexes reported in the literature [28].

6. It was proved that the antiproliferative activity of many of the synthesized complexes is associated with induction of apoptosis.

3.8.3. Activity of Pd(0) olefin complexes with purine-based NHCs toward ovarian cancer lines

The antiproliferative activity of Pd(0) olefin compounds was tested on A2780 (cisplatin-sensitive) and A2780-R (cisplatin-resistant) tumour lines. A stock solution in DMSO (50 mM) was prepared for each compound and the working solutions were obtained by diluting the stock solution with ethanol (complexes **15-24)** or water (bis-PTA complexes **25-28**).

The stability of complexes was preliminarily checked in D_2O (**25-28**) or dmso-d6 (**15-24**): after 48 hours at room temperature no degradation and no ligand replacement was observed. The antiproliferative activity data are reported in Table 3.7, expressed as IC_{50}.

Complex	**IC_{50} (μM)**	
	A2780	**A2780-R**
Cisplatin	0.6 ± 0.1	6 ± 1
15a	8 ± 3	34 ± 2
15b	5.4 ± 0.8	5.4 ± 0.1
15d	4.8 ± 0.7	6.1 ± 0.5
16a	4.7 ± 0.4	4.7 ± 0.3
17a	0.8 ± 0.2	4.8 ± 0.2
19a	6.3 ± 0.8	48.4 ± 0.6
19b	5.0 ± 0.7	38.7 ± 0.9
19d	4.4 ± 0.9	6.7 ± 0.3
20a	5.5 ± 0.2	3.8 ± 0.7
21a	37 ± 3	23.9 ± 0.3
23a	6.7 ± 0.2	51.3 ± 0.4
23b	10 ± 0.2	49.4 ± 0.7
23d	5.7 ± 0.4	43.9 ± 0.9
24a	4.7 ± 0.6	1.1 ± 0.1
25	31 ± 1	0.8 ± 0.2
26	2.9 ± 0.5	5.4 ± 0.5
27	31 ± 1	8.7 ± 0.1

Table 3.7 Effects of Pd(0) olefin complexes on the proliferation of A2780 and A2780-R cells (72h).

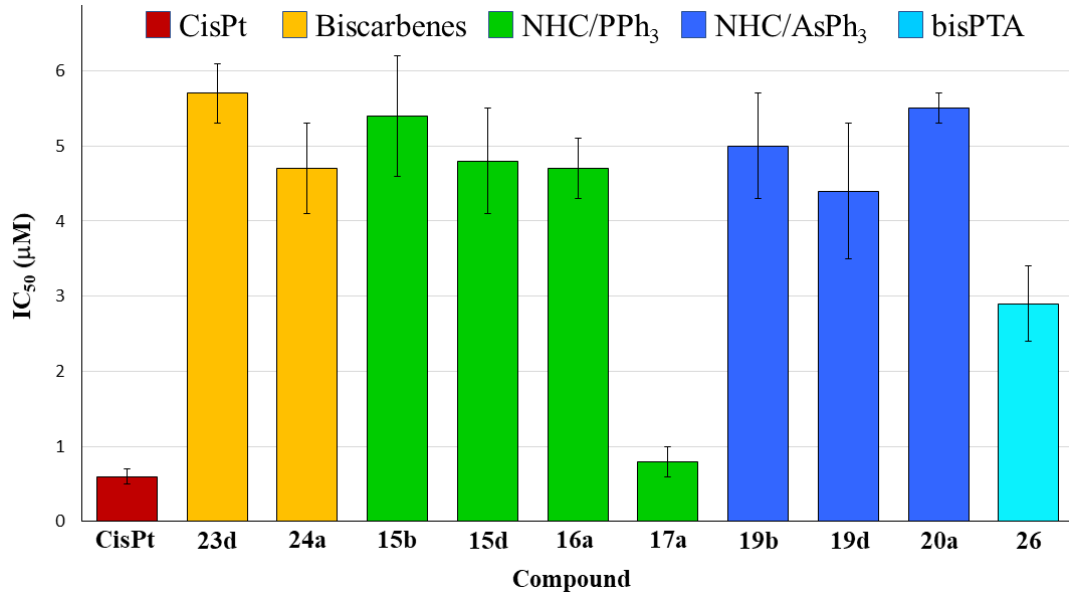

Fig. 3.83 Pd(0) olefin complexes with IC_{50}<6 µM on A2780 cell line.

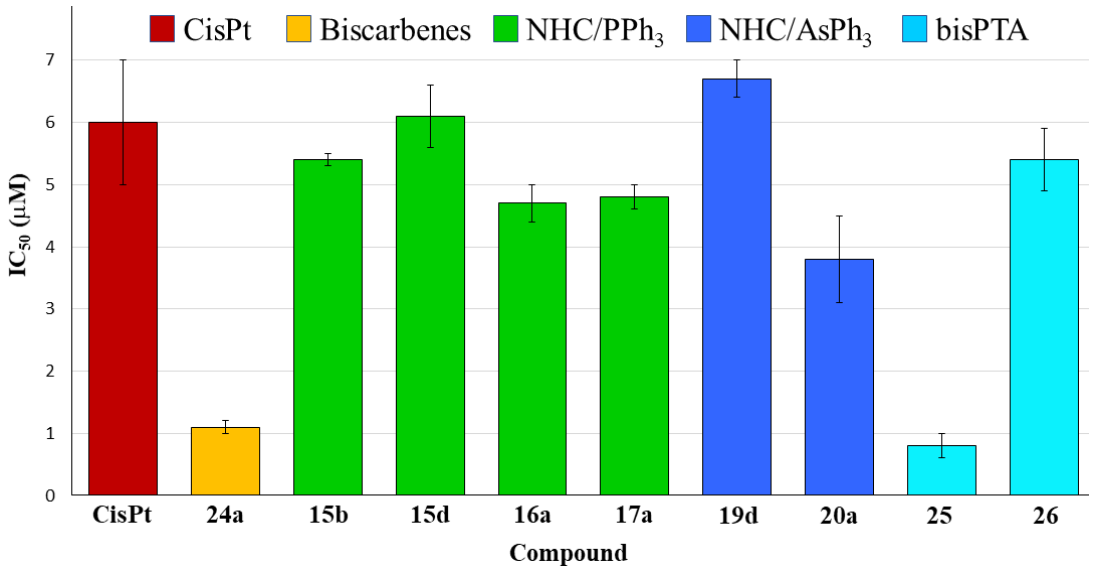

Fig. 3.84 Pd(0) olefin complexes with IC_{50}<8 µM on A2780-R cell line.

From the analysis of IC_{50} values, we can propose the following general considerations:

1. The compounds having a carbene and a triphenylphosphine ligand (mixed NHC/PPh_3 complexes) show the best antiproliferative activity on both cell lines. A similar result has been obtained with the Pd (II) allyl complexes (see paragraph 3.8.1).

2. As for the A2780 line (cisPt sensitive) only one complex (**17a**) shows activity comparable to that of cisplatin, while for A2780-R line, the number of compounds able to equal its performance is higher (**15b**, **15d**, **16a**, **17a**, **19d**, **20a** and **26**); two of the synthesized complexes (**24a** and **25**) are definitely better than cisplatin. The results of compound **25** appear particularly interesting for the water-solubility of the complex, an important feature for a potential biomedical agent.

3. With regard to the A2780 line, the change of the cordinated olefin in complexes with the same spectator ligands does not influence the activity of the complex. Likewise, maintaining the same type of olefin (tmetc) and changing the type of carbene ligand, there are no substantial differences in terms of activity.

4. With regard to the A2780-R line, for the same spectator ligands, the most efficient complexs are those coordinating fumaronitrile and maleic anhydride. On the other hand, complexes with tmetc are poorly active, with the sole exception of the bis-PTA complex.

5. Comparing the IC_{50} values obtained in the two different lines, we can observe that compounds coordinating the fumaronitrile maintain their antiproliferative activity. A similar trend is found in the complexes with maleic anhydride. The analogous complexes with tmetc, except for **15b**, **15d** and **19d**, instead reduce their activity passing from the cisplatin-sensitive line to the resistant one.

Pro-apoptotic effect

In Table 3.8 the percentage of total apoptosis was reported for some representative compounds (**15b**, **16a**, **17a, 20a, 24a, 25** and **26**) and each data was compared to the analysis of untreated cells (negative control, C-), in which the observed total apoptosis was less than 5%.

COMPLEX	Total apoptosis (%)	
	A2780	A2780-R
C-	3.7	10.9
Cisplatin	19.5 (0.6 μM) 16.9 (1.2 μM)	48.1 (6 μM) 68.0 (12 μM)
15b	4.4 (6 μM) 6.7 (9 μM)	8.3 (5 μM) 10.0 (9 μM)
16a	41.8 (5 μM) 88.2 (8 μM)	13.7 (5 μM) 35.3 (8 μM)
17a	6.9 (0.8 μM) 10.0 (1.2 μM)	15.2 (5 μM) 22.5 (8 μM)
20a	7.7 (6 μM) 14.8 (10 μM)	23.6 (4 μM) 13.2 (8 μM)
24a	64.4 (5 μM) 98.8 (8 μM)	48.1 (6 μM) 68.0 (12 μM)
25	7.2 (30 μM) 58.8 (70 μM)	10.8 (0.9 μM) 14.0 (1.4 μM)
26	6.8 (3 μM) 62.9 (7 μM)	23.2 (3 μM) 33.8 (8 μM)

Table 3.8 Pro-apoptotic effects of Pd(0) olefin complexes (C-: untreated cells)

The analysis of the results obtained for the A2780 line shows that compounds **16a**, **24a** and **26** have a good pro-apoptotic activity at concentrations between 5 and 8 μM. In particular, the total apoptosis (early and late) remains between 63% and 99%.

Also in the case of the A2780-R cell line, complexes **16a**, **24a** and **26** are those with the greater percentages of total apoptosis; however, the value between 30 and 35% is smaller than that found for the cisplatin-sensitive line.

3.9. Conclusions

In this chapter we have presented the synthesis and characterization of palladium η^3-allyl, η^2-olefin and palladacyclopentadienyl complexes containing purine-based NHC ligands. These complexes, which are stable both in the solid state and in solution, were tested toward ovarian cancer cell lines both cisplatin-sensitive and cisplatin-resistant. The results of the antiproliferative activity have highlighted that η^3-allyl palladium and palladacyclopentadienyl complexes are generally more active than η^2-olefn palladium (0) derivatives. Among the most active species, η^3-allyl complexes containing a NHC ligand and a triphenylphosphine and mixed NHC/PTA palladacyclopentadienyl compounds are especially promising. In fact, they display an excellent antiproliferative activity on the ovarian cancer lines and, at the same time, they are almost inactive on normal cells.

Moreover, the analysis of the proapoptotic activity showed that the most active complexes are able to promote programmed cell death (apoptosis). This process, unlike necrosis, is preferred because the system can recycle the cellular material avoiding or reducing inflammatory processes.

Encouraged by the results regarding the compounds with purine-based NHCs, we decided to extend our study also to η^3-allyl-palladium and palladacyclopentadienyl complexes stabilized by other types of NHCs. The synthesis of these classes of compounds and their biological activity will be presented in the successive chapters.

3.10. References

[1] (a) T.A.K. Al-Allaf, L.J. Rashan, *Eur. J. Med. Chem.*, 1998, **33**, 817; (b) A. Valentini, F. Conforti, A. Crispini, A. De Martino, R. Condello, C. Stellitano, G. Rotillo, M. Ghedini, G. Federici, S. Bernardini, D. Pucci, *J. Med. Chem.*, 2009, **52**, 484; (c) A. Monney, M. Albrecht, *Coord. Chem. Rev.*, 2013, **257**, 2420; d) M. Tanaka, H. Kataoka, S. Yano, H. Ohi, K. Kawamoto, T. Shibahara, T. Mizoshita, Y. Mori, S. Tanida, T. Kamiya, T. Joh, *BMC Cancer*, 2013, **13**, 327.

[2] H. Rosemeyer, *Chem. Biodivers.*, 2004, **1** (3), 361.

[3] T.W. Stone, H.A. Simmonds, *Purines: Basic and Clinical Aspects*. Springer Netherlands, 1991.

[4] J.W. Daly, *Cell. Mol. Life Sci.*, 2007, **64**, 2153.

[5] T.T. Hansel, R.C. Tennant, A.J. Tan, L.A. Higgins, H. Neighbour, E.M. Erin, P.J. Barnes, *Drugs Today*, 2004, **40**, 55.

[6] (a) D. Petch, R.J. Anderson, A. Cunningham, S.E. George, D.E. Hibbs, R. Liu, S.P. Mackay, A. Paul, D.A.P. Small, P.W. Groundwater, *Bioorg. Med. Chem.*, 2012, **20**, 5901; (b) C. Siering, H. Kerschbaumer, M. Nieger, S. R. Waldvogel, *Org. Lett.*, 2006, **8**, 1471; (c) F. G. Lupascu, O. M. Dragostin, L. Foia, D. Lupascu, L. Profire, *Molecules*, 2013, **18**, 9684.

[7] (a) E.I. Ivanov, G.D. Kalayanov, I.M. Yaroshchenko, D.E. Stepanov, *Khim. Geterotsikl. Soedin*, 1989, **11**, 1570; (b) J. Schutz, W.A. Herrmann, *J. Organomet. Chem.*, 2004, **689**, 2995.

[8] E. Mohammadi, B. Movassagh, *J. Mol. Cat. A*, 2016, **418**, 158.

[9] V.R. Landaeta, R.E. Rodriguez-Lugo, E.N. Rodriguez-Arias, D.S. Coll-Gomez, T. Gonzalez, *Transition Met. Chem.*, 2010, **35**, 165.

[10] J. Schutz, W.A. Herrmann, *J. Organomet. Chem.*, 2004, **689**, 2995.

[11] J.J. Zhang, J.K. Muenzner, M.A. Abu El Maaty, B. Karge, R. Schobert, S. Wolfl, I. Ott, *Dalton Trans.*, 2016, **45**, 13161.

[12] (a) A.K. Nebioglu, A. Melaiye, K.M Hindi, S. Durmus, M.J. Panzner, L.A. Hogue, R.J. Mallet, C.E. Hovis, M. Coughenour, S.D. Crosby, A. Milsted, D.L. Ely, C.A. Tessier, C.L. Cannon, W.J. Youngs, *J. Med. Chem.*, 2006, **49**, 6811; (b) H.A. Mohamed, B.R.M. Lake, T. Laing, R.M. Phillips, C.E. Willians, *Dalton Trans.*, 2015, **44**, 7563.

[13] K.M. Hindi, M.J. Panzner, C.A. Tessier, C.L. Cannon, W.J. Youngs, *Chem. Rev.*, 2009, **109** (8), 3859.

[14] A. Szadkowska, S. Staszko, E. Zaorska, R. Pawlowski, *RSC Adv.*, 2016, **6**, 44248.

[15] (a) J.J. Zhang, C.M. Che, I. Ott, *J. Organomet. Chem.*, 2015, **782**, 37; (b) M. Skander, P. Retailleau, B. Bourriè, L. Schio, P. Mailliet, A. Marinetti, *J. Med. Chem.*, 2010, **53**, 2146.

[16] B. Bertrand, L. Stefan, M. Pirrotta, D. Monchaud, E. Bodio, P. Richard, P.L. Gendre, E. Warmerdam, M.H. De Jager, G.M.M. Groothuis, M. Picquet, A. Casini, *Inorg. Chem.*, 2014, **53**, 2296.

[17] E. Mohammadi, B. Movassagh, *J. Organomet. Chem.*, 2016, **822**, 62.

[18] H. E. Affsprung, V.S. Archer, *Anal. Chem.*, 1964, **36 (13)**, 2512-2513; (b) M.J. Smith, S.E. Manahan, *Anal. Chim. Acta*, **48**, 1969, 315.

[19] P. de Fremont, N.M. Scott, E.D. Stevens, T. Ramnial, O.C. Lightbody, C.L.B. Macdonald, J.A.C. Clyburne, C.D. Abernethy, S.P. Nolan, *Organometallics*, 2005, **24**, 6301.

[20] I. J. B. Lin, C. S. Vasam, *Coord. Chem. Rev.*, 2007, **251**, 642.

[21] L. Canovese, F. Visentin, G. Chessa, P. Uguagliati, G. Bandoli, *Organometallics*, 2005, **24**, 3297.

[22] S. N. Sluijter, S. Warsink, M. Lutzc, C. J. Elsevier, *Dalton Trans.*, 2013, **42**, 7365.

[23] (a) L. Canovese, F. Visentin, G. Chessa, P. Uguagliati, A. Dolmella, *J. Organomet. Chem*, 2000, **601**, 1; (b) L. Canovese, F. Visentin, P. Uguagliati, B. Crociani, *J. Chem. Soc. Dalton Trans.*, 1996, 1921; (c) L. Canovese, C. Santo, F. Visentin, *Organometallics*, 2008, **27**, 3577; (d) L. Canovese, F. Visentin, C. Biz, T. Scattolin, C. Santo, V. Bertolasi, *Polyhedron*, 2015, **102**, 94.

[24] (a) L. Canovese, F. Visentin, G. Chessa, P. Uguagliati, C. Levi, A. Dolmella, *Organometallics*, 2005, **24**, 5537; (b) L. Canovese, F. Visentin, P. Uguagliati, G. Chessa, A. Pesce, *J. Organomet. Chem.*, 1998, **566**, 61.

[25] L. Canovese, C. Santo, T. Scattolin, F. Visentin, V. Bertolasi, J. *Organomet. Chem.*, 2015, **794**, 288.

[26] (a) E. Guerrero, S. Miranda, S. Luttenberg, N. Frohlich, J.M. Koenen, F. Mohr, E. Cerrada, M. Laguna, A. Mendia, *Inorg. Chem.*, 2013, **52**, 6635; (b) M. Carreira, R. Calvo-Sanjuaı`n, M. Sanauı`, I. Marzo, M. Contel, *Organometallics*, 2012, **31**, 5772.

[27] ECACC (*European Collection of authenticated cell cultures*) (http://www.pheculture collections.org.uk/products/celllines/generalcell/detail.jsp?refId=93112519&collection=ecac c_gc).

[28] T.T. Fong, C. Lock, C.Y. Chung, Y.E. Fung, P. Chow, P. Wan, C. Che, *Angew. Chem. Int. Ed.*, 2016, **55**, 11935.

4

Pd complexes with “Classical” NHCs and Bridged BisNHCs

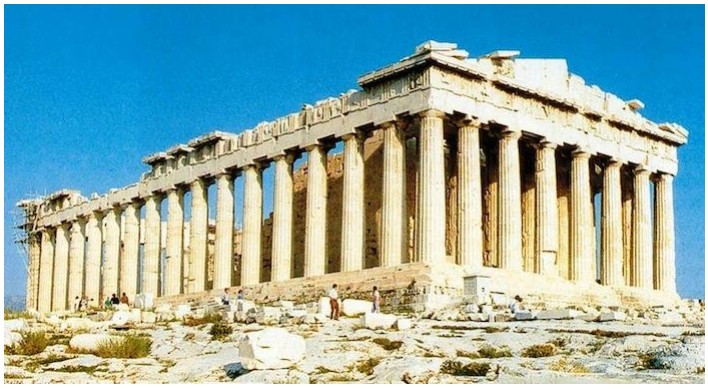


In this chapter the synthesis and evaluation of the antitumor activity of complexes bearing imidazole derived NHC ligands and η^3-allyl-Pd(II) or palladacyclopentadienyl organometallic fragments will be examined. As already stated, these classes of compounds, seem to be more promising than the Pd (0) olefin derivatives. In addition to the results related to their synthesis and biological activity, some connected kinetic and thermodynamic aspects will be discussed in detail.

Their anticancer activity has been evaluated not only against ovarian carcinoma lines but also toward lung, colon cancer and malignant melanoma lines. Moreover, a possible correlation between their antiproliferative activity and structure will be hypothesized.

Finally, the activity of the examined complexes toward healthy cell (fibroblasts) and some tests aimed at identifying the main bio-target and the probable mechanism of action of some particularly promising compounds, will be discussed.

The figures proposed at the beginning of the chapter are related to these sources: https://rickardha.deviantart.com/art/Roman-Bridge-363826754 and http://greece.greekreporter.com/2014/07/14/10-must-see-ancient-greek-temples/

4.1. Introduction

As mentioned in paragraph 1.4, the most common ("classical") *N*-Heterocyclic Carbene ligands are obtained by functionalization of imidazole (Fig. 4.1).

Fig. 4.1 General structure of NHC derived from the imidazole ring.

It was also emphasized that the bulkiness of such ligands can be easily modified by the steric demand of the substituents R whereas their electronic characteristics are of difficult modulation, since R substituents are not directly linked to the carbenic carbon and summing up NHCs act basically as strong σ-donor ligands. However, the versatility of these ligands can be increased by the inclusion of R substituents bearing another coordinating function. Thus, the presence of one or more additional donor atoms renders these species potentially bi- or poly-dentate ligands. Moreover, from another point of view, additional donor atoms may act as free Lewis bases and interact with sites present in the biological environment.

In this chapter, the classical alkyl and aryl imidazoles together with the NHC ligands characterized by thioethers (C-S ligands) or pyridine (C-N ligands) residue will be described (Fig. 4.2).

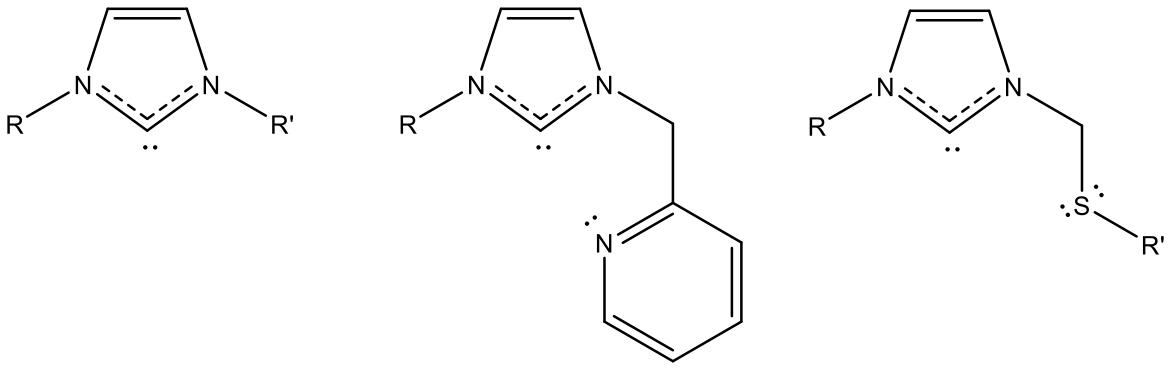

Fig. 4.2 Structure of NHC and hemi-labile NHC-pyridine or NHC-thioether ligands.

As a part of the whole work, the synthesis of complexes with bidentate biscarbene ligands will be dealt with (Fig. 4.3). In this respect, it is important to know that the nature of the bridging group **Y** is a crucial element in determining the coordination mode (chelate vs. bridging).

Generally speaking, these compounds are good σ-donor ligands and moreover, thanks to the chelating effect, they bind very strongly the metal center.

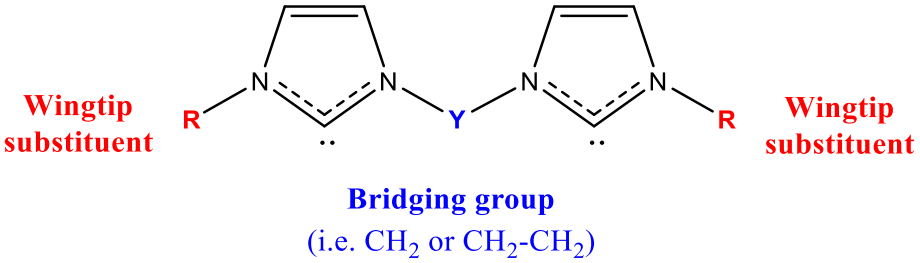

Fig. 4.3 Structure of bidentate bisNHCs.

In this regard, many examples of palladium and other transition metals derivatives stabilized by this class of ligands are well known [1]. The catalytic activity [2] and the optical properties (i.e. photoluminescence) of these species [3] have been extensively explored, whereas their biological activity has been remarkably less studied [4]. As an example, some compounds present in the literature and their applications are reported in Fig. 4.4.

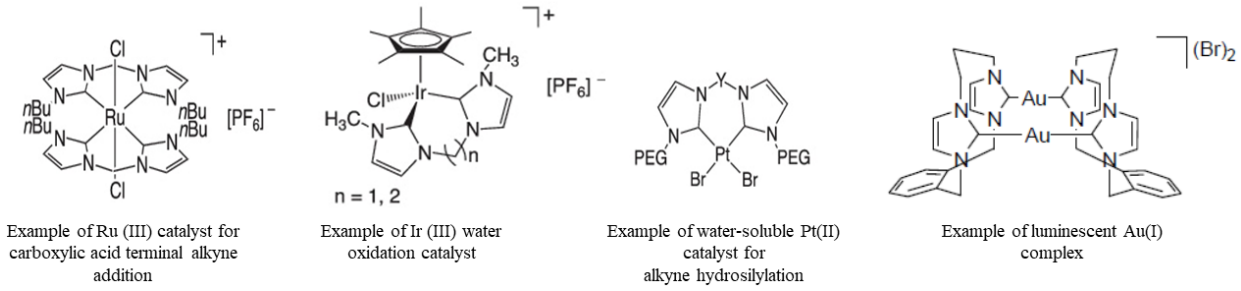

Fig. 4.4 Structure of bidentate bisNHC complexes with catalytic and optical proprieties [131-133].

In the following paragraphs the multi-step synthesis of complexes bearing imidazole derivatives will be discussed.

4.2. Synthesis of the imidazolium and bisimidazolium salts

The imidazolium salts used as precursors of the NHC ligands described in this chapter can be divided into four categories (Fig. 4.5).

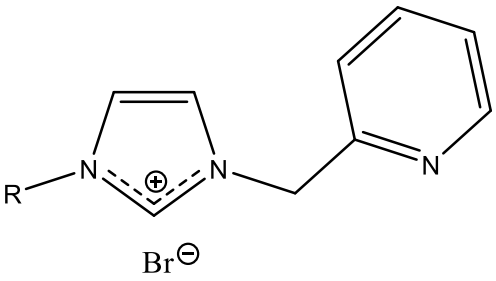

$Br^{\ominus}$

R= CH_3, Mes **(29a-b)**

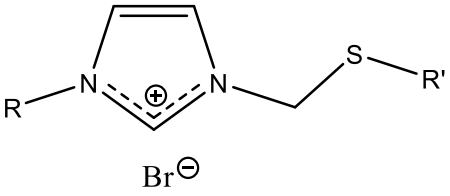

$Br^{\ominus}$

R= CH_3	R'= CH_3	**(30a)**
R= CH_3	R'= Ph	**(30b)**
R= Mes	R'= CH_3	**(30c)**
R= Mes	R'= Ph	**(30d)**

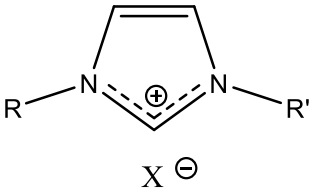

$X^{\ominus}$

R= CH_2Tol	R'= CH_2Tol	X= Br	**(31a)**
R= Mes	R'= Mes	X= Cl	**(31b)**
R= CH_3	R'= Bn	X= Br	**(31c)**
R= CH_3	R'= CH_2Tol	X= Br	**(31d)**

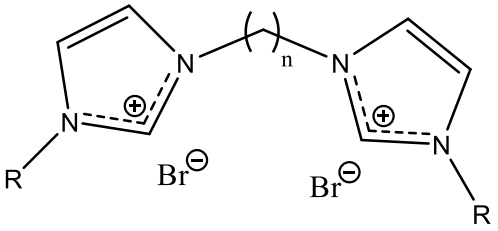

$Br^{\ominus}$ $Br^{\ominus}$

R= Bn	n= 1, 2	**(34a-b)**
R= Mes	n= 1, 2	**(34c-d)**
R= CH_3	n= 1, 2	**(34e-f)**

Fig. 4.5

The synthesis of compounds with one imidazole ring, apart from the commercially available IMesHCl (compound **31b**), was carried out by reacting an imidazole derivative (Me-Imidazole, Mes-Imidazole [5] or TolCH_2-Imidazole [6]) with a suitable alkylating agent (alkyl chlorides or bromides), under the experimental conditions shown in Scheme 4.1 [7].

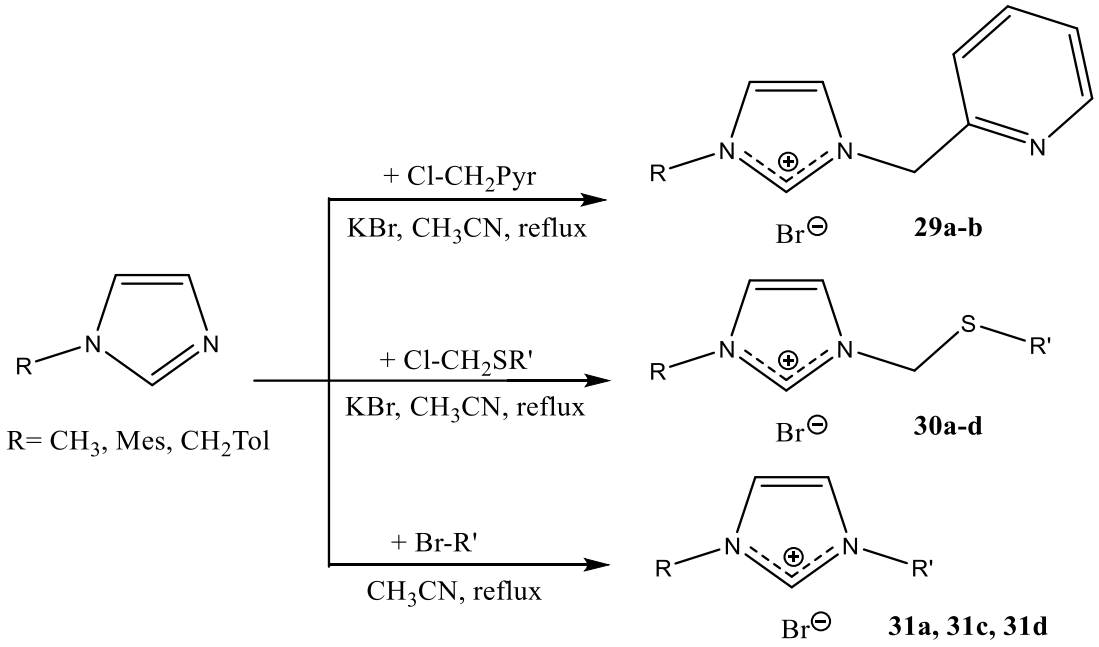

Scheme 4.1

The bis-imidazolium salts (**34a-d**) were prepared starting from Methyl-Imidazole, Benzyl-Imidazole or Mesityl-Imidazole by reaction with dibromo-methane or dibromo-ethane as reported by Lee and co-workers, according to the Scheme 4.2 [8].

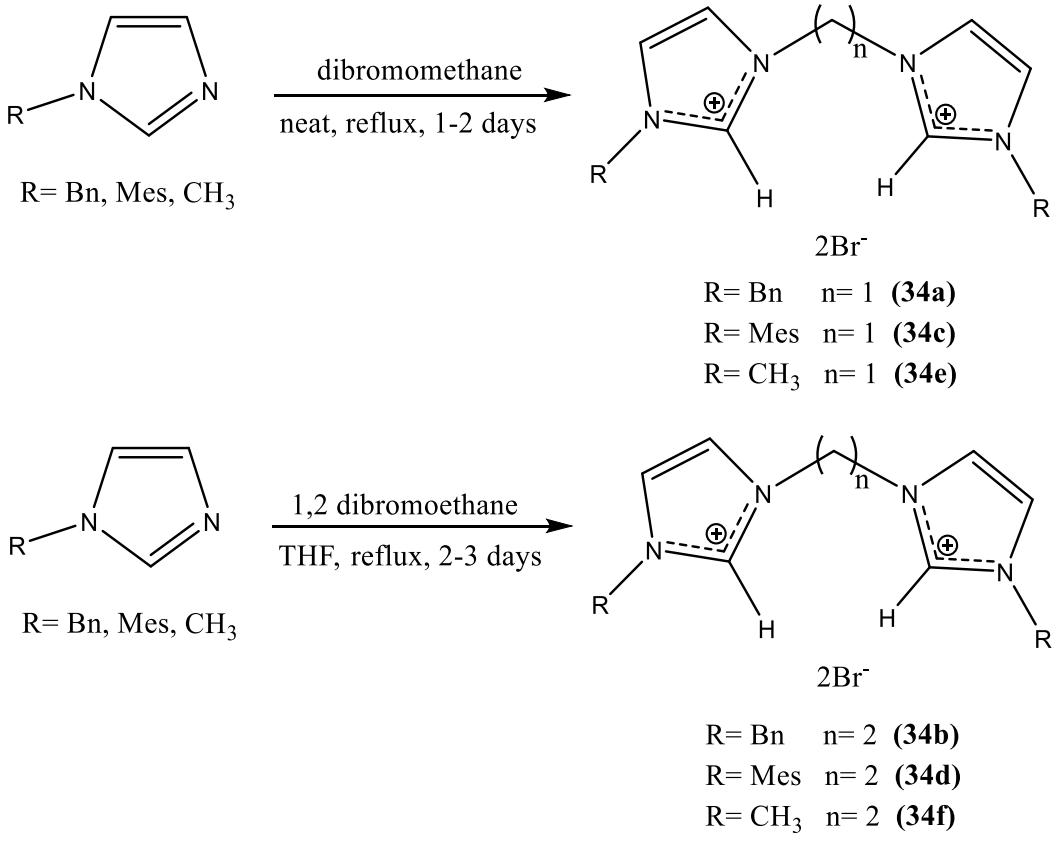

Scheme 4.2

4.3. Synthesis of the silver-NHC complexes

The synthesis of the silver complexes bearing only one imidazole unit, was carried out according to the protocols reported in the literature [7d-e], by reacting the imidazolium salts **29a-b**, **30a-d** and **31a-d** with 0.5 equivalents of silver oxide under the experimental conditions shown in Scheme 4.3.

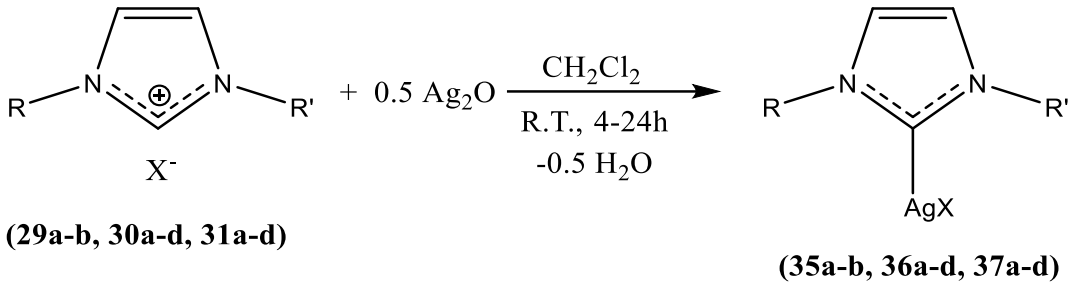

(29a-b, 30a-d, 31a-d) **(35a-b, 36a-d, 37a-d)**

Scheme 4.3

The reaction progress is evidenced by the progressive dissolution of the silver oxide. From the ^{1}H-NMR spectra of the isolated complexes, it is possible to observe the disappearance of the peak at ca. 9-11 ppm related to the NCHN proton (Fig. 4.6) whereas, in the ^{13}C-NMR spectra, the appearance of the signal of the coordinated carbenic carbon at about 170-190 ppm, is detected.

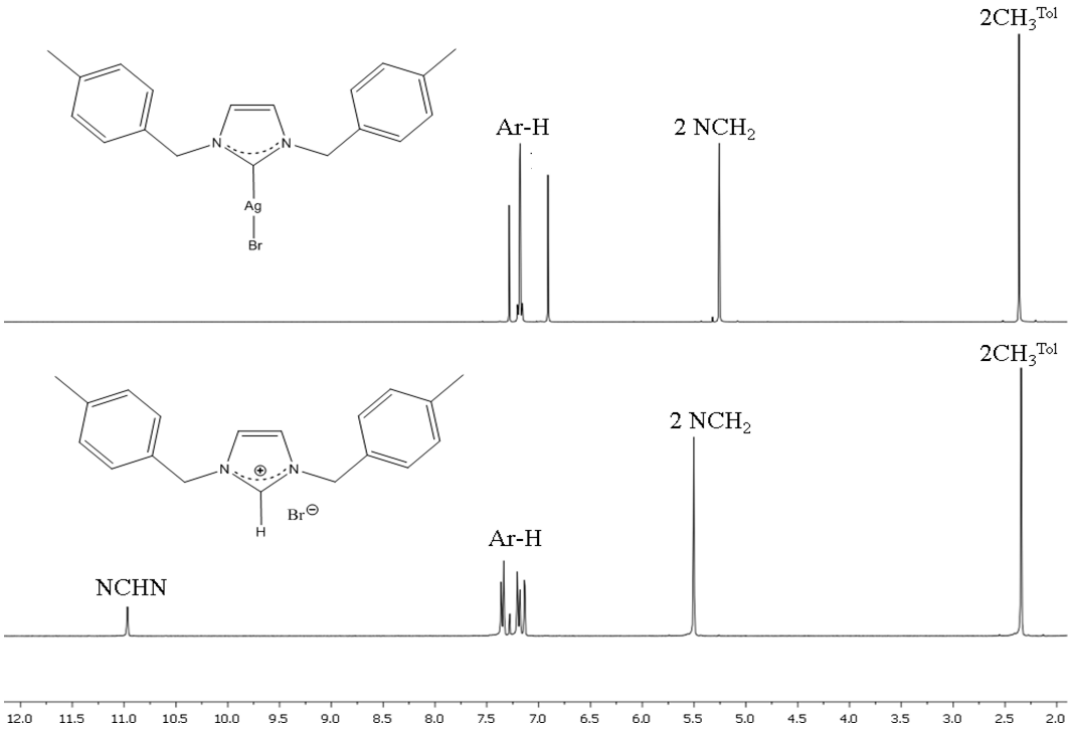

*Fig. 4.6 ^{1}H-NMR spectra of the silver complex **37a** and the imidazolium salt **31a** (T=298K, $CDCl_3$).*

The synthesis of the complexes with two imidazole units (bidentate bisNHC silver complexes), was carried out following the protocol reported by Slaughter and Chen [9]. Thus, the bisimidazolium salts **34a-f** were reacted with 1 equivalent of Ag_2O in methanol, in the case of the compounds with the methyl or benzyl residue, or in dichloromethane for compounds with the mesityl as wingtip substituent (Scheme 4.4.).

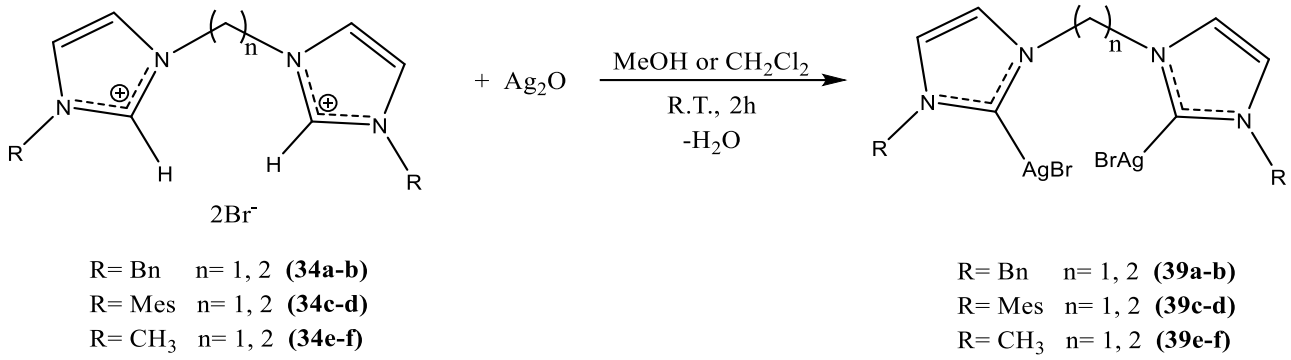

R= Bn n= 1, 2 **(34a-b)**
R= Mes n= 1, 2 **(34c-d)**
R= CH_3 n= 1, 2 **(34e-f)**

R= Bn n= 1, 2 **(39a-b)**
R= Mes n= 1, 2 **(39c-d)**
R= CH_3 n= 1, 2 **(39e-f)**

Scheme 4.4

The ^{1}H-NMR spectra show the disappearance of the central imidazole proton at ca. 9-11 ppm (see Fig. 4.7) and, in the ^{13}C-NMR spectra, the simultaneous appearance of the coordinated carbenic carbon signal between 170 and 190 ppm, is observed.

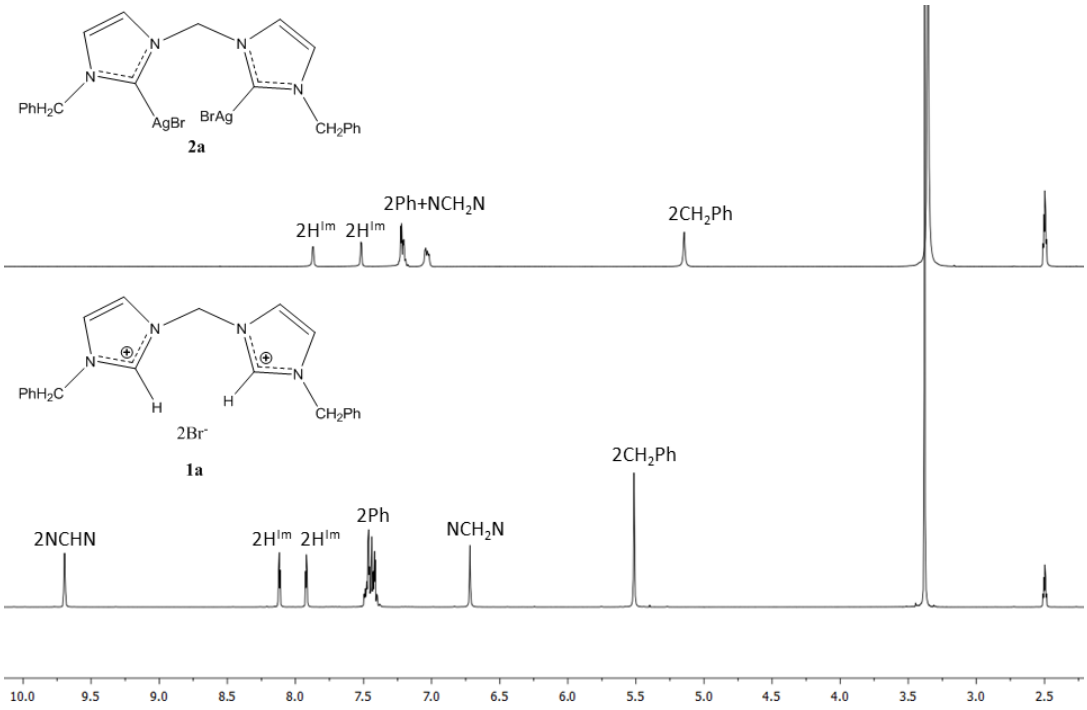

*Fig. 4.7 ^{1}H-NMR spectra of the silver complex **39a** and the imidazolium salt **34a** (T=298K, d_6-DMSO).*

It should be noted that the complexes with the mesityl group (**34c-d**) are present in solution as a mixture of oligomers, as pointed out in an article published by Slaughter and co-workers [9b].

4.4. Synthesis of palladacyclopentadienyl complexes

As already reported in section 3.6, the palladacyclopentadienyl complexes are generally obtained by addition of a bidentate ligand or two monodentate ligands to the polymeric precursor $[PdC_4(COOCH_3)_4]_n$. In the following section we will describe in detail the synthesis and characteristics of the palladacyclopentadienyl complexes reported in Fig. 4.8.

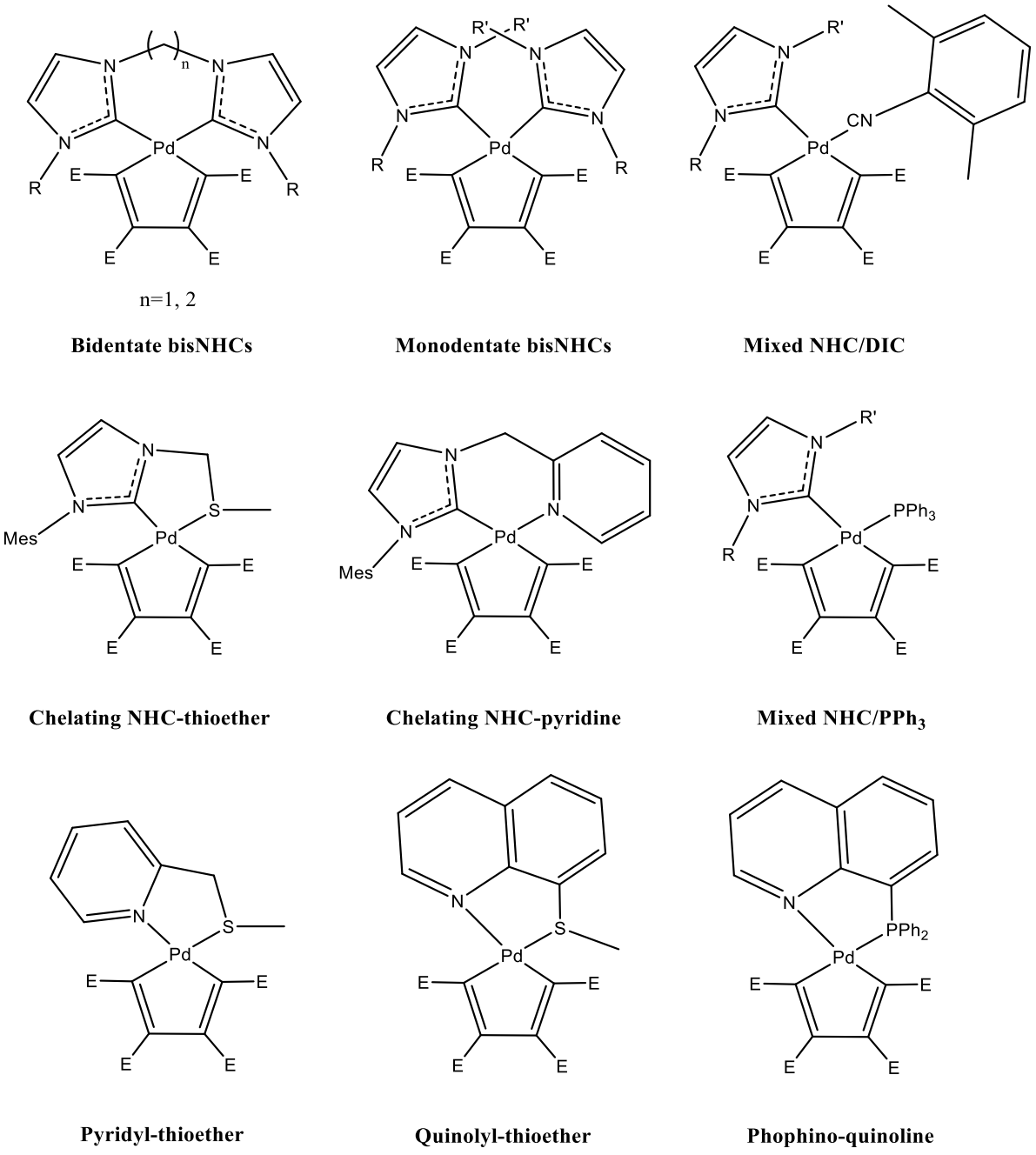

Fig. 4.8

4.4.1. Palladacyclopentadienyl complexes bearing bidentate bisNHCs

The possibility of inserting a bidentate bis-NHC ligand into the palladacyclopentadienyl fragment was preliminarily assessed by tests carried out in NMR tube. The following scheme 4.5 summarizes the results.

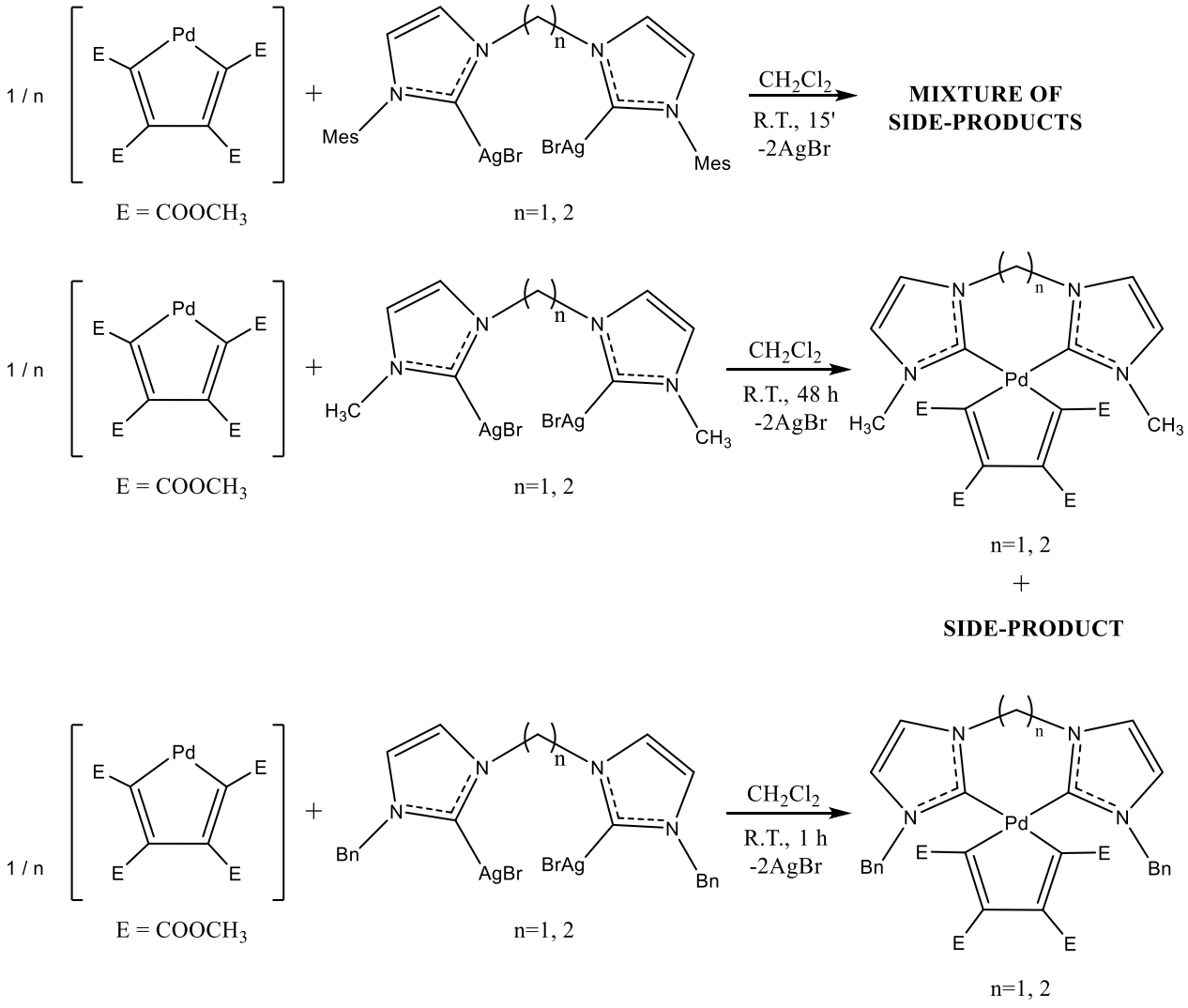

Scheme 4.5

These tests suggest that the exclusive formation of a pure product is possible only in the case of the bis-carbene with a benzyl as wingtip substituent.

The bis-carbene with the mesityl substituent, yields mixtures of products of difficult identification probably owing to its high steric bulkiness (Fig. 4.9).

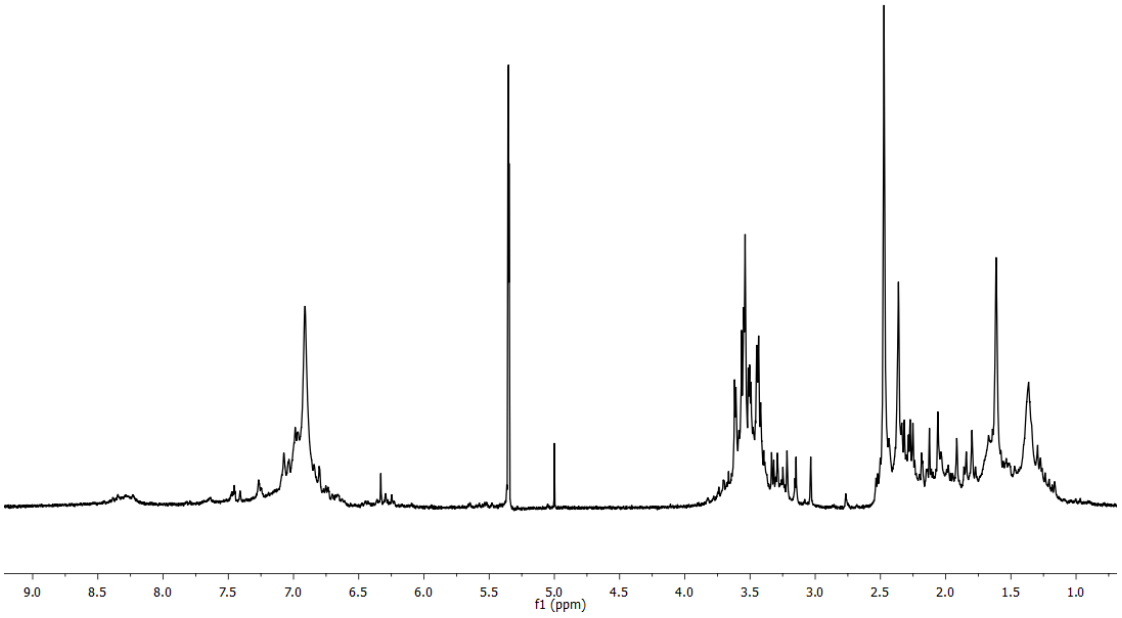

Fig. 4.9 ^{1}H-NMR spectra of the reaction between $[PdC_4(COOCH_3)_4]_n$ and the silver complex $[(MesImCH_2ImMes)Ag_2Br_2]$ in CD_2Cl_2 at T = 298 K.

The tests carried out with substrates having the methyl group as wingtips, indicate that the desired product is initially formed, but subsequently one side-product and traces of decomposition products are detected in the NMR spectra. After 48 hours, an equilibrium between the two species in the ratio (product/main side-product) of about 40/60 is reached (Fig. 4.10).

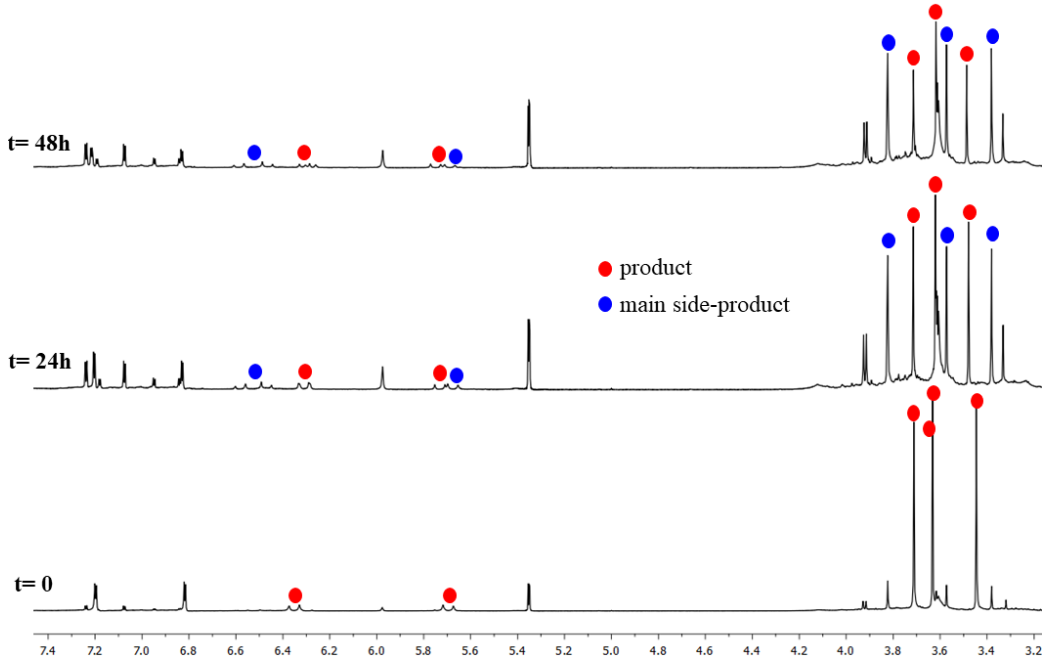

Fig. 4.10 ^{1}H-NMR spectra of the reaction between $[PdC_4(COOCH_3)_4]_n$ and the silver complex $[(CH_3ImCH_2ImCH_3)Ag_2Br_2]$ in CD_2Cl_2 at T = 298 K.

From the analysis of the NMR spectra (Fig. 4.10), we can argue that the main side-product shows the same number of signals than that of the product of interest and it should therefore be a species with a high degree of symmetry. Our formulated hypothesis suggests the formation of a dimeric species, in which the bidentate bisNHC acts as a bridged ligand between the two palladacyclopentadienyl fragments. Two different structures are possible for this dimeric species (Fig 4.11) and, between the two, the compound **B** (C_s symmetry) is more stable than the sterically hindered complex **A**, as confirmed by DFT calculations ($\Delta G° = 14.6$ kcal/mol).

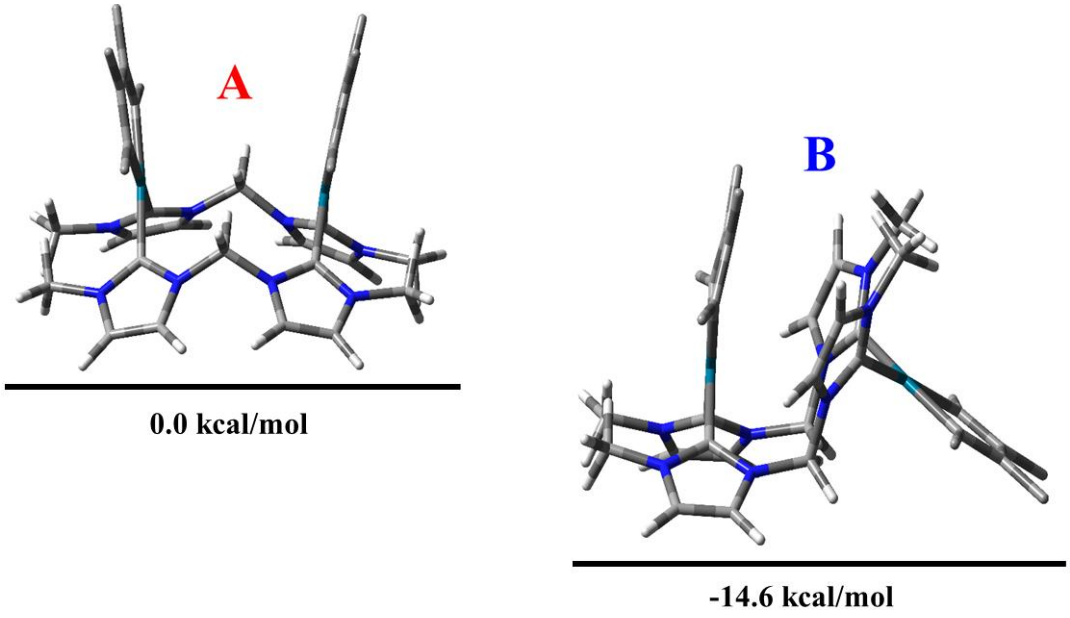

Fig. 4.11 Representation of the two isomers of the dimeric species by means of DFT calculations (COOCH$_3$ groups are not shown to simplify the figure).

Complex **B** is also slightly more stable than the wanted monomeric species ($\Delta G° = -0.9$ kcal/mol). Such difference in energy justifies the coexistence of the monomer and the dimer observed by NMR spectroscopy (Scheme 4.6).

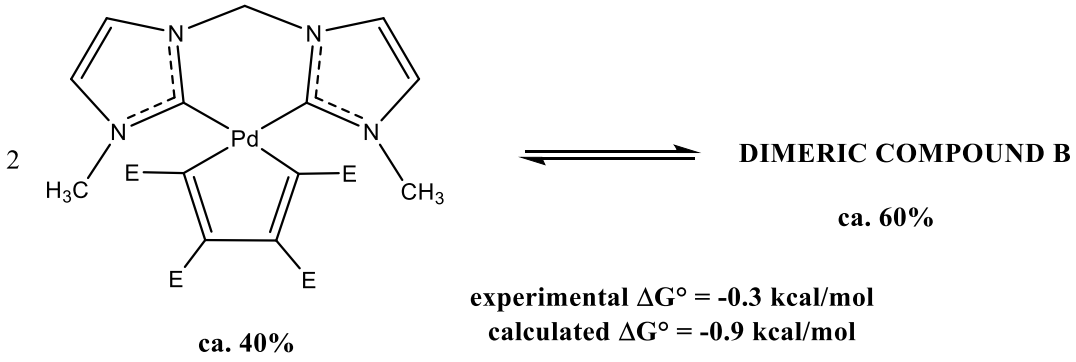

Scheme 4.6

The synthesis of the substrates bearing the bidentate NHC ligand with the benzyl wingtip groups and the palladacyclopentadienyl fragment (complexes **40a-b)**, carried out under the conditions reported in Scheme 4.7, was successfully performed.

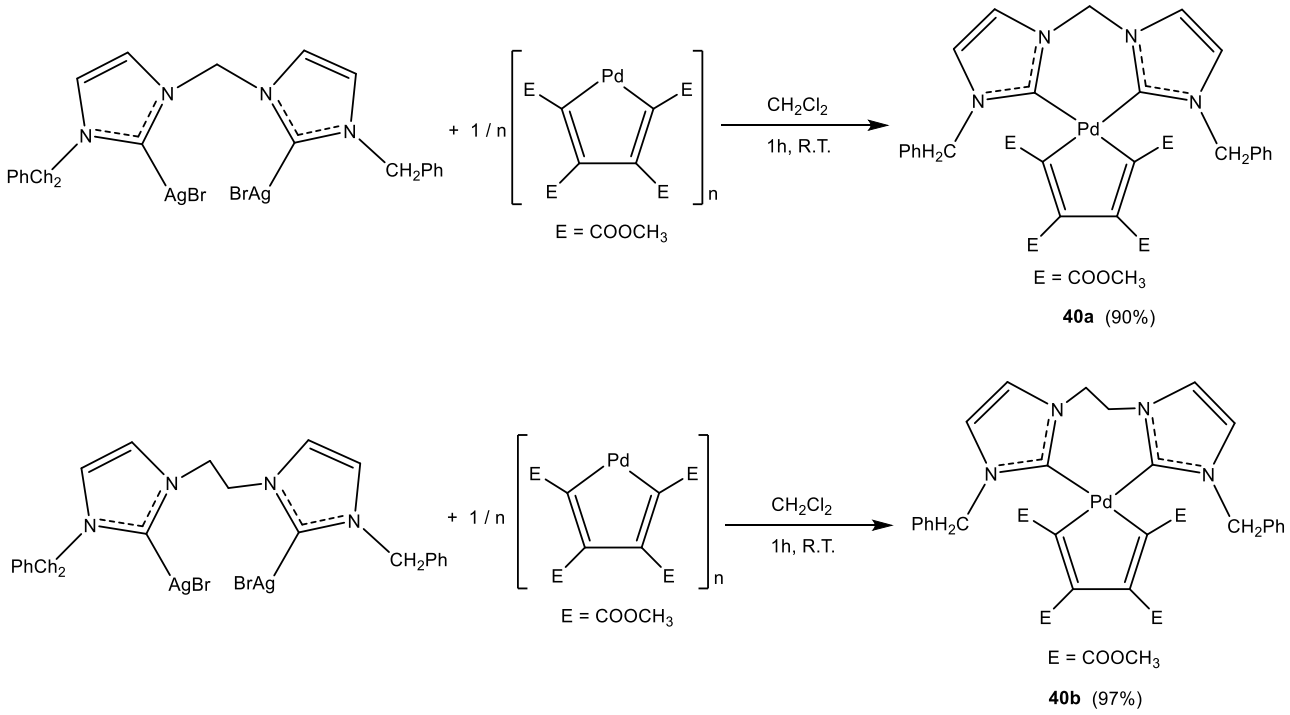

Scheme 4.7

The final compounds were isolated, after filtration of the AgBr, by precipitation from a CH_2Cl_2/ Et_2O mixture and characterized by elemental analysis, NMR and IR spectroscopy.

As for the compound **40a**, in the ^{1}H-NMR spectra (Fig. 4.12) we observe:

- The presence, between 3 and 4 ppm, of two signals ascribable to the two distinct pairs of OCH_3 groups.
- The presence of two AB systems, one between 5 and 6 ppm (J = 15 Hz) related to the methylene protons of the terminal benzyl groups, the other, between 6 and 6.5 ppm (J = 13.6 Hz), ascribable to the methylene bridged protons between the two carbenic fragments.

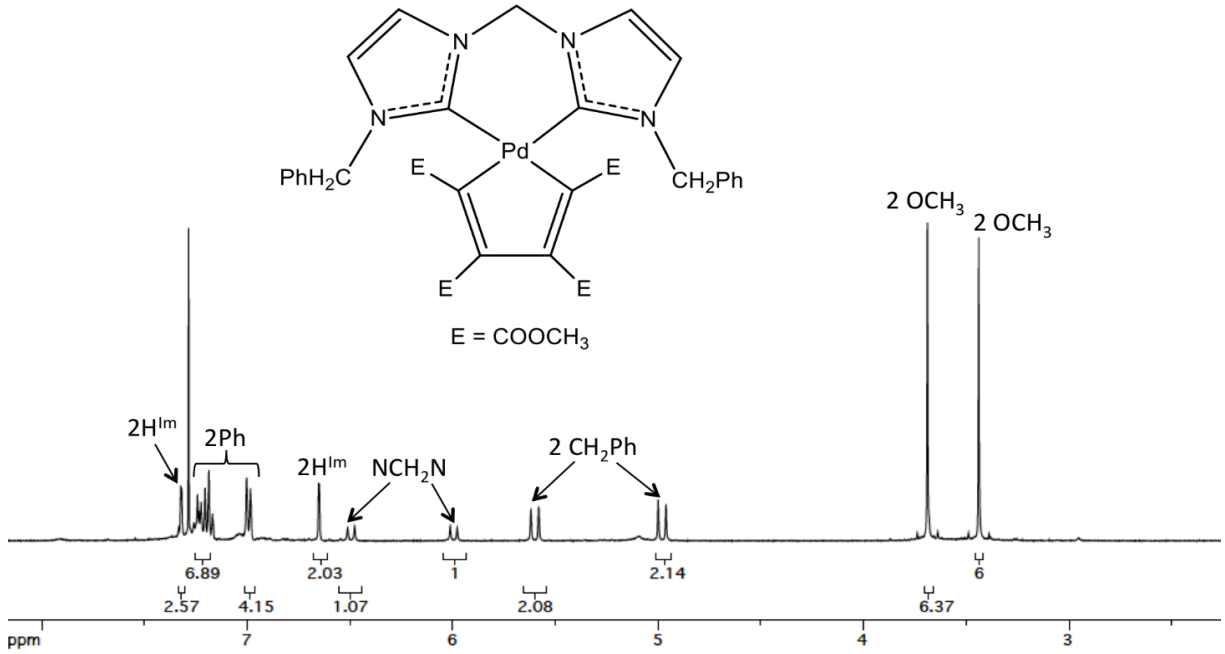

*Fig. 4.12 [1]H-NMR spectrum of the complex **40a** (T=298K, $CDCl_3$).*

The [1]H-NMR spectrum (Fig. 4.13) of the compound **40b** shows the presence of the two distinct groups of OCH_3 protons between 3 and 4 ppm (similarly to compound **40a)**, an AB system at about 5.2 ppm (J = 15.4 Hz) related to the methylene protons of the lateral benzyl groups and two multiplets at about 4.3 and 5.3 ppm ascribable to the protons of the ethylene bridge.

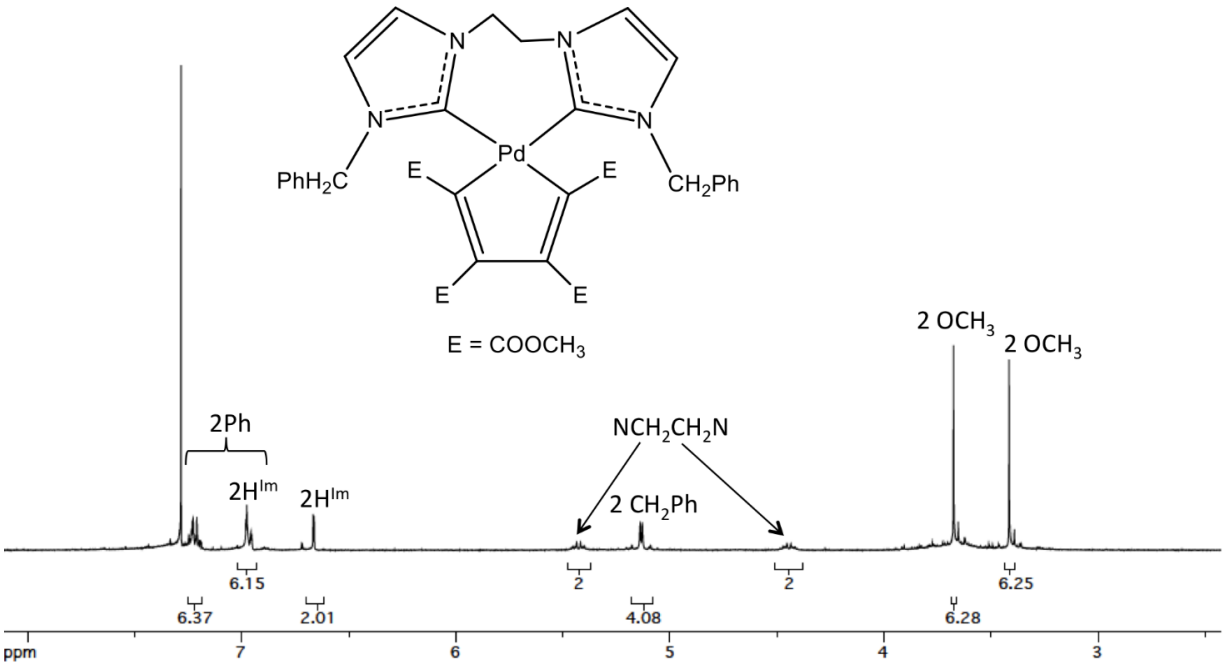

*Fig. 4.13 [1]H-NMR spectrum of the complex **40b** (T=298K, $CDCl_3$).*

In the $^{13}C\{^{1}H\}$-NMR spectra (Figs. 4.14 and 4.15) it is possible to identify the signals ascribable to the two different pairs of the $COOCH_3$ and $\underline{C}(COOCH_3)$ groups and that of the carbenic carbon at about 180 ppm.

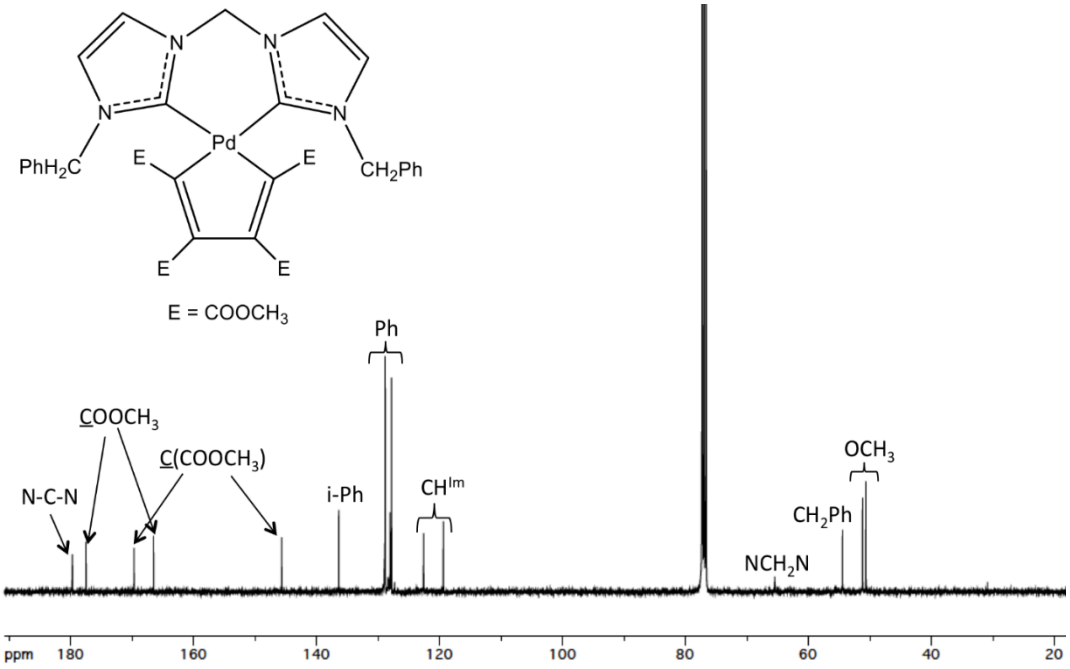

*Fig. 4.14 $^{13}C\{^{1}H\}$-NMR spectrum of the complex **40a** (T=298K, $CDCl_3$).*

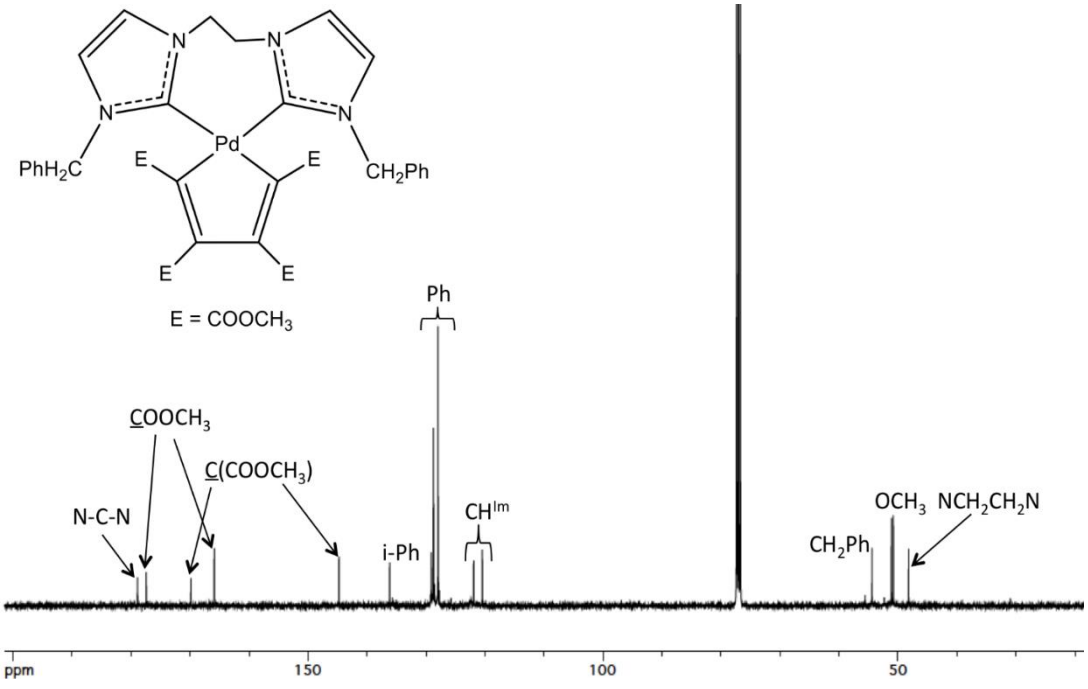

*Fig. 4.15 $^{13}C\{^{1}H\}$-NMR spectrum of the complex **40b** (T=298K, $CDCl_3$).*

The IR spectra show the presence of strong bands between 1730 and 1680 cm^{-1} ($\upsilon_{C=O}$) of the carbonyl groups of the cyclopalladate fragment.

The structures inferred by the interpretation of the IR and NMR spectra, were confirmed in the case of complex **40a** by single crystal X-ray diffraction (Fig. 4.16).

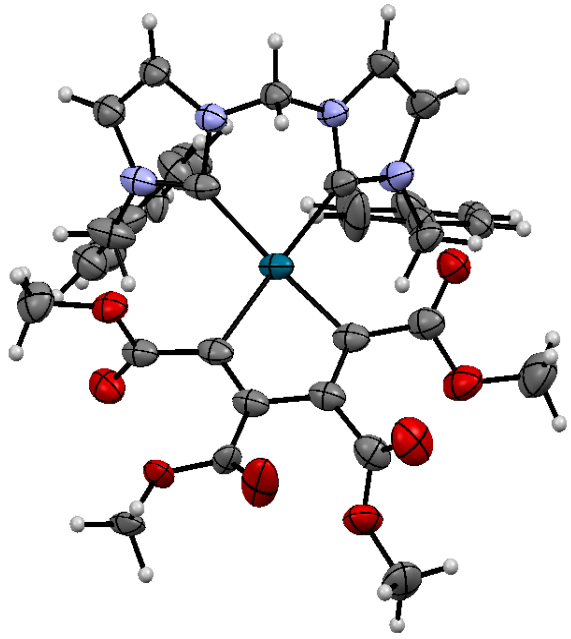

*Fig. 4.16 Ellipsoid representation of **40a** crystal ASU contents (50% probability).*

4.4.2. Palladacyclopentadienyl complexes bearing two monodentate NHCs

Palladacyclopentadienyl derivatives stabilized by two monocoordinated carbene ligands represent a category of complexes similar to those previously described. Similarly to the complexes with chelating bisNHCs, the choice of the R substituents at the monocoordinated carbene is very important for the success of the reactions. In particular, it has been observed that in the case of carbene substituted by one benzyl group and one bulkier group (i.e. mesityl or 2,6-diisopropylphenyl), the synthesis of the biscarbene is impossible owing to high steric demand [10]. Conversely, this kind of reactions gives good results when carbenes bearing less bulky substituents are used. The addition of two equivalents of the silver complexes **35a**, **36a** or **37c** to a solution of $[PdC_4(COOCH_3)_4]_n$ in dichloromethane is sufficient to promote transmetallation, as can be deduced by the progressive precipitation of AgBr (Scheme 4.8).

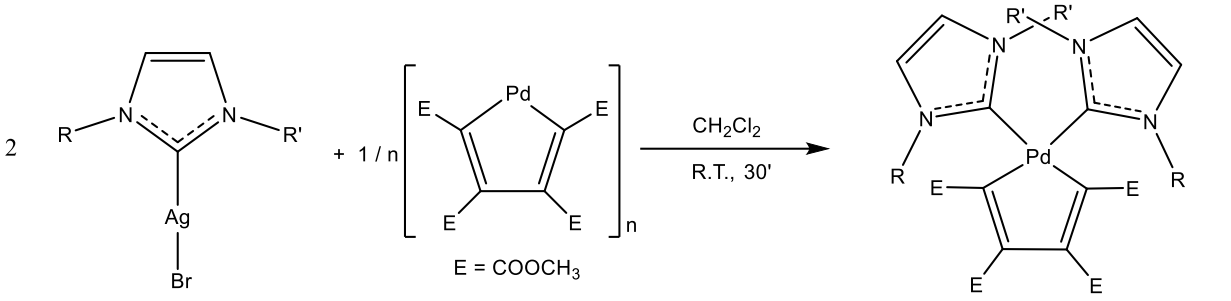

R= CH_3 R'= CH_2Py (**35a**)
R= CH_3 R'= CH_2SCH_3 (**36a**)
R= CH_3 R'= CH_2Ph (**37c**)

R= CH_3 R'= CH_2Py (**41a**)
R= CH_3 R'= CH_2SCH_3 (**41b**)
R= CH_3 R'= CH_2Ph (**41c**)

Scheme 4.8

The characterization of the products by NMR spectroscopy reveals the presence of a pairs of atropoisomers (*syn* and *anti*) for each compound, caused by the hindered rotation of the carbene ligands about the Pd-C bond (Fig. 4.17).

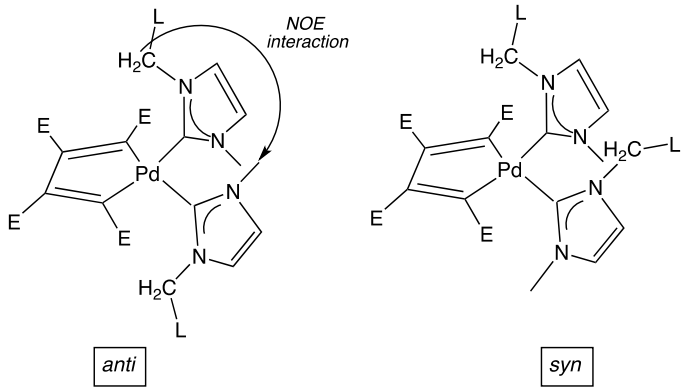

Fig. 4.17

The ^{1}H-NMR spectra reveal the presence of two signals related to the two pairs of OCH_3 groups of the palladacycle and AX or AB systems ascribable to the methylene protons NCH_2, for each atropoisomer (Fig 4.18).

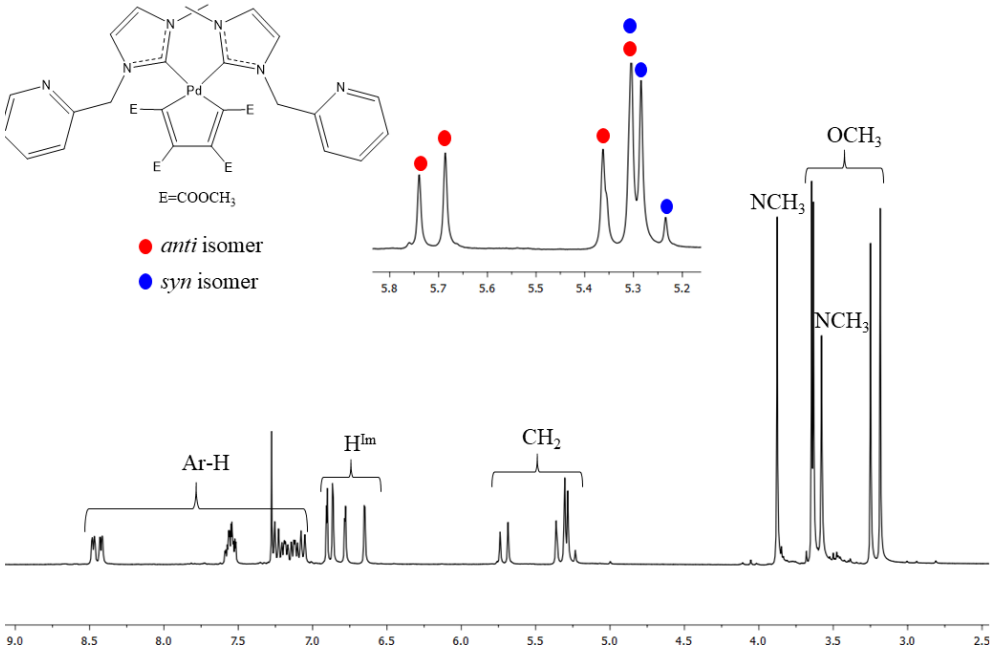

*Fig. 4.18 ^{1}H-NMR spectrum of the complex **41a** (T=298K, $CDCl_3$).*

In the ^{13}C-NMR and in the bidimensional HMBC and HMQC spectra (see Fig. 4.19), the two carbenic carbons (one for each atropoisomer) are always well distinguishable at about 180 ppm.

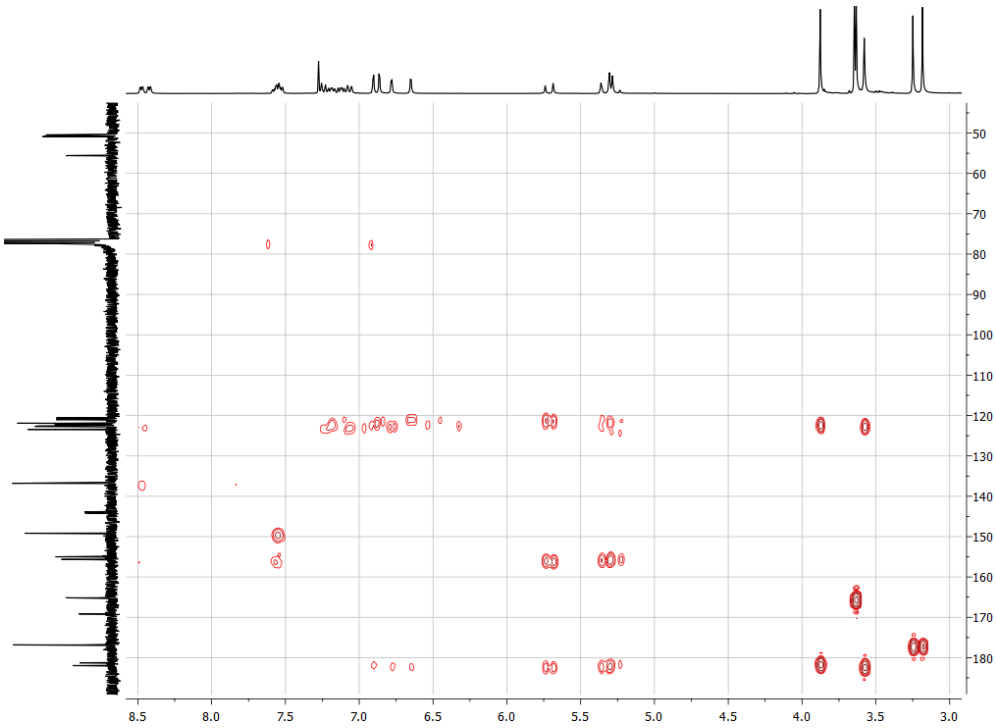

*Fig. 4.19 HMBC spectrum of the complex **41a** (T=298K, $CDCl_3$).*

The assignment of the peaks ascribable to the *syn* and *anti* isomers is based on the NOESY spectra (Fig. 4.20), where an intense cross-peak between the protons of the methyl substituent and one of the two methylene protons (*anti* isomer), was observed.

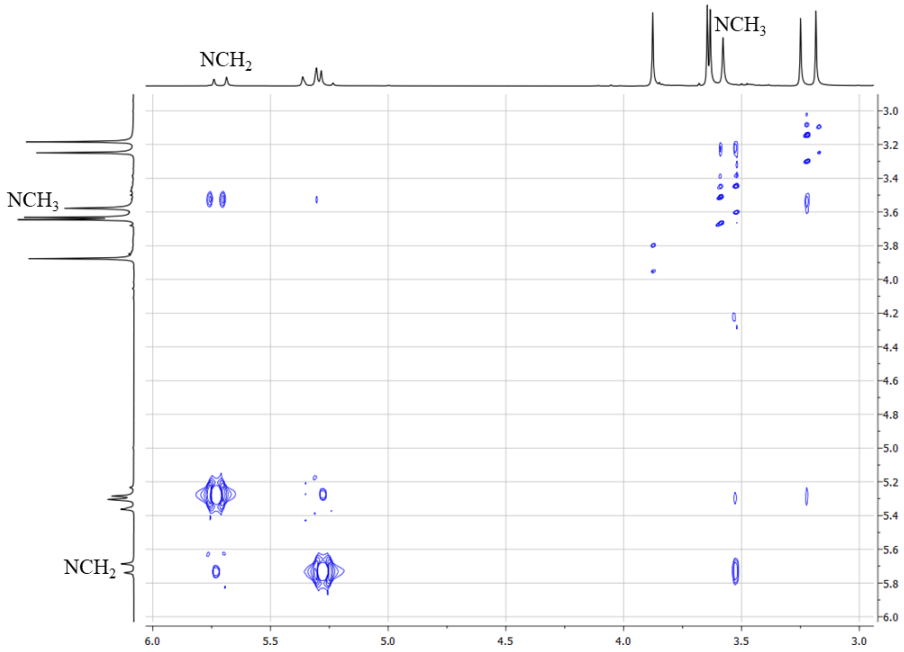

*Fig. 4.20 NOESY spectrum of the complex **41a** (T=298K, $CDCl_3$).*

At equilibrium, the ratio between the two isomers is summarized in table 4.1.

COMPOUND	***anti*/*syn***
41 a	3.6
41 b	2.0
41 c	2.8

Table 4.1

In the case of compound **41a** it was also possible to obtain its solid-state structure by single crystal X-ray diffraction (Fig. 4.21).

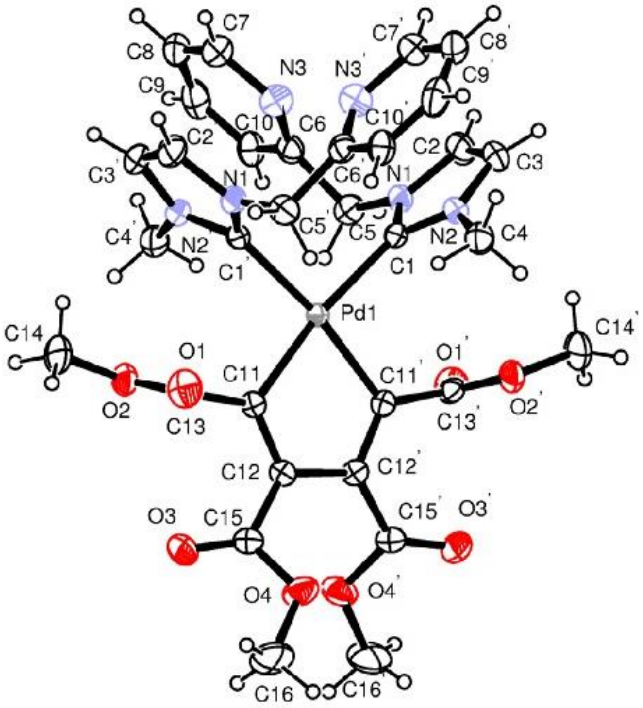

*Fig. 4.21 Ellipsoid representation of **41a** crystal ASU contents (50% probability).*

4.4.3. Palladacyclopentadienyl complexes with chelating NHC-thioether or NHC-pyridine ligands

Another class of ligands taken into consideration is represented by the hemi-labile NHC-thioether and NHC-pyridine ligands.

The corresponding palladacyclopentadienyl complexes (**42** and **43**) were synthesized by reacting one equivalent of the silver compounds **35a-b** and **36c** with the polymeric precursor $[PdC_4(COOCH_3)_4]_n$, under the conditions indicated in Scheme 4.9.

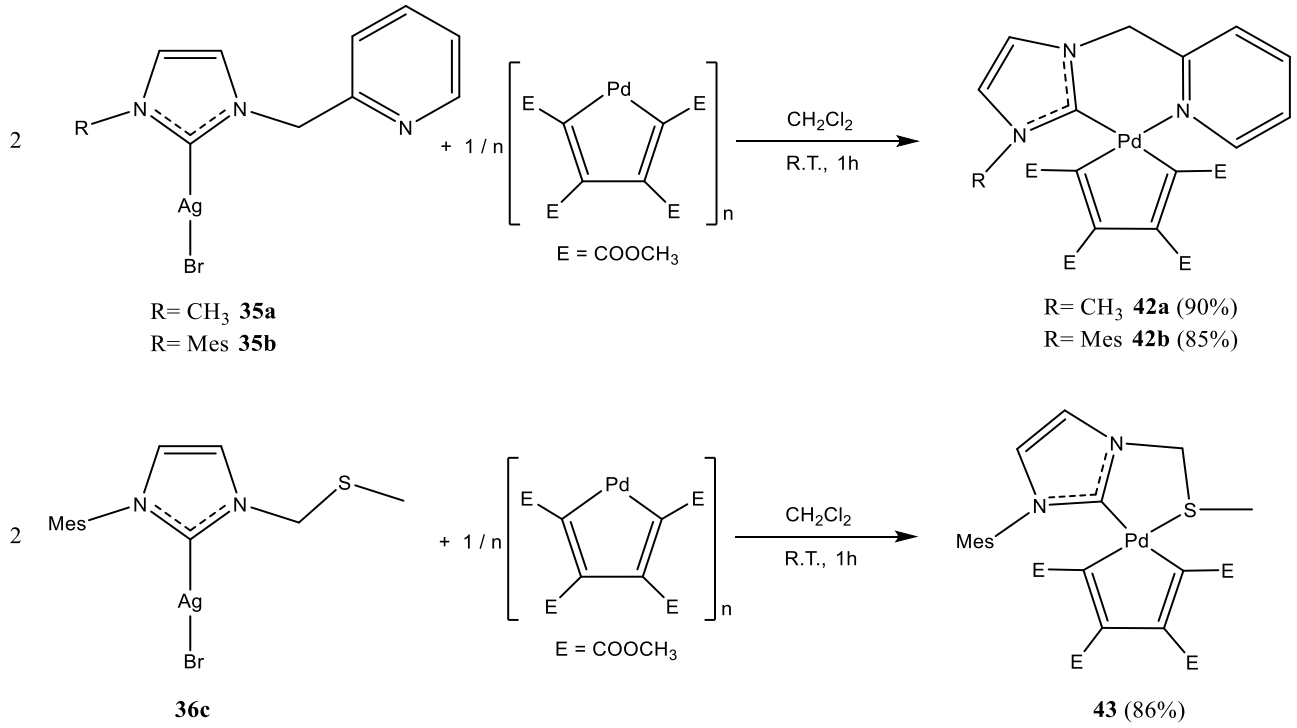

Scheme 4.9

This class of compounds was synthesized with the purpose of verify whether the presence of a labile coordinative site (pyridine nitrogen or thioether sulphur) might affect the biological activity of the system. As a matter of fact, such complexes may interact with soft bio-ligands (i.e. glutathione) and form *in vivo* some species with enhanced or reduced activity if compared to that of the starting compounds.

Species **42** and **43** were fully characterized by IR and NMR spectroscopic techniques and elemental analysis.

The ^{1}H-NMR and ^{13}C-NMR spectra of the complex **42b** (Figs. 4.22 and 4.23) confirming the hypothesized structure, are shown below.

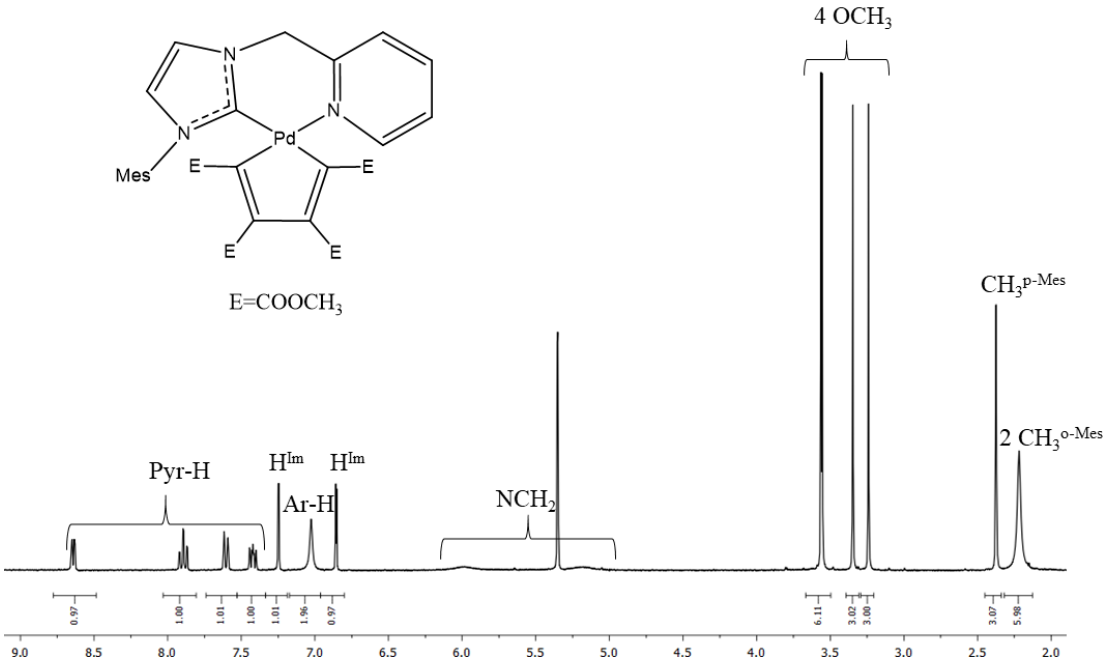

*Fig. 4.22 ^{1}H-NMR spectrum of the complex **42b** (T=298K, CD_2Cl_2).*

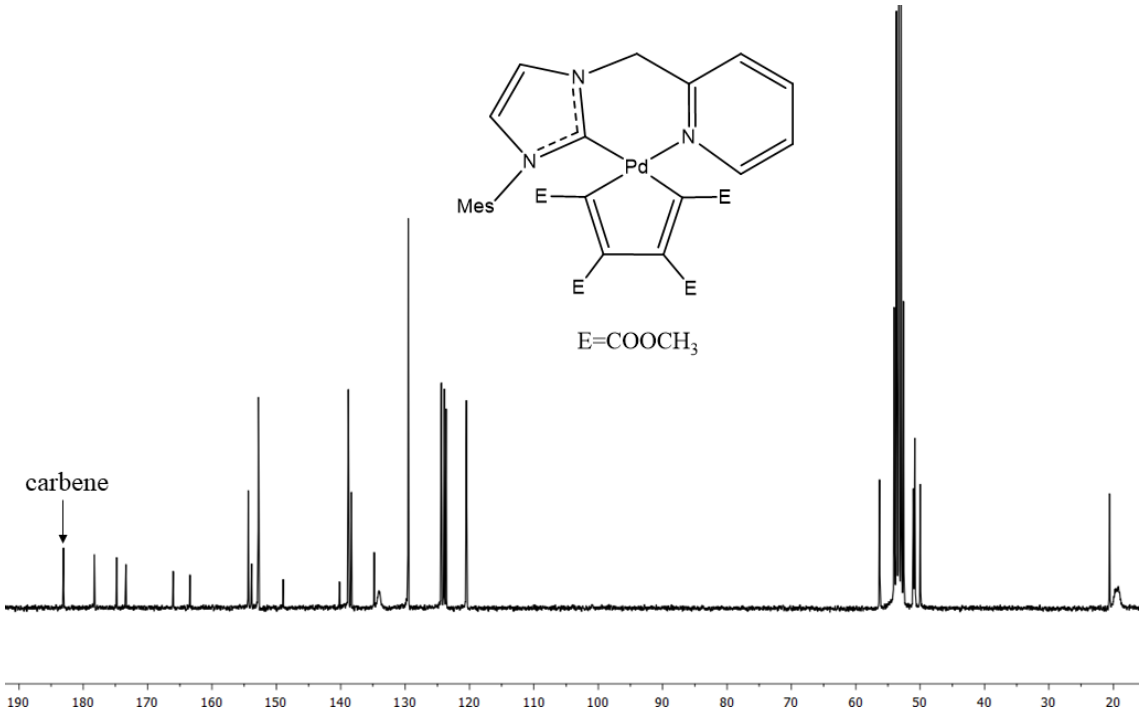

*Fig. 4.23 ^{13}C{^{1}H}-NMR spectrum of the complex **42b** (T=298K, CD_2Cl_2).*

For the compound **42a** it was also possible to obtain its solid-state structure by single crystal X-ray diffraction (Fig. 4.24).

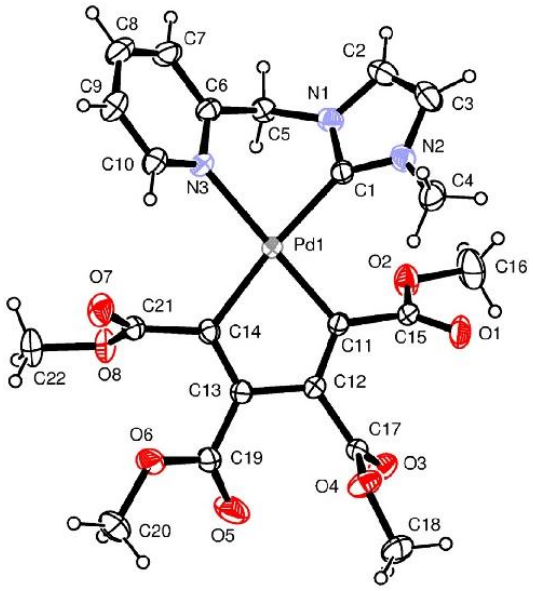

*Fig. 4.24 Ellipsoid representation of **42a** crystal ASU contents (50% probability).*

In some articles of our research group, the reactivity of the palladacyclopentadienyl complexes toward halogens and interhalogens [10, 11] was studied and, in one case, the formation of an unprecedented compound was observed when the complexes **42a-b**, bearing hemilabile NHC-pyridine ligands, are reacted with one equivalent of iodine [11e].

In particular, it was firstly observed the formation of the expected σ-butadienyl product (oxidative addition of I_2 followed by stereoselective reductive elimination) and subsequently, with different rate depending on the R substituent of the carbenic fragment, the exclusive formation of a zwitterionic species with a chelating ligand consisting in a 10-terms ring and two iodides coordinated in t*rans* to the palladium (Scheme 4.10 and Fig. 4.25).

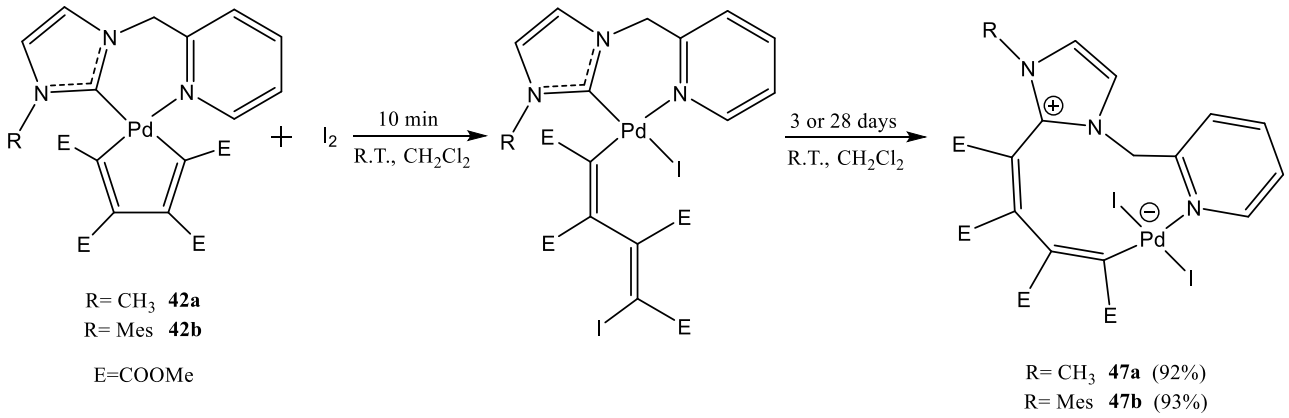

Scheme 4.10

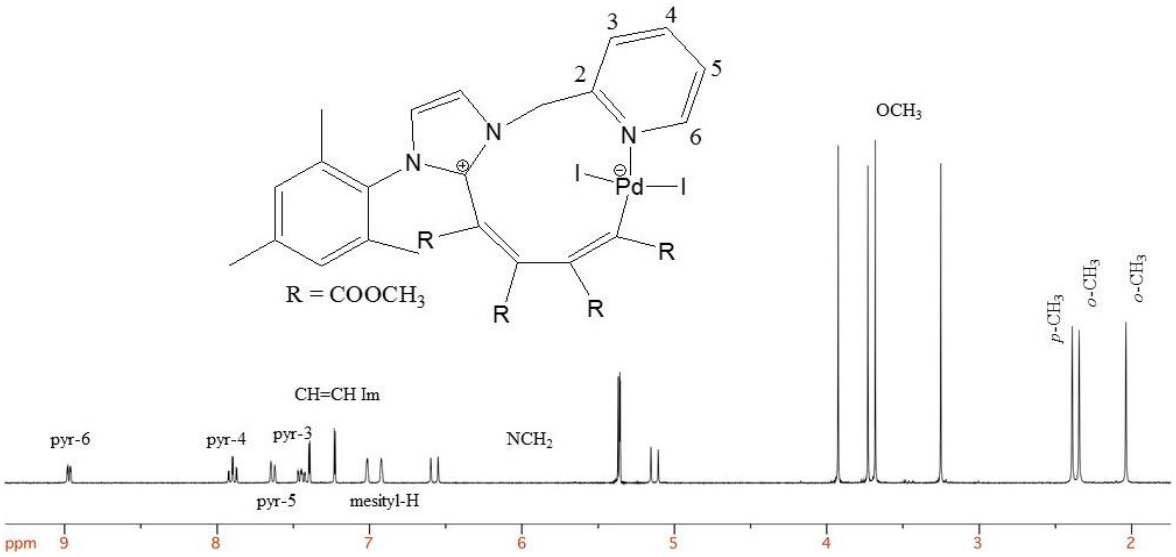

*Fig. 4.25 ^{1}H-NMR spectrum of the complex **42b** (T=298K, CD_2Cl_2).*

For this process a reaction mechanism was also proposed on the basis of kinetic studies carried out by NMR spectroscopy and theoretical DFT calculations (Scheme 4.11).

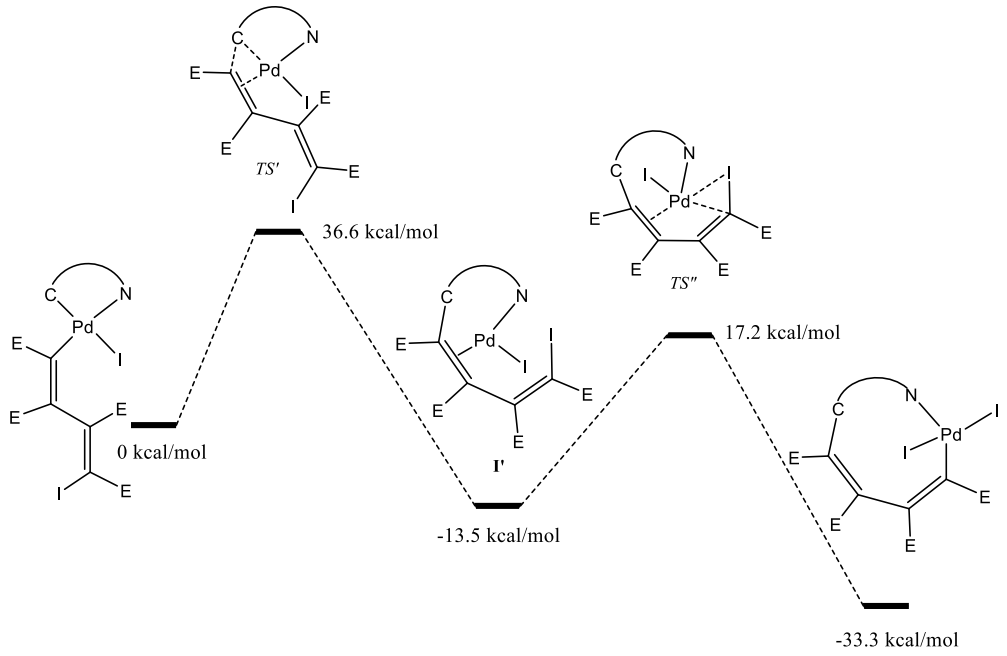

*Scheme 4.10 Computed energies for the reaction between complex **42a** and I_2, starting from the related σ-butadienyl intermediate.*

The final species **47a-b** were characterized by IR and NMR techniques, but it was the achievement of the X-ray structure for the complex **47b** that defined its nature (Fig. 4.26).

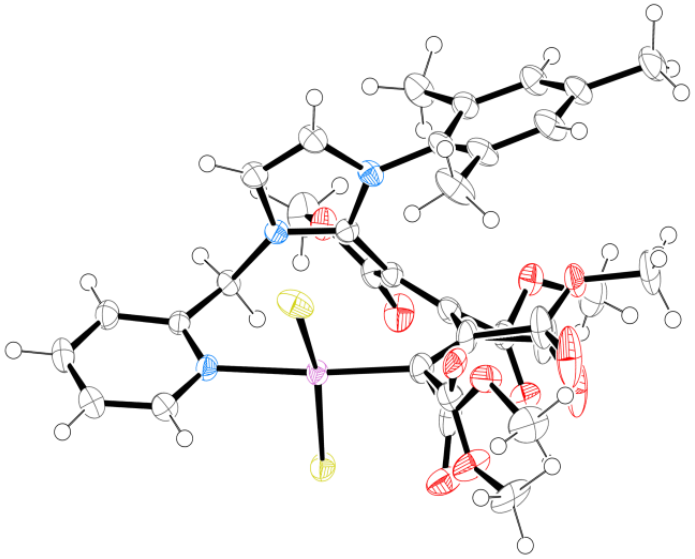

*Fig. 4.26 Ellipsoid representation of **47b** crystal ASU contents (50% probability).*

These complexes, as will be reported in the following section 4.5, have been tested *in vitro* because they structurally belong to one of the classes of palladium compounds that have shown a good antitumor activity (see section 1.3.6). These are *trans*-PdX_2L_2 compounds, widely studied and summarized in the review published in 2014 by Fairlamb and Kapdi [12].

4.4.4. Mixed NHC/PPh_3 palladacyclopentadienyl complexes

As already stated, it is possible to synthesize palladacyclopentadienyl complexes bearing one purine-based NHCs and one triphenylphosphine.

Compounds **44a-b**, bearing classical NHCs, were synthesized in good yields and purity following a similar protocol. In Scheme 4.11 the synthesized complexes are reported.

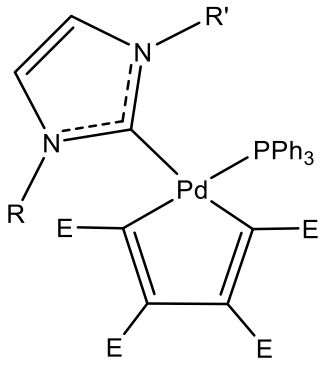

E=$COOCH_3$	R= CH_3	R'= CH_2Py	**44a**
E=$COOCH_3$	R= CH_3	R'= Bn	**44b**

Scheme 4.11

The first mixed NHC/PPh_3 compound synthesized was **44a**, taking advantage of the easy displacement of the labile pyridine nitrogen by the entering phosphine (Scheme 4.12).

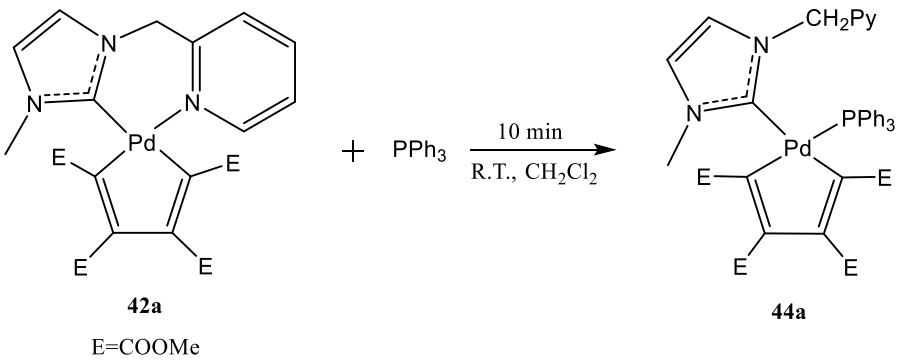

42a

E=COOMe

44a

Scheme 4.12

A more general approach, including complexes with carbene ligands without a second coordinating labile function, was subsequently developed [10].

In fact, the addition of one equivalent of PPh_3 and one of the silver carbene complex to the polymeric precursor $[PdC_4(COOCH_3)_4]_n$, selectively leads to the formation of the NHC/PPh_3 mixed complexes **44a-b**.

In principle, this procedure does not guarantee the exclusive formation of the mixed derivative since the "homoleptic" complexes containing two phosphine or two carbene ligands could also be produced at the same time.

However, DFT theoretical calculations have shown that the exclusive formation of the mixed derivative is favourable from the thermodynamic point of view (Scheme 4.13) [10].

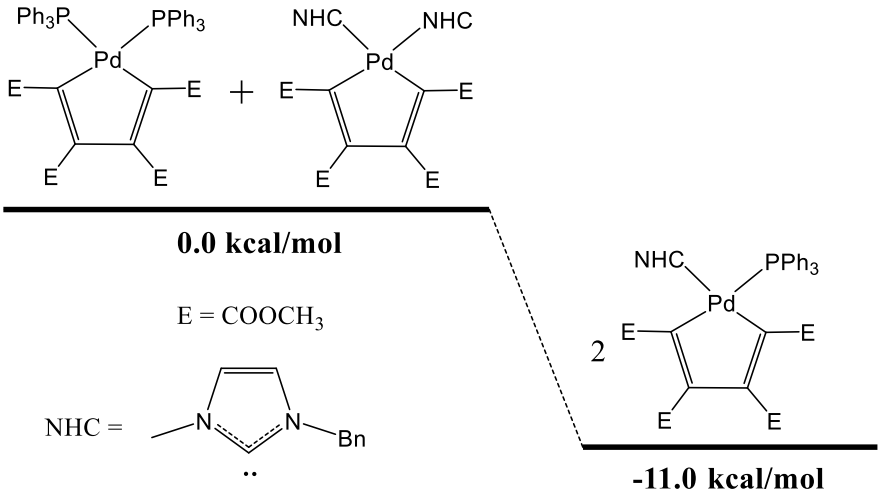

Scheme 4.13 Computed energies (ΔG°) related to the "homoleptic" and mixed NHC/PPh_3 complexes.

Nevertheless, the possibility that the reaction might be under kinetic control, requires that the operating conditions giving the selective obtainment of the mixed species have to be in any case experimentally verified.

Preliminary tests suggest the following indications:

1. The mixed derivatives are selectively obtained by adding to the solution of the $[PdC_4(COOCH_3)_4]_n$ precursor a solution containing both triphenylphosphine and the silver carbene complex.
2. An alternative is represented by the addition of the silver carbene complex and then of triphenylphosphine, but this approach firstly yields a mixture of the two "homoleptic" complexes and only after, very slowly and partially (decomposition processes cannot be easily controlled), gives the mixed product.

The effect of the two different protocols was interpreted and described according to Scheme 4.14.

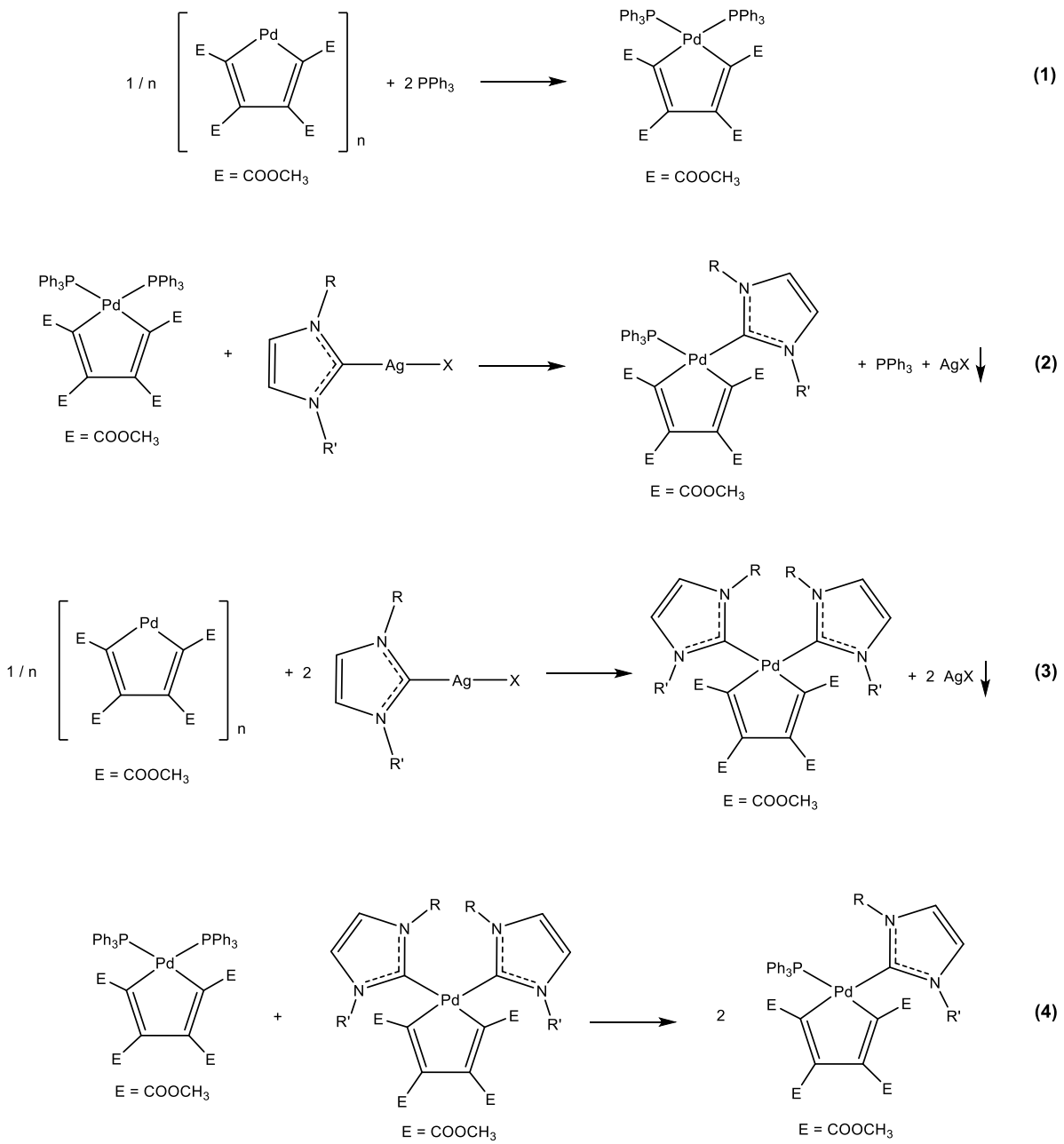

Scheme 4.14 Possible competitive processes involving the polymer precursor, the phosphine and the carbene ligand present in the reaction environment.

The four described reactions are all clearly possible, but we have to suppose that the processes (1) and (2) must be faster than the processes (3) and (4).

In fact, the preliminary addition of triphenylphosphine only, or combined with the silver carbene complex, leads to the formation of the desired product according to the reactions (1) and (2), without the slower process (3) is simultaneously activated.

Conversely, if we first add the silver carbene complex to the palladacyclic precursor, the biscarbene complex is obtained (reaction (3)); the subsequent addition of one equivalent of phosphine leads to the formation of the bis-phosphinic derivative by reaction with the unreacted palladacyclic precursor

(reaction (1)). The conversion of these two compounds into the mixed derivative is eventually gradually obtained by means of the slow reaction (4).

Once defined the synthesis protocol, the mixed complexes **44a-b** were obtained in one hour with good yields (Scheme 4.15).

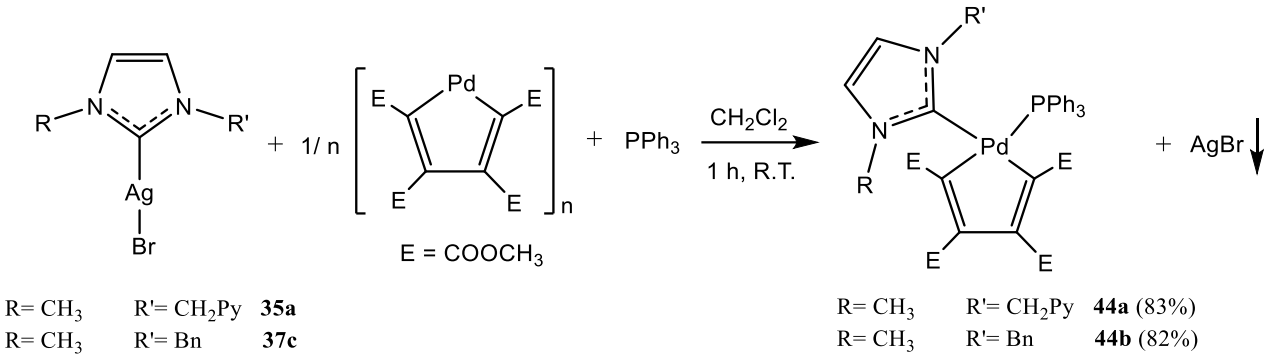

Scheme 4.15

These products were characterized by NMR spectroscopy. In particular, the presence of only one species is well evidenced by the single peak observed in the $^{31}P\{^{1}H\}$-NMR spectra, resonating at about 26-27 ppm. In the ^{1}H-NMR (Fig. 4.27) and $^{13}C\{^{1}H\}$-NMR (Fig. 4.28) spectra, owing to the presence of two different spectator ligands, four different signals ascribable to $COOCH_3$ ester groups can be detected.

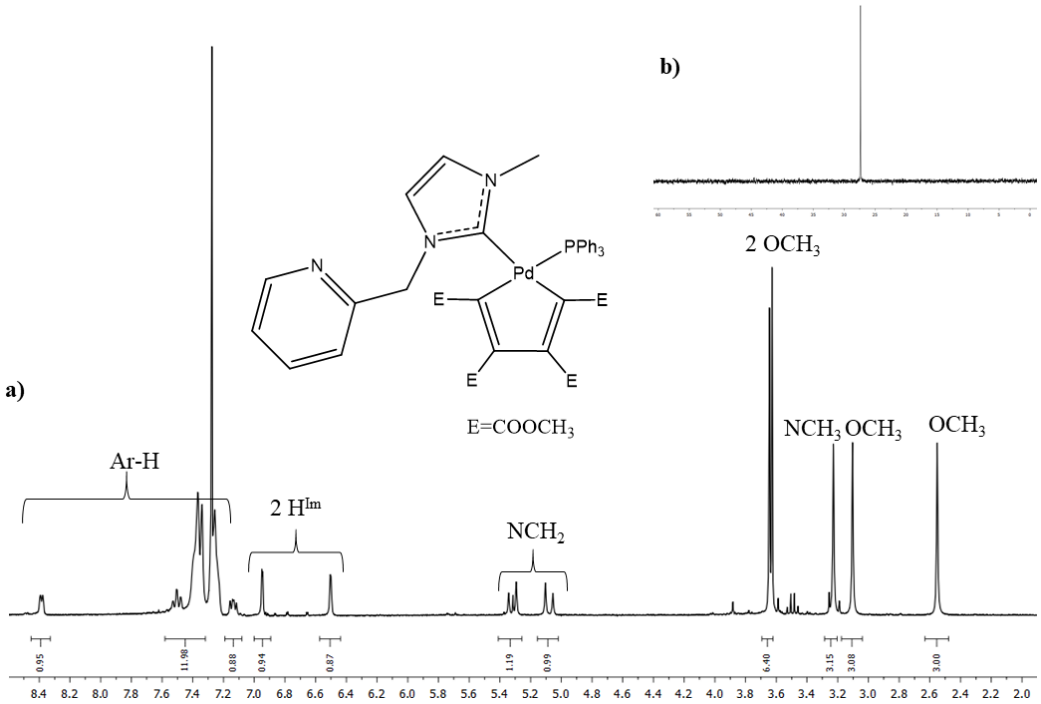

*Fig. 4.27 ^{1}H-NMR (a) and $^{31}P\{^{1}H\}$-NMR (b) spectra of the complex **44a** in CDCl3 at T = 298 K.*

Moreover, the signal ascribable to the carbene carbon at about 180 ppm is present in all $^{13}C\{^{1}H\}$-NMR spectra of all the synthesized derivatives and, due to the coupling with the phosphorus of the adjacent phosphine ligand, it appears as a doublet ($J_{C\text{-}P} \approx 16$ Hz) (Fig. 4.28).

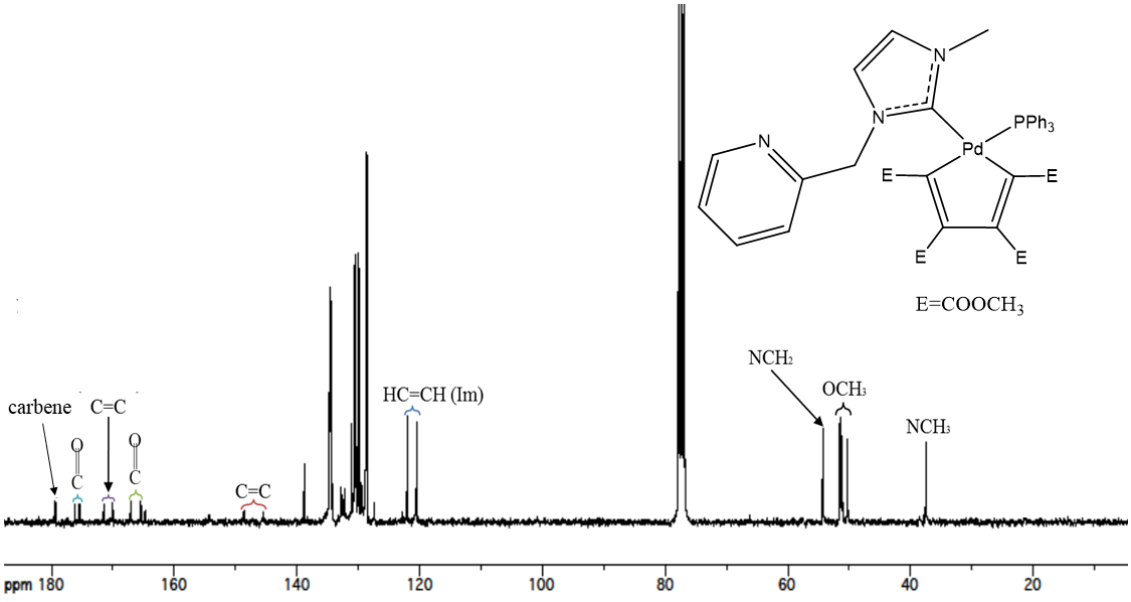

*Fig. 4.28 $^{13}C\{^{1}H\}$-NMR spectra of the complex **44a** in $CDCl_3$ at T = 298 K.*

4.4.5. Mixed NHC/DIC palladacyclopentadienyl complexes

The same methodology was adopted for the synthesis of the mixed NHC/DIC palladacyclopentadienyl complexes.

A test carried out in NMR tube, by adding to a solution of the $[PdC_4(COOCH_3)_4]_n$ precursor another solution containing one equivalent of the silver complex **37d** and one equivalent of DIC, indicated the formation after few minutes of a mixture of the mixed derivative and of the two "bis-DIC" and "bis-NHC" complexes. However, it was observed the progressive transformation of the two compounds with the same spectator ligand into the mixed derivative in about 48 hours, without detecting perceptible decomposition (Fig. 4.29).

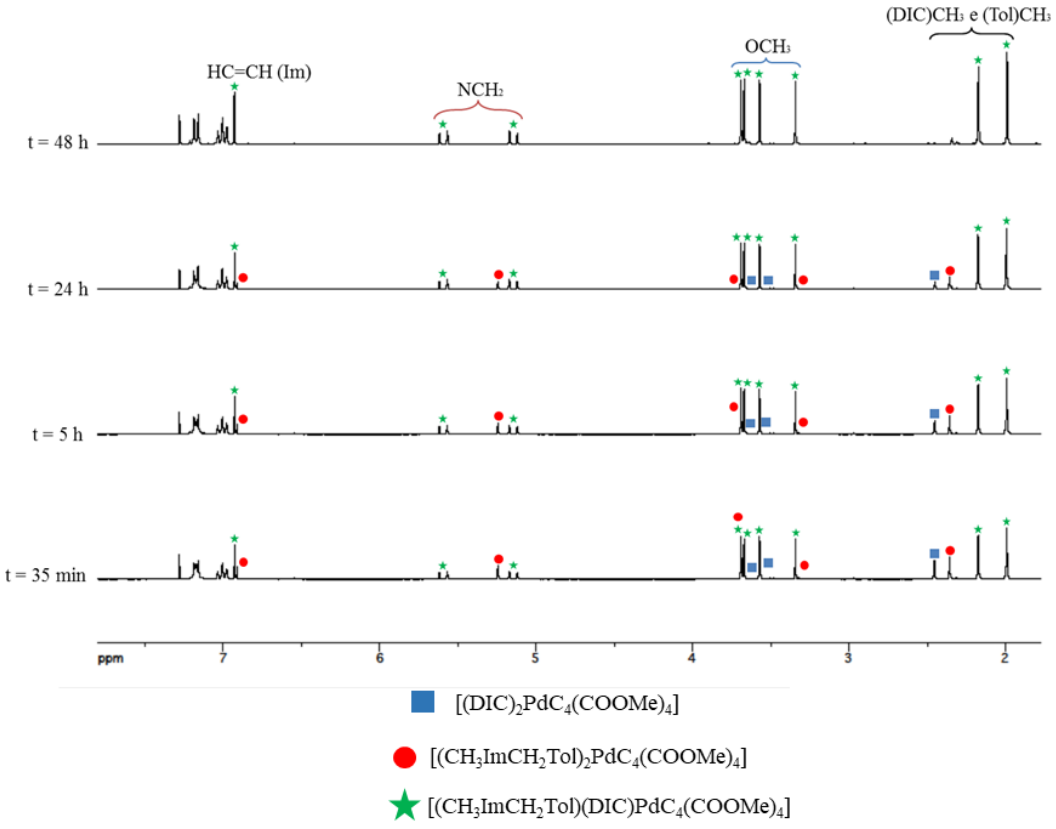

*Fig. 4.29 ^{1}H-NMR spectra of the reaction between $[PdC_4(COOCH_3)_4]_n$, DIC and the silver complex **37d** in $CDCl_3$ at T = 298 K.*

On the basis of a reaction scheme similar to that reported in the former Scheme 4.14, it is apparent that in this case the processes (3) and (2) must be of comparable rate, whereas the process (4) probably remains significantly slower than the other three. This scheme explains the initial presence in solution of all the three possible palladacyclometallated species and the subsequent slow achievement of the mixed derivative (Scheme 4.15).

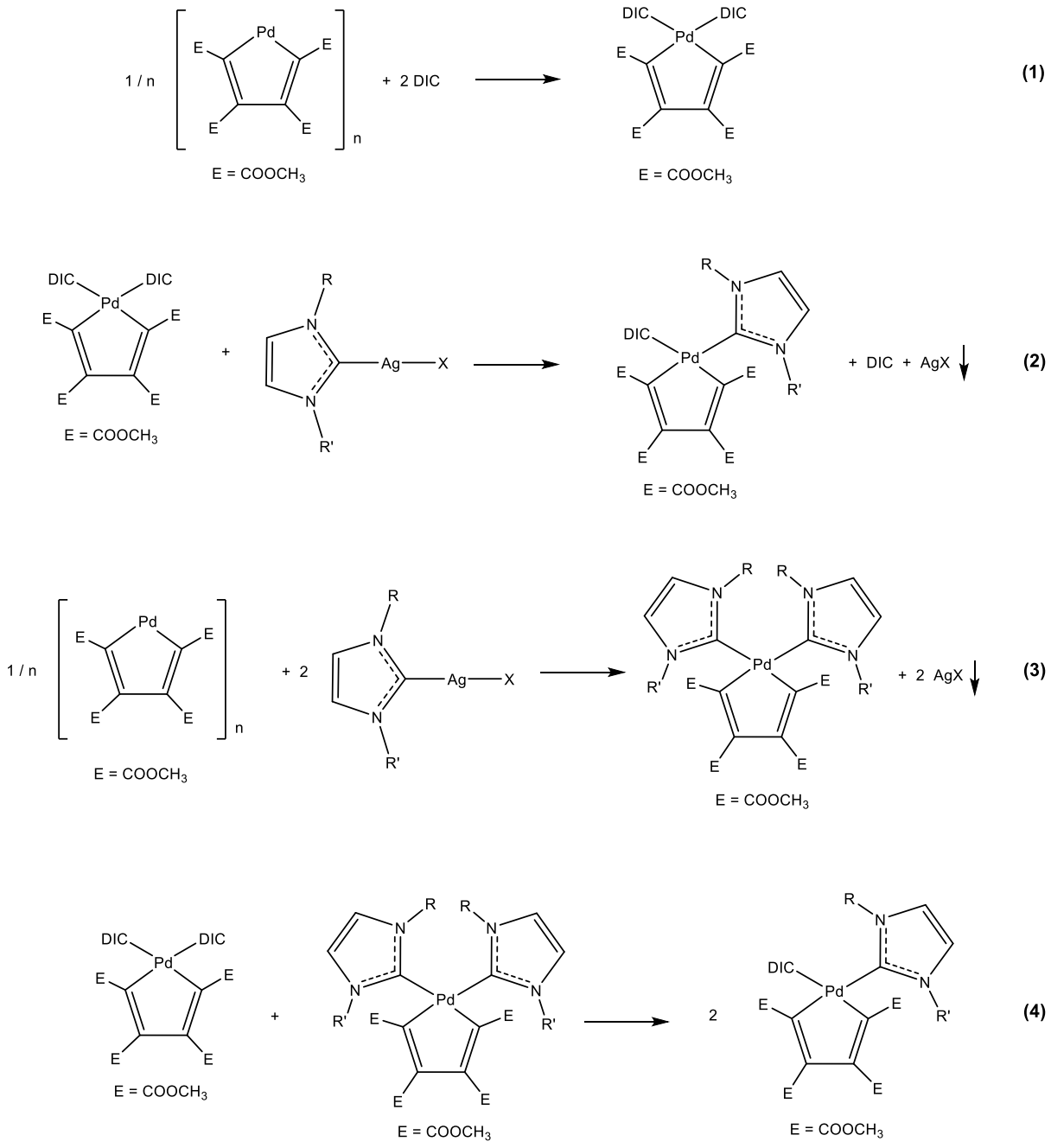

Scheme 4.15 Possible competitive processes involving the polymer precursor, DIC and the carbene ligand present in the reaction environment.

It can be concluded that the synthesis of the mixed NHC/DIC complex, needs a considerably lengthening of the reaction times with respect to that necessary with phosphines. Once defined these experimental conditions, the complexes can be easily separated from the reaction mixture and selectively isolated in good yields (Scheme 4.16).

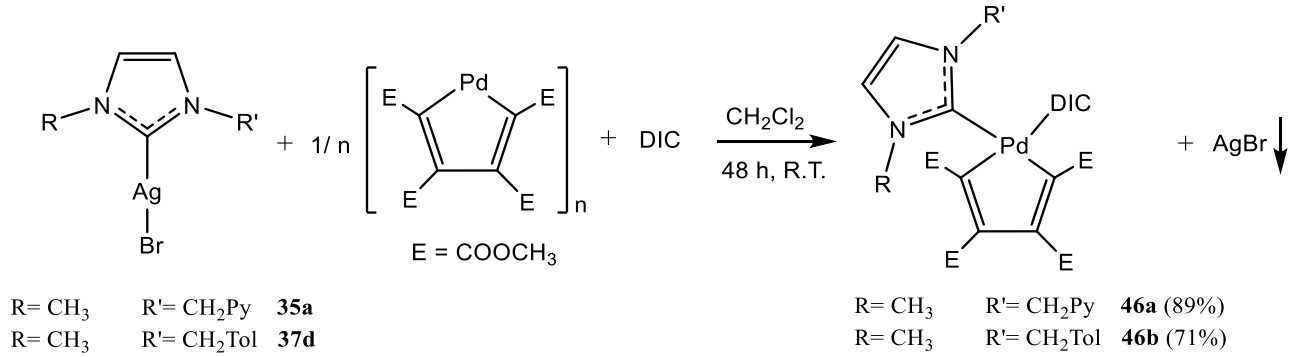

Scheme 4.16

In the ^{1}H-NMR spectra, the signals of the two different ligands (isocyanide and carbene) are clearly identifiable. The two benzyl protons resonate as a pair of doublets, again as a consequence of the hindered rotation about the Pd-carbenic carbon bond. Finally, the presence of the palladacyclopentadienyl fragment is confirmed by the four different peaks ascribable to the OCH_3 groups (Fig. 4.30).

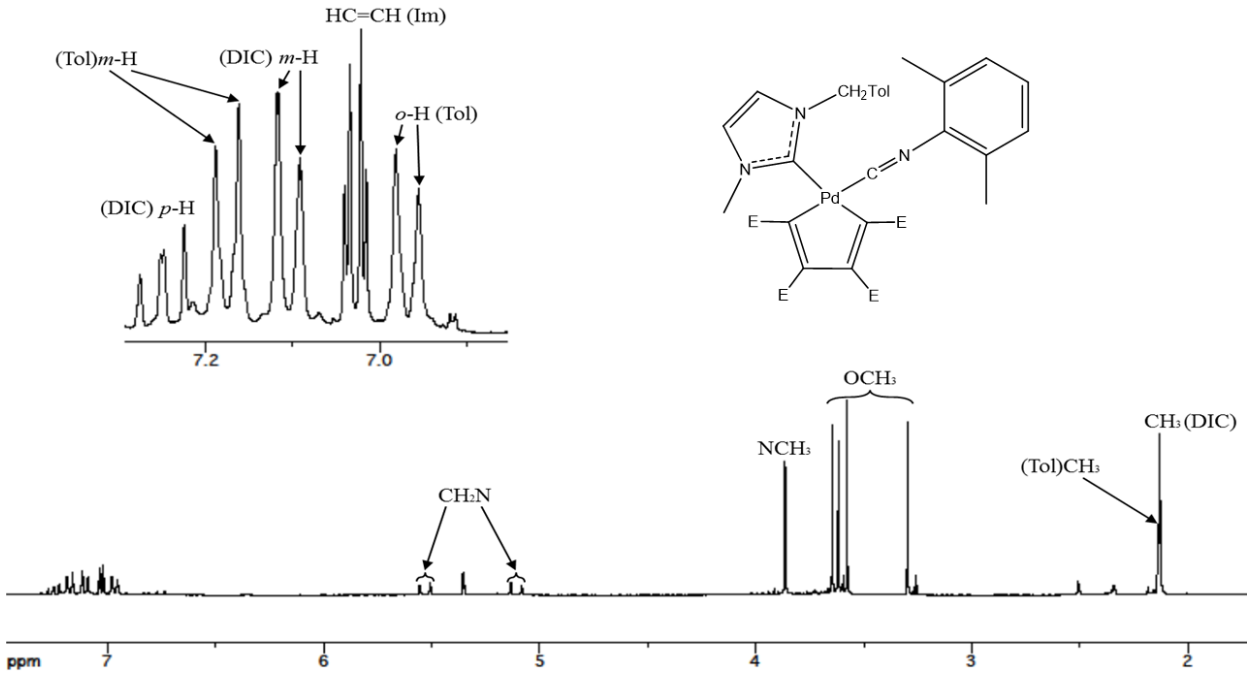

*Fig. 4.30 ^{1}H-NMR spectrum of the complex **46b** in CD_2Cl_2 at T = 298 K.*

In the $^{13}C\{^{1}H\}$-NMR spectra, it is possible to observe the weak signal of the isocyanide carbon atom (at about 150 ppm) and the coordinated carbene signal at about 178 ppm (Fig. 4.31).

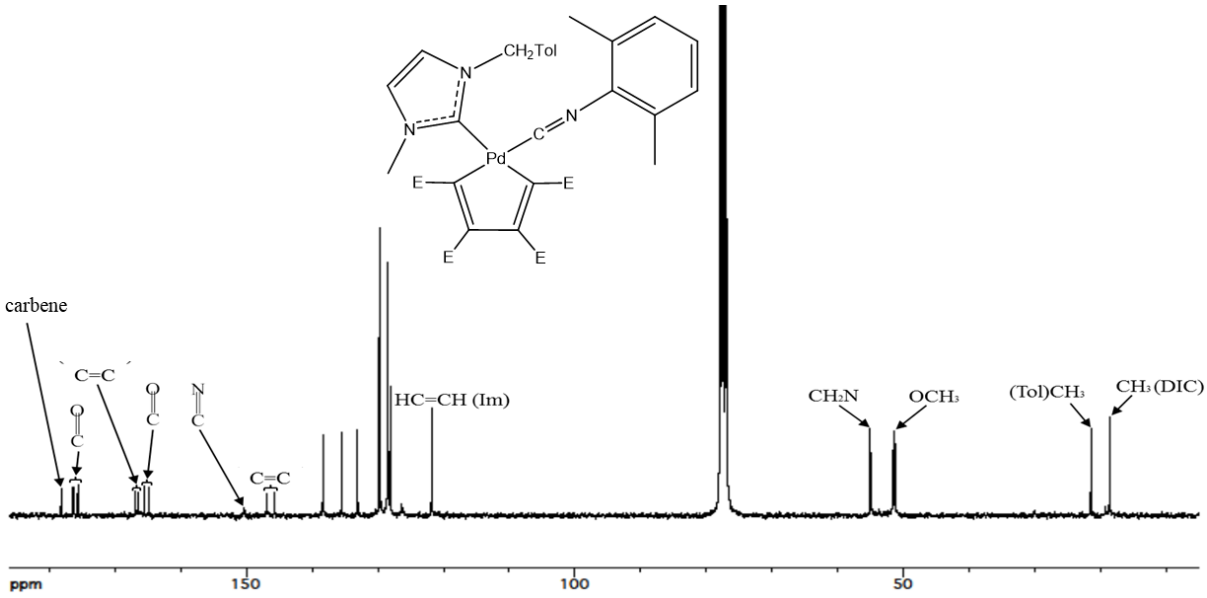

*Fig. 4.31 $^{13}C\{^{1}H\}$-NMR spectrum of the complex **46b** in $CDCl_3$ at T = 298 K.*

4.4.6. Palladacyclopentadienyl bearing chelating N-S and N-P ligands

The last class of palladacyclopentadienyl compounds, synthesized by published protocols [11b, 11d, 13], whose antiproliferative activity has been evaluated, are stabilized by bidentate N-S (pyridyl-thioethers or thioquinolines) and N-P (phosphoquinolines) ligands. This category of complexes has been synthesized according to the conditions reported in the Scheme 4.17 and, it is worth noting that among all those described hitherto, they bear the most labile ancillary ligands.

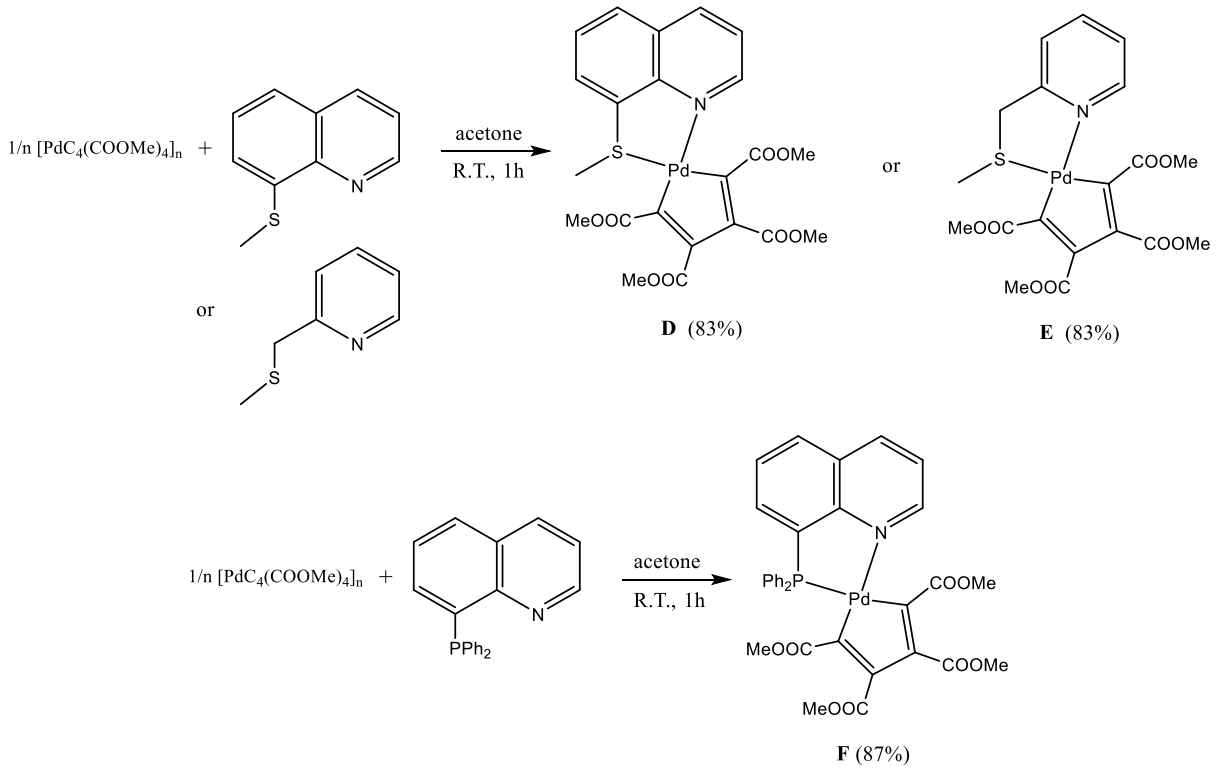

Scheme 4.17

4.5. Antiproliferative activity and biological assays on palladacyclopentadienyl complexes

In this paragraph the antiproliferative activity of the palladacyclopentadienyl compounds described in the previous section (see Fig 4.8), will be examined on different human tumor lines.
These studies, as well as those reported in the next chapters, were carried out by the molecular biology research group of dr. Flavio Rizzolio at the "Centro di Riferimento Oncologico" (CRO) of Aviano.
In particular, the following cancer lines have been considered:

- A2780 and A2780-R: human ovarian carcinoma (sensitive and resistant to cisplatin), already studied in the case of compounds containing purine-based NHCs (paragraph 3.8) [14].
- OVCAR5: human ovarian carcinoma (Cisplatin sensitive) from a 67-year-old woman not previously treated with any pharmacological therapy [15].
- A549: human lung cancer (adenocarcinomic human alveolar basal epithelial cells) from a 58-year-old Caucasian male [16].
- A375: human malignant melanoma, a solid tumor from a 54-year-old female [17].
- DLD1: human colon adenocarcinoma removed from a female subject [18].

In order to verify the selectivity of these palladium complexes *versus* cancer cells, normal human fibroblasts MRC-5 (derived from lung tissue of at 14-week-old aborted Caucasian male fetus) were also tested.

4.5.1. Antiproliferative activity of palladacyclopentadienyl compounds on different cancer cell lines and fibroblasts.

The fibroblasts and the tumor lines were treated with DMSO solutions of the palladacyclopentadienyl compounds (10 mM stock solutions), suitably diluted in the culture medium; their antiproliferative activities are expressed as IC_{50} (μM) and reported in table 4.2.

Preliminarily, the stability of the examined palladacyclopentadienyl complexes was checked in 1:1 dmso-d6/D_2O solution (**42**, **43**, **46** and **D-F**) or dmso-d6 (**40**, **41**, **44** and **47**) by NMR spectroscopy: after 48 hours at room temperature no degradation and no ligand replacement was observed.

Class of compound	Compound	IC_{50} (μM)						
		A2780	A2780-R	OVCAR5	A549	A375	DLD1	MRC-5
Cisplatin	Cisplatin	0.81±0.06	9±3	0.84±0.04	6±3	4.7±0.4	19±4	14±1
Bidentate bisNHCs	40a	0.039±0.006	2.8±0.6	0.30±0.07	>100	0.3±0.1	>100	>100
	40b	0.46±0.05	7±5	0.49±0.09	>100	2.5±0.7	>100	>100
Monodentate bisNHCs	41a	2.6±0.4	12±3	7±2	>100	9±5	7±1	>100
	41b	0.58±0.03	4.4±0.3	13±3	>100	10.2±0.1	34±15	>100
	41c	46±11	31±1	0.13±0.07	>100	19±16	0.10±0.09	>100
NHC-CH_2Py	42b	2.7±0.2	>100	52±26	>100	24±9	>100	>100
NHC-CH_2SR	43	3.7±0.2	4.4±0.9	1.79±0.06	>100	2±2	>100	>100
Mixed NHC/PPh_3	44a	3.9±0.6	3.4±0.8	1±1	0.05±0.02	29±7	>100	>100
	44b	0.33±0.08	1.3±0.4	1.2±0.4	17±9	4.4±0.3	4.7±0.9	4.7±0.2
Mixed NHC/DIC	46a	2.6±0.4	3.9±0.6	13±2	0.24±0.09	4.9±0.9	7±2	>100
	46b	1.0±0.2	0.6±0.2	3.5±0.4	2.8±0.2	5.6±0.5	5.2±0.7	4.8±0.2
Zwitterionic species	47a	5.8±0.6	>100	6.8±0.6	>100	2±1	>100	>100
	47b	0.51±0.04	1.12±0.04	4.4±0.9	3.5±0.3	0.3±0.2	4.4±0.7	>100
Chelating N-P and N-S	D	98±49	>100	>100	>100	>100	>100	>100
	E	10±2	28±3	>100	>100	>100	>100	>100
	F	16±5	>100	>100	>100	37±3	>100	>100

Table 4.2 In vitro antiproliferative IC_{50} values (μM, 72 h) of the palladacyclopentadienyl complexes toward human cell lines of ovarian cancer (A2780 and OVCAR5), the cisplatin resistant clone (A2780-R), lung cancer (A549), malignant melanoma (A375), colon cancer (DLD1) and normal lung fibroblast (MRC-5).

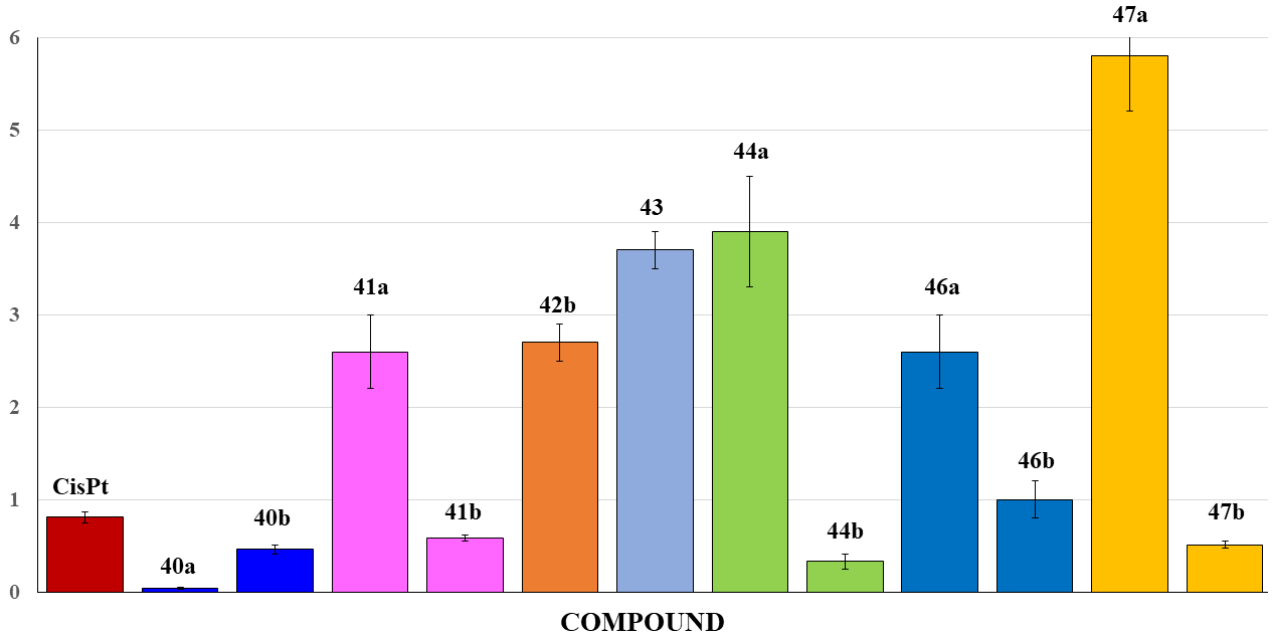

Fig. 4.32 Palladacyclopentadienyl complexes with IC_{50}<8 μM on A2780 cell line.

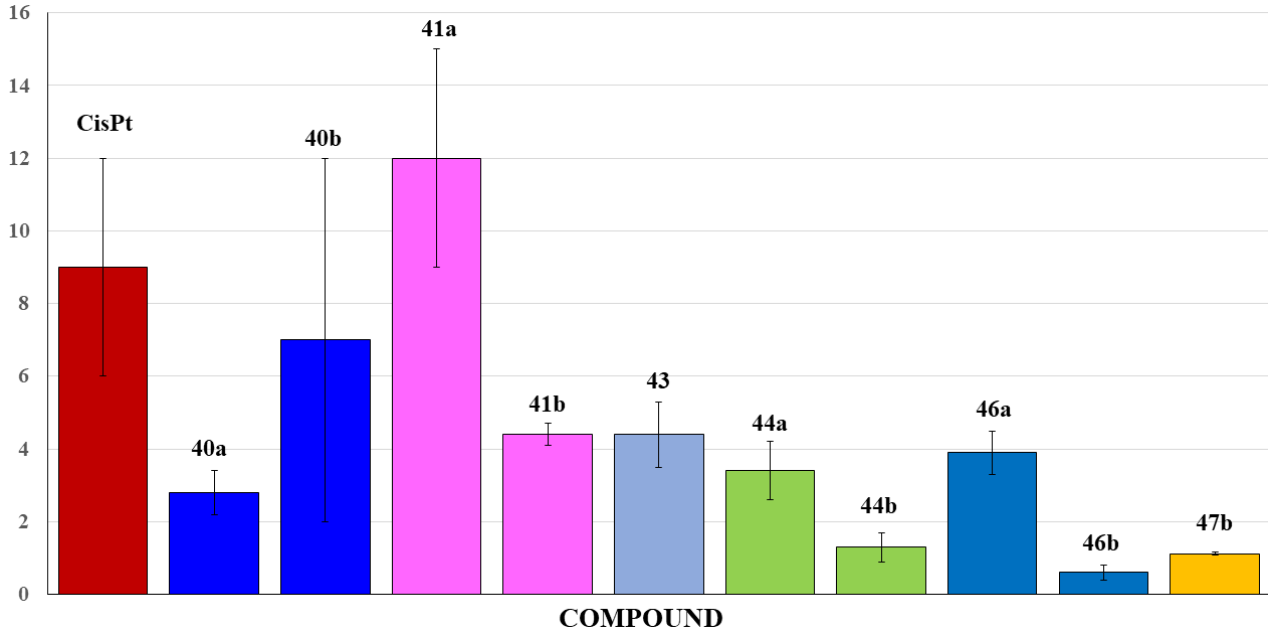

Fig. 4.33 Palladacyclopentadienyl complexes with IC_{50}<18 μM on A2780-R cell line.

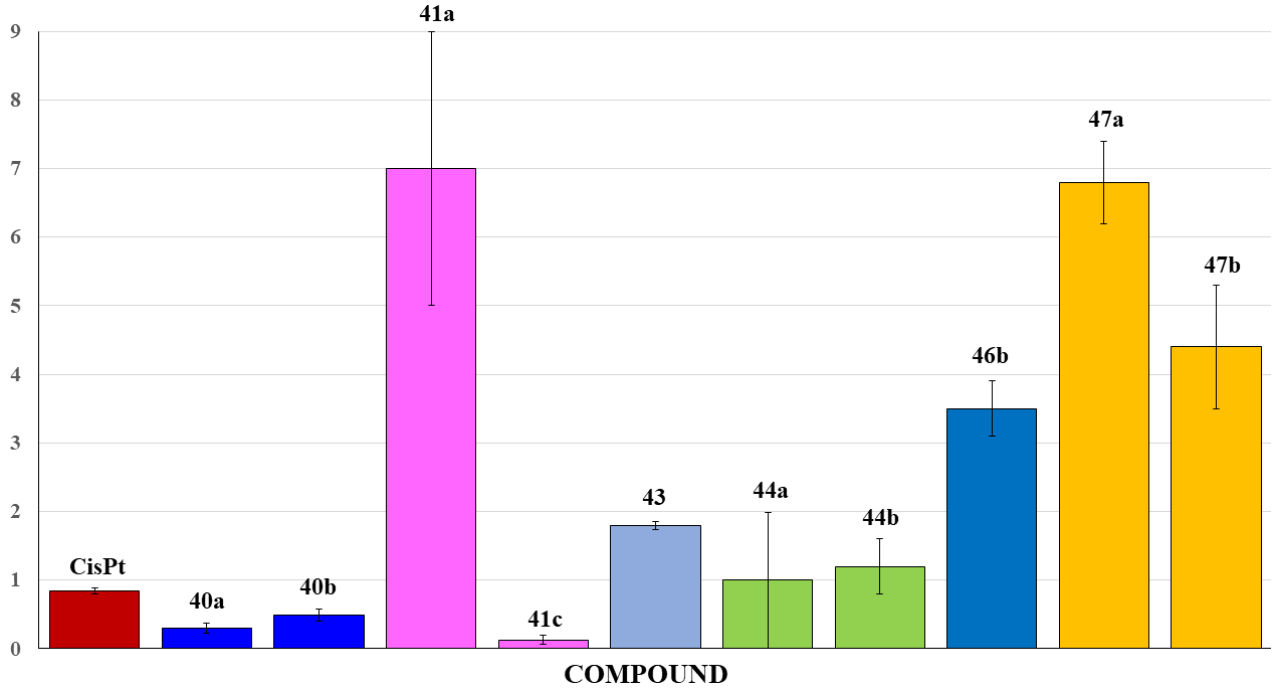

Fig. 4.34 Palladacyclopentadienyl complexes with IC_{50}<8 μM on OVCAR5 cell line.

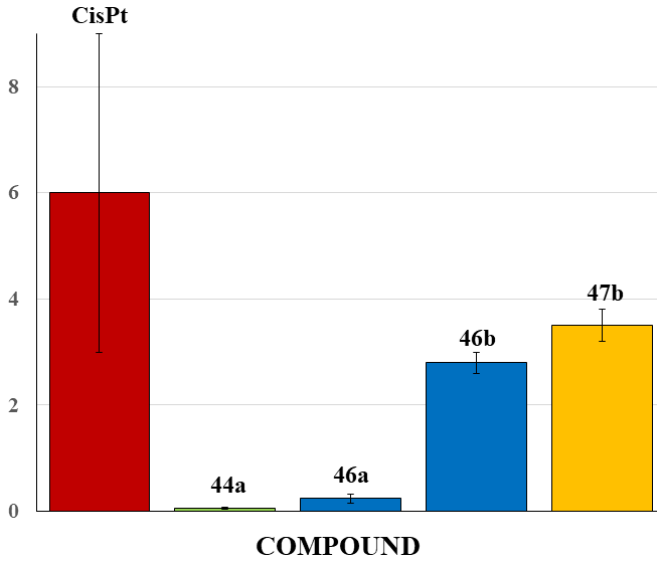

Fig. 4.35 Palladacyclopentadienyl complexes with IC_{50}<8 μM on A549 cell line.

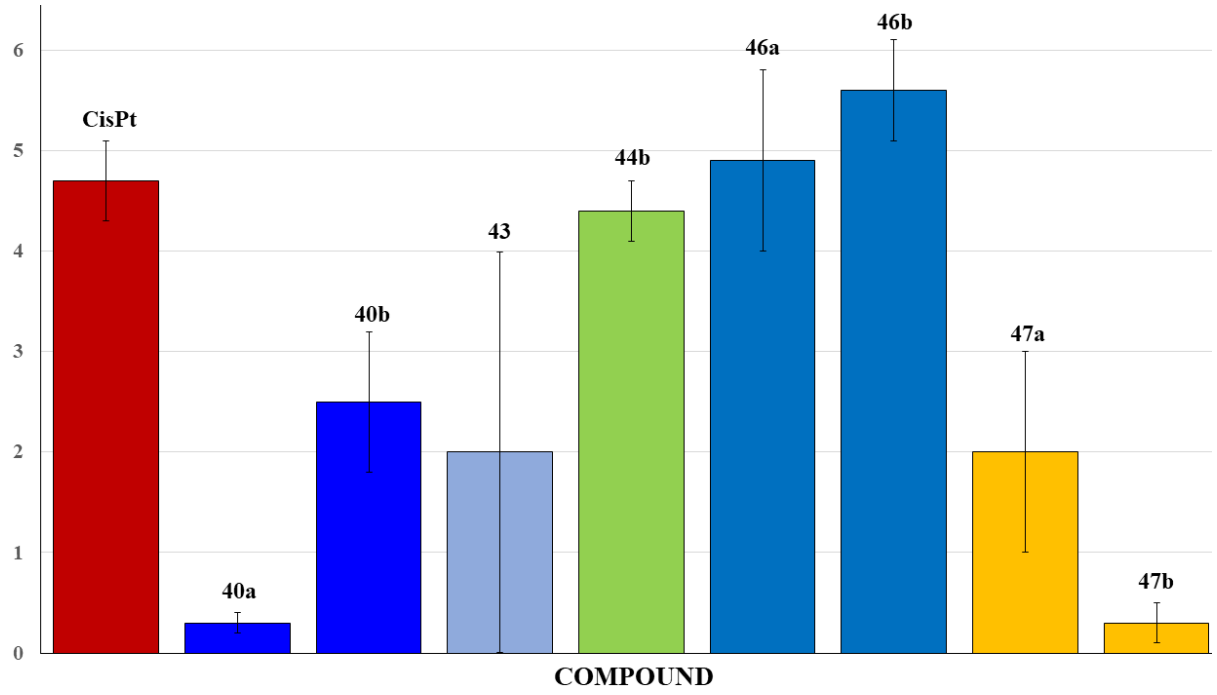

Fig. 4.36 Palladacyclopentadienyl complexes with IC_{50}<6μM on A375 cell line.

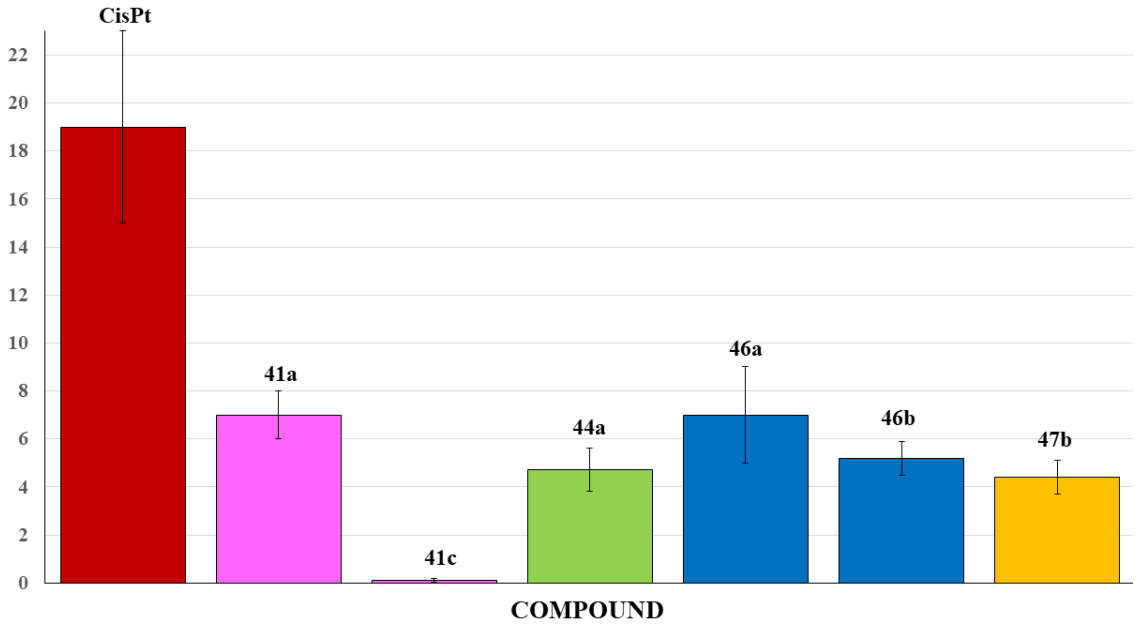

Fig. 4.37 Palladacyclopentadienyl complexes with IC_{50}<20 μM on DLD1 cell line.

From the analysis of IC_{50} values it is possible to propose the following considerations:

- All the examined species, except for compounds **44b** and **46b**, are substantially inactive toward healthy cells (IC_{50}> 100 μM on fibroblasts). This feature, if accompanied by a good activity toward the tumor lines, is of fundamental importance.
- For the cisplatin-sensitive ovarian cancer lines (A2780 and OVCAR5) the most active compounds are those bearing: *i)* chelating bisNHCs (**40a-b**) ligands, *ii)* two NHC ligands (**41b**

and **41c**, respectively active in the A2780 and OVCAR5 lines), *iii)* mixed NHC/PPh_3 (**44b**) and NHC/DIC (**46b**) ligands and *iv)* the zwitterionic complex **47b**.

- For the cisplatin-resistant ovarian cancer line A2780-R, the active compounds are those bearing: *i)* chelating bisNHCs (**40a-b**), *ii)* the biscarbene complex **41b**, *iii)* the complex with the pyridylcarbene ligand **43**, *iv)* all the mixed NHC/PPh_3 and NHC/DIC complexes (**44a-b** and **46a-b**) and *v)* the zwitterionic compound **47b**.
- On the lung cancer line (A549), only the mixed NHC/PPh_3 and NHC/DIC compounds (**44a-b** and **46a-b**) and the zwitterionic complex **47b** are active. Particularly interesting is the compound **44a** which shows an IC_{50} about 100 times lower than to cisplatin.
- As for the malignant melanoma (A375 line) the most active compounds are those bearing: *i)* chelating bisNHCs (**40a-b**), *ii)* mixed NHC/PPh_3 and NHC/DIC ligands (**44a-b** and **46a-b**) and *iii)* the zwitterionic complexes **47a- b**.
- For the colon adenocarcinoma (DLD1 line) the compounds that have a significant activity are those bearing: *i)* two carbene ligands (**41a-c**), ii) mixed NHC/PPh_3 and NHC/DIC complexes (**44b** and **46b**) and iii) the zwitterionic species **47b**.
- Complexes with chelating N-S and N-P ligands (**D**-**F**) are poorly active or inactive toward all the lines taken into consideration.

4.5.2. Reactivity of complexes with reduced L-glutathione (GSH)

In order to verify whether the different activity of the palladacyclopentadienyl complexes may be ascribed to the different lability of their ancillary ligands, some reactivity tests were performed with reduced glutathione (GSH). This tripeptide, as already mentioned in the introductory chapter, is one of the main potential soft bio-ligands present in the cellular environment and can potentially coordinate on the metal centre replacing one or more ligands present in the starting complex.
The tests carried out by us, using 2 mM and 10 mM concentrations respectively of complex and glutathione, have shown that:

1. The complexes bearing chelating or two monodentate carbene ligands (**40**-**41**) and the mixed NHC/DIC complexes (**46**) are stable for 48 h in the presence of reduced glutathione.
2. The mixed NHC/PPh_3 complexes (**44**) and that stabilized by the phosphinoquinoline ligand DPPQ (**D**), undergo substitution of PPh_3 and of phosphinoquinoline moiety within 24 hours, respectively. It is noteworthy that in both cases the phosphine ligand is converted into the corresponding phosphine oxide.

3. After the addition of GSH, the complexes bearing chelating carbene ligands (NHC-pyridine (**42**) and NHC-thioether (**43**)) undergo the fast displacement of the labile heteroatom arm. The system does not further evolve and the carbene group remains coordinated to the palladium centre.
4. In the complexes with thioquinoline and pyridylthioether (TMQ and $PyrCH_2SCH_3$, complexes **E-F**), glutathione immediately replaces the bidentate ligands.
5. In no case it is possible to observe any reaction between the palladacyclopentadienyl residue and glutathione.

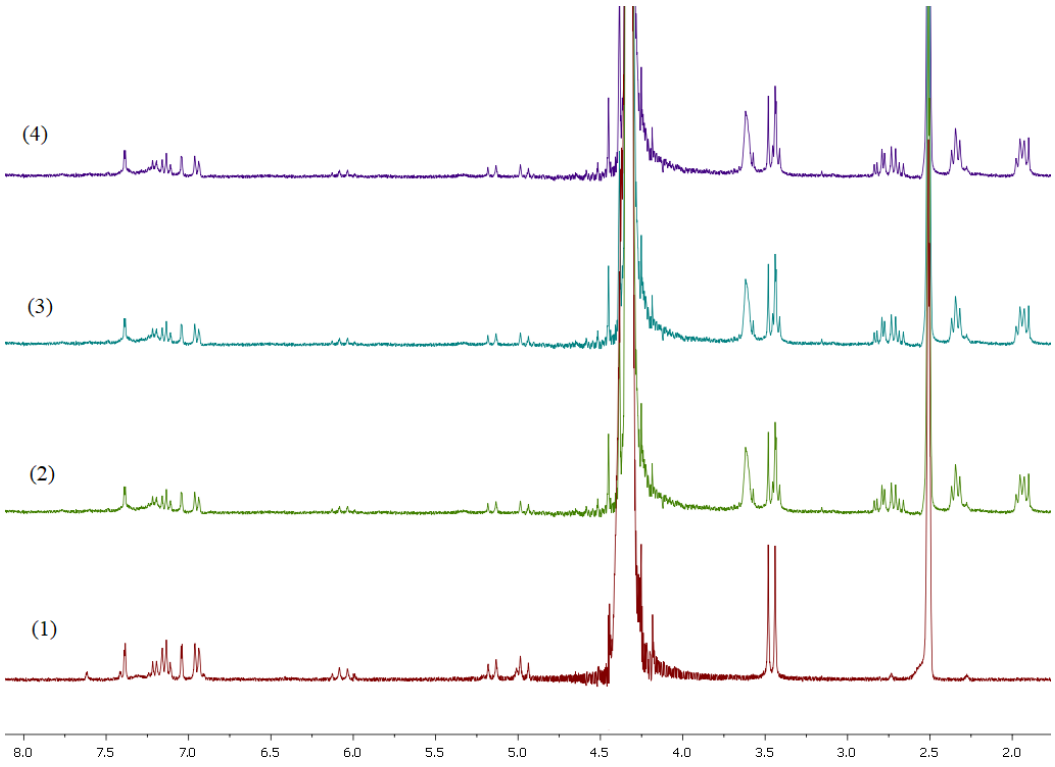

*Fig. 4.38 H^1-NMR spectra (298K) of complex **40a** in DMSO-d6/D_2O (1) and after the addition of GSH, recorded at different time: t=0 (2), 24h (3), 48h (4).*

In summary, the mixed NHC/DIC complexes and those bearing two carbene ligands retain their structure (Fig. 4.38). On the contrary, the remaining complexes undergo partial or total ligand substitution by GSH.

These reactivity tests allow us to make further considerations in relation to the biological data reported in Table 4.2.

In particular, we can observe that generally the most active compounds have spectator ligands firmly anchored to the metal center (chelating bisNHCs, bisNHCs, mixed NHC/PPh_3 or NHC/DIC), whereas species that do not contain at least one coordinated carbene (chelating N-S and N-P ligands) are poorly active or inactive.

In this regard, the most interesting compounds we have identified are:

- Complex **40a**, which is particularly active on ovarian cancer lines (A2780, OVCAR5 and A2780-R).
- Complex **41c**, which is particularly active on the OVCAR5 line (ovarian carcinoma) and above all DLD1 (colon adenocarcinoma).
- Complexes **44a** and **46a**, which are very active on the A549 line (lung carcinoma).
- The zwitterionic complex **47b**, which displays a good/excellent activity in all the lines taken into consideration.

Since this work is particularly focused on ovarian cancer, a more in-depth study on the activity of the promising complex **40a** will be proposed below.
In particular, the cellular uptake data and the results of specific biological tests, aimed at identify the main biological target of this compound, will be presented.

4.5.3. Uptake analysis

In order to verify whether the activity of the examined complexes may be influenced by the different cellular uptake, we have compared the uptake percentage of the efficient complex **40a** and the virtually inactive complex **E,** on the A2780 cell line.
The collected data showed that the greater activity of **40a** ($IC_{50} \approx 0.04$ μM) with respect to **E** ($IC_{50} \approx$ 98 μM) is ascribable also to the higher uptake level (ca. 60% vs 0.6%), determined close to the IC_{50} value.

4.5.4. Biological tests for the determination of the biological target

To better understand the main mechanism of action of compound **40a**, all the cell-based experiments were performed following different time points.
As reported in some recently published works, one of the possible main targets for palladium complexes is DNA [12, 19].
To test the interaction between this important biomolecule and compound **40a**, as a sensitive marker for DNA double-strand breaks, the phosphorylation of Ser139 of Histone H2AX was evaluated. In fact, after DNA damage, the phosphorylation at Ser139 helps to recruit the DNA repair machine and apoptotic proteins to dispatch their function [20]. As shown in Figure 4.39, the complex is active already at 40 nM (IC_{50} value) and after only 3 hours the phosphorylation of Ser139-Histone H2AX starts to accumulate in the nucleus.

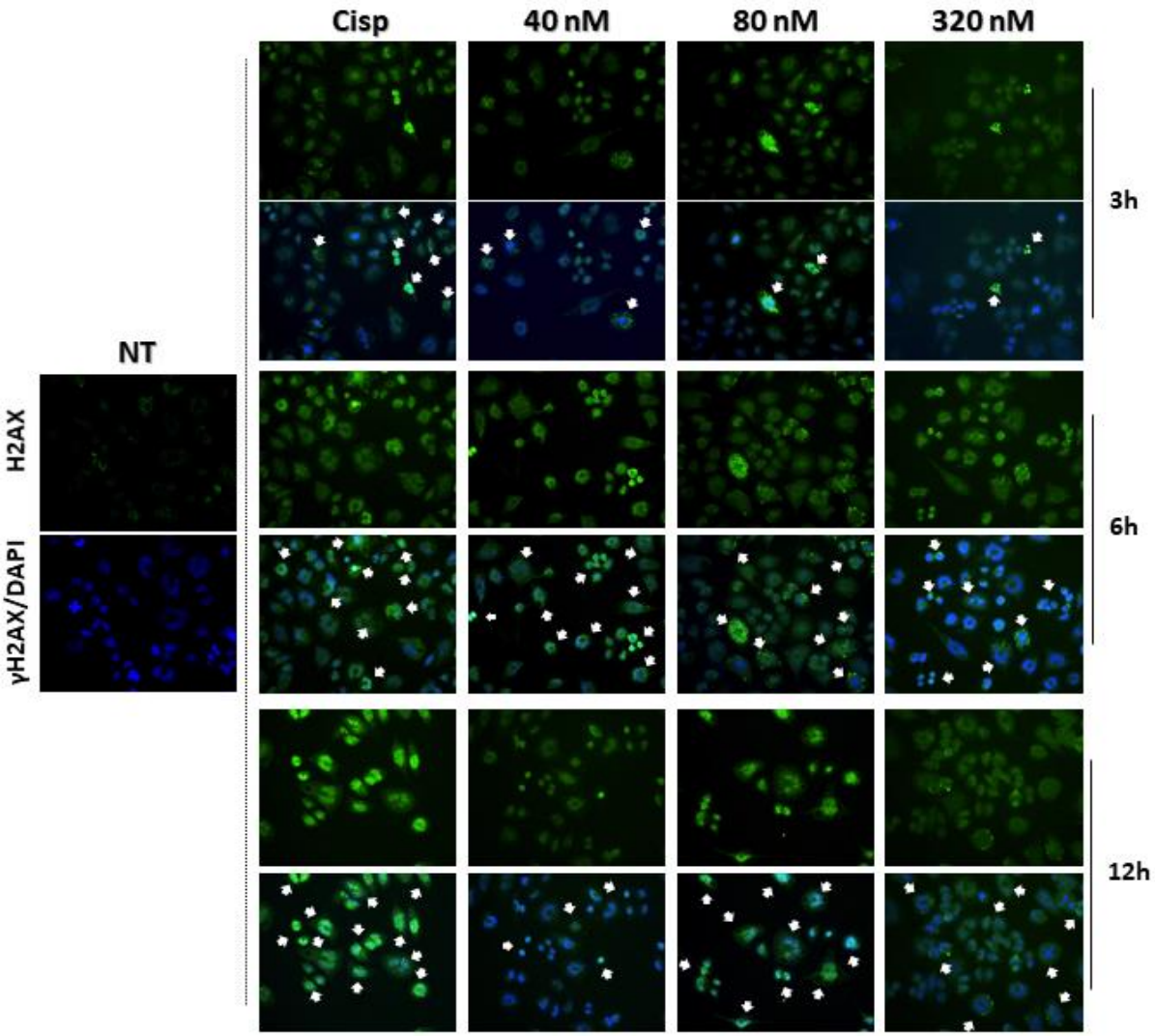

*Fig. 4.39 Assay for DNA double-strand breaks. After incubation of A2780 cells with compound **40a** (40nM, 80nM, 320nM), cisplatin (10μM) or control (non-treated) for 3h, 6h or 12h, they were stained with anti-phospho-histone H2AX antibody and detected with Alexa Fluor® 488-conjugated secondary antibody (green). A2780 cells were also stained with DAPI for visualization of nucleus (blue). White arrows are rapresentative foci formation (accumulation of phospho-histone H2AX in the nucleus) showing that compound **40a** induces DNA double-strand breaks 3 hours after treatment compared to the untreated cells.*

Following the DNA damage, cells activate the apoptotic pathway by inducing the release of cytochrome C, a conserved electron-transport protein which is part of the respiratory chain of mitochondria. This early event was studied by immunofluorescence.

After 6-12 hours, in the A2780 cells treated with compound **40a**, the cytochrome C appears to be translocated from the mitochondria to the cytoplasm as a diffuse cytoplasmic staining pattern (Fig. 4.40).

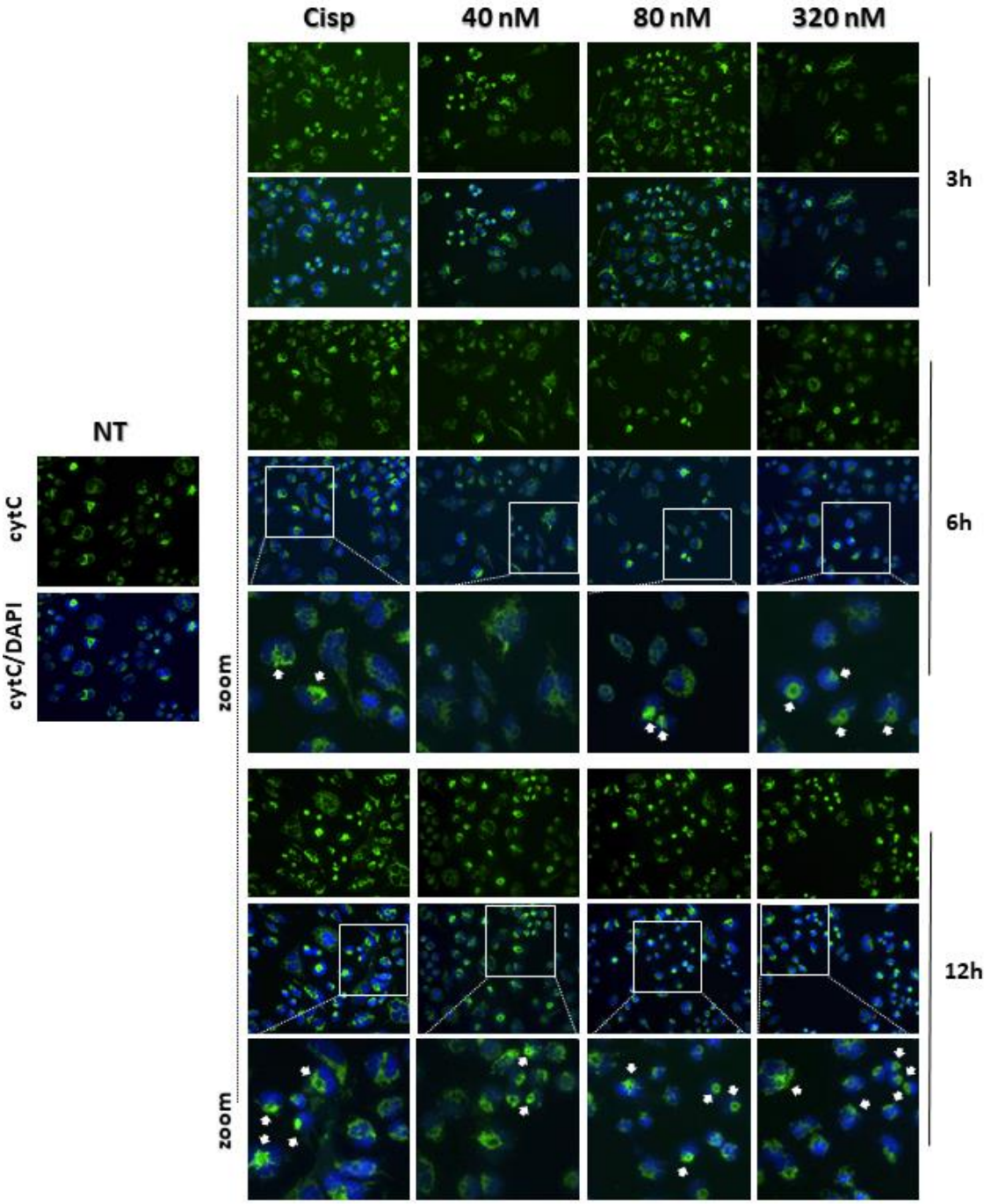

Fig. 4.40 Assay for the release of cytochrome C. After incubation of A2780 cells with compound ***40a*** *(40nM, 80nM, 320nM), cisplatin (10µM) or control (non-treated) for 3h, 6h or 12h, they were stained with anti-cytochrome c antibody detected with Alexa Fluor® 488-conjugated secondary antibody (green). A2780 cells were also stained with DAPI for visualization of nucleus (blue). White arrows indicate a selection of apoptotic cells showing that compound* ***40a****, similar to cisplatin, induces the translocation of cytochrome c from mitochondria to cytoplasm (diffuse cytoplasmic staining pattern) 6-12 hours after treatment compared to the untreated cells showing a pointed or massive staining pattern.*

After the release of cytochrome C, cells activate the caspase cascade to induce the apoptosis process. The induction of caspase 3/7 was assessed at different time points and concentration of compound **40a.** Starting from 40 nM of such compound, cells displayed a high level of caspase 3/7 compared to untreated cells (Fig. 4.41).

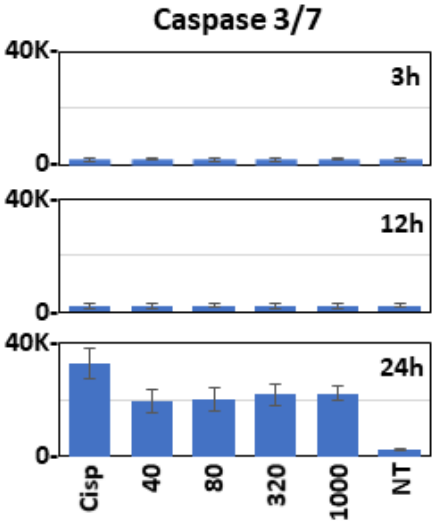

*Fig. 4.41 Effect of compound **40a** on caspase-3 and caspase-7 activities after incubation of A2780 cells with compound **40a** (40nM, 80nM, 320nM), cisplatin (10µM) or control (non-treated) for 3h, 12h, 24h. After 24 hours of treatment with compound **40a**, A2780 cells, similar to cisplatin effect, showed a high level of caspase-3 and caspase-7 activation compared to untreated cells.*

To confirm that the complex **40a** acts mainly and effectively on the DNA, causing only afterwards damage in the other regions of the cell, a test aimed at indentify after how long the damage occurs on the mitochondrial membrane has been carried out.

In this regard, the cyclopalladated compounds recently published by Fong and co-workers, mainly act against this membrane and only marginally cause DNA damage in the early hours of exposure to the drug by the cell [21].

The assay for mitochondrial membrane potential that we performed, showed that it is possible to see clear membrane damage only after 24 hours from the treatment of the A2780 cells with compound **40a** (Fig. 4.42). This evidence suggests that damage to the mitochondria occurs as a result of DNA damage (evident as early as 3 hours) and activation of apoptosis pathways.

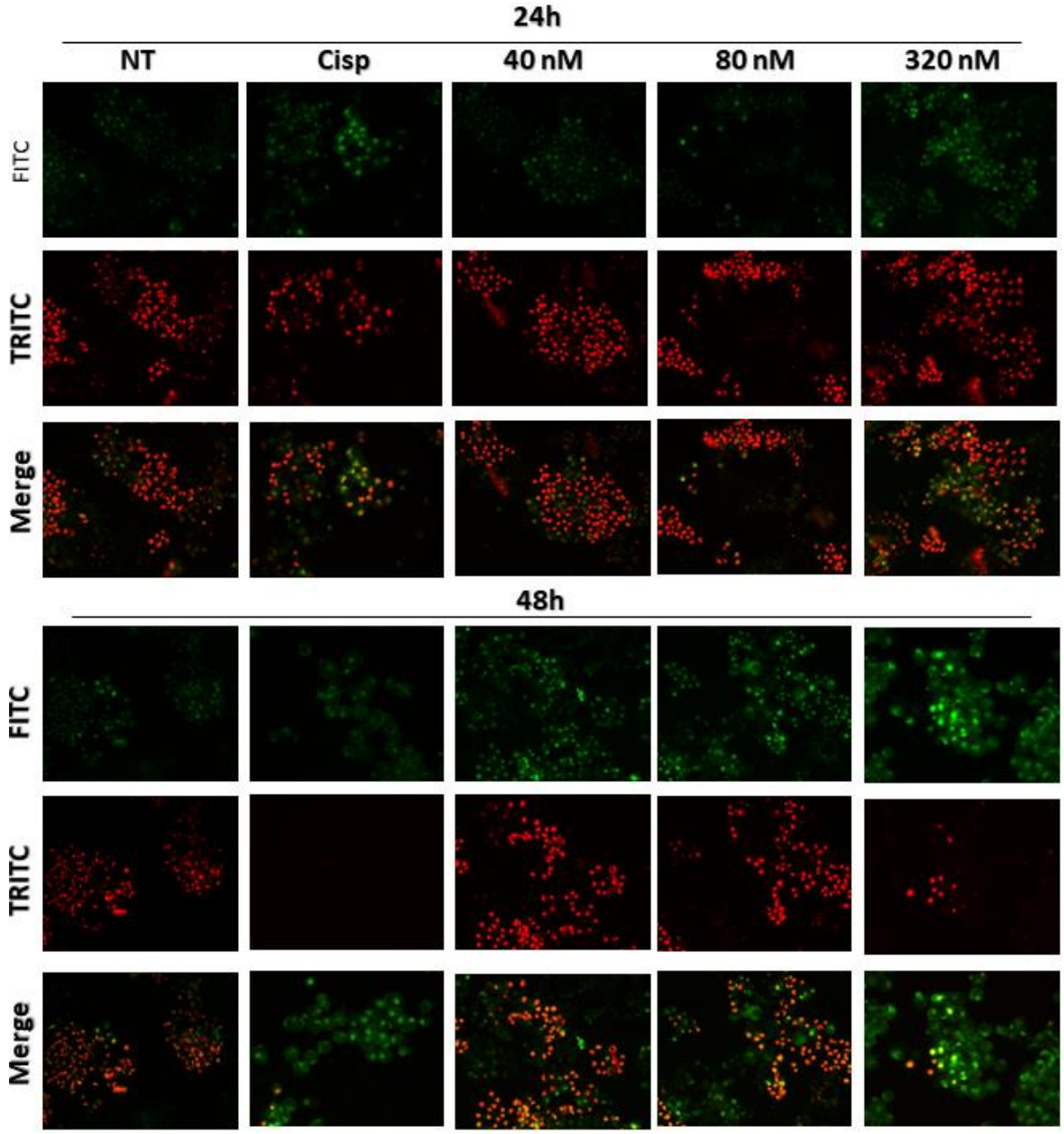

*Fig. 4.42 Assay for mitochondrial membrane potential. After incubation of A2780 cells with compound **40a** (40nM, 80nM, 320nM), cisplatin (10µM) or control (non-treated) for 24h or 48h, they were stained with JC-1 dye. Untreated cells showing red J-aggregate fluorescence indicated hyperpolarized membrane potentials. Cells treated with cisplatin showing cytoplasmic diffusion of green monomer fluorescence indicated depolarized membrane potentials. Cells treated with compound **40a** show a progressive loss of red J-aggregate fluorescence (hyperpolarized membrane potentials) and cytoplasmic diffusion of green monomer (depolarized membrane potentials) 24 hours after treatment of A2780 cells compared to untreated cells.*

4.6. Synthesis of η^3-allyl palladium complexes

Analogously to that described in the previous paragraphs about the palladacyclopentadienyl complexes, it was decided to test *in vitro* the cationic η^3-allyl palladium complexes synthesized by our research group and summarized in Figure 4.43.

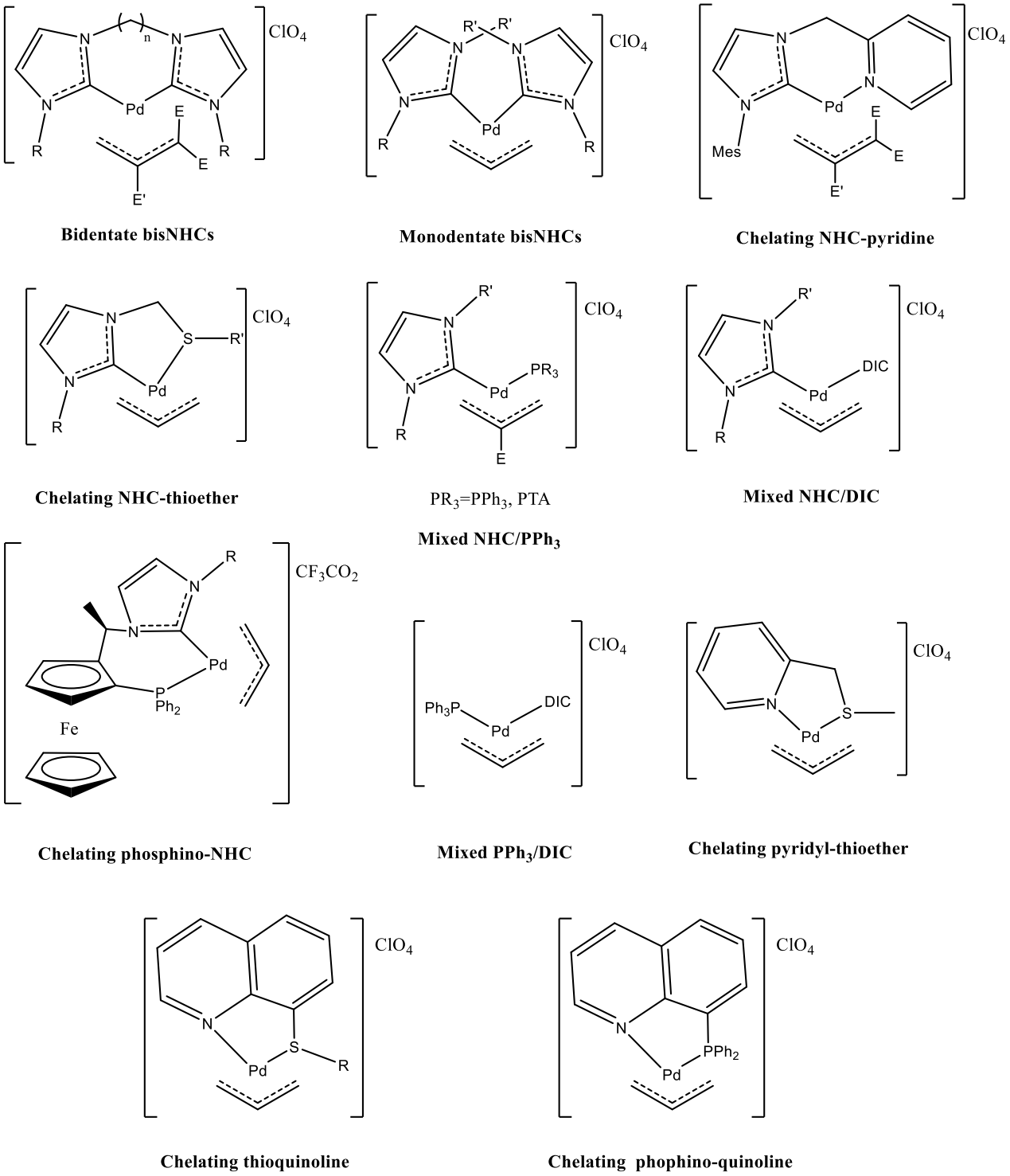

Fig. 4.43

4.6.1. η^3-allyl palladium complexes bearing bidentate bisNHCs

The synthesis of cationic η^3-allyl palladium compounds containing chelating biscarbene ligands was carried out following a synthetic strategy different from that proposed by Elsevier and co-workers, who synthesized the allyl derivatives by reacting the dimeric precursor $[Pd(\mu\text{-}Cl)(\eta^3\text{-allyl})]_2$ with the silver carbene complexes **39a-f** [22] (Scheme 4.18).

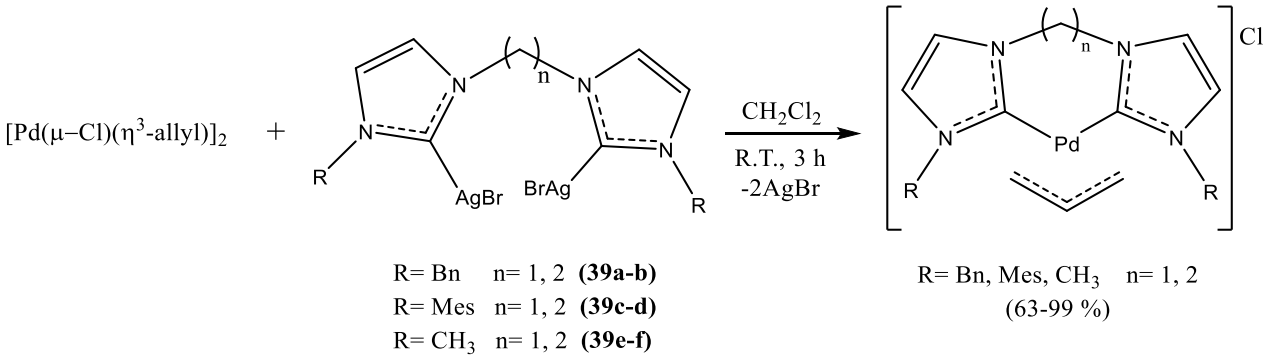

Scheme 4.18

In order to extend the synthesis to the complexes with two monodentate NHCs and obtain compounds with perchlorate as counterion, in uniformity with the other categories of allyl complexes that will be discussed, it was decided to synthesize allyl palladium precursors with a labile pyridyl-thioether ligand (Me-PyCH_2SPh), and subsequently carry out the transmetallation with the silver complexes **39a-f** (Scheme 4.19).

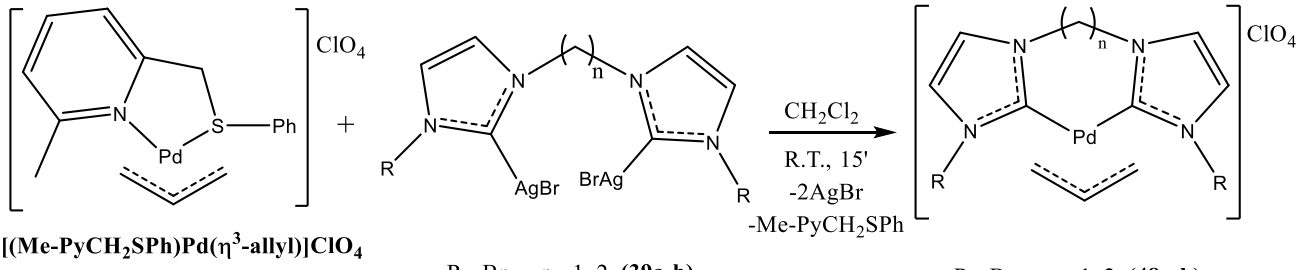

Scheme 4.19

All these compounds were selectively obtained and isolated as solids, by precipitation from dichloromethane/diethyl ether mixture, and exhaustively characterized by NMR, IR and elementary analysis techniques.

4.6.1.1. Complexes with R = methyl or benzyl

Complexes **48a-b** and **48g-h** were obtained as single species, since the rearrangement of the methylene or ethylene spacer up and down to the main coordination plane is free and therefore no isomers are observed. Due to the symmetry of these species, in the ^{1}H-NMR spectra (Fig. 4.44) we can notice the presence of:

- The *central* allyl proton between 5.2 and 5.4 ppm as a multiplet.
- The *anti* allyl protons, as one doublet, between 2.7 and 2.9 ppm (J ≈ 13 Hz).
- The *syn* allyl protons, as one doublet, between 3.8 and 4.3 ppm (J ≈ 7-8 Hz).
- The methylene bridge protons as an AB system between 6 and 7 ppm (J ≈ 13 Hz) in the case of complexes **48a** and **48g**.
- The ethylene bridge protons as a multiplet between 4.5 and 5 ppm in the case of complexes **48b** and **48h**.
- The signals ascribable to the methyl substituents at about 3.7 ppm (singlet) in the case of complexes **48a-b** or the methylene protons of the benzyl substituents between 5 and 5.3 ppm (singlet) in the case of compounds **48g-h**.

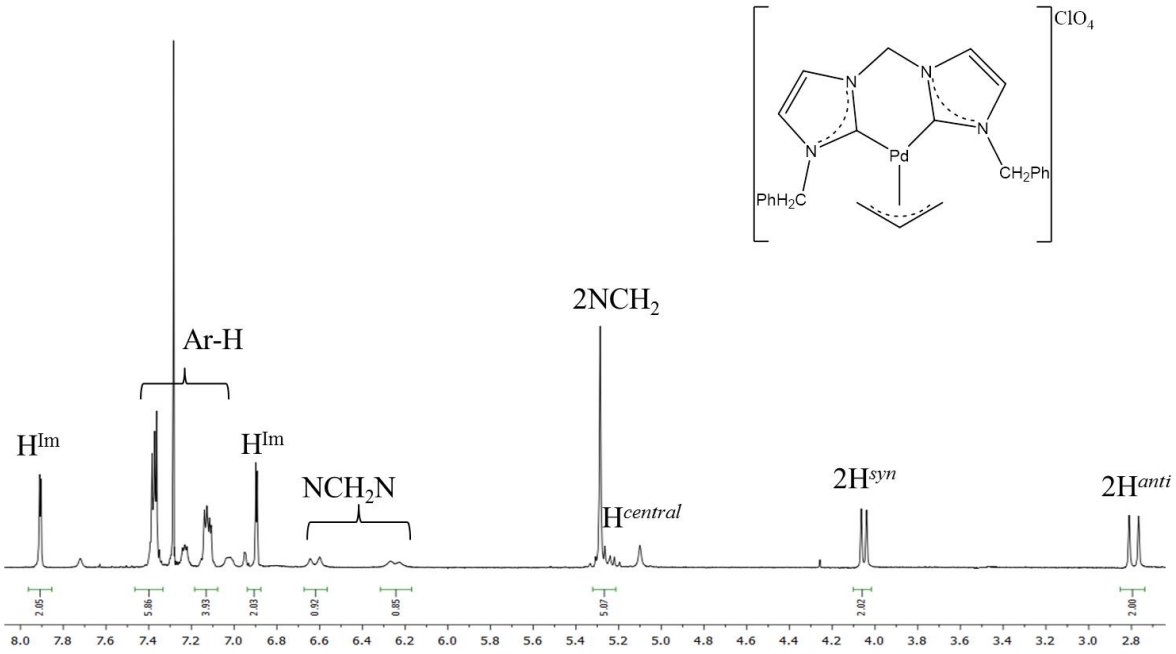

*Fig. 4.44 ^{1}H-NMR spectrum of the complex **48a** in $CDCl_3$ at T = 298 K.*

As for the ^{13}C-NMR spectra (Fig. 4.45), in addition to the signals related to the methyl or benzyl substituents and of the aromatic carbons, we can observe:

- A single signal for the *terminal* allyl carbons at about 58-59 ppm.
- The signal of the *central* allyl carbon at about 119 ppm.

- The signal of the methylene spacer carbon (NCH_2N) at about 62-63 ppm in the case of species **48a** and **48g** or the ethylene spacer carbon (NCH_2CH_2N) at about 48 ppm in the case of complexes **48b** and **48h**.

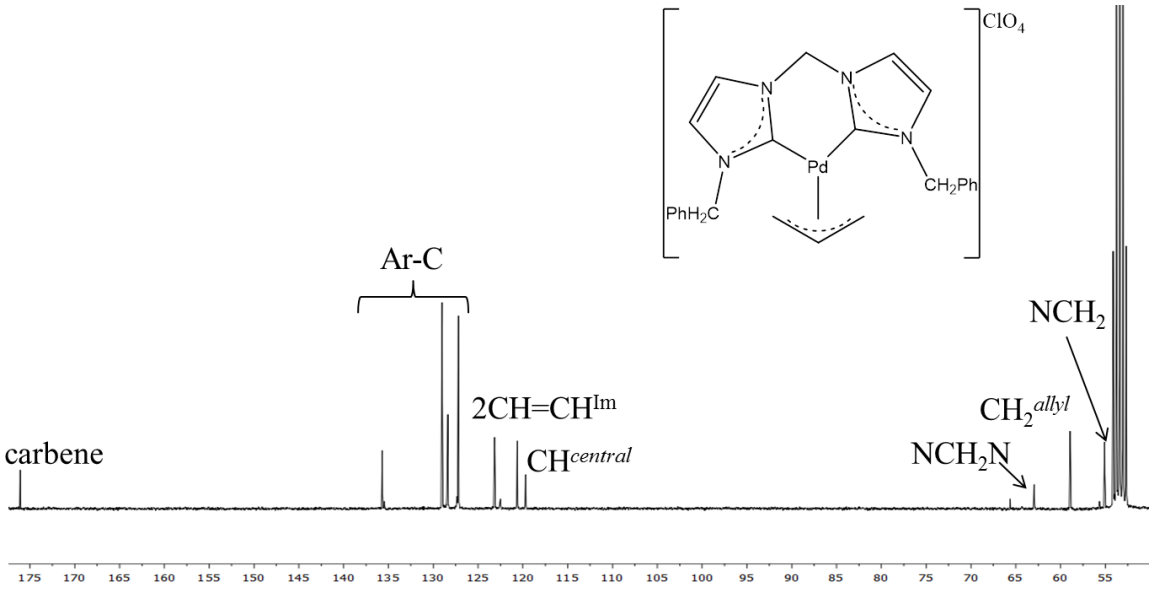

*Fig. 4.45 $^{13}C\{^1H\}$-NMR spectrum of the complex **48a** in CD_2Cl_2 at T = 298 K.*

4.6.1.2. Complexes with R = mesityl

The synthesized complexes bearing the mesityl as lateral substituent, unlike the previous ones, are all present as a pair of atropoisomers. In fact, the ensuing high steric hindrance prevents the free movement with respect to the main coordination plane of the spacer and favours the formation of the two possible atropoisomers *exo* and *endo*, as shown in Figure 4.46.

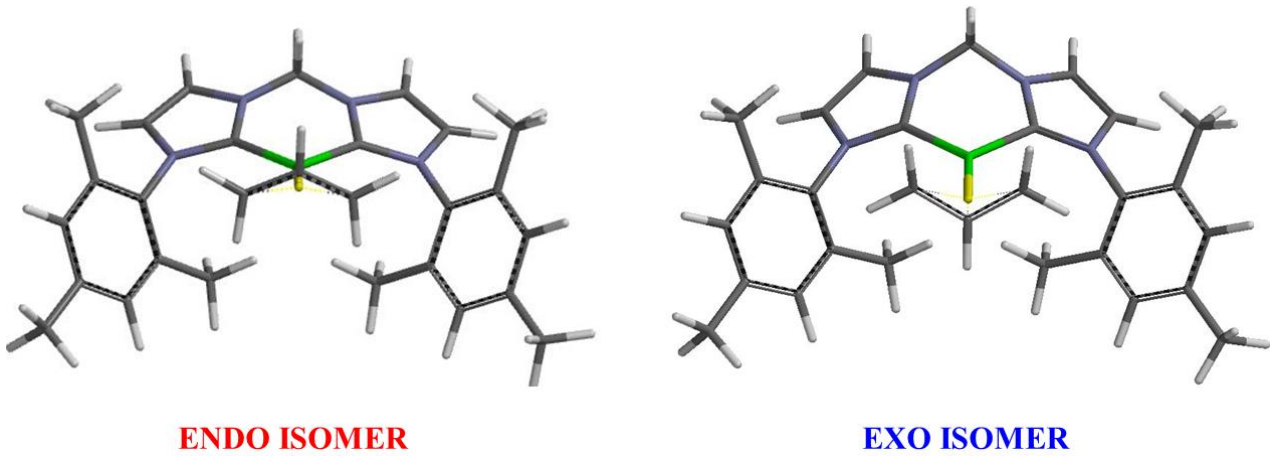

*Fig. 4.46 Representation of the two atropoisomers for complex **4c** by means of DFT calculations.*

Consequently, the doubling of all the NMR signals is observed. In particular, for each atropoisomer, it is possible to notice the presence in ^{1}H-NMR spectra (Fig. 4.47) of:

- A doublet (J ≈ 13 Hz) between 1.5 and 2 ppm related to the *anti* allyl protons.
- A doublet (J ≈ 8 Hz) between 3 and 3.2 ppm for the *syn* allyl protons.
- A multiplet between 4.5 and 5 ppm for the *central* allyl proton.
- A multiplet at about 5 ppm for the ethylene spacer of the complex **48d** or an AB system (J ≈ 13 Hz) between 6 and 7 ppm ascribable to the methylene spacer (complex **48c**).
- Three different methyl signals ascribable to the mesityl substituent.

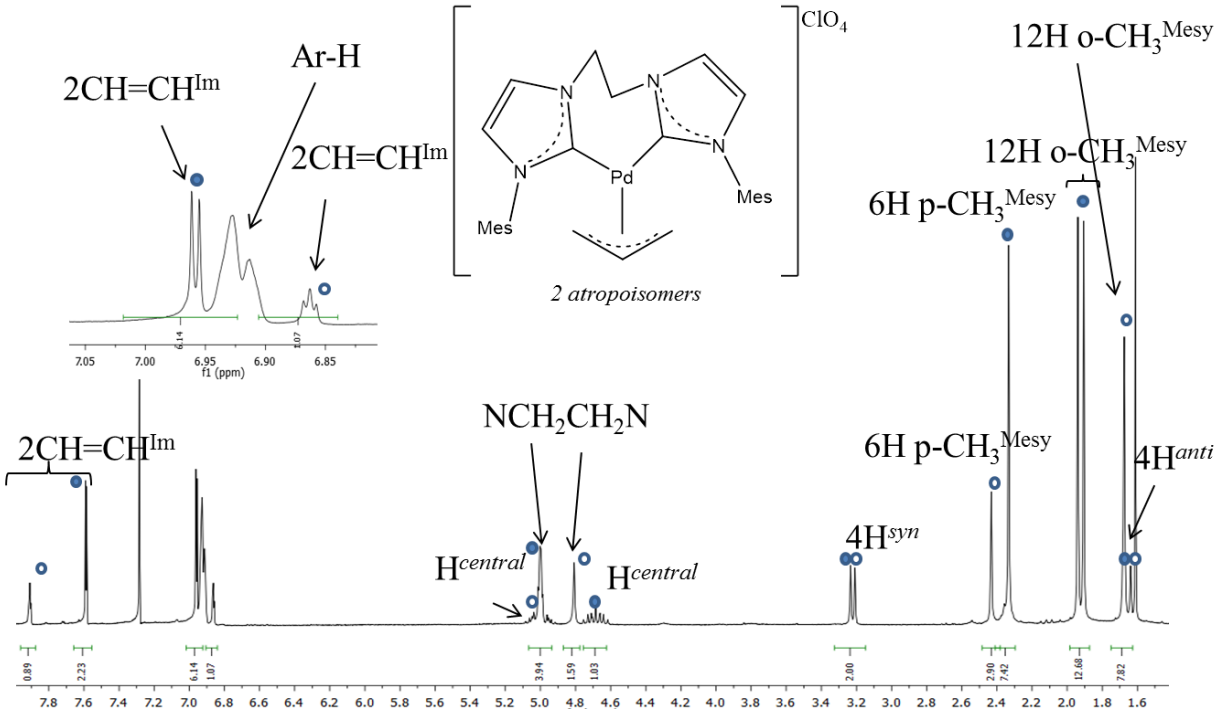

*Fig. 4.47 ^{1}H-NMR spectrum of the complex **48d** in $CDCl_3$ at T = 298 K.*

In the ^{13}C-NMR spectra it is possible to observe the presence of two signals, one for each isomer, ascribable to the coordinated carbenic carbon at about 176 ppm.

For analogues compounds with the chloride counterion, a single set of signals is present in the NMR spectra, as reported by Elsevier and co-workers [22]. This fact can be easily explained by previous experience, suggesting that the presence of nucleophiles in solution tends to promote the η^3- η^1-η^3 isomerization process and thus the interconversion between the two atropoisomers [23].

In the biological environment, in which chlorides and other nucleophiles are present, the allyl complexes present as a pair of atropoisomers, can easily interconvert throughout the η^3- η^1-η^3 isomerization process.

The marked tendency of the compounds **48c-d** to precipitate as microcrystals of excellent purity prompted us to synthesize chelating biscarbene complexes bearing the 2-methylallyl or the 1,1-dimethyl-allyl moieties and the carbene substituted by the mesityl fragment.

It is well known that the introduction of substituents (i.e. methyl or phenyl groups) on the allyl moiety heavily influences the reactivity of the derived compounds. This aspect could be exploited for the modulation of the reactivity of complexes in biological environment as can be deduced by the values of the kinetic constants related to the nucleophilic attack of amines on differently substituted allyl fragment, in complexes bearing the same spectator ligand (Scheme 4.20) [24].

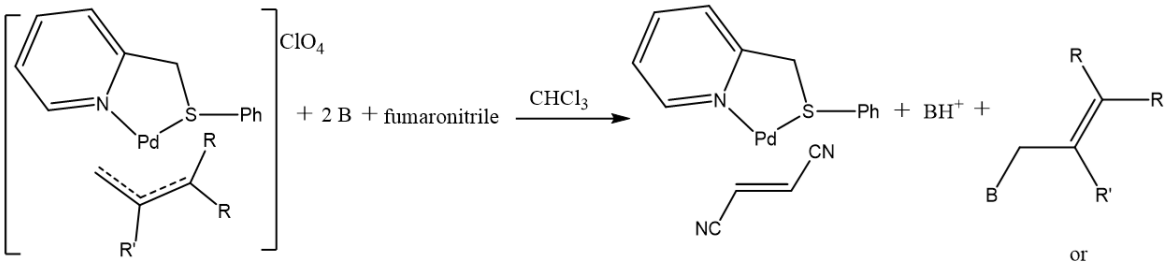

R= H R'=H **(1a*)**
R= H R'=CH_3 **(1b*)**
R= CH_3 R'=H **(1c*)**

Complex	Second order rate constant (k_2, $mol^{-1}dm^3s^{-1}$) at 25 °C		
	B = Piperidine	B = Diethylamine	B = Morpholine
1a*	3.9±0.3	0.78±0.02	1.19±0.03
1b*	0.106±0.004	(3.3±0.2)·10^{-2}	(8.8±0.2)·10^{-3}
1c*	0.163±0.002	(2.03±0.08)·10^{-2}	(1.5±0.2)·10^{-2}

Scheme 4.20

From the table of Scheme 4.20 it is possible to infer how the introduction of a methyl in the central or peripheral position of the allyl fragment considerably slows down the rate of the nucleophilic attack of the amines. Thus, complexes **48e-f** were synthesized following a protocol similar to that previously used in the case of the derivatives bearing the unsubstituted allyl fragment (Scheme 4.21).

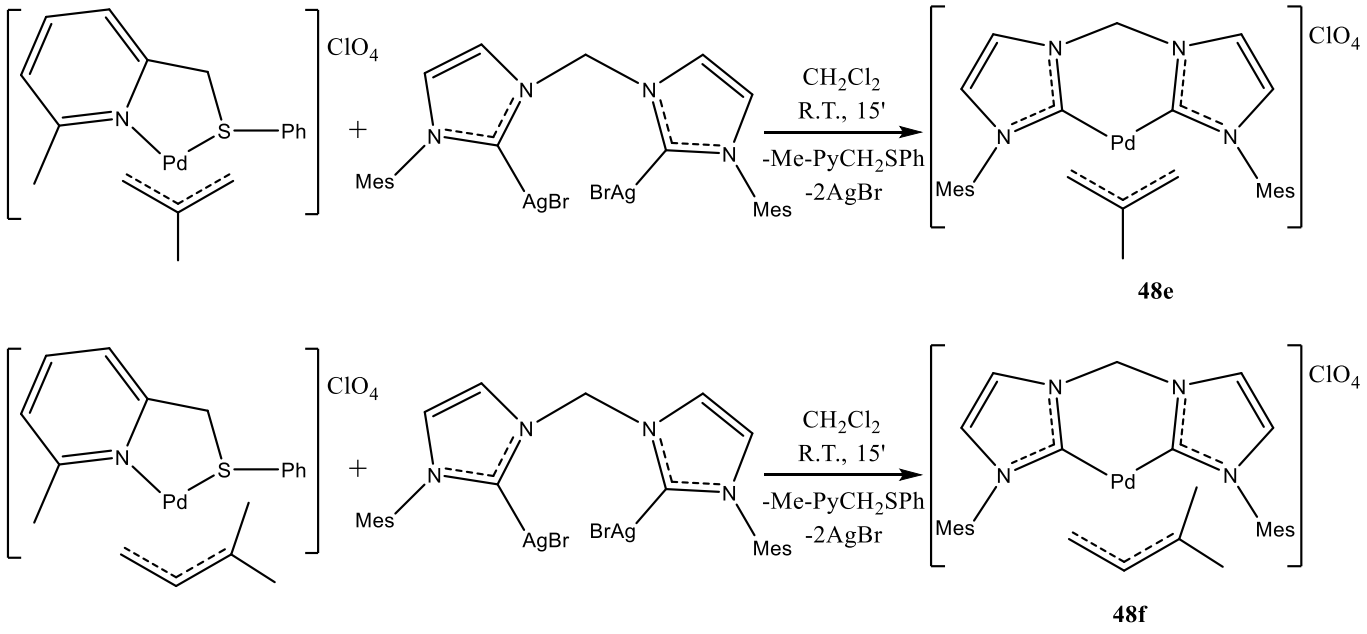

Scheme 4.21

The ^{1}H-NMR spectrum of compound **48e** (Fig. 4.48) shows, for each atropoisomer, the presence of:

- A singlet at about 2 ppm related to the *anti* allyl protons.
- A singlet at about 2.5 ppm ascribable to the *syn* allyl protons.
- A singlet between 1 and 1.5 ppm traceable back to the methyl substituent of the allyl fragment and an AB system (J ≈ 13 Hz) between 6.5 and 7 ppm related to the NCH_2N spacer.
- Three different methyl signals for the mesityl substituent between 1.5 and 2.5 ppm.

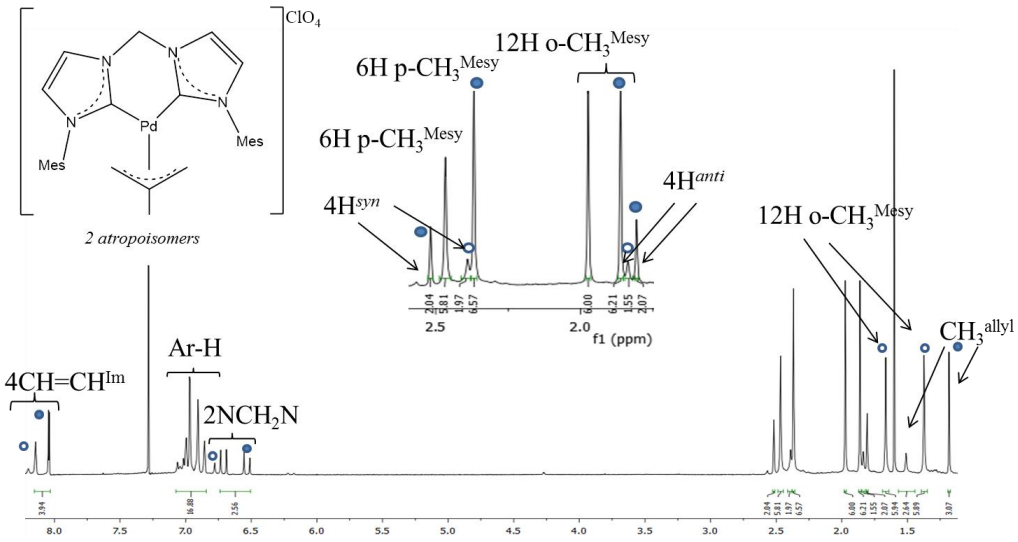

*Fig. 4.48 ^{1}H-NMR spectrum of the complex **48e** in $CDCl_3$ at T = 298 K.*

At variance with complexes **48a-d**, the ^{13}C-NMR spectra of complexes **48e-f** show the signal of central allyl carbon at about 130 ppm (Δδ ≈10 ppm downfield with respect to the complex **48c**), whereas the coordinated carbenic carbon resonates at about 177 ppm.

For the complex **48e** it was also possible to obtain its solid-state structure by single crystal X-ray diffraction (Fig. 4.49).

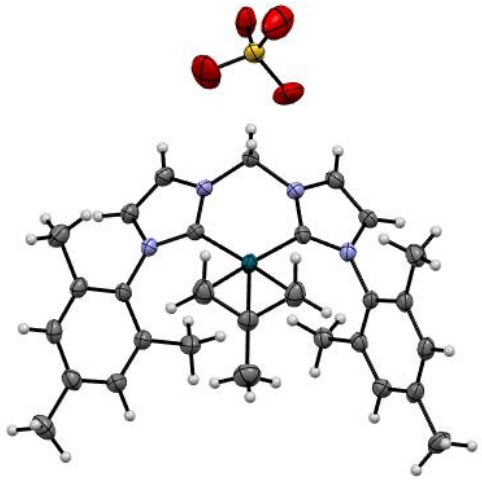

*Fig. 4.49 Ellipsoid representation of **48e** crystal ASU contents (50% probability).*

In contrast to the previously cases, the reaction between the precursor [(Me-PyCH$_2$SPh)Pd(1,1-dimethyl-η^3-C$_3$H$_3$)]ClO$_4$ and the silver complex **39c** is not selective at room temperature nor at 233K (Scheme 4.22).

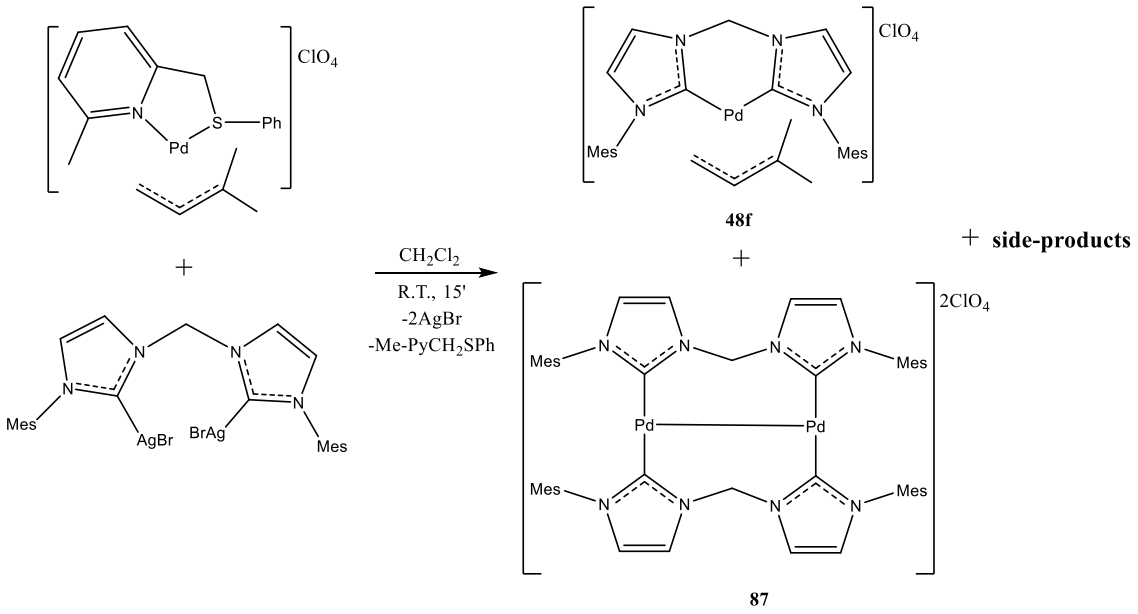

Scheme 4.22

As a matter of fact, a compound present in solution at 25% does not present signals traceable back to the allyl fragment in its NMR spectra.

Such compound, that was separated from the starting mixture by selective precipitation (in a 1 : 2 mixture of dichloromethane/diethylether, set at 5 °C for 24 h), is stable both in solid and in solution. According to the data obtained by X-ray diffraction, this side product (compound **87**) is a dinuclear complex of Pd(I) containing a Pd-Pd bond and stabilized by two bridged bis-NHCs (Fig. 4.50).

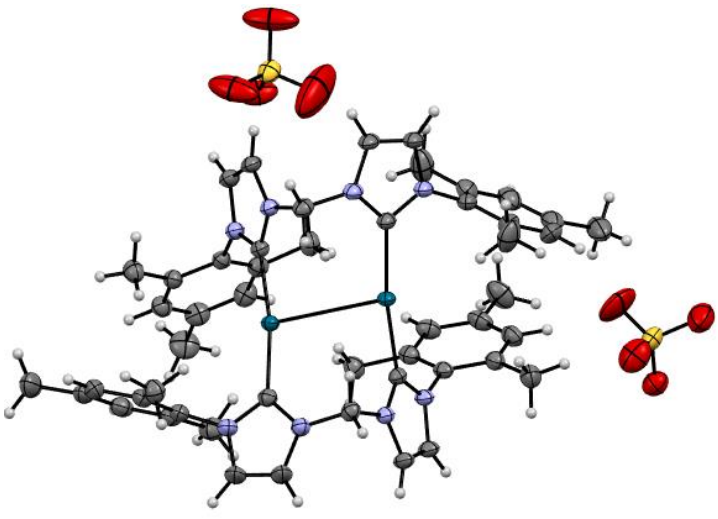

*Fig. 4.50 Ellipsoid representation of **87** crystal ASU contents (50% probability).*

Remarkably, palladium complexes in oxidation state +1 are quite rare and the most important examples are reported in figure 4.51.

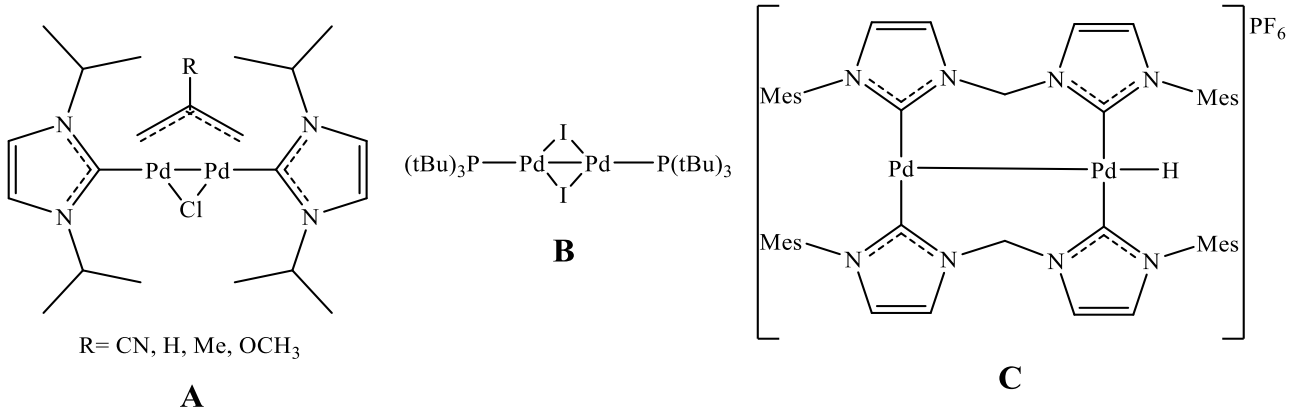

Fig. 4.51

Among the described species, the neutral allyl Pd (I) complexes **A**, reported on the left of Fig. 4.46, were firstly observed as decomposition products of Pd (II) allyl complexes used in some catalytic processes [25]. Subsequently they were selectively obtained by means of a synthetic strategy developed by Hazari and co-workers [26]. The neutral Pd (I) species **B** have recently been successfully used as catalysts in cross-coupling reactions [27], whereas the complex reported on the right side of figure 4.51 (compound **C**) is very similar to that we synthesized [28]. However, at variance with our complex, is difficult to handle because its high instability as a solid (air sensitive) and in solution.

The Pd(I) complex **87** was also fully characterized by NMR spectroscopy and elemental analysis.

In the ^{1}H-NMR spectrum (Fig. 4.52) it is possible to detect:

- The methyl substituents of the mesityl groups within 1.2 and 2.4 ppm.
- An AB system (J = 13.6 Hz) ascribable to the methylene bridges within 6.5 and 7.3 ppm.
- The aromatic protons between 6.9 and 8 ppm.

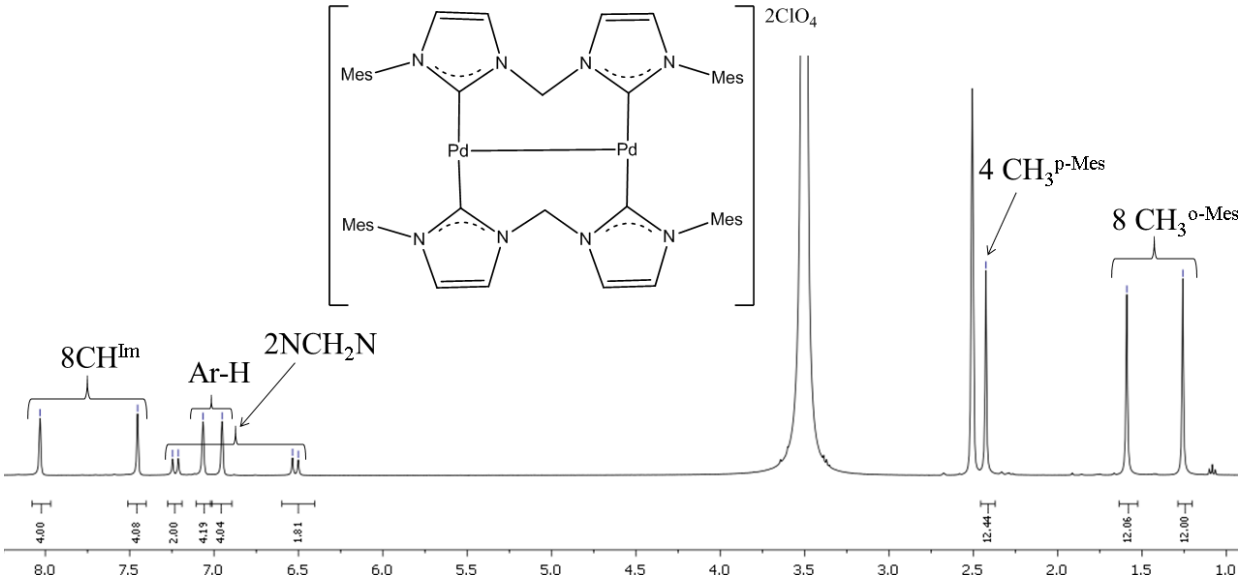

*Fig. 4.52 [1]H-NMR spectrum of the complex **87** in d[6]-DMSO at T = 298 K.*

In the [13]C-NMR spectrum (Fig. 4.53) the presence of the signal ascribable to the coordinated carbenic carbon at about 183 ppm was observed.

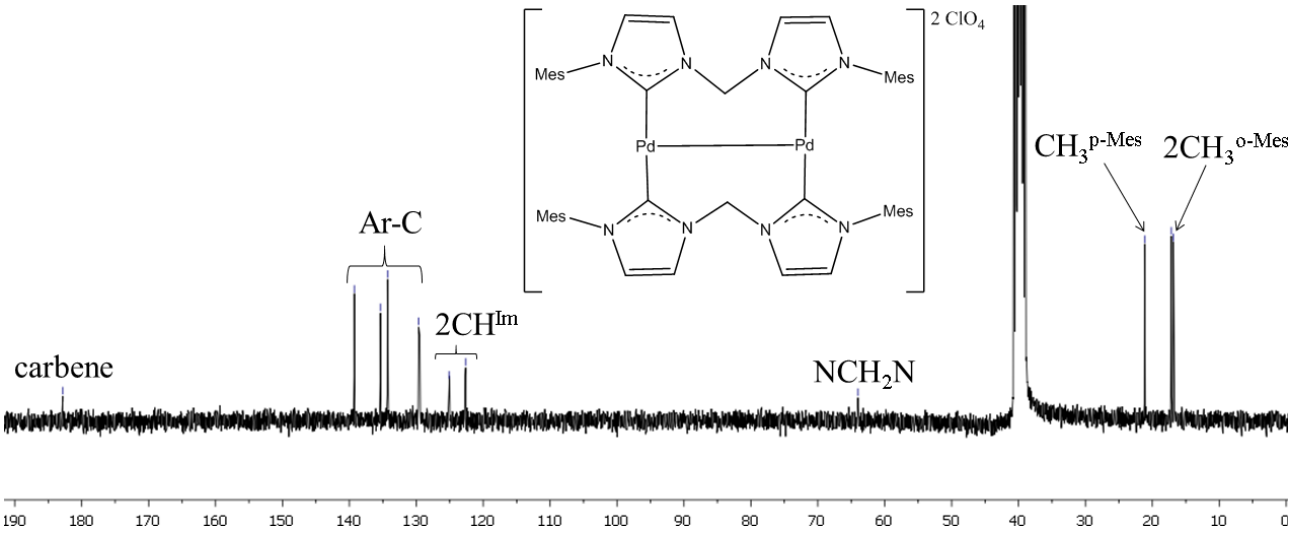

*Fig. 4.53 [13]C{[1]H}-NMR spectrum of the complex **87** in d[6]-DMSO at T = 298 K.*

The expected allyl complex **48f**, once separated from the dimeric species **87**, is stable in solution and, for each atropoisomer, the [1]H-NMR spectra show (Fig. 4.54):

- A doublet of doublets at about 4.5 ppm related to the *central* allyl proton.
- A doublet at about 1.5 ppm ascribable to the *anti* allyl proton (J ≈ 12 Hz) and a doublet at about 2.5 ppm traceable back to the *syn* allyl proton (J ≈ 6 Hz).
- Two singlets between 0.5 and 1.5 ppm related to the terminal allyl methyl groups.
- An AB system between 6 and 7 ppm ascribable to the NCH_2N spacer.

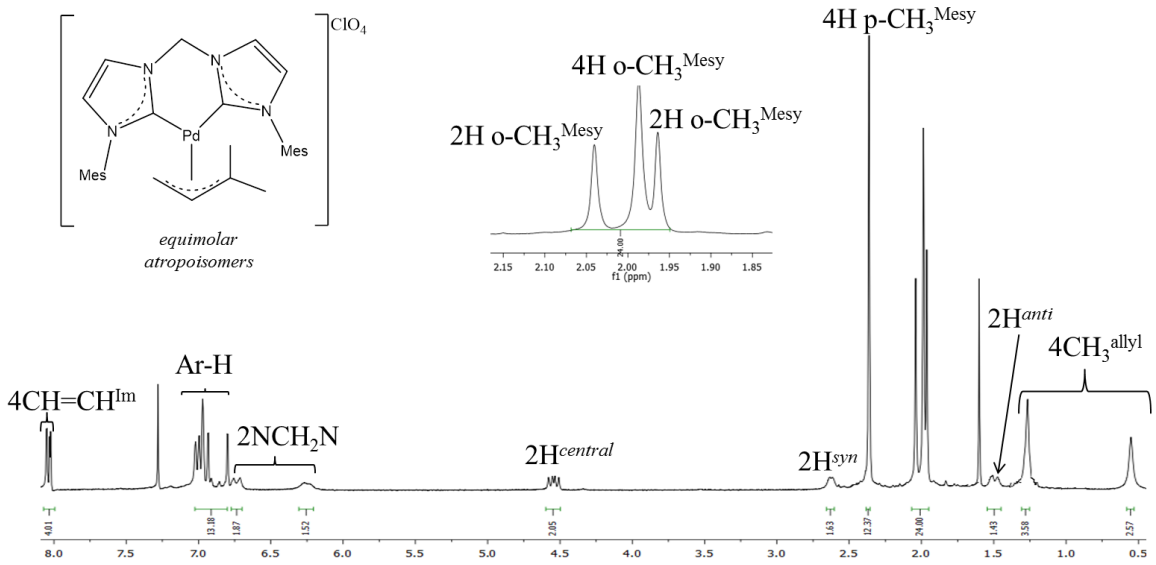

*Fig. 4.54 ^{1}H-NMR spectrum of the complex **48f** in $CDCl_3$ at T = 298 K.*

Finally, in the ^{13}C-NMR spectra (Fig. 4.55) it is possible to observe, for each species, the signal of the carbenic carbon between 175 and 180 ppm and all the other signals related to the allyl fragment and biscarbene ligand.

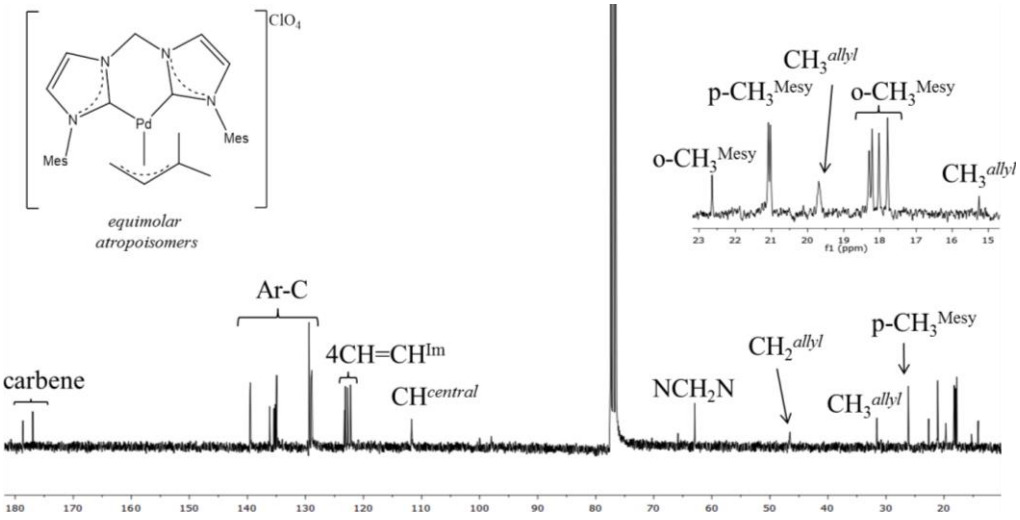

*Fig. 4.55 ^{13}C{^{1}H}-NMR spectrum of the complex **48f** in $CDCl_3$ at T = 298 K.*

4.6.2. η^3-allyl palladium complexes bearing two monodentate NHCs

In analogy to what reported in the previous paragraph, some η^3-allyl palladium species stabilized by two monodentate carbenes were also synthesized. In particular, starting from the [(MePyCH$_2$SPh)Pd(η^3-allyl)]ClO$_4$ precursor and according to the following scheme, the compounds **49a-d** have been synthesized in good yields and purity (Scheme 4.23).

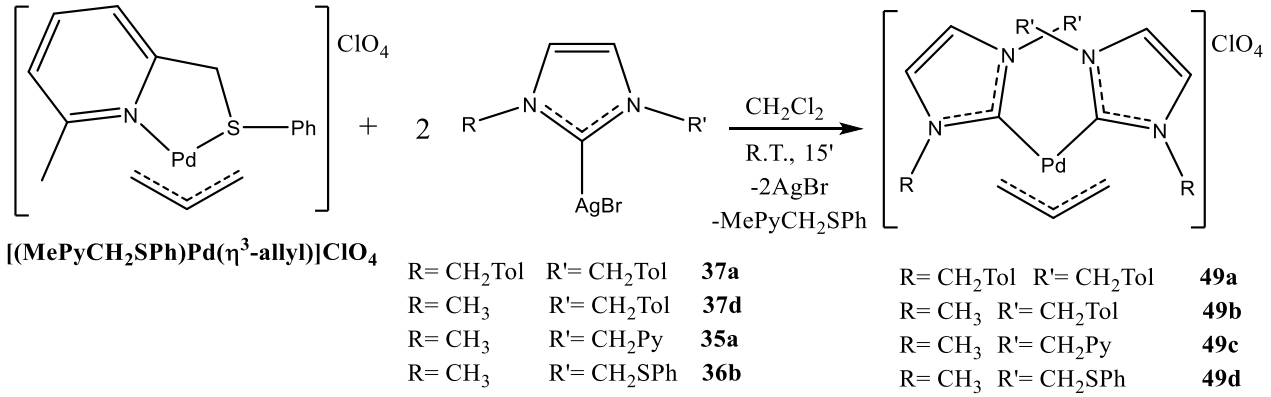

[(MePyCH$_2$SPh)Pd(η^3-allyl)]ClO$_4$

R= CH_2Tol	R'= CH_2Tol	**37a**
R= CH_3	R'= CH_2Tol	**37d**
R= CH_3	R'= CH_2Py	**35a**
R= CH_3	R'= CH_2SPh	**36b**

R= CH_2Tol	R'= CH_2Tol	**49a**
R= CH_3	R'= CH_2Tol	**49b**
R= CH_3	R'= CH_2Py	**49c**
R= CH_3	R'= CH_2SPh	**49d**

Scheme 4.23

The success of the reactions was confirmed by NMR spectroscopy. The use of symmetric or asymmetric carbenes allowed in all cases to observe in solution at RT a single species (no atropoisomers) owing to the free rotation about the Pd-carbene bond of the spectator ligands.

In the ^{1}H-NMR spectra (Fig. 4.56) it is possible to detect the presence of:

- A doublet at about 2.4-2.6 ppm ascribable to the *anti* allyl protons.
- A doublet at about 3.6-3.8 ppm ascribable to the *syn* allyl protons.
- A multiplet between 5 and 5.5 ppm ascribable to the *central* allyl proton.

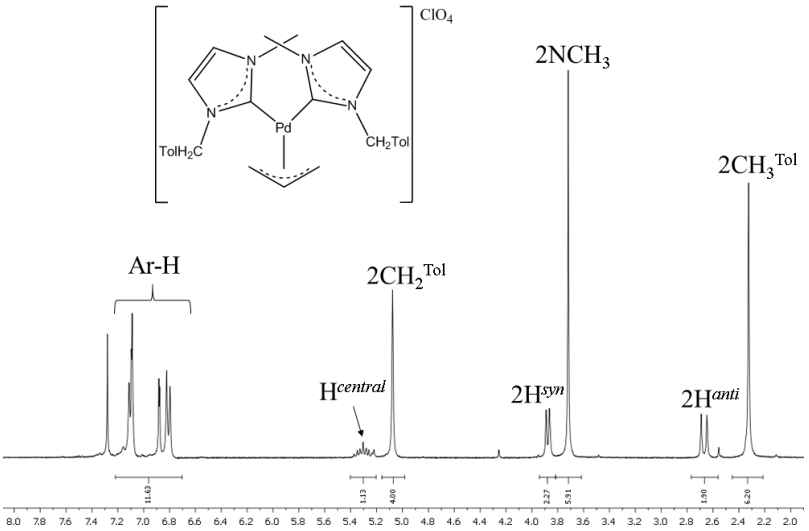

*Fig. 4.56 ^{1}H-NMR spectrum of the complex **49b** in $CDCl_3$ at T = 298 K.*

In the ^{13}C-NMR spectra (Fig. 4.57), in addition to the typical signals of the allyl fragment and of the NHC substituents, the peak of the coordinated carbenic carbon at about 177 ppm was detected.

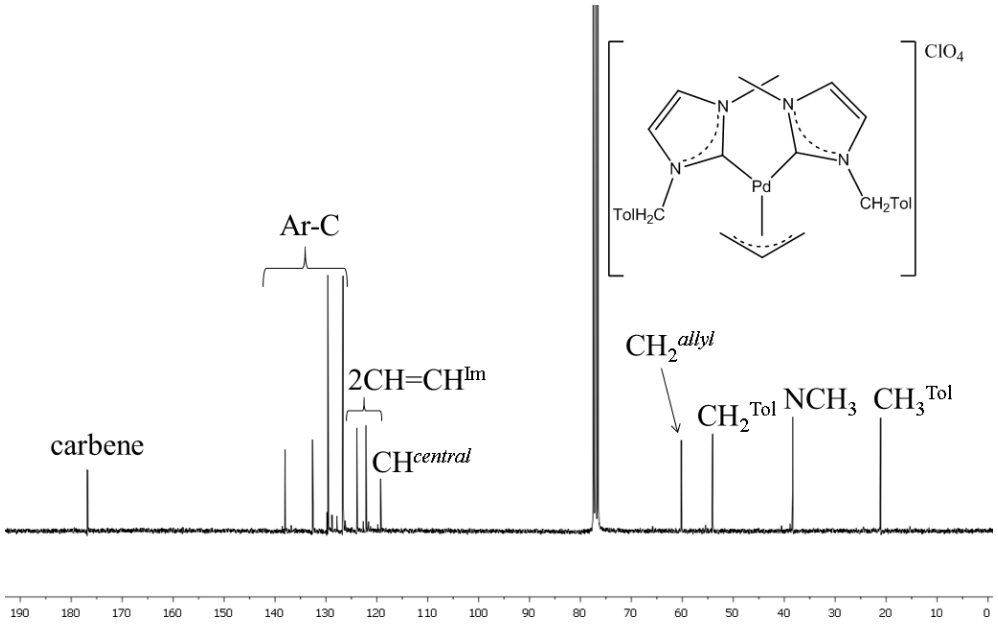

*Fig. 4.57 $^{13}C\{^1H\}$-NMR spectrum of the complex **49b** in $CDCl_3$ at T = 298 K.*

In one case (complex **49d**), the structure obtained by X-ray diffraction has been previously reported (Fig. 4.58) [29]. In the cited work, the synthesis of this class of compounds was carried out by transmetallation between the allyl complex containing the NHC-thioether bidentate ligand (complex **55**, see paragraph 4.6.3) and the silver complex **36b** exploiting the displacement of the labile wing (thioether) with the consequent formation of the biscarbene complex **49d**.

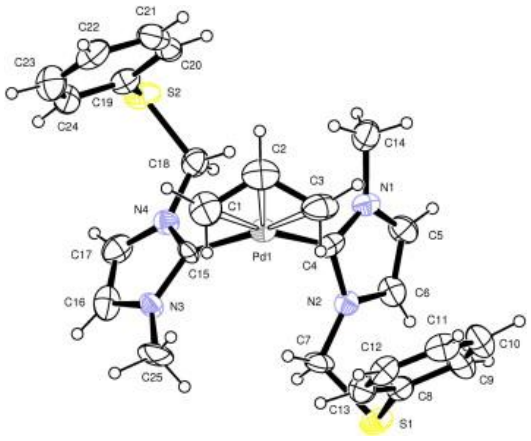

*Fig. 4.58 Ellipsoid representation of **49d** crystal ASU contents (50% probability).*

In conclusion, it is important to underline how the success of the reactions is heavily influenced by the steric demand. In fact, the concomitant coordination of two carbene each containing two mesityl substituents was an unsuccessful (Scheme 4.24) and a number of by-products is formed; among them

it is possible to observe the linear Pd (0) complex stabilized by two carbenic fragments (the signals coincide with those reported in the spectra of the product isolated by Herrmann and co-workers [30]) and the neutral allyl complex [(IMes)Pd(Cl)(η^3-allyl)].

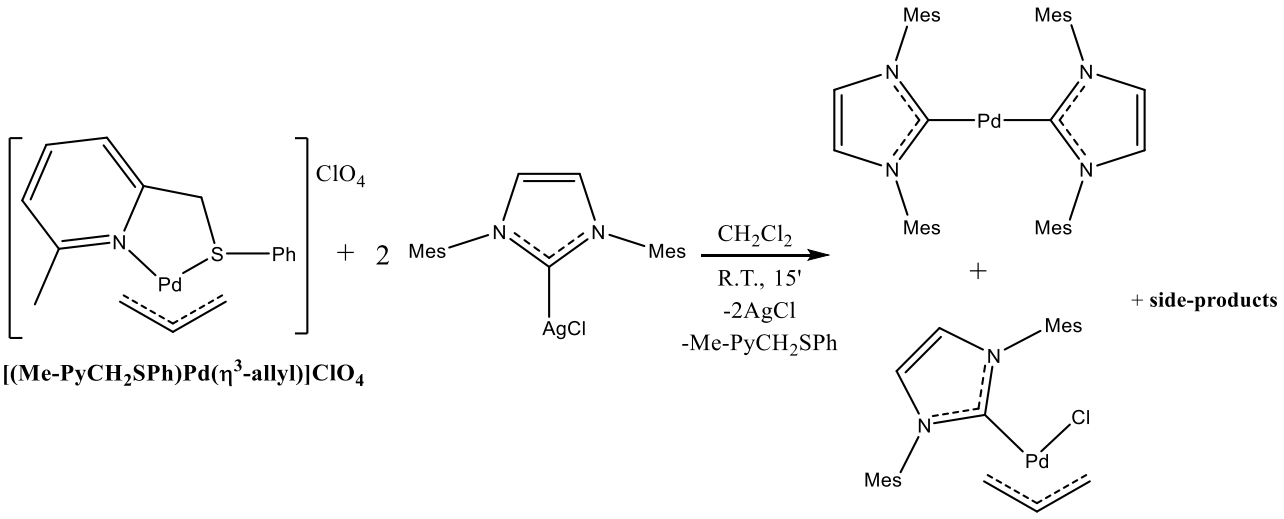

[(Me-PyCH$_2$SPh)Pd(η^3-allyl)]ClO$_4$

Scheme 4.24

4.6.3. η^3-allyl palladium complexes with chelating NHC-thioether or NHC-pyridine ligands

Another category of allyl complexes synthesized exhibits as bidentate ligand a carbene with a thioether or pyridine wing.

According to Scheme 4.25, these complexes were prepared by reaction between the $[Pd(\mu\text{-}Cl)(\eta^3\text{-allyl})]_2$ precursor and the silver complexes **35b** and **36b-d**, in the presence of sodium perchlorate (dissolved in a 1/3 dichloromethane/methanol mixture) as dechlorinating agent.

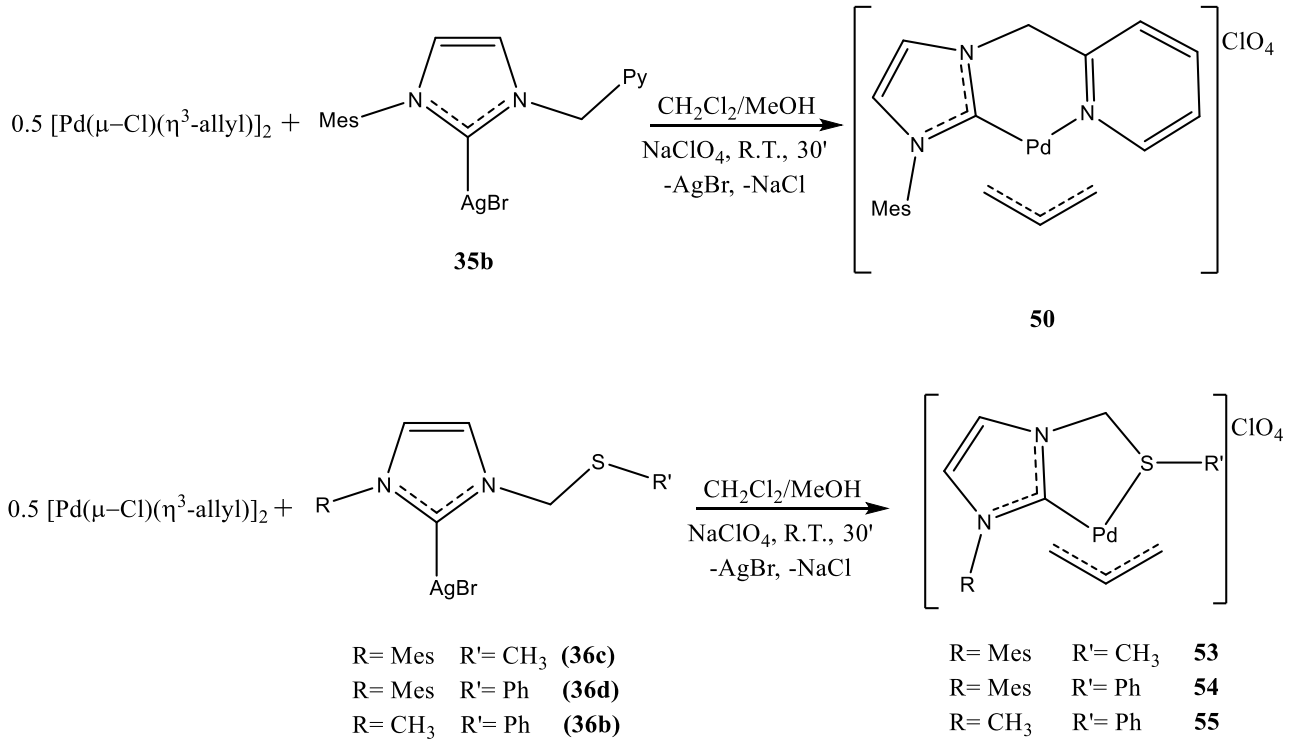

Scheme 4.25

The success of the reactions is evidenced by the coherence among the NMR spectra and the elementary analyses with the wanted structures.

In particular, owing to the asymmetry of the spectator ligand, the ^{1}H-NMR spectra show five signals related to the allyl fragment, together with the signals ascribable to the carbene fragment (Fig. 4.59).

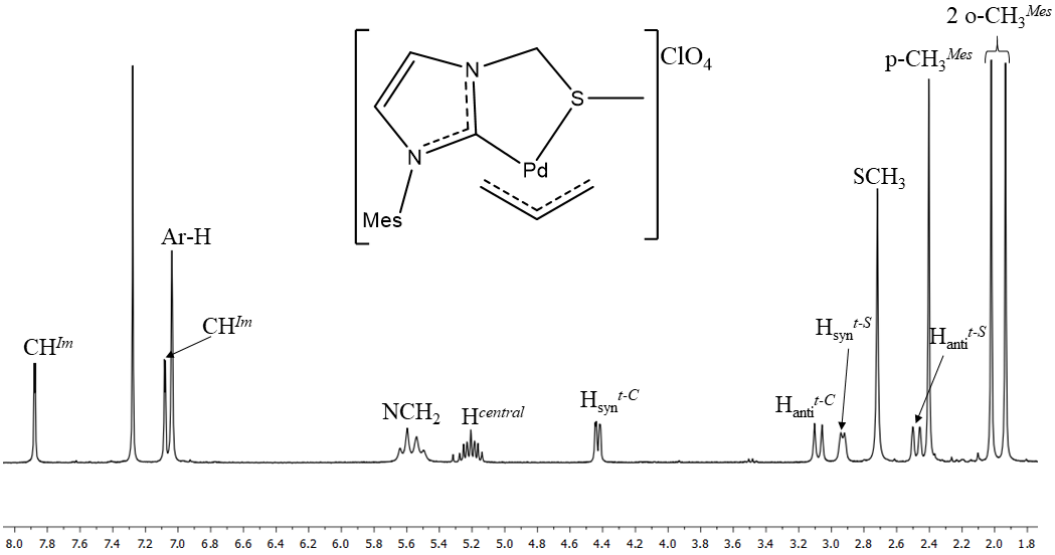

*Fig. 4.59 ^{1}H-NMR spectrum of the complex **53** in $CDCl_3$ at T = 298 K.*

Likewise, in the ^{13}C-NMR spectra (Fig. 4.60), the signals of the three different allyl carbons and that of the coordinated carbenic carbon can be found.

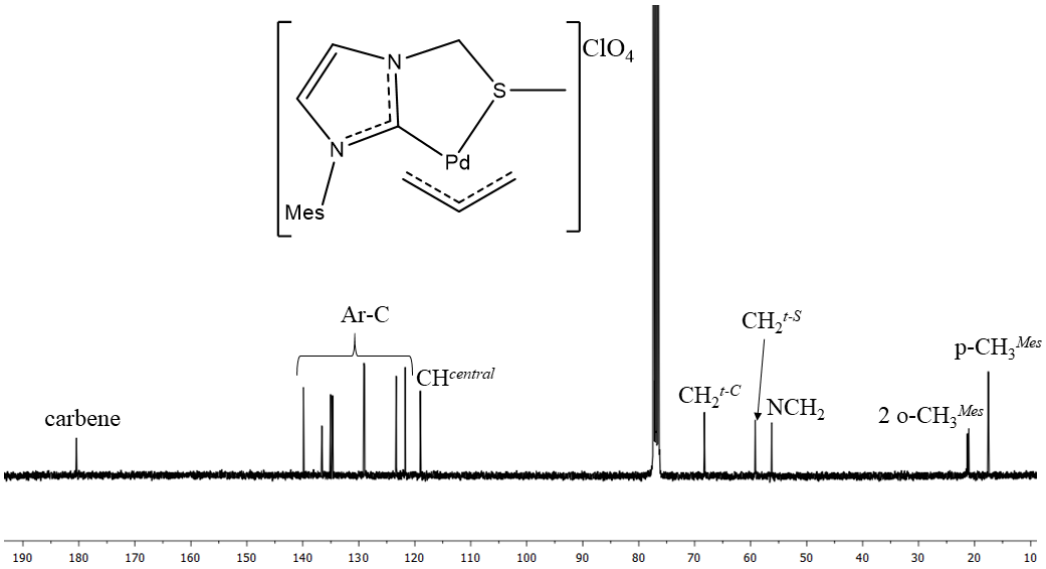

*Fig. 4.60 $^{13}C\{^{1}H\}$-NMR spectrum of the complex **53** in $CDCl_3$ at T = 298 K*

In the case of the carbenes with the pyridine wing, the complexes **51** and **52**, bearing the 2-methylallyl and 1,1-dimethylallyl fragments, were synthesized (Scheme 4.26).

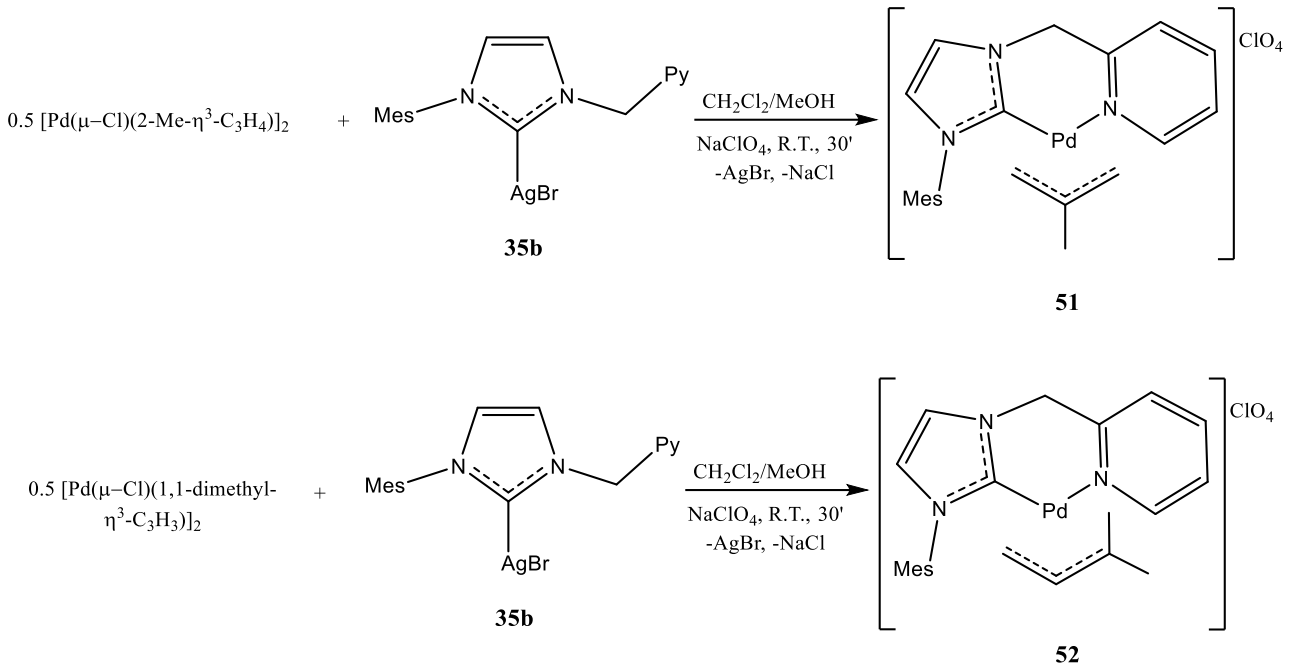

Scheme 4.26

As can be seen in Fig. 4.61, the NMR spectra indicate the presence of only one species with the two methyl groups of the allyl fragment *trans* to the carbene (complex **52)**. Likewise, the synthesis of complex **51** was successful and in both cases characterized by very high yield.

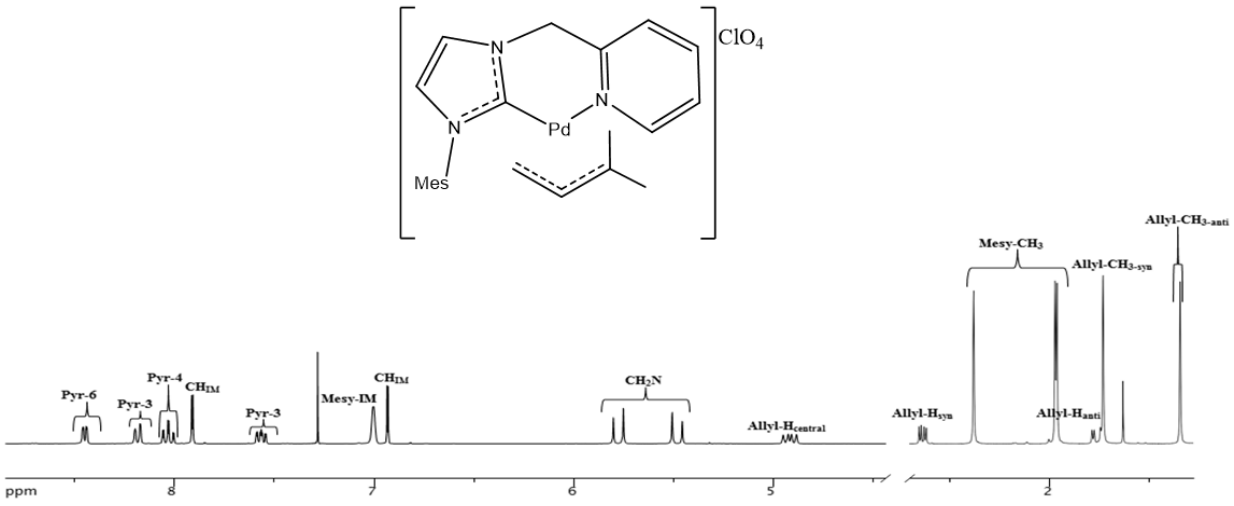

*Fig. 4.61 ^{1}H-NMR spectrum of the complex **52** in $CDCl_3$ at T = 298 K.*

4.6.4. Mixed NHC/PPh_3, NHC/PTA, NHC/DIC and PPh_3/DIC η^3-allyl palladium complexes

Similarly to the cases previously discussed (see paragraphs 3.5 and 4.4) related to the compounds containing purine-based NHCs and palladacyclopentadienyl complexes, respectively, it was decided to synthesize η^3-allyl palladium complexes bearing two different types of spectator ligands. In particular, the synthesis of mixed NHC/PPh_3, NHC/PTA, NHC/DIC and DIC/PPh_3 complexes was carried out.

At variance with the palladacyclopentadienyl mixed complexes described so far (section 4.4), the following reactions (*vide infra*) are characterized by a favourable thermodynamic and a short reaction time (max 1 hour).

4.6.4.1. Mixed NHC/PPh_3 complexes

The complexes bearing one carbene and one triphenylphosphine (**59**-**68**) were synthesized according to the conditions reported in the following scheme (Scheme 4.27).

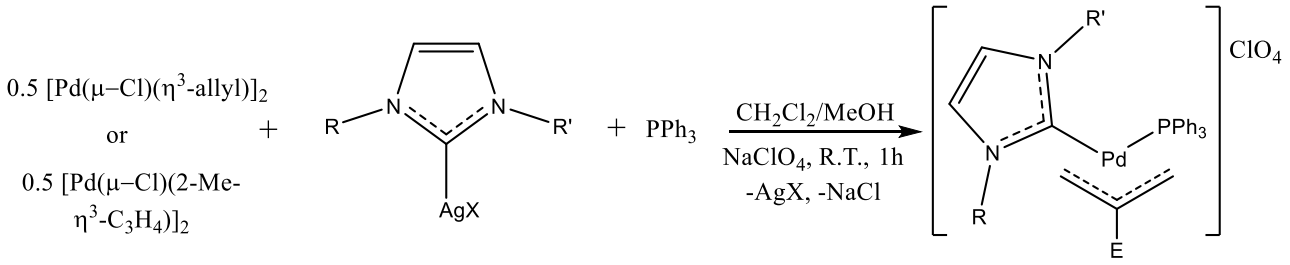

R= CH_2Tol	R'= CH_2Tol	**37a**
R= Mes	R'= Mes	**37b**
R= CH_3	R'= Bn	**37c**
R= CH_3	R'= CH_2Py	**35a**
R= Mes	R'= CH_2Py	**35b**
R= CH_3	R'= CH_2SPh	**36b**
R= Mes	R'= CH_2SPh	**36d**
R= Mes	R'= CH_2SCH_3	**36c**

R= CH_2Tol	R'= CH_2Tol	E= H	**59**
R= CH_2Tol	R'= CH_2Tol	E=CH_3	**60**
R= Mes	R'= Mes	E= H	**61**
R= Mes	R'= Mes	E=CH_3	**62**
R= CH_3	R'= Bn	E=H	**63**
R= CH_3	R'= CH_2Py	E=H	**64**
R= Mes	R'= CH_2Py	E=H	**65**
R= CH_3	R'= CH_2SPh	E=H	**66**
R= Mes	R'= CH_2SPh	E=H	**67**
R= Mes	R'= CH_2SCH_3	E=H	**68**

Scheme 4.27

The complexes with symmetric NHC ligands were obtained as single species, characterized by a peak observed at about 23 ppm in the ^{31}P-NMR spectra ($\Delta\delta \approx 30$ ppm downfield compared to the uncoordinated triphenylphosphine). The ^{1}H-NMR spectra (Fig. 4.62) show five distinct allylic signals, with the *syn* and *anti* protons *trans* to phosphine resonating as doublets of doublets (or multiplets), owing to their coupling with phosphorus.

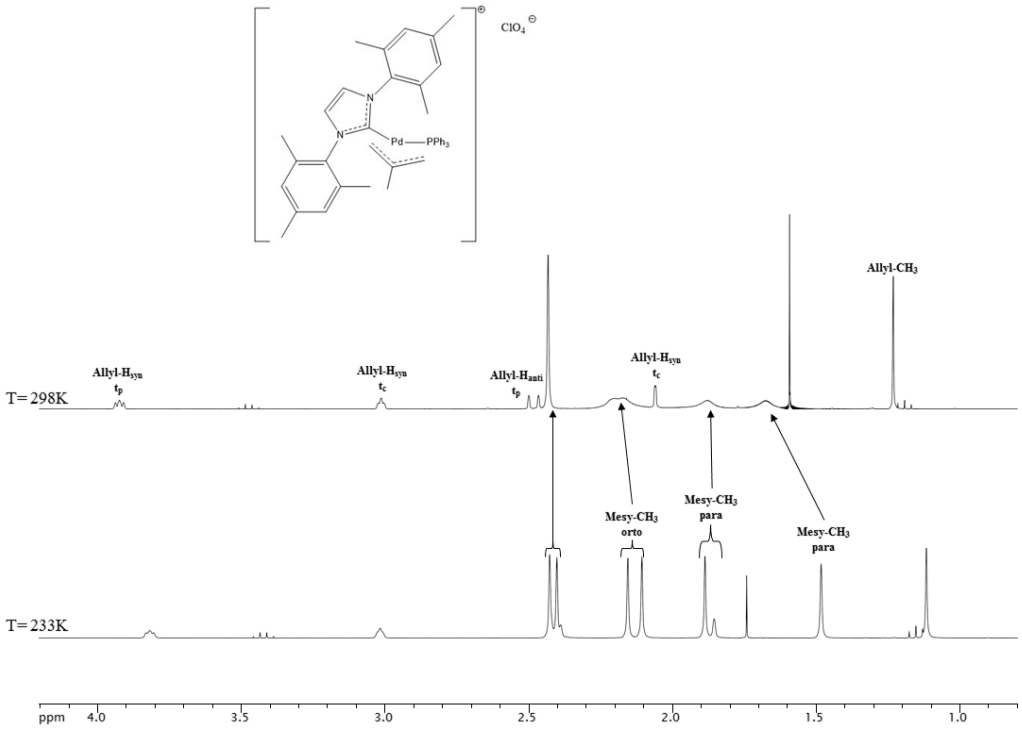

*Fig. 4.62 ^{1}H-NMR spectrum of the complex **62** in $CDCl_3$ at T = 298 K.*

The ^{13}C-NMR spectra (Fig. 4.63), show the doublet ascribable to the carbenic carbon at about 180 ppm ($J_{C\text{-}P}$ = 15 Hz) and the two different terminal allyl carbons at very similar frequencies (similar *trans influence* between carbene and phosphine) with the carbon *trans* to phosphine resonating as a doublet ($J_{C\text{-}P} \approx 30$ Hz).

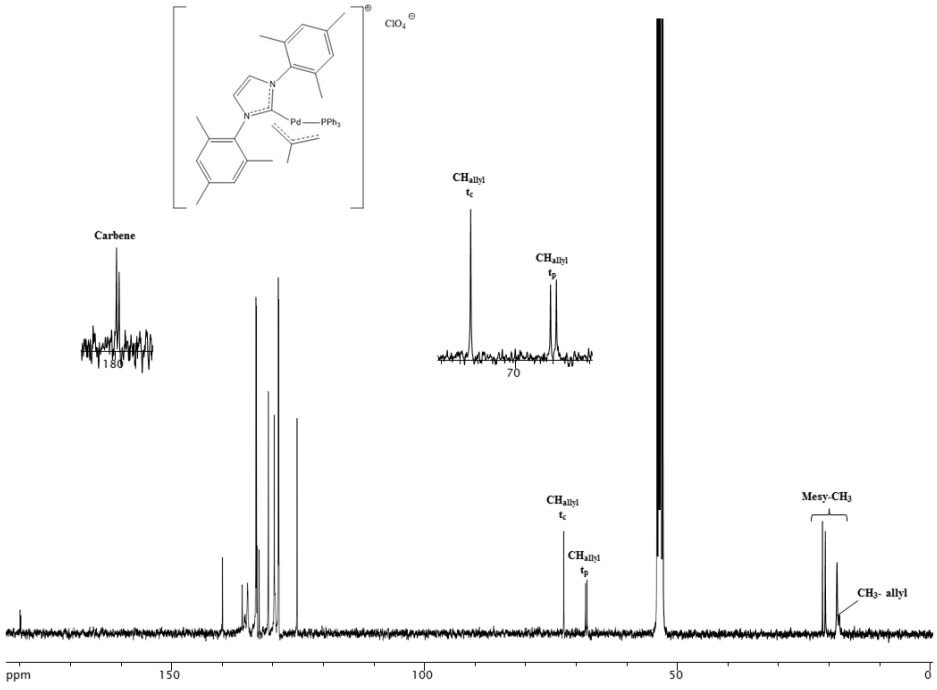

*Fig. 4.63 $^{13}C\{^{1}H\}$-NMR spectrum of the complex **62** in $CDCl_3$ at T = 298 K.*

As for the complexes bearing an asymmetric NHC, the formation of pairs of atropoisomers due to the hindered rotation at RT about the Pd-C bond, and the consequent doubling of the signals in ^{1}H-NMR and ^{13}C-NMR spectra, as reported in figure 4.64 are observed.

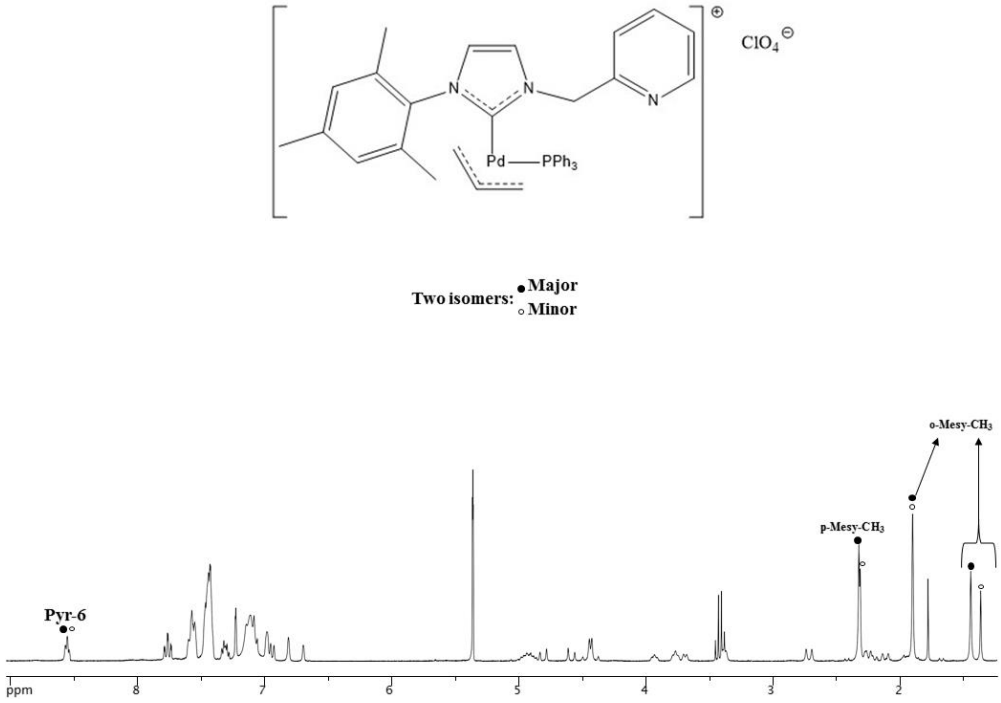

*Fig. 4.64 ^{1}H-NMR spectrum of the complex **65** in $CDCl_3$ at T = 298 K.*

In the case of the compound **60** it was also possible to obtain its solid-state structure by single crystal X-ray diffraction (Fig. 4.65).

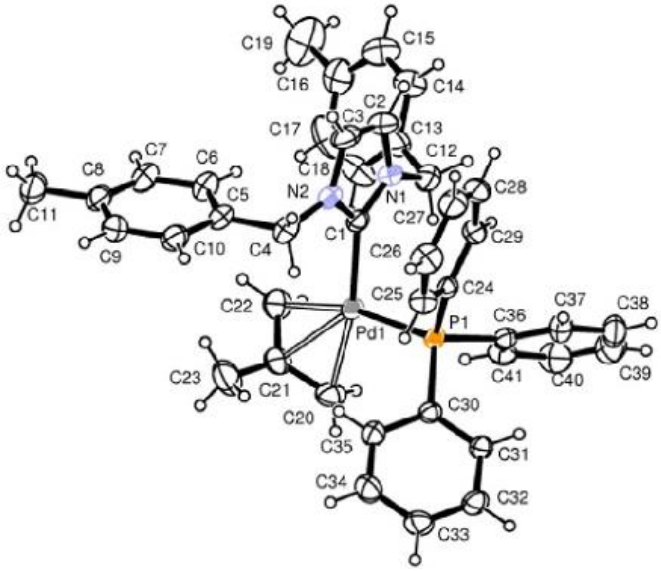

*Fig. 4.65 Ellipsoid representation of **60** crystal ASU contents (50% probability).*

4.6.4.2. Mixed NHC/PTA complexes

The mixed NHC/PTA complexes can be distinguished into two categories:

a) Complexes with NHCs without a side coordinating function.

b) Complexes with NHCs with a side coordinating function.

The first kind of derivatives were prepared by a similar protocol than that of the complexes with triphenylphosphine. Therefore, the allyl precursors $[Pd(\mu\text{-}Cl)(\eta^3\text{-allyl})]_2$ or $[Pd(\mu\text{-}Cl)(\eta^3\text{-2-Me-allyl})]_2$ were reacted with the silver complex **37b**, and subsequentely treated with the dechlorinating agent $NaClO_4$ and PTA (Scheme 4.28).

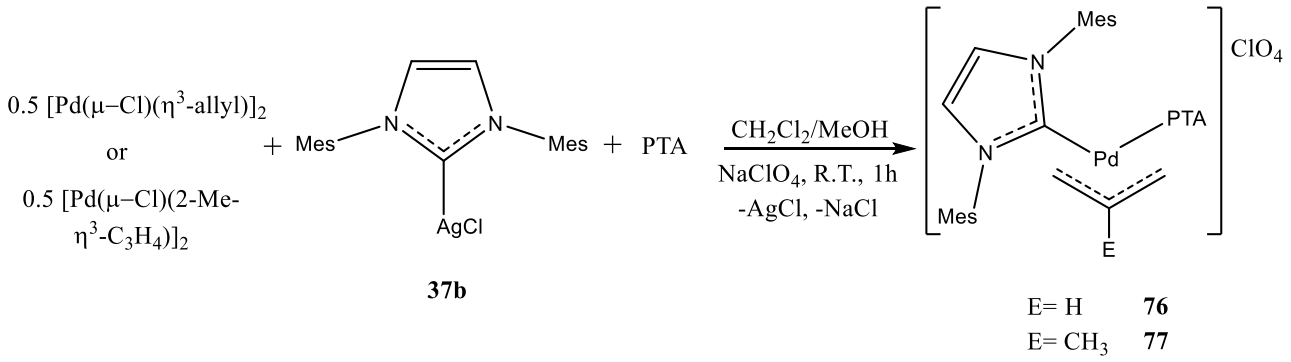

Scheme 4.28

The NMR spectra confirm the coordination of both PTA and carbene ligand (Fig. 4.66).

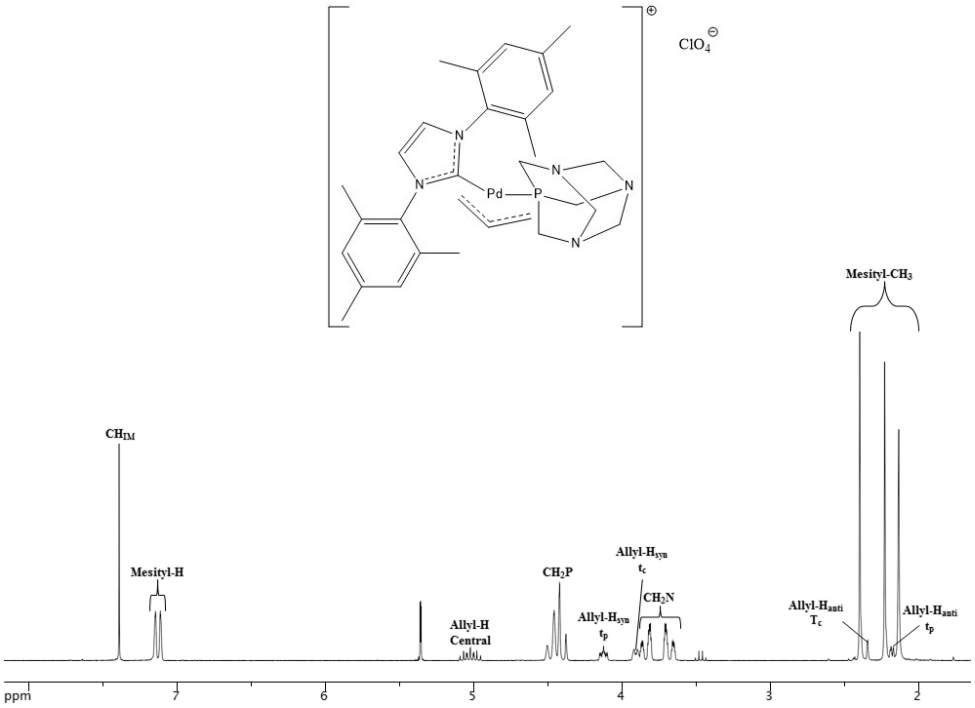

*Fig. 4.66 ^{1}H-NMR spectrum of the complex **76** in $CDCl_3$ at T = 298 K.*

The synthesis of mixed NHC/PTA complexes with carbenes bearing a pyridine or thioether wing, were carried out in two separated steps. The starting C-S or C-N chelated compounds were first prepared, according to the synthesis reported in the previous paragraph 4.6.3, and subsequently the labile pyridine or thioether wing was displaced by PTA. However, these reactions are not selective, and hence, only the complex **78** was obtained pure.

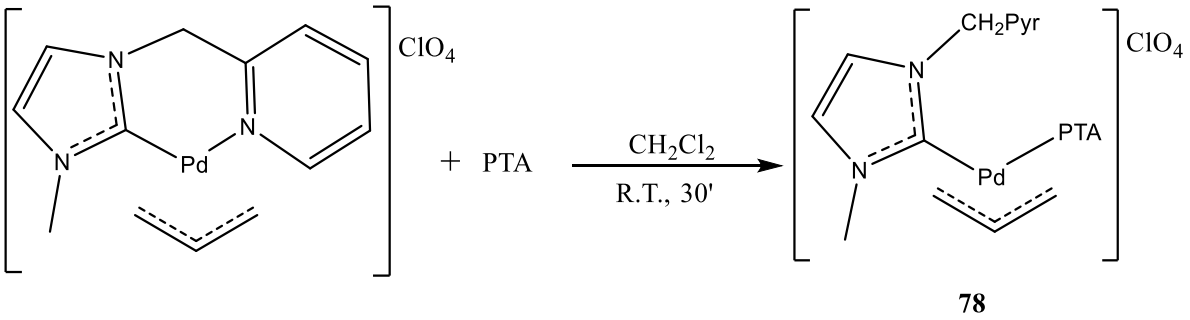

78

Scheme 4.29

4.6.4.3. Mixed NHC/DIC and mixed PPh_3/DIC complexes

The synthesis of mixed NHC/DIC and PPh_3/DIC complexes **85** and **86** was carried out following published protocol synthetically summarized in Scheme 4.30 [31].

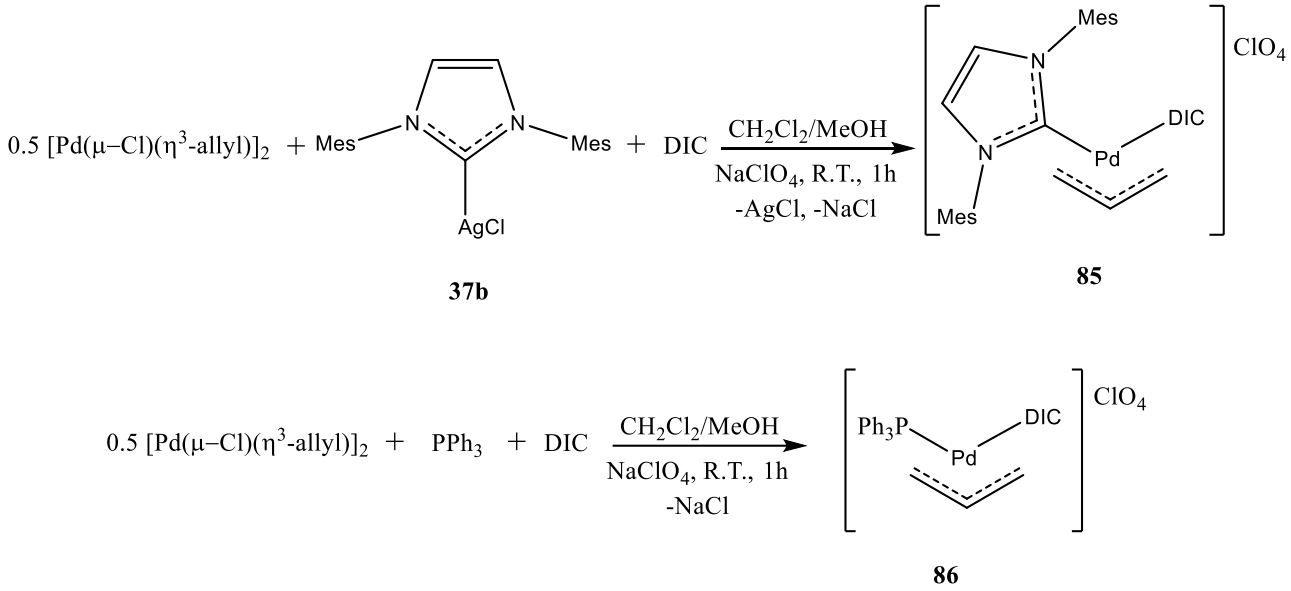

Scheme 4.30

In the NMR spectra of the products (see Rif. [31]), all the signals of the carbene (or triphenylphosphine) ligand and of the isocyanide ligand, are found.

Remarkably, in the case of complex **85** it was possible in the past to collect its solid-state structure obtained by single crystal X-ray diffraction (Fig. 4.67).

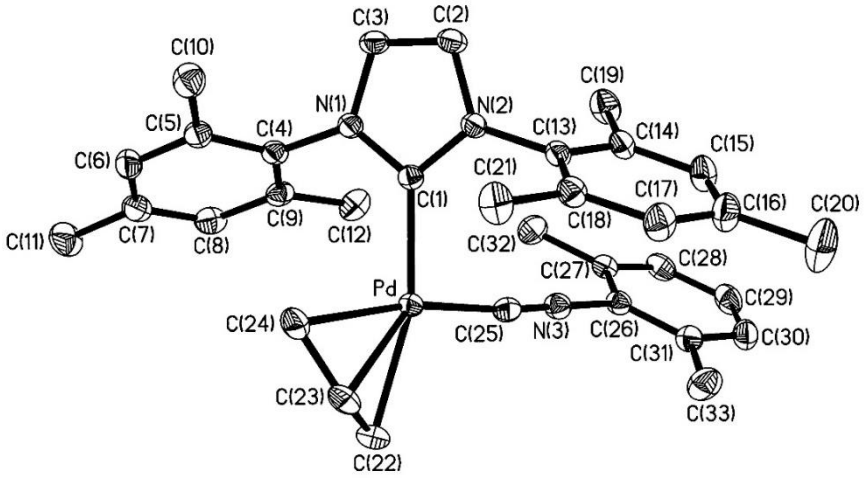

*Fig. 4.67 Ellipsoid representation of **85** crystal ASU contents (50% probability).*

4.6.5. η^3-allyl palladium complexes bearing chelating phosphino-carbene ligands

Another category of η^3-allyl complexes described in this chapter is characterized by chelating phosphino-carbenes as ancillary ligands. This class of molecules, whose synthesis was reported by Togni and Visentin in 2007 [32] is synthetically depicted in scheme 4.31. The interest about such compounds stems on the fact that they contain strong chelating C-P ligands and a residue deriving from the ferrocene, whose antitumor activity has been extensively studied as reported in the introductory section 1.3.2.

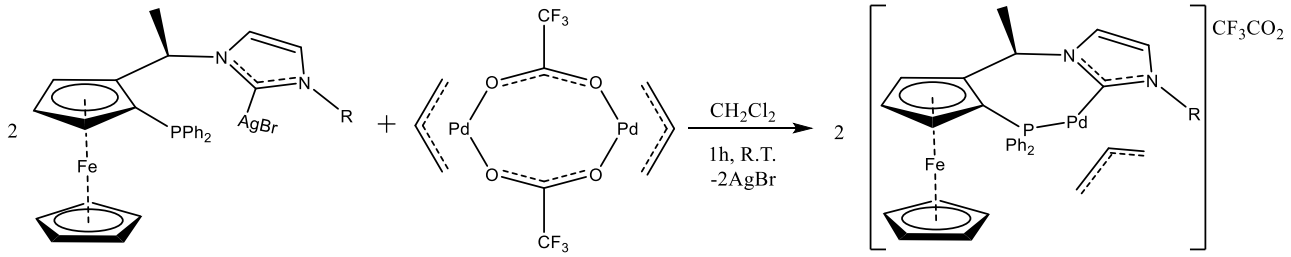

R= Me **G**
R= t-Bu **H**

Scheme 4.31

These complexes with a chiral C-P ligand form pairs of atropoisomers (*endo* and *exo*) observable in the reaction mixture (Fig. 4.68). As reported in the original work, they were successfully characterized by NMR, IR and elemental analysis.

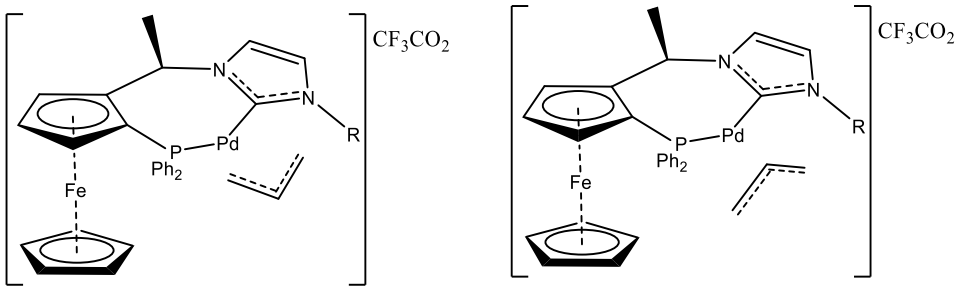

endo isomer *exo* isomer

Fig. 4.68

4.6.6. η^3-allyl palladium complexes bearing chelating N-P and N-S ligands

The last class of allyl compounds exposed, is characterized by bidentate N-S (pyridyl thioethers or thioquinolines) or N-P (phosphinoquinolines) as spectator ligands.

The compounds taken into consideration are summarized in Scheme 4.32, together with the corresponding synthetic protocol so far reported [24, 33].

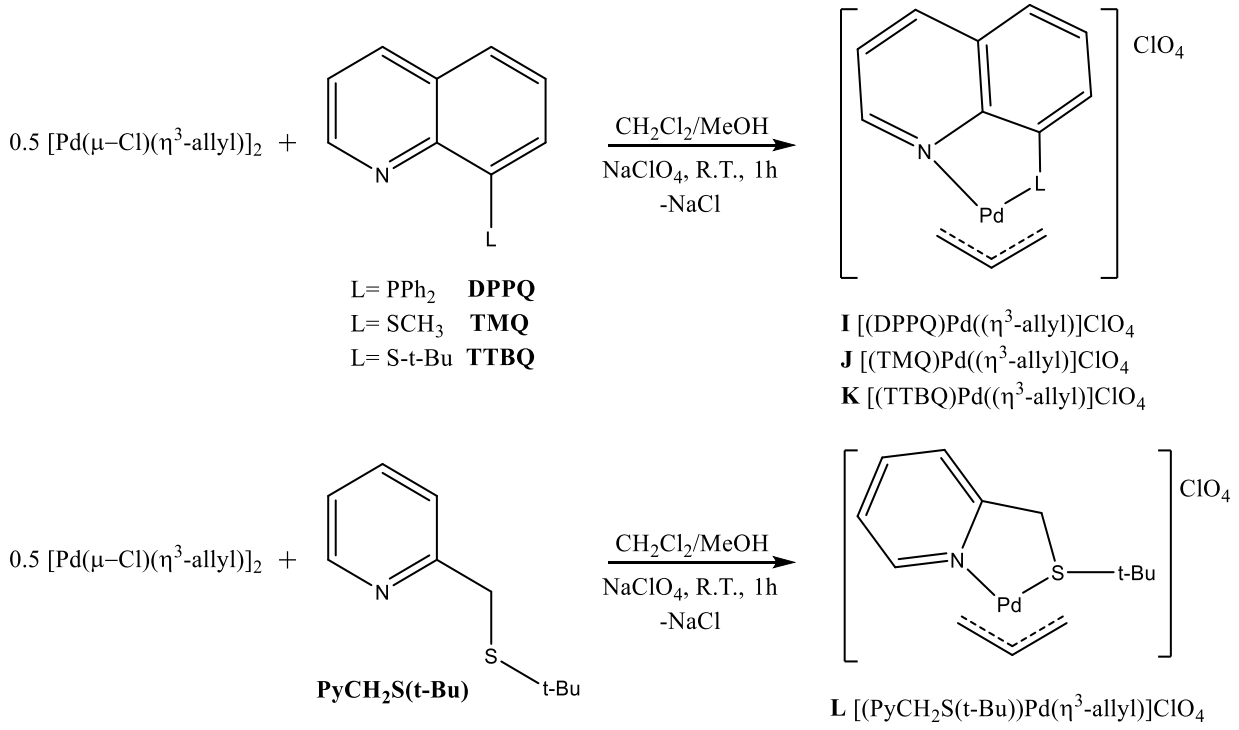

Scheme 4.32

As stated in the previously cited papers, they have been exhaustively characterized by NMR and IR spectroscopic techniques, as well as by the solid-state structures obtained by single crystal X-ray diffraction (Fig. 4.69).

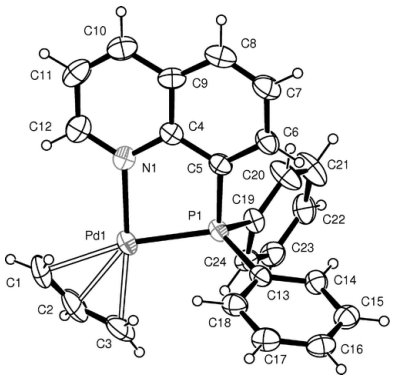

*Fig. 4.69 Ellipsoid representation of the complex **F** [(DPPQ)Pd(η^3-allyl)]ClO_4) crystal ASU contents (50% probability).*

4.7. Antiproliferative activity of allyl palladium complexes

The antiproliferative activity of the allyl palladium complexes and the Pd(I) dimeric species was firstly tested on A2780 and A2780-R cancer lines and toward MRC-5 fibroblasts (Table 4.3).
The preliminary stability tests in DMSO-d6 or DMSO-d6/D_2O mixtures have shown that these molecules have a good stability in solution.

Class of compound	Compound	IC_{50} (μM)		
		A2780	A2780-R	MRC-5
Cisplatin	**Cisplatin**	0.81±0.06	9 ± 3	14 ± 1
Bidentate bisNHCs	**48b**	0.3 ± 0.1	0.4 ± 0.1	3.1 ± 0.1
	48c	0.16 ±0.02	0.08 ± 0.04	0.28 ± 0.03
	48f	0.09 ± 0.02	0.027 ± 0.03	0.27 ± 0.08
Monodentate bisNHCs	**49b**	0.08 ± 0.06	0.25 ± 0.07	2.4 ± 0.8
	49c	0.37 ± 0.08	4.8 ± 0.8	>100
Hemilabile NHCs	**50**	0.013 ± 0.002	0.030 ± 0.009	0.04 ± 0.01
	53	0.019 ± 0.001	0.12 ± 0.05	1.7 ± 0.4
Mixed NHC/PPh_3	**61**	0.013 ± 0.003	0.12 ± 0.01	0.017 ± 0.001
	62	0.26 ± 0.02	0.4 ± 0.2	0.55 ± 0.12
	63	0.034 ± 0.007	0.42 ± 0.04	0.34 ± 0.04
Mixed NHC/PTA	**76**	0.020 ± 0.005	0.033 ± 0.003	3.8 ± 0.3
Mixed NHC/DIC	**85**	0.004 ± 0.001	0.021 ± 0.003	0.022 ± 0.001
Mixed DIC/PPh_3	**86**	0.24 ± 0.07	2.0 ± 0.4	>100
Pd(I) dimer	**87**	0.031 ± 0.008	2.3 ± 0.3	>100
Chelating NHC-P	**G**	0.025 ± 0.007	0.31 ± 0.09	0.23 ± 0.01
	H	0.1 ± 0.1	0.40 ± 0.02	0.35 ± 0.09
Chelating N-P and N-S	**I**	0.020 ± 0.003	0.08 ± 0.04	0.26 ± 0.05
	J	2.6 ± 0.3	2.4 ± 0.6	>100
	K	1.8 ± 0.2	4.1 ± 0.4	35 ± 8
	L	2.1 ± 0.6	4.5 ± 0.7	>100

Table 4.3

From the antiproliferative activity data, concerning most of the synthesized compounds (some data are not yet available), it is possible to make the following considerations:

1. All tested compounds, except for those indicated with the abbreviations **J**, **K** and **L**, are significantly more active than cisplatin toward the A2780 and A2780-R lines.

2. This high cytotoxicity seems quite indipendent of the nature of the spectator ligands and therefore it may be credited reasonably to the η^3-allyl-Pd(II) fragment.

3. Unfortunately, most of these allyl compounds are cytotoxic even on healthy cells (MRC-5), with IC_{50} values often comparable to those obtained for the tumor lines. Important exceptions are the bis-NHC complex **49c** (with two pyridil-nitrogen free), the mixed PPh_3/DIC complex **86** and the complexes with chelating N-S ligands (**J**, **K** and **L**). The allyl complex coordinating one carbene ligand (IMes) and one PTA molecule (compound **76**) is also interesting since, despite its moderate cytotoxic toward healthy cells ($IC_{50} \approx 4$ μM), it is more active than cisplatin in both tumor lines of about two orders of magnitude.
4. The Pd (I) dimeric species **87,** even though not containing the allylic fragment, shows an high antiproliferative activity toward both cisplatin sensitive A2780 and cisplatin resistant A2780-R cell lines. Its low toxicity to MRC-5 fibroblasts (IC_{50} >100 μM) renders this compound particularly promising.

As shown in Table 4.4, extending the analysis (for now only on some compounds) toward other tumor lines it is possible to notice how this class of compounds is generally very cytotoxic even on these types of neoplasms.

Compound	**IC_{50} (μM)**			
	OVCAR5	**A549**	**A375**	**DLD1**
Cisplatin	0.84 ± 0.04	6 ± 3	4.7 ± 0.4	19 ± 4
50	0.031 ± 0.008	0.06 ± 0.06	0.01 ± 0.009	0.33 ± 0.08
53	0.38 ± 0.08	0.07 ± 0.02	0.022 ± 0.002	0.29 ± 0.02
61	0.29 ± 0.06	0.36 ± 0.04	0.141 ± 0.009	0.40 ± 0.04
63	0.034 ± 0.005	0.4 ± 0.2	0.36 ± 0.04	0.40 ± 0.08
86	4 ± 1	1.32 ± 0.06	3.0 ± 0.5	4.2 ± 0.7
G	0.23 ± 0.01	0.49 ± 0.03	0.20 ± 0.03	3.5 ± 0.2
H	0.35 ± 0.09	0.17 ± 0.08	0.6 ± 0.1	3.26 ± 0.03
I	0.27 ± 0.02	0.10 ± 0.03	0.023 ± 0.004	0.023 ± 0.002
J	7 ± 2	5 ± 1	4.5 ± 0.7	>100
K	>100	3.2 ± 2	3 ± 1	>100
L	8 ± 1	4 ± 2	4.5 ± 0.1	>100

Table 4.4 In vitro antiproliferative IC_{50} values (μM, 72 h) of the η^3-allyl-Pd(II) complexes toward human cell lines of ovarian cancer (OVCAR5), lung cancer (A549), malignant melanoma (A375) and colon cancer (DLD1).

4.8. Conclusions

In this chapter it was described the synthesis and characterization of allyl and palladacyclopentadienyl complexes (and their derivatives) stabilized by *N*-Heterocyclic Carbenes deriving from the functionalization of imidazole.

For these compounds, the antiproliferative activity was studied toward different tumor lines (ovarian carcinoma, colon cancer, lung cancer and malignant melanoma), showing that the allyl compounds are generally much more active than those containing the palladacyclopentadienyl fragment. However, this greater activity often involves a greater cytotoxicity even on healthy cells. In any case, it was possible to identify some species with marked antitumor activity and low cytotoxicity on fibroblasts (Fig. 4.72).

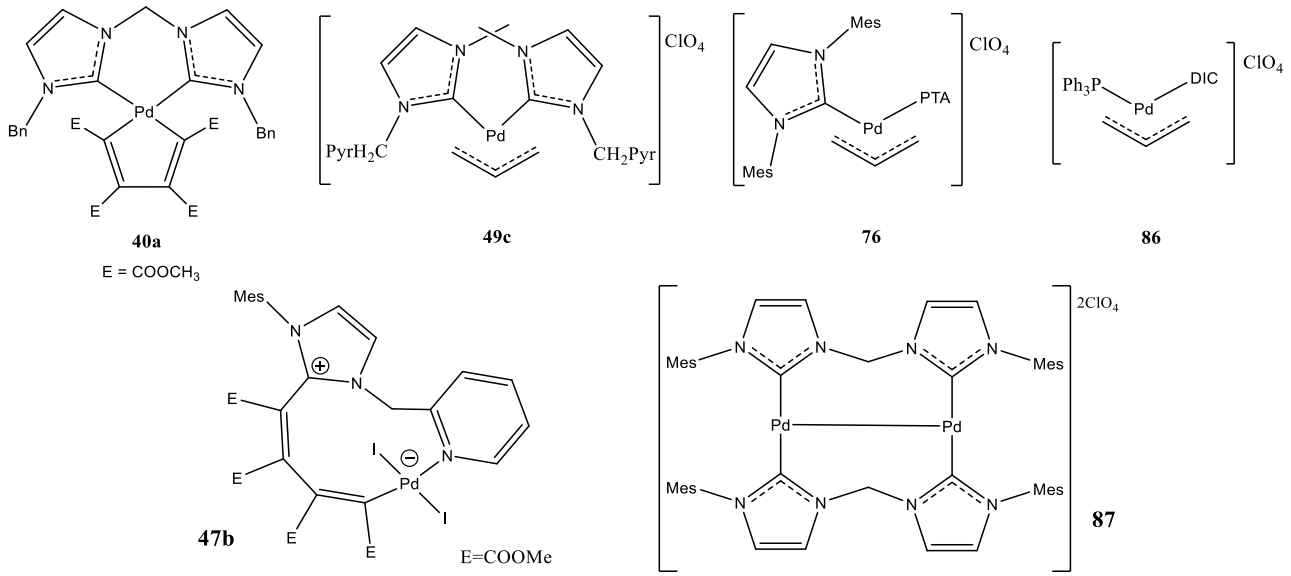

Fig. 4.72

For one of these promising compounds (**40a**), some specific biological tests have allowed to identify DNA as the main bio-target. The high stability of the palladacyclopentadienyl fragment and the strong coordinating capability of the biscarbene ligand, (no substitution reaction was observed in presence of excess of glutathione) probably permit to this compound to remain intact in the biological environment; therefore it is reasonable to suppose that its binding with the DNA occurs through non-covalent interactions with the polynucleotide chain (intercalation).

Finally, compounds **47b** and **87** (Fig. 4.72) are interesting both from the structural point of view and for their antiproliferative activity. In fact, from the preliminary results, they are very active against the investigated cancer lines and inactive toward healthy cells.

4.9. References

[1] M. G. Gardiner, C. C. Ho, *Coord. Chem. Rev.*, 2018, **375**, 373.

[2] (a) M. Nirmala, G. Saranya, P. Viswanathamurthi, R. Bertani, P. Sgarbossa, J. G. Malecki, *J. Organomet. Chem.*, 2017, **831**, 1; (b) D. Munz, C. Allolio, D. Meyer, M. Micksch, L. Roessner, T. Strabner, *J. Organomet. Chem.*, 2015, **798**, 330; (c) M.V. Baker, D.H. Brown, P.V. Simpson, B.W. Skelton, A.H. White, C.C. Williams, *J. Organomet. Chem.*, 2006, **691**, 5845; (d) A. Biffis, M. Cipani, E. Bressan, C. Tubaro, C. Graiff, Al. Venzo, *Organometallics*, 2014, 33, 2182.

[3] (a) M. Baron, C. Tubaro, M. Basato, A. Biffis, C. Graiff, A. Poater, L. Cavallo, N. Armaroli, G. Accorsi, *Inorg. Chem.*, 2012, **51**, 1778; (b) Y. Liu, K. S. Kjaer, L. A. Fredin, P. Chábera, T. Harlang, S. E. Canton, S. Lidin, J. Zhang, R. Lomoth, K. E. Bergquist, *Chem. Eur. J.*, 2014, **21**, 3628; (c) Y. Liu, P. Persson, V. Sundström, K. Wärnmark, *Acc. Chem. Res.*, 2016, **49**, 1477; (d) M. Saitoh, A. L. Balch, J. Yuasa, T. Kawai, *Inorg. Chem.*, 2010, **49**, 7129.

[4] (a) P. J. Barnard, E. Wedlock, M. V. Baker, S. J. Berners-Price, D. A. Joyce, B. W. Skelton, J. H. Steer, *Angew. Chem. Int. Ed.*, 2006, **45**, 5966; (b) M. Baron, S. Bellemin-Laponnaz, C. Tubaro, M. Basato, S. Bogialli, A. Dolmella, *J. Inorg. Biochem.*, 2014, **141**, 94.

[5] S. Warsink, U. Chang, J. J. Weigand, P. Hauwert, J. Chen, C. Elsevier, *Organometallics*, 2010, **29**, 4555.

[6] U. E. Hille, C. Zimmer, C. A. Vock, R. W. Hartmann, *ACS Med. Chem. Lett.*, 2011, **2**, 2.

[7] (a) S.-T. Liu, C.-I. Lee, C.-F. Fu, C.-H. Chen, Y.-H. Liu, C.J. Elsevier, S.-M. Peng, J.-T. Chen, *Organometallics*, 2009, **28**, 6597; (b) (h) A.A.D. Tulloch, A.A. Danoupolos, S. Winston, S. Khleinhenz, G. Eastham, *J. Chem. Soc., Dalton Trans.*, 2000, 4499; (c) J. Liu, J. Chen, J. Zaho, Y. Zhao, H. Zhang, Synthesis, 2003, 2661; (d) L. Canovese, F. Visentin, T. Scattolin, C. Santo, V. Bertolasi, *Polyhedron*, 2016, **119**, 377; (e) L. Canovese, F. Visentin, C. Levi, C. Santo, V. Bertolasi, *Inorganica Chim. Acta*, 2012, **390**, 105.

[8] H. M. Lee, C. Y. Lu, C. Y. Chen, W. L. Chen, H. C. Lin, P. L. Chiu, P. Y. Cheng, *Tetrahedron*, 2004, **27**, 5807–5825.

[9] (a) Y. Cheng, X. Lu, H. Xu, Y. Li, X. Chen, Z. Xue, *Inorganica Chimica Acta*, 2010, **363**, 430-437; (b) Y. A. Wanniarachchi, M. A. Khan, L. M. Slaughter, *Organometallics*, 2004, **23**, 5881-5884.

[10] L. Canovese, C. Santo, T. Scattolin, F. Visentin, V. Bertolasi, J. *Organomet. Chem.*, 2015, **794**, 288.

[11] L. Canovese, F. Visentin, T. Scattolin, C. Santo, V. Bertolasi, J. *Organomet. Chem.*, 2016, **808**, 48; (b) L. Canovese, F. Visentin, T. Scattolin, C. Santo, V. Bertolasi, *Polyhedron*, 2016,

113, 25; (c) T. Scattolin, F. Visentin, C. Santo, V. Bertolasi, L. Canovese, *Dalton Trans.*, 2016, **45**, 11560; (d) L. Canovese, F. Visentin, T. Scattolin, C. Santo, V. Bertolasi, *Dalton Trans.*, 2015, **44**, 15049; (e) F. Visentin, C. Santo, T. Scattolin, N. Demitri, L. Canovese, *Dalton Trans.*, 2017, **46**,10399.

[12] A.R. Kapdi, I.J.S. Fairlamb, *Chem. Soc. Rev.*, 2014, **43**, 4751.

[13] L. Canovese, F. Visentin, G. Chessa, C. Levi, P. Uguagliati, A. Dolmella, G. Bandoli, *Organometallics*, 2006, **25**, 5355.

[14] ECACC (*European Collection of authenticated cell cultures*) (http://www.pheculture collections.org.uk/products/celllines/generalcell/detail.jsp?refId=93112519&collection=ecacc_gc).

[15] COLT Cancer database (http://dpsc.ccbr.utoronto.ca/cancer/getcellline.pl?cellline=OVCA5)

[16] K.A. Foster, C.G. Oster, M.M. Mayer, M.L. Avery, K.L. Audus, *Experimental Cell Research*, 1998, **243** (2), 359.

[17] https://www.imanislife.com/collections/cell-lines/a375-cells/.

[18] D. Ahmed, P.W Eide, I.A. Eilertsen, S.A. Danielsen, M. Eknæs, M. Hektoen, G.E. Lind, R.A. Lothe, *Oncogenesis*, 2013, **2** (9), e71.

[19] M.E.H. Mazumder, P. Beale, C. Chan, J.Q.Yu, F. Huq, *ChemMedChem*, 2012, **7**, 1.

[20] Y.R. Adamski, J. Chen, *FEBS Letters*, 2010, **584**, 1873.

[21] T.T. Fong, C. Lock, C.Y. Chung, Y.E. Fung, P. Chow, P. Wan, C. Che, *Angew. Chem. Int. Ed.*, 2016, **55**, 11935.

[22] S. N. Sluijter, S. Warsink, M. Lutzc, C. J. Elsevier, *Dalton Trans.*, 2013, **42**, 7365.

[23] S. Hansson, P.O. Norrby, M.P.T. Sjogren, B. Akermark, M.E. Cucciolito, F. Giordano, A. Vitagliano, *Organometallics*, 1993, **12**, 4940.

[24] L. Canovese, F. Visentin, P. Uguagliati, G. Chessa, A. Pesce, *J. Organomet. Chem*, 1998, **566**, 61.

[25] D. P. Hruszkewycz, D. Balcells, L. M. Guard, N. Hazari, M. Tilset, *J. Am. Chem. Soc.*, 2014, **136**, 7300.

[26] D. P. Hruszkewycz, L. M. Guard, D. Balcells, N. Feldman, N. Hazari, M. Tilset, *Organometallics*, 2015, **34**, 381.

[27] (a) M. Aufiero, T. Scattolin, F. Proutière, F. Schoenebeck, *Organometallics*, 2015, **34**, 5191; (b) T. Scattolin, E. Senoi, Q. Guo, F. Schoenebeck, *Angew. Chem. Int. Ed.*, 2018, **57**, 12425.

[28] P. D. W. Boyd, A. J. Edwards, M. G. Gardiner, C. C. Ho, M.H. Lemée-Cailleau, D. S. McGuinness, A. Riapanitra, J. W. Steed, D.N. Stringer, B. F. Yates, *Angew. Chem. Int. Ed.*, 2010, **49**, 6315.

[29] L. Canovese, F. Visentin, C. Levi, C. Santo, V. Bertolasi, *J. Organomet. Chem*, 2013, **732**, 27.

[30] V.P.W. Bohm, C.W.K. Gstottmayr, T. Weskamp, W.A. Herrmann, *J. Organomet. Chem*, 2000, **595**, 186.

[31] (a) L. Canovese, F. Visentin, C. Levi, A. Dolmella, *Dalton Trans.*, 2011, **40**, 966; (b) L. Canovese, F. Visentin, C. Levi, C. Santo, V. Bertolasi, *Inorganica Chimica Acta*, 2011, **378**, 239.

[32] F. Visentin, A. Togni, *Organometallics*, 2007, **26**, 3746.

[33] L. Canovese, F. Visentin, C. Santo, G. Chessa, V. Bertolasi, *Organometallics*, 2010, **29**, 3027.

[34] (a) J. Tsuji, *Palladium reagent and catalysts*, John Wiley and sons, 1995, 5; (b) L. Canovese, F. Visentin, C. Levi, C. Santo, V. Bertolasi, *J. Organomet. Chem.*, 2013, **732**, 27; (c) L. Canovese, F. Visentin, T. Scattolin, C. Santo, V. Bertolasi, *Polyhedron*, 2016, **119**, 377; (d) L. Canovese, G. Chessa, F. Visentin, *Inorganica Chim. Acta*, 2010, **363**, 3426; (e) L. Canovese, F. Visentin, C. Santo, G. Chessa, V. Bertolasi, *Organometallics*, 2010, **29**, 3027; (f) L. Canovese, F. Visentin, C. Levi, A. Dolmella, *Dalton Trans.*, 2011, **40**, 966; (g) L. Canovese, F. Visentin, C. Levi, C. Santo, V. Bertolasi, *Inorganica Chim. Acta*, 2011, **378**, 239; (h) L. Canovese, F. Visentin, C. Levi, C. Santo, V. Bertolasi, *J. Organomet. Chem.*, 2013, **732**, 27.

5

Carbohydrate based NHC complexes

As seen in the previous chapter, complexes with carbene ligands deriving from alkyl imidazoles or bidentate biscarbene ligands, display an interesting activity toward different tumour lines but in many cases they are cytotoxic toward fibroblasts. The introduction of one or more glycosidic units could improve the selectivity of such compounds, on the basis of the well-known Warburg effect, which is for example the basis of the PET technique as will be explained in detail later.

As a matter of fact, glucose and its derivatives tend to accumulate preferentially in tumour cells rather into the healthy ones. After a brief general introduction about carbohydrates, the following section will deal with the synthesis and antitumor activity of Pd (II) complexes stabilized by carbohydrate-based NHC ligands.

The figure proposed at the beginning of the chapter is related to this source:
https://news.usc.edu/117042/from-mother-to-baby-secondhand-sugars-can-pass-through-breast-milk/

5.1. Introduction [1,2]

5.1.1. Carbohydrates: General aspects

Carbohydrates are the most abundant class of organic molecules in nature and are one of the three main components of living cells, along with amino acids and lipids. Carbohydrates have numerous biological functions: they represent an important source of energy (through their oxidation, in non-photosynthetic cells), an indispensable structural component of the cellulose and cartilage and also play a fundamental role in the immune and reproductive systems.

They can be divided into three main classes: monosaccharides, oligosaccharides and polysaccharides. The simplest carbohydrates are called monosaccharides and are substantially polyhydroxy aldehydes or polyhydroxy ketones (or substances that generate such compounds by hydrolysis) having from four to nine carbon atoms in their chain (five or six for the most part).

Apart dihydroxyacetone, all monosaccharides contain one or more asymmetric carbon atoms (stereogenic centers) and are therefore often present in nature in several optically active isomeric forms. A classic way to represent the structure and therefore the configuration of the monosaccharides is the use of the so-called "Fisher projections" [3]. For instance, the "Fisher projections" of the glyceraldehyde, the simplest aldose, display only one stereogenic center and therefore two optical isomers (enantiomers), called D- and L-glyceraldehyde (Fig. 5.1).

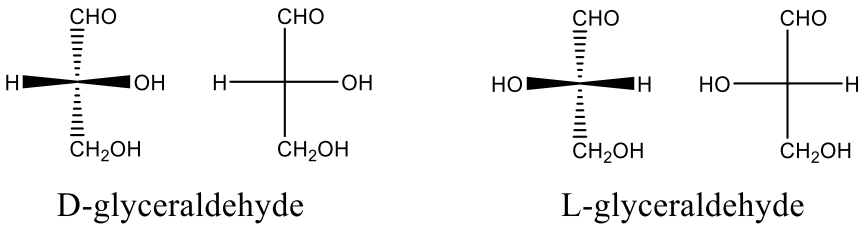

Fig. 5.1

Monosaccharides can be divided in two categories i.e. D- or L-isomers on the basis of the their stereogenic center furthest from the carbonyl group having the same configuration of that of the D- or L- glyceraldehyde, respectively. Most of the hexoses present in living organisms are D-isomers (Fig. 5.2).

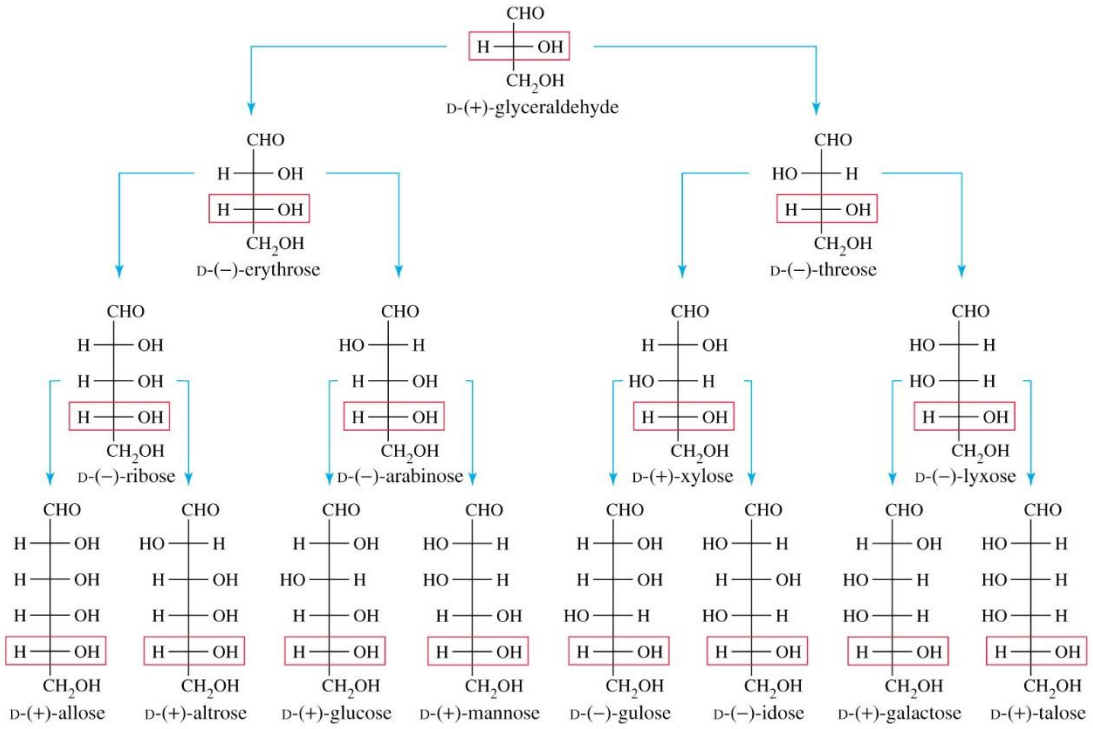

Fig. 5.2. The D-family of aldoses.

In aqueous solution, the aldotetroses and all the other monosaccharides with five or more carbon atoms assume a cyclic form, due to the reaction between the carbonyl group and a hydroxyl group belonging to the chain. This reaction produces an additional stereogenic center which can assume two different configurations called α and β (Fig. 5.3).

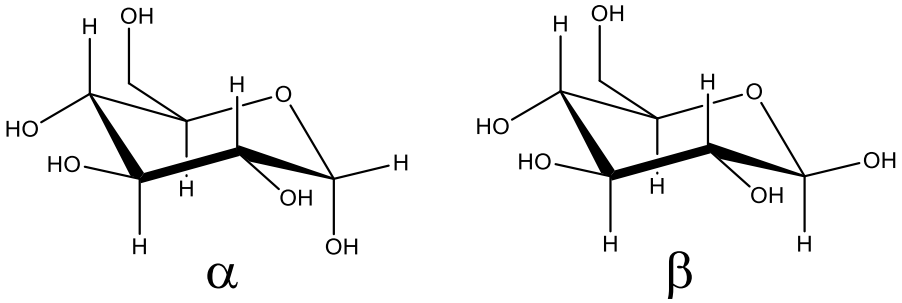

Fig. 5.3. Structure of α- and β-D-glucose.

These cyclic forms are also called hemiacetal or hemiketal, depending on their starting molecule which can be an aldehyde or a ketone. Their structures can be traced back to those of the pyran, if they form a six-term ring (pyranoses), or furan if they form a five-term ring (furanoses). The isomeric forms (α or β) differing only for the configuration of the hemiacetal (or hemiketal) carbon are called anomeric forms.

5.1.2. Anomeric effect and anomerization [2]

In 1928 Pascu discovered that the β-anomers of the acetylated and alkylated glucose anomerize in the presence of Brönsted acids (i.e. H_2SO_4) or Lewis acids (i.e. $SnCl_4$ or BF_3) to give mixtures of α and β forms [4].

The effect leading to the reposition of an aglycone (substituent on the anomeric carbon) from the equatorial to the more crowded axial position, is called direct anomeric effect. According to Corey and Edward, this relocation can be traced back to the interaction between dipoles associated to the hemiacetalic oxygen atom with that bound to C-1 (Fig. 5.4).

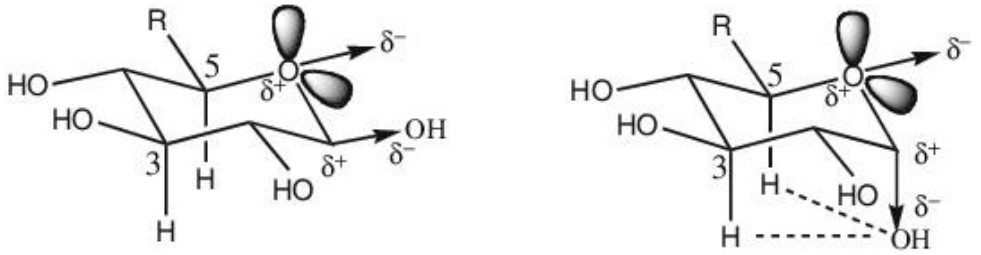

Fig. 5.4

In the case of imidazolic aglycones it can be represented as follows (Scheme 5.1):

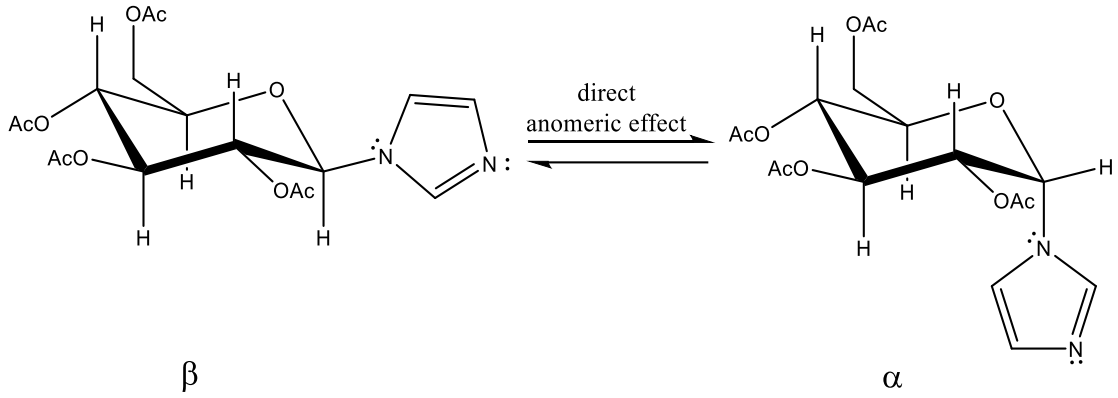

Scheme 5.1

The opposite phenomenon, observed in the case of an aglycone bound to the monosaccharide by an electron-withdrawing group or a positive atom, is called "reverse anomeric effect" and is typical of the imidazolium salts (Scheme 5.2).

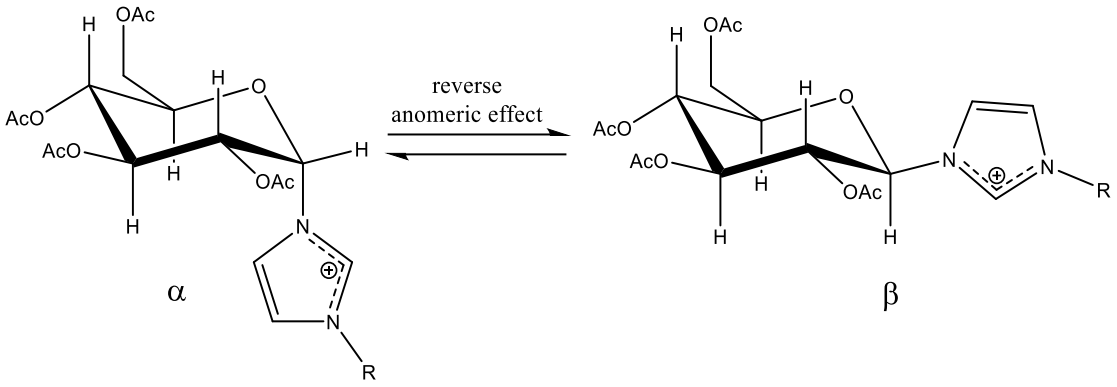

Scheme 5.2

Therefore, anomerization is the process that promotes the attainment of the thermodynamic equilibrium between anomers and obviously depends from the relative energy between the species under examination. This process is catalysed by Brönsted or Lewis acids and is more conspicuous in the presence of polar protic solvents. The mechanisms of anomerization can be approximately distinguished in two categories: mutarotation and anomerization in the strict sense of the term.

5.1.2.1. Mutarotation

The mutarotation is a process possible in the presence of water and favored by the presence of acids or bases. It involves the passage from the closed hemiacetal to the open form, rotation about the C1-C2 bond and hemiacetal reclosing, as reported in Scheme 5.3.

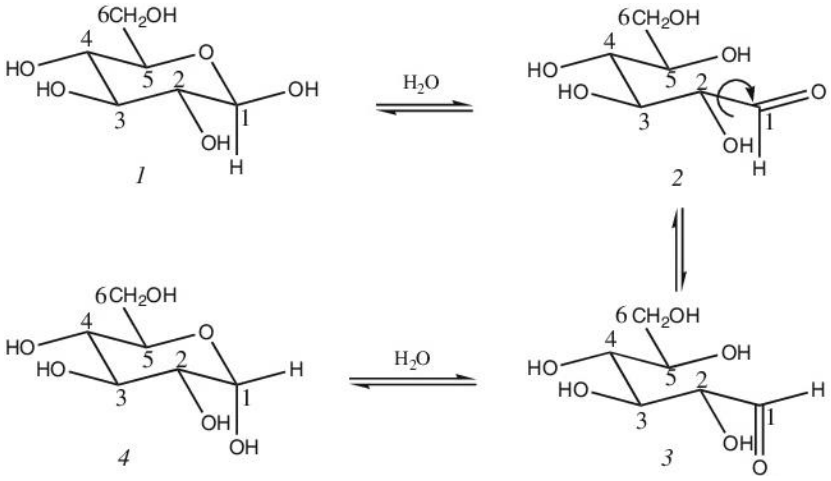

Scheme 5.3

5.1.2.2. Anomerization

The transformation from α to β anomer (or vice versa) without passing through the open form of the sugar is called anomerization in the strict sense. The difference with the mutarotation is that it can be promoted only by Brönsted or Lewis acids and does not necessarily require water or protic polar solvents. The mechanisms proposed for such a transformation are summarized in Scheme 5.4:

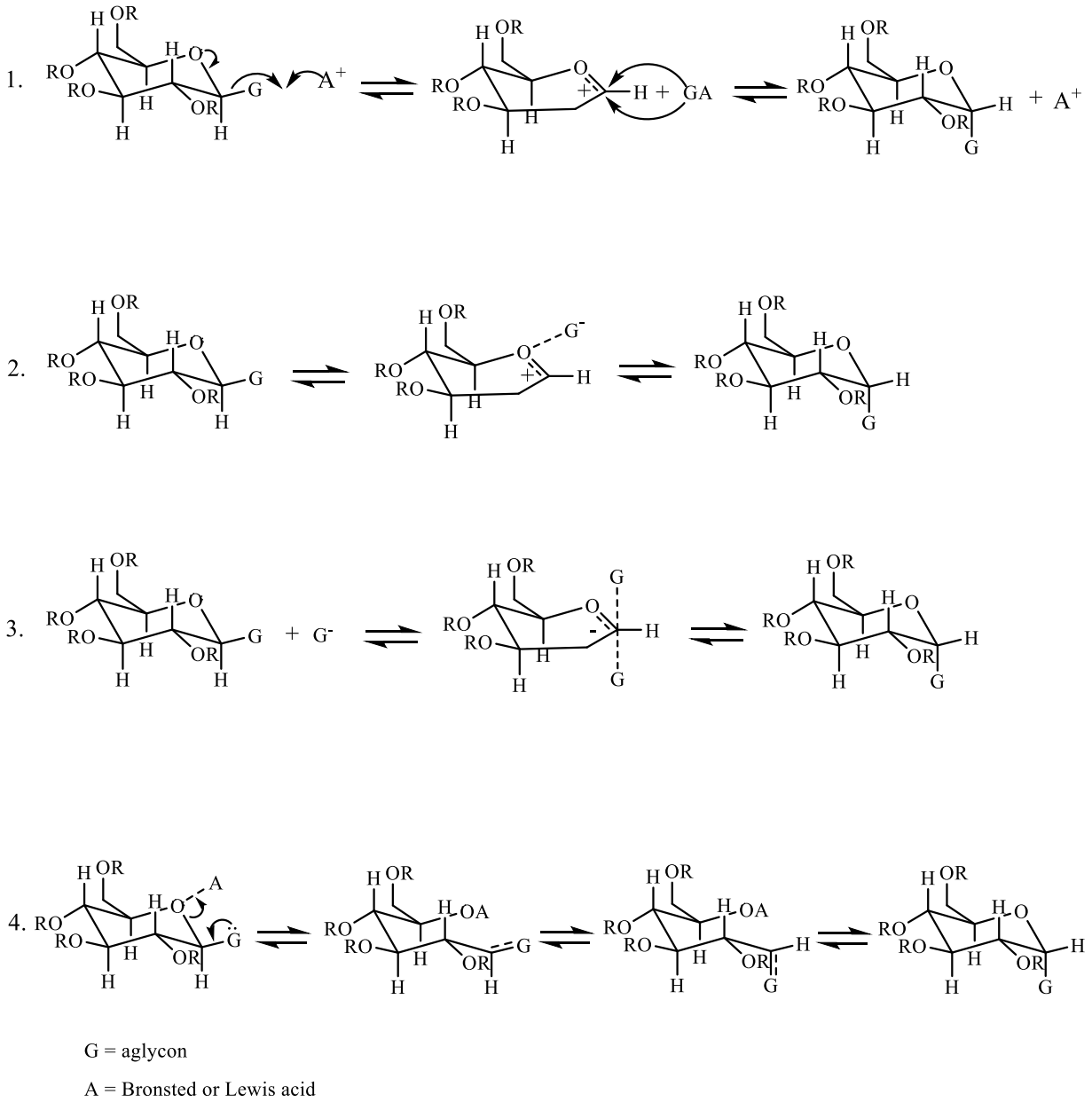

Scheme 5.4

In the case of the processes which will be described later, the most probable is mechanism 4, which is promoted by the interaction between the metal centers (Ag and/or Pd) and the hemiacetalic oxygen.

5.1.3. Metal-based compounds with glycosidic groups and Warburg effect

Unlike the differentiated normal cells, which exploit the mitochondrial oxidative phosphorylation as their primary source of energy, most tumour cells prefer to acquire energy by a mechanism not very clear yet, which is based on the aerobic glycolysis, an inefficient process producing adenosine-5'-triphosphate (ATP) [5].

This phenomenon is called "Warburg effect", and its most important expression is the significant increase of the uptake and incorporation of nutrients in tumour cells if compared to the healthy ones. In important works by Warburg (1920) and others [5, 6], the remarkable uptake and consumption of glucose taking place in tumour cells have been highlighted and the increased acidity interpreted on the basis of the different way to metabolize the sugar with consequent production of lactic acid.

These findings have subsequently led many research groups to employ glucose and its derivatives to identify tumour masses (i.e. PET) and/or to selectively damage them (by the introduction of glycosidic fragments into potential chemotherapeutic agents).

In the field of diagnostics, PET (*Positron Emission Tomography*) allow to obtain maps of the functional processes occurring inside the body, at variance with the Computerized Tomography (CT) and the Magnetic Resonance Imaging (MRI) which provide only morphological information. Obviously, the three cited techniques are often complementary.

PET technique exploits the great tendency of the tumor masses (up to 200 times compared to healthy tissues) to absorb the radiopharmaceutical ^{18}F-fluoroglucose (^{18}F-FDG), permitting us to acquire images in marked contrast with those of the areas not affected by cancer (Fig. 5.5) [7].

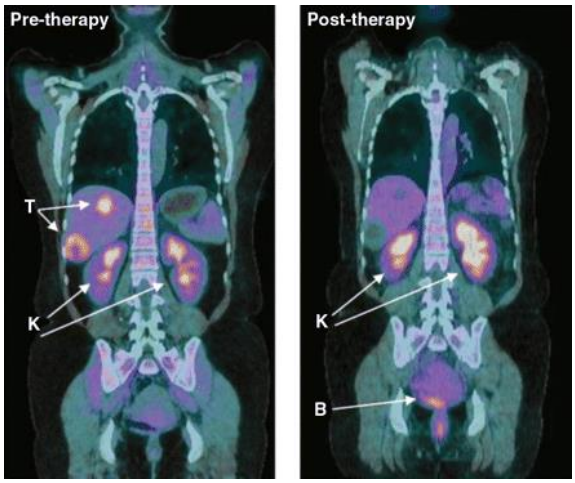

Fig. 5.5 The tumor (T) is readily visualized by FDG-PET/CT before therapy (left). After 4 weeks of therapy (right), the tumor shows no uptake of FDG despite persistent abnormalities on CT. Excess FDG is excreted in the urine, and therefore the kidneys (K) and bladder (B) are also visualized as labelled [5].

In the last decades several transition metal complexes containing glycosidic units have been synthesized and some of their biological properties, such as the antiproliferative activity against different tumors, studied.

The most important example is the [2,3,4,6-tetra-*O*-acetyl-1-(thio-κ*S*)-β-D-glucopyranosato]-(triethylphosphane)gold(I), usually called Auranofin (Fig. 5.6).

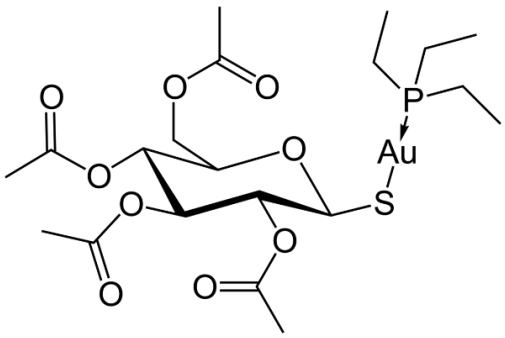

Fig. 5.6. Chemical structure of Auranofin

This compound was approved by the FDA in 1985 as a drug against rheumatoid arthritis [8] and in the same year, Mirabelli and co-workers studied its antitumor activity. The mechanisms of action are still debated, and the main target seems to be Thioredoxine reductase (TrxK), a key enzyme overexpressed by tumor cells. Auranofin reacts selectively with the selenium of the selenocysteine covalently bound to the TrxK, and in that way inhibits the enzyme [9]. This kind of inhibition induces the cell apoptosis through a "cascade" mechanism.

In 2016, phase I and II of clinical trials for the treatment of chronic lymphocytic leukemia (CLL) with Auranofin were successfully completed [10].

In the case of palladium few compounds containing glycosidic units are known, but the results of *in vitro* tests are encouraging (Fig. 5.7) [11].

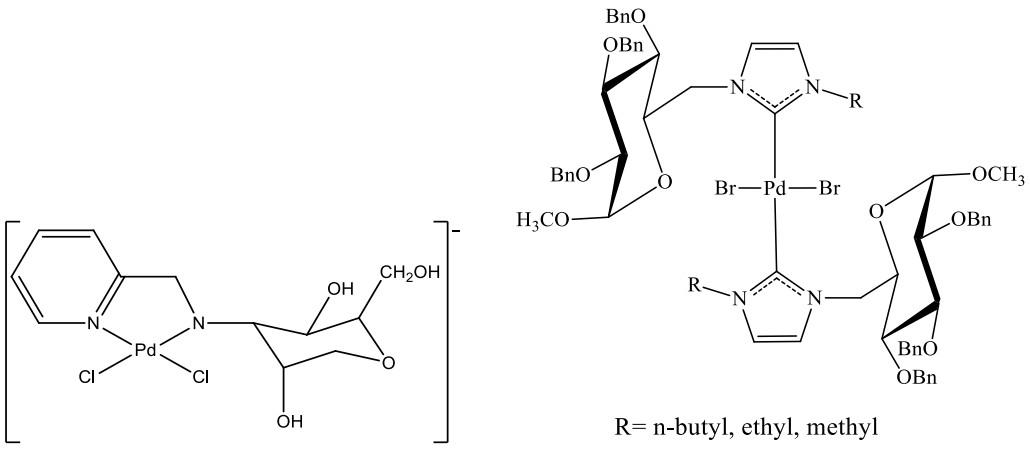

Fig. 5.7

These facts prompt us to try the synthesis of new organometallic palladium compounds bearing NHC with glycosidic substituents. In particular, the interesting results described in the previous chapters induces us to focus our attention on palladacyclopentadienyl and η^3-allyl complexes. Our hope is that the introduction of a glycosidic fragment could improve the selectivity of the modified complexes against tumour cells.

5.2. Synthesis of 2,3,4,6-tetra-O-acetyl-α-D-glucopyranosyl bromide

The first step of the synthesis of the compounds which will be discussed in this chapter is the protection of the α-D-glucose hydroxyl groups in positions 2, 3, 4 and 6 with acetyl groups (esterification reaction) and the simultaneous activation of the anomeric carbon (position 1) by bromination. This step was carried out by reacting at room temperature, α-D-glucose, acetic anhydride and acetyl bromide in the presence of a small amount of $HClO_4$ [12] (Scheme 5.5).

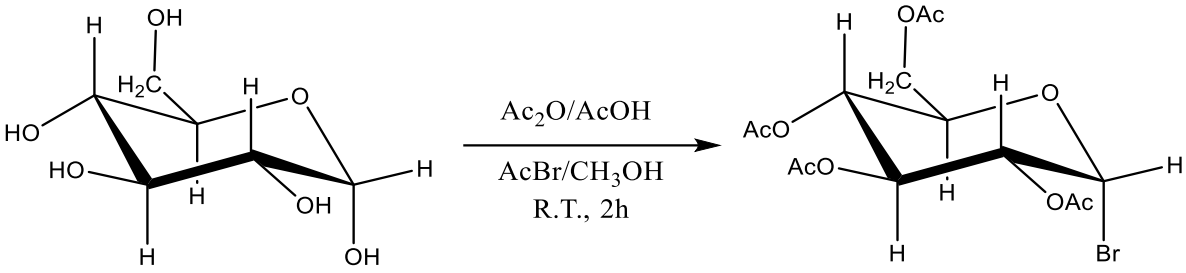

α-D-glucopyranose

2,3,4,6-tetra-O-acetyl-α-D-glucopyranosyl bromide

(99%)

Scheme 5.5

The ensuing compound can be easily identified from its ^{1}H-NMR spectrum (Fig. 5.8), showing:

- Four different singlets ascribable to the OCH_3 groups, within 2 and 2.1 ppm.
- The CH and CH_2 protons of the glycoside within 4.1 and 6.6 ppm. In particular, the proton in position 1, relative to the anomeric carbon, is present as a doublet at about 6.6 ppm and will be of fundamental importance for the interpretation of the spectra of the compounds which will be discussed later.

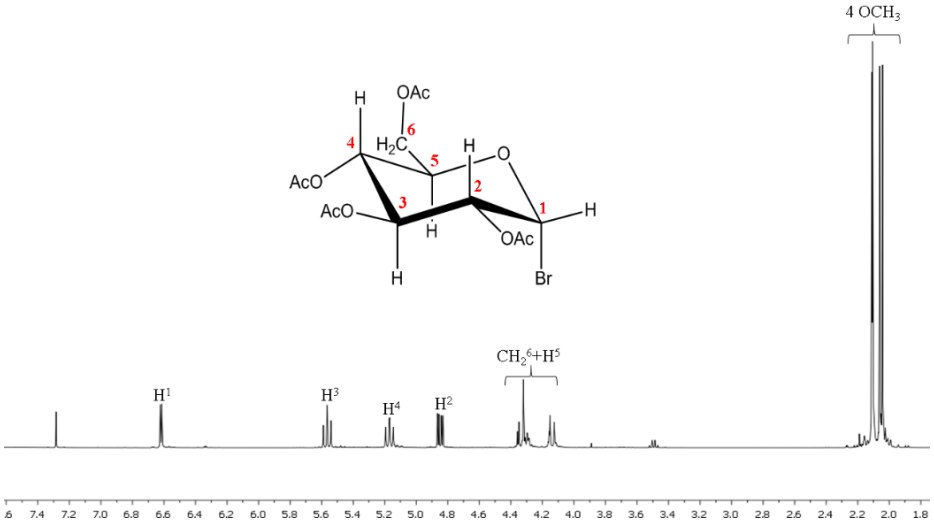

Fig. 5.8. ^{1}H-NMR spectrum of 2,3,4,6-tetra-O-acetyl-α-D-glucopyranosyl bromide ($CDCl_3$).

In the $^{13}C\{^{1}H\}$-NMR spectrum (Fig. 5.9), the following signals are observed:

- Four OCH_3 groups at about 20.5 ppm.
- CH_2 in position 6 at about 61 ppm.
- Five glycosidic CH between 67 and 87 ppm.
- Four carbonyl carbons at about 170 ppm.

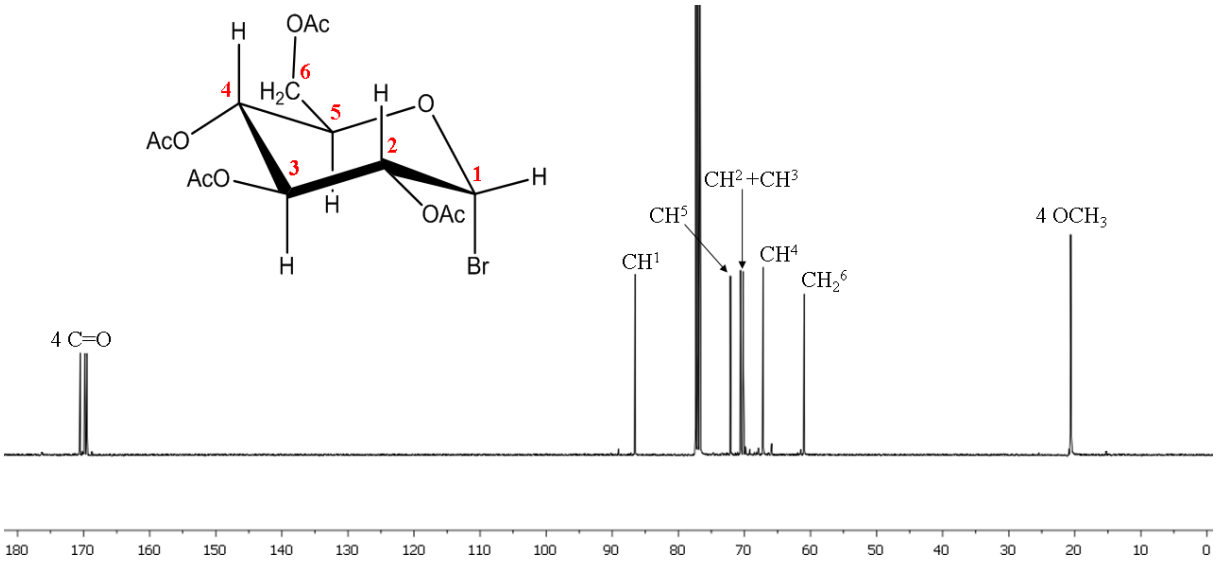

Fig. 5.9. $^{13}C\{^{1}H\}$-NMR spectrum of 2,3,4,6-tetra-O-acetyl-α-D-glucopyranosyl bromide ($CDCl_3$)

5.3. Synthesis of 1-(2,3,4,6-tetra-O-acetyl-β-D-glucopyranosyl) imidazole

The nucleophilic substitution between the 2,3,4,6-tetra-O-acetyl-α-D-glucopyranosyl bromide and the imidazole is strategic for the final synthesis of the target complexes bearing *N*-Heterocyclic Carbenes. The reaction was carried out using imidazole in excess, following the conditions of Scheme 5.6 [13].

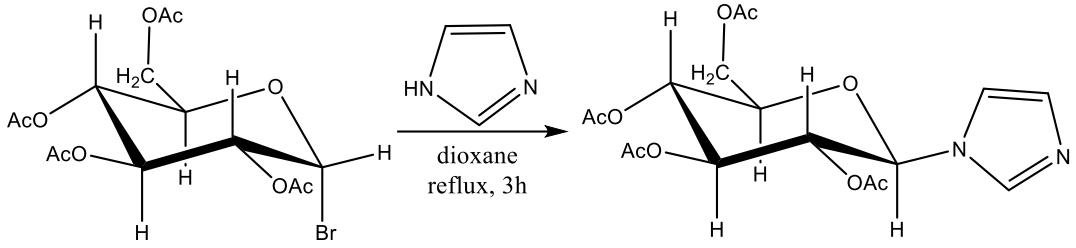

2,3,4,6-tetra-O-acetyl-α-D-glucopyranosyl bromide

1-(2,3,4,6-tetra-O-acetyl-β-D-glucopyranosyl) imidazole

(53%)

Scheme 5.6

The imidazole derivative can be easily precipitated by addition of water to the reaction mixture. Since the employed reaction is a SN_2 nucleophilic substitution, it was possible to observe the inversion of the configuration of the anomeric carbon (from α to β). The final compound was characterized exhaustively by ^{1}H-NMR spectroscopy. In particular, in the ^{1}H-NMR spectrum (Fig. 5.10) it is possible to observe the presence of:

- Four signals ascribable to the OCH_3 groups within 1.9 and 2.1 ppm.
- CH and CH_2 glycosidic protons within 3.5 and 5.5 ppm.
- The imidazolic proton (NCHN) at about 7.7 ppm.

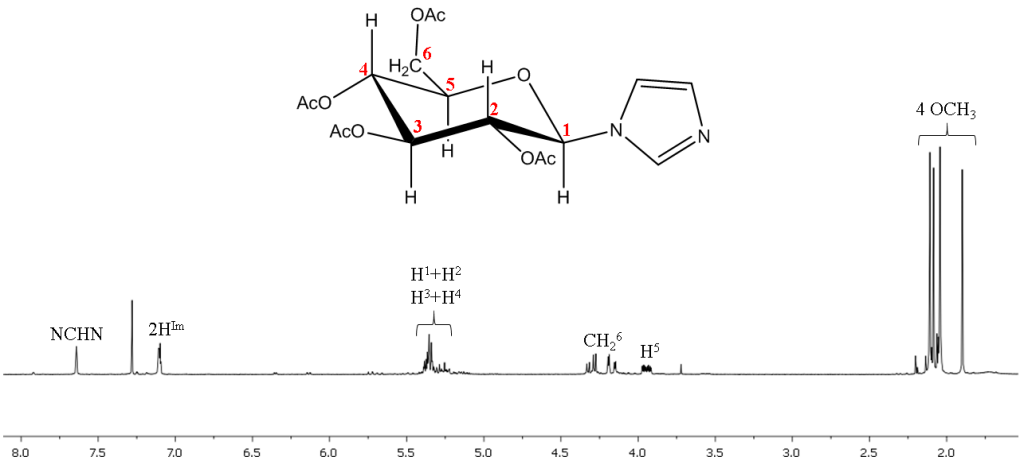

Fig. 5.10. ^{1}H-NMR spectrum of 1-(2,3,4,6-tetra-O-acetyl-α-D-glucopyranosyl)imidazole.

5.4. Synthesis of imidazolium salts

The corresponding imidazolium salts can be easily obtained by alkylation of the non-functionalized nitrogen (quaternization) of the above described compound. In particular, as highlighted in Scheme 5.7, the reaction of the imidazole with *n*-butyl bromide or methyl iodide, yields the imidazolium salts **33a** and **33b**, respectively [13].

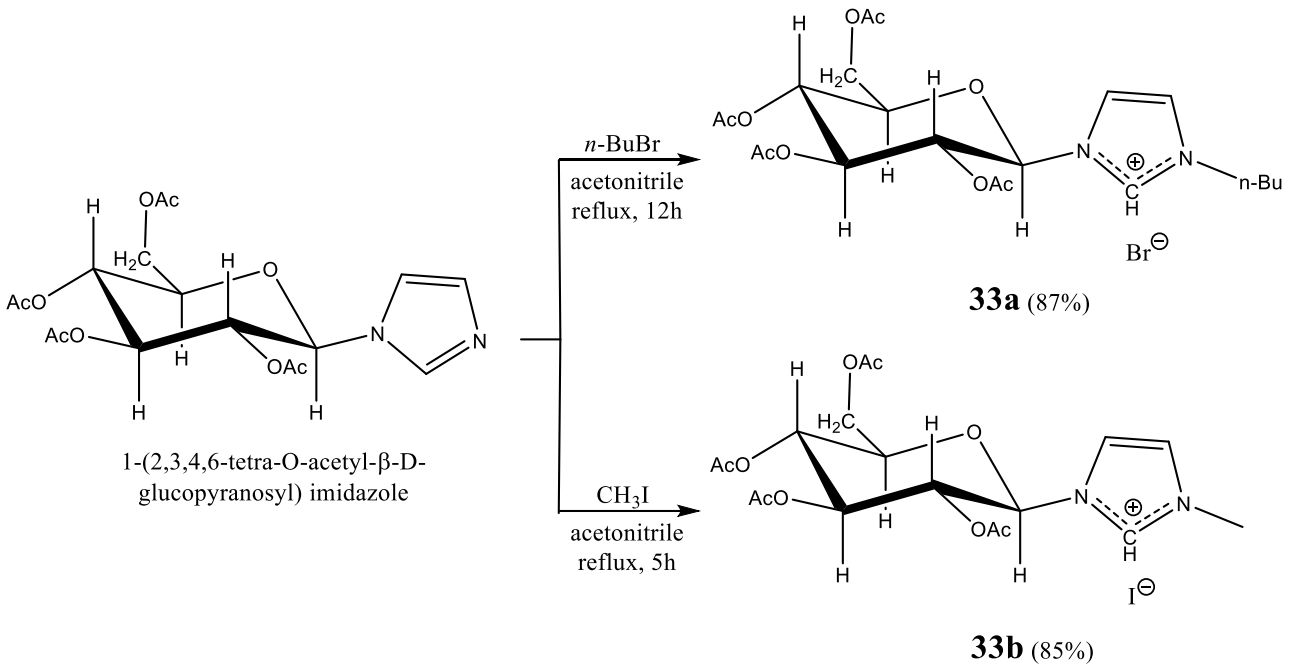

Scheme 5.7

The imidazolium salt **33a** requires a purification on a chromatographic column whereas compound **33b** was isolated by precipitation from a CH_2Cl_2/Et_2O mixture.

From the ^{1}H-NMR spectra (Figs. 5.11 and 5.12) of the compounds, it is possible to observe the presence of:

- The CH and CH_2 glycosidic protons within 4 and 7 ppm. In particular, the proton in position 1 resonates as doublet at about 6.5 ppm.
- The imidazolium proton NCHN within 10.5 and 11 ppm ($\Delta\delta \approx 3$ ppm with respect to the starting imidazole).
- The butyl substituent signals within 1 and 2 ppm ($CH_2^{2'}$, $CH_2^{3'}$, $CH_3^{4'}$) and the CH_2 directly bound to the imidazole nitrogen ($CH_2^{1'}$) at about 4 ppm, in the case of the imidazolium salt **33a**.
- The NCH_3 signal at 4.3 ppm in the case of compound **33b**.

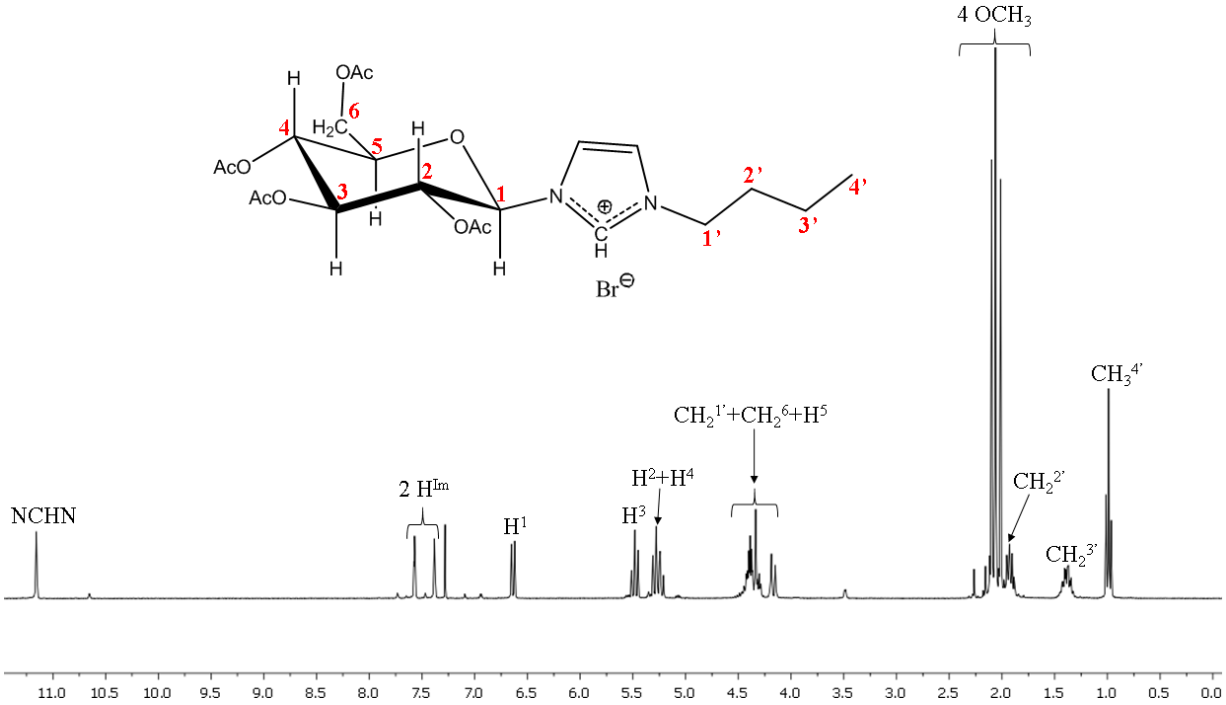

Fig. 5.11. ^{1}*H-NMR spectrum of the imidazolium salt* ***33a*** *(T=298K, $CDCl_3$).*

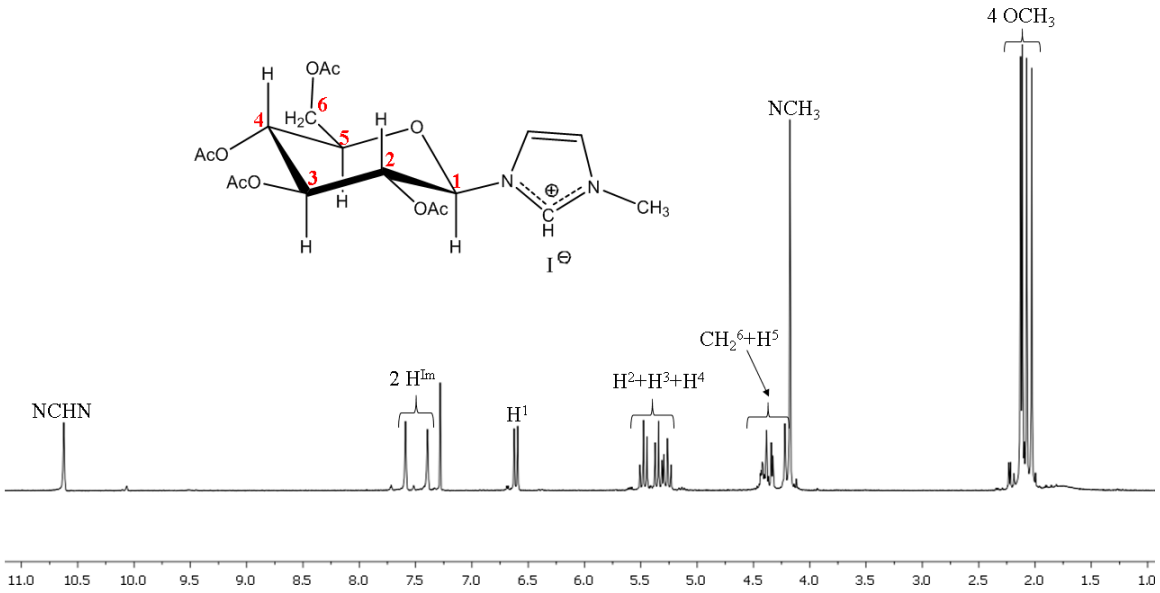

Fig. 5.12. ^{1}*H-NMR spectrum of the imidazolium salt* ***33b*** *(T=298K, $CDCl_3$).*

In the $^{13}C\{^{1}H\}$-NMR spectra (Fig. 5.13), it is possible to observe:

- The signals of the carbonyl carbons at about 170 ppm.
- The NCHN imidazolic carbon signal at about 135-140 ppm.
- The CH and CH_2 glycosidic signals within 60 and 90 ppm.
- The signals of the OCH_3 groups at about 21 ppm.

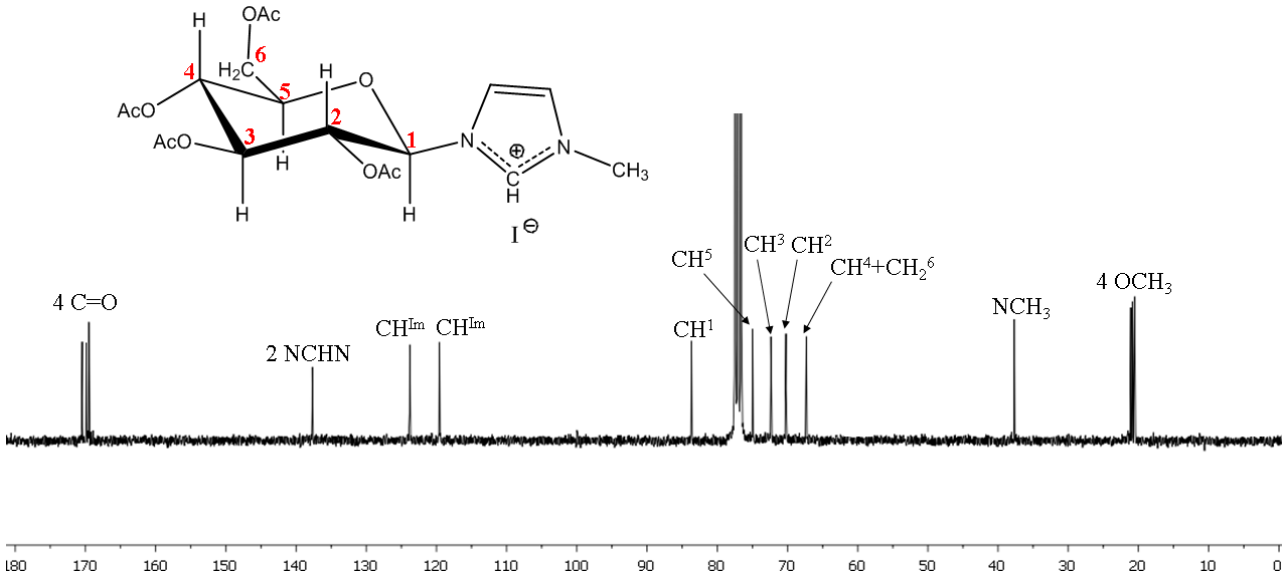

Fig. 5.13. $^{13}C\{^{1}H\}$*-NMR spectrum of the imidazolium salt* ***33b*** *(T=298K,* $CDCl_3$*).*

The synthesis of the imidazolium salt bearing a mesityl substituent was carried out by direct reaction between the 2,3,4,6-tetra-O-acetyl-α-D-glucopyranosyl bromide, mesityl imidazole and silver triflate (Scheme 5.8). The reaction was carried out in reflux of acetonitrile for 16 hours [14].

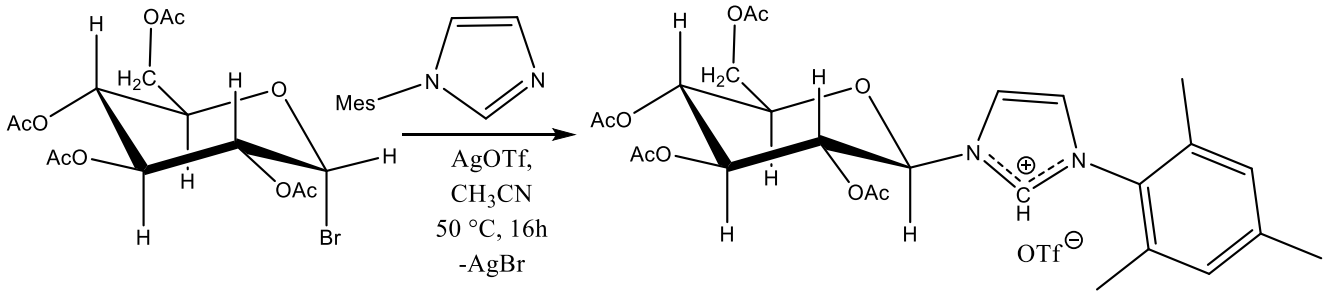

2,3,4,6-tetra-O-acetyl-α-D-glucopyranosyl bromide

1-(2',3',4',6'-tetra-O-acetyl-β-D-glucopyranosyl)-3-mesityl imidazolium triflate

(34%)

Scheme 5.8

The product was isolated by precipitation from a dichloromethane/diethylether mixture. In order to favour the successive synthetic steps, the triflate was replaced with chloride by the ion-exchange resin DOWEX-21KCl (Scheme 5.9).

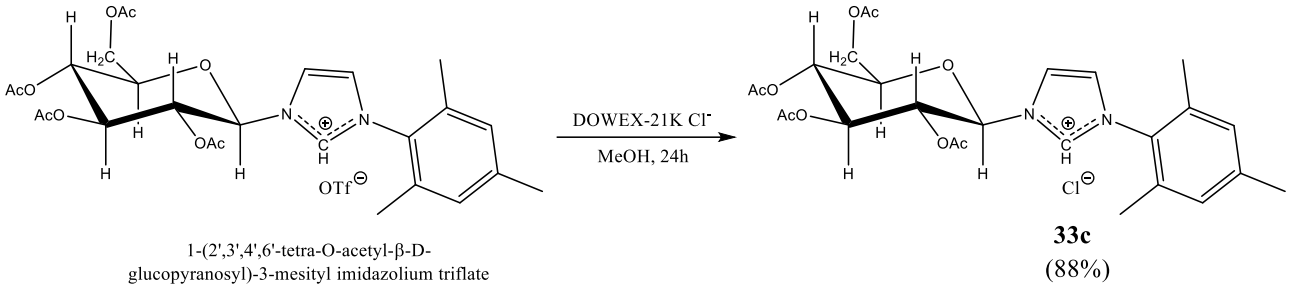

1-(2',3',4',6'-tetra-O-acetyl-β-D-glucopyranosyl)-3-mesityl imidazolium triflate

33c
(88%)

Scheme 5.9

At variance with its triflate precursor, the derivative **33c** is present in solution as two anomers (α and β), in ca. 60:40 ratio. The anomerization was most likely promoted by the interaction between the compound and the resin (interaction with acidic sites in a polar protic solvent). The co-presence of the two anomers is unequivocally attested by the duplication of all the signals in the ^{1}H-NMR and ^{13}C-NMR spectra.

In ^{1}H-NMR spectra (Fig. 5.14) we can see in detail:

- The imidazole protons at about 11 and 8.5 ppm.
- The glycosidic proton in position 1 (one for each anomer) resonant as a doublet at 7.3 ppm.
- The other CH glycosidic protons within 4.2 and 5.6 ppm.
- The signals of the methyl groups of the acetyls and of the mesityl substituents within 2 and 2.4 ppm.

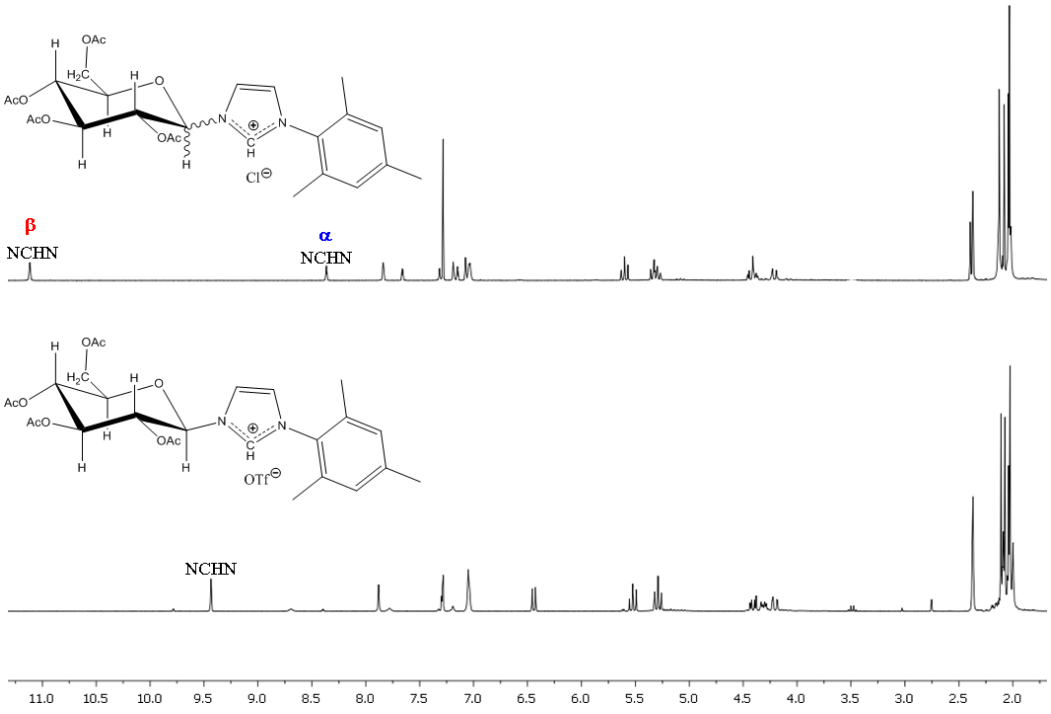

*Fig. 5.14. ^{1}H-NMR spectra of **33c** and the starting imidazolium salt (T=298K, $CDCl_3$)-*

The $^{13}C\{^{1}H\}$-NMR spectrum (Fig. 5.15) of compound **33c** shows signals similar to those already recorded in the case of compounds **33a** and **33b**. In addition, those of the carbons of the methyl substituents of the mesityl group resonating within 17 and 21 ppm and the aromatic carbons at 130-140 ppm are observed.

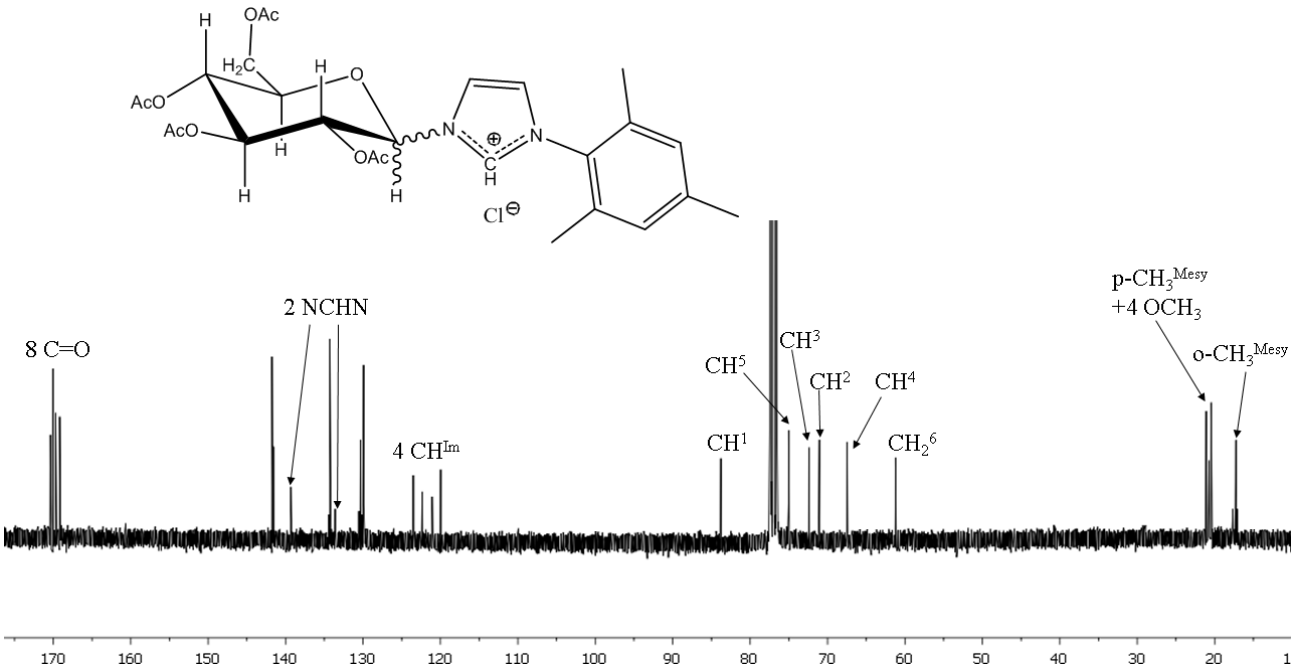

*Fig. 5.15. $^{13}C\{^{1}H\}$-NMR spectrum of the imidazolium salt **33c** (T=298K, $CDCl_3$).*

Finally, in the IR spectra (Fig 5.16) the disappearance of the signals at 639 cm^{-1} (S=O bending) and at 1200-1300 cm^{-1} (S=O and C-F triflate stretchings) are observed.

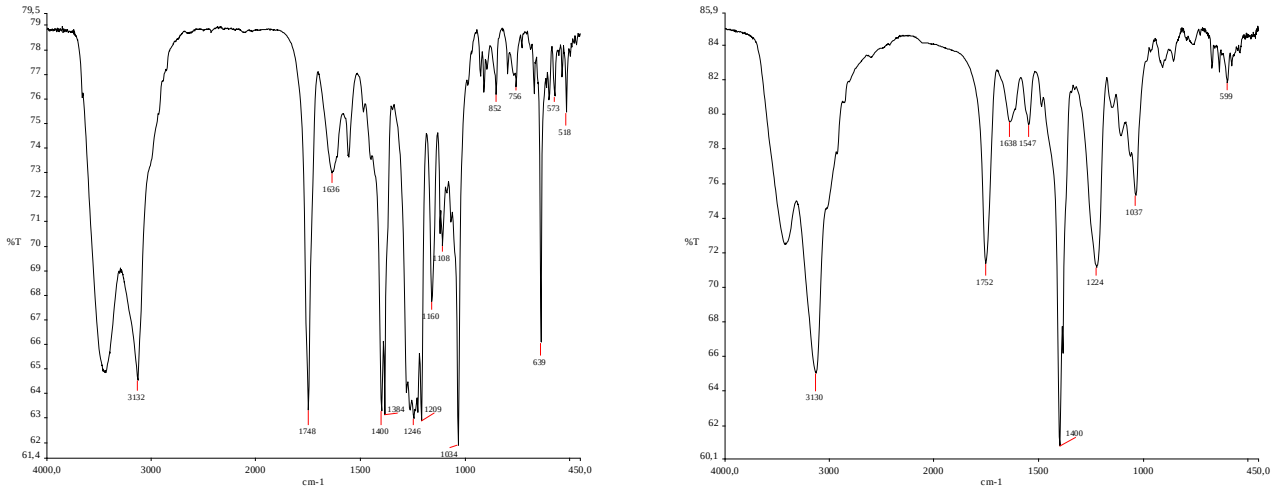

*Fig. 5.16. IR spectra (in KBr) of **33c** (right) and the starting imidazolium salt (left).*

5.5. Synthesis of Silver(I) complexes

The Ag(I) carbene complexes **38a-c** were obtained by reacting the imidazolium salts **33a-c** with silver oxide according to the conditions reported in Scheme 5.10.

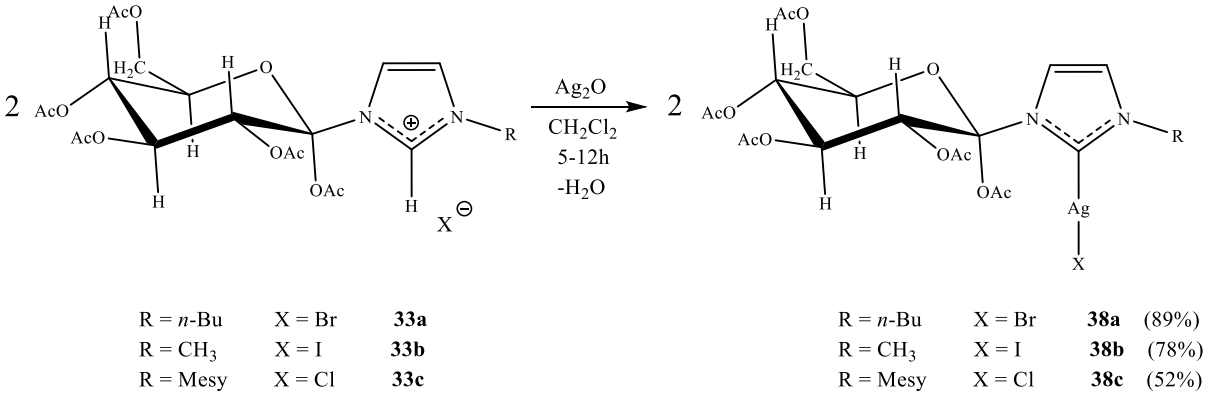

R = *n*-Bu	X = Br	**33a**	R = *n*-Bu	X = Br	**38a** (89%)
R = CH_3	X = I	**33b**	R = CH_3	X = I	**38b** (78%)
R = Mesy	X = Cl	**33c**	R = Mesy	X = Cl	**38c** (52%)

Scheme 5.10

The reactions were carried out in anhydrous dichloromethane, under inert atmosphere (Ar), in the dark for a time ranging from 5 to 12 hours, as entailed by the R substituent. In all cases, the reaction advancement is revealed by the progressive dissolution of the silver oxide. The products were isolated in good yields by precipitation with diethyl ether from the reaction mixture. The novel compounds **38a-c**, in analogy with similar Ag (I) complexes reported in the literature [15], should be formulated as $[Ag(NHC)_2][AgX_2]$. All the investigated complexes have been characterized by NMR and IR spectroscopy and are present as a single isomer, independently of the presence of one or two anomers in the starting imidazolium salts.

In the NMR spectra it is possible to observe:

- The disappearance, in the ^{1}H-NMR spectra (Fig. 5.17), of the peak ascribable to the imidazolic proton NCHN between 8 and 11 ppm.
- The typical coordinated carbenic carbon signal between 180 and 190 ppm in the $^{13}C\{^1H\}$-NMR spectra (Fig. 5.18).

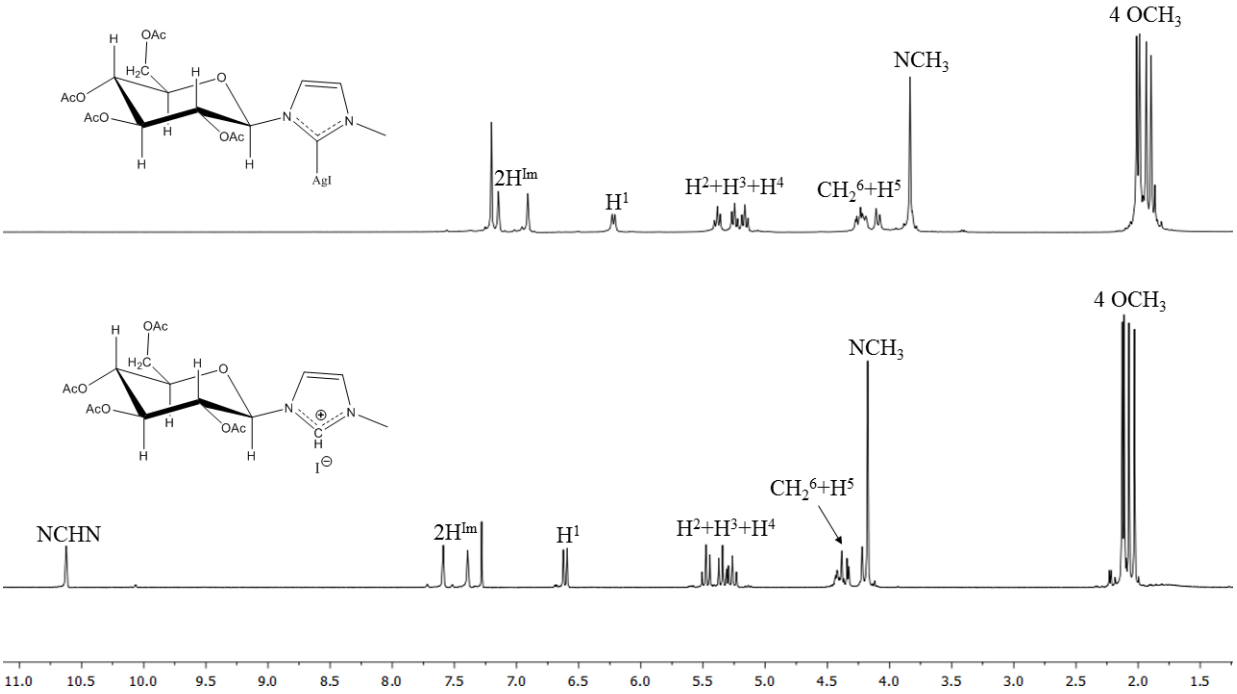

*Fig. 5.17. ^{1}H-NMR spectra of the silver complex **38b** and the imidazolium salt **33b** (T=298K, $CDCl_3$).*

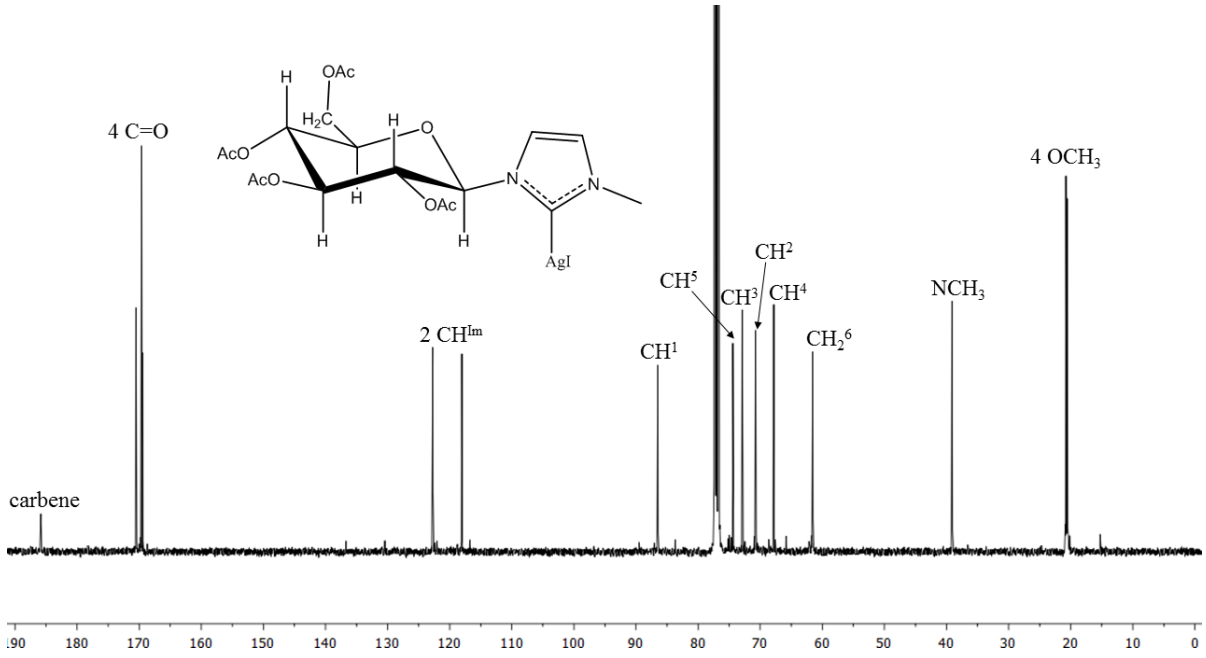

*Fig. 5.18. $^{13}C\{^{1}H\}$-NMR spectrum of the silver complex **38b** (T=298K, $CDCl_3$).*

5.6. Synthesis of the η^3-allyl Pd(II) complexes

5.6.1. Neutral η^3-allyl Pd(II) complexes

The reaction between the precursor $[Pd(\mu\text{-}Cl)(\eta^3\text{-allyl})]_2$ with the silver complexes **38a-c** yields the neutral η^3-allyl complexes **56a-c** together with the precipitation of the corresponding silver halide, that constitutes the real driving force of the entire process (Scheme 5.11).

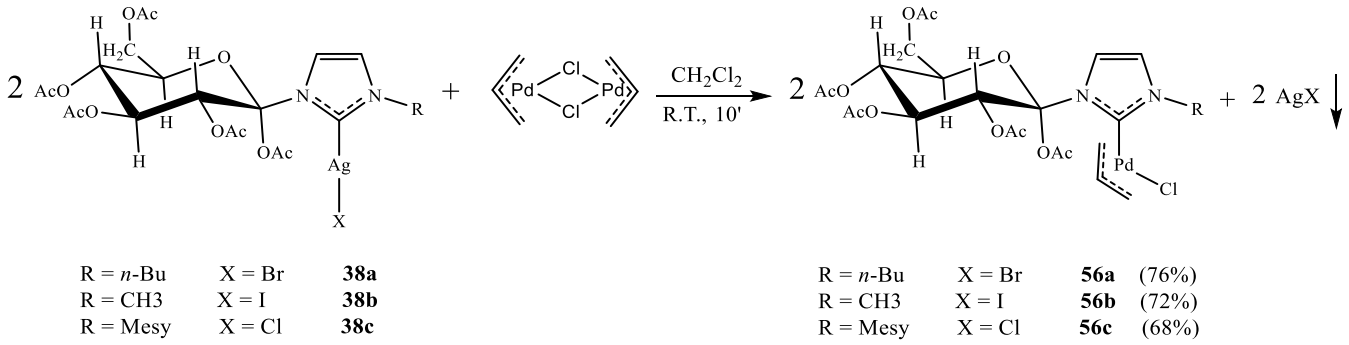

R = *n*-Bu	X = Br	**38a**	R = *n*-Bu	X = Br	**56a** (76%)
R = CH3	X = I	**38b**	R = CH3	X = I	**56b** (72%)
R = Mesy	X = Cl	**38c**	R = Mesy	X = Cl	**56c** (68%)

Scheme 5.11

The final complexes were obtained in good yields by treatment of the reaction residue with a diethylether/*n*-hexane mixture.

^{1}H-NMR spectra at 298 K reveal that each product consists of two anomers. The anomerization is most likely promoted by the presence in the reaction mixture of the metal centers Pd (II) and Ag (I), which can act as Lewis acids (see section 5.1).

The complexes under examination, having two different spectator ligands (Cl^- and NHC), present five different proton signals (for each anomer) related to the η^3-allyl fragment ($H^{syn}_{t\text{-}Cl}$, $H^{syn}_{t\text{-}C}$, $H^{anti}_{t\text{-}Cl}$, $H^{anti}_{t\text{-}C}$ and $H^{central}$), in addition to the typical signals of the carbenic moiety.

Thus, for each anomer, in the ^{1}H-NMR spectra (Figs. 5.19 and 5.20) it is possible to identify:

- The acetyl OCH_3 signals resonant as singlets within 2 and 2.1 ppm.
- The $H^{anti}_{t\text{-}Cl}$ and $H^{anti}_{t\text{-}C}$ doublets ($J \approx 12\text{-}13$ Hz) within 2.5 and 3.4 ppm, respectively.
- The $H^{syn}_{t\text{-}Cl}$ and $H^{syn}_{t\text{-}C}$ doublets ($J \approx 5\text{-}7$ Hz) within 3.5 and 4.4 ppm, respectively.
- The $H^{central}$ signal as a multiplet at about 5.5 ppm.
- The CH and CH_2 glycosidic signals within 4 and 6.3 ppm. In particular, the two doublets at about 6.2 ppm ($2H^1$) is indicative of the two different anomeric species.
- The signal of the methyl, *n*-butyl and mesityl substituents slightly displaced with respect to those of the starting Ag (I) complexes.

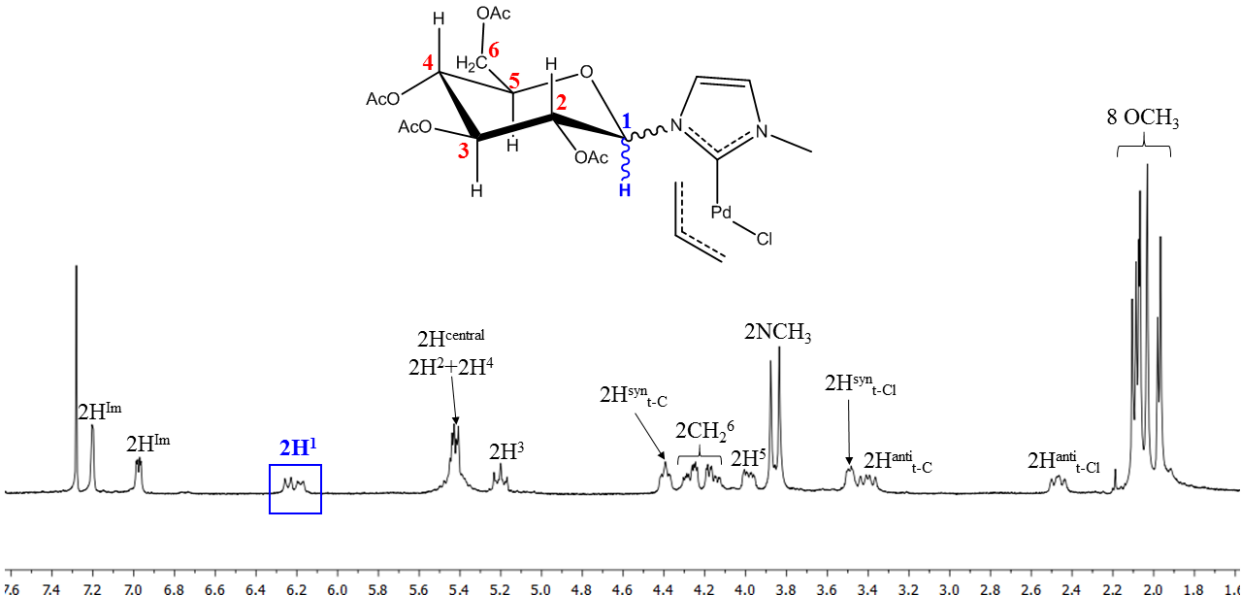

*Fig.5.19. [1]H-NMR spectrum of the complex **56b** (T=298K, $CDCl_3$).*

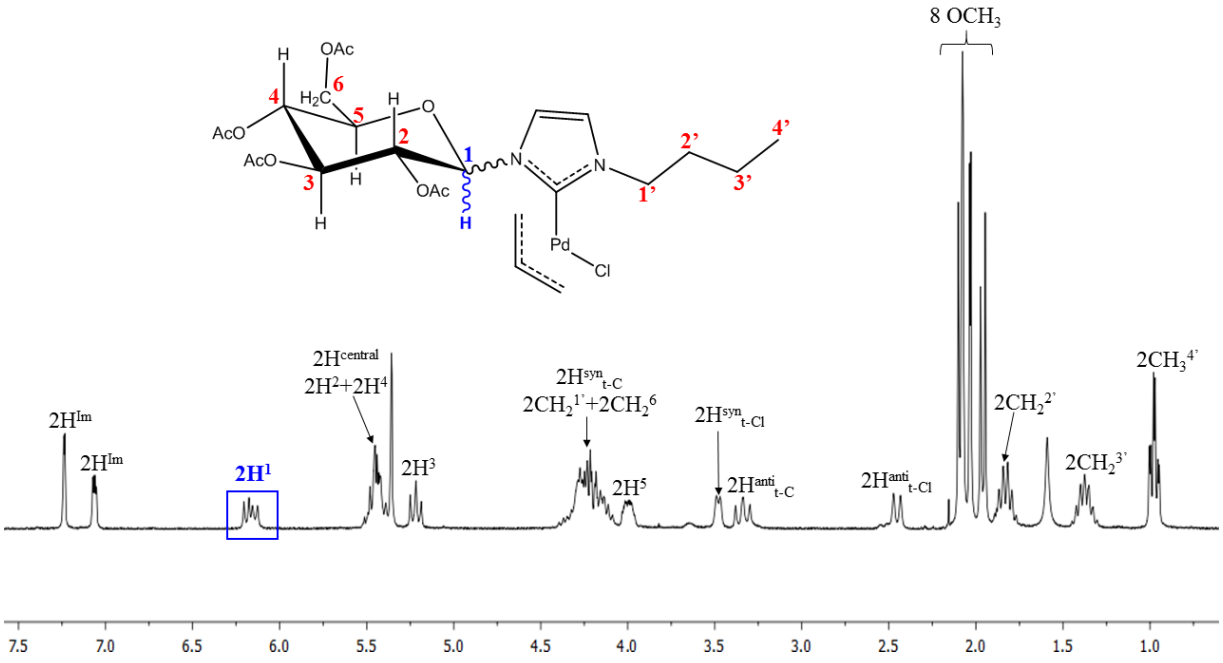

*Fig. 5.20. [1]H-NMR spectrum of the complex **56a** (T=298K, $CDCl_3$).*

The assignment of the proton signals was achieved by means of two-dimensional COSY technique (Fig. 5.21).

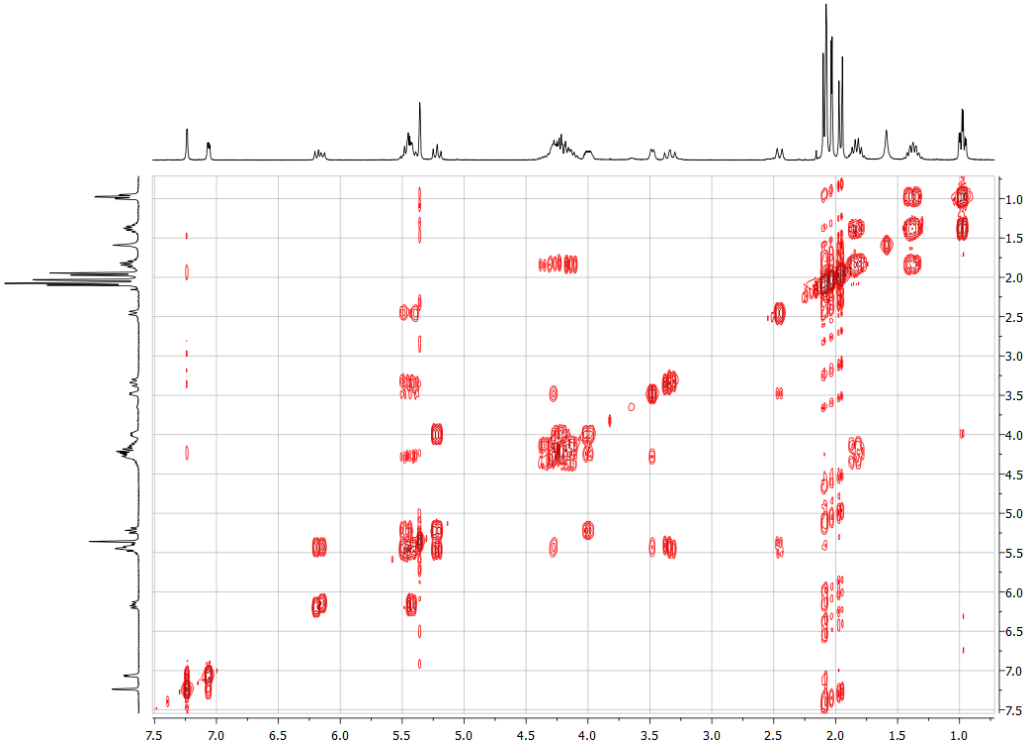

*Fig. 5.21. COSY spectrum of the complex **56a** (T=298K, $CDCl_3$)*

By means of the NOESY spectra (Fig. 5.23), using as reference the H^1 protons, it was possible to attribute the proton signals to the two different anomeric species. In particular, as shown by DFT theoretical calculations, the spatial distance between the protons H^1 and H^2 (Fig. 5.22) is different in different anomers, being of about 2.9 Å and 2.3 Å for anomer β and α, respectively. Therefore, it is possible to discriminate between anomers on the basis of the Nuclear Overhauser Effect (NOE), which is generally evident under 3 Å. Thus, the cross-peak less intense was assigned to β anomer.

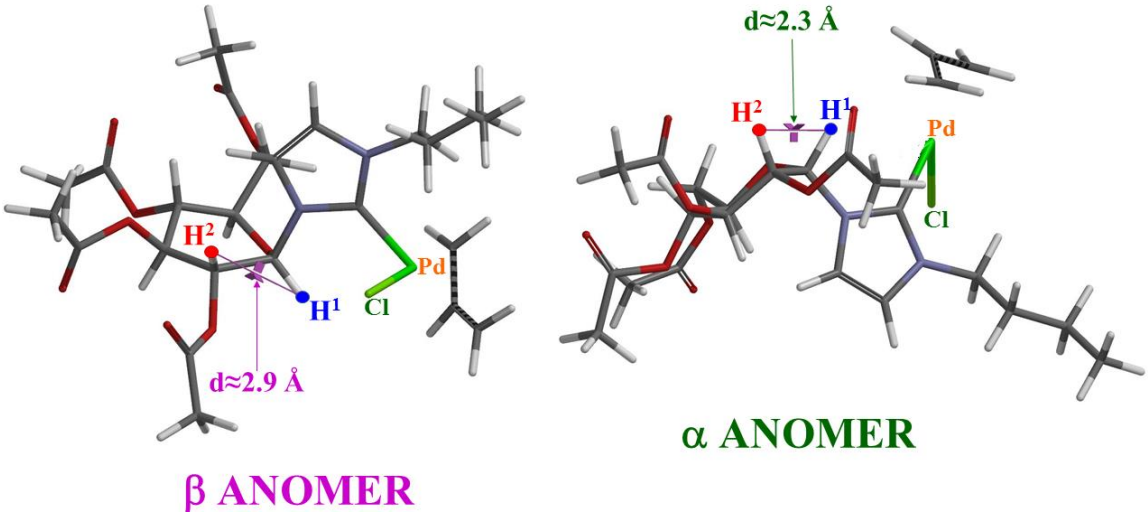

*Fig. 5.22. Representation of the two anomers of compound **56a** (DFT calculations).*

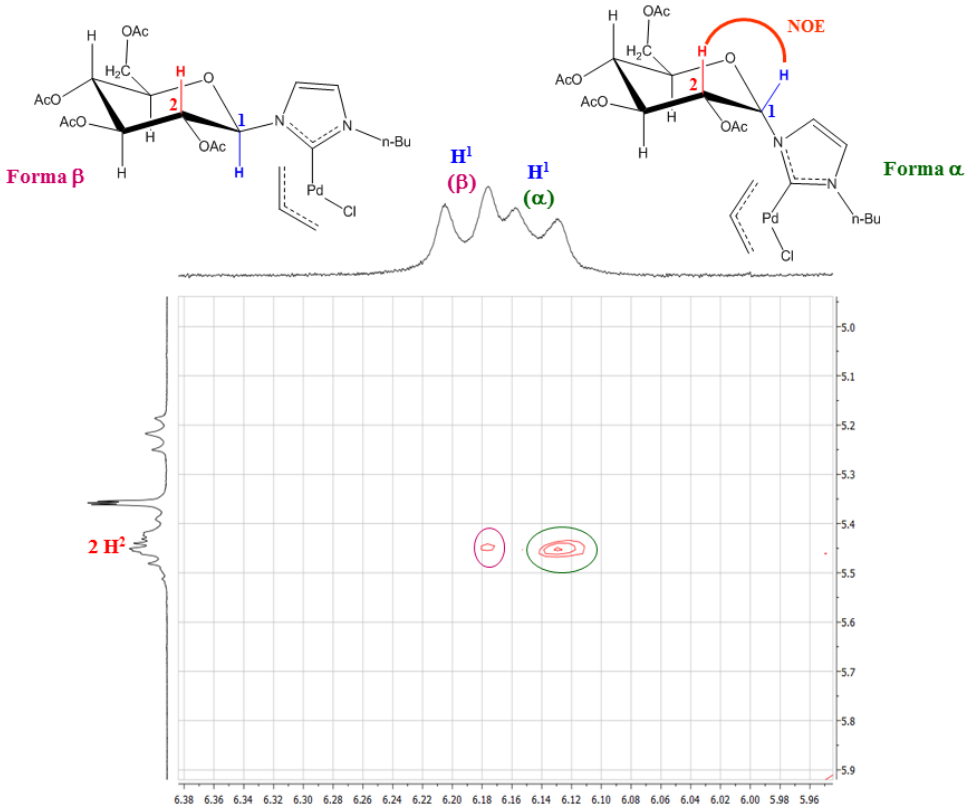

*Fig. 5.23 Relevant part of the NOESY spectrum of the complex **56a** (T=298K, $CDCl_3$).*

By recording the ^{1}H-NMR spectra at low temperature (193-233 K) it was possible to freeze the rotation about the Pd-carbene bond with the consequent visualization of the signals related to four different species, two atropoisomers (*exo* and *endo*) for each anomer (α e β) (Fig. 5.24).

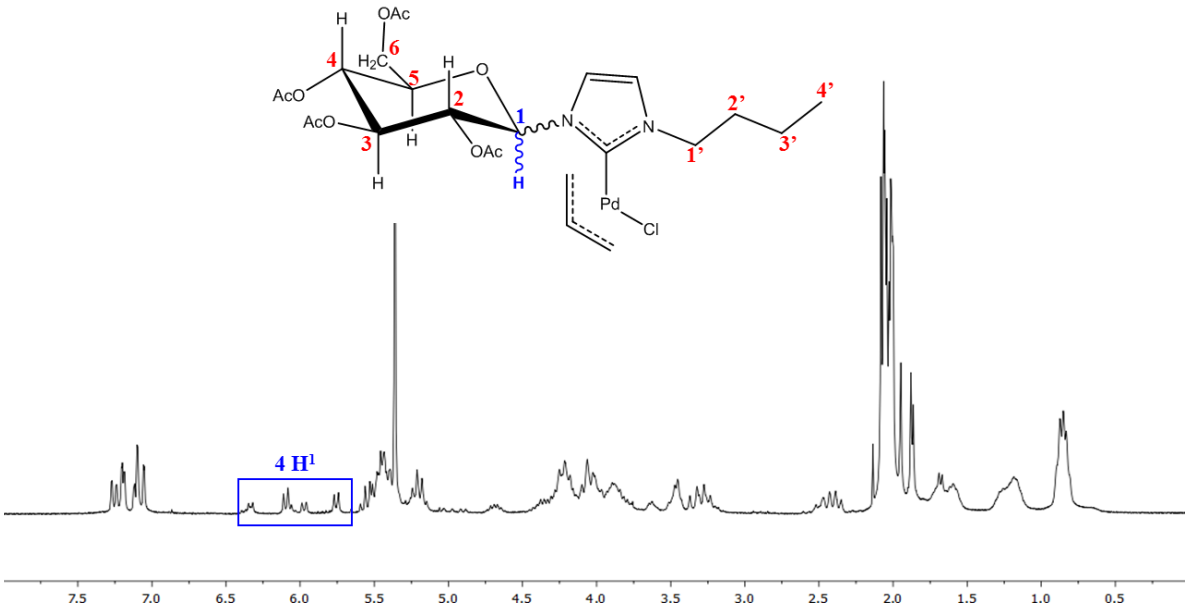

*Fig. 5.24 ^{1}H-NMR spectrum of the complex **56a** (T=193K, CD_2Cl_2).*

The two atropoisomers are distinguishable as a consequence of the mutual position of the R substituent (i.e. *n*-butyl for the compound **56a**) with respect to the central proton of the allyl group. As a matter of fact, the allyl central proton and the R group may be on the same or opposite side with respect of the main coordination plane which is identified by the palladium, the carbenic carbon and the chloride ligand. As can be seen in Fig. 5.25, atropoisomers *exo* are characterized by a reduced steric hindrance and therefore are the most abundant in solution. For instance, the ratio between the *exo* and *endo* species in complex **56a** is *exo:endo* ≈ 80/20 as can be deduced from the spectra recorded at 193K (see Fig 5.24).

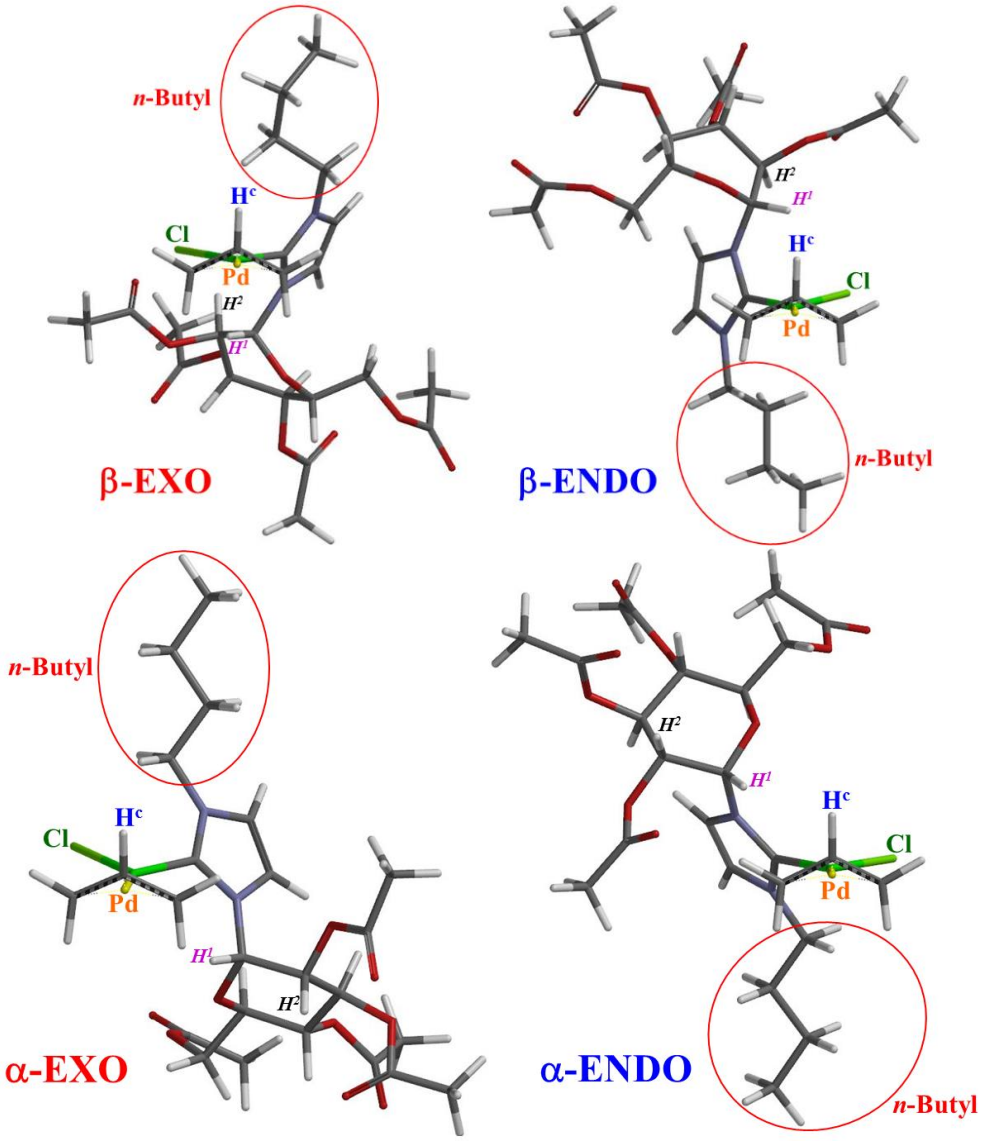

*Fig. 5.25 Representation of the four atropoisomers of the complex **56a** (DFT calculations).*

The NMR characterization was completed by the analysis of the $^{13}C\{^{1}H\}$-NMR spectra (Fig. 5.26) where, for each anomer, it is possible to observe:

- The signal of the carbenic carbon at 180-185 ppm.
- The signal of central allyl carbon at about 115 ppm.
- The signal of the allyl carbon *trans* to carbene at about 73 ppm.
- The signal of the allyl carbon *trans* to chloride at about 49 ppm.

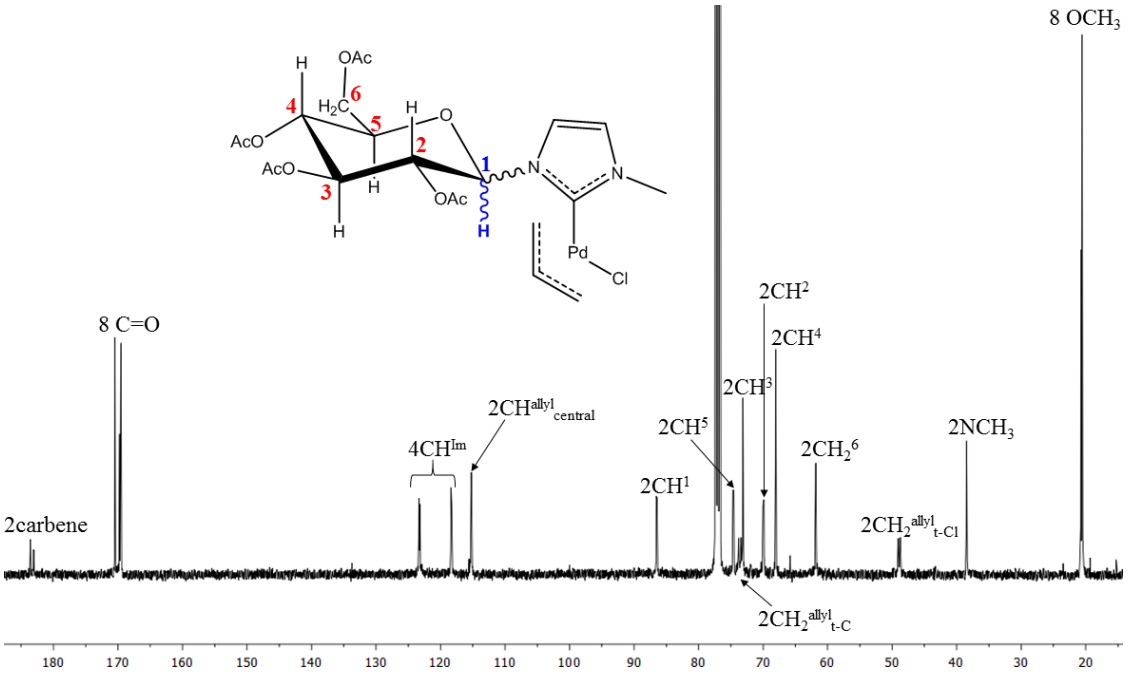

*Fig. 5.26 $^{13}C\{^{1}H\}$-NMR spectrum of the complex **56b** (T=298K, $CDCl_3$).*

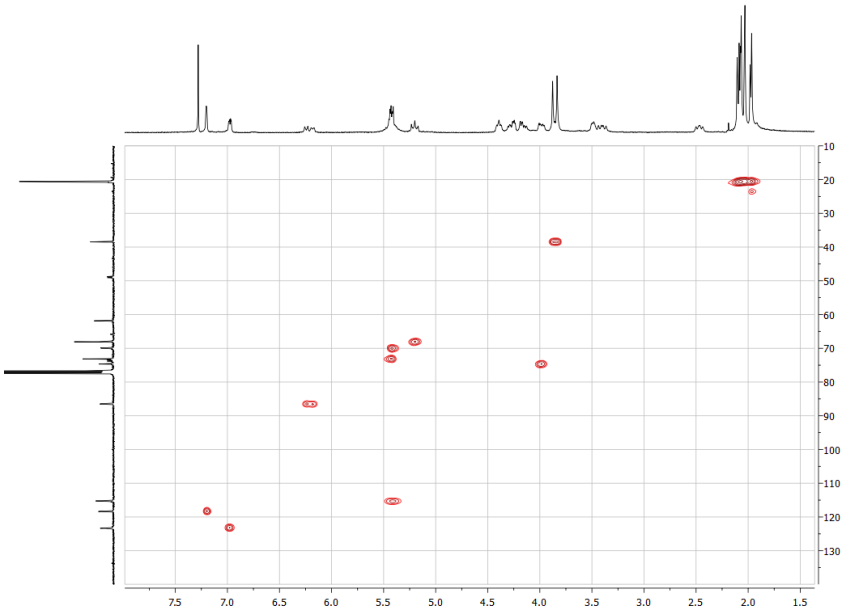

*Fig. 5.27 HSQC spectrum of the complex **56b** (T=298K, $CDCl_3$).*

5.6.2. Mixed NHC/PPh_3 η^3-allyl Pd(II) complexes

The high antiproliferative activity exerted by the allyl complexes stabilized by classic NHC ligand and triphenylphosphine (paragraph 4.7), encouraged us to synthesize compounds bearing triphenylphosphine and carbohydrate-based carbenes. We hoped to maintain similar activity against the tumour lines but to decrease the cytotoxicity generally detected versus the fibroblasts lines (healthy cells).

Therefore, the cationic complexes **69a-c** were obtained by dehalogenation with $NaClO_4$ and addition of triphenylphosphine [16] to the neutral **56a-c** allyl complexes (Scheme 5.12).

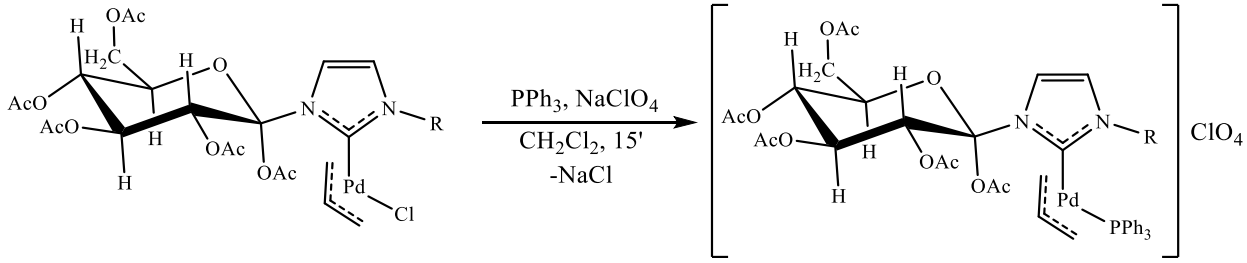

R = *n*-Bu **56a**
R = CH_3 **56b**
R = Mesy **56c**

R = *n*-Bu **69a** (83%)
R = CH_3 **69b** (85%)
R = Mesy **69c** (88%)

Scheme 5.12

The reactions were carried out by adding to a solution in dichloromethane of the complexes **56a-c**, one equivalent of PPh_3 and subsequently an excess of $NaClO_4 \cdot H_2O$ (dissolved separately in a 3:1 mixture of dichloromethane/methanol). The precipitation of NaCl attests the progress of the reaction. After the removal of the solvent, the residue was dissolved in dichloromethane and the inorganic salts filtered off on Celite filter. The final products were then easily isolated by precipitation induced by the addition of diethyl ether and *n*-hexane.

At variance with the neutral compounds **56a-c**, the presence in solution of the four different isomers (two atropoisomers for each anomer) is observed already at room temperature, since the triphenylphosphine prevents the rotation about the Pd-C bond of the NHC fragment. Therefore, in the $^{31}P\{^1H\}$-NMR spectra (Fig. 5.28) the four signals, located in a range between 25 and 27 ppm (with a $\Delta\delta \approx 30$ ppm with respect to the uncoordinated PPh_3) are always observed. From the $^{31}P\{^1H\}$-NMR spectra, it is possible to notice that the abundance of the anomeric species is more or less the same, whereas the atropoisomers present different concentration.

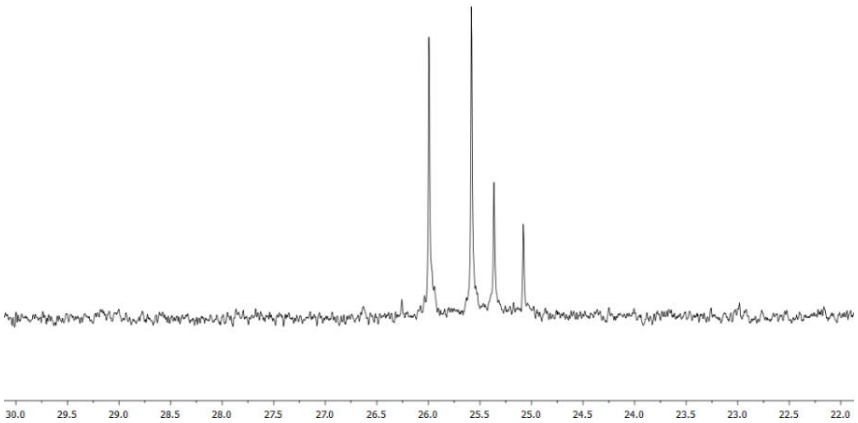

*Fig. 5.28 $^{31}P\{^{1}H\}$-NMR spectrum of the complex **69b** (T=298K, $CDCl_3$).*

In the ^{1}H-NMR spectra (Fig. 5.29), for each species, we can identify:

- The $H^{anti}_{t\text{-}C}$ signal as doublet (J ≈ 12-13 Hz) at about 3.2 ppm.
- The $H^{anti}_{t\text{-}P}$ signal as multiplet at about 3.4-3.6 ppm.
- The $H^{syn}_{t\text{-}C}$ signal as doublet (J ≈ 3-4 Hz) at 3.6-3.8 ppm.
- The $H^{syn}_{t\text{-}P}$ signal as multiplet between 4.0 and 4.4 ppm.
- The $H^{central}$ signal as multiplet at about 5.8-6.0 ppm.

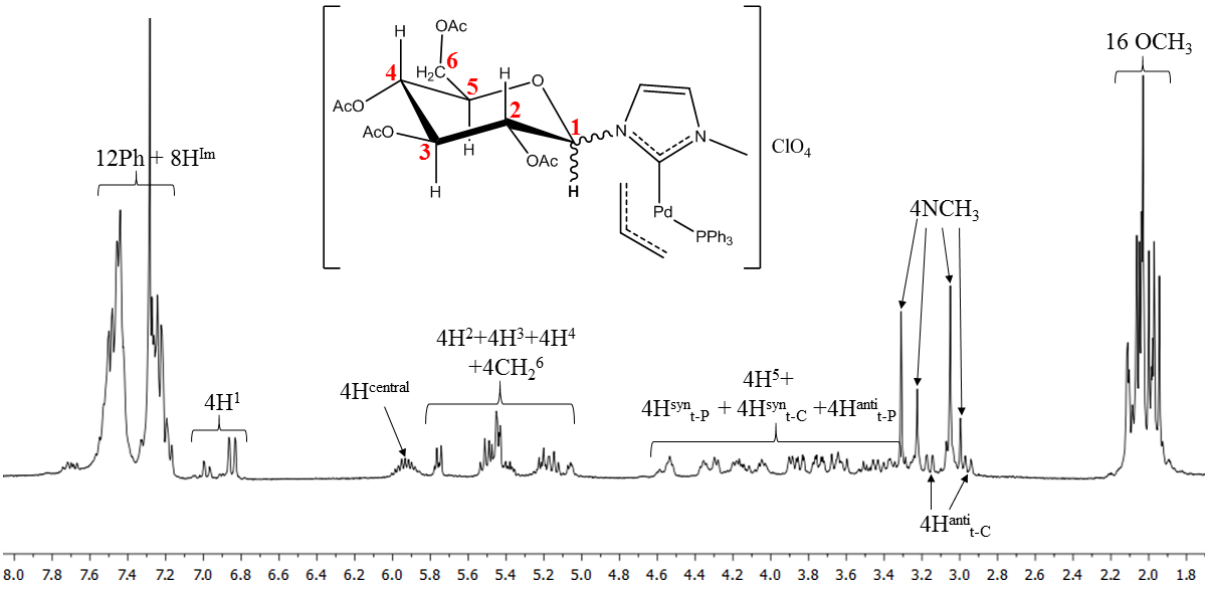

*Fig. 5.29 ^{1}H-NMR spectrum of the complex **69b** (T=298K, $CDCl_3$).*

In the $^{13}C\{^1H\}$-NMR spectra (Fig. 5.30), for each isomer, we can observe:

- At about 180 ppm the signal ascribable to the carbenic carbon, resonating as a doublet ($J_{CP} \approx$ 20 Hz).
- A doublet ($J_{CP} \approx$ 25-30 Hz) at about 69 ppm related to the CH_2 allyl *trans* to the phosphine.
- A singlet at about 74 ppm related to the CH_2 allyl *trans* to the carbene.
- A singlet, at about 120-125 ppm, related to the central allyl carbon.

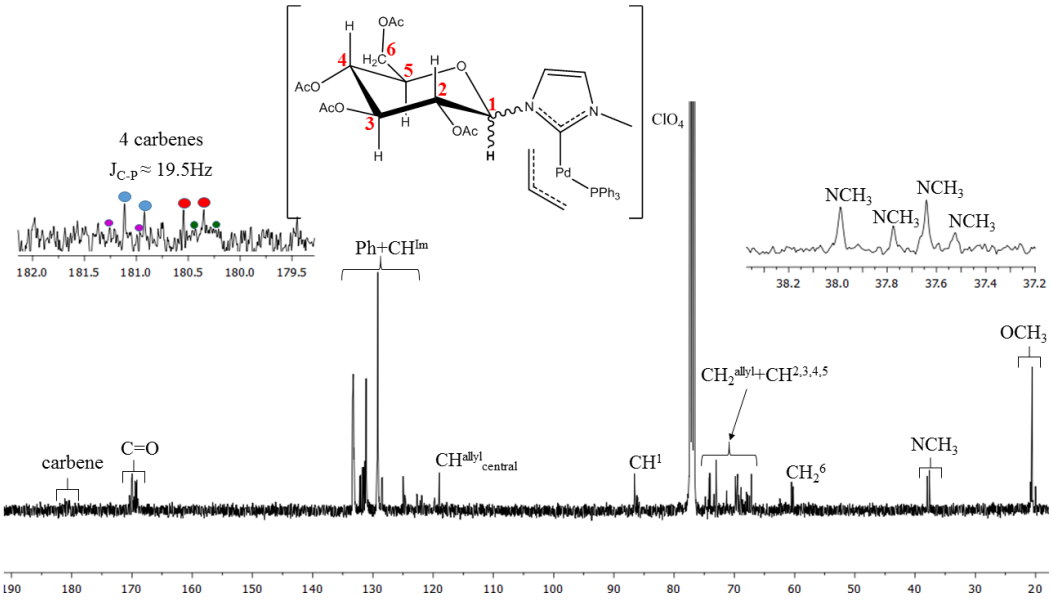

*Fig. 5.30 $^{13}C\{^1H\}$-NMR spectrum of the complex **69b** (T=298K, $CDCl_3$).*

In the IR spectra (Fig. 5.31), the C=O and C-O stretching at about 1750 and 1231 cm^{-1} are respectively observed, whereas the Cl-O stretching of the perchlorate counterion is detected at approximately 1100 cm^{-1}.

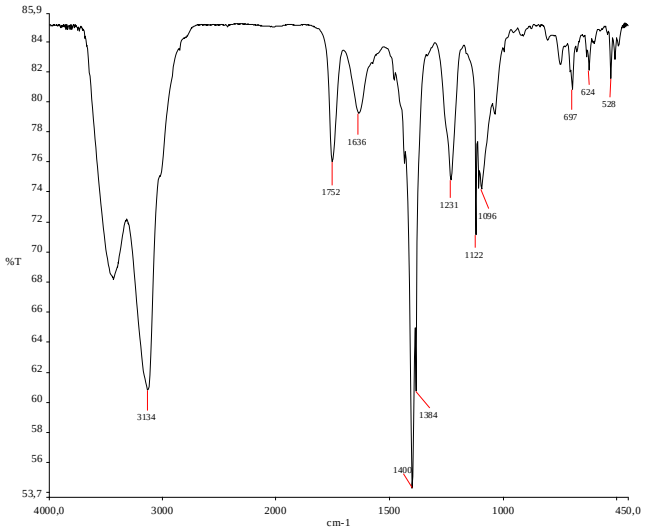

*Fig. 5.31 IR spectrum (in KBr) of the complex **69b.***

5.7. Mixed NHC/PPh_3 palladacyclopentadienyl complexes

The mixed compounds **45a-c** were synthesized in good yields by reacting, in dichloromethane at room temperature, the $[PdC_4(COOCH_3)_4]_n$ precursor, one equivalent of PPh_3 and one equivalent of the Ag (I) complexes **38a-c** (Scheme 5.13).

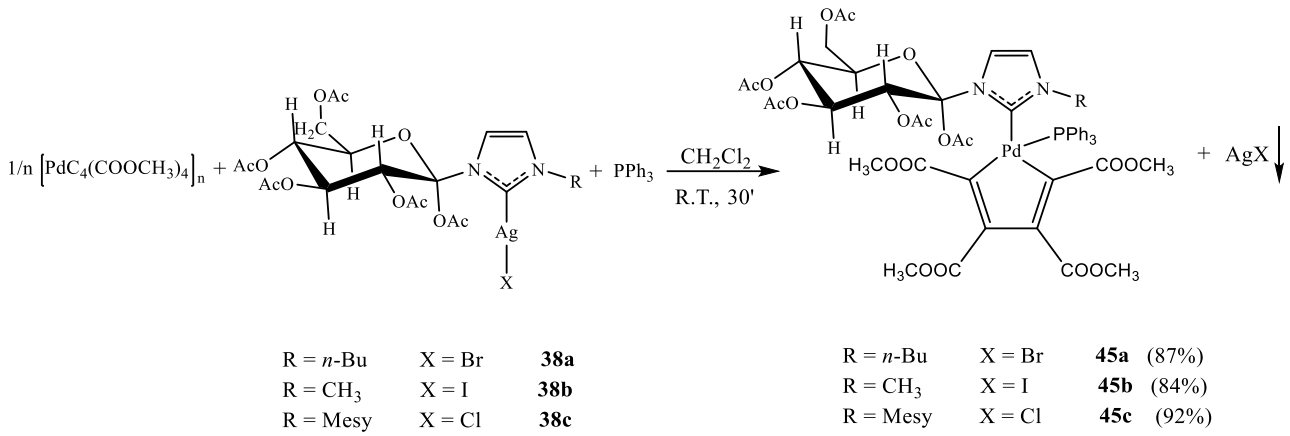

Scheme 5.13

The products were isolated, after the removal of the silver halide, by precipitation with diethylether and *n*-hexane. The ensuing complexes (**45a-c**), analyzed by NMR and IR spectroscopy, always formed a mixture of two different anomers (α and β). It is worth noting that, on the contrary of the mixed NHC/PPh_3 allyl complexes, in this case a potential hindered rotation around the Pd-carbene bond should not produce atropoisomers, being the palladacyclopentadienyl fragment symmetric with respect to the main coordination plane.

Consistently, in the $^{31}P\{^1H\}$-NMR spectra (Fig. 5.32) the presence of two singlets related to the triphenylphosphine coordinated to two different anomers, is detected. As can be seen, the mentioned singlets have a comparable intensity and resonate within the 24-26 ppm range.

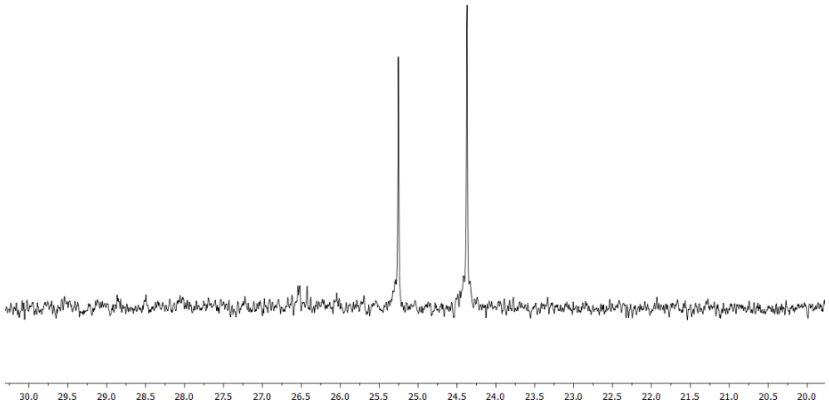

*Fig. 5.32 $^{31}P\{^1H\}$-NMR spectrum of the complex **45b** (T=298K, $CDCl_3$).*

In the ^{1}H-NMR spectra (Fig. 5.33), beside the signals of the carbenic substituents (*n*-Bu, Me or Mesityl), we observe for each anomer:

- Four different OCH_3 singlets at about 2 ppm ascribable to the acetyl groups present in the glycosidic substituent.
- Four different singlets within 2.5 and 4 ppm assigned to the OCH_3 of the palladacyclopentadienyl fragment.
- The signals ascribable to the CH and CH_2 of the glycosidic protons within 3 and 6.5 ppm.

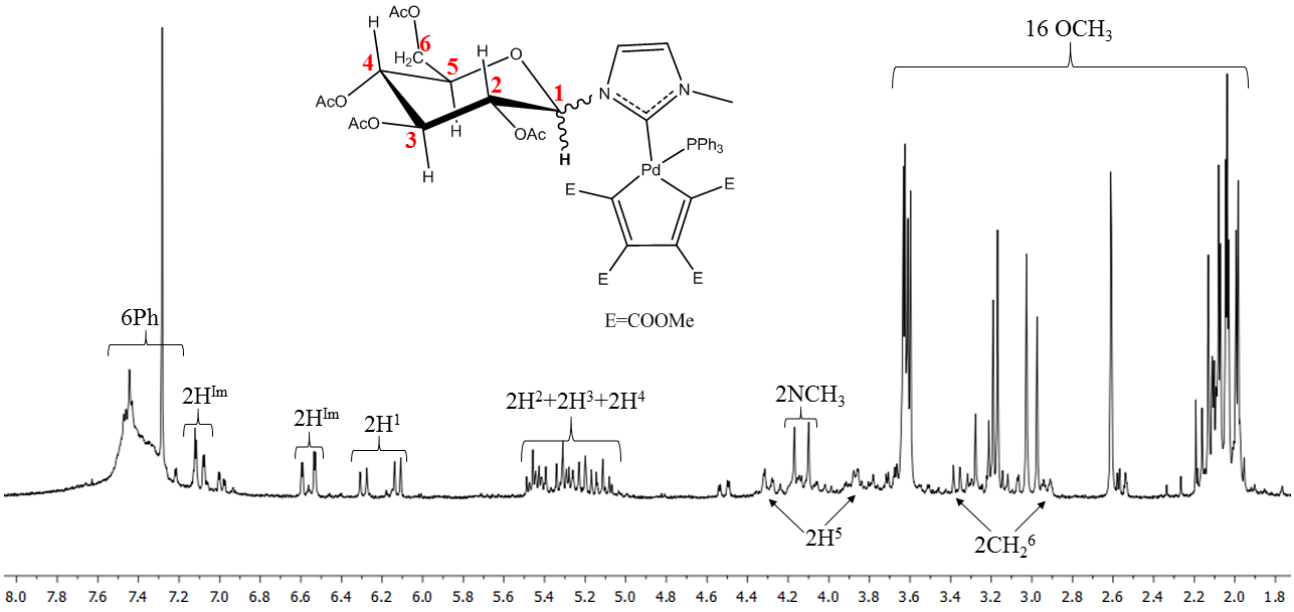

*Fig. 5.33 ^{1}H-NMR spectrum of the complex **45b** (T = 298 K, $CDCl_3$).*

In the ^{13}C{^{1}H}-NMR spectra (Fig. 5.34), recorded at 243 K (owing to the partial decomposition of the complexes at RT), we observe:

- The OCH_3 signals of the glycosidic fragment at about 20 ppm.
- The OCH_3 signals of the palladacyclopentadienyl fragment at about 50 ppm.
- The carbonyl signals, related to both the glycosidic fragment and palladacycle, at about 170 ppm.
- The typical signal of the coordinated carbene carbon at about 182 ppm, resonating as a doublet due to the J^2 coupling with the phosphorus of the triphenylphosphine ($J_{C\text{-}P} \approx 20$ Hz).

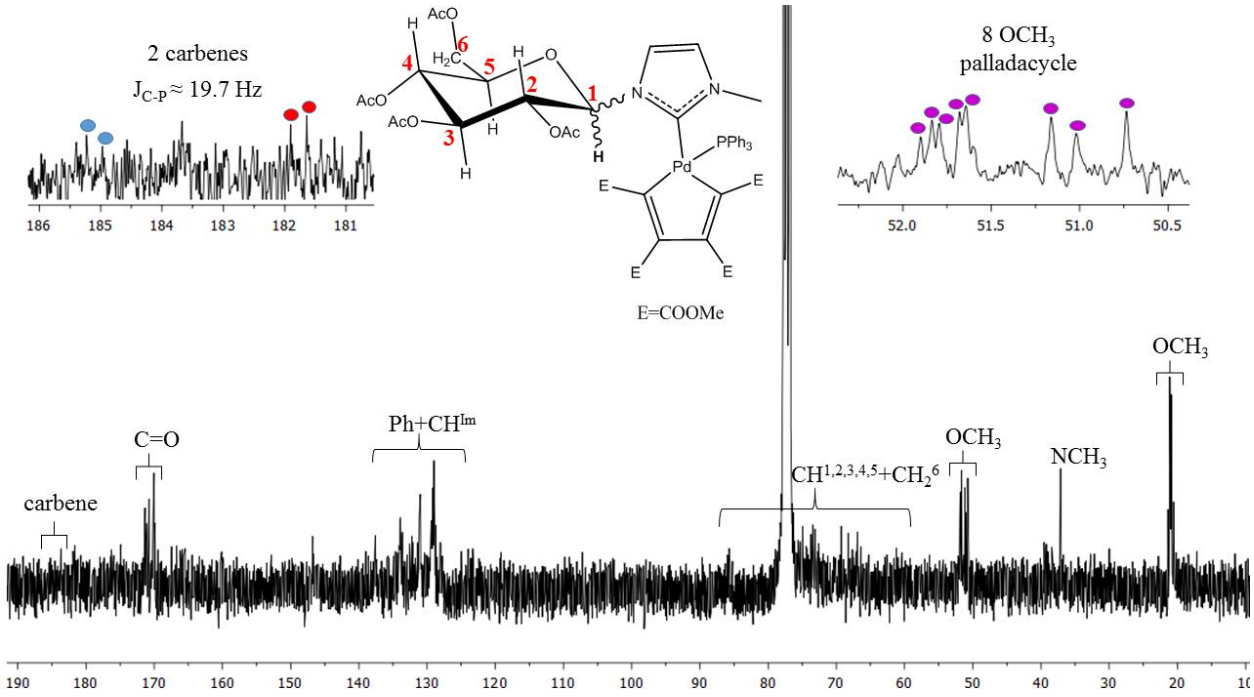

*Fig. 5.34 $^{13}C\{^1H\}$-NMR spectrum of the complex **45b** (T=298K, $CDCl_3$).*

5.8. Antiproliferative activity: preliminary results

The antiproliferative activity of the allyl compounds bearing a carbohydrate-based NHC and PPh_3 was preliminary analyzed on A2780 line and on MRC-5 fibroblasts. The results for compound **69c** are reported in table 5.1 (the triplicated data are not yet available for the remaining compounds).

COMPLEX	**IC_{50} (μM)**	
	A2780	**MRC-5**
Cisplatin	0.81 ± 0.06	14 ± 1
69c	0.31 ± 0.03	3.9 ± 0.2

Table 5.1

As reported in Table 5.1, compound **69c** is more active than cisplatin on the A2780 cancer line. Furthermore, a slight selectivity of action emerges analysing the data on fibroblasts. The IC_{50} value determined for healthy cells is one order of magnitude higher compared to the A2780 line.
Anyway, in order to accurately evaluate the selectivity of these species and therefore the possible presence of the Warburg effect, as stressed in the numerous works concerning this phenomenon [5-9], it will be necessary to await the results of the *in vivo* tests.

5.9. Conclusions

In this chapter a synthetic protocol for the synthesis of novel Pd (II) allyl and palladacyclopentadienyl complexes containing carbohydrate-based NHC ligands has been proposed.
In particular, the stable cationic species **69a-c** (mixed NHC/PPh_3 complexes), were obtained from the neutral allyl complexes **56a-c.**
These compounds were synthesized as a mixture of four isomers, due to the anomerization (presence of alpha and beta isomers) and the hindered rotation around the Pd-carbene bond (formation of atropoisomers).
The antiproliferative activity of these compounds toward the A2780 ovarian cancer line showed, in the preliminary results (compound **69c**), a better activity compared to cisplatin. Furthermore, this species has a slight selectivity toward cancer cells compared to healthy cells. In order to better evaluate the degree of selectivity of this class of compounds, also based on the well-known Warburg effect, *in vivo* studies will be carried out in the future.

5.10. References

[1] D. L. Nelson, M. M. Cox, *Lehninger Principles of Biochemistry*, W. H. Freeman & Co., 6th edn, 2012, 243-274.

[2] M. Miljkovic', *Carbohydrates: Synthesis, mechanisms and stereoelectronic effects*, Springer, 2009, 1-109.

[3] E. Fischer, *Chemische Berichte*, 1891, **24**, 2683.

[4] (a) E. Pacsu, *Chemische Berichte*, 1928, **61**, 1508; (b) B. Lindberg, *Arkiv Kemi, Mineral. Geol. Ser. B*, 1944, **18** (9), 1.

[5] M.G. Vander Heiden, L.C. Cantley, C.B. Thompson, *Science*, 2009, **324**, 1029.

[6] (a) O. Warburg, *Science*, 1956, **123**, 309; (b) M.V. Liberti, J.W. Locasale, *Trends in Biochemical Sciences*, 2016, **41** (3), 211; (c) J.S. Bertram, *Molecular Aspects of Medicine*, 2001, **21**, 167.

[7] (a) M.E. Phelps, *PET: physics, instrumentation, and scanners*, Springer, 2006, 8–10; (b) H. Young, R. Baum, U. Cremerius, *European Journal of Cancer*, 1999, **35** (13), 1773.

[8] (a) W.O. Foye, T.L. Lemke, D.A. Williams, *Foye's principles of medicinal chemistry*, Lippincott Williams & Wilkins, 6th edn, 2008, 989.

[9] (a) A.G. Cox, K.K. Brown, E.S.J. Arner, M.B. Hampton, *Biochemical Pharmacology*, 2008, **76**, 1097; (b) K. Becker, S. Gromer, R.H. Schirmer, S. Müller, *European Journal of Biochemistry*, 2000, **267**, 6118; (c) T. Sandalova, L. Zhong, Y. Lindqvist, A. Holmgren, G. Schneider, *Proceedings of the National Academy of Sciences U.S.A.*, 2001, **98**, 9533; (d) A. Bindoli, M. P. Rigobello, G. Scutari, C. Gabbiani, A. Casini, L. Messori, *Coord. Chem. Rev.*, 2009, **253**, 1692; (e) A. Casini, C. Gabbiani, F. Sorrentino, M. P. Rigobello, A. Bindoli, T. J. Geldbach, A. Marrone, N. Re, C. G. Hartinger, P. J. Dyson, L. Messori, *J. Med. Chem.*, 2008, **51**, 6773; (f) A. Casini, L. Messori, *Current Topics in Medicinal Chemistry*, 2011, **11**, 2647, (g) C. Gabbiani, G. Mastrobuoni, F. Sorrentino, B. Dani, M.P. Rigobello, A. Bindoli, M.A. Cinellu, G. Pieraccini, L. Messori, A. Casini, *Med. Chem. Comm.*, 2011, **2**, 50.

[10] https://clinicaltrials.gov/ct2/show/NCT01747798.

[11] (a) F. Tewes, A. Schlecker, K. Harms, F. Glorius, *J. Organomet. Chem.*, 2007, **692**, 4593; (b) C. Yang, P. Lin, F. Liu, I.J.B. Lin, *Organometallics*, 2010, **29**, 5959; (c) M. Tanaka, H. Kataoka, S. Yano, H. Ohi, K. Kawamoto, T. Shibahara, T. Mizoshita, Y. Mori, S. Tanida, T. Kamiya, T. Joh, *BMC Cancer*, 2013, **13**, 327.

[12] M. Hunsen, D.A. Long, C.R. D'Ardenne, A.L. Smith, *Carbohydr. Res.*, 2005, **340**, 2670.

[13] Z. Zhou, J. Qiu, L. Xie, F. Du, G. Xu, Y. Xie, Q. Ling, *Catal. Lett.*, 2014, **144**, 1911.

[14] F. Tewes, A. Schlecker, K. Harms, F. Glorius, *J. Organomet. Chem.*, 2007, **692**, 4593.

[15] T. Nishioka, T. Shibata, I. Kinoshita, *Organometallics*, 2007, **26**, 1126.

[16] L. Canovese, F. Visentin, T. Scattolin, C. Santo, V. Bertolasi, *Polyhedron*, 2016, **119**, 377.

[17] L. Canovese, C. Santo, T. Scattolin, F. Visentin, V. Bertolasi, J. *Organomet. Chem.*, 2015, **794**, 288.

6

Pd(II) complexes bearing *N*-Trifluoromethyl NHCs

The last class of compounds which has been synthesized and studied under its antiproliferative activity, is constituted by η^3-allyl palladium complexes stabilized by *N*-trifluoromethyl NHC ligands. The synthesis of such compounds was carried out during the Ph.D. period spent at the Polytechnic of Zurich (ETH Zurich) under the supervision of prof. Antonio Togni.

CF_3 is a very important group under pharmacological aspect and interesting from the electronic point of view owing to its strong electron-withdrawing nature, promoting remarkable π-backdonation when present as a substituent in the NHC ligands. In this chapter we will discuss how to insert the CF_3 group into our molecules following a protocol recently developed by the group of prof. Togni.

In particular, it was decided to synthesize the mixed NHC/PPh_3 and NHC/PTA complexes, which have already given excellent biological results as shown in the previous chapters.

The figure proposed at the beginning of the chapter is related to this source: http://www.1zoom.me/en/wallpaper/455190/z6781/

6.1. Introduction

This section will give an overview on *i)* the importance of the CF_3 in compounds of pharmaceutical interest, *ii)* the main processes of insertion of this group into the molecules of interest (trifluoromethylation reactions) and finally *iii)* the characteristics acquired by the carbene fragment bearing this kind of substituent.

6.1.1. Trifluoromethyl and polyfluorinated groups in medicinal chemistry

The importance of fluorine and polyfluorinated groups in medicinal chemistry is highlighted by a large number of published articles on this topic and also by commercially available drugs and biologically active compounds containing at least one fluorine atom [1, 2].

Although fluorine represents the most abundant halogen on earth, only a dozen fluorinated organic compounds have been identified in nature [3].

The introduction of fluorine-containing groups into organic molecules significantly changes the chemical, physical and biological properties of these species. For these reasons organofluorine structures have received much interest in medicinal, pharmaceutical, agricultural chemistry and material sciences [1b].

As an example, we report 8 drugs bearing the CF_3 group, among the 200 most successful, available on the market (US, 2012) (Fig. 6.1).

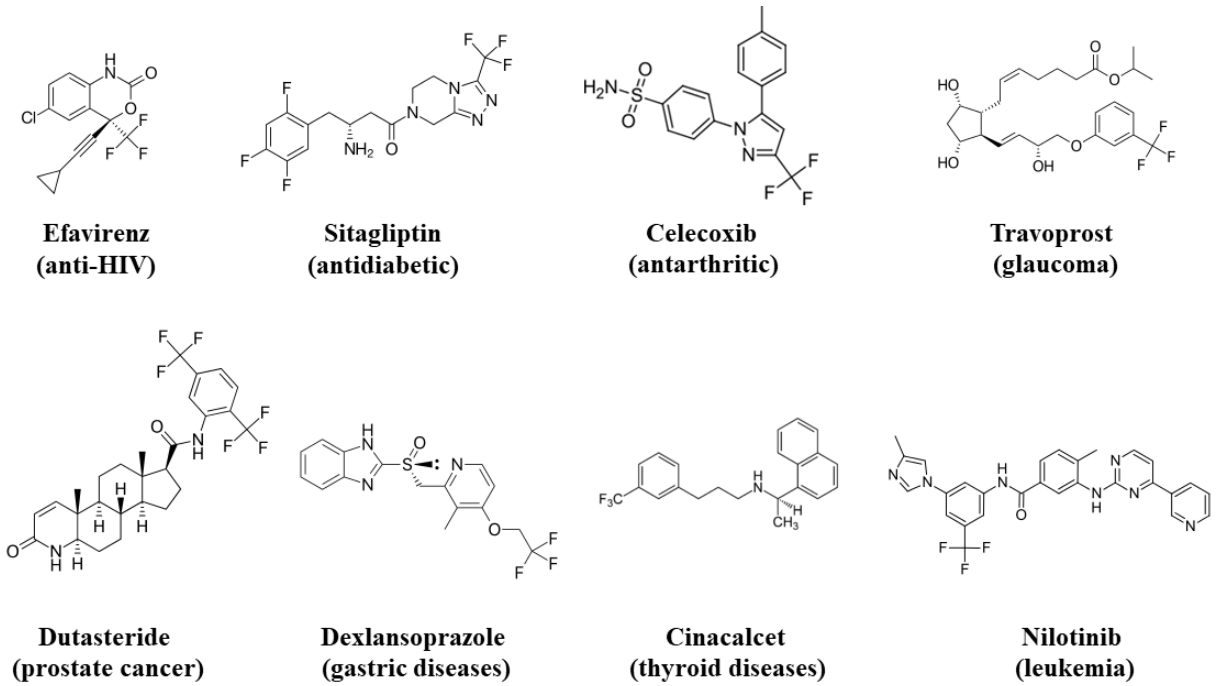

Fig. 6.1

Furthermore, the interest has also been focused on the OCF_3 and SCF_3 groups, which have very similar properties than CF_3 [4].

The effect of fluorine on the lipophilicity of compounds mainly depends on the number of fluorine atoms inserted and on their position in the molecule. For instance, fluorination of aromatic rings considerably increases the lipophilicity of the derivatives [5].

Table 6.1 shows the influence on the Hansch-Leo hydrophobic parameter π, derived from the octanol/water partition coefficients P_X and P_H, of different groups on the generic C_6F_5X compound [6].

Hydrophobic parameter [π_X= log(P_X/P_H) (octanol/water)] for C_6F_5X compounds			
X	**π_X**	**X**	**π_X**
OH	-0.67	SCH_3	0.61
F	0.14	SCF_3	1.44
CH_3	0.56	CH_3CO	0.02
CF_3	0.88	CF_3CO	0.55
OCH_3	-0.02	CH_3SO_2	-1.63
OCF_3	1.04	CF_3SO_2	0.55

Table 6.1 [5]

Moreover, the perfluorinated groups confer a remarkable stability to their derived systems, owing to the strength of the C-F bond. For instance, chloride or methyl groups can undergo metabolic oxidation whereas the CF_3 group and analogues are stable toward this type of degradation and therefore used as valid alternative (bioisostere groups) [7].

Recently, thanks to the ^{19}F-NMR spectroscopy it was possible to study the affinity of some libraries of fluorinated compounds toward particular regions of target receptors, eventually suggesting the drugs design once the main receptor was individuated [8].

The interest toward the perfluorinated substituents and in particular for the CF_3 group is also the result of numerous methods currently available for their introduction into the systems of interest as will be illustrated in the following paragraph.

6.1.2. Synthetic methodologies for the introduction of the trifluoromethyl group

The first method describing the insertion of a CF_3 group into an organic molecule is attributed to Frédéric Swarts, that in 1892 published the reaction between trichlorophenylmethane and SbF_3 (subsequently replaced by HF in the 1930s) to give $PhCF_2Cl$ and $PhCF_3$ [9]. The reaction between CF_3I and iodobenzene in the presence of copper, was instead the first example reported in the literature of a stoichiometric coupling (McLoughlin-Thrower, 1968, see Scheme 6.1) [10].

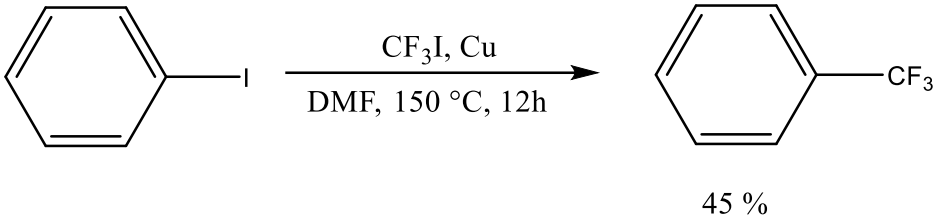

Scheme 6.1

Later, the first catalytic coupling between iodoarenes, trifluoroethylsilane, copper iodide (0.1 eq) and 1.10-phenanthroline was published by Oishi and co-workers in 2009 (Scheme 6.2) [11].

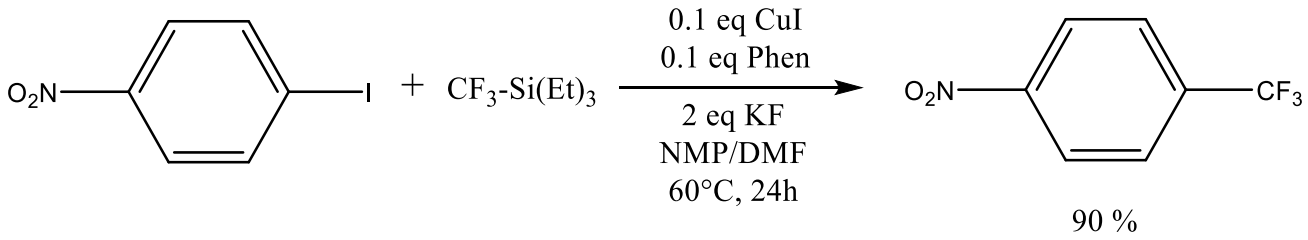

Scheme 6.2

The palladium-catalysed process in which aryl halides and (trifluoromethyl)triethylsilane were reacted in the presence of the dimeric species $[Pd(\mu\text{-}Cl)(\eta^3\text{-allyl})]_2$ was later published [12].
It is now important to remind that the trifluoromethylation reactions can be divided into three broad categories:

- Radical trifluoromethylations.
- Nucleophilic trifluoromethylations.
- Electrophilic trifluoromethylations.

In the radical trifluoromethylations the formation of the free trifluoromethyl radical [13] is the key step and such a species is much more reactive than the methyl radical [14]. One typical reagent is represented by the CF_3I/triethylborane combination (Scheme 6.3) [15].

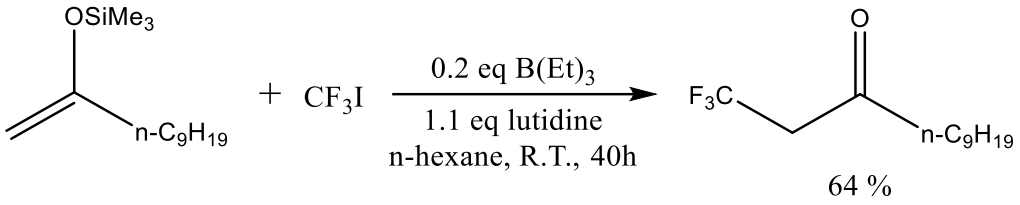

Scheme 6.3

More recently, other processes have been developed for the production of radicals similar to CF_3 as for instance OCF_3 (trifluoromethoxylation reaction, see Scheme 6.4) [4b].

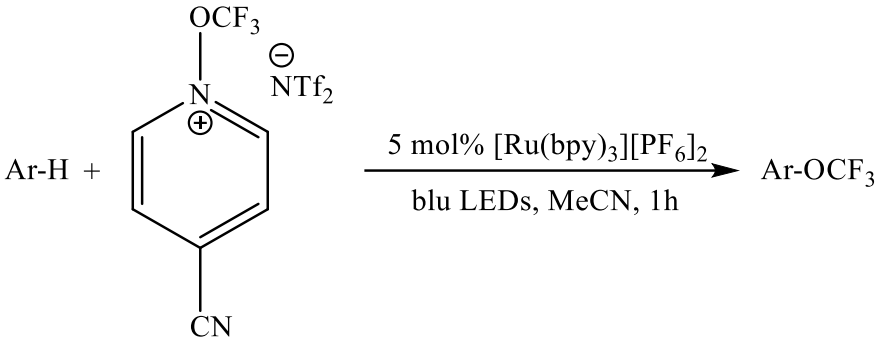

Scheme 6.4

In the nucleophilic trifluoromethylation processes the active species is the CF_3^- anion, which is a very reactive species, and hence this type of process can be often difficult. This anion was isolated with the $[K(18\text{-crown-6})]^+$ counterion from Prakash and co-workers [16]. An example of nucleophilic trifluoromethylation characterized by CF_3Cu as intermediate is reported below (Scheme 6.5) [17].

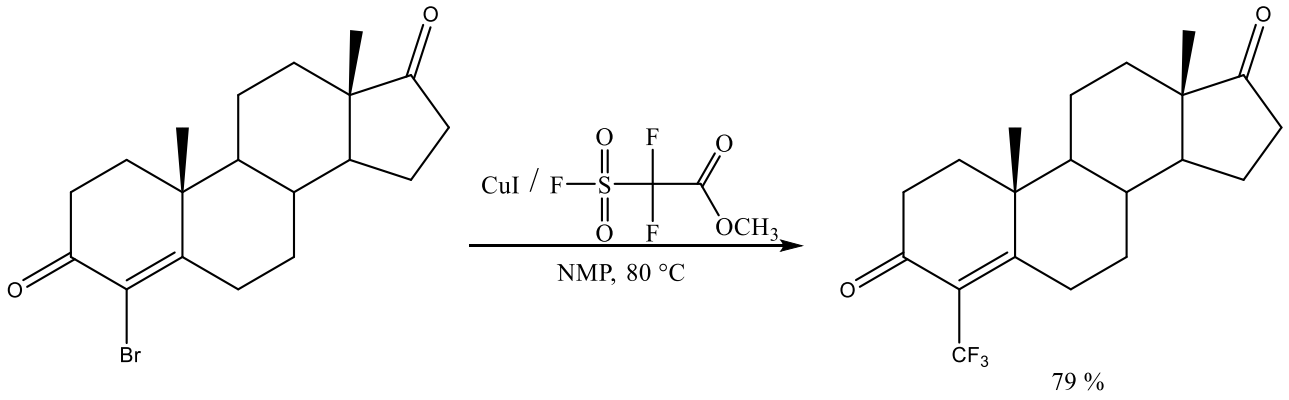

Scheme 6.5

In the electrophilic trifluoromethylations the key step is the extremely difficult production of the CF_3^+ cation.

The first reagent used in this aim was the diaryl(trifluoromethyl)sulfonium salt [Ar_2SCF_3] [SbF_6], and its application for the functionalization of thiophenolates was exposed in detail in 1984 (Fig. 6.2) [18]. Analogous reagents with the sulphur replaced by oxygen, selenium or tellurium are also available [19].

For this broad category of reagents anilines, pyridines and triphenylphosphine were examined as substrates.

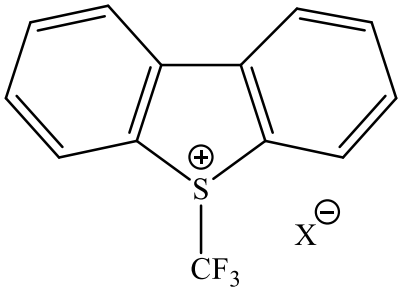

X = OTf, BF_4

Fig. 6.2

A second important category of trifluoromethyl donors is represented by hypervalent iodine (III)-CF_3 reagents, firstly published by Togni and co-workers [20]. This sort of reagents has been used with a huge number of substrates, among them thiols [20a], alcohols [20a], phosphines [20a], arenes and (hetero) arenes [21], unactivated olefins [22] and unsaturated carboxylic acids [23], are worthy of mention.

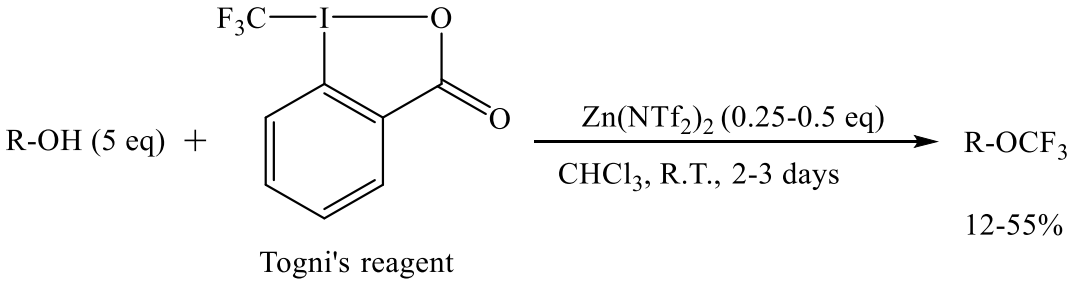

Scheme 6.6 [20a]

For both the electrophilic and nucleophilic trifluoromethylations, some examples of enantioselective processes are known. One of these processes proposed by Allen and co-workers is reported below (Scheme 6.7) [24].

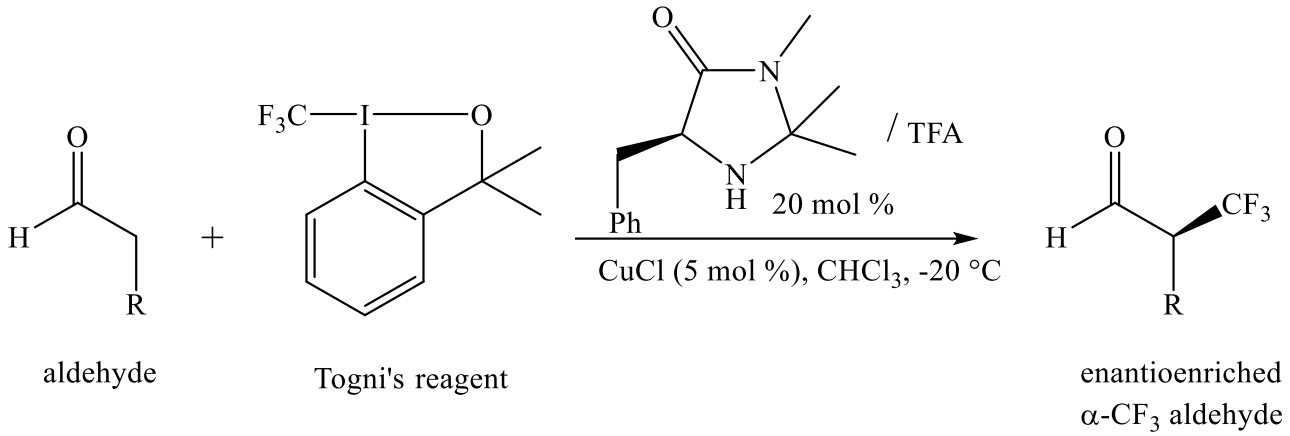

Scheme 6.7 [24e]

6.1.3. *N*-Trifluoromethyl NHC ligands

This last introductory section will show and discuss the main characteristics of *N*-Heterocyclic Carbenes functionalized with the CF_3 group (*N*-trifluoromethyl NHCs).

As reported in the introductory section concerning the *N*-Heterocyclic Carbene ligands (section 1.4), their success, in the field of catalysis, is due to their excellent σ-electron donating properties, which leads to the formation of very strong metal-carbene bonds, thereby increasing the stability and activity of the catalysts [25]. Recent works have however demonstrated the catalytic importance of the π-backdonation, which can be increased by using electron-withdrawing groups as substituent at the nitrogen [26]. For instance, a great π-backdonation renders the metal more electron-deficient and makes processes such as π-acid catalysed cyclizations easier [27].

An excellent example is the work by Alcarazo et al. where, by tuning the π-acceptor properties of the NHCs, they were able to selectively modulate the result of three distinct gold (I)-catalysed processes [28].

From a theoretical point of view, Gusev and co-workers were able to calculate by DFT simulations, the Tolman electronic parameter (TEP) related to different NHC ligands in the $[Ni(CO)_3(NHC)]$ complexes taken as a model [29]. The study also examined ligands not synthesized yet, such as N-bistrifluoromethyl NHC $ImN(CF_3)_2$ (Fig 6.3).

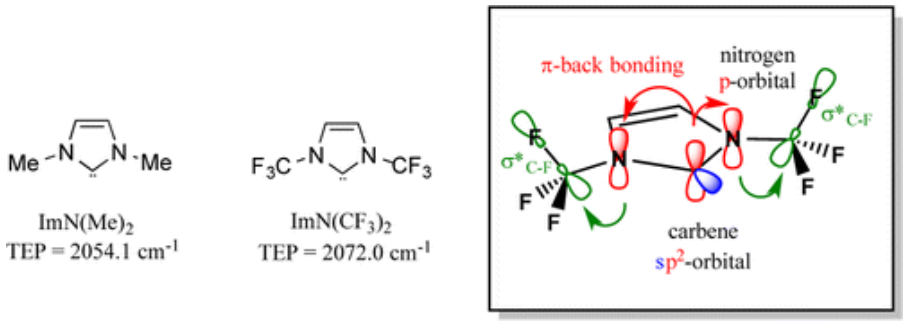

Fig. 6.3

These studies have shown that this ligand is a significantly weaker donor than the *N*-methyl analogue ($ImN(Me)_2$). As a matter of fact, there is a partial donation of electron density from the lone pairs of the nitrogen atoms to the $\sigma^*_{C\text{-}F}$ antibonding orbital, which decreases the π-donation of the nitrogen atoms to the empty p_π orbital of the carbenic carbon.

Togni and co-workers published in 2015 the first example of complexes with *N*-trifluoromethyl NHC ligands [30] obtained from trifluorobenzimidazole, which is synthesized on a large scale by electrophilic *N*-trifluoromethylation of benzimidazole [20a, 31]. The latter can be finally functionalized by alkyl or aryl groups, to give the corresponding imidazolium salts (Scheme 6.8) [30].

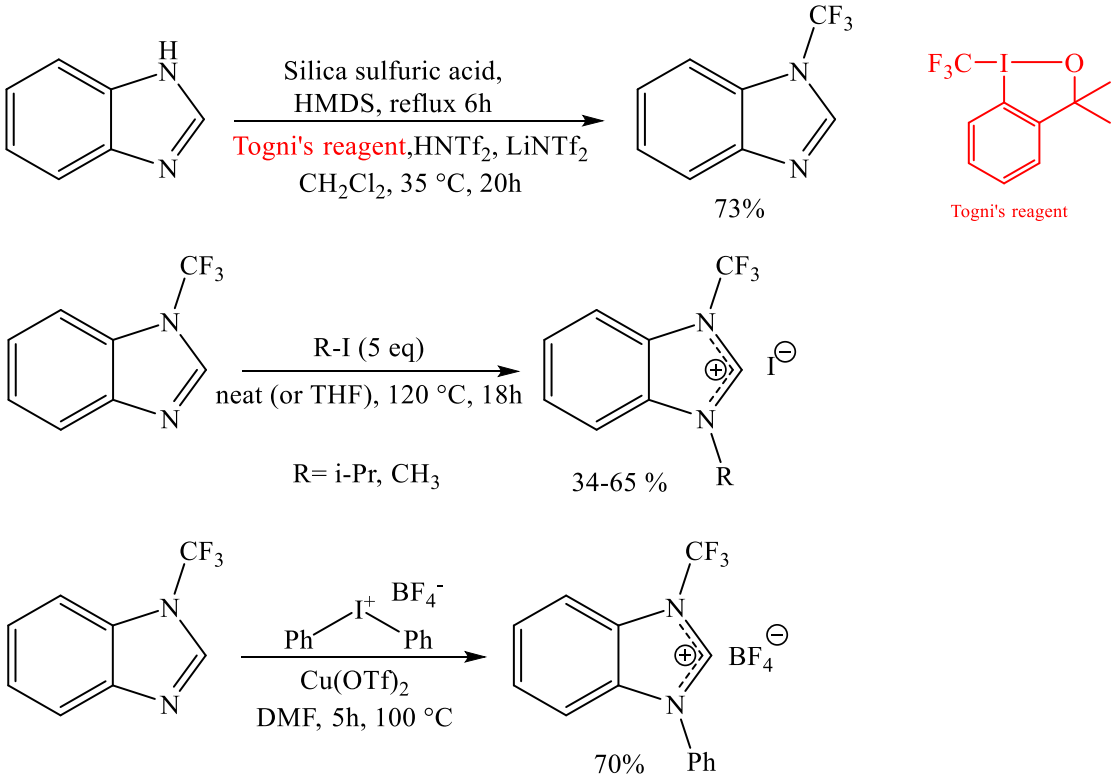

Scheme 6.8

These imidazolium salts react with metallic precursors (i.e. $[Rh(COD)Cl]_2$, $[RuCl_2(=CHPh)(PCy_3)_2]$ or [Au(DMS)Cl]) in the presence of a base (i.e. K_2CO_3) to give the final carbene species, which are efficient catalysts in the metathesis of the olefins (Ru complexes [32]) or in the hydroalkoxylation of olefins (Au (I) complexes (Scheme 6.9) [30]).

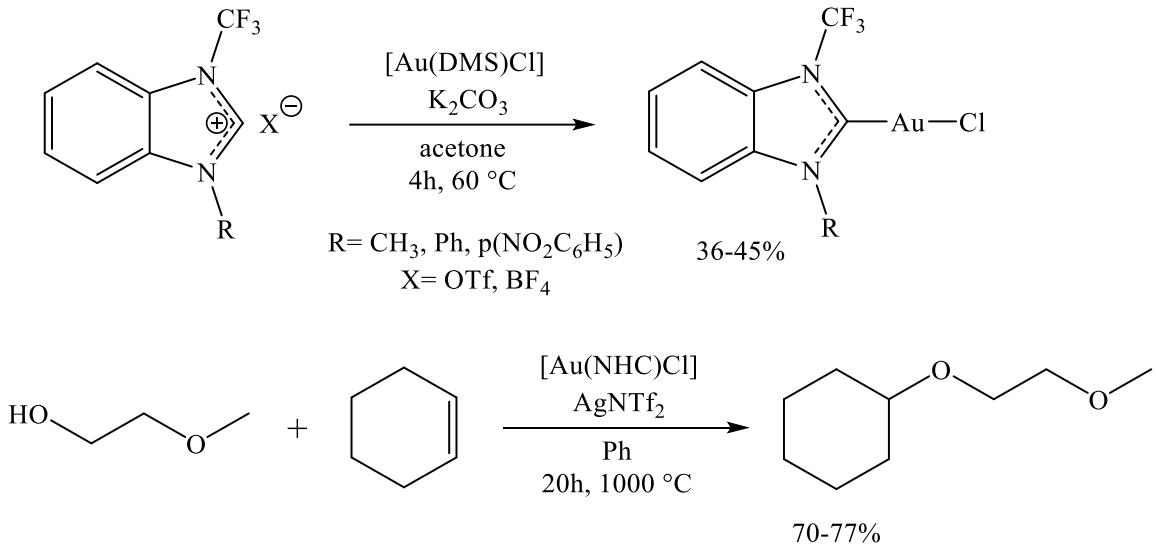

Scheme 6.9

6.2. *N*-trifluoromethyl benzimidazolium salts

As already mentioned in the previous paragraph (section 6.1.3), it is possible to synthesize the *N*-trifluoromethyl benzimidazole by electrophilic trifluoromethylation, with the protocol developed by Togni and co-workers [20a, 31]. This neutral compound reacts with a suitable alkylating agent to give the corresponding imidazolium salt.

In this work, for reasons which will be explained later, we have only synthesized imidazolium salts bearing tetrafluoroborate as counterion, following the conditions shown in Scheme 6.10.

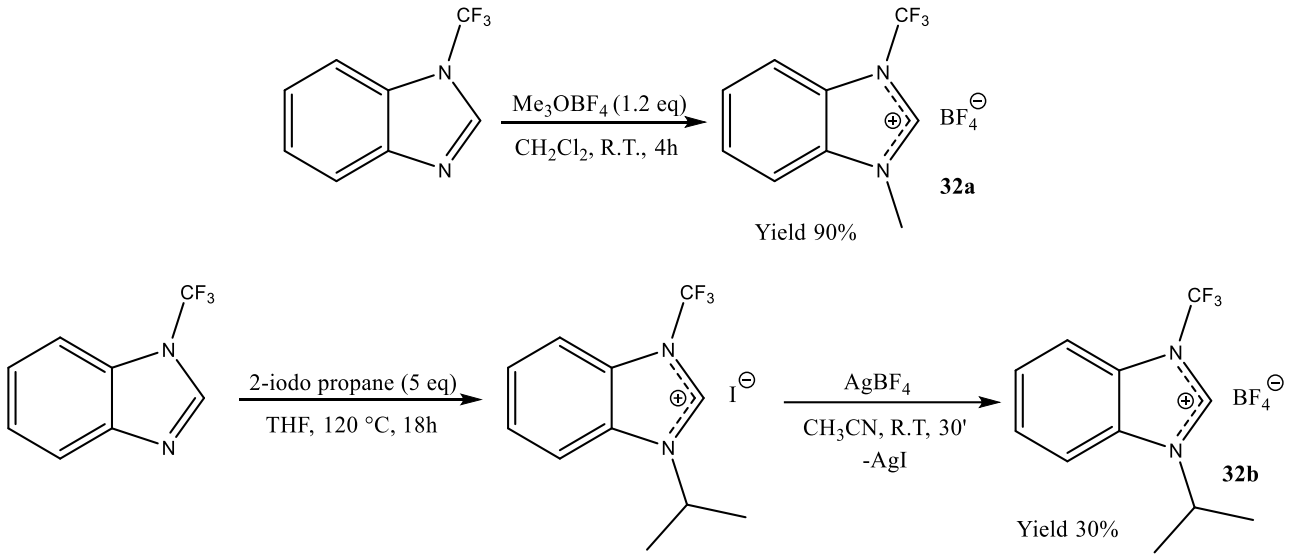

Scheme 6.10

In order to obtain the methylated derivative **32a**, the trifluorobenzimidazole was reacted in dichloromethane with the Meerwein's salt (Me_3OBF_4) under controlled atmosphere.

Owing to the commercial unavailability of the $(iPr)_3OBF_4$ species, the introduction of the isopropyl substituent was achieved by the synthesis of the iodide derivative according to the method already reported in the literature [30], first followed by the I^-/BF_4^- counterion-exchange using silver tetrafluoroborate as a dehalogenizing agent. After the filtration of AgI, the desired product was easily isolated.

The successful result of the reactions is proved by the presence in the ^{1}H-NMR spectra (Fig. 6.4) of all the signals of benzimidazole and those of the inserted methyl or isopropyl substituents. Moreover, in the ^{19}F-NMR spectra are present two sets of signals (Fig. 6.5). In more detail:

- A singlet at ca. -59 ppm related to the CF_3 group.
- Two singlets at ca. -152 ppm ascribable to the tetrafluoroborate counterion ($^{10}BF_4$ and $^{11}BF_4$).

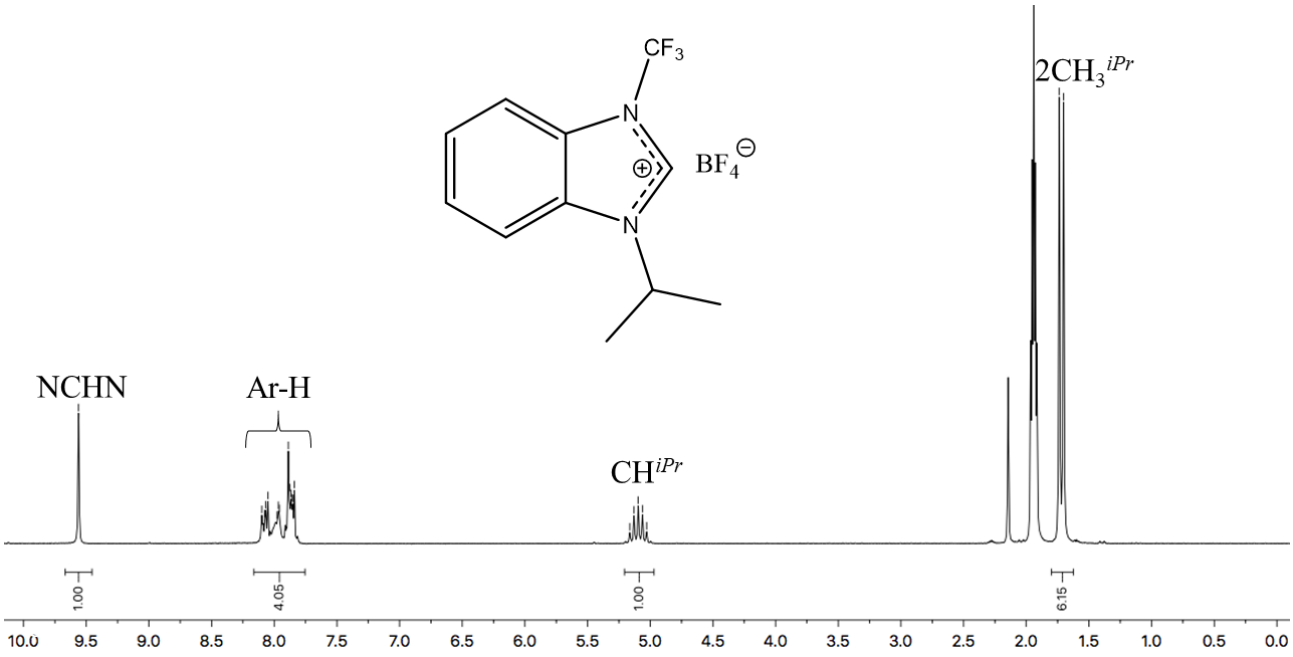

*Fig. 6.4 ^{1}H-NMR spectrum of the imidazolium salt **32b** (T=298K, CD_3CN).*

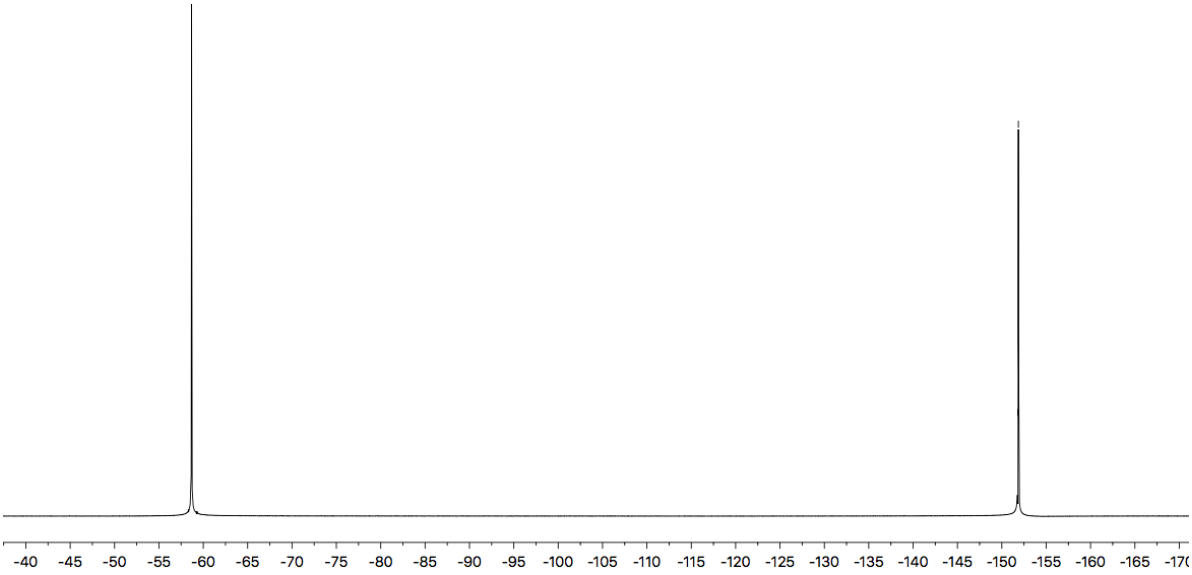

*Fig. 6.5 ^{19}F{^{1}H}-NMR spectrum of the imidazolium salt **32b** (T=298K, CD_3CN).*

Finally, the synthesis of the phenyl derivative **32c** was carried out following the Ullmann method reported in literature and consisting in the coupling between the N-trifluoromethyl benzimidazole and $(Ph_2I)BF_4$ in the presence of $Cu(OTf)_2$ as a catalyst (Scheme 6.11) [30].

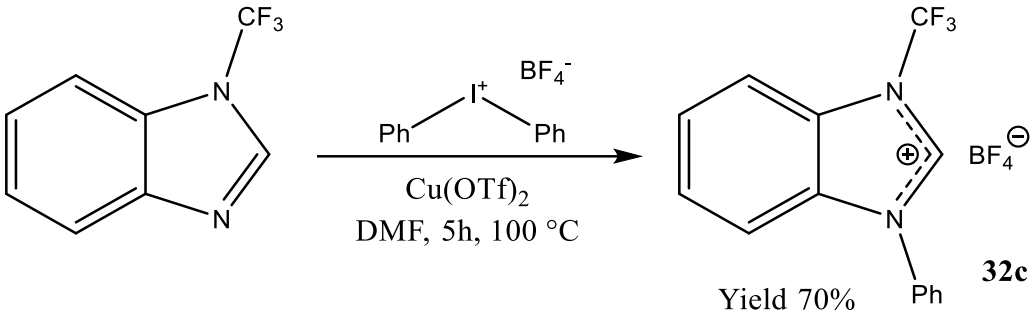

32c

Scheme 6.11

6.3. Palladium (II) η^3-allyl complexes bearing *N*-trifluoromethyl NHCs

Owing to the promising antiproliferative activity against several tumor lines obtained in the case of the allyl complexes (paragraphs 3.8, 4.7 and 5.8), we decided to synthesize some palladium complexes bearing the allyl fragment and the *N*-trifluoromethyl NHC ligands.

Preliminary tests have shown that silver compounds bearing these ligands are of not easy isolation. These species are in fact not very stable and of difficult manipulation. It was therefore decided to carry out one-pot reactions by reacting in acetonitrile for seven hours the starting imidazolium salt with 0.5 equivalents of silver oxide and subsequently, adding to the reaction mixture the palladium allyl precursor of interest.

Further preliminary tests have highlighted the difficulty of the selective synthesis of η^3-allyl complexes bearing two *N*-trifluoromethyl NHCs (biscarbene complexes). On the contrary, the synthesis of mixed palladium allyl derivatives bearing one *N*-trifluoromethyl carbene and one phosphine ligand (PPh_3 or PTA) was successful achieved with high yields according to the experimental condition of Scheme 6.12.

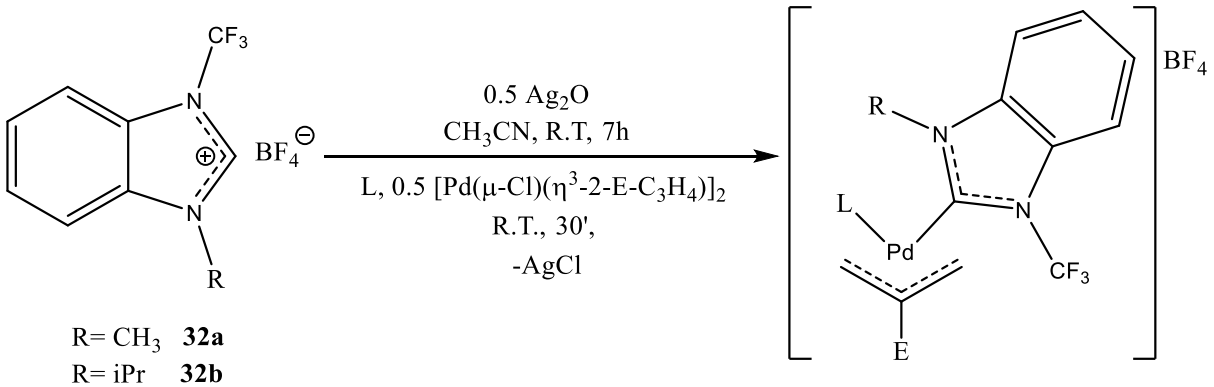

R= CH_3 **32a**
R= iPr **32b**
R= Ph **32c**

Yield (70-94%)

L=PPh_3	R= CH_3	E = H, CH_3	**70, 71**
L=PPh_3	R= iPr	E = H, CH_3	**72, 73**
L=PPh_3	R= Ph	E = H, CH_3	**74, 75**
L=PTA	R= CH_3	E = H, CH_3	**79, 80**
L=PTA	R= iPr	E = H, CH_3	**81, 82**
L=PTA	R= Ph	E = H, CH_3	**83, 84**

Scheme 6.12

All the investigated complexes, owing to the hindered rotation about the Pd-carbene bond, are again present in solution as a pair of atropoisomers (Fig. 6.6). As a matter of fact, it is possible to observe in the NMR spectra the doubling of all the characteristic signals of these molecules.

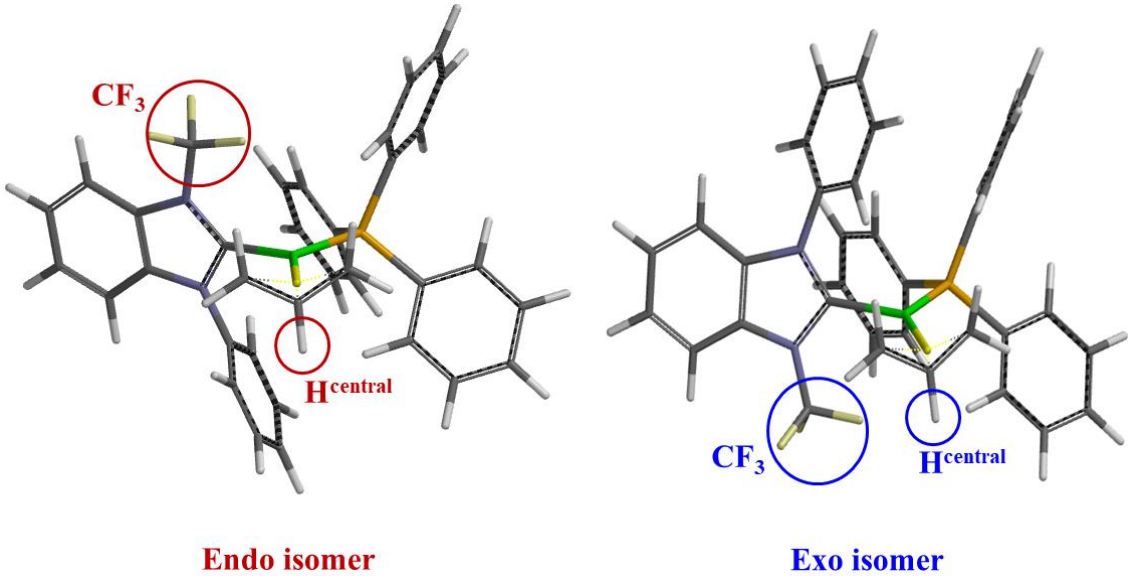

*Fig. 6.6. Representation of the two atropoisomers related to compound **74** (DFT calculations).*

6.3.1. Mixed NHC/PPh_3 complexes

The ^{1}H-NMR spectra of the mixed NHC/PPh_3 complexes, show the presence in solution of two atropoisomer each complex (Fig. 6.7). In particular, the following peaks are observed:

- The signals of the *anti* allyl proton *trans* to carbene within 2.5 and 3.5 ppm (doublet, with J ≈ 13 Hz, in the case of the complexes bearing η^3-allyl fragment or a singlet for those with the η^3-2-Me-allyl group).
- The signals of the *anti* allyl proton *trans* to phosphorus within 3 and 4 ppm (doublet of doublets, with $J_1 \approx 13$ Hz and $J_2 \approx 10$ Hz, in the case of compounds bearing the η^3-allyl fragment or a doublet, with J ≈ 12 Hz, for those with the η^3-2-Me-allyl group).
- The signals of the *syn* allyl proton *trans* to carbene within 3.8 and 4.5 ppm (doublet, with J ≈ 7 Hz, for the compounds bearing the η^3-allyl fragment or a singlet for those with the η^3-2-Me-allyl group).
- The signals of the *syn* allyl proton *trans* to phosphorus within 4.2 and 4.8 ppm (doublet of doublets, with $J_1 \approx 7$ Hz and $J_2 \approx 7$ Hz, for the compounds bearing the η^3-allyl fragment or a broad doublet for those with the η^3-2-Me-allyl fragment).

- The signals of the *central* allyl proton within 5.5 and 6.5 ppm for the compounds bearing the η^3-allyl fragment (multiplet) or a singlet at ca. 2 ppm of the *central* methyl group for those with the η^3-2-Me-allyl fragment.

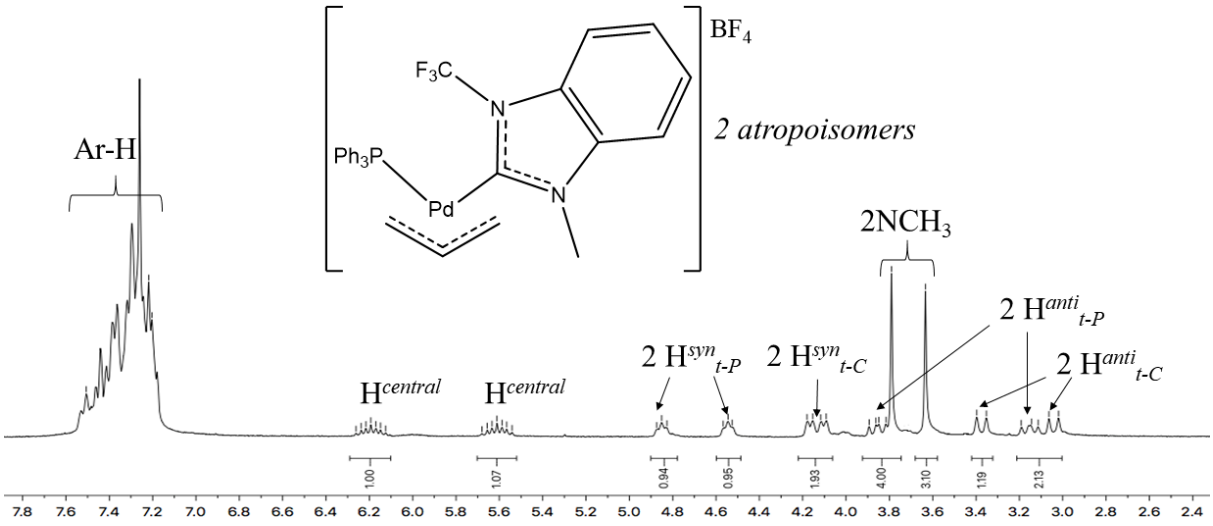

*Fig. 6.7 ^{1}H-NMR spectrum of the complex **70** (T=298K, $CDCl_3$).*

The $^{31}P\{^1H\}$-NMR (Fig. 6.8) spectra show two narrow quartets at about 25 ppm (one for each isomer), due to the coupling through the space between the phosphorus and the fluorine nuclei of the CF_3 group ($J_{P\text{-}F}$=1-4 Hz).

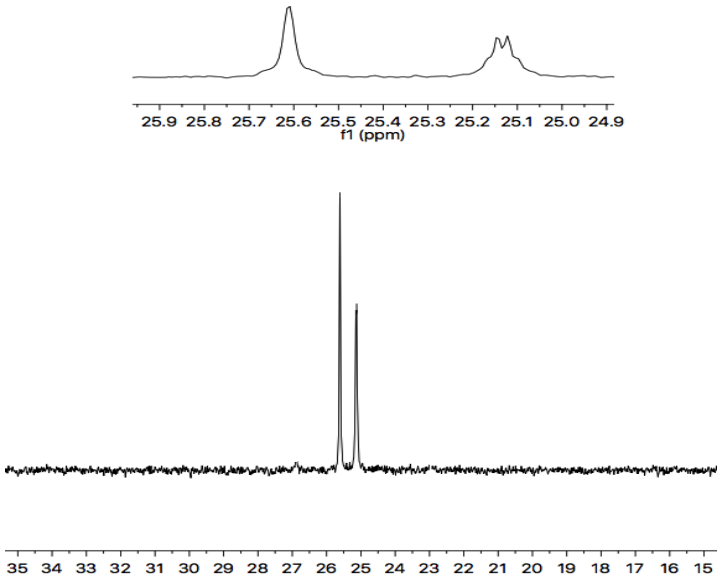

*Figure 6.8 $^{31}P\{^1H\}$-NMR spectrum of the complex **70** (T=298K, $CDCl_3$).*

The $^{19}F\{^{1}H\}$-NMR spectra (Fig. 6.9), show two narrow doublets (one for each isomer) at about -55 ppm (J_{P-F} = 1-4 Hz) related to the CF_3 group and the tetrafluoroborate counterion signals at about -153 ppm.

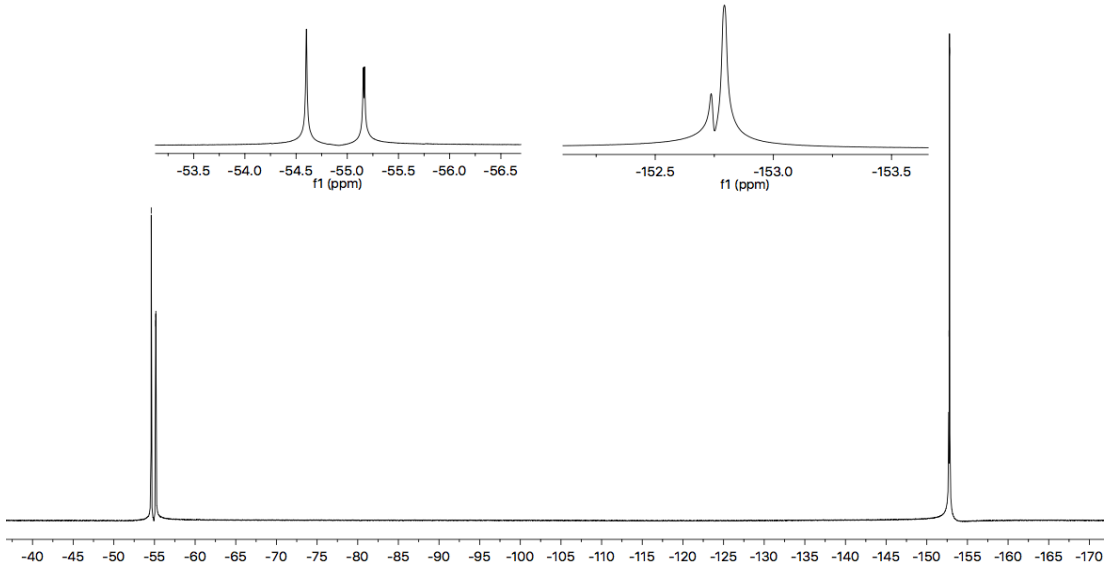

*Fig. 6.9 $^{19}F\{^{1}H\}$-NMR spectrum of the complex **70** (T=298K, $CDCl_3$).*

In the ^{13}C-NMR spectra (Fig. 6.10), in addition to the typical signals of the allyl carbons, it is possible to see the signal of the coordinated carbene carbon at about 190 ppm resonating as a multiplet (coupling with the phosphorus and fluorine nuclei).

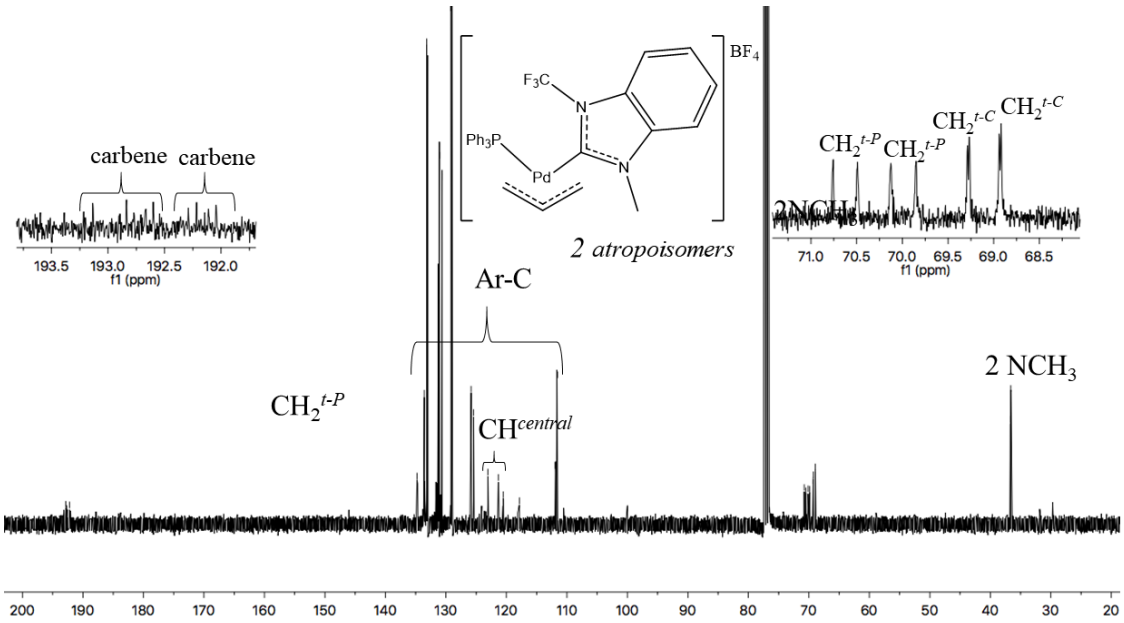

*Fig. 6.10. $^{39}C\{^{1}H\}$-NMR spectrum of the complex **70** (T=298K, $CDCl_3$).*

Finally, in the case of the compound **74** it was possible to obtain the structure of the single crystal, by X-ray diffraction (Fig. 6.11).

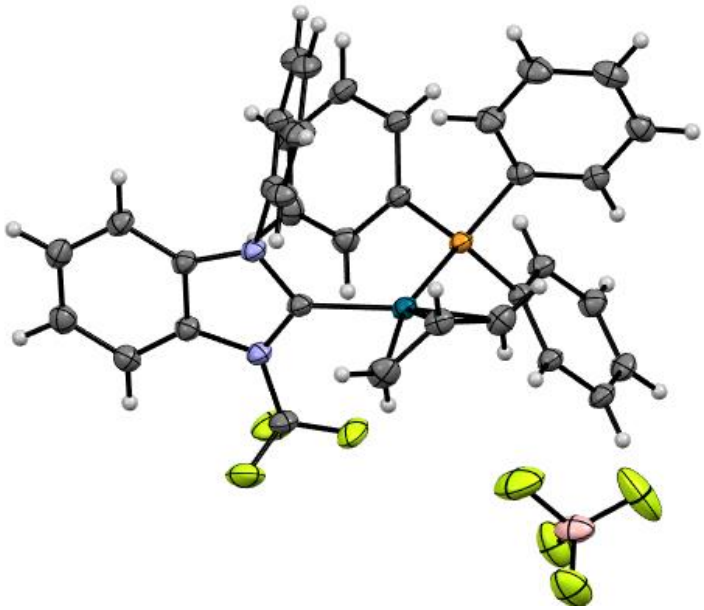

*Fig. 6.11 Ellipsoid representation of **74** crystal ASU contents (50% probability).*

6.3.2. Mixed NHC/PTA complexes

The ^{1}H-NMR spectra of the mixed NHC/PTA complexes show the presence in solution of two atropoisomer each complex (Fig. 6.12). In particular, the following signals are observed:

- The signals of the *anti* allyl proton *trans* to carbene within 2.5 and 3.0 ppm (doublet, with J ≈ 13 Hz, for the compounds bearing the η^3-allyl fragment or a singlet for those with the η^3-2-Me-allyl fragment).
- The signals of the *anti* allyl proton in *trans* to phosphorus within 3 and 3.5 ppm (multiplet for the compounds bearing the η^3-allyl fragment or a doublet, with J ≈ 9 Hz, for those with the η^3-2-Me-allyl fragment).
- The signals of the *syn* allyl protons and the NCH_2N/NCH_2P systems within 4 and 5 ppm.
- The signals at ca. 5.5 ppm of the *central* allyl proton for the compounds bearing the η^3-allyl fragment (multiplet) or a singlet at ca. 1.8 ppm of the *central* methyl group for those with the η^3-2-Me-allyl fragment.

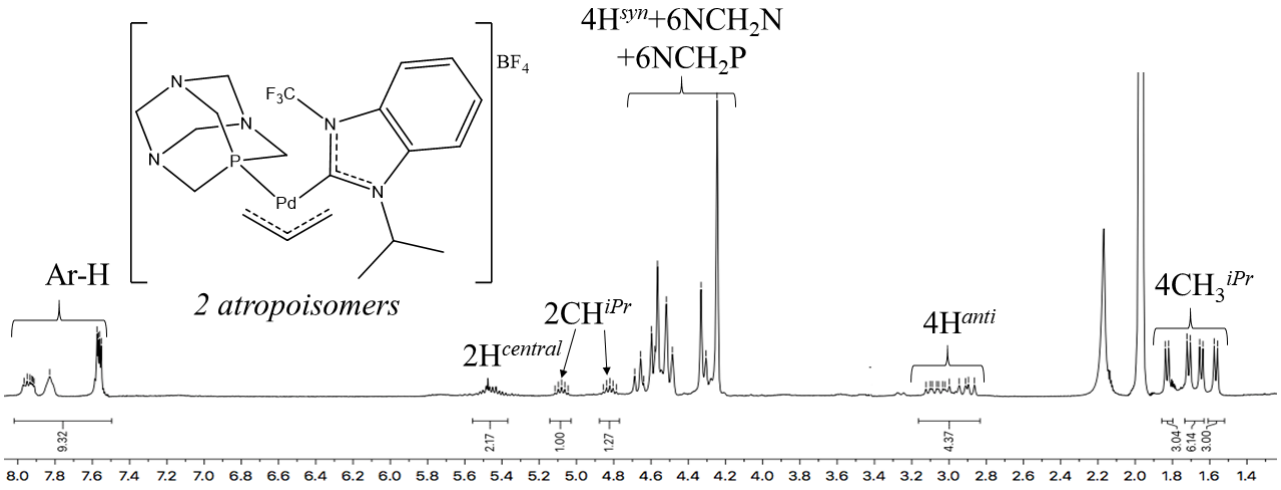

*Fig. 6.12 ^{1}H-NMR spectrum of the complex **81** (T=298K, CD_3CN).*

The $^{31}P\{^{1}H\}$-NMR (Fig. 6.13) spectra show two superimposed quartets (one for each isomer) at about -58 ppm with a J_{P-F}=1-5 Hz.

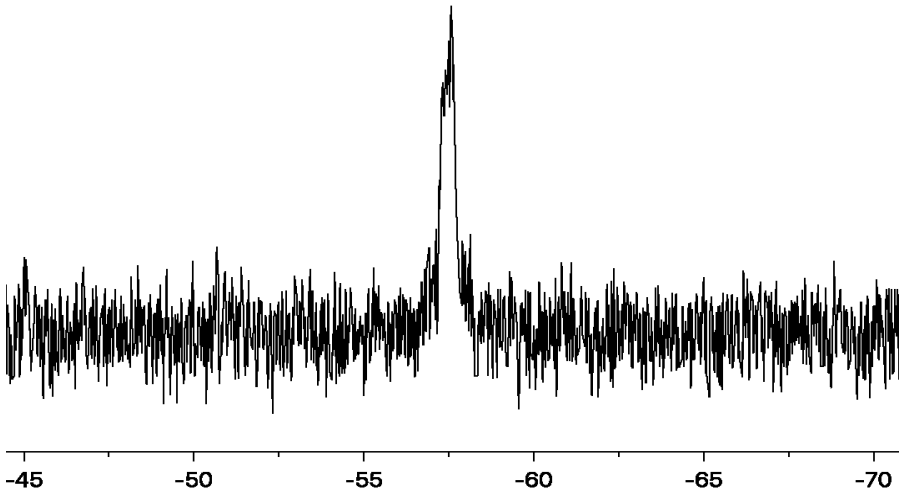

*Fig. 6.13 $^{31}P\{^{1}H\}$-NMR spectrum of the complex **81** (T=298K, CD_3CN).*

The $^{19}F\{^{1}H\}$-NMR spectra (Fig. 6.14) show two narrow doublets (one for each isomer) at about -56 ppm (J_{P-F} = 1-4 Hz) related to the CF_3 group and that of the tetrafluoroborate counterion at about -152 ppm.

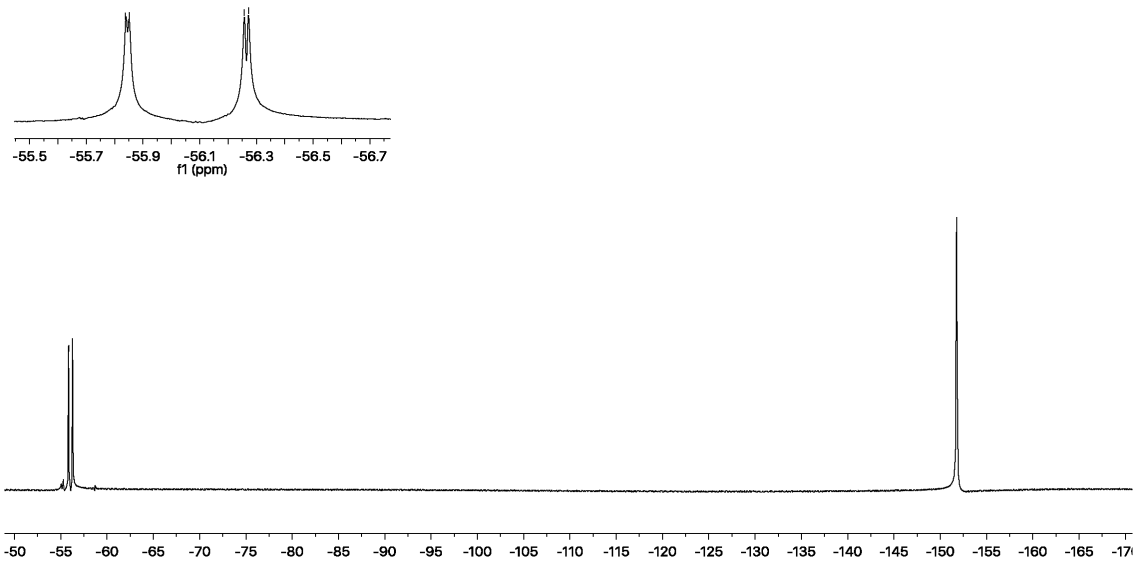

*Fig. 6.14 $^{19}F\{^{1}H\}$-NMR spectrum of the complex **81** (T=298K, CD_3CN).*

Finally, the ^{13}C-NMR spectra (Fig. 6.15) show the typical signals of the allyl carbons and that of the coordinated carbene carbon at about 190 ppm resonating as a multiplet (coupling with the phosphorus and fluorine nuclei).

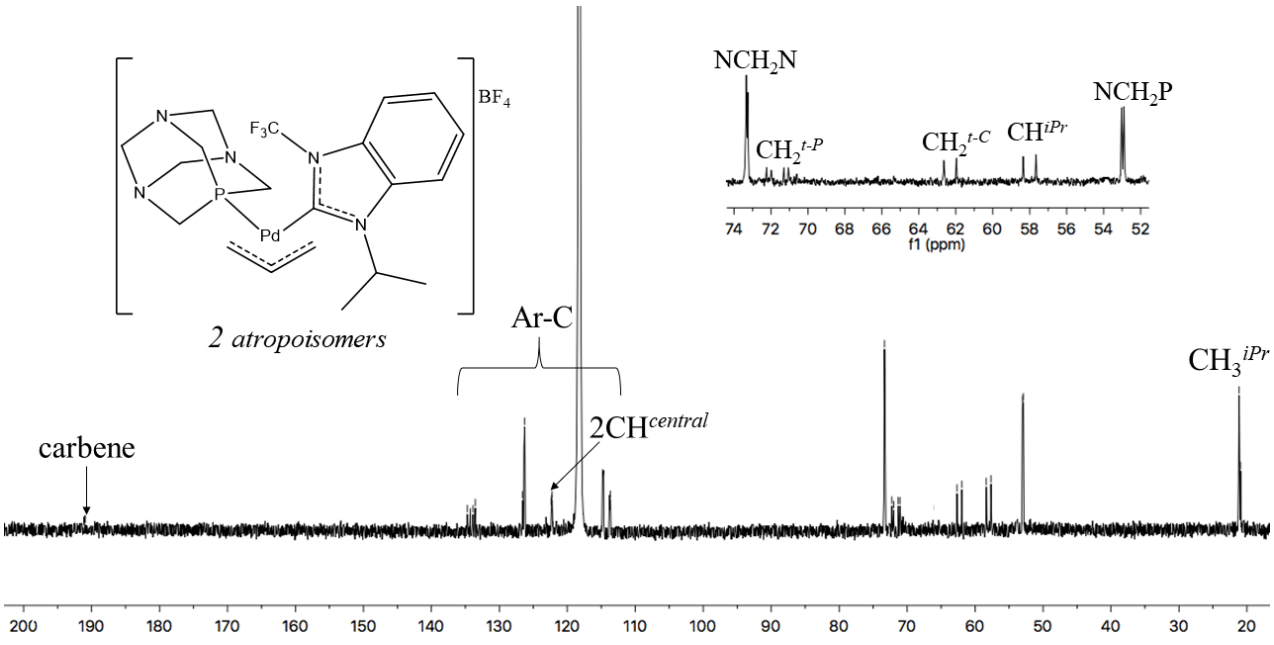

*Fig. 6.15 $^{39}C\{^{1}H\}$-NMR spectrum of the complex **81** (T=298K, CD_3CN).*

6.4. Antiproliferative activity and biological assays

The antiproliferative activity of the allyl compounds described in this chapter was determined *in vitro* toward healthy cells (MRC-5 fibroblasts) and several tumor lines. The final results are summarized in table 6.2 and visualized in figures 6.16-6.21.

COMPOUND	IC_{50} (μM)						
	A2780	A2780-R	OVCAR5	A549	A375	DLD1	MRC-5
Cisplatin	0.81±0.06	9±3	0.84±0.04	6±3	4.7±0.4	19±4	14±1
70	0.03±0.01	0.051±0.004	0.26±0.03	0.18±0.09	0.041±0.003	0.28±0.06	0.28±0.01
71	0.14±0.03	0.08±0.02	0.30±0.05	0.14±0.06	0.083±0.009	0.31±0.04	1.8±0.6
72	0.024±0.002	0.027±0.004	0.20±0.06	0.17±0.01	0.045±0.005	0.28±0.01	0.30±0.05
73	0.18±0.05	0.12±0.02	0.5±0.1	0.32±0.05	0.24±0.02	0.50±0.09	1.5±0.3
79	0.23±0.07	0.9±0.2	10±1	10±3	0.286±0.006	1.11±0.09	>100
80	0.25±0.01	1.4±0.1	6±1	2.1±0.1	1.7±0.3	48±29	>100
81	0.30±0.02	0.22±0.05	2.8±0.7	1.37±0.09	0.34±0.06	3±1	>100
82	0.76±0.01	1.3±0.1	6.3±0.7	2.5±0.1	2.7±0.8	5.4±0.5	>100

*Table 6.2 In vitro antiproliferative IC_{50} values (μM, 72 h) of complexes **70-82** toward human cell lines of ovarian cancer (A2780 and OVCAR5), the cisplatin resistant clone (A2780-R), lung cancer (A549), malignant melanoma (A375), colon cancer (DLD1) and normal lung fibroblast (MRC-5).*

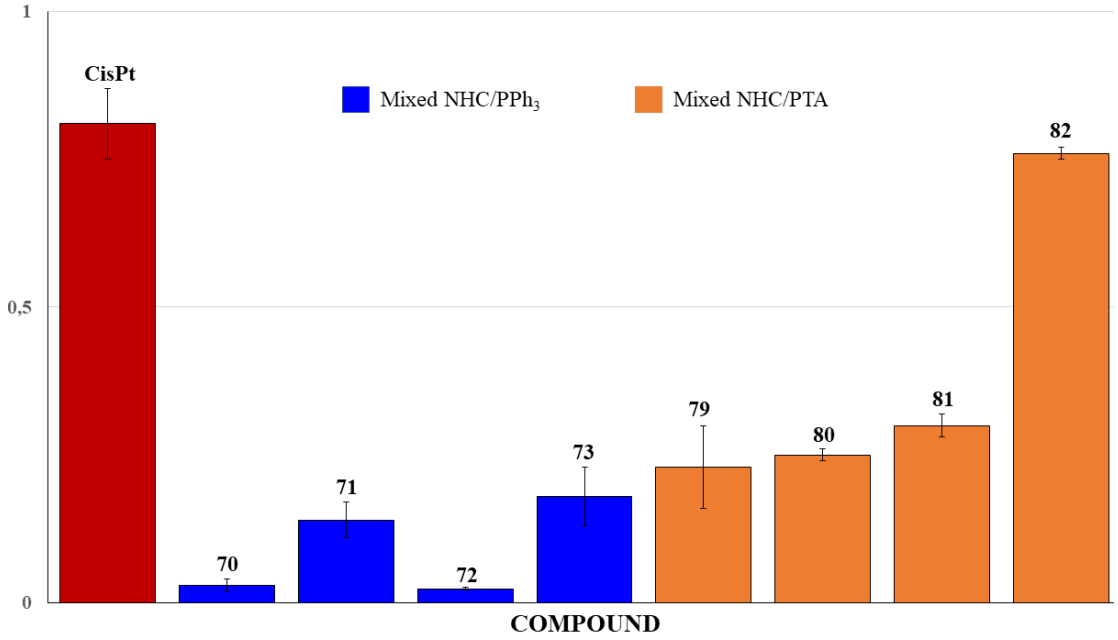

Fig. 6.16 Antiproliferative activity on A2780 cell line.

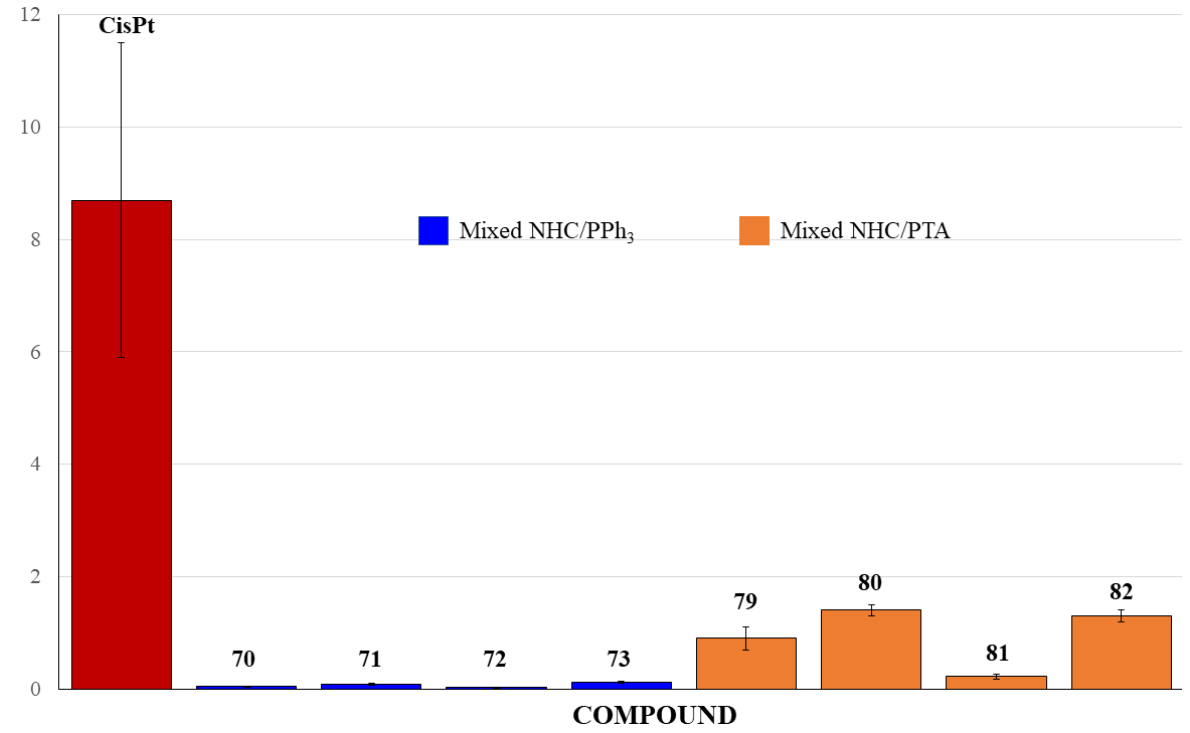

Fig. 6.17 Antiproliferative activity on A2780-R cell line.

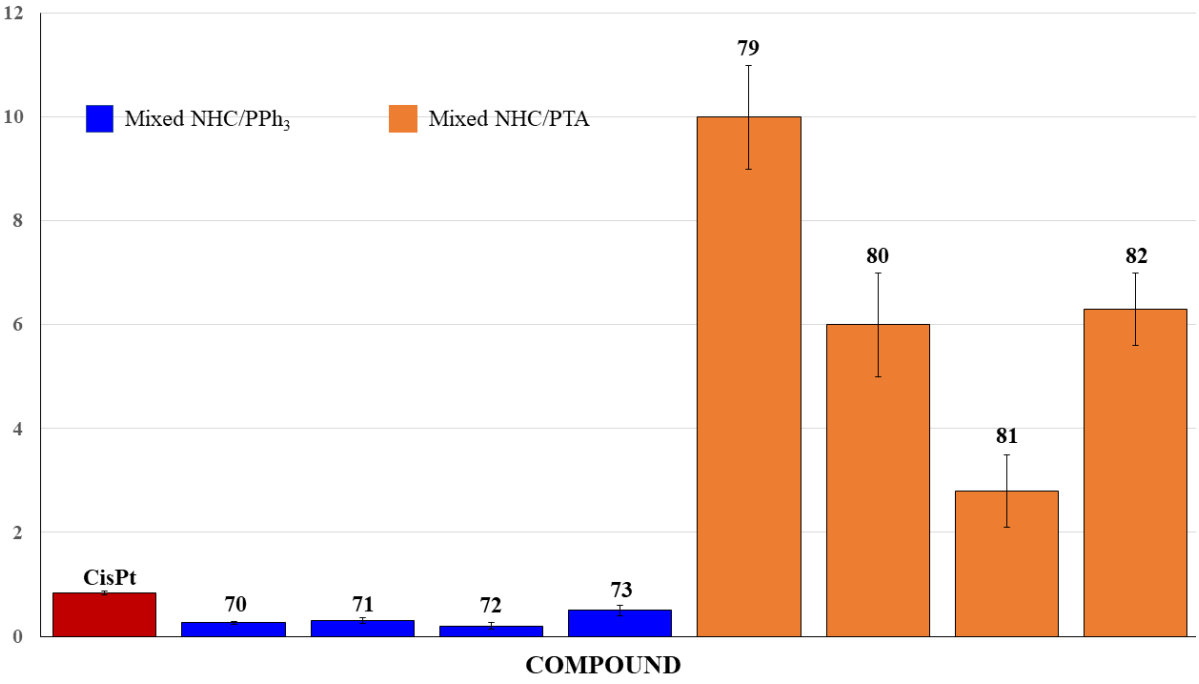

Fig. 6.18 Antiproliferative activity on OVCAR5 cell line.

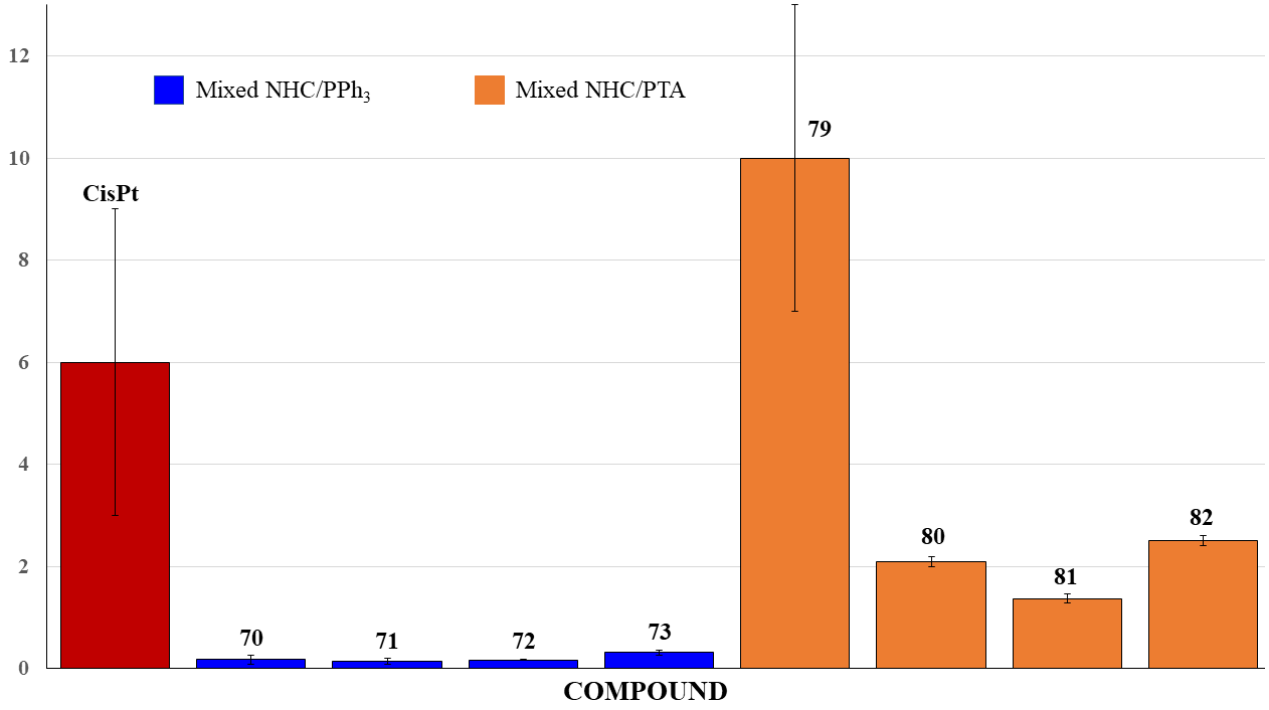

Fig. 6.19 Antiproliferative activity on A549 cell line.

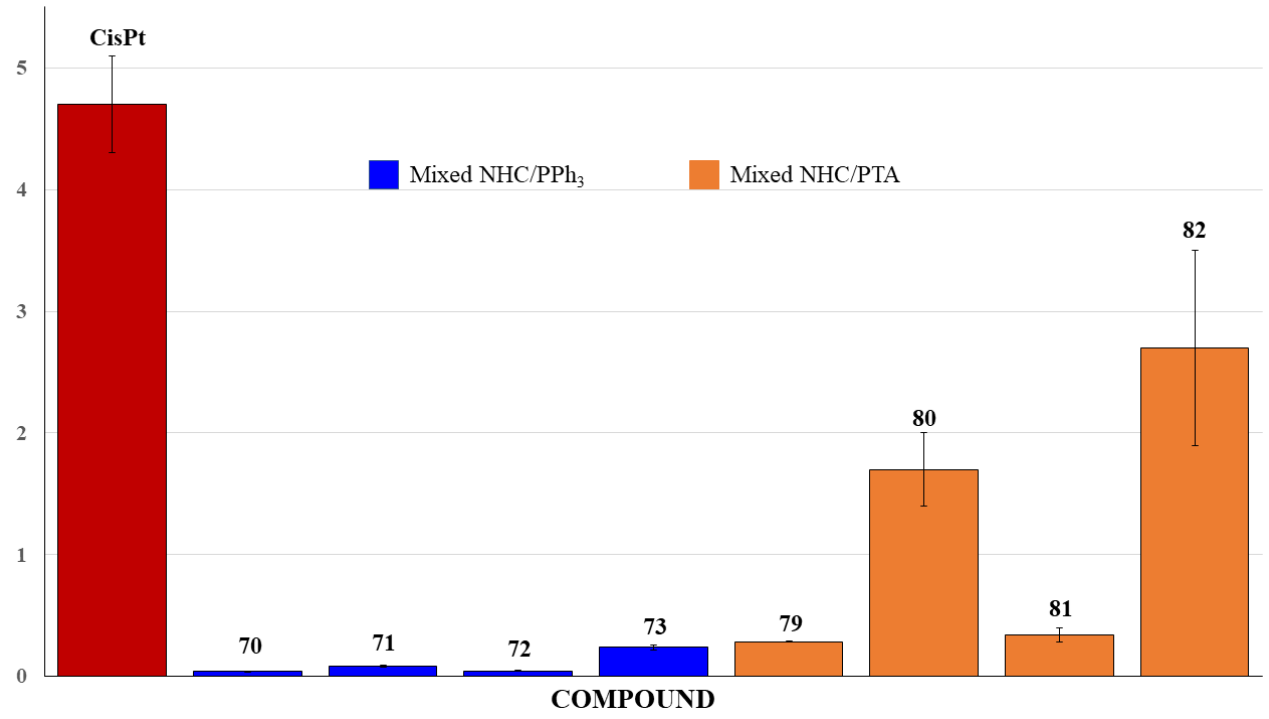

Fig. 6.20 Antiproliferative activity on A375cell line.

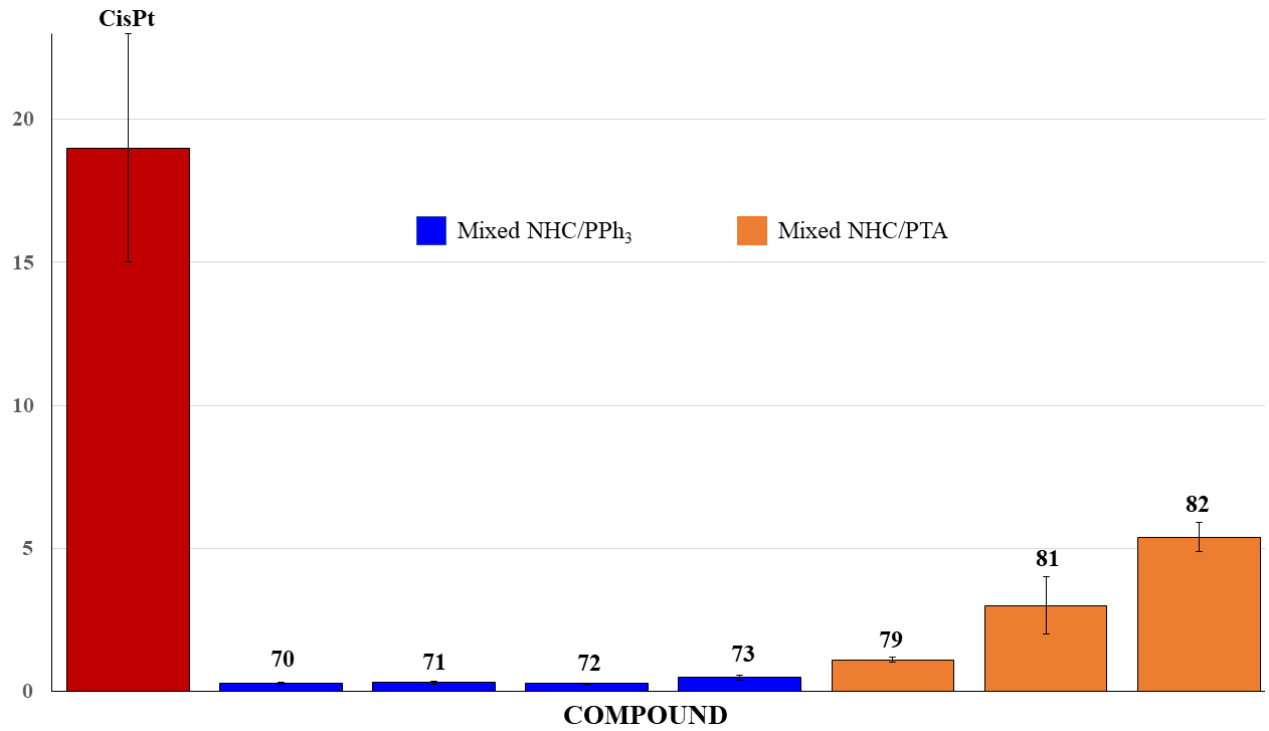

Fig. 6.21 Antiproliferative activity on DLD1 cell line (compound 80 has been omitted).

On the basis of these results, we can propose the following considerations:

1. These compounds, except for some rare cases, appears to be more active than cisplatin in all the tumor lines taken into consideration.
2. The mixed NHC/PPh_3 compounds (**70**-**75**) are in most cases more active than the mixed NHC/PTA homologues (**79**-**84**).
3. For the same spectator ligands, the complexes with the η^3-2-Me-allyl organometallic fragment are generally less active than those containing the η^3-allyl fragment.
4. Mixed NHC/PTA compounds, even if they show a slightly lower activity compared to NHC/PPh_3 homologues, have the advantage of being almost inactive toward healthy cell lines (IC_{50}> 100 μM on fibroblasts).

6.5. Conclusions

In this chapter the synthesis of cationic complexes of Pd (II), stabilized by *N*-trifluoromethyl NHC ligands and phosphines (PTA or PPh_3) was described.

The new compounds were completely characterized by spectroscopic techniques (IR and NMR), elemental analysis and X-ray diffraction (for compound **75**).

Their antiproliferative activity was assayed on several tumor lines, showing in most cases a higher effectiveness than cisplatin.

In particular, the mixed NHC/PTA complexes are very interesting since, in addition to a good antiproliferative activity on the examined tumor lines, do not seem particularly cytotoxic on healthy cells (IC_{50}> 100 μM on MRC-5 fibroblasts).

6.6. References

[1] (a) M. Bassetto, S. Ferla, F. Pertusati, *Future Med. Chem.*, 2015, **7(4)**, 527; (b) P. Shah, A. D. Westwell, *Journal of Enzyme Inhibition and Medicinal Chemistry*, 2007; **22(5)**, 527.

[2] (a) N.A. Meanwell N A., *J. Med. Chem.*, 2010, **54(8)**, 2529; (b) J. Wang, M. Sánchez-Roselló, J.L. Aceña, E. Al, *Chem. Rev.* 2014, **114(4)**, 2432.; (c) S. Purser, P.R. Moore, S. Swallow, V. Gouverneur, *Chem. Soc. Rev.*, 2008, **37**, 320.

[3] D. O'Hagan, D.B. Harper, *J. Fluor. Chem.*, 1999, **100**, 127.

[4] (a) G. Teverovskiy, D.S. Surry, S.L. Buchwald, Angew. Chem. Int. Ed., 2011, **50**, 7312; (b) B.J. Jelier, Pascal F. Tripet, E. Pietrasiak, I. Franzoni, G. Jeschke, A. Togni, *Angew. Chem. Int. Ed.*, 2018, **57**, 1.

[5] B.E. Smart, *J. Fluor. Chem.*, 2001, **109(1)**, 3.

[6] (a) C. Hansch, A. Leo, *Fundamentals and Applications in Chemistry and Biology*, American Chemical Society, Washington, DC, 1995; (b) C. Hansch, A. Leo, D. Hoekman, *Hydrophobic, Electronic and Steric Constants*, ACS Professional Reference Book, American Chemical Society, Washington, DC, 1995.

[7] B.K. Park, N.R. Kitteringham, P.M. O'Neill, *Annu. Rev. Pharmacol. Toxicol.*, 2001, **41**, 443.

[8] C. Dalvit, A. Vulpetti, *Chem. Med. Chem.*, 2012, **7(2)**, 262.

[9] Swarts, *Acad. Roy. Belg.*, 1892, **3** (24), 474.

[10] V.C.R. McLoughlin, J. Thrower, *Tetrahedron*, 1969, **25** (24), 5921.

[11] M. Oishi, H. Kondo, H. Amii, *Chem. Commun.*, 2009, **14**, 1909.

[12] E.J. Cho, T.D. Senecal, T. Kinzel, Y. Zhang, D.A. Watson, S.L. Buchwald, *Science*, 2010, **328** (5986), 1679.

[13] J. Ma, D. Cahard, *J. Fluor. Chem.*, 2007, **128** (9), 975.

[14] A. Studer, *Angew. Chem. Int. Ed.*, 2012, **51** (36), 8950.

[15] K. Miura, Y. Takeyama, K. Oshima, K. Utimoto, *Bulletin of the Chemical Society of Japan*, 1991, **64** (5), 1542.

[16] G.K. Prakash, F. Wang, Z. Zhang, R. Haiges, M. Rahm, K.O. Christe, T. Mathew, G.A. Olah, *Angew. Chem. Int. Ed.*, 2014, **53** (43), 11575.

[17] X. Fei, W. Tian, K. Ding, Y. Wang, C. Qing-Yun, *Org. Synth.*, 2010, **87** (87), 126.

[18] L.M. Yagupolskii, N.V. Kondratenko, G.N. Timofeeva, *J. Org. Chem.*, 1984, **20**, 103.

[19] (a) U. Teruo, I. Sumi, *Tetrahedron Letters*, 1990, **31** (25), 3579; (b) T. Umemoto, S. Ishihara, *J. Am. Chem. Soc.*, 1993, **115** (6), 2156.

[20] (a) J. Charpentier, N. Früh, A. Togni, *Chem. Rev.*, 2015, **115**, 650; (b) P. Eisenberger, S. Gischig, A. Togni, *Chemistry: A European Journal*, 2006, **12** (9), 2579; (c) I. Kieltsch, P.

Eisenberger, A. Togni, *Angew. Chem. Int. Ed.*, 2007, **46** (5), 754; (d) P. Eisenberger, I. Kieltsch, N. Armanino, A. Togni, *Chem. Commun*., 2008, **13**, 1575; (e) K. Stanek, R. Koller, A. Togni, *J. Org. Chem.*, 2008, **73** (19), 7678.

[21] P. Eisenberger, I. Kieltsch, R. Koller, K. Stanek, A. Togni, *Org. Synth.*, 2011, **88**, 168.

[22] A.T. Parsons, S.L. Buchwald, *Angew. Chem. Int. Ed.*, 2011, **50** (39), 9120.

[23] Z. He, T. Luo, M. Hu, Y. Cao, J. Hu, *Angew. Chem. Int. Ed.*, 2012, **51** (16), 3944.

[24] (a) K. Iseki, T. Nagai, Y. Kobayashi, *Tetrahedron Letters*, 1994, **35** (19), 3137; (b) S. Caron, N. Do, P. Arpin, A. Larivée, *Synthesis*, 2003, **11**, 1693; (c) T. Umemoto, K. Adachi, *J. Org. Chem.*, 1994, **59** (19), 5692; (d) D.A. Nagib, M.E. Scott, D.W.C. MacMillan, *J. Am. Chem. Soc.*, 2009, **131** (31), 10875; (e) A.E. Allen, D.W.C. MacMillan, *J. Am. Chem. Soc.*, 2010, **132** (14), 4986; (f) Q. Deng, H. Wadepohl, L.H. Gade, *J. Am. Chem. Soc.*, 2012, **134** (26), 10769.

[25] (a) H. Jacobsen, A. Correa, A. Poater, C. Costabile, L. Cavallo, *Coord. Chem. Rev.*, 2009, **253**, 687; (b) U. Radius, F.M. Bickelhaupt, *Coord. Chem. Rev.*, 2009, **253**, 678 ; (c) S. Díez-González, S.P. Nolan, *Coord. Chem. Rev.*, 2007, **251**, 874 ; (d) W.A. Herrmann, C. Köcher, *Angew. Chem. Int. Ed.*, 1997, **36**, 2162.

[26] (a) D.J. Nelson, S.P. Nolan, *Chem. Soc. Rev.*, 2013, **42**, 6723; (b) D. Marchione, L. Belpassi, G. Bistoni, A. Macchioni, F. Tarantelli, D. Zuccaccia, *Organometallics*, 2014, **33**, 4200; (c) A. Liske, K. Verlinden, H. Buhl, K. Schaper, C. Ganter, *Organometallics*, 2013, **32**, 5269.

[27] (a) O.S. Morozov, A.V. Lunchev, A.A. Bush, A.A. Tukov, A.F. Asachenko, V.N. Khrustalev, S.S. Zalesskiy, A.P. Ananikov, A.S. Nechaev, *Chem. Eur. J.*, 2014, **20**, 6162; (b) T. Sato, Y. Hirose, D. Yoshioka, T. Shimojo, S. Oi, *Chem. Eur. J.*, 2013, **19**, 15710; (c) T. Sato, Y. Hirose, D. Yoshioka, S. Oi, *Organometallics*, 2012, **31**, 6995; (d) X. Zeng, G.D. Frey, R. Kinjo, B. Donadieu, G. Bertrand, *J. Am. Chem. Soc.*, 2009, **131**, 8690.

[28] M. Alcarazo, T. Stork, A. Anoop, W. Thiel, A. Fürstner, *Angew. Chem. Int. Ed.*, 2010, **49**, 2542.

[29] D.G. Gusev, *Organometallics*, 2009, **28**, 6458.

[30] P.S. Engl, R. Senn, E. Otth, A. Togni, *Organometallics*, 2015, **34**, 1384.

[31] K. Niedermann, N. Früh, R. Senn, B. Czarniecki, R. Verel, A. Togni, *Angew. Chem., Int. Ed.*, 2011, **50**, 1059.

[32] (a) P.S. Engl, A. Fedorov, C. Copéret, A. Togni, *Organometallics*, 2016, **35**, 887; (b) P.S. Engl, C.B. Santiago, C.P. Gordon, L.W. Liao, A. Fedorov, C. Copéret, M.S. Sigman, A. Togni, *J. Am. Chem. Soc.*, 2017, **139**, 13117.

7

Conclusions and future perspectives

This work reports the synthesis and characterization of about one hundred palladium compounds in three different oxidation states (0, +1 and +2), stabilized by six different types of *N*-Heterocyclic Carbenes and bearing three different organometallic fragments (Fig 7.1).

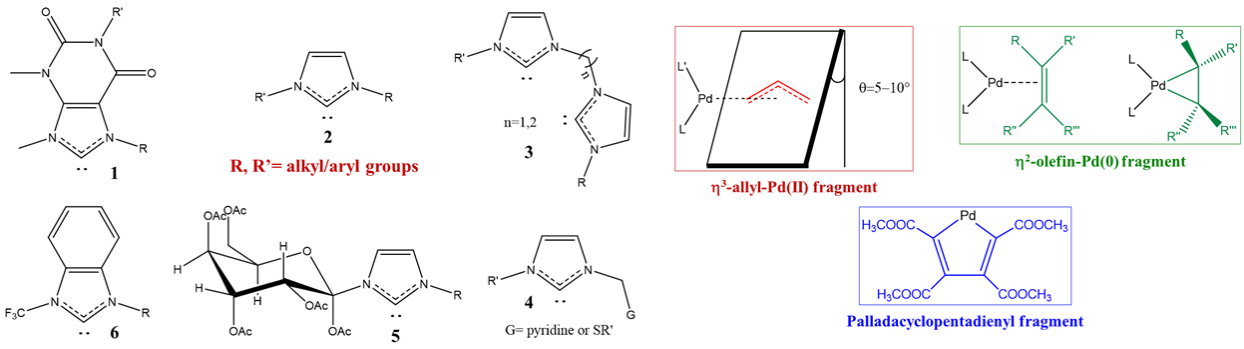

Fig. 7.1

The figure proposed at the beginning of the chapter is related to this source: https://de.fotolia.com/

The synthetic strategies used and the features of products obtained have been discussed in detail both from the kinetic and thermodynamic point of view, sometimes with the support of DFT theoretical calculations.

All compounds were subsequently tested *in vitro* on several tumor lines (mainly of ovarian carcinoma) and, in order to verify their selectivity toward cancer cells, also on lung fibroblast lines.

From this screening it is possible to deduce that the antiproliferative activity promoted by these complexes is mainly dependent on the type of organometallic fragment involved.

The nature of the organometallic function (η^3-allyl-Pd(II), palladacyclopentadienyl or η^2-olefin-Pd(0)) seems to play a fundamental role in the interactions of the palladium complexes with biological systems and consequently in the definition of their cytotoxicity. In particular, it has been observed that compounds containing the allyl residue are generally more active than the palladacyclopentadienyl complexes and much more active toward tumor cells than those coordinating an olefin.

In any case, it was possible to verify that for the same organometallic fragment, the choice of the spectator ligands somehow allows a rough modulation of the antiproliferative activity of the complex and its selectivity toward cancer cells.

Therefore, at the end of this systematic work we have been able to identify eight molecules (or sub-categories of molecules) showing high antiproliferative activity against the examined cancer lines and, at the same time, low cytotoxicity toward healthy cells (Figs. 7.2 and 7.3).

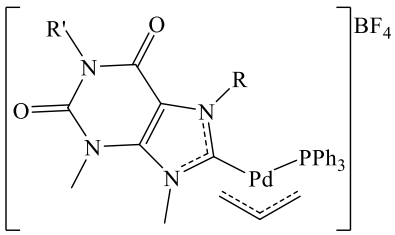

6a-d R = CH_3, Bn, Phprop; R'= CH_3, Bn

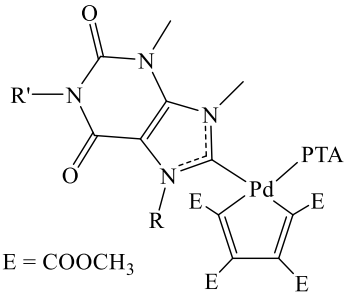

12a-d R = CH_3, Bn; R'= CH_3, Bn

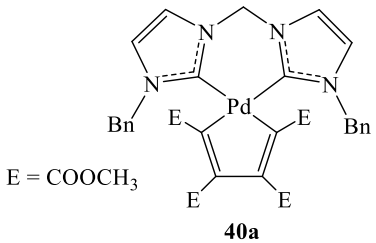

40a

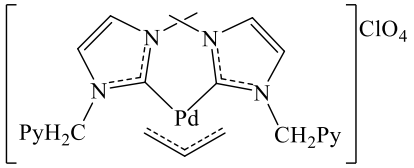

49c

Fig. 7.2

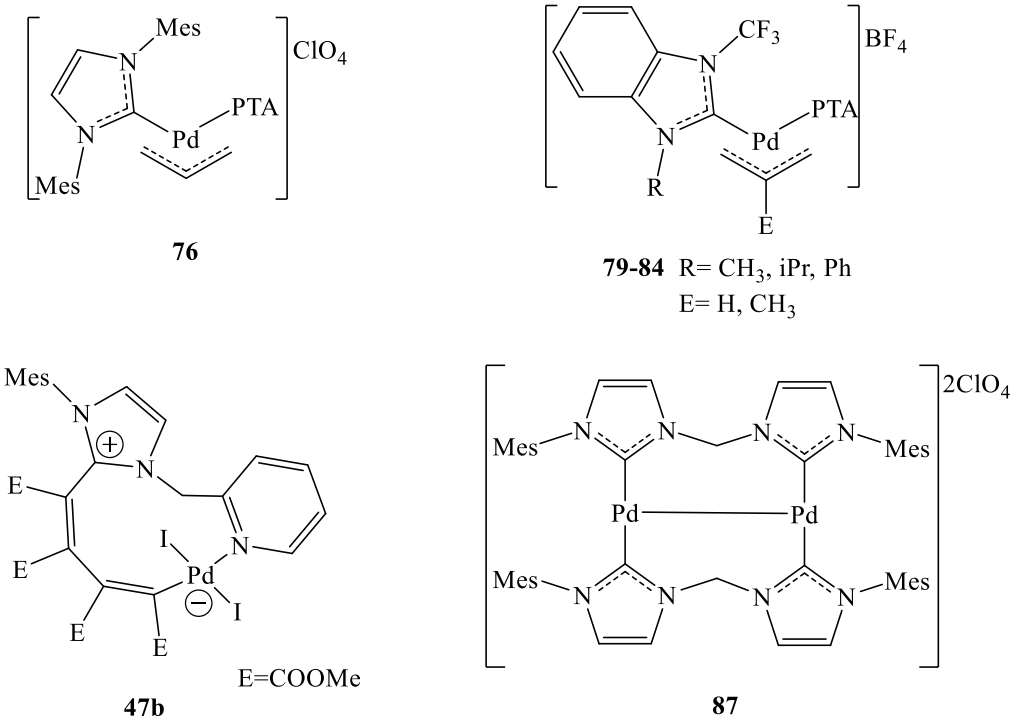

Fig. 7.3

Two of these compounds (**47b** and **87**) do not contains any of the three organometallic fragments peculiar of this work, but are their derivatives or by-products and deserve attention even for their original structure.

For one of the most promising complex, the biscarbene compound **40a,** it was possible to identify the DNA as primary target and define the sequence of events that leads to the death of tumor cell for apoptosis.

Our program for the future is extends the studies on mechanism of action also to the other complexes reported in figures 7.2-7.3 and finally tests their behaviour *in vivo*, in order to understand the real potential of this kind of molecules as new possible anticancer agents for chemotherapy.

8

Publications and communications at conferences

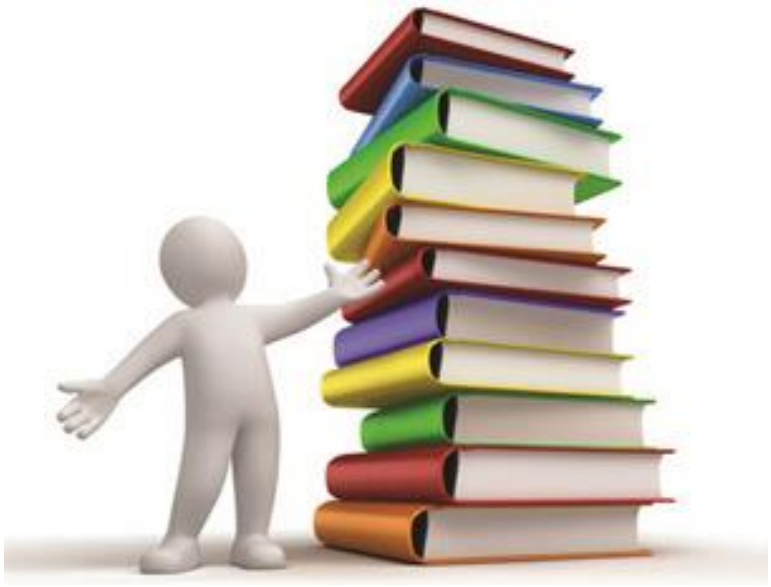

PUBBLICATIONS

1. Luciano Canovese, Fabiano Visentin, Chiara Biz, Thomas Scattolin, Claudio Santo, Valerio Bertolasi, *Journal of Organometallic Chemistry*, 786 (**2015**), 21-30.
2. Luciano Canovese, Fabiano Visentin, Thomas Scattolin, Claudio Santo, Valerio Bertolasi, *Journal of Organometallic Chemistry*, 794 (**2015**), 288-3000.
3. Luciano Canovese, Fabiano Visentin, Thomas Scattolin, Claudio Santo, Valerio Bertolasi, *Dalton Transactions*, 44 (**2015**), 15049-15058.
4. Luciano Canovese, Fabiano Visentin, Chiara Biz, Thomas Scattolin, Claudio Santo, Valerio Bertolasi, *Polyhedron*, 102 (**2015**), 94-102.
5. Luciano Canovese, Fabiano Visentin, Thomas Scattolin, Claudio Santo, Valerio Bertolasi, *Journal of Organometallic Chemistry*, 808 (**2016**), 48-56.
6. Thomas Scattolin, Fabiano Visentin, Claudio Santo, Valerio Bertolasi, Luciano Canovese, *Dalton Transactions*, 45 (**2016**), 11560-11567.

The figure proposed at the beginning of the chapter is related to this source: https://de.fotolia.com/

7. Luciano Canovese, Fabiano Visentin, Thomas Scattolin, Claudio Santo, Valerio Bertolasi, *Polyhedron*, 113 (**2016**), 25-34.
8. Luciano Canovese, Fabiano Visentin, Thomas Scattolin, Claudio Santo, Valerio Bertolasi, *Polyhedron*, 119 (**2016**), 377-386.
9. Thomas Scattolin, Fabiano Visentin, Claudio Santo, Valerio Bertolasi, Luciano Canovese, *Dalton Transactions*, 46 (**2017**), 5210-5217.
10. Luciano Canovese, Fabiano Visentin, Thomas Scattolin, Claudio Santo, Valerio Bertolasi, *Polyhedron*, 129 (**2017**), 229-239.
11. Fabiano Visentin, Claudio Santo, Thomas Scattolin, Nicola Demitri, Luciano Canovese, *Dalton Transactions*, 46 (**2017**), 10399-10407.
12. Luciano Canovese, Thomas Scattolin, Fabiano Visentin, Claudio Santo, *Journal of Organometallic Chemistry*, 834 (**2017**), 10-21.
13. Thomas Scattolin, Luciano Canovese, Fabiano Visentin, Stefano Paganelli, Patrizia Canton, Nicola Demitri, *Applied Organometallic Chemistry*, 32 (**2018**), e4034.
14. Luciano Canovese, Fabiano Visentin, Thomas Scattolin, Claudio Santo, Valerio Bertolasi, *Polyhedron*, 144 (**2018**), 131-143.
15. Thomas Scattolin, Luciano Canovese, Fabiano Visentin, Claudio Santo, Nicola Demitri, *Polyhedron*, 154 (**2018**), 382-389.
16. Thomas Scattolin, Isabella Caligiuri, Luciano Canovese, Nicola Demitri, Roberto Gambari, Ilaria Lampronti, Flavio Rizzolio, Claudio Santo, Fabiano Visentin, *Dalton Transactions*, 47 (**2018**), 13616–13630.

COMMUNICATIONS AT CONFERENCES

1. XXXVII National Conference of Organic Chemistry (Venice, 2016). Title of presentation: *A simple and alternative way for the methylation of functionalized purine bases.*
2. XLIV National Conference of Theoretical and Computational Chemistry (Pisa, 2016). Title of presentation: *Computational investigations on the unexpected extrusion of molecular iodine in Pd(II) σ-butadienyl complexes.*
3. XLIV National Conference of Inorganic Chemistry (Padua, 2016). Title of presentation: *Halogen metathesis in Pd(II) σ-butadienyl complexes.*
4. XVI Workshop on PharmacoBioMetallics (Messina, 2016). Title of presentation: *Synthesis, characterization and antiproliferative activity of theophylline-based Pd(II) allyl complexes.*
5. XI edition of the International School of Organometallic Chemistry (San Benedetto del Tronto, 2017). Title of presentation: *Reactivity of palladacyclopentadienyl complexes toward halide addition. The influence of the ancillary ligand.*
6. XLVI National Conference of Inorganic Chemistry (Bologna, 2018). Title of presentation: *Palladium Purine-based N-Heterocyclic carbene complexes: Synthesis and antiproliferative activity against human ovarian cancer cell lines.*

Member of the local organizing committe of the XXXVII National Conference of Organic Chemistry, 18-22 September 2016 (Venice).

9

Experimental section

In the experimental section the synthesis and characterization of all the compounds will be reported in detail. The synthesis of the final palladium complexes, the silver carbene precursors and the different imidazolium salts used, will be described.

In this chapter the details related to the X-ray diffraction measurements, the functionals and basis sets used in the DFT theoretical calculations, the protocols followed in the biological tests about the antiproliferative and pro-apoptotic activity, and the tests aimed at determining the main biological target will be reported.

The figure proposed at the beginning of the chapter is related to this source:
https://www.inquisitr.com/1790394/12-high-school-students-5-faculty-hospitalized-following-chemistry-lab-mishap-in-new-jersey/

9.1. Solvents and reagents

The solvents CH_2Cl_2 and CH_3CN were distilled over CaH_2, whereas acetone was refluxed over 4Å molecular sieves and distilled. Palladium precursors $[PdC_4(COOCH_3)_4]_n$ [1], [Pd(Me-PyCH$_2$SPh)(η^2-olefin)] (η^2-olefin = ma, fn, tmetc), [Pd(TMQ-Me)(η^2-dmfu)] [2], [Pd(Me-PyCH$_2$SPh)(η^3-C_3H_5)] ClO_4, [Pd(Me-PyCH$_2$SPh)(η^3-2-MeC_3H_4)]ClO_4 and [Pd(Me-PyCH$_2$SPh) (η^3-1,1-dimethylC_3H_3)] ClO_4 [3] were prepared according to published procedures. All other solvents and chemicals were commercial grade products and used as purchased.

9.2. Instruments

- NMR spectra were recorded on a Bruker Avance 400 or 300 MHz spectrometer; chemical shifts (δ) are reported in ppm related to the residual solvent signals.
- IR spectra (KBr) were recorded on a Perkin–Elmer Spectrum One spectrophotometer.
- IR spectra (neat) were recorded on a Thermo Fischer Scientific Nicolet 6700 FT-IR equipped with PIKE Technologies Gladi ATR or on a PerkinElmer BX II using ATR FT-IR technology.
- ICP–MS measurements were carried out by a Nexion 350X mass spectrometer (Perkin−Elmer) interfaced with a plasma torch in KED (Kinetic Energy Discrimination) procedure with He as collision gas.
- ESI–MS analysis were performed using a LCQ–Duo (Thermo−Finnigan) operating in positive ion mode. Instrumental parameters: capillary voltage 10 V, spray voltage 4.5 kV, capillary temperature 200 °C, mass scan range from 150 to 2000 amu, N_2 was used as sheath gas and the He pressure inside the trap was kept constant. The pressure directly read by an ion gauge (in the absence of N_2 stream) was 1.33 × 10−5 Torr. Sample solutions were prepared by dissolving the compounds in acetonitrile and directly infused into the ESI source by a syringe pump at 8 μL min−1 flow rate.
- Elemental analysis was carried out using an Elemental CHN ‘CUBO Micro Vario’ analyzer.

9.3. Computational details

The geometrical optimization of the complexes was carried out without symmetry constraints, using the hyper-GGA functional M06 [4, 5] in combination with polarized triple-ζ-quality basis sets (LAN2TZ(f)) [6, 7] and relativistic pseudopotential for the Pd atoms, a polarized double-ζ-quality basis set (LANL2DZdp)[8] with diffuse functions for the halogen atoms and a polarized double-ζ-quality basis set (6-31G(d,p)) for the other elements.

Solvent effects (dichloromethane, ε = 8.93) were included using CPCM [9, 10].

The "restricted" formalism was applied in all the calculations. By means of the stationary points characterized by IR simulation, the zero-point vibrational energies and thermodynamic parameters were obtained [11]. The software used was Gaussian 09 [12] and all the computational work was carried out on Intel based × 86-64 workstations.

9.4. *In vitro* cytotoxic activity

9.4.1. Growth inhibition assays (ovarian cancer lines)

Cell growth inhibition assays were carried out using three human ovarian cancer cell lines, A2780, A2780-R and SKOV-3. A2780 cells are cisplatin-sensitive whereas A2780-R and SKOV-3 cells are cisplatin-resistant. Cell lines were obtained from ATCC (Manassas, VA) and maintained in RPMI 1640, supplemented with 10% fetal bovine serum (FBS), penicillin (100 Units mL^{-1}), streptomycin (100 μg mL^{-1}) and glutamine (2 mM) (complete medium); the pH of the medium was 7.2 and the incubation was performed at 37°C in a 5% CO_2 atmosphere. Adherent cells were routinely used at 70% of confluence and passaged every 3 days by treatment with 0.05% trypsin-EDTA (Lonza).

Pure derivatives were added at serial dilutions and incubated for 3 days. After this time, cells were washed with PBS 1X and detached with trypsin. Cells were suspended in physiological solution and counted with a Z2 Coulter Counter (Coulter Electronics, Hialeah, FL, USA). The cell number/ml was determined as IC_{50} after 3 days of culture, when untreated cells are in log phase of cell growth [13, 14]. All stock solutions were diluted in complete medium to give final concentrations. Cisplatin was employed as a control for the cisplatin-sensitive A2780, and for the cisplatin-resistant SKOV3. Untreated cells were placed in every plate as negative control. The cells were exposed to the compounds in 1000 μL total volume, for 72 hours.

9.4.2. Apoptosis assays

Annexin V and Dead Cell assays on IB3-1 cells, untreated and treated for 72 h with increasing doses of Pd-complexes, were performed with the Muse cell analyzer (Millipore, Billerica, MA, USA) method, according to the instructions supplied by the manufacturer. This procedure utilizes Annexin V to detect PS (PhosphatidylSerine) on the external membrane of apoptotic cells. A dead cell marker is also used as indicator of cell membrane structural integrity. Four populations of cells can be distinguished using this assay: live, early apoptotic, late apoptotic and dead cells. Cells were washed with sterile PBS 1X, tripsinized, resuspended in the original medium and diluted (1:2) with the one step addition of the Muse Annexin V & Dead Cell reagent. After incubation of 20 min at room temperature, samples were analyzed, using Triton X 0.01%, as positive control [15]. Data from prepared samples are acquired and recorded utilizing the Annexin V and Dead Cell Software Module (Millipore, Billerica, MA, USA).

9.4.3. Immunofluorescence microscopy

Cells were seeded at a density of 2×10^5 cells/mL on coverslip glass (pre-treated with poly-D-Lysine, 1µg/mL) inserted in 6-well plates. After overnight culture at 37°C and 5% CO_2, cells were treated with different concentrations of compound 1 (40nM, 80nM, 320nM or 1µM) or cisplatin (10 µM) for 3, 6, and 12h for γH2AX antibody and for 3, 6, 12 and 24h for cytochrome c antibody. Cells were fixed in 4% paraformaldehyde/PBS (20 min, RT), permeabilized with 0.3 % Triton X-100/PBS (15min, RT) and blocked in 8% BSA/PBS (1h, RT). Cells were stained with mouse monoclonal anti-phospho-histone H2AX antibody (1:100 dilution in 1% BSA/PBS, at 4 °C, ON) or with mouse monoclonal anti-cytochrome c antibody (1:100 dilution in 1% BSA/PBS, at 4 °C, ON) that were obtained respectively from Millipore (Cat. # 05-636; Burlington, MA, US) and Cell signalling Technology (Cat. # 12963; Danvers, MA, US), and labelled with secondary antibodies (Alexa Fluor® 488 dye, 1:1000 dilution, RT, 2h) obtained from Cell signalling Technology (Cat. # 4408; Danvers, MA, US). To visualize DNA, cells were stained with DAPI 1mg/µL (1:1000 dilution in PBS, at 4 °C, 1min). Cells were washed three times with 1 × PBS after all incubations. All the coverslips were mounted in fluorSave™ reagent (Cat. # 345789; Millipore: Burlington, MA, US), the cells were examined with a Nikon Eclipse Ti fluorescence microscope, and the images were analysed with NIS Elements software version 3.0 (Nikon: Shinagawa, Tokyo, Japan).

9.4.4. Mitochondrial membrane potential measurement

Cells were seeded at a density of 2.5 × 10^4 cells/mL (compound 1) or 5 × 10^5 cells/mL (cisplatin) in triplicate on 6-well plates. After incubation overnight at 37°C in 5% CO2, cells were treated with different concentrations of compound 1 (40nM, 80nM, 320nM or 1µM) or cisplatin (10 µM) for 24, 48, and 72h. Working staining solution was prepared from the JC-1 powdered dye provided from Invitrogen (Cat. # T3168; Waltham, MA, US). in dimethyl sulfoxide (DMSO) at 1 mg/mL, which was then added to the cells (10µg/mL according to JC-1 cell staining conditions). Incubation was carried out at 37°C in 5% CO_2 incubator for 10 minutes. Cells were washed with 1× PBS, examined with a Nikon Eclipse Ti fluorescence microscope, and the images were analysed with NIS Elements software version 3.0 (Nikon: Shinagawa, Tokyo, Japan). JC-1 exists either as a diffuse green-fluorescent monomer at depolarized membrane potentials (altered) or as an orange-fluorescent J-aggregate at hyperpolarized membrane potentials (normal).

9.4.5. Caspase-3/7 activity detection

The expression of caspase-3/7 were determined by Caspase-Glo™ 3/7 Assay (Cat. # G8091; Promega: Madison, WI, US). Cells were seeded at a density of 10^5 cells/mL on 6-well plates. After incubation overnight at 37°C in 5% CO2, cells were treated with different concentrations of compound 1 (40nM, 80nM, 320nM or 1µM) or cisplatin (10 µM) for 24, 48, and 72h. Cells were collected by trypsinization and centrifugation. Cell lysis buffer (Tris HCl 1M pH 8, NaCl 5M, 10% glycerol, 1% NP-40, EDTA 0.5M) with Sodium orthovanadate 2mM (Cat. # S6508-50G, Sigma-Aldrich: St. Louis, MO, US), Sodium fluoride 5mM (Cat. # S7920-100G, Sigma-Aldrich: St. Louis, MO, US) and EDTA-free protease inhibitors 25x (Cat. # 04693132001, Roche: Basel, Switzerland). The cellular protein content was quantified by the Eppendorf BioPhotometer (Hamburg, Germany). The assay was performed in 1:1 ratio of Caspase-Glo® 3/7 reagent volume to protein extracts (40 µg) in triplicate in 96-well plate. The plate was incubated at RT for 30min. Luminescence was recorded using Tecan M1000 PRO instrument (Männedorf, Zürich, Switzerland).

9.5. Crystal data

9.5.1. Data collected at the University of Ferrara (prof. Valerio Bertolasi)

The crystal data for complexes **41a**, **42a**, **49d**, **60** and **85** were collected at room temperature using a Nonius Kappa CCD diffractometer with graphite monochromated Mo-Kα radiation. The data sets were integrated with the Denzo-SMN package [16] and corrected for Lorentz, polarization and absorption effects (SORTAV) [17]. The structure was solved by direct methods using the SIR97 [18] system of programs and refined using full-matrix least-squares with all non-hydrogen atoms anisotropically and hydrogens included on calculated positions, riding on their carrier atoms. In some cases, the program SQUEEZE was used to cancel out the effects of the disordered solvent. SQUEEZE is part of the PLATON program system which attempts to remove mathematically the effects of disordered solvent [19]. All calculations were performed using PLATON [19], SHELXL-97 [20] and PARST [21] implemented in WINGX [22] system of programs.

9.5.2. Data collected at the Elettra Synchrotron of Trieste (dr. Nicola Demitri)

The crystal data for complexes **4b**, **6a**, **10d**, **11b**, **26**, **40a**, **47b**, **48e, 74** and **87** were collected at 100K at the XRD1 beamline of the Elettra Synchrotron, Trieste (Italy) [23]. The data sets were integrated and corrected for Lorentz and polarization effects with the XDS package [24]. Data have been scaled using CCP4 Aimless code [25]. The structures were solved by direct methods using SHELXT program [26] and refined using full−matrix least−squares with all non−hydrogen atoms anisotropically and hydrogens included on calculated positions, riding on their carrier atoms. Geometric restrains on bond lengths and angles (DFIX, DANG) have been used in **7** models for disordered fragments (i.e. solvent CH_2Cl_2 molecule and BF_4^- ion). All calculations were performed using SHELXL−2017/1 [27]. The Coot program was used for structure building [28]. Pictures were prepared using Ortep3 [29] software.

9.6. Synthesis of compounds derived from functionalized purine bases

9.6.1. General procedure for the synthesis of alkyl-functionalized theophylline and theobromine (1)

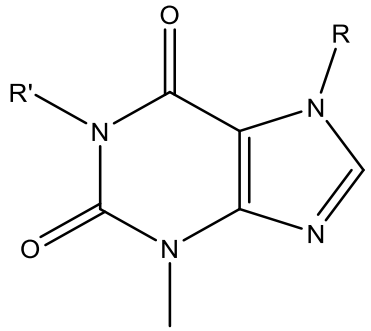

1a R= CH_3 R'= CH_3 (commercial caffeine)
1b R= CH_2Ph R'= CH_3
1c R= $CH_2C{\equiv}CPh$ R'= CH_3
1d R= CH_3 R'= CH_2Ph

1 g (5.55 mmol) of the starting xanthine (theophylline or theobromine) and 1.15 g (8.33 mmol) of K_2CO_3, were suspended in DMF (20 mL) in a 250 ml flask. To the suspension, 2 equivalents (11.1 mmol) of the appropriate alkyl halide (benzyl bromide for **1b** and **1d** and phenyl propargyl chloride for **1c**) were added and the resulting mixture was vigorously stirred overnight at R.T. The compounds were precipitated by addition of H_2O (ca. 100 mL).

7-benzyl-1,3-dimethylxanthine (1b)

White solid, yield 93 %.

^{1}H-NMR (400 MHz, $CDCl_3$, T=298K, ppm) δ: 3.43 (s, 3H, N-CH_3), 3.60 (s, 3H, N-CH_3), 5.52 (s, 2H, N-CH_2), 7.30-7.40 (m, 5H, Ph), 7.58 (s, 1H, NCHN).

^{13}C{^{1}H}-NMR ($CDCl_3$, T=298K, ppm) δ: 28.0 (N-CH_3), 29.8 (N-CH_3), 50.3 (N-CH_2), 107.0 (C^5), 128.0, 128.7, 129.1, 135.4 (C_{Ph}), 140.9 (N-CH-N), 148.9 (C^4), 151.7 (C=O), 155.3 (C=O).

ESI-MS (CH_3CN): m/z Calcd. for $C_{14}H_{15}N_4O_2$ $[M+H]^+$ 271.12; found: 271.06.

Anal. Calcd. for $C_{14}H_{14}N_4O_2$: C 62.21, H 5.22, N 20.73. Found: C 62.32, H 5.14, N 20.64.

7-phenylpropargyl-1,3-dimethylxanthine (1c)

Pink solid, yield 95 %.

^{1}H-NMR (400 MHz, $CDCl_3$, T=298K, ppm) δ: 3.45 (s, 3H, N-CH_3), 3.63 (s, 3H, N-CH_3), 5.42 (s, 2H, N-CH_2), 7.32-7.50 (m, 5H, Ph), 7.94 (s, 1H, NCHN).

^{13}C{^{1}H}-NMR ($CDCl_3$, T=298K, ppm) δ: 28.0 (N-CH_3), 29.8 (N-CH_3), 37.4 (N-CH_2), 80.5 (≡C-CH_2), 87.6 (≡C-Ph), 106.8 (C^5), 121.5, 128.5, 129.2, 131.9 (C_{Ph}), 140.6 (N-CH-N), 148.9 (C^4), 151.7 (C=O), 155.3 (C=O).

ESI-MS (CH_3CN): m/z Calcd. for $C_{16}H_{15}N_4O_2$ $[M+H]^+$ 295.12; found: 294.98.

Anal. Calcd. for $C_{16}H_{14}N_4O_2$: C 65.30, H 4.79, N 19.04. Found: C 65.49, H 4.83, N 18.89.

1-benzyl-3,7-dimethylxanthine (1d)

White solid, yield 95 %.

^{1}H-NMR (400 MHz, $CDCl_3$, T=298K, ppm) δ: 3.59 (s, 3H, N-CH_3), 4.00 (s, 3H, N-CH_3), 5.22 (s, 2H, N-CH_2), 7.25-7.55 (m, 5H, Ph), 7.51 (s, 1H, NCHN).

^{13}C{^{1}H}-NMR ($CDCl_3$, T=298K, ppm) δ: 29.8 (N-CH_3), 33.6 (N-CH_3), 44.5 (N-CH_2), 107.7 (C^5), 127.5, 128.4, 128.8, 137.3 (C_{Ph}), 141.5 (N-CH-N), 148.9 (C^4), 151.6 (C=O), 155.3 (C=O).

ESI ESI-MS (CH_3CN): m/z Calcd. for $C_{14}H_{15}N_4O_2$ $[M+H]^+$ 271.12; found: 271.14.

Anal. Calcd. for $C_{14}H_{14}N_4O_2$: C 62.21, H 5.22, N 20.73. Found: C 62.45, H 5.07, N 20.99.

9.6.2. General procedure for the synthesis of the imidazolium salts from caffeine and functionalized theophylline and theobromine with BF_4 as counterion (2)

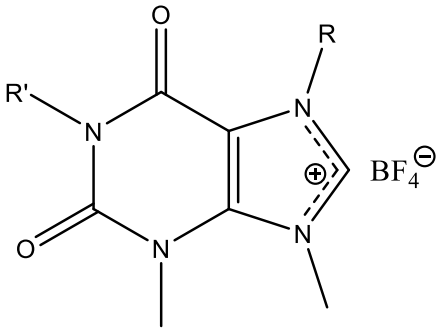

2a R= CH_3 R'= CH_3
2b R= CH_2Ph R'= CH_3
2c R= $CH_2C{\equiv}CPh$ R'= CH_3
2d R= CH_3 R'= CH_2Ph

1.8 mmol of functionalized xanthine **1a-d** (**1a** = commercial caffeine) was dissolved in ca. 25 mL of CH_3CN into a 50 mL flask. In the case of incomplete dissolution ultrasounds or moderate heating may be useful. One equivalent (1.8 mmol) of Me_3OBF_4 was added to the clear solution which was stirred for 5 min. Na_2CO_3 (ca. 100 mg) was then added to the mixture which was stirred again for 45 min. Further addition of 0.6 equivalents (1.1 mmol) of Me_3OBF_4 and 10 min of additional stirring led to virtual completion. The excess of base Na_2CO_3 and the $NaBF_4$ formed were filtered off and the solvent completely removed under reduced pressure. The solid was washed with three aliquots of a 2:1 mixture of Et_2O/CH_2Cl_2 on a sintered glass filter, dried under vacuum and characterized.

1,3,7,9-tetramethylxanthinium tetrafluoroborate (2a)

White solid, yield 97 %. mp = 132-133 °C

^{1}H-NMR (400 MHz, CD_3CN, T=298K, ppm) δ: 3.35 (s, 3H, N-CH_3), 3.74 (s, 3H, N-CH_3), 4.08 (s, 6H, 2N-CH_3), 8.47 (s, 1H, NCHN).

^{13}C{^{1}H}-NMR (CD_3CN, T=298K, ppm) δ: 28.7 (N-CH_3), 31.8 (N-CH_3), 36.3 (N-CH_3), 37.6 (N-CH_3), 109.1 (C^5), 139.3(N-CH-N), 140.2 (C^4), 151.1 (C=O), 154.2 (C=O).

ESI-MS (CH_3CN): m/z Calcd. for $C_9H_{13}N_4O_2$ $[M]^+$ 209.10; found: 209.07.

Anal. Calcd. for $C_9H_{13}BF_4N_4O_2$: C 36.52, H 4.43, N 18.93. Found: C 36.74, H 4.61, N 18.88

7-benzyl-1,3,9-trimethylxanthinium tetrafluoroborate (2b)

White solid, yield 91 %. mp = 251-253 °C

^{1}H-NMR (400 MHz, CD_3CN, T=298K, ppm) δ: 3.33 (s, 3H, N-CH_3), 3.73 (s, 3H, N-CH_3), 4.06 (s, 3H, N-CH_3), 5.70 (s, 2H, N-CH_2), 7.45-7.48 (m, 5H, Ph), 8.56 (s, 1H, NCHN).

^{13}C{^{1}H}-NMR (CD_3CN, T=298K, ppm) δ: 28.8 (N-CH_3), 31.8 (N-CH_3), 37.9 (N-CH_3), 52.7 (N-CH_2), 108.4 (C^5), 129.2, 129.7, 129.8, 133.9 (C_{Ph}), 138.9(N-CH-N), 140.6 (C^4), 151.0 (C=O), 154.0 (C=O).

ESI-MS (CH_3CN): m/z Calcd. for $C_{15}H_{17}N_4O_2$ $[M]^+$ 285.13; found: 285.04.

Anal. Calcd. for $C_{15}H_{17}BF_4N_4O_2$: C 48.41, H 4.60, N 15.06. Found: C 48.39, H 4.64, N 15.18.

7-phenylpropargyl-1,3,9-trimethylxanthinium tetrafluoroborate (2c)

White solid, yield 92 % (612 mg). mp = 231 °C

^{1}H-NMR (400 MHz, CD_3CN, T=298K, ppm) δ: 3.37 (s, 3H, N-CH_3), 3.76 (s, 3H, N-CH_3), 4.14 (s, 3H, N-CH_3), 5.57 (s, 2H, N-CH_2), 7.42-7.60 (m, 5H, Ph), 8.85 (s, 1H, NCHN). ^{13}C{^{1}H}-NMR (CD_3CN, T=298K, ppm) δ: 28.8 (N-CH_3), 31.9 (N-CH_3), 37.9 (N-CH_3), 40.7 (N-CH_2), 79.2 (≡$\underline{C}$-CH_2), 89.4 (≡$\underline{C}$-Ph), 108.3 (C^5), 121.6, 129.4, 130.4, 132.5 (C_{Ph}), 138.8 (N-CH-N), 140.6 (C^4), 151.0 (C=O), 154.0 (C=O).

ESI-MS (CH_3CN): m/z Calcd. for $C_{17}H_{17}N_4O_2$ $[M]^+$ 309.13; found: 309.02.

Anal. Calcd. for $C_{17}H_{17}BF_4N_4O_2$: C 51.54, H 4.33, N 14.14. Found: C 51.73, H 4.28, N 14.31.

1-benzyl-3,7,9-trimethylxanthinium tetrafluoroborate (2d)

White solid, yield 94 % (621 mg). mp = 171-172 °C

^{1}H-NMR (400 MHz, CD_3CN, T=298K, ppm) δ: 3.74 (s, 3H, N-CH_3), 4.08 (s, 3H, N-CH_3), 4.09 (s, 3H, N-CH_3), 5.17 (s, 2H, N-CH_2), 7.28-7.42 (m, 5H, Ph), 8.48 (s, 1H, NCHN).

^{13}C{^{1}H}-NMR (CD_3CN, T=298K, ppm) δ: 31.9 (N-CH_3), 36.4 (N-CH_3), 37.6 (N-CH_3), 45.6 (N-CH_2), 109.2 (C^5), 128.3, 128.6, 129.1, 137.1 (C_{Ph}), 139.4 (N-CH-N), 140.5 (C^4), 151.0 (C=O), 154.1 (C=O).

ESI-MS (CH_3CN): m/z Calcd. for $C_{15}H_{17}N_4O_2$ $[M]^+$ 285.13; found: 285.11.

Anal. Calcd. for $C_{15}H_{17}BF_4N_4O_2$: C 48.41, H 4.60, N 15.06. Found: C 48.65, H 4.72, N 15.14.

9.6.3. Synthesis of the imidazolium salts from caffeine and functionalized theophylline and theobromine with chloride as counterion (3)

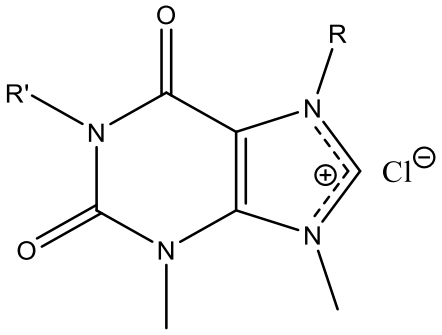

3a R= CH_3 R'= CH_3
3b R= CH_2Ph R'= CH_3
3d R= CH_3 R'= CH_2Ph

1,3,7,9-tetramethylxanthinium chloride (3a)

In a 500 mL flask 0.3562 g (1.203 mmol) of the imidazolium salt **2a** was dissolved in ca. 200 mL of water. The resulting solution was treated with 503.9 mg (1.203 mmol) of $AsPh_4Cl$ and stirred at R.T. for 30 min. The precipitated $AsPh_4BF_4$ was removed by filtration on a millipore membrane filter and the solvent was removed under reduced pressure.

The white solid was washed with ca. 20 mL of dichloromethane and filtered off on a gooch.

0.2933 g of **3a** was obtained (yield 99%).

^{1}H-NMR (400 MHz, CD_3CN, T = 298K, ppm) δ: 3.34 (s, 3H, NCH_3), 3.75 (s, 3H, NCH_3), 4.13 (s, 3H, NCH_3), 4.21 (s, 3H, NCH_3), 10.03 (s, 1H, NCHN).

^{13}C{^{1}H}-NMR (CD_3CN, T = 298K, ppm) δ: 28.6 (CH_3, NCH_3), 31.8 (CH_3, NCH_3), 36.2 (CH_3, NCH_3), 37.5 (CH_3, NCH_3), 108.8 (C, C^5), 140.1 (C, C^4), 140.4(CH, N-CH-N), 151.1 (C, C=O), 154.2 (C, C=O).

IR (KBr): $\nu_{C=O}$ = 1719 cm^{-1}, 1675 cm^{-1}, ν_{C-O} = 1304 cm^{-1}, 1264 cm^{-1}

7-benzyl-1,3,9-trimethylxanthinium tetrafluoroborate (3b)

Compound **3b** was prepared in analogues manner as that described for **3a** starting from 0.4004 g (1.076 mmol) of **2b** and 0.4506 g of $AsPh_4Cl$ (1.076 mmol).

0.3434 g (yield 98%) of **3b** was obtained.

^{1}H-NMR (400 MHz, CD_3CN, T = 298K, ppm) δ: 3.33 (s, 3H, NCH_3), 3.73 (s, 3H, NCH_3), 4.10 (s, 3H, NCH_3), 5.72 (s, 2H, NCH_2), 7.44-7.50 (m, 5H, Ph), 8.92 (s, 1H, NCHN).

$^{13}C\{^{1}H\}$-NMR (CD_3CN, T = 298K, ppm) δ: 28.2 (CH_3, NCH_3), 31.2 (CH_3, NCH_3), 37.3 (CH_3, NCH_3), 52.0 (CH_2, NCH_2), 107.8 (C, C^5), 128.6-133.4 (Ph), 138.6 (CH, NCHN), 140.0 (C, C^4), 150.4 (C, C=O), 153.4 (C, C=O).

IR (KBr): $\nu_{C=O}$ = 1717 cm^{-1}, 1671 cm^{-1}, ν_{C-O} = 1267 cm^{-1}

1-benzyl-3,7,9-trimethylxanthinium tetrafluoroborate (3d)

Compound **3c** was prepared in analogues manner as that described for **3a** starting from 0.3512 g (0.9438 mmol) of **2d** and 0.3952 g of $AsPh_4Cl$ (0.9438 mmol).

0.3021 g (yield 99%) of **3d** was obtained.

^{1}H-NMR (400 MHz, CD_3CN, T = 298K, ppm) δ: 3.73 (s, 3H, NCH_3), 4.09 (s, 3H, NCH_3), 4.10 (s, 3H, NCH_3), 5.16 (s, 2H, NCH_2), 7.33-7.39 (m, 5H, Ph), 8.82 (s, 1H, NCHN).

$^{13}C\{^{1}H\}$-NMR (CD_3CN, T = 298K, ppm) δ: 31.3 (CH_3, NCH_3), 35.8 (CH_3, NCH_3), 37.0 (CH_3, NCH_3), 45.0 (CH_2, NCH_2), 108.6 (C, C^5), 127.7-136.5 (Ph), 139.0 (CH, NCHN), 139.8 (C, C^4), 150.4 (C, C=O), 153.5 (C, C=O).

IR (KBr): $\nu_{C=O}$ = 1722 cm^{-1}, 1674 cm^{-1}

9.6.4. Synthesis of silver bis(purine-based NHC) complexes with BF_4 as counterion (4)

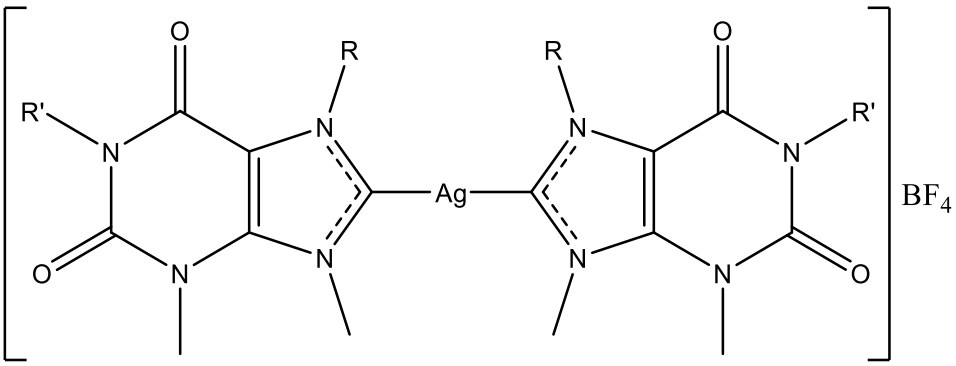

4a R= CH_3 R'= CH_3
4b R= CH_2Ph R'= CH_3
4c R= $CH_2C{\equiv}CPh$ R'= CH_3
4d R= CH_3 R'= CH_2Ph

Synthesis of 1:1 mixture of 4a and $AgBF_4$

0.1967 g (0.6644 mmol) of the imidazolium salt **2a** was dissolved in 30 mL of anhydrous CH_3CN in a 100 mL two-necked flask and 0.0924 g (0.3987 mmol) of Ag_2O was added under inert atmosphere (Ar). The mixture was stirred for 28 h at R.T. in the dark.

The solution was filtered on millipore membrane filter to remove the Ag_2O in excess. The resulting clear solution was concentrated under vacuum and the title complex precipitated by addition of diethylether. The white complex was filtered off on a gooch, repeatedly washed with diethylether and *n*–pentane and dried under vacuum.

0.2463 g (yield 92%) of 1:1 mixture of **4a** and $AgBF_4$ was obtained.

^{1}H-NMR (400 MHz, CD_3CN, T = 298K, ppm) δ: 3.33 (s, 6H, $2NCH_3$), 3.77 (s, 6H, $2NCH_3$), 4.10 (s, 6H, $2NCH_3$), 4.16 (s, 6H, $2NCH_3$).

^{13}C{^{1}H}-NMR (CD_3CN, T = 298K, ppm) δ: 28.7 (CH_3, NCH_3), 32.2 (CH_3, NCH_3), 38.7 (CH_3, NCH_3), 40.1 (CH_3, NCH_3), 110.3 (C, C^5), 141.5 (C, C^4), 151.8 (C, C=O), 154.6 (C, C=O), 187.4 (C, carbene).

IR (KBr): ν_{CO} = 1703, 1662 cm^{-1}, ν_{BF} =1053, 1086 cm^{-1}

Synthesis of 1:1 mixture of 4b and $AgBF_4$

The 1:1 mixture of **4b** and $AgBF_4$ was prepared in analogues manner as that described for **4a**/$AgBF_4$, with a reaction time of 24 hours, starting from 0.1564 g of **2b** and 0.0584 g of Ag_2O.

0.2077 g (yield 96%) of 1:1 mixture of **4b** and $AgBF_4$ was obtained.

^{1}H-NMR (400 MHz, CD_3CN, T = 298K, ppm) δ: 3.30 (s, 6H, $2NCH_3$), 3.76 (s, 6H, $2NCH_3$), 4.08 (s, 6H, $2NCH_3$), 5.66 (s, 4H, $2NCH_2$), 7.28-7.33 (m, 10H, 2Ph).

$^{13}C\{^{1}H\}$-NMR (CD_3CN, T = 298K, ppm) δ: 27.9 (CH_3, NCH_3), 31.4 (CH_3, NCH_3), 39.6 (CH_3, NCH_3), 53.2 (CH_2, NCH_2), 109.0 (C, C^5), 127.4-136.7 (Ph), 141.0 (C, C^4), 150.9 (C, C=O), 153.6 (C, C=O), 187.1 (C, carbene).

IR (KBr): ν_{CO} = 1711, 1668 cm^{-1}, ν_{BF} =1046, 1084 cm^{-1}

Synthesis of 1:1 mixture of 4c and $AgBF_4$

The 1:1 mixture of **4c** and $AgBF_4$ was prepared in analogues manner as that described for **4a**/$AgBF_4$, with a reaction time of 24 hours, starting from 0.2218 g of **2c** and 0.0779 g of Ag_2O.

0.2569 g (yield 91%) of 1:1 mixture of **4c** and $AgBF_4$ was obtained.

^{1}H-NMR (400 MHz, CD_3CN, T=298K, ppm) δ: 3.35 (s, 6H, $2NCH_3$), 3.70 (s, 6H, $2NCH_3$), 4.03 (s, 6H, $2NCH_3$), 5.40 (s, 4H, $2NCH_2$), 7.27-7.43 (m, 10H, 2Ph).

$^{13}C\{^{1}H\}$-NMR (CD_3CN, T=298K, ppm) δ: 27.9 (CH_3, NCH_3), 31.4 (CH_3, NCH_3), 40.1 (CH_2, NCH_2), 40.2 (CH_3, NCH_3), 82.5 (C, CH_2-C≡), 88.7 (C, Ph-C≡), 108.7 (C, C^5), 121.3-131.8 (Ph), 140.4 (C, C^4), 150.7 (C, C=O), 153.5 (C, C=O), 187.1 (C, carbene).

IR (KBr): $\nu_{C\equiv C}$= 2218 cm^{-1}, ν_{CO}= 1710, 1668 cm^{-1}, ν_{BF}=1054 cm^{-1}.

Synthesis of 1:1 mixture of 4d and $AgBF_4$

The 1:1 mixture of **4d** and $AgBF_4$ was prepared in analogues manner as that described for **4a**/$AgBF_4$, with a reaction time of 24 hours, starting from 0.1505 g of **2d** and 0.0562 g of Ag_2O.

0.1801 g (yield 93%) of 1:1 mixture of **4d** and $AgBF_4$ was obtained.

^{1}H-NMR (400 MHz, CD_3CN, T = 298K, ppm) δ: 3.77 (s, 6H, $2NCH_3$), 4.10 (s, 6H, $2NCH_3$), 4.15 (s, 6H, $2NCH_3$), 5.16 (s, 4H, $2NCH_2$), 7.28-7.40 (m, 10H, 2Ph).

$^{13}C\{^{1}H\}$-NMR (CD_3CN, T = 298K, ppm) δ: 32.1 (CH_3, NCH_3), 38.5 (CH_3, NCH_3), 39.9 (CH_3, NCH_3), 45.3 (CH_2, NCH_2), 110.2 (C, C^5), 128.0-137.8 (Ph), 141.6 (C, C^4), 151.6 (C, C=O), 154.3 (C, C=O), 187.5 (C, carbene).

IR (KBr): ν_{CO} = 1709, 1665 cm^{-1}, ν_{BF} =1050 and 1085 cm^{-1}

9.6.5. Synthesis of the silver bis(purine-based NHC) complexes with $AgCl_2$ as counterion (5)

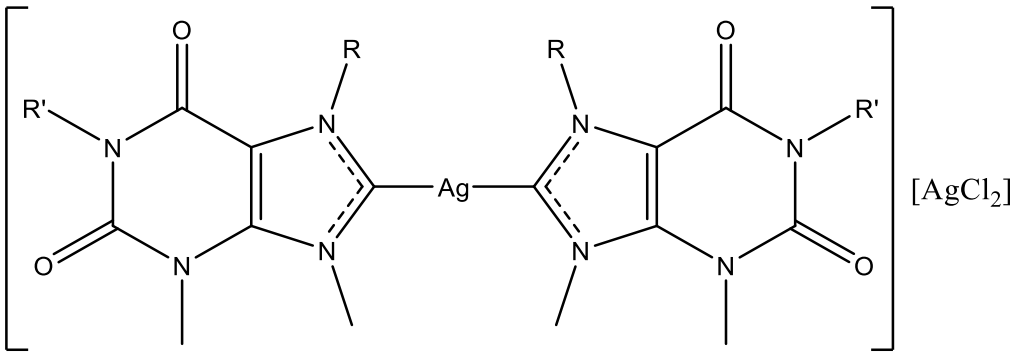

5a R= CH_3 R'= CH_3
5b R= CH_2Ph R'= CH_3
5d R= CH_3 R'= CH_2Ph

Synthesis of the complex 5a

0.1425 g (0.5824 mmol) of the imidazolium salt **3a** was dissolved in 35 mL of anhydrous CH_3CN in a 100 mL two-necked flask and 0.0742 g (0.3203 mmol) of Ag_2O was added under inert atmosphere (Ar). The mixture was stirred for 4 h at R.T. in the dark and the solvent was subsequently removed under reduced pressure.

The solid was dissolved in ca. 200 mL of dichloromethane and the resulting mixture was filtered on millipore membrane filter to remove the Ag_2O in excess. The clear solution was concentrated under vacuum and the title complex precipitated by addition of diethylether.

The white complex was filtered off on a gooch, repeatedly washed with diethylether and *n*–pentane. 0.1214 g (yield 60%) of **5a** was obtained.

^{1}H-NMR (400 MHz, CD_2Cl_2, T = 298K, ppm) δ: 3.41 (s, 6H, $2NCH_3$), 3.84 (s, 6H, $2NCH_3$), 4.17 (s, 6H, $2NCH_3$), 4.24 (s, 6H, $2NCH_3$).

^{13}C{^{1}H}-NMR (d^6-DMSO, T = 298K, ppm) δ: 28.7 (CH_3, NCH_3), 31.2 (CH_3, NCH_3), 32.0 (CH_3, NCH_3), 38.3 (CH_3, NCH_3), 109.3 (C, C^5), 140.9 (C, C^4), 151.0 (C, C=O), 153.7 (C, C=O), 207.0 (C, carbene).

ESI-MS (CH_3CN): m/z 525.04 $[Ag(NHC)_2]^+$.

IR (KBr): $\nu_{C=O}$ = 1709 cm^{-1}, 1669 cm^{-1}

Synthesis of the complex 5b

Complex **5b** was prepared in analogues manner as that described for **5a** starting from 0.3434 g (1.071 mmol) of **3b**, and 0.1303 g (0.5620 mmol) of Ag_2O.

0.3069 g (yield 67%) of **5b** was obtained.

^{1}H-NMR (400 MHz, $CDCl_3$, T = 298K, ppm) δ: 3.31 (s, 6H, $2NCH_3$), 3.73 (s, 6H, $2NCH_3$), 4.16 (s, 6H, $2NCH_3$), 5.62 (s, 4H, $2NCH_2$), 7.20-7.41 (m, 10H, 2Ph).

^{13}C{^{1}H}-NMR ($CDCl_3$, T = 298K, ppm) δ: 28.8 (CH_3, NCH_3), 32.0 (CH_3, NCH_3), 40.1 (CH_3, NCH_3), 54.1 (CH_2, NCH_2), 109.1 (C, C^5), 128.3-135.5 (Ph), 140.3 (C, C^4), 150.6 (C, C=O), 153.1 (C, C=O), 188.1 (C, carbene).

ESI-MS (CH_3CN): m/z 677.11 $[Ag(NHC)_2]^+$.

IR (KBr): $\nu_{C=O}$ = 1713 cm^{-1}, 1673 cm^{-1}

Synthesis of the complex 5d

Complex **5d** was prepared in analogues manner as that described for **5a** starting from 0.1341 g (0.4181 mmol) of **3d**, and 0.0509 g (0.2195 mmol) of Ag_2O.

0.1249 g (yield 70%) of **5d** was obtained.

^{1}H-NMR (400 MHz, $CDCl_3$, T = 298K, ppm) δ: 3.83 (s, 6H, $2NCH_3$), 4.15 (s, 6H, $2NCH_3$), 4.19 (s, 6H, $2NCH_3$), 5.19 (s, 4H, $2NCH_2$), 7.29-7.50 (m, 10H, 2Ph).

^{13}C{^{1}H}-NMR (d^6-DMSO, T = 298K, ppm) δ: 31.2 (CH_3, NCH_3), 32.1 (CH_3, NCH_3), 38.3 (CH_2, NCH_2), 109.3 (C, C^5), 127.7-137.3 (Ph), 141.3 (C, C^4), 150.9 (C, C=O), 153.5 (C, C=O), 206.9 (C, carbene).

ESI-MS (CH_3CN): m/z 677.08 $[Ag(NHC)_2]^+$.

IR (KBr): $\nu_{C=O}$ = 1711 cm^{-1}, 1674 cm^{-1}

9.6.6. Synthesis of the mixed purine-based NHC/PPh_3 palladium η^3-allyl complexes (6)

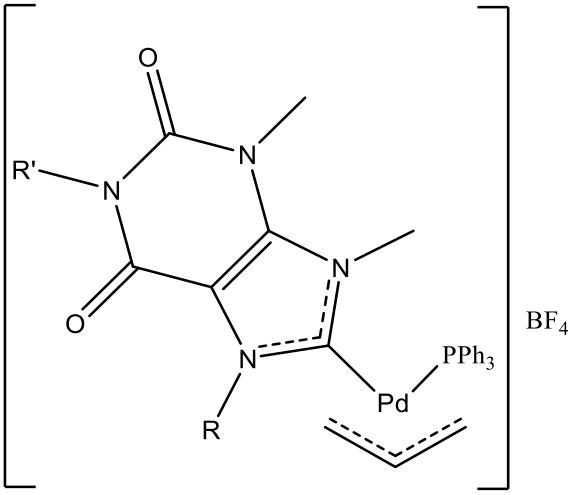

6a R= CH_3 R'= CH_3
6b R= CH_2Ph R'= CH_3
6c R= $CH_2C{\equiv}CPh$ R'= CH_3
6d R= CH_3 R'= CH_2Ph

Synthesis of the complex 6a

0.0195 g (0.053 mmol) of the $[Pd(\mu\text{-}Cl)(\eta^3\text{-}C_3H_5)]_2$ dimer and 0.0279 g (0.106 mmol) of PPh_3 were dissolved in ca. 20 mL of anhydrous CH_3CN in a 50 mL two-necked flask under inert atmosphere (Ar). The resulting mixture was treated with 0.0388 g (0.048 mmol) of **4a**/$AgBF_4$ and stirred at RT for ca. 15 min.

The precipitated AgCl was removed by filtration on a millipore membrane filter.

Addition of diethylether to the concentrated solution yields the precipitation of the complex **6a** as a yellow solid which was filtered off on a gooch and washed with *n*-pentane.

0.0576 g of **6a** was obtained (yield 85%).

^{1}H-NMR (400 MHz, T=298K, $CDCl_3$, ppm) δ: 3.16 (d, 1H, J= 13.4 Hz, *anti* allyl-H *trans* C), 3.26 (d, 1H, J= 13.7 Hz, *anti* allyl-H *trans* C), 3.27 (m, 1H, *anti* allyl-H *trans* P), 3.38 (s, 6H, $2NCH_3$), 3.59 (s, 6H, $2NCH_3$), 3.61 (s, 6H, $2NCH_3$), 3.68 (m, 1H, *anti* allyl-H *trans* P), 3.76 (s, 3H, NCH_3), 3.78 (s, 3H, NCH_3), 4.11 (d, 1H, J= 8.4 Hz, *syn* allyl-H *trans* C), 4.19 (d, 1H, J= 7.6 Hz, *syn* allyl-H *trans* C), 4.59 (dd, 1H, $J_{H\text{-}H}$=$J_{H\text{-}P}$= 5.9 Hz, *syn* allyl-H *trans* P), 4.80 (dt, 1H, $J_{H\text{-}H}$=$J_{H\text{-}P}$= 6.6 Hz, *syn* allyl-H *trans* P), 5.71 (m, 1H, *central* allyl-H), 5.99 (m, 1H, *central* allyl-H), 7.25-7.53 (m, 30H, 6Ph). ^{13}C{^{1}H}-NMR (T=298K, $CDCl_3$, ppm) δ: 28.6 (CH_3, NCH_3), 31.7 (CH_3, NCH_3), 36.9 (CH_3, NCH_3), 37.1 (CH_3, NCH_3), 38.7 (CH_3, NCH_3), 38.9 (CH_3, NCH_3), 68.5 (d, CH_2, $J_{C\text{-}P}$= 28.5 Hz, allyl *trans P*), 69.3 (d, CH_2, $J_{C\text{-}P}$= 27.6 Hz, allyl *trans P*), 69.4 (d, CH_2, $J_{C\text{-}P}$= 1.8 Hz, allyl *trans C*), 69.4 (d, CH_2, $J_{C\text{-}P}$= 1.7 Hz, allyl *trans C*), 110.4 (C, C^5), 110.6 (C, C^5), 121.4 (d, CH, $J_{C\text{-}P}$= 5.4 Hz, *central* allyl), 122.8 (d, CH, $J_{C\text{-}P}$= 5.1 Hz, *central* allyl), 129.2-133.2 (Ph), 141.0 (C, C^4), 141.1 (C, C^4), 150.4

(C, C=O), 153.0 (C, C=O), 185.8 (d, C, J_{C-P}= 19.7 Hz, carbene), 186.2 (d, C, J_{C-P}= 19.3 Hz, carbene). $^{31}P\{^{1}H\}$-NMR (T=298K, $CDCl_3$, ppm) δ: 25.9, 25.8.

IR (KBr): ν_{CO}= 1709, 1668 cm^{-1}, ν_{BF}=1059 cm^{-1}.

Anal. Calcd. for $C_{30}H_{32}BF_4N_4O_2PPd$: C 51.12, H 4.58, N 7.95. Found: C 51.42, H 4.32, N 8.10.

Synthesis of the complex 6b

Complex **6b** was prepared in analogues manner as that described for **6a** starting from 0.0144 g of $[Pd(\mu\text{-}Cl)(\eta^3\text{-allyl})]_2$, 0.0358 g of **4b**/$AgBF_4$ and 0.0196 g of PPh_3.

0.0511 g (yield 88%) of **6b** was obtained.

^{1}H-NMR (400 MHz, T=298K, $CDCl_3$, ppm) δ: 2.38 (m, 1H, *anti* allyl-H *trans* P), 2.93 (d, 1H, J= 13.6 Hz, *anti* allyl-H *trans* C), 3.17 (d, 1H, J= 13.4 Hz, *anti* allyl-H *trans* C), 3.40 (s, 3H, NCH_3), 3.42 (s, 3H, NCH_3), 3.60 (m, 1H, *anti* allyl-H *trans* P), 3.62 (s, 3H, NCH_3), 3.63 (s, 3H, NCH_3), 3.86 (s, 3H, NCH_3), 3.96 (dd, 1H, J_{H-H} = 6.8 Hz, J_{H-P} = 6.8 Hz, *syn* allyl-H *trans* P), 4.09 (d, 1H, J= 6.4 Hz, *syn* allyl-H *trans* C), 4.19 (d, 1H, J= 6.1 Hz, *syn* allyl-H *trans* C), 4.70 (dd, 1H, J_{H-H} = 7.7 Hz, J_{H-P} = 7.7 Hz, *syn* allyl-H *trans* P), 4.80 and 5.57 (AB system, 2H, J=14.8 Hz, NCH_2), 5.03 and 5.63 (AB system, 2H, J=15.0 Hz, NCH_2), 5.22 (m, 1H, *central* allyl-H), 5.97 (m, 1H, *central* allyl-H), 7.00-7.60 (m, 40H, 8Ph).

$^{13}C\{^{1}H\}$-NMR (T=298K, $CDCl_3$, ppm) δ: 28.7 (CH_3, NCH_3), 28.8 (CH_3, NCH_3), 31.9 (CH_3, NCH_3), 39.3 (CH_3, NCH_3), 39.5 (CH_3, NCH_3), 52.4 (CH_2, NCH_2), 52.7 (CH_2, NCH_2), 68.6 (d, CH_2, J_{C-P}= 1.9 Hz, allyl *trans*-C), 68.7 (d, CH_2, J_{C-P}= 1.8 Hz, allyl *trans*-C), 70.1 (d, CH_2, J_{C-P}= 27.7 Hz, allyl *trans*-P), 70.8 (d, CH_2, J_{C-P}= 27.8 Hz, allyl *trans*-P), 110.1 (C, C^5), 110.3 (C, C^5), 121.0 (CH, *central* allyl), 122.8 (CH, *central* allyl), 127.2-135.3 (Ph), 141.1 (C^4), 141.3 (C^4), 143.7 (Ph), 150.3 (C, C=O), 150.4 (C, C=O), 152.8 (C, C=O), 152.9 (C, C=O), 187.5 (d, C, J_{C-P}= 18.5 Hz, carbene), 187.8 (d, C, J_{C-P}= 18.4 Hz, carbene). $^{31}P\{^{1}H\}$-NMR (T=298K, $CDCl_3$, ppm) δ: 25.6, 26.3

IR (KBr): ν_{CO}= 1709, 1668 cm^{-1}, ν_{BF}=1056 cm^{-1}

Anal. Calcd. for $C_{36}H_{36}BF_4N_4O_2PPd$: C 55.37, H 4.65, N 7.17. Found: C 55.12, H 4.80, N 7.38.

Synthesis of the complex 6c

Complex **6c** was prepared in analogues manner as that described for **6a** starting from 0.0160 g of $[Pd(\mu\text{-}Cl)(\eta^3\text{-allyl})]_2$, 0.0418 g of **4c**/$AgBF_4$ and 0.0218 g of PPh_3.

0.0559 g (yield 84%) of **6c** was obtained.

^{1}H-NMR (400 MHz, T=298K, $CDCl_3$, ppm) δ: 2.97 (d, 1H, J= 13.3 Hz, *anti* allyl-H *trans* C), 3.20 (d, 1H, J= 12.8 Hz, *anti* allyl-H *trans* C), 3.36 (m, 1H, *anti* allyl-H *trans* P), 3.42 (s, 6H, $2NCH_3$), 3.61 (s, 3H, NCH_3), 3.62 (s, 3H, NCH_3), 3.68 (s, 3H, NCH_3), 3.76 (m, 1H, *anti* allyl-H *trans* P), 3.82 (s, 3H, NCH_3), 4.04 (d, 1H, J= 6.1 Hz, *syn* allyl-H *trans* C), 4.22 (d, 1H, J= 6.4 Hz, *syn* allyl-H *trans*

C), 4.71 (dd, 1H, J_{H-H} = 6.0 Hz, J_{H-P} = 6.8 Hz,, *syn* allyl-H *trans* P), 4.82 and 5.28 (AB system, 2H, J=17.2 Hz, NCH_2), 4.88 and 5.47 (AB system, 2H, J=17.6 Hz, NCH_2), 4.89 (m, 1H, *syn* allyl-H *trans* P), 5.63 (m, 1H, *central* allyl-H), 6.03 (m, 2H, *central* allyl-H), 7.15-7.46 (m, 40H, 8Ph). $^{13}C\{^1H\}$-NMR (T=298K, $CDCl_3$, ppm) δ: 28.7 (CH_3, NCH_3), 31.8 (CH_3, NCH_3), 39.4 (CH_3, NCH_3), 40.0 (CH_2, NCH_2), 68.9 (CH_2, allyl *trans*-C), 69.3 (CH_2, allyl *trans*-C), 69.9 (d, CH_2, J_{C-P}= 27.5 Hz, allyl *trans*-P), 70.4 (d, CH_2, J_{C-P}= 27.6 Hz, allyl *trans*-P), 81.6 (C, ≡C-CH_2), 81.9 (C, ≡C-CH_2), 86.5 (C, ≡C-Ph), 87.4 (C, ≡C-Ph), 109.6 (C, C^5), 109.7 (C, C^5), 121.4 (d, CH, J_{C-P}= 5.1 Hz, *central* allyl), 122.7 (d, CH, J_{C-P}= 5.2 Hz, *central* allyl), 128.4-134.0 (Ph), 141.2 (C, C^4), 150.4 (C, C=O), 152.6 (C, C=O), 152.7 (C, C=O), 187.3 (d, C, J_{C-P}= 18.8 Hz, carbene), 187.7 (d, C, J_{C-P}= 18.5 Hz, carbene). $^{31}P\{^1H\}$-NMR (T=298K, $CDCl_3$, ppm) δ: 25.4, 25.9.

IR (KBr): ν_{CO}= 1709, 1667 cm^{-1}, ν_{BF}=1058 cm^{-1}

Anal. Calcd. for $C_{38}H_{36}BF_4N_4O_2PPd$: C 56.70, H 4.51, N 6.96. Found: C 56.52, H 4.78, N 7.12.

Synthesis of the complex 6d

Complex **6d** was prepared in analogues manner as that described for **6a** starting from 0.0154 g of $[Pd(\mu\text{-}Cl)(\eta^3\text{-allyl})]_2$, 0.0383 g of **4d**/$AgBF_4$ and 0.0210 g of PPh_3.

0.0522 g (yield 84%) of **6d** was obtained.

^1H-NMR (400 MHz, T=298K, $CDCl_3$, ppm) δ: 3.13 (d, 1H, J= 13.4 Hz, *anti* allyl-H *trans* C), 3.28 (d+m, 2H, J= 13.2 Hz, *anti* allyl-H *trans* C), 3.29 (m, 1H, *anti* allyl-H *trans* P), 3.58 (s, 3H, NCH_3), 3.59 (s, 3H, NCH_3), 3.60 (s, 3H, NCH_3), 3.62 (s, 3H, NCH_3), 3.68 (m, 1H, *anti* allyl-H *trans* P), 3.74 (s, 3H, NCH_3), 3.81 (s, 3H, NCH_3), 4.13 (d, 1H, J= 7.4 Hz, *syn* allyl-H *trans* C), 4.21 (d, 1H, J= 7.8 Hz, *syn* allyl-H *trans* C), 4.58 (dd, 1H, J_{H-H}=J_{H-P}= 5.2 Hz, *syn* allyl-H *trans* P), 4.79 (dd, 1H, J_{H-H} = 5.5 Hz, J_{H-P} = 5.5 Hz, *syn* allyl-H *trans* P), 5.15 (s, 4H, 2 NCH_2), 5.70 (m, 1H, *central* allyl-H), 5.99 (m, 1H, *central* allyl-H), 7.25-7.47 (m, 40H, 8Ph). $^{13}C\{^1H\}$-NMR (T=298K, $CDCl_3$, ppm) δ: 31.8 (CH_3, NCH_3), 36.9 (CH_3, NCH_3), 37.0 (CH_3, NCH_3), 38.7 (CH_3, NCH_3), 38.9 (CH_3, NCH_3), 45.1 (CH_2, NCH_2), 68.3 (d, CH_2, J_{C-P}= 28.4 Hz, allyl *trans*-P), 69.1 (d, CH_2, J_{C-P}= 28.1 Hz, allyl *trans*-P), 69.2 (d, CH_2, J_{C-P}= 1.7 Hz, allyl *trans*-C), 69.4 (d, CH_2, J_{C-P}= 1.9 Hz, allyl *trans*-C), 110.7 (C, C^5), 121.3 (d, CH, J_{C-P}= 5.5 Hz, *central* allyl), 122.8 (d, CH, J_{C-P}= 5.3 Hz, *central* allyl), 127.9-136.4 (Ph), 141.0 (C, C^4), 141.1 (C, C^4), 150.2 (C, C=O), 152.7 (C, C=O), 186.1 (d, C, J_{C-P}= 19.3 Hz, carbene), 186.5 (d, C, J_{C-P}= 19.4 Hz, carbene). $^{31}P\{^1H\}$-NMR (T=298K, $CDCl_3$, ppm) δ: 25.9, 26.0.

IR (KBr): ν_{CO}= 1707, 1668 cm^{-1}, ν_{BF}=1056 cm^{-1}.

Anal. Calcd. for $C_{36}H_{36}BF_4N_4O_2PPd$: C 55.37, H 4.65, N 7.17. Found: C 55.22, H 4.58, N 7.42.

9.6.7. Synthesis of mixed purine-based NHC/TPPTS palladium η^3-allyl complexes (7)

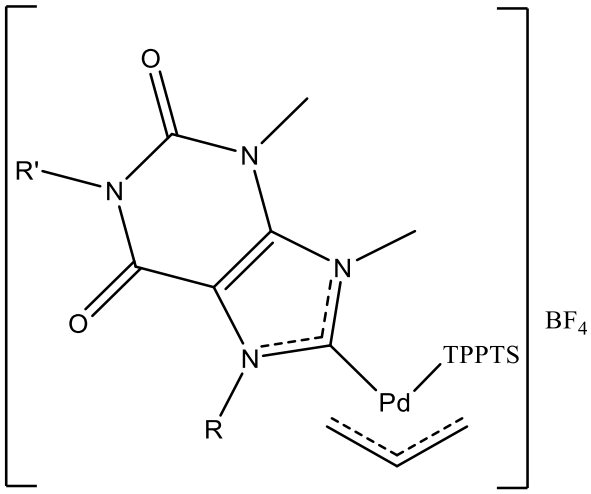

7a R= CH_3 R'= CH_3
7b R= CH_2Ph R'= CH_3
7d R= CH_3 R'= CH_2Ph

Synthesis of the complex 7a

0.0571g (0.0999 mmol) of TPPTS (3,3′,3″–phosphinetriyltribenzenesulfonate) was dissolved in 40 mL of CH_3CN and 7 mL of water in a two-necked flask under inert atmosphere (Ar).

To the resulting solution 0.0239g (0.0653 mmol) of the dimer $[Pd(\mu\text{-}Cl)(\eta^3\text{-allyl})]_2$ and 0.0352g (0.0873 mmol) of **4a**/ $AgBF_4$ were added and the final mixture stirred at RT for ca. 1 h.

The precipitated AgCl was removed by filtration on a millipore membrane filter.

The solution was dried under vacuum and the residue treated with 5 mL of diethylether and 5 mL of CH_2Cl_2 yielding the complex **7a** as brownish solid that was filtered off on a gooch, washed with *n*–pentane and dried under vacuum.

0.0763g (yield 86%) of **7a** was obtained.

^{1}H-NMR (400 MHz, T = 298K, D_2O, ppm) δ: 3.17 (d, 1H, J = 13.3 Hz, *anti* allyl-H *trans*-C), 3.23 (s, 6H, $2NCH_3$), 3.29 (d, 1H, J = 13.2 Hz, *anti* allyl-H *trans*-C), 3.40 (s, 3H, NCH_3), 3.41 (dd = t, 2H, $J_{H\text{-}H} = J_{H\text{-}P}$ = 10.0 Hz, 2*anti* allyl-H *trans*-P), 3.57 (s, 3H, NCH_3), 3.58 (s, 6H, $2NCH_3$), 3.67 (s, 3H, NCH_3), 3.84 (s, 3H, NCH_3), 4.39 (d, 1H, J = 7.4 Hz, *syn* allyl-H *trans*-C), 4.47 (d, 1H, J = 8.1 Hz, *syn* allyl-H *trans*-C), 4.61 (dd = t, 2H, $J_{H\text{-}H} = J_{H\text{-}P}$ = 6.1 Hz, 2*syn* allyl-H *trans*-P), 5.82 (m, 2H, 2*central* allyl-H), 7.45-7.90 (m, 24H, $6PhSO_3Na$).

$^{31}P\{^1H\}$-NMR (T = 298K, D_2O, ppm) δ: 28.3, 28.5

$^{13}C\{^1H\}$-NMR (T = 298K, D_2O, ppm) δ: 28.4 (CH_3, NCH_3), 31.8 (CH_3, NCH_3), 36.6 (CH_3, NCH_3), 36.8 (CH_3, NCH_3), 38.3 (CH_3, NCH_3), 38.4 (CH_3, NCH_3), 68.2 (d, CH_2, $J_{C\text{-}P}$ = 28.4 Hz, 2 allyl *trans*-P), 69.5 (CH_2, allyl *trans*-C), 69.8 (CH_2, allyl *trans*-C), 111.1 (C, C^5), 111.3 (C, C^5), 122.6 (CH,

central allyl), 128.3-136.4 and 143.7-143.8 (Ph), 141.5 (C, C^4), 141.7 (C, C^4), 151.8 (C, C=O), 154.3 (C, C=O), 185.3 (d, C, J_{C-P} = 20.0 Hz, carbene), 185.4 (d, C, J_{C-P} = 19.9 Hz, carbene).

IR (KBr): ν_{CO} = 1705, 1664 cm^{-1}, ν_{BF} =1035, 1095 cm^{-1}

Anal. Calcd. for $C_{30}H_{29}BF_4N_4Na_3O_{11}PPdS_3$: C 35.64, H 2.89, N 5.54. Found: C 35.72, H 2.80, N 5.52.

Synthesis of the complex 7b

Complex **7b** was prepared in analogues manner as that described for **7a** starting from 0.0153 g of $[Pd(\mu\text{-}Cl)(\eta^3\text{-allyl})]_2$, 0.0475 g of TPPTS and 0.0348 g of **4b**/$AgBF_4$.

0.0708 g (yield 90%) of **7b** was obtained.

^{1}H-NMR (400 MHz, T = 298K, D_2O, ppm) δ: 3.18 (d, 1H, J = 13.8 Hz, *anti* allyl-H *trans*-C), 3.27 (d, 1H, J = 13.3 Hz, *anti* allyl-H *trans*-C), 3.41 (dd = t, 2H, $J_{H-H} = J_{H-P}$ = 11.5 Hz, 2*anti* allyl-H *trans*-P), 3.41 (s, 3H, NCH_3), 3.57 (s, 3H, NCH_3), 3.58 (s, 3H, NCH_3), 3.59 (s, 3H, NCH_3), 3.67 (s, 3H, NCH_3), 3.84 (s, 3H, NCH_3), 4.43 (d, 1H, J = 7.1 Hz, *syn* allyl-H *trans*-C), 4.49 (d, 1H, J = 7.0 Hz, *syn* allyl-H *trans*-C), 4.62 (dd, 2H, J = 7.9, J = 5.7 Hz, 2*syn* allyl-H *trans*-P), 4.99 and 5.09 (2AB system, 4H, J = 15.5 Hz, $2NCH_2$), 5.86 (m, 2H, 2*central* allyl-H), 7.27-7.87 (m, 34H, $6PhSO_3Na$+2Ph).

$^{31}P\{^1H\}$-NMR (T = 298K, D_2O, ppm) δ: 28.5, 28.8

$^{13}C\{^1H\}$-NMR (T = 298K, D_2O, ppm) δ: 31.9 (CH_3, NCH_3), 36.7 (CH_3, NCH_3), 36.9 (CH_3, NCH_3), 38.3(CH_3, NCH_3), 38.5 (CH_3, NCH_3), 45.2 (CH_2, NCH_2), 68.2 (d, CH_2, J_{C-P} = 28.4 Hz, allyl *trans*-P), 68.4 (d, CH_2, J_{C-P} = 29.0 Hz, allyl *trans*-P), 69.5 (CH_2, allyl *trans*-C), 69.6 (CH_2, allyl *trans*-C), 111.1 (C, C^5), 111.2 (C, C^5), 122.4 (d, CH, J_{C-P} = 5.2 Hz, *central* allyl), and 122.5 (d, CH, J_{C-P} = 5.6 Hz, *central* allyl), 127.2-136.3 (Ph), 141.7 (C, C^4), 141.8 (C, C^4), 143.7 and 143.8 (Ph), 151.5 (C, C=O), 153.9 (C, C=O), 186.0 (d, C, J_{C-P} = 19.8 Hz, carbene), 186.1 (d, C, J_{C-P} = 20.0 Hz, carbene).

IR (KBr): ν_{CO} = 1706, 1666 cm^{-1}, ν_{BF} =1036, 1084 cm^{-1}

Anal. Calcd. for $C_{36}H_{33}BF_4N_4Na_3O_{11}PPdS_3$: C 39.78, H 3.06, N 5.15. Found: C 39.72, H 3.13, N 5.24.

Synthesis of the complex 7c

Complex **7c** was prepared in analogues manner as that described for **7a** starting from 0.0154 g of $[Pd(\mu\text{-}Cl)(\eta^3\text{-allyl})]_2$, 0.0478 g of TPPTS and 0.0350 g of **4c**/$AgBF_4$.

0.0698 g (yield 88%) of **7c** was obtained.

^{1}H-NMR (400 MHz, T = 298K, D_2O, ppm) δ: 3.03 (d, 1H, J = 13.3 Hz, *anti* allyl-H *trans*-C), 3.11 (d, 1H, J = 13.4 Hz, *anti* allyl-H *trans*-C), 3.24 (s, 3H, NCH_3), 3.25 (s, 3H, NCH_3), 3.28 (m, 2H, 2*anti* allyl-H *trans*-P), 3.58 (s, 3H, NCH_3), 3.62 (s, 3H, NCH_3), 3.64 (s, 3H, NCH_3), 3.85 (s, 3H, NCH_3), 4.07 (dd = t, 1H, J = 5.4 Hz, *syn* allyl-H *trans*-P), 4.33 (d, 1H, J = 7.1 Hz, 2*syn* allyl-H *trans*-C), 4.34

(d, 1H, J =7.6 Hz, *syn* allyl-H *trans*-C), 4.48 (dd = t, 1H, $J_{H-H} = J_{H-P} = 4.7$ Hz, *syn* allyl-H *trans*-P), 4.93 and 5.25 (AB system, 2H, J = 15.4 Hz, NCH_2), 5.17 and 5.35 (AB system, 2H, J = 14.5 Hz, NCH_2), 5.44 (m, 1H, *central* allyl-H), 5.78 (m, 1H, *central* allyl-H), 6.97-7.90 (m, 34H, $6PhSO_3Na$+2Ph).

$^{31}P\{^1H\}$-NMR (T = 298K, D_2O, ppm) δ: 27.6, 28.1

$^{13}C\{^1H\}$-NMR (T = 298K, D_2O, ppm) δ: 28.4 (CH_3, NCH_3), 31.9 (CH_3, NCH_3), 38.9 (CH_3, NCH_3), 39.0 (CH_3, NCH_3), 52.4 (CH_2, NCH_2), 52.6 (CH_2, NCH_2), 68.9 (d, CH_2, J_{C-P} = 28.5 Hz, allyl *trans*-P), 69.1 (d, CH_2, J_{C-P} = 27.8 Hz, allyl *trans*-P), 69.8 (CH_2, allyl *trans*-C), 69.9 (CH_2, allyl *trans*-C), 111.1 (C, C^5), 111.4 (C, C^5), 122.2 (CH, *central* allyl), 122.3 (CH, *central* allyl), 126.6-136.3 and 143.7 (Ph), 141.8 (C, C^4), 151.8 (C, C=O), 154.1 (C, C=O), 187.3 (d, C, J_{C-P} = 19.4 Hz, carbene), 187.4 (d, C, J_{C-P} = 19.0 Hz, carbene).

IR (KBr): ν_{CO} = 1703, 1663 cm^{-1}, ν_{BF} =1036, 1084 cm^{-1}

Anal. Calcd. for $C_{36}H_{33}BF_4N_4Na_3O_{11}PPdS_3$: C 39.78, H 3.06, N 5.15. Found: C 39.84, H 3.11, N 5.20.

9.6.8. Synthesis of mixed purine-based NHC/PTA palladium η^3-allyl complexes (8)

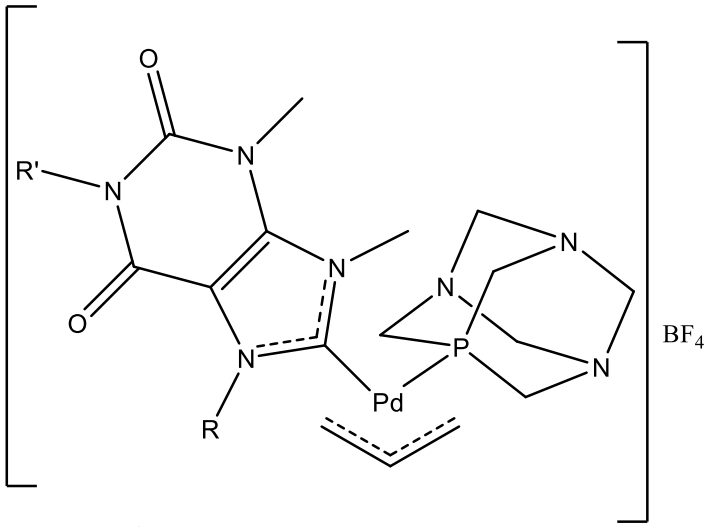

8a R= CH_3 R'= CH_3
8b R= CH_2Ph R'= CH_3
8d R= CH_3 R'= CH_2Ph

Synthesis of the complex 8a

0.0411 g (0.112 mmol) of the dimer $[Pd(\mu\text{-}Cl)(\eta^3\text{-}C_3H_5)]_2$ and 0.0353 g (0.224 mmol) of PTA (1,3,5-triaza-7-phosphadamantane) were dissolved in ca. 30 mL of anhydrous CH_3CN in a 100 mL two-necked flask under inert atmosphere (Ar). The resulting mixture was treated with 0.0787 g (0.0975 mmol) of **4a**/$AgBF_4$ and stirred at RT for ca. 1 h.

The precipitated AgCl was removed by filtration on a millipore membrane filter.

The solution was dried under vacuum and the residue treated with 2 mL of CH_2Cl_2.

Addition of diethylether to the concentrated solution yields the precipitation of the complex **8a** as a brownish solid which was filtered off on a gooch, washed with *n*-pentane and dried under vacuum. 0.0991 g of **8a** was obtained (yield 97%).

^{1}H-NMR (400 MHz, T=298K, D_2O, ppm) δ: 2.88 (d, 2H, J= 13.2 Hz, 2 *anti* allyl-H *trans*-C), 3.15 (m, 2H, 2 *anti* allyl-H *trans*-P), 3.32 (s, 3H, NCH_3), 3.33 (s, 3H, NCH_3), 3.74 (s, 3H, NCH_3), 3.77 (s, 3H, NCH_3), 3.80 (s, 3H, NCH_3), 3.87 (s, 3H, NCH_3), 3.92 (s, 3H, NCH_3), 4.05 (s, 3H, NCH_3), 4.21 (s, 12H, 6 NCH_2P_{PTA}), 4.38 (d, 2H, J= 7.4 Hz, 2 *syn* allyl-H *trans*-C), 4.47 (m, 2H, 2 *syn* allyl-H *trans*-P), 4.55 (m, 12H, 6 NCH_2N_{PTA}), 5.48 (m, 2H, 2 *central* allyl-H). $^{13}C\{^1H\}$-NMR (T=298K, D_2O, ppm) δ: 28.4 (CH_3, NCH_3), 31.8 (CH_3, NCH_3), 36.7 (CH_3, NCH_3), 36.9 (CH_3, NCH_3), 38.2 (CH_3, NCH_3), 38.4 (CH_3, NCH_3), 50.3 (CH_2, NCH_2P, $J_{C\text{-}P}$ =13.6 Hz), 62.7 (CH_2, allyl *trans*-C), 62.8 (CH_2, allyl *trans*-C), 68.9 (d, CH_2, $J_{C\text{-}P}$= 4.8 Hz, allyl *trans*-P), 69.2 (d, CH_2, $J_{C\text{-}P}$= 5.2 Hz, allyl *trans*-P), 70.7 (CH_2, NCH_2N), 70.8 (CH_2, NCH_2N), 111.2 (C, C^5), 111.4 (C, C^5), 121.9 (CH, *central* allyl),

122.0 (CH, *central* allyl), 141.8 (C, C^4), 141.9 (C, C^4), 151.8 (C, C=O), 154.5 (C, C=O), 183.9 (C, J_{C-P}= 21.2 Hz, carbene). $^{31}P\{^1H\}$-NMR (T=298K, D_2O, ppm) δ: -52.4

IR (KBr): ν_{CO}= 1704, 1665 cm^{-1}, ν_{BF}=1031, 1084 cm^{-1}.

Anal. Calcd. for $C_{18}H_{29}BF_4N_7O_2PPd$: C 36.05, H 4.87, N 16.35. Found: C 36.34, H 4.97, N 16.14.

Synthesis of the complex 8b

Complex **8b** was prepared in analogues manner as that described for **8a** starting from 0.0353 g of $[Pd(\mu\text{-}Cl)(\eta^3\text{-allyl})]_2$, 0.0804 g of **4b**/$AgBF_4$ and 0.0304 g of PTA.

0.0925 g (yield 82%) of **8b** was obtained.

^1H-NMR (400 MHz, T=298K, D_2O, ppm) δ: 2.76 (m, 2H, 2 *anti* allyl-H *trans*-C), 3.06 (m, 2H, 2 *anti* allyl-H *trans*-P), 3.28 (s, 3H, NCH_3), 3.29 (s, 3H, NCH_3), 3.72 (s, 6H, 3 NCH_2P_{PTA}), 3.75 (s, 6H, 3 NCH_2P_{PTA}), 3.77 (s, 3H, NCH_3), 3.80 (s, 3H, NCH_3), 3.88 (s, 3H, NCH_3), 4.06 (s, 3H, NCH_3), 4.27-4.70 (m, 16 H, 6 NCH_2N_{PTA} and 2 *syn* allyl-H *trans*-C and 2 *syn* allyl-H *trans*-P), 5.07 and 5.64 (AB system, 2H, J=15.4 Hz, NCH_2), 5.29 and 5.76 (AB system, 2H, J=15.7 Hz, NCH_2), 5.36 (m, 2H, 2 *central* allyl-H), 6.81-7.36 (m, 10H, 2Ph). $^{13}C\{^1H\}$-NMR (T=298K, D_2O, ppm) δ: 28.5 (CH_3, NCH_3), 31.9 (CH_3, NCH_3), 38.6 (CH_3, NCH_3), 38.9 (CH_3, NCH_3), 49.9 (d, CH_2, J= 13.5 Hz, NCH_2P), 50.0 (d, CH_2, J= 13.6 Hz, NCH_2P), 52.5 (CH_2, NCH_2), 52.7 (CH_2, NCH_2), 62.6 (CH_2, allyl *trans*-C), 63.0 (CH_2, allyl *trans*-C), 69.4 (d, CH_2, J_{C-P}= 26.7 Hz, allyl *trans*-P), 69.9 (d, CH_2, J_{C-P}= 27.8 Hz, allyl *trans*-P), 70.4 (CH_2, NCH_2N_{PTA}) 70.5 (CH_2, NCH_2N), 111.1 (C, C^5), 111.4 (C, C^5), 121.9 (CH, *central* allyl), 126.9-136.7 (Ph), 141.8 (C, C^4), 141.9 (C, C^4), 151.8 (C, C=O), 154.2 (C, C=O), 186.0 (d, C, J_{C-P}= 20.4, carbene), 186.1 (d, C, J_{C-P}= 20.5 Hz, carbene). $^{31}P\{^1H\}$-NMR (T=298K, D_2O, ppm) δ: -54.1, -54.0.

IR (KBr): ν_{CO}= 1705, 1664 cm^{-1}, ν_{BF}=1035, 1083 cm^{-1}

Anal. Calcd. for $C_{24}H_{33}BF_4N_7O_2PPd$: C 42.66, H 4.92, N 14.51. Found: C 42.82, H 4.78, N 14.22.

Synthesis of the complex 8d

Complex **8d** was prepared in analogues manner as that described for **8a** starting from 0.0352 g of $[Pd(\mu\text{-}Cl)(\eta^3\text{-allyl})]_2$, 0.0800 g of **4d**/$AgBF_4$ and 0.0301 g of PTA.

0.1057 g (yield 94%) of **8d** was obtained.

^1H-NMR (400 MHz, T=298K, D_2O, ppm) δ: 2.83 (d, J= 13.8 Hz, 2H, 2 *anti* allyl-H *trans*-C), 3.07 (m, 2H, 2 *anti* allyl-H *trans*-P), 3.69 (s, 3H, NCH_3), 3.70 (s, 3H, NCH_3), 3.73 (s, 3H, NCH_3), 3.82 (s, 3H, NCH_3), 3.87 (s, 3H, NCH_3), 4.01 (s, 3H, NCH_3), 4.15 (s, 6H, 3 NCH_2P_{PTA}), 4.27 (s, 6H, 3 NCH_2P_{PTA}), 4.32 (d, J = 6.6 Hz, 2H, 2 *syn* allyl-H *trans*-C), 4.45 (m, 2H, 2 *syn* allyl-H *trans*-P), 4.50-4.70 (m, 12H, 6 NCH_2P_{PTA}), 5.10 (2s, 4H, 2 N-CH_2), 5.42 (m, 2H, 2 *central* allyl-H), 7.25-7.30 (m, 10H, 2Ph).

$^{13}C\{^{1}H\}$-NMR (T=298K, D_2O, ppm) δ: 31.9 (CH_3, NCH_3), 36.8 (CH_3, NCH_3), 37.1 (CH_3, NCH_3), 38.2 (CH_3, NCH_3), 38.5 (CH_3, NCH_3), 45.2 (CH_2, NCH_2), 50.3 (d, CH_2, J_{C-P}= 13.8 Hz, NCH_2P), 51.1 (d, CH_2, J_{C-P}= 15.4 Hz, NCH_2P), 62.8 (CH_2, allyl *trans*-C), 62.9 (CH_2, allyl *trans*-C), 69.2 (d, CH_2, J_{C-P}= 27.7 Hz, allyl *trans*-P), 70.8 (CH_2, NCH_2N), 71.3 (d, CH_2, J_{C-P}= 26.2 Hz, allyl *trans*-P), 111.4 (C^5), 122.0 (CH, *central* allyl), 123.0 (CH, *central* allyl), 127.2-136.2 (Ph), 142.3 (C, C^4), 151.6 (C, C=O), 154.2 (C, C=O), 184.2 (d, C, J_{C-P}= 19.0 Hz, carbene), 184.3 (d, C, J_{C-P}= 19.8 Hz, carbene). $^{31}P\{^{1}H\}$-NMR (T=298K, D_2O, ppm) δ: -54.2, -53.1.

IR (KBr): ν_{CO}= 1708, 1668 cm^{-1}, ν_{BF}=1062, 1084 cm^{-1}

Anal. Calcd. for $C_{24}H_{33}BF_4N_7O_2PPd$: C 42.66, H 4.92, N 14.51. Found: C 42.52, H 4.99, N 14.32.

9.6.9. Synthesis of mixed purine-based NHC/DIC palladium η^3-allyl complexes (9)

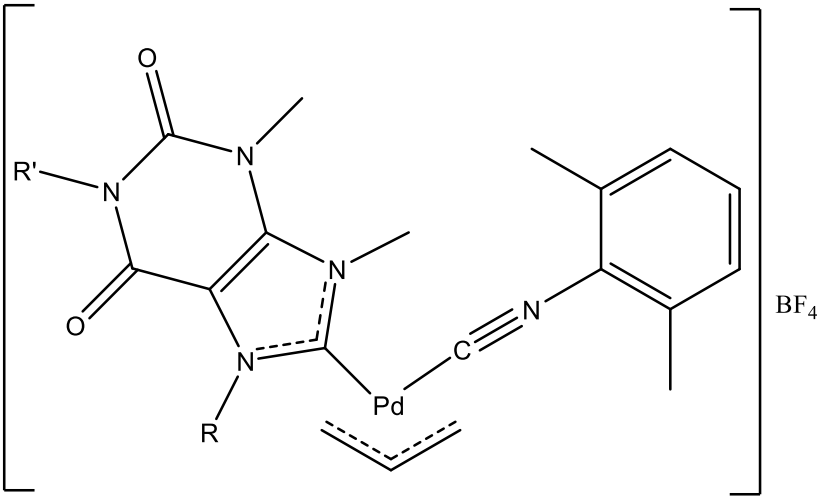

9a R= CH_3 R'= CH_3
9b R= CH_2Ph R'= CH_3
9d R= CH_3 R'= CH_2Ph

Synthesis of the complex 9a

0.0173 g (0.047 mmol) of the dimer $[Pd(\mu\text{-}Cl)(\eta^3\text{-}C_3H_5)]_2$ and 0.0124 g (0.094 mmol) of DIC (2,6-dimethylphenyl isocyanide) were dissolved in ca. 20 mL of anhydrous CH_3CN in a 50 mL two-necked flask under inert atmosphere (Ar). The resulting mixture was treated with 0.0344 g (0.043 mmol) of **4a**/$AgBF_4$ and stirred at RT for ca. 15 min.

The precipitated AgCl was removed by filtration on a millipore membrane filter.

Addition of diethylether to the concentrated solution yields the precipitation of the complex **9a** as a brownish solid which was filtered off on a gooch and washed with *n*-pentane.

0.0431 g of **9a** was obtained (yield 88%).

^{1}H-NMR (400 MHz, T=298K, $CDCl_3$, ppm) δ: 2.41 (s, 6H, $2CH_3^{DIC}$), 3.20 (d, 1H, J= 13.3 Hz, *anti* allyl-H), 3.40 (s, 3H, NCH_3), 3.41 (d, 1H, J= 12.7 Hz, *anti* allyl-H), 3.88 (s, 3H, NCH_3), 4.05 (s, 3H, NCH_3), 4.20 (s, 3H, NCH_3), 4.47 (d, 1H, J= 6.4 Hz, *syn* allyl-H), 4.79 (d, 1H, J= 7.5 Hz, *syn* allyl-H), 5.72 (m, 1H, *central* allyl-H), 7.17-7.31 (m, 3H, Ph^{DIC}). $^{13}C\{^1H\}$-NMR (T=298K, $CDCl_3$, ppm) δ: 18.7 (CH_3, CH_3^{DIC}), 28.6 (CH_3, NCH_3), 32.0 (CH_3, NCH_3), 37.5 (CH_3, NCH_3), 39.3 (CH_3, NCH_3), 65.0 (CH_2, allyl-C), 69.3 (CH_2, allyl-C), 110.8 (C, C^5), 122.2 (*central* allyl), 128.4-135.6 (Ph), 141.4 (C, C^4), 150.6 (C, C=O), 150.7 (C, CN^{DIC}), 153.4 (C, C=O), 181.5 (C, carbene).

IR (KBr): ν_{CN}=2175 cm^{-1}, ν_{CO}= 1706, 1665 cm^{-1}, ν_{BF}=1056 cm^{-1}.

Anal. Calcd. for $C_{21}H_{26}BF_4N_5O_2Pd$: C 43.97, H 4.57, N 12.21. Found: C 44.24, H 4.77, N 12.04.

Synthesis of the complex 9b

Complex **9b** was prepared in analogues manner as that described for **9a** starting from 0.0180 g of $[Pd(\mu\text{-}Cl)(\eta^3\text{-allyl})]_2$, 0.0428 g of **4b**/$AgBF_4$ and 0.128 g of DIC.

0.0491 g (yield 85%) of **9b** was obtained.

^{1}H-NMR (400 MHz, T=298K, $CDCl_3$, ppm) δ: 2.36 (s, 6H, $2CH_3^{DIC}$), 3.42 (s, 3H, NCH_3), 3.48 (bd, 2H, 2*anti* allyl-H), 3.91 (s, 3H, NCH_3), 4.24 (bd, 1H, s*yn* allyl-H), 4.25 (s, 3H, NCH_3), 4.67 (d, 1H, J= 7.5 Hz, *syn* allyl-H), 5.65 (s, 2H, NCH_2), 5.73 (m, 1H, *central* allyl-H), 7.16-7.33 (m, 8H, Ph and Ph^{DIC}). $^{13}C\{^1H\}$-NMR (T=298K, $CDCl_3$, ppm) δ: 18.8 (CH_3, CH_3^{DIC}), 28.7 (CH_3, NCH_3), 32.1 (CH_3, NCH_3), 39.9 (CH_3, NCH_3), 53.0 (CH_2, NCH_2), 65.5 (CH_2, allyl-C), 110.6 (C, C^5), 121.9 (CH, *central* allyl), 127.5-135.9 (Ph), 141.5 (C, C^4), 150.5 (C, C=O), 150.7 (C, CN^{DIC}), 153.2 (C, C=O), 183.5 (C, carbene).

IR (KBr): ν_{CN}=2175 cm^{-1}, ν_{CO}= 1709, 1670 cm^{-1}, ν_{BF}=1057 cm^{-1}.

Anal. Calcd. for $C_{27}H_{30}BF_4N_5O_2Pd$: C 49.91, H 4.65, N 10.78. Found: C 49.84, H 4.83, N 10.90.

Synthesis of the complex 9d

Complex **9d** was prepared in analogues manner as that described for **9a** starting from 0.0184 g of $[Pd(\mu\text{-}Cl)(\eta^3\text{-allyl})]_2$, 0.0437 g of **4d**/$AgBF_4$ and 0.0131 g of DIC.

0.0543 g (yield 92%) of **9d** was obtained.

^{1}H-NMR (400 MHz, T=298K, $CDCl_3$, ppm) δ: 2.41 (s, 6H, $2CH_3^{DIC}$), 3.19 (d, 1H, J= 13.5 Hz, *anti* allyl-H), 3.41 (d, 1H, J= 12.5 Hz, *anti* allyl-H), 3.86 (s, 3H, NCH_3), 4.05 (s, 3H, NCH_3), 4.19 (s, 3H, NCH_3), 4.47 (d, 1H, J= 7.1 Hz, *syn* allyl-H), 4.78 (d, 1H, J= 7.5 Hz, *syn* allyl-H), 5.18 (s, 2H, NCH_2), 5.72 (m, 1H, *central* allyl-H), 7.17-7.49 (m, 8H, Ph and Ph^{DIC}). $^{13}C\{^1H\}$-NMR (T=298K, $CDCl_3$, ppm) δ: 18.8 (CH_3, CH_3^{DIC}), 32.0 (CH_3, NCH_3), 37.5 (CH_3, NCH_3), 39.3 (CH_3, NCH_3), 45.2 (CH_2, NCH_2), 64.9 (CH_2, allyl-C), 110.9 (C, C^5), 122.2 (CH, *central* allyl), 127.8-136.3 (Ph), 141.5 (C, C^4), 150.5 (C, C=O), 150.6 (C, CN^{DIC}), 153.2 (C, C=O), 181.8 (C, carbene).

IR (KBr): ν_{CN}=2173 cm^{-1}, ν_{CO}= 1707, 1665 cm^{-1}, ν_{BF}=1056 cm^{-1}.

Anal. Calcd. for $C_{27}H_{30}BF_4N_5O_2Pd$: C 49.91, H 4.65, N 10.78. Found: C 50.04, H 4.51, N 10.95.

9.6.10. Synthesis of the Bis(purine-based NHC) palladium η^3-allyl complexes (10)

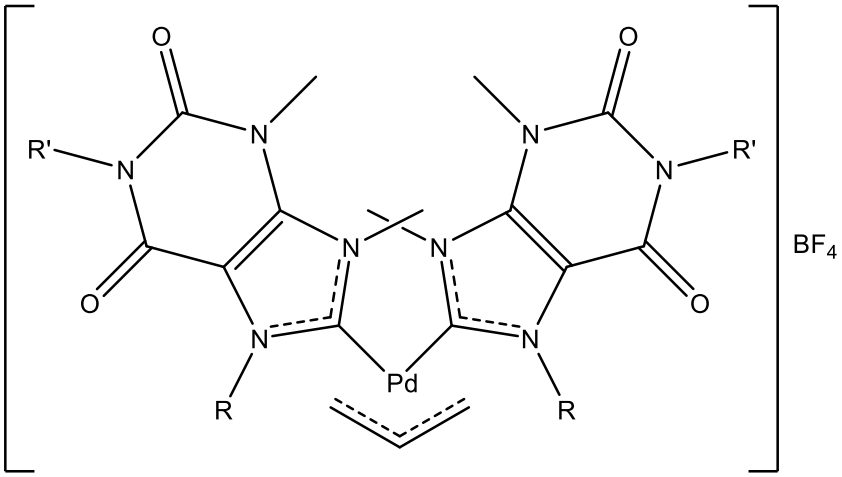

10a R= CH_3 R'= CH_3
10b R= CH_2Ph R'= CH_3
10c R= $CH_2C{\equiv}CPh$ R'= CH_3
10d R= CH_3 R'= CH_2Ph

Synthesis of the complex 10a

0.0156 g (0.086 mmol) of the dimer $[Pd(\mu\text{-}Cl)(\eta^3\text{-}C_3H_5)]_2$ was dissolved in ca. 20 mL of anhydrous CH_3CN in a 50 mL two necked flask under inert atmosphere (Ar).

The resulting mixture was treated with 0.0690 g (0.171 mmol) of **4a**/$AgBF_4$, 0.0142 g (0.086 mmol) of KI and stirred at RT for ca. 15 min. The precipitated AgCl and AgI were removed by filtration on a millipore membrane filter. Addition of diethylether to the concentrated solution yields the precipitation of the complex **10a** as a white solid which was filtered off on a gooch and washed with *n*-pentane.

0.0446 g of **10a** was obtained (yield 80%).

^{1}H-NMR (400 MHz, T=298K, CD_3CN, ppm) δ: 2.95 (d, 2H, J= 13.3 Hz, *anti* allyl-H), 3.30 (s, 6H, NCH_3), 3.73 (s, 6H, NCH_3), 3.93 (s, 6H, NCH_3), 4.02 (s, 6H, NCH_3), 4.12 (d, 2H, J= 7.4 Hz, *syn* allyl-H), 5.59 (m, 1H, *central* allyl-H). $^{13}C\{^1H\}$-NMR (T=298K, CD_3CN, ppm) δ: 28.4 (CH_3, NCH_3), 32.0 (CH_3, NCH_3), 37.7 (CH_3, NCH_3), 39.4 (CH_3, NCH_3), 61.6 (CH_2, allyl-C), 110.9 (C, C^5), 121.0 (CH, *central* allyl), 141.9 (C, C^4), 151.4 (C, C=O), 153.9 (C, C=O), 184.9 (C, carbene).

IR (KBr): ν_{CO}= 1706, 1668 cm^{-1}, ν_{BF}=1053 cm^{-1}.

Anal. Calcd. for $C_{21}H_{29}BF_4N_8O_4Pd$: C 38.76, H 4.49, N 17.22. Found: C 38.50, H 4.82, N 17.35.

Synthesis of the complex 10b

Complex **10b** was prepared in analogues manner as that described for **10a** starting from 0.0157 g of [Pd(μ-Cl)(η^3-allyl)]$_2$, 0.0822 g of **4b**/$AgBF_4$ and 0.0142 g of KI.

0.0599 g (yield 87%) of **10b** was obtained.

^{1}H-NMR (400 MHz, T=298K, CD_3CN, ppm) δ: 2.79 (d, 2H, J= 13.2 Hz, *anti* allyl-H), 3.23 (s, 6H, NCH_3), 3.68 (s, 6H, NCH_3), 3.97 (s, 6H, NCH_3), 3.97 (bd, 2H, *syn* allyl-H), 5.39-5.61 (m, 5H, NCH_2 and *central* allyl-H), 6.94-7.24 (m, 10H, 2Ph).

^{13}C{^{1}H}-NMR (T=298K, CD_3CN, ppm) δ: 28.3 (CH_3, NCH_3), 31.9 (CH_3, NCH_3), 39.6 (CH_3, NCH_3), 53.0 (CH_2, NCH_2), 65.9 (CH_2, allyl-C), 110.4 (C, C^5), 121.2 (CH, *central* allyl), 125.7-137.2 (Ph), 142.0 (C, C^4), 151.2 (C, C=O), 153.2 (C, C=O), 185.3 (C, carbene).

IR (KBr): ν_{CO}= 1709, 1664 cm^{-1}, ν_{BF}=1058 cm^{-1}.

Anal. Calcd. for $C_{33}H_{37}BF_4N_8O_4Pd$: C 49.36, H 4.64, N 13.96. Found: C 49.57, H 4.12, N 14.22.

Synthesis of the complex 10c

Complex **10c** was prepared in analogues manner as that described for **10a** starting from 0.0157 g of [Pd(μ-Cl)(η^3-allyl)]$_2$, 0.0863 g of **4c**/$AgBF_4$ and 0.0142 g of KI.

0.0592g (yield 81%) of **10c** was obtained.

^{1}H-NMR (400 MHz, T=298K, CD_3CN, ppm) δ: 3.02 (s, 6H, NCH_3), 3.03 (d, 2H, J= 13.4 Hz, *anti* allyl-H), 3.53 (s, 6H, NCH_3), 4.20 (m, 8H, NCH_3 and *syn* allyl-H), 5.44 (bs, 4H, NCH_2), 5.66 (m, 1H, *central* allyl-H), 7.16-7.48 (m, 10H, 2Ph). ^{13}C{^{1}H}-NMR (T=298K, CD_3CN, ppm) δ: 28.4 (CH_3, NCH_3), 31.9 (CH_3, NCH_3), 39.8 (CH_3, NCH_3), 41.1 (CH_2, NCH_2), 65.9 (CH_2, allyl-C), 83.8 (CH_2-C≡), 84.7 (C, Ph-C≡), 110.4 (C, C^5), 121.6 (CH, *central* allyl), 121.9-131.0 (Ph), 141.7 (C, C^4), 150.5 (C, C=O), 153.4 (C, C=O), 185.5 (C, carbene).

IR (KBr): ν_{CO}= 1706, 1667 cm^{-1}, ν_{BF}=1056 cm^{-1}.

Anal. Calcd. for $C_{37}H_{37}BF_4N_8O_4Pd$: C 52.22, H 4.38, N 13.17. Found: C 52.37, H 4.10, N 13.55.

Synthesis of the complex 10d

Complex **10d** was prepared in analogues manner as that described for **10a** starting from 0.0154 g of [Pd(μ-Cl)(η^3-allyl)]$_2$, 0.0806 g of **4d**/$AgBF_4$ and 0.0139 g of KI.

0.0595 g (yield 88%) of **10d** was obtained.

^{1}H-NMR (400 MHz, T=298K, CD_3CN, ppm) δ: 2.96 (d, 2H, J= 13.3 Hz, *anti* allyl-H), 3.73 (s, 6H, NCH_3), 3.93 (s, 6H, NCH_3), 4.02 (s, 6H, NCH_3), 4.13 (d, 2H, J= 7.4 Hz, 2 *syn* allyl-H), 5.13 (s, 4H, NCH_2), 5.59 (m, 1H, *central* allyl-H), 7.28-7.39 (m, 10H, 2Ph).

$^{13}C\{^{1}H\}$-NMR (T=298K, CD_3CN, ppm) δ: 31.5 (CH_3, NCH_3), 37.2 (CH_3, NCH_3), 38.8 (CH_3, NCH_3), 44.6 (CH_2, NCH_2), 61.1 (CH_2, allyl-C), 110.4 (C, C^5), 120.4 (CH, *central* allyl), 127.4-137.3 (Ph), 141.5 (C, C^4), 150.7 (C, C=O), 153.2 (C, C=O), 184.7 (C, carbene).

IR (KBr): ν_{CO}= 1708, 1667 cm^{-1}, ν_{BF}=1058 cm^{-1}.

Anal. Calcd. for $C_{33}H_{37}BF_4N_8O_4Pd$: C 49.36, H 4.64, N 13.96. Found: C 49.61, H 4.17, N 14.05.

9.6.11. Synthesis of mixed purine-based NHC/PPh_3 pallacyclopentadienyl complexes (11)

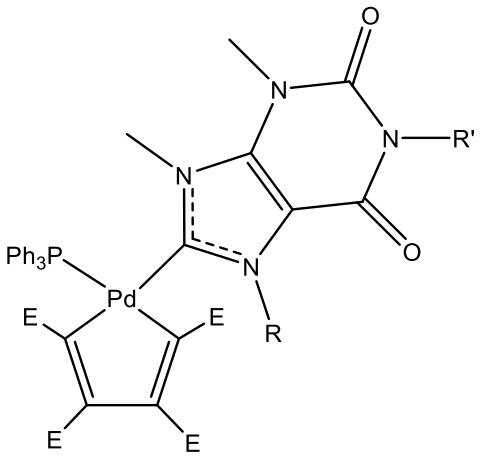

11a R= CH_3 R'= CH_3
11b R= CH_2Ph R'= CH_3
11d R= CH_3 R'= CH_2Ph

Synthesis of the complex 11a

0.0279 g (0.0713 mmol) of the polymeric precursor $[PdC_4(COOCH_3)_4]_n$ was dissolved in 5 mL of anhydrous dichloromethane in a 100 mL two necked flask under inert atmosphere (Ar). To this solution a mixture constituted by 0.0218 g (0.0310 mmol) of the silver complex **5a** and 0.0171 g (0.0651 mmol) of PPh_3 dissolved in ca. 30 mL of anhydrous dichloromethane, was added.

The mixture was stirred at R.T. for 1 h and subsequently the precipitated AgCl was removed by filtration on a millipore membrane filter.

Addition of diethylether to the concentrated solution yields the precipitation of the complex **11a** as a yellow solid which was filtered off on a gooch and washed with *n*-pentane.

0.0509 g of **11a** was obtained (yield 83%).

^{1}H-NMR (400 MHz, $CDCl_3$, T=298K, ppm) δ: 2.53 (s, 3H, OCH_3), 3.25 (s, 3H, OCH_3), 3.36 (s, 3H, NCH_3), 3.48 (s, 3H, NCH_3), 3.63 (s, 3H, OCH_3), 3.65 (s, 3H, OCH_3), 3.76 (s, 3H, NCH_3), 3.82 (s, 3H, NCH_3), 7.32-7.51 (m, 15H, 3Ph).

^{13}C{^{1}H}-NMR ($CDCl_3$, T = 298K, ppm) δ: 28.6 (CH_3, NCH_3), 31.5 (CH_3, NCH_3), 36.6 (CH_3, NCH_3), 38.2 (CH_3, NCH_3), 50.0 (CH_3, OCH_3), 50.8 (CH_3, OCH_3), 51.2 (CH_3, OCH_3), 51.3 (CH_3, OCH_3), 109.7 (C, C^5), 128.3-134.1 (Ph), 140.2 (C, C^4), 145.9 (d, C, J_{C-P} = 5.4 Hz, C-$COOCH_3$), 148.8 (d, C, J_{C-P} = 7.0 Hz, C-$COOCH_3$), 150.2 (C, C=O), 152.7 (C, C=O), 164.0-166.4 (C, $COOCH_3$), 168.1 (C, C-$COOCH_3$), 169.6 (C, C-$COOCH_3$), 174.9 (d, C, J_{C-P} = 4.9 Hz, $COOCH_3$), 175.6 (d, C, J_{C-P} = 5.3 Hz, $COOCH_3$), 189.1 (d, C, J_{C-P} = 15.8 Hz, carbene).

^{31}P{^{1}H}-NMR ($CDCl_3$, T = 298K, ppm) δ: 26.1

IR (KBr): $\nu_{C=O}$ = 1730 cm^{-1} - 1692 cm^{-1}, ν_{C-O} = 1212 cm^{-1}

Synthesis of the complex 11b

Complex **11b** was prepared in analogues manner as that described for **11a** starting from 0.0267 g of $[PdC_4(COOCH_3)_4]_n$, 0.0265 g of **5b** and 0.0163 g of PPh_3.

0.0552 g (yield 86%) of **11b** was obtained.

^{1}H-NMR (400 MHz, $CDCl_3$, T = 298K, ppm) δ: 2.56 (s, 3H, OCH_3), 3.04 (s, 3H, OCH_3), 3.38 (s, 3H, NCH_3), 3.46 (s, 3H, NCH_3), 3.63 (s, 3H, OCH_3), 3.64 (s, 3H, OCH_3), 3.85 (s, 3H, NCH_3), 5.40 and 5.50 (AB system, 2H, J = 14.2 Hz, NCH_2), 7.12-7.52 (m, 20H, 4Ph).

^{13}C{^{1}H}-NMR ($CDCl_3$, T = 298K, ppm) δ: 28.7 (CH_3, NCH_3), 31.8 (CH_3, NCH_3), 39.0 (CH_3, NCH_3), 50.0 (CH_3, OCH_3), 50.9 (CH_3, OCH_3), 51.2 (CH_3, OCH_3), 51.3 (CH_3, OCH_3), 53.6 (CH_2, NCH_2), 109.5 (C, C^5), 128.2-134.7 (Ph), 140.9 (C, C^4), 148.8 (d, C, J_{C-P}= 5.6 Hz, C-$COOCH_3$), 149.0 (d, C, J_{C-P}= 7.3 Hz, C-$COOCH_3$), 150.3 (C, C=O), 152.7 (C, C=O), 164.9-165.1 (C, $COOCH_3$), 166.0 (C, C-$COOCH_3$), 166.4 (C, C-$COOCH_3$), 174.5 (d, C, J_{C-P}= 5.2 Hz, $COOCH_3$), 174.9 (d, C, J_{C-P}= 6.4 Hz, $COOCH_3$), 189.4 (d, C, J_{C-P}= 15.5 Hz, carbene).

^{31}P{^{1}H}-NMR ($CDCl_3$, T = 298K, ppm) δ: 25.1

IR (KBr): $\nu_{C=O}$ = 1710 cm^{-1}, 1670 cm^{-1}, ν_{C-O} = 1208 cm^{-1}

Synthesis of the complex 11d

Complex **11d** was prepared in analogues manner as that described for **11a** starting from 0.0355 g of $[PdC_4(COOCH_3)_4]_n$, 0.0353 g of **5d** and 0.0217 g of PPh_3.

0.0729 g (yield 85%) of **11d** was obtained.

^{1}H-NMR (400 MHz, $CDCl_3$, T = 298K, ppm) δ: 2.53 (s, 3H, OCH_3), 3.24 (s, 3H, OCH_3), 3.48 (s, 3H, NCH_3), 3.63 (s, 3H, OCH_3), 3.65 (s, 3H, OCH_3), 3.80 (s, 6H, $2NCH_3$), 5.08 and 5.13 (AB system, 2H, J = 14.5 Hz, NCH_2), 7.24-7.50 (m, 20H, 4Ph). ^{13}C{^{1}H}-NMR ($CDCl_3$, T = 298K, ppm) δ: 31.6 (CH_3, NCH_3), 36.6 (CH_3, NCH_3), 38.3 (CH_3, NCH_3), 45.0 (CH_2, NCH_2), 49.9 (CH_3, OCH_3), 50.8 (CH_3, OCH_3), 51.2 (CH_3, OCH_3), 51.3 (CH_3, OCH_3), 109.9 (C, C^5), 128.0-136.5 (Ph), 140.1 (C, C^4), 145.9 (d, C, J_{C-P} = 5.5 Hz, C-$COOCH_3$), 148.8 (d, C, J_{C-P} = 7.1 Hz, C-$COOCH_3$), 150.1 (C, C=O), 152.5 (C, C=O), 164.1-166.3 (C, $COOCH_3$), 168.1 (C, C-$COOCH_3$), 169.2 (C, C-$COOCH_3$), 174.3 (d, C, J_{C-P} = 5.5 Hz, $COOCH_3$), 175.6 (d, C, J_{C-P} = 5.5 Hz, $COOCH_3$), 189.4 (d, C, J_{C-P} = 16.0 Hz, carbene). ^{31}P{^{1}H}-NMR ($CDCl_3$, T=298K, ppm) δ: 26.2

IR (KBr): $\nu_{C=O}$ = 1699 cm^{-1}, 1674 cm^{-1}, ν_{C-O} = 1205 cm^{-1}

9.6.12. Synthesis of mixed purine-based NHC/PTA pallacyclopentadienyl complexes (12)

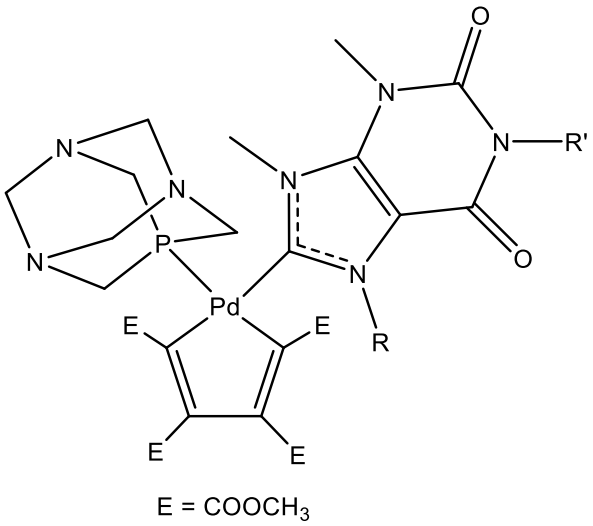

12a R= CH_3 R'= CH_3
12b R= CH_2Ph R'= CH_3
12d R= CH_3 R'= CH_2Ph

Synthesis of the complex 12a

0.0578 g (0.148 mmol) of the polymeric precursor $[PdC_4(COOCH_3)_4]_n$ was dissolved in 5 mL of anhydrous dichloromethane in a 100 mL two-necked flask under inert atmosphere (Ar). To this solution a mixture constituted by 0.0452 g (0.0643 mmol) of the silver complex **5a** and 0.0212 g (0.135 mmol) of PTA (1,3,5-triaza-7-phosphadamantane) dissolved in ca. 25 mL of anhydrous dichloromethane, was added. The mixture was stirred at R.T. for 1 h and subsequently the precipitated AgCl was removed by filtration on a millipore membrane filter. Addition of diethylether to the concentrated solution yields the precipitation of the complex **12a** as a brownish solid which was filtered off on a gooch and washed with *n*-pentane. 0.1019 g of **12a** was obtained (yield 91%).

^{1}H-NMR (400 MHz, $CDCl_3$, T = 298K, ppm) δ: 3.28 (s, 3H, OCH_3), 3.42 (s, 3H, NCH_3), 3.61 (s, 3H, OCH_3), 3.68 (s, 3H, OCH_3), 3.80 (s, 3H, OCH_3), 3.84 (s, 3H, NCH_3), 4.00 (d, 6H, J = 2.1 Hz, $3NCH_2P$), 4.04 (s, 3H, NCH_3), 4.20 (s, 3H, NCH_3), 4.49 (s, 6H, $3NCH_2N$).

^{13}C{^{1}H}-NMR ($CDCl_3$, T = 298K, ppm) δ: 28.7 (CH_3, NCH_3), 32.0 (CH_3, NCH_3), 37.0 (CH_3, NCH_3), 38.9 (CH_3, NCH_3), 50.9 (CH_3, OCH_3), 51.1 (d, CH_2, J_{C-P} = 10.2 Hz, NCH_2P), 51.2 (CH_3, OCH_3), 51.4 (CH_3, OCH_3), 51.6 (CH_3, OCH_3), 73.1 (d, CH_2, J_{C-P} = 6.4 Hz, NCH_2N), 110.1 (C, C^5), 140.6 (C, C^4), 164.3-165.0 (C, $\underline{C}OOCH_3$), 165.4 (C, $\underline{C}$-$COOCH_3$), 168.7 (C, $\underline{C}$-$COOCH_3$), 175.1 (d, C, J_{C-P} = 5.7 Hz, $\underline{C}OOCH_3$), 177.3 (d, C, J_{C-P} = 5.8 Hz, $\underline{C}OOCH_3$), 186.9 (d, C, J_{C-P} = 18.4 Hz, carbene).

^{31}P{^{1}H}-NMR ($CDCl_3$, T = 298K, ppm) δ: -64.8

IR (KBr): $\nu_{C=O}$ = 1711 cm^{-1}, 1672 cm^{-1}, ν_{C-O} = 1206 cm^{-1}

Synthesis of the complex 12b

Complex **12b** was prepared in analogues manner as that described for **12a** starting from 0.0290 g of $[PdC_4(COOCH_3)_4]_n$, 0.0276 g of **5b** and 0.0112 g of PTA (1,3,5-triaza-7-phosphadamantane). 0.0556 g (yield 90%) of **12b** was obtained.

^{1}H-NMR (400 MHz, $CDCl_3$, T = 298K, ppm) δ: 3.23 (s, 3H, OCH_3), 3.40 (s, 9H, $3NCH_2P$+NCH_3), 3.53 (s, 3H, OCH_3), 3.61 (s, 3H, OCH_3), 3.71 (s, 3H, OCH_3), 3.78 (s, 3H, NCH_3), 4.14 (s, 3H, NCH_3), 4.06 and 4.20 (AB system, 6H, J = 14.8 Hz, $3NCH_2N$), 5.19 and 6.02 (AB system, 2H, J = 13.4 Hz, NCH_2), 7.34-7.44 (m, 5H, Ph).

^{13}C{^{1}H}-NMR ($CDCl_3$, T = 298K, ppm) δ: 28.8 (CH_3, NCH_3), 32.2 (CH_3, NCH_3), 39.3 (CH_3, NCH_3), 50.1 (d, CH_2, J_{C-P} = 10.0 Hz, NCH_2P), 51.0 (CH_3, OCH_3), 51.3 (CH_3, OCH_3), 51.4 (CH_3, OCH_3), 51.6 (CH_3, OCH_3), 52.8 (CH_2, NCH_2), 72.7 (d, CH_2, J_{C-P} = 6.5 Hz, NCH_2N), 110.1 (C, C^5), 128.6-136.5 (Ph), 140.6 (C, C^4), 164.7-165.2 (C, $\underline{C}OOCH_3$), 166.6 (C, $\underline{C}$-$COOCH_3$), 167.7 (C, $\underline{C}$-$COOCH_3$), 175.1 (d, C, J_{C-P} = 5.5 Hz, $\underline{C}OOCH_3$), 177.3 (d, C, J_{C-P} = 5.9 Hz, $\underline{C}OOCH_3$), 188.0 (d, C, J_{C-P} = 17.5 Hz, carbene). ^{31}P{^{1}H}-NMR ($CDCl_3$, T=298K, ppm) δ: -66.7

IR (KBr): $\nu_{C=O}$ = 1709 cm^{-1}, 1670 cm^{-1}, ν_{C-O} = 1242 cm^{-1}, 1207cm^{-1}

Synthesis of the complex 12d

Complex **12d** was prepared in analogues manner as that described for **12a** starting from 0.0287 g of $[PdC_4(COOCH_3)_4]_n$, 0.0286 g of **5d** and 0.0105 g of PTA (1,3,5-triaza-7-phosphadamantane). 0.0564 g (yield 92%) of **12d** was obtained.

^{1}H-NMR (400 MHz, $CDCl_3$, T = 298K, ppm) δ: 3.24 (s, 3H, OCH_3), 3.60 (s, 3H, OCH_3), 3.68 (s, 3H, OCH_3), 3.80 (s, 3H, OCH_3), 3.82 (s, 3H, NCH_3), 4.00 (d, 6H, J = 2.0 Hz, $3NCH_2P$), 4.04 (s, 3H, NCH_3), 4.20 (s, 3H, NCH_3), 4.48 (s, 6H, $3NCH_2N$), 5.18 (s, 2H, NCH_2), 7.32-7.50 (m, 5H, Ph).

^{13}C{^{1}H}-NMR ($CDCl_3$, T = 298K, ppm) δ: 32.0 (CH_3, NCH_3), 37.0 (CH_3, NCH_3), 39.0 (CH_3, NCH_3), 45.3 (CH_2, NCH_2), 50.9 (CH_3, OCH_3), 51.1 (d, CH_2, J_{C-P} = 10.3 Hz, NCH_2P), 51.3 (CH_3, OCH_3), 51.4 (CH_3, OCH_3), 51.6 (CH_3, OCH_3), 73.1 (d, CH_2, J_{C-P} = 6.4 Hz, NCH_2N), 110.1 (C, C^5), 128.0-136.2 (Ph), 140.8 (C, C^4), 163.6-164.3 (C, $\underline{C}OOCH_3$), 165.4 (C, $\underline{C}$-$COOCH_3$), 168.9 (C, $\underline{C}$-$COOCH_3$), 175.1 (d, C, J_{C-P} = 5.5 Hz, $\underline{C}OOCH_3$), 177.3 (d, C, J_{C-P} = 5.7 Hz, $\underline{C}OOCH_3$), 186.0 (d, C, J_{C-P} = 18.7 Hz, carbene). ^{31}P{^{1}H}-NMR ($CDCl_3$, T = 298K, ppm) δ: -64.8

IR (KBr): $\nu_{C=O}$ = 1710 cm^{-1}, 1672 cm^{-1}, ν_{C-O} = 1243 cm^{-1}, 1207 cm^{-1}

9.6.13. Synthesis of mixed purine-based NHC/DIC pallacyclopentadienyl complexes (13)

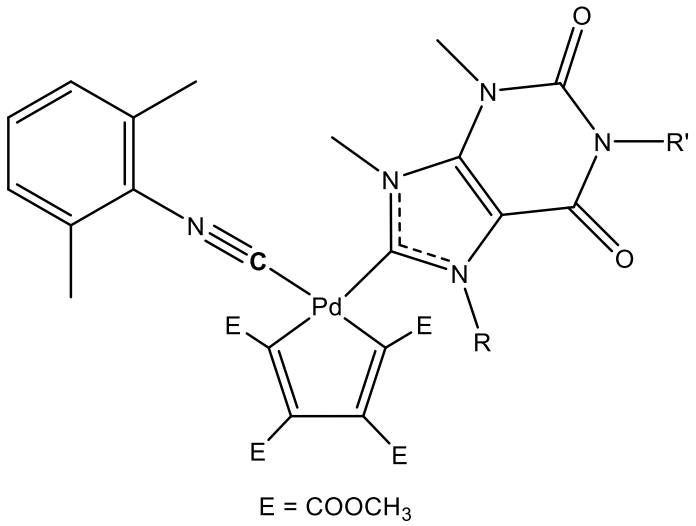

13a R= CH_3 R'= CH_3
13b R= CH_2Ph R'= CH_3
13d R= CH_3 R'= CH_2Ph

Synthesis of the complex 13a

0.0438 g (0.112 mmol) of the polymeric precursor $[PdC_4(COOCH_3)_4]_n$ was dissolved in 5 mL of anhydrous dichloromethane in a 100 mL two-necked flask under inert atmosphere (Ar). To this solution a mixture constituted by 0.0394 g (0.0560 mmol) of the silver complex **5a** and 0.0147 g (0.112 mmol) of 2,6-dimethylphenyl isocyanide (DIC) dissolved in ca. 25 mL of anhydrous dichloromethane, was added. The mixture was stirred at R.T. for 48 h and subsequently the precipitated AgCl was removed by filtration on a millipore membrane filter.

Addition of diethylether to the concentrated solution yields the precipitation of the complex **13a** as a yellow solid which was filtered off on a gooch and washed with *n*-pentane.

0.0731 g of **13a** was obtained (yield 89%).

^{1}H-NMR (400 MHz, $CDCl_3$, T = 298K, ppm) δ: 2.35 (s, 6H, $2CH_3^{DIC}$), 3.34 (s, 3H, OCH_3), 3.41 (s, 3H, NCH_3), 3.58 (s, 3H, OCH_3), 3.61 (s, 3H, OCH_3), 3.69 (s, 3H, OCH_3), 3.83 (s, 3H, NCH_3), 4.14 (s, 3H, NCH_3), 4.30 (s, 3H, NCH_3), 7.12 (d, 2H, J= 8.1 Hz, $2H^{meta}$), 7.23 (t, 1H, J= 8.1 Hz, H^{para}).

^{13}C{^{1}H}-NMR ($CDCl_3$, T = 298K, ppm) δ: 18.5 (CH_3, CH_3^{DIC}), 28.6 (CH_3, NCH_3), 32.0 (CH_3, NCH_3), 37.1 (CH_3, NCH_3), 39.0 (CH_3, NCH_3), 51.0 (CH_3, OCH_3), 51.3 (CH_3, OCH_3), 110.1 (C, C^5), 128.2-135.1 (Ph^{DIC}), 140.6 (C, C^4), 145.9 (C, C-$COOCH_3$), 147.7 (C, C-$COOCH_3$), 149.0 (C, CN), 150.5 (C, C=O), 153.1 (C, C=O), 164.3 (C, $COOCH_3$), 164.5 (C, $COOCH_3$), 164.8 (C, C-$COOCH_3$), 166.5 (C, C-$COOCH_3$), 174.9 (C, $COOCH_3$), 175.6 (C, $COOCH_3$), 185.8 (C, carbene).

IR (KBr): $\nu_{C=N}$ = 2176 cm^{-1}, $\nu_{C=O}$ = 1710 cm^{-1}, 1670 cm^{-1}, ν_{C-O} = 1207 cm^{-1}

Synthesis of the complex 13b

Complex **13b** was prepared in analogues manner as that described for **13a** starting from 0.0348 g of $[PdC_4(COOCH_3)_4]_n$, 0.0381 g of **5b** and 0.0117 g of 2,6-dimethylphenyl isocyanide (DIC).
0.0602 g (yield 84%) of **13b** was obtained.
^{1}H-NMR (400 MHz, $CDCl_3$, T = 298K, ppm) δ: 2.11 (s, 6H, $2CH_3^{DIC}$), 3.29 (s, 3H, OCH_3), 3.35 (s, 3H, NCH_3), 3.56 (s, 3H, OCH_3), 3.66 (s, 3H, OCH_3), 3.70 (s, 3H, OCH_3), 3.84 (s, 3H, NCH_3), 4.33 (s, 3H, NCH_3), 5.60 and 5.94 (AB system, 2H, J = 14.7 Hz, NCH_2), 7.04-7.44 (m, 8H, Ph^{DIC}, Ph^{Bn}).
^{13}C{^{1}H}-NMR ($CDCl_3$, T = 298K, ppm) δ: 18.4 (CH_3, CH_3^{DIC}), 28.7 (CH_3, NCH_3), 32.0 (CH_3, NCH_3), 39.3 (CH_3, NCH_3), 51.0 (CH_3, OCH_3), 51.1 (CH_3, OCH_3), 51.3 (CH_3, OCH_3), 51.4 (CH_3, OCH_3), 53.1 (CH_2, NCH_2), 109.7 (C, C^5), 128.0-135.9 (Ph), 140.7 (C, C^4), 145.7 (C, C-$COOCH_3$), 148.2 (C, C-$COOCH_3$), 149.1 (C, CN), 150.5 (C, C=O), 152.8 (C, C=O), 163.7 (C, $COOCH_3$), 164.6 (C, $COOCH_3$), 164.8 (C, C-$COOCH_3$), 166.9 (C, C-$COOCH_3$), 174.9 (C, $COOCH_3$), 175.5 (C, $COOCH_3$), 187.4 (C, carbene).
IR (KBr): $\nu_{C=N}$ = 2177 cm^{-1}, $\nu_{C=O}$ = 1710 cm^{-1}, 1670 cm^{-1}, ν_{C-O} = 1208 cm^{-1}

Synthesis of the complex 13d

Complex **13d** was prepared in analogues manner as that described for **13a** starting from 0.0313 g of $[PdC_4(COOCH_3)_4]_n$, 0.0343 g of **5d** and 0.0105 g of 2,6-dimethylphenyl isocyanide (DIC).
0.0564 g (yield 87%) of **13d** was obtained.
^{1}H-NMR (400 MHz, $CDCl_3$, T = 298K, ppm) δ: 2.35 (s, 6H, $2CH_3^{DIC}$), 3.32 (s, 3H, OCH_3), 3.57 (s, 3H, NCH_3), 3.65 (s, 3H, OCH_3), 3.69 (s, 3H, OCH_3), 3.81 (s, 3H, OCH_3), 4.15 (s, 3H, NCH_3), 4.28 (s, 3H, NCH_3), 5.14 and 5.20 (AB system, 2H, J = 13.8 Hz, NCH_2), 7.10-7.48 (m, 8H, Ph^{DIC}, Ph^{Bn}).
^{13}C{^{1}H}-NMR ($CDCl_3$, T = 298K, ppm) δ: 18.6 (CH_3, CH_3^{DIC}), 32.0 (CH_3, NCH_3), 37.1 (CH_3, NCH_3), 39.0 (CH_3, NCH_3), 45.2 (CH_2, NCH_2), 51.0 (CH_3, OCH_3), 51.3 (CH_3, OCH_3), 51.4 (CH_3, OCH_3), 110.2 (C, C^5), 128.0-136.3 (Ph), 140.7 (C, C^4), 145.8 (C, C-$COOCH_3$), 147.7 (C, C-$COOCH_3$), 149.0 (C, CN), 150.4 (C, C=O), 153.0 (C, C=O), 164.2 (C, $COOCH_3$), 164.5 (C, $COOCH_3$), 164.8 (C, C-$COOCH_3$), 166.4 (C, C-$COOCH_3$), 174.9 (C, $COOCH_3$), 175.6 (C, $COOCH_3$), 186.0 (C, carbene).
IR (KBr): $\nu_{C=N}$ = 2178 cm^{-1}, $\nu_{C=O}$ = 1710 cm^{-1}, 1675 cm^{-1}, ν_{C-O} = 1205 cm^{-1}

9.6.14. Synthesis of Bis(purine-based NHC) palladacyclopentadienyl complexes (14)

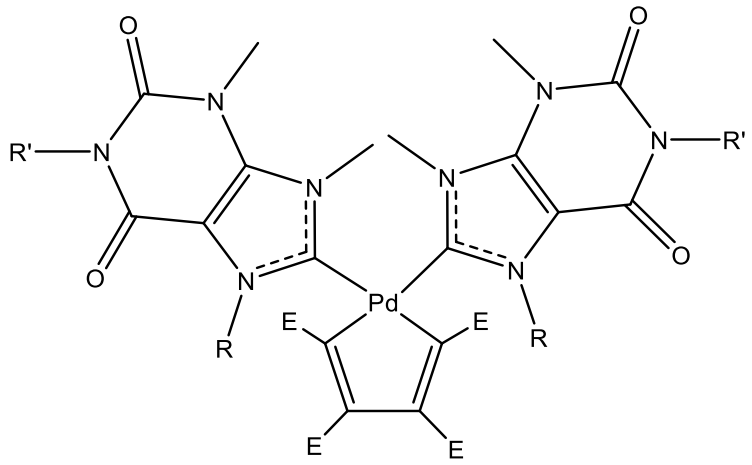

14a R= CH_3 R'= CH_3
14b R= CH_2Ph R'= CH_3
14d R= CH_3 R'= CH_2Ph

Synthesis of the complex 14a

0.0182 g (0.0466 mmol) of the polymeric precursor $[PdC_4(COOCH_3)_4]_n$ was dissolved in 5 mL of anhydrous dichloromethane in a 100 mL two-necked flask under inert atmosphere (Ar). To this solution a mixture constituted by 0.0273 g (0.0388 mmol) of the silver complex **5a** dissolved in ca. 25 mL of anhydrous dichloromethane, was added.

The mixture was stirred at R.T. for 1 h and subsequently the precipitated AgCl was removed by filtration on a millipore membrane filter.

Addition of diethylether to the concentrated solution yields the precipitation of the complex **14a** as a yellow solid which was filtered off on a gooch and washed with *n*-pentane.

0.0213 g of **14a** was obtained (yield 70%).

^{1}H-NMR (400 MHz, CD_2Cl_2, T = 298K, ppm) δ: 3.30 (s, 12H, 4 OCH_3), 3.36 (s, 12H, 4NCH_3), 3.61 (s, 12H, 4 OCH_3), 3.78 (s, 6H, 2NCH_3), 3.79 (s, 6H, 2NCH_3), 4.11 (s, 6H, 2NCH_3), 4.15 (s, 6H, 2NCH_3), 4.32 (s, 6H, 2NCH_3), 4.34 (s, 6H, 2NCH_3).

^{13}C{^{1}H}-NMR (CD_2Cl_2, T = 298K, ppm) δ: 28.3 (CH_3, NCH_3), 31.8 (CH_3, NCH_3), 37.2 (CH_3, NCH_3), 37.4 (CH_3, NCH_3), 39.2 (CH_3, NCH_3), 39.3 (CH_3, NCH_3), 50.6 (CH_3, OCH_3), 51.0 (CH_3, OCH_3), 109.8 (C, C^5), 140.5 (C, C^4), 144.6 (C, <u>C</u>-$COOCH_3$), 150.6 (C, C=O), 153.0 (C, C=O), 164.8 (C, <u>C</u>$OOCH_3$), 164.9 (C, <u>C</u>$OOCH_3$), 167.1 (C, <u>C</u>-$COOCH_3$), 167.2 (C, <u>C</u>-$COOCH_3$), 175.7 (C, <u>C</u>$OOCH_3$), 175.9 (C, <u>C</u>$OOCH_3$), 188.1 (C, carbene), 188.4 (C, carbene).

IR (KBr): $\nu_{C=O}$ = 1710 cm^{-1}, 1672 cm^{-1}, ν_{C-O} = 1209 cm^{-1}

Synthesis of the complex 14b

Complex **14b** was prepared in analogues manner as that described for **14a** starting from 0.0194 g of $[PdC_4(COOCH_3)_4]_n$ and 0.0354 g of **5b**.

0.0363 g (yield 91%) of **14b** was obtained.

^{1}H-NMR (400 MHz, CD_2Cl_2, T = 298K, ppm) δ: 3.27 (s, 12H, 4 OCH_3), 3.29 (s, 12H, 4NCH_3), 3.43 (s, 6H, 2NCH_3), 3.61 (s, 6H, 2 OCH_3), 3.63 (s, 6H, 2 OCH_3), 3.75 (s, 6H, 2NCH_3), 3.79 (s, 6H, 2NCH_3), 4.32 (s, 6H, 2NCH_3), 4.98 and 5.40 (AB system, 4H, J = 15.5 Hz, 2NCH_2), 5.77 and 5.85 (AB system, 4H, J = 16.3 Hz, 2NCH_2), 6.90-7.33 (m, 20H, 4Ph).

^{13}C{^{1}H}-NMR (CD_2Cl_2, T = 298K, ppm) δ: 28.3 (CH_3, NCH_3), 31.5 (CH_3, NCH_3), 31.9 (CH_3, NCH_3), 38.4 (CH_3, NCH_3), 39.4 (CH_3, NCH_3), 50.6 (CH_3, OCH_3), 51.0 (CH_3, OCH_3), 52.7 (CH_2, NCH_2), 109.0 (C, C^5), 109.5 (C, C^5), 125.1-136.7 (Ph), 140.7 (C, C^4), 140.8 (C, C^4), 145.1 (C, C-$COOCH_3$), 145.2 (C, C-$COOCH_3$), 150.4 (C, C=O), 150.5 (C, C=O), 152.3 (C, C=O), 164.8 (C, $COOCH_3$), 165.1 (C, $COOCH_3$), 166.7 (C, C-$COOCH_3$), 167.1 (C, C-$COOCH_3$), 175.4 (C, $COOCH_3$), 188.6 (C, carbene), 189.1 (C, carbene).

IR (KBr): $\nu_{C=O}$ = 1710 cm^{-1}, 1668 cm^{-1}, ν_{C-O} = 1206 cm^{-1}

Synthesis of the complex 14d

Complex **14d** was prepared in analogues manner as that described for **14a** starting from 0.0283 g of $[PdC_4(COOCH_3)_4]_n$ and 0.0516 g of **5d**.

0.0551 g (yield 80%) of **14d** was obtained.

^{1}H-NMR (400 MHz, $CDCl_3$, T = 298K, ppm) δ: 3.28 (s, 6H, 2 OCH_3), 3.31 (s, 6H, 2 OCH_3), 3.62 (s, 6H, 2 OCH_3), 3.64 (s, 6H, 2 OCH_3), 3.74 (s, 6H, 2NCH_3), 3.78 (s, 6H, 2NCH_3), 4.09 (s, 6H, 2NCH_3), 4.13 (s, 6H, 2NCH_3), 4.35 (s, 6H, 2NCH_3), 4.36 (s, 6H, 2NCH_3), 5.14 (m, 8H, 4NCH_2), 7.27-7.40 (m, 20H, 4Ph).

^{13}C{^{1}H}-NMR ($CDCl_3$, T = 298K, ppm) δ: 31.9 (CH_3, NCH_3), 32.0 (CH_3, NCH_3), 37.4 (CH_3, NCH_3), 37.6 (CH_3, NCH_3), 39.4 (CH_3, NCH_3), 39.6 (CH_3, NCH_3), 45.1 (CH_2, NCH_2), 50.8 (CH_3, OCH_3), 51.3 (CH_3, OCH_3), 109.9 (C, C^5), 127.9-136.3 (Ph), 140.7 (C, C^4), 140.8 (C, C^4), 145.0 (C, C-$COOCH_3$), 145.3 (C, C-$COOCH_3$), 150.4 (C, C=O), 152.9 (C, C=O), 165.0 (C, $COOCH_3$), 165.2 (C, $COOCH_3$), 166.6 (C, C-$COOCH_3$), 166.9 (C, C-$COOCH_3$), 176.1 (C, $COOCH_3$), 176.2 (C, $COOCH_3$), 188.3 (C, carbene), 189.1 (C, carbene).

IR (KBr): $\nu_{C=O}$ = 1709 cm^{-1}, 1671 cm^{-1}, ν_{C-O} = 1208 cm^{-1}

9.6.15. Synthesis of mixed purine-based NHC/PPh_3 palladium η^2-olefin complexes (15-18)

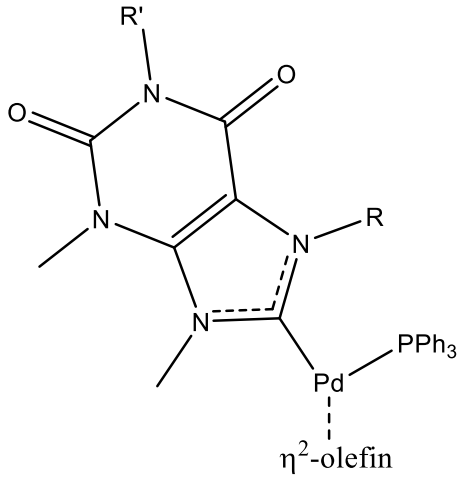

15a R= CH_3 R'= CH_3 η^2-olefin = tmetc
15b R= CH_2Ph R'= CH_3 η^2-olefin = tmetc
15d R= CH_3 R'= CH_2Ph η^2-olefin = tmetc
16a R= CH_3 R'= CH_3 η^2-olefin = fn
17a R= CH_3 R'= CH_3 η^2-olefin = ma
18a R= CH_3 R'= CH_3 η^2-olefin = dmfu

Synthesis of the complex 15a

0.0500 g (0.086 mmol) of the precursor [Pd(Me-$PyCH_2SPh$)(η^2-tmetc)] was dissolved in 10 mL of anhydrous dichloromethane in a 50 mL two-necked flask under inert atmosphere (Ar). To this solution a mixture constituted by 0.0302 g (0.043 mmol) of the silver complex **5a** and 0.0225 g (0.086 mmol) of PPh_3 dissolved in ca. 15 mL of anhydrous dichloromethane, was added.

The mixture was stirred at R.T. for 1 h and subsequently the precipitated AgCl was removed by filtration on a millipore membrane filter. The solvent was removed under reduced pressure and the yellow solid was washed with ca. 10 mL of diethylether and filtered off on a gooch.

0.0641 g of **15a** was obtained (yield 80%).

^{1}H-NMR (400 MHz, CD_2Cl_2, T=298K, ppm) δ: 3.35 (s, 3H, NCH_3), 3.46 (s, 3H, OCH_3), 3.48 (s, 3H, NCH_3), 3.56 (s, 3H, OCH_3), 3.61 (s, 3H, OCH_3), 3.62 (s, 3H, OCH_3), 3.70 (s, 3H, NCH_3), 3.71 (s, 3H, NCH_3), 7.34-7.44 (m, 15H, 3Ph).

^{13}C{^{1}H}-NMR (CD_2Cl_2, T=298K, ppm) δ: 28.2 (CH_3, NCH_3), 31.4 (CH_3, NCH_3), 36.5 (CH_3, NCH_3), 38.1 (CH_3, NCH_3), 51.3 (CH_3, OCH_3), 51.5 (CH_3, OCH_3), 51.6 (CH_3, OCH_3), 51.9 (CH_3, OCH_3), 110.1 (C, C^5), 128.1-134.6 (Ph), 140.2 (C, C^4), 150.5 (C, C=O), 152.9 (C, C=O), 169.8-170.4 (C, $\underline{C}OOCH_3$), 196.5 (d, C, J_{C-P} = 15.1 Hz, carbene).

^{31}P{^{1}H}-NMR (CD_2Cl_2, T=298K, ppm) δ: 29.4

IR (KBr): $\nu_{C=O}$= 1725, 1709, 1694, 1668 cm^{-1}

Synthesis of the complex 15b

Complex **15b** was prepared in analogues manner as that described for **15a** starting from 0.0377 g of [Pd(Me-PyCH$_2$SPh)(η^2-tmetc)], 0.0170 g of PPh$_3$ and 0.0277 g of **5b**.

0.0473 g (yield 80%) of **15b** was obtained.

^{1}H-NMR (400 MHz, CDCl$_3$, T=298K, ppm) δ: 3.11 (s, 3H, OCH$_3$), 3.38 (s, 3H, NCH$_3$), 3.41 (s, 3H, NCH$_3$), 3.52 (s, 3H, OCH$_3$), 3.64 (s, 3H, OCH$_3$), 3.71 (s, 3H, NCH$_3$), 3.72 (s, 3H, OCH$_3$), 5.25 and 5.85 (AB system, 2H, J= 13.9 Hz, NCH$_2$), 6.71-7.61 (m, 20H, 4Ph).

^{13}C{^{1}H}-NMR (CDCl$_3$, T=298K, ppm) δ: 28.7 (CH$_3$, NCH$_3$), 31.8 (CH$_3$, NCH$_3$), 38.4 (CH$_3$, NCH$_3$), 51.0 (CH$_3$, OCH$_3$), 52.0 (CH$_3$, OCH$_3$), 52.5 (CH$_3$, OCH$_3$), 52.6 (CH$_3$, OCH$_3$), 53.4 (CH$_2$, NCH$_2$), 61.9 (C, C=C *trans*-C), 64.0 (d, C, J_{C-P} = 37.6 Hz, C=C *trans*-P), 109.4 (C, C^5), 127.9-136.2 (Ph), 140.7 (C, C^4), 150.6 (C, C=O), 152.9 (C, C=O), 169.8-170.4 (C, COOCH$_3$) 198.5 (d, C, J_{C-P} = 14.4 Hz, carbene).

^{31}P{^{1}H}-NMR (CDCl$_3$, T=298K, ppm) δ: 26.9

IR (KBr): $\nu_{C=O}$= 1704, 1666 cm^{-1}

Synthesis of the complex 15d

Complex **15d** was prepared in analogues manner as that described for **15a** starting from 0.0500 g of [Pd(NSPM)(η^2-tmetc)], 0.0225 g of PPh$_3$ and 0.0367 g of **5d**.

0.0604 g (yield 77%) of **15d** was obtained.

^{1}H-NMR (400 MHz, CDCl$_3$, T=298K, ppm) δ: 3.47 (s, 3H, OCH$_3$), 3.53 (s, 3H, NCH$_3$), 3.55 (s, 3H, OCH$_3$), 3.65 (s, 3H, OCH$_3$), 3.67 (s, 3H, OCH$_3$), 3.73 (s, 3H, NCH$_3$), 3.74 (s, 3H, NCH$_3$), 5.15 (s, 2H, NCH$_2$), 7.32-7.46 (m, 20H, 4Ph).

^{13}C{^{1}H}-NMR (CDCl$_3$, T=298K, ppm) δ: 31.5 (CH$_3$, NCH$_3$), 36.8 (CH$_3$, NCH$_3$), 38.5 (CH$_3$, NCH$_3$), 45.0 (CH$_2$, NCH$_2$), 51.5 (CH$_3$, OCH$_3$), 51.9 (CH$_3$, OCH$_3$), 52.1 (CH$_3$, OCH$_3$), 52.5 (CH$_3$, OCH$_3$), 61.9 (d, C, J_{C-P} = 2.1 Hz, C=C *trans*-C), 63.8 (d, C, J_{C-P} = 36.9 Hz, C=C *trans*-P), 110.2 (C, C^5), 127.8-136.6 (Ph), 140.2 (C, C^4), 150.4 (C, C=O), 152.7 (C, C=O), 169.8-170.4 (C, COOCH$_3$),197.4 (d, C, J_{C-P} = 15.8 Hz, carbene).

^{31}P{^{1}H}-NMR (CDCl$_3$, T=298K, ppm) δ: 29.2

IR (KBr): $\nu_{C=O}$= 1706, 1668 cm^{-1}

Synthesis of the complex 16a

0.0450 g (0.112 mmol) of the precursor [Pd(Me-PyCH$_2$SPh)(η^2-fn)] was dissolved in 10 mL of anhydrous dichloromethane in a 50 mL two necked flask under inert atmosphere (Ar). To this solution a mixture constituted by 0.0396 g (0.056 mmol) of the silver complex **5a** and 0.0295 g (0.112 mmol) of PPh$_3$ dissolved in ca. 15 mL of anhydrous dichloromethane, was added.

The mixture was stirred at R.T. for 1 h and subsequently the precipitated AgCl was removed by filtration on a millipore membrane filter.

Addition of diethylether to the concentrated solution yields the precipitation of the complex **16a** as a yellow solid which was filtered off on a gooch and washed with *n*-pentane.

0.0597 g of **16a** was obtained (yield 81%).

^{1}H-NMR (400 MHz, $CDCl_3$, T=298K, ppm) δ: 2.90 (dd, J_{H-H} = 9.4 Hz, J_{H-P} = 3.4 Hz, 1H, CH=CH *trans*-P), 3.01 (d, J_{H-H} = 9.4 Hz, 1H, CH=CH *trans*-C), 3.40 (s, 3H, NCH_3), 3.61 (s, 3H, NCH_3), 3.69 (s, 3H, NCH_3), 3.78 (s, 3H, NCH_3), 7.33-7.42 (m, 15H, 3Ph).

^{13}C{^{1}H}-NMR ($CDCl_3$, T=298K, ppm) δ: 22.5 (d, CH, J_{C-P} = 3.4 Hz, CH=CH *trans*-C), 22.9 (d, CH, J_{C-P} = 37.8 Hz, CH=CH *trans*-P), 28.6 (CH_3, NCH_3), 31.6 (CH_3, NCH_3), 37.0 (CH_3, NCH_3), 38.0 (CH_3, NCH_3), 110.2 (C, C^5), 123.2 (d, C, J_{C-P} = 2.6 Hz, CN *trans*-C), 123.8 (d, C, J_{C-P} = 8.0 Hz, CN *trans*-P), 128.6-134.5 (Ph), 140.3 (C, C^4), 150.6 (C, C=O), 152.9 (C, C=O), 198.5 (d, C, J_{C-P} = 11.7 Hz, carbene).

^{31}P{^{1}H}-NMR ($CDCl_3$, T=298K, ppm) δ: 27.9

IR (KBr): ν_{CN}= 2191 cm^{-1}, ν_{CO}= 1807, 1667 cm^{-1}

Synthesis of the complex 17a

0.0500 g (0.119 mmol) of the precursor [Pd(Me-PyCH_2SPh)(η^2-ma)] was dissolved in 10 mL of anhydrous dichloromethane in a 50 mL two-necked flask under inert atmosphere (Ar). To this solution a mixture constituted by 0.0419 g (0.059 mmol) of the silver complex **5a** and 0.0312 g (0.119 mmol) of PPh_3 dissolved in ca. 15 mL of anhydrous dichloromethane, was added.

The mixture was stirred at R.T. for 1 h and subsequently the precipitated AgCl was removed by filtration on a millipore membrane filter. Addition of diethylether to the concentrated solution yields the precipitation of the complex **17a** as a yellow solid which was filtered off on a gooch and washed with *n*-pentane. 0.0594 g of **17a** was obtained (yield 74%).

^{1}H-NMR (400 MHz, $CDCl_3$, T=298K, ppm) δ: 3.39 (s, 3H, NCH_3), 3.60 (s, 3H, NCH_3), 3.65 (s, 6H, 2NCH_3), 3.99 (dd, J_{H-H} = 3.9 Hz, J_{H-P} = 2.9 Hz, 1H, CH=CH *trans*-C), 4.22 (dd, J_{H-H} = 3.9 Hz, J_{H-P} = 9.8 Hz, 1H, CH=CH *trans*-P), 7.31-7.41 (m, 15H, 3Ph).

^{13}C{^{1}H}-NMR ($CDCl_3$, T=298K, ppm) δ: 28.6 (CH_3, NCH_3), 31.6 (CH_3, NCH_3), 36.9 (CH_3, NCH_3), 38.0 (CH_3, NCH_3), 45.6 (CH, CH=CH *trans*-C), 47.5 (d, CH, J_{C-P} = 27.8 Hz, CH=CH *trans*-P), 110.2 (C, C^5), 128.6-134.3 (Ph), 140.3 (C, C^4), 150.5 (C, C=O), 152.9 (C, C=O), 172.3 (d, C, J_{C-P} = 1.9 Hz, C=O^{ma} *trans*-C), 172.7 (d, C, J_{C-P} = 5.2 Hz, C=O^{ma} *trans*-P), 198.4 (d, C, J_{C-P} = 14.5 Hz, carbene).

^{31}P{^{1}H}-NMR ($CDCl_3$, T=298K, ppm) δ: 30.4

IR (KBr): $\nu_{C=O}$= 1790, 1722, 1704, 1665 cm^{-1} ν_{C-O}= 1224 cm^{-1}

Synthesis of the complex 18a

0.0400 g (0.091 mmol) of the precursor [Pd(TMQ-Me)(η^2-dmfu)] were dissolved in 10 mL of anhydrous dichloromethane in a 50 mL two necked flask under inert atmosphere (Ar) at -40°C. To this solution a mixture constituted by 0.0297 g (0.042 mmol) of the silver complex **5a** and 0.0238 g (0.091mmol) of PPh_3 dissolved in ca. 15 mL of anhydrous dichloromethane, was added.

The mixture was stirred at -40°C for 30 min and subsequently the precipitated AgCl was removed by filtration on a millipore membrane filter.

Addition of diethylether to the concentrated solution yields the precipitation of the complex **18a** as a brownish solid which was filtered off on a gooch and washed with *n*-pentane.

0.0422 g of **18a** was obtained (yield 64%).

^{1}H-NMR (400 MHz, $CDCl_3$, T=298K, ppm) δ: 3.17 (s, 3H, NCH_3), 3.39 (s, 3H, NCH_3), 3.54 (s, 3H, NCH_3), 3.57 (s, 3H, NCH_3), 3.97 (dd, J_{H-H} = 9.5 Hz, J_{H-P} = 2.6 Hz, 1H, CH=CH *trans*-P), 4.08 (d, J_{H-H} = 9.5 Hz, 1H, CH=CH *trans*-C), 7.30-7.34 (m, 15H, 3Ph).

^{13}C{^{1}H}-NMR ($CDCl_3$, T=243K, ppm) δ: 28.9 (CH_3, NCH_3), 31.7 (CH_3, NCH_3), 36.8 (CH_3, NCH_3), 37.7 (CH_3, OCH_3), 38.7 (CH_3, NCH_3), 50.6 (CH, $CH=CH^{dmfu}$), 51.5 (CH, $CH=CH^{dmfu}$), 110.0 (C, C^5), 128.4-135.0 (Ph), 140.0 (C, C^4), 150.5 (C, C=O), 153.0 (C, C=O), 174.7 (C, $C=O^{dmfu}$), 198.5 (d, C, J_{C-P} = 14.3 Hz, carbene).

^{31}P{^{1}H}-NMR ($CDCl_3$, T=298K, ppm) δ: 29.7

IR (KBr): $\nu_{C=O}$= 1662 cm^{-1}

9.6.16. Synthesis of mixed purine-based NHC/$AsPh_3$ palladium η^2-olefin complexes (19-22)

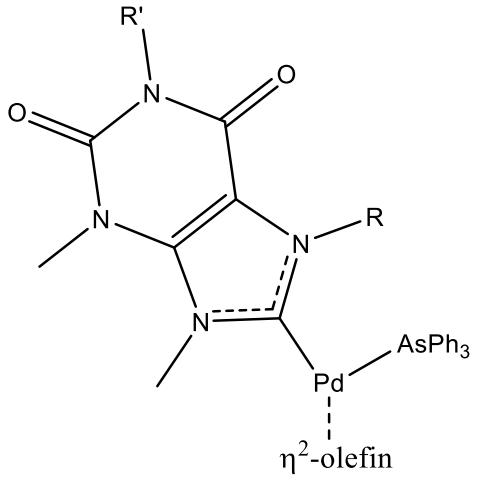

19a R= CH_3 R'= CH_3 η^2-olefin = tmetc
19b R= CH_2Ph R'= CH_3 η^2-olefin = tmetc
19d R= CH_3 R'= CH_2Ph η^2-olefin = tmetc
20a R= CH_3 R'= CH_3 η^2-olefin = fn
21a R= CH_3 R'= CH_3 η^2-olefin = ma
22a R= CH_3 R'= CH_3 η^2-olefin = dmfu

Synthesis of the complex 19a

0.0500 g (0.086 mmol) of the precursor [Pd(Me-$PyCH_2SPh$)(η^2-tmetc)] was dissolved in 10 mL of anhydrous dichloromethane in a 50 mL two-necked flask under inert atmosphere (Ar). To this solution a mixture constituted by 0.0302 g (0.043 mmol) of the silver complex **5a** and 0.0263 g (0.086 mmol) of $AsPh_3$ dissolved in ca. 15 mL of anhydrous dichloromethane, was added.

The mixture was stirred at R.T. for 1 h and subsequently the precipitated AgCl was removed by filtration on a millipore membrane filter. The solvent was removed under reduced pressure and the yellow solid was washed with ca. 10 mL of diethylether and filtered off on a gooch.

0.0626 g of **19a** was obtained (yield 83%).

^{1}H-NMR (400 MHz, $CDCl_3$, T=298K, ppm) δ: 3.37 (s, 3H, NCH_3), 3.47 (s, 3H, OCH_3), 3.53 (s, 3H, NCH_3), 3.58 (s, 3H, OCH_3), 3.65 (s, 3H, OCH_3), 3.68 (s, 3H, OCH_3), 3.75 (s, 3H, NCH_3), 3.78 (s, 3H, NCH_3), 7.28-7.42 (m, 15H, 3Ph).

^{13}C{^{1}H}-NMR ($CDCl_3$, T=298K, ppm) δ: 28.5 (CH_3, NCH_3), 31.5 (CH_3, NCH_3), 36.9 (CH_3, NCH_3), 38.5 (CH_3, NCH_3), 51.6 (CH_3, OCH_3), 52.0 (CH_3, OCH_3), 52.1 (CH_3, OCH_3), 52.5 (CH_3, OCH_3), 61.0 (C, C=C), 64.1 (C, C=C), 110.1 (C, C^5), 128.7-136.5 (Ph), 140.2 (C, C^4), 150.5 (C, C=O), 153.0 (C, C=O), 169.7 (C, $\underline{C}OOCH_3$), 169.8 (C, $\underline{C}OOCH_3$), 170.0 (C, $\underline{C}OOCH_3$), 170.5 (C, $\underline{C}OOCH_3$), 197.1 (C, carbene). IR (KBr): $\nu_{C=O}$= 1707, 1667 cm^{-1}

Synthesis of the complex 19b

Complex **19b** was prepared in analogues manner as that described for **19a** starting from 0.0430 g of [Pd(Me-PyCH$_2$SPh)(η^2-tmetc)], 0.0226 g of AsPh$_3$ and 0.0316 g of **5b**.

0.0542 g (yield 77%) of **19b** was obtained.

^{1}H-NMR (400 MHz, CDCl$_3$, T=298K, ppm) δ: 3.08 (s, 3H, OCH$_3$), 3.33 (s, 3H, NCH$_3$), 3.44 (s, 3H, NCH$_3$), 3.60 (s, 3H, OCH$_3$), 3.71 (s, 3H, OCH$_3$), 3.75 (s, 3H, NCH$_3$), 3.78 (s, 3H, OCH$_3$), 5.25 and 5.89 (AB system, 2H, J= 13.6 Hz, NCH$_2$), 6.68-7.74 (m, 20H, 4Ph).

^{13}C{^{1}H}-NMR (CDCl$_3$, T=298K, ppm) δ: 28.7 (CH$_3$, NCH$_3$), 31.7 (CH$_3$, NCH$_3$), 38.5 (CH$_3$, NCH$_3$), 50.9 (CH$_3$, OCH$_3$), 52.0 (CH$_3$, OCH$_3$), 52.1 (CH$_2$, NCH$_2$), 52.2 (CH$_3$, OCH$_3$), 52.6 (CH$_3$, OCH$_3$), 61.0 (C, C=C), 64.2 (C, C=C), 109.3 (C, C^5), 128.0-136.3 (Ph), 140.5 (C, C^4), 150.5 (C, C=O), 153.0 (C, C=O), 169.8 (C, COOCH$_3$), 170.1 (C, COOCH$_3$), 170.2 (C, COOCH$_3$), 170.4 (C, COOCH$_3$), 198.4 (C, carbene).

IR (KBr): $\nu_{C=O}$= 1707, 1670 cm^{-1}

Synthesis of the complex 19d

Complex **19d** was prepared in analogues manner as that described for **19a** starting from 0.0500 g of [Pd(NSPM)(η^2-tmetc)], 0.0263 g of AsPh$_3$ and 0.0367 g of **5d**.

0.0631g (yield 77%) of **19d** was obtained.

^{1}H-NMR (400 MHz, CDCl$_3$, T=298K, ppm) δ: 3.47 (s, 3H, OCH$_3$), 3.51 (s, 3H, NCH$_3$), 3.58 (s, 3H, OCH$_3$), 3.66 (s, 3H, OCH$_3$), 3.69 (s, 3H, OCH$_3$), 3.78 (s, 3H, NCH$_3$), 3.79 (s, 3H, NCH$_3$), 5.14 (s, 2H, NCH$_2$), 7.26-7.48 (m, 20H, 4Ph).

^{13}C{^{1}H}-NMR (CDCl$_3$, T=298K, ppm) δ: 31.5 (CH$_3$, NCH$_3$), 36.9 (CH$_3$, NCH$_3$), 38.6 (CH$_3$, NCH$_3$), 44.9 (CH$_2$, NCH$_2$), 51.6 (CH$_3$, OCH$_3$), 52.1 (CH$_3$, OCH$_3$), 52.2 (CH$_3$, OCH$_3$), 52.5 (CH$_3$, OCH$_3$), 61.0 (C, C=C), 64.0 (C, C=C), 110.1 (C, C^5), 127.9-136.6 (Ph), 140.1 (C, C^4), 150.4 (C, C=O), 152.7 (C, C=O), 169.7 (C, COOCH$_3$), 169.8 (C, COOCH$_3$), 170.0 (C, COOCH$_3$), 170.4 (C, COOCH$_3$), 197.2 (C, carbene).

IR (KBr): $\nu_{C=O}$= 1708, 1670 cm^{-1}

Synthesis of the complex 20a

0.0452 g (0.113 mmol) of the precursor [Pd(Me-PyCH$_2$SPh)(η^2-fn)] was dissolved in 10 mL of anhydrous dichloromethane in a 50 mL two necked flask under inert atmosphere (Ar). To this solution a mixture constituted by 0.0397 g (0.056 mmol) of the silver complex **5a** and 0.0346 g (0.113 mmol) of AsPh$_3$ dissolved in ca. 15 mL of anhydrous dichloromethane, was added.

The mixture was stirred at R.T. for 1 h and subsequently the precipitated AgCl was removed by filtration on a millipore membrane filter.

Addition of diethylether to the concentrated solution yields the precipitation of the complex **20a** as a yellow solid which was filtered off on a gooch and washed with *n*-pentane.

0.0582 g of **20a** was obtained (yield 74%).

^{1}H-NMR (400 MHz, $CDCl_3$, T=298K, ppm) δ: 3.02 (d, J_{H-H} = 9.3 Hz, 1H, CH=CH), 3.16 (d, J_{H-H} = 9.4 Hz, 1H, CH=CH), 3.40 (s, 3H, NCH_3), 3.61 (s, 3H, NCH_3), 3.75 (s, 3H, NCH_3), 3.84 (s, 3H, NCH_3), 7.36-7.40 (m, 15H, 3Ph).

^{13}C{^{1}H}-NMR ($CDCl_3$, T=298K, ppm) δ: 20.7 (CH, CH=CH), 23.1 (CH, CH=CH), 28.6 (CH_3, NCH_3), 31.6 (CH_3, NCH_3), 37.1 (CH_3, NCH_3), 38.2 (CH_3, NCH_3), 110.2 (C, C^5), 123.1 (C, CN), 123.3 (C, CN), 129.1-136.1 (Ph), 140.2 (C, C^4), 150.5 (C, C=O), 152.9 (C, C=O), 198.0 (C, carbene).

IR (KBr): ν_{CN}= 2191 cm^{-1}, $\nu_{C=O}$= 1708, 1667 cm^{-1}

Synthesis of the complex 21a

0.0500 g (0.119 mmol) of the precursor [Pd(Me-PyCH_2SPh)(η^2-ma)] was dissolved in 10 mL of anhydrous dichloromethane in a 50 mL two necked flask under inert atmosphere (Ar). To this solution a mixture constituted by 0.0419 g (0.059 mmol) of the silver complex **5a** and 0.0365 g (0.119 mmol) of $AsPh_3$ dissolved in ca. 15 mL of anhydrous dichloromethane, was added.

The mixture was stirred at R.T. for 1 h and subsequently the precipitated AgCl was removed by filtration on a millipore membrane filter.

Addition of diethylether to the concentrated solution yields the precipitation of the complex **21a** as a yellow solid which was filtered off on a gooch and washed with *n*-pentane.

0.0673 g of **21a** was obtained (yield 79%).

^{1}H-NMR (400 MHz, $CDCl_3$, T=298K, ppm) δ: 3.39 (s, 3H, NCH_3), 3.59 (s, 3H, NCH_3), 3.70 (s, 3H, NCH_3), 3.72 (s, 3H, NCH_3), 4.13 (d, J = 3.9 Hz, 1H, CH=CH), 4.33 (d, J = 3.9 Hz, 1H, CH=CH), 7.32-7.41 (m, 15H, 3Ph).

^{13}C{^{1}H}-NMR ($CDCl_3$, T=298K, ppm) δ: 28.6 (CH_3, NCH_3), 31.6 (CH_3, NCH_3), 37.1 (CH_3, NCH_3), 38.2 (CH_3, NCH_3), 44.0 (CH, CH=CH), 47.6 (d, CH, CH=CH), 110.2 (C, C^5), 128.8-136.1 (Ph), 140.3 (C, C^4), 150.5 (C, C=O), 152.9 (C, C=O), 172.3 (C, C=O^{ma}), 172.4 (C, C=O^{ma}), 197.9 (C, carbene).

IR (KBr): $\nu_{C=O}$= 1788, 1725, 1695 cm^{-1} ν_{C-O}=1220 cm^{-1}

Synthesis of the complex 22a

0.0400 g (0.091 mmol) of the precursor [Pd(TMQ-Me)(η^2-dmfu)] was dissolved in 10 mL of anhydrous dichloromethane in a 50 mL two necked flask under inert atmosphere (Ar) at -40°C. To this solution a mixture constituted by 0.0297 g (0.042 mmol) of the silver complex **5a** and 0.0278 g (0.091mmol) of $AsPh_3$ dissolved in ca. 15 mL of anhydrous dichloromethane, was added.

The mixture was stirred at -40°C for 30 min and subsequently the precipitated AgCl was removed by

filtration on a millipore membrane filter.

Addition of diethylether to the concentrated solution yields the precipitation of the complex **18a** as a brownish solid which was filtered off on a gooch and washed with *n*-pentane.

0.0529 g of **18a** was obtained (yield 76%).

^{1}H-NMR (400 MHz, $CDCl_3$, T=298K, ppm) δ: 3.20 (s, 3H, OCH_3), 3.39 (s, 3H, NCH_3), 3.56 (s, 6H, NCH_3+OCH_3), 3.71 (s, 3H, NCH_3), 3.76 (s, 3H, NCH_3), 4.08 (d, J = 10.0 Hz, 1H, CH=CH), 4.22 (d, J = 10.0 Hz, 1H, CH=CH), 7.32-7.37 (m, 15H, 3Ph).

^{13}C{^{1}H}-NMR ($CDCl_3$, T=243K, ppm) δ: 28.9 (CH_3, NCH_3), 31.6 (CH_3, NCH_3), 37.0 (CH_3, NCH_3), 37.9 (CH_3, NCH_3), 45.5 (CH, CH=CH), 48.2 (CH, CH=CH), 50.6 (CH_3, OCH_3), 51.6 (CH_3, OCH_3), 109.9 (C, C^5), 128.6-137.0 (Ph), 140.0 (C, C^4), 150.5 (C, C=O), 153.1 (C, C=O), 174.7 (C, $C=O^{dmfu}$), 174.8 (C, $C=O^{dmfu}$), 194.5 (C, carbene).

IR (KBr): $\nu_{C=O}$= 1709, 1665 cm^{-1} ν_{C-O}= 1289 cm^{-1}

9.6.17. Synthesis of Bis(purine-based NHC) palladium olefin complexes (23-24)

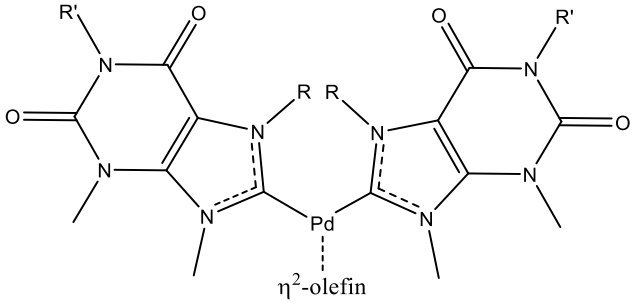

23a R= CH_3 R'= CH_3 η^2-olefin= tmetc
23b R= CH_2Ph R'= CH_3 η^2-olefin= tmetc
23d R= CH_3 R'= CH_2Ph η^2-olefin= tmetc
24a R= CH_3 R'= CH_3 η^2-olefin= fn

Synthesis of the complex 23a

0.0386 g (0.066 mmol) of the precursor [Pd(Me-PyCH_2SPh)(η^2-tmetc)] was dissolved in 25 mL of anhydrous dichloromethane in a 100 mL two-necked flask under inert atmosphere (Ar). Subsequently 0.0466 g (0.066 mmol) of the silver complex **5a**, was added. The mixture was stirred at R.T. for 1 h and the precipitated AgCl was removed by filtration on a millipore membrane filter.

The solvent was removed under reduced pressure and the yellow solid was washed with ca. 10 mL of diethylether and filtered off on a gooch.

0.0516 g of **23a** was obtained (yield 99%).

^{1}H-NMR (400 MHz, $CDCl_3$, T=298K, ppm) δ: 3.39 (s, 6H, 2NCH_3), 3.65 (s, 12H, 4 OCH_3), 3.80 (s, 6H, 2NCH_3), 4.07 (s, 6H, 2NCH_3), 4.34 (s, 6H, 2NCH_3).

^{13}C{^{1}H}-NMR ($CDCl_3$, T=298K, ppm) δ: 28.5 (CH_3, NCH_3), 31.8 (CH_3, NCH_3), 37.2 (CH_3, NCH_3), 39.4 (CH_3, NCH_3), 52.2 (CH_3, OCH_3), 58.2 (C, C=C), 110.4 (C, C^5), 140.5 (C, C^4), 150.7 (C, C=O), 153.2 (C, C=O), 170.8 (C, $\underline{C}OOCH_3$), 197.0 (C, carbene).

IR (KBr): $\nu_{C=O}$= 1706, 1668 cm^{-1}

Synthesis of the complex 23b

Complex **23b** was prepared in analogues manner as that described for **23a** starting from 0.0500 g of [Pd(Me-PyCH_2SPh)(η^2-tmetc)] and 0.0735 g of **5b**. 0.0722 g (yield 86%) of **23b** was obtained.

^{1}H-NMR (400 MHz, $CDCl_3$, T=298K, ppm) δ: 3.28 (s, 6H, 2NCH_3), 3.43 (s, 6H, 2NCH_3), 3.63 (s, 12H, 4 OCH_3), 3.68 (s, 6H, 2NCH_3), 5.79 (s, 4H, 2NCH_2), 6.88-6.91 and 7.22-7.24 (m, 10H, 2Ph).

^{13}C{^{1}H}-NMR ($CDCl_3$, T=298K, ppm) δ: 28.5 (CH_3, NCH_3), 31.5 (CH_3, NCH_3), 38.8 (CH_3, NCH_3), 52.2 (CH_3, OCH_3), 52.3 (CH_2, NCH_2), 58.4 (C, C=C), 109.5 (C, C^5), 125.3-137.3 (Ph), 140.9 (C, C^4), 150.6 (C, C=O), 152.4 (C, C=O), 170.8 (C, $\underline{C}OOCH_3$), 197.4 (C, carbene).

IR (KBr): $\nu_{C=O}$= 1708, 1668 cm^{-1}

Synthesis of the complex 23d

Complex **23d** was prepared in analogues manner as that described for **23a** starting from 0.0500 g of [Pd(Me-PyCH$_2$SPh)(η^2-tmetc)] and 0.0735 g of **5d**.

0.0765 g (yield 95%) of **23d** was obtained.

^{1}H-NMR (400 MHz, $CDCl_3$, T=298K, ppm) δ: 3.64 (s, 12H, 4 OCH_3), 3.77 (s, 6H, 2NCH_3), 4.07 (s, 6H, 2NCH_3), 4.31 (s, 6H, 2NCH_3), 5.14 (s, 4H, 2NCH_2), 7.31-7.35 (m, 10H, 2Ph).

^{13}C{^{1}H}-NMR ($CDCl_3$, T=298K, ppm) δ: 31.8 (CH_3, NCH_3), 37.3 (CH_3, NCH_3), 39.4 (CH_3, NCH_3), 45.0 (CH_2, NCH_2), 52.2 (CH_3, OCH_3), 58.3 (C, C=C), 110.4 (C, C^5), 127.8-136.4 (Ph), 140.6 (C, C^4), 150.6 (C, C=O), 153.0 (C, C=O), 170.8 (C, $\underline{C}OOCH_3$), 197.1 (C, carbene).

IR (KBr): ν_{CO}= 1707, 1668 cm^{-1}

Synthesis of the complex 24a

0.0333 g (0.083 mmol) of the precursor [Pd(Me-PyCH$_2$SPh)(η^2-fn)] was dissolved in 25 mL of anhydrous dichloromethane in a 100 mL two-necked flask under inert atmosphere (Ar). Subsequently 0.0585 g (0.083 mmol) of the silver complex **5a**, was added. The mixture was stirred at R.T. for 1 h and the precipitated AgCl was removed by filtration on a millipore membrane filter.

Addition of diethylether to the concentrated solution yields the precipitation of the complex **24a** as a yellow solid which was filtered off on a gooch and washed with *n*-pentane.

0.0516 g of **24a** was obtained (yield 99%).

^{1}H-NMR (400 MHz, $CDCl_3$, T=298K, ppm) δ: 2.58 (s, 2H, CH=CH), 3.40 (s, 6H, 2NCH_3), 3.82 (s, 6H, 2NCH_3), 4.11 (s, 6H, 2NCH_3), 4.31 (s, 6H, 2NCH_3).

^{13}C{^{1}H}-NMR ($CDCl_3$, T=298K, ppm) δ: 16.3 (CH, CH=CH), 28.6 (CH_3, NCH_3), 31.9 (CH_3, NCH_3), 37.3 (CH_3, NCH_3), 38.8 (CH_3, NCH_3), 110.4 (C, C^5), 125.1 (C, CN), 140.5 (C, C^4), 150.7 (C, C=O), 153.1 (C, C=O), 198.3 (C, carbene).

IR (KBr): ν_{CN}= 2192 cm^{-1}, ν_{CO}= 1709, 1666 cm^{-1}

9.6.18. Synthesis of Bis(PTA) palladium olefin complexes (25-28)

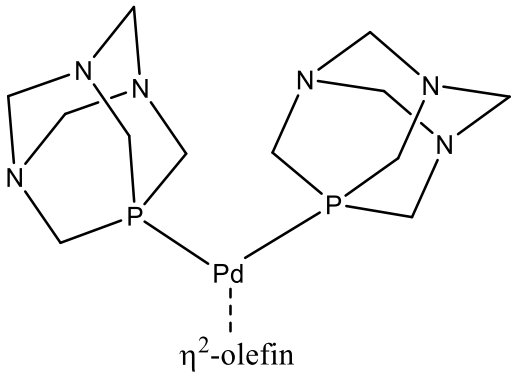

25 η^2-tmetc
26 η^2-fn
27 η^2-am
28 η^2-dmfu

Synthesis of the complex 25

0.0500 g (0.086 mmol) of the precursor [Pd(Me-PyCH$_2$SPh)(η^2-tmetc)] was dissolved in 25 mL of anhydrous dichloromethane in a 100 mL two necked flask under inert atmosphere (Ar). Subsequently 0.0270 g (0.171 mmol) of PTA (1,3,5-triaza-7-phosphadamantane), was added. The mixture was stirred at R.T. for 30 min and the addition of diethylether to the concentrated solution yields the precipitation of the complex **25** as a yellow solid which was filtered off on a gooch and washed with *n*-pentane.

0.0533 g of **25** was obtained (yield 91%).

^{1}H-NMR (400 MHz, CDCl$_3$, T=298K, ppm) δ: 3.62 (s, 12H, 4 OCH$_3$), 4.08 and 4.12 (AB system, J= 12.3 Hz, 12H, 3NCH$_2$P), 4.48 and 4.52 (AB system, J= 13.7 Hz, 12H, 3NCH$_2$N).

^{13}C{^{1}H}-NMR (CDCl$_3$, T=298K, ppm) δ: 52.4 (CH$_3$, OCH$_3$), 53.5 (d, CH$_2$, J_{C-P} = 9.2 Hz, NCH$_2$P), 67.2 (d, J_{C-P} = 3.4 Hz, C=C), 73.5 (d, CH$_2$, J_{C-P} = 6.5 Hz, NCH$_2$N), 168.7 (d, C, J_{C-P} = 11.7 Hz, COOCH$_3$). ^{31}P{^{1}H}-NMR (CDCl$_3$, T=298K, ppm) δ: -61.0

IR (KBr): $\nu_{C=O}$= 1722, 1670 cm^{-1}

Synthesis of the complex 26

0.0500 g (0.125 mmol) of the precursor [Pd(Me-PyCH$_2$SPh)(η^2-fn)] was dissolved in 25 mL of anhydrous dichloromethane in a 100 mL two necked flask under inert atmosphere (Ar). Subsequently 0.0393 g (0.250 mmol) of PTA (1,3,5-triaza-7-phosphadamantane), was added. The mixture was stirred at R.T. for 30 min and the addition of diethylether to the concentrated solution yields the precipitation of the complex **26** as a yellow solid which was filtered off on a gooch and washed with *n*-pentane.

0.0610 g of **26** was obtained (yield 98%).

^{1}H-NMR (400 MHz, $CDCl_3$, T=298K, ppm) δ: 3.00 (s, 2H, CH=CH), 4.19 and 4.23 (AB system, J= 10.3 Hz, 12H, $3NCH_2P$), 4.60 and 4.64 (AB system, J= 14.6 Hz, 12H, $3NCH_2N$).

$^{13}C\{^{1}H\}$-NMR ($CDCl_3$, T=298K, ppm) δ: 26.9 (CH, CH=CH), 53.6 (d, CH_2, J_{C-P} = 7.6 Hz, NCH_2P), 73.5 (d, CH_2, J_{C-P} = 6.2 Hz, NCH_2N), 121.1 (C, CN).

$^{31}P\{^{1}H\}$-NMR ($CDCl_3$, T=298K, ppm) δ: -63.7

IR (KBr): ν_{CN}= 2199 cm^{-1}

Synthesis of the complex 27

0.0500 g (0.119 mmol) of the precursor [Pd(Me-$PyCH_2SPh$)(η^2-ma)] was dissolved in 25 mL of anhydrous dichloromethane in a 100 mL two necked flask under inert atmosphere (Ar). Subsequently 0.0374 g (0.238 mmol) of PTA (1,3,5-triaza-7-phosphadamantane), was added. The mixture was stirred at R.T. for 30 min and the addition of diethylether to the concentrated solution yields the precipitation of the complex **27** as a yellow solid which was filtered off on a gooch and washed with *n*-pentane.

0.0577 g of **27** was obtained (yield 93%).

^{1}H-NMR (400 MHz, $CDCl_3$, T=298K, ppm) δ: 4.16 (m, 14H, $3NCH_2P$+CH=CH), 4.58 and 4.62 (AB system, J= 14.7 Hz, 12H, $3NCH_2N$).

$^{13}C\{^{1}H\}$-NMR ($CDCl_3$, T=298K, ppm) δ: 50.8 (CH, CH=CH), 53.4 (d, CH_2, J_{C-P} = 8.0 Hz, NCH_2P), 73.4 (d, CH_2, J_{C-P} = 6.3 Hz, NCH_2N), 170.5 (C, $\underline{C}OOCH_3$).

$^{31}P\{^{1}H\}$-NMR ($CDCl_3$, T=298K, ppm) δ: -62.2

IR (KBr): $\nu_{C=O}$= 1783, 1717, 1637 cm^{-1} ν_{C-O}= 1240 cm^{-1}

Synthesis of the complex 28

0.0400 g (0.091 mmol) of the precursor [Pd(TMQ-Me)(η^2-dmfu)] was dissolved in 25 mL of anhydrous dichloromethane in a 50 mL two necked flask under inert atmosphere (Ar) at -40°C. To this solution 0.0286 g (0.182 mmol) of of PTA (1,3,5-triaza-7-phosphadamantane), was added. The mixture was stirred at -40°C for 30 min and the addition of diethylether to the concentrated solution yields the precipitation of the complex **28** as a yellow solid which was filtered off on a gooch and washed with *n*-pentane.

0.0464 g of **28** was obtained (yield 90%).

^{1}H-NMR (400 MHz, $CDCl_3$, T=298K, ppm) δ: 3.66 (s, 6H, 2 OCH_3), 3.99 (d, J= 5.8 Hz, 2H, CH=CH), 4.06 and 4.15 (AB system, J= 15.2 Hz, 12H, $3NCH_2P$), 4.57 and 4.61 (AB system, J= 20.1 Hz, 12H, $3NCH_2N$). $^{31}P\{^{1}H\}$-NMR ($CDCl_3$, T=298K, ppm) δ: -61.3

$^{13}C\{^{1}H\}$-NMR ($CDCl_3$, T=243K, selected peaks ppm) δ: 51.6 (CH_3, OCH_3), 53.2 (d, CH_2, J_{C-P} = 4.7 Hz, NCH_2P), 73.2 (CH_2, NCH_2N), 173.1 (C, $\underline{C}OOCH_3$).

IR (KBr): $\nu_{C=O}$= 1672, 1632 cm^{-1} ν_{C-O}= 1241 cm^{-1}

9.7. Synthesis of compounds derived from functionalized imidazole and benzimidazole

9.7.1. Synthesis of imidazolium salts with pyridyl or thioether groups (29-30)

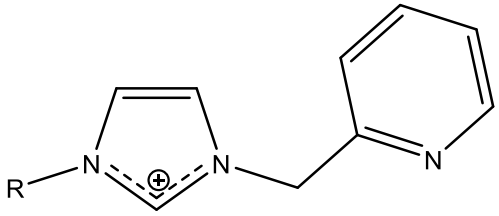

$Br^{\ominus}$

R= CH_3 **(29a)**
R= Mes **(29b)**

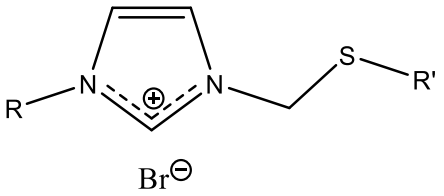

$Br^{\ominus}$

R= CH_3 R'= CH_3 **(30a)**
R= CH_3 R'= Ph **(30b)**
R= Mes R'= CH_3 **(30c)**
R= Mes R'= Ph **(30d)**

Imidazolium salts **29** and **30** were synthesized according to published procedures [30, 31].

9.7.2. Synthesis of imidazolium salts with alkyl and aryl groups (31)

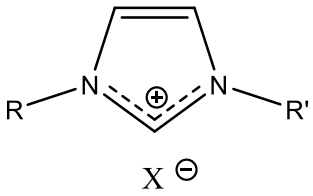

$X^{\ominus}$

R= CH_2Tol R'= CH_2Tol X= Br **(31a)**
R= Mes R'= Mes X= Cl **(31b)**
R= CH_3 R'= Bn X= Br **(31c)**
R= CH_3 R'= CH_2Tol X= Br **(31d)**

Synthesis of 31a

3.647 g (21.0 mmol) of 1-(4-methylbenzyl)-1H-imidazole was dissolved in 50 ml of anhydrous CH_3CN in a two-necked flask and 3.5 g (34.0 mmol) of NaBr and 3 ml (23.0 mmol) of 1-(chloromethyl)-4-methylbenzene were added in rapid sequence under inert atmosphere (Ar). The resulting mixture was refluxed for 36 h and eventually the residual salts were filtered off and repeatedly washed with CH_2Cl_2 on a gooch. The clear solution was concentrated under vacuum and the title compound was precipitated as white powder by addition of diethylether. The compound was filtered off on a gooch, repeatedly washed with diethylether and dried under vacuum.

6.62 g (yield 88%) of the ligand were obtained.

^{1}H NMR ($CDCl_3$, T = 298 K, ppm) d: 2.33 (s, 3H, tol-CH_3), 5.50 (s, 2H, N-CH_2), 7.15 (d, J = 1.6 Hz, 2H, CH=CH^{Im}), 7.17–7.2 (m, 2H, Ph), 7.33–7.36 (m, 2H, Ph), 10.98 (bt, 1H, NCHN).

^{13}C{^{1}H}-NMR ($CDCl_3$, T = 298 K, ppm) d: 21.1 (CH_3, Ph-CH_3), 53.3 (CH_2, N-CH_2), 121.4 (CH, CH=CH^{Im}), 129.0 (CH, Tol o-C), 129.5 (CH, Tol i-C), 130.0 (CH, Tol m-C), 139.6 (CH, Tol p-C), 137.2 (CH, NCHN).

Anal. Calc. for $C_{19}H_{21}BrN_2$: C, 63.87; H, 5.92; N, 7.84. Found: C, 63.99; H, 5.87; N, 7.71%.

Synthesis of 31b-d

The imidazolium salt **31b** (IMes·HCl) was commercial grade product, whereas the compounds **31c** and **31d** were synthesized according to published procedures [32, 31c].

9.7.3. Synthesis of imidazolium salts derived from trifluoromethyl benzimidazole (32)

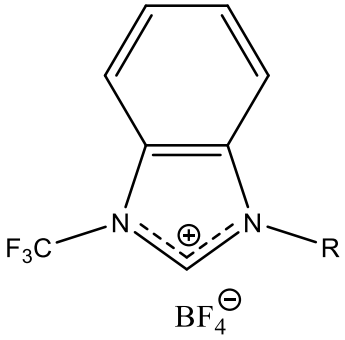

R= CH_3 **(32a)**
R= i-Pr **(32b)**
R= Ph **(32c)**

Synthesis of 32a

A 25 mL Schlenk was charged with 0.0925 g of Me_3OBF_4 (0.625 mmol) and CH_2Cl_2 (8 mL). Subsequently, a solution constituted by 0.0970 g of 1-(Trifluoromethyl)-1H-benzo[d]imidazole (0.521 mmol) and 2 mL of CH_2Cl_2, was added dropwise. The reaction mixture was stirred at room temperature for 4h and the precipitated was filtered off and washed with dichloromethane and diethylether. The product was obtained as a white solid (0.1351 mg, 90%).

^{1}H NMR (CD_3CN, T = 298 K, ppm) δ: 4.19 (s, 3H, NCH_3), 7.89–8.05 (m, 4H, ArH), 9.60 (s, 1H, NCHN).

^{19}F{^{1}H}-NMR (CD_3CN, T = 298 K, ppm) δ: -58.7 (CF_3), -151.9 ($^{10}BF_4$), -152.0 ($^{11}BF_4$).

^{13}C{^{1}H}-NMR (CD_3CN, T = 298 K, ppm) δ: 35.5 (CH_3, NCH_3), 114.1 (q, J = 1.7 Hz, CH), 115.7 (CH), 118.4 (q, C, J = 268.8 Hz, CF_3), 128.4 (C), 129.8 (CH), 130.7 (CH), 133.3 (C), 142.0 (CH, NCHN).

Anal. Calc. for $C_9H_8BF_7N_2$: C, 37.54; H, 2.80; N, 9.73. Found: C, 37.60; H, 2.78; N, 9.75%.

Synthesis of 32b

0.3221 g (0.9044 mmol) of 3-isopropyl-1-(trifluoromethyl)-1H-benzo[d]imidazol-3-ium iodide, synthesized according to published procedures [33] was dissolved in 15 mL of anhydrous acetonitrile. Subsequently 176.1 mg (0.9044 mmol) of $AgBF_4$, were added and the resulting mixture was stirred at R.T. for 30', filtered on millipore membrane filter and concentrated under vacuum. The final product precipitated as a pale-yellow solid by addition of diethylether and was filtered off on a gooch. 270.0 mg of **32b** was obtained (yield 93%).

^{1}H NMR (CD_3CN, T = 298 K, ppm) δ: 1.73 (d, J = 6.7 Hz,6H, $CH(\underline{CH_3})_2$), 5.12 (d, J = 6.7 Hz, 1H, $\underline{CH}(CH_3)_2$), 7.85–8.10 (m, 4H, ArH), 9.57 (s, 1H, NCHN).

^{19}F{^{1}H}-NMR (CD_3CN, T = 298 K, ppm) δ: -58.7 (CF_3), -151.8 ($^{10}BF_4$), -151.9 ($^{11}BF_4$).

^{13}C{^{1}H}-NMR (CD_3CN, T = 298 K, ppm) δ: 21.7 (CH_3, CH_3^{iPr}), 54.4 (CH, $\underline{CH}(CH_3)_2$), 114.5 (m, CH), 116.0 (CH), 128.8 (C), 129.6 (CH), 130.6 (CH), 132.1 (C), 140.1 (CH, NCHN).

Anal. Calc. for $C_{11}H_{12}BF_7N_2$: C, 41.81; H, 3.83; N, 8.86. Found: C, 41.84; H, 3.80; N, 8.91%.

Synthesis of 32c

Imidazolium salt **32c** was synthesized according to published procedures [33].

9.7.4. Synthesis of imidazolium salts with glucopiranosidic groups (33)

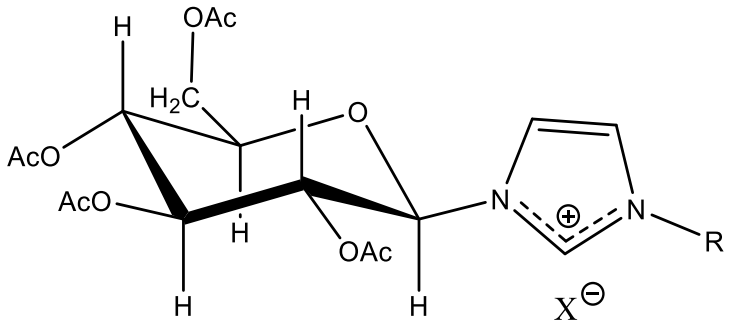

R= *n*-Bu X= Br **(33a)**
R= CH_3 X= I **(33b)**
R= Mes X= Cl **(33c)**

Synthesis of 33a

Imidazolium salt **33a** was synthesized according to published procedures [34].

Synthesis of 33b

0.9330 g of 1-(2,3,4,6-tetra-O-acetyl-β-D-glucopyranosyl)imidazole, synthesized according to published procedures [34], and 2.8 g (1 mL, 0.02 mol) of methyl iodide were dissolved in 25 mL of anhydrous acetonitrile. The mixture was stirred at reflux for 4 h and subsequently the solvent was removed under reduced pressure. The brownish solid obtained was dissolved in ca. 3 mL of dichloromethane and the addition of diethyleter induced the precipitation of the final product that was filtered off on a gooch.

1.07 g of **33b** was obtained (yield 85%).

^{1}H-NMR (300 MHz, $CDCl_3$, T = 298 K, ppm) δ: 2.03 (s, 3H, OCH_3), 2.07 (s, 3H, OCH_3), 2.11 (s, 3H, OCH_3), 2.12 (s, 3H, OCH_3), 4.21 (s, 3H, N-CH_3), 4.22-4.43 (m, 3H, H^5+ CH_2^6), 5.26 (t, 1H, J= 9.2 Hz, H^4), 5.34 (t, 1H, J= 9.2 Hz, H^2), 5.48 (t, 1H, J= 9.2 Hz, H^3), 6.61 (d, 1H, J= 9.2 Hz, H^1), 7.42 (d, 1H, J= 2.0 Hz, H^{Im}), 7.60 (t, 1H, J= 2.0 Hz, H^{Im}), 10.57 (s, 1H, NCHN).

^{13}C{^{1}H}-NMR ($CDCl_3$, T = 298 K, ppm) δ: 20.5 (CH_3, OCH_3), 20.6 (CH_3, OCH_3), 20.9 (CH_3, OCH_3), 21.1 (CH_3, OCH_3), 37.7 (CH_3, NCH_3), 61.1 (CH_2, CH_2^6), 67.3 (CH, CH^4), 71.2 (CH, CH^2), 72.4 (CH, CH^3), 75.0 (CH, CH^5), 83.7 (CH, CH^1), 119.6 (CH, CH^{Im}), 123.8 (CH, CH^{Im}), 137.7 (CH, NCHN), 169.4 (C, C=O), 169.5 (C, C=O), 169.9 (C, C=O), 170.5 (C, C=O).

Synthesis of 33c

0.405 g (0.608 mmol) of 1-(2,3,4,6-Tetra-O-acetyl-β-D-glucopyranosyl)-3-(mesityl)imidazolium triflate, synthesized according to published procedures [35], was dissolved in 25 mL of methanol. To this solution 2g of DOWEX 21K Cl exchange resin was added and the system was stirred for 24h at R.T. Subsequently the solvent was removed under vacuum and the solid obtained was dissolved in ca. 3 mL of dichloromethane. The addition of diethyleter induced the precipitation of the final product that was filtered off on a gooch.

0.2454 g of **33c** was obtained (yield 73%).

<u>β Anomer (60%):</u>

^{1}H-NMR (300 MHz, $CDCl_3$, T = 298 K, ppm) δ: 2.02-2.13 (m, 18H, 4 OCH_3 + 2 *o*-CH_3^{Mes}), 2.37 (s, 3H, *p*-CH_3^{Mes}), 4.19-4.44 (m, 3H, H^5+ CH_2^6), 5.27-5.36 (m, 2H, H^2+H^4), 5.60 (t, 1H, J= 9.3 Hz, H^3), 7.30 (d, 1H, J= 9.3 Hz, H^1), 7.66 (d, 1H, J= 2.0 Hz, H^{Im}), 7.84 (t, 1H, J= 2.0 Hz, H^{Im}), 11.12 (s, 1H, NCHN).

^{13}C{^{1}H}-NMR ($CDCl_3$, T = 298 K, ppm) δ: 17.3 (CH_3, *o*-CH_3^{Mes}), 20.4 (CH_3, OCH_3), 20.5 (CH_3, OCH_3), 20.6 (CH_3, OCH_3), 20.7 (CH_3, OCH_3), 21.1 (CH_3, *p*-CH_3^{Mes}), 61.2 (CH_2, CH_2^6), 67.5 (CH, CH^4), 71.1 (CH, CH^2), 72.4 (CH, CH^3), 75.0 (CH, CH^5), 83.8 (CH, CH^1), 120.0 (CH, CH^{Im}), 123.5 (CH, CH^{Im}), 129.9 (CH, *m*-CH^{Mes}), 134.3 (C, *o*-C^{Mes}), 139.3 (CH, NCHN), 141.6 (C, *i*-C^{Mes}), 141.8 (C, *p*-C^{Mes}), 169.2 (C, C=O), 169.7 (C, C=O), 170.1 (C, C=O), 170.4 (C, C=O).

α Anomer (40%):

^{1}H-NMR (300 MHz, $CDCl_3$, T = 298 K, ppm) δ: 2.02-2.13 (m, 18H, 4 OCH_3 + 2 *o*-CH_3^{Mes}), 2.39 (s, 3H, *p*-CH_3^{Mes}), 4.19-4.44 (m, 3H, H^5+ CH_2^6), 5.27-5.36 (m, 2H, H^2+H^4), 5.60 (t, 1H, J= 9.3 Hz, H^3), 7.30 (d, 1H, J= 9.3 Hz, H^1), 7.15 (d, 1H, J= 2.0 Hz, H^{Im}), 7.19 (t, 1H, J= 2.0 Hz, H^{Im}), 8.36 (s, 1H, NCHN).

^{13}C{^{1}H}-NMR ($CDCl_3$, T = 298 K, ppm) δ: 17.3 (CH_3, *o*-CH_3^{Mes}), 20.4 (CH_3, OCH_3), 20.5 (CH_3, OCH_3), 20.6 (CH_3, OCH_3), 20.7 (CH_3, OCH_3), 21.1 (CH_3, *p*-CH_3^{Mes}), 61.2 (CH_2, CH_2^6), 67.5 (CH, CH^4), 71.1 (CH, CH^2), 72.4 (CH, CH^3), 75.0 (CH, CH^5), 83.8 (CH, CH^1), 121.1 (CH, CH^{Im}), 122.3 (CH, CH^{Im}), 130.2 (CH, *m*-CH^{Mes}), 133.6 (CH, NCHN), 134.3 (C, *o*-C^{Mes}), 141.6 (C, *i*-C^{Mes}), 141.8 (C, *p*-C^{Mes}), 169.2 (C, C=O), 169.7 (C, C=O), 170.1 (C, C=O), 170.4 (C, C=O).

9.7.5. Synthesis of bis-imidazolium salts (34):

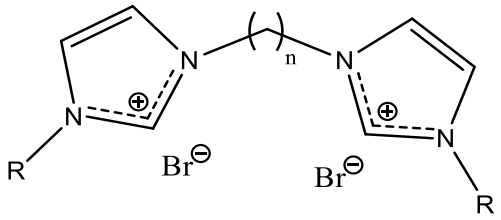

R= Bn n=1 **(34a)**
R= Bn n=2 **(34b)**
R= Mes n=1 **(34c)**
R= Mes n=2 **(34d)**
R= CH_3 n=1 **(34e)**
R= CH_3 n=2 **(34f)**

Imidazolium salts **34a-f** were synthesized according to published procedures [36].

9.7.6. Synthesis of silver complexes bearing NHC with pyridyl and thioether groups (35-36)

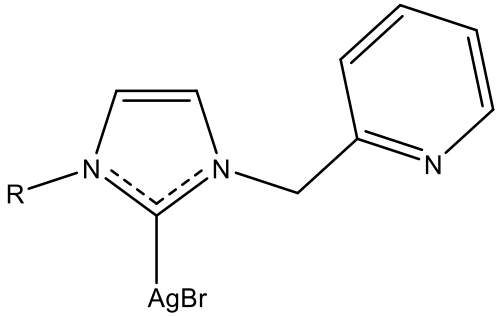

R= CH_3 **(35a)**
R= Mes **(35b)**

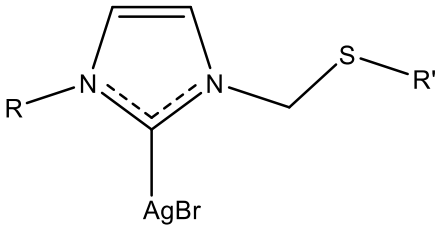

R= CH_3 R'= CH_3 **(36a)**
R= CH_3 R'= Ph **(36b)**
R= Mes R'= CH_3 **(36c)**
R= Mes R'= Ph **(36d)**

Complexes **35a-b** and **36a-b** were synthesized according to published procedures [30, 31].

9.7.7. Synthesis of silver complexes bearing NHC with alkyl and aryl groups (37)

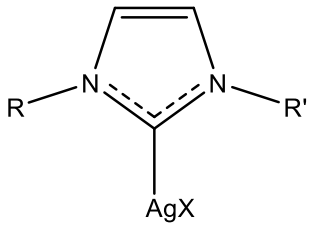

X= Br R= CH_2Tol R'= CH_2Tol **(37a)**
X= Cl R= Mes R'= Mes **(37b)**
X= Br R= CH_3 R'= Bn **(37c)**
X= Br R= CH_3 R'= CH_2Tol **(37d)**

Synthesis of 37a

0.400 g (1.12 mmol) of **31a** was dissolved in 30 ml of anhydrous CH_2Cl_2 in a two-necked flask and 0.1557 g (0.672 mmol) of Ag_2O was added under inert atmosphere (Ar).

The mixture was stirred overnight at RT in the dark. The solution was filtered on millipore membrane filter, concentrated under vacuum and the title complex precipitated by addition of diethylether.

The white complex was filtered off on a gooch, repeatedly washed with diethylether and *n*-pentane and dried under vacuum.

0.4893 g (yield 94%) of complex **37a** was obtained.

^{1}H-NMR ($CDCl_3$, T = 298 K, ppm) d: 2.35 (s, 6H, tol-CH_3), 5.25 (s, 4H, N-CH_2), 6.90 (s, 2H, CH=CH Im), 7.16–7.17 (m, 8H, tol-H).

^{13}C{^{1}H}NMR ($CDCl_3$, T = 298 K, ppm) d: 21.1 (CH_3, Ph-CH_3), 55.5 (CH_2, N-CH_2), 121.2 (CH, $CH=CH^{Im}$), 127.8 (CH, Tol o-C), 129.7 (CH, Tol m-C), 132.3 (CH, Tol i-C), 138.5 (CH, Tol p-C), 180.8 (C, carbene).

Anal. Calc. for $C_{19}H_{20}AgBrN_2$: C, 49.17; H, 4.34; N, 6.04. Found: C, 49.33; H, 4.19, N, 6.21%.

Synthesis of 37b-d

Complexes **37b**, **37c** and **37d** were synthesized according to published procedures [32, 31c].

9.7.8. Synthesis of silver complexes from imidazolium salts with glucopiranosidic group (38)

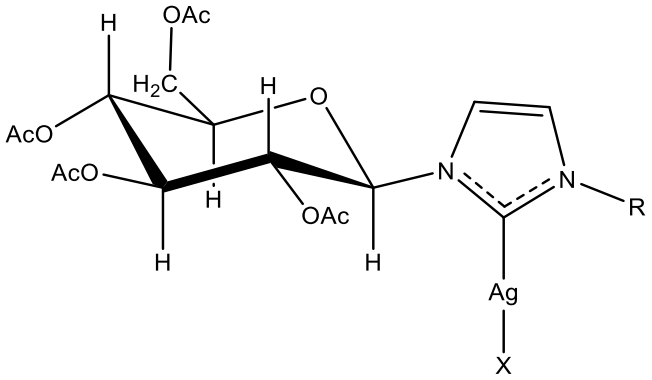

R= *n*-Bu X= Br **(38a)**
R= CH_3 X= I **(38b)**
R= Mes X= Cl **(38c)**

Synthesis of the complex 38a

0.2020 g (0.377 mmol) of **33a** was dissolved in 25 ml of anhydrous CH_2Cl_2 in a two-necked flask and 0.0524 g (0.226 mmol) of Ag_2O was added under inert atmosphere (Ar).

The mixture was stirred for 5 hours at RT in the dark and subsequently transferred in a 250 mL flask with the addition of ca. 150 mL of CH_2Cl_2. The solution was filtered on millipore membrane filter, concentrated under vacuum and the title complex precipitated by addition of diethylether.

The pale-yellow complex was filtered off on a gooch, repeatedly washed with diethylether and *n*-pentane and dried under vacuum.

0.2159 g of **38a** was obtained (yield 89%).

^{1}H-NMR (300 MHz, $CDCl_3$, T = 298 K, ppm) δ: 0.96 (t, 3H, J= 7.3 Hz, $CH_3^{4'}$), 1.33 (m, 2H, $CH_2^{3'}$), 1.79 (m, 2H, $CH_2^{2'}$), 1.96 (s, 3H, OCH_3), 2.02 (s, 3H, OCH_3), 2.08 (s, 3H, OCH_3), 2.11 (s, 3H, OCH_3), 4.11-4.37 (m, 5H, H^5+$CH_2^{1'}$+CH_2^6), 5.21-5.29 (m, 2H, H^2+H^4), 5.44 (t, 1H, J= 9.3 Hz, H^3), 6.62 (d, 1H, J= 9.3 Hz, H^1), 7.04 (d, 1H, J= 1.8 Hz, H^{Im}), 7.25 (d, 1H, J= 1.8 Hz, H^{Im}).

^{13}C{^{1}H}-NMR ($CDCl_3$, T = 298 K, ppm) δ: 13.6 (CH_3, $CH_3^{4'}$), 19.5 (CH_2, $CH_2^{3'}$), 20.4 (CH_3, OCH_3), 20.5 (CH_3, OCH_3), 20.6 (CH_3, OCH_3), 20.7 (CH_3, OCH_3), 33.2 (CH_2, $CH_2^{2'}$), 55.3 (CH_2, $CH_2^{1'}$), 61.6 (CH_2, CH_2^6), 67.7 (CH, CH^4), 71.0 (CH, CH^2), 72.5 (CH, CH^3), 74.9 (CH, CH^5), 87.5 (CH, CH^1), 118.4 (CH, CH^{Im}), 121.9 (CH, CH^{Im}), 169.1 (C, C=O), 169.5 (C, C=O), 169.6 (C, C=O), 170.5 (C, C=O), 179.9 (C, carbene). IR(KBr): $\nu_{C=O}$ = 1754cm^{-1}, ν_{C-O} = 1230 cm^{-1}.

Synthesis of the complex 38b

Complex **38b** was prepared in analogues manner as that described for **38a** starting from 0.2020 g of **33b** and 0.0524 g of Ag_2O.

0.1878 g (yield 78%) of **38b** was obtained.

^{1}H-NMR (300 MHz, $CDCl_3$, T = 298 K, ppm) δ: 1.99 (s, 3H, OCH_3), 2.03 (s, 3H, OCH_3), 2.09 (s, 3H, OCH_3), 2.11 (s, 3H, OCH_3), 3.91 (s, 3H, NCH_3), 4.16-4.38 (m, 3H, H^5+CH_2^6), 5.16 (t, 1H, J= 9.3 Hz, H^4), 5.25 (t, 1H, J= 9.3 Hz, H^2), 5.38 (t, 1H, J= 9.3 Hz, H^3), 6.12 (d, 1H, J= 9.2 Hz, H^1), 7.01 (d, 1H, J= 1.8 Hz, H^{Im}), 7.24 (d, 1H, J= 1.8 Hz, H^{Im}).

^{13}C{^{1}H}-NMR ($CDCl_3$, T = 298 K, ppm) δ: 20.5 (CH_3, OCH_3), 20.6 (CH_3, OCH_3), 20.7 (CH_3, OCH_3), 20.8 (CH_3, OCH_3), 39.1 (CH_3, NCH_3), 61.5 (CH_2, CH_2^6), 67.8 (CH, CH^4), 70.8 (CH, CH^2), 72.9 (CH, CH^3), 74.4 (CH, CH^5), 86.5 (CH, CH^1), 118.1 (CH, CH^{Im}), 122.7 (CH, CH^{Im}), 169.4 (C, C=O), 169.5 (C, C=O), 169.6 (C, C=O), 170.5 (C, C=O), 185.8 (C, carbene).

IR(KBr): $\nu_{C=O}$ = 1752cm^{-1}, ν_{C-O} = 1228 cm^{-1}.

Synthesis of the complex 38c

Complex **38c** was prepared in analogues manner as that described for **38a** starting from 0.1073 g of **33c** and 0.0270 g of Ag_2O.

0.0661 g (yield 52%) of **38c** was obtained.

^{1}H-NMR (300 MHz, $CDCl_3$, T = 298 K, ppm) δ: 1.92 (s, 3H, *p*-CH_3^{Mes}), 1.98 (s, 3H, *o*-CH_3^{Mes}), 2.02 (s, 3H, *o*-CH_3^{Mes}), 2.05 (s, 3H, OCH_3), 2.11 (s, 3H, OCH_3), 2.15 (s, 3H, OCH_3), 2.35 (s, 3H, OCH_3), 4.07 (m, 1H, H^5), 4.21-4.42 (m, 2H, CH_2^6), 5.25-5.37 (m, 2H, H^2+H^4), 5.45 (t, 1H, J= 9.4 Hz, H^3), 5.77 (d, 1H, J= 9.3 Hz, H^1), 6.99 (m, 2H, *m*-CH^{Mes}), 7.02 (t, 1H, J= 1.9 Hz, H^{Im}), 7.44 (t, 1H, J= 1.9 Hz, H^{Im}).

^{13}C{^{1}H}-NMR ($CDCl_3$, T = 298 K, ppm) δ: 17.3 (CH_3, *p*-CH_3^{Me}), 20.4 (CH_3, *o*-CH_3^{Mes}), 20.5 (CH_3, OCH_3), 20.6 (CH_3, OCH_3), 20.8 (CH_3, OCH_3), 21.1 (CH_3, OCH_3), 61.5 (CH_2, CH_2^6), 67.6 (CH, CH^4), 71.1 (CH, CH^2), 72.3 (CH, CH^3), 75.1 (CH, CH^5), 87.8 (CH, CH^1), 118.5 (CH, CH^{Im}), 124.0 (CH, CH^{Im}), 129.6-140.0 (Ph), 169.0 (C, C=O), 169.4 (C, C=O), 169.6 (C, C=O), 170.5 (C, C=O), 180.4 (C, carbene).

IR(KBr): $\nu_{C=O}$ = 1754cm^{-1}, ν_{C-O} = 1231 cm^{-1}.

9.7.9. Synthesis of silver complexes with chelating bis(NHC) (39)

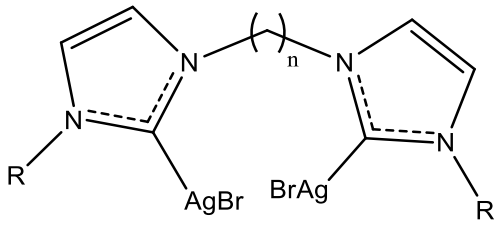

R= Bn n=1 **(39a)**
R= Bn n=2 **(39b)**
R= Mes n=1 **(39c)**
R= Mes n=2 **(39d)**
R= CH_3 n=1 **(39e)**
R= CH_3 n=2 **(39f)**

Synthesis of the complex 39a

0.2693 g (0.549 mmol) of the imidazolium salt **34a** was dissolved in 35 mL of anhydrous methanol in a 100 mL two necked flask and 0.1655 g (0.7140 mmol) of Ag_2O was added under inert atmosphere (Ar). The mixture was stirred for 2 h at R.T. in the dark and the resulting mixture was filtered on millipore membrane filter to eliminate the Ag_2O in excess. The solvent was removed under vacuum and the brownish solid obtained was suspended in ca. 3 mL of dichloromethane. The product was precipitated by addition of diethylether and filtered off on a gooch.

0.2445 g of **39a** was obtained (yield 63%).

^{1}H-NMR (300 MHz, d_6-DMSO, T = 298 K, ppm) δ: 5.18 (s, 4H, 2$\underline{CH_2}$Ph), 7.05 (s, 2H, 2CH^{Im}), 7.04-7.23 (m, 10H, 2Ph), 7.54 (s, 2H, 2CH^{Im}), 7.93 (s, 2H, NCH_2N).

^{13}C{^{1}H}-NMR (d_6-DMSO, T = 298 K, ppm) δ: 54.9 (CH_2, $\underline{CH_2}$Ph), 63.4 (CH_2, NCH_2N), 123.0 (CH, CH^{Im}), 123.5 (CH, CH^{Im}), 127.5-137.1 (Ph), 182.6 (C, carbene).

Synthesis of the complex 39b

Complex **39b** was prepared in analogues manner as that described for **39a** starting from 0.252 g of **34b** and 0.150 g of Ag_2O.

0.212 g (yield 59%) of **39b** was obtained.

^{1}H-NMR (300 MHz, d_6-DMSO, T = 298 K, ppm) δ: 4.65 (s, 4H, NCH_2CH_2N), 5.17 (s, 4H, 2$\underline{CH_2}$Ph), 6.98-7.26 (m, 10H, 2Ph), 7.45 (d, 2H, J= 1.8 Hz, 2CH^{Im}), 7.48 (d, 2H, J= 1.8 Hz, 2CH^{Im}).

^{13}C{^{1}H}-NMR (d_6-DMSO, T = 298 K, ppm) δ: 51.5 (CH_2, NCH_2CH_2N), 54.5 (CH_2, $\underline{CH_2}$Ph), 122.9 (CH, CH^{Im}), 123.3 (CH, CH^{Im}), 127.4-137.5 (Ph), 180.8 (C, carbene).

Synthesis of 39c-f

Complexes **39c-f** were synthesized according to published procedures [37].

9.7.10. Synthesis of palladacyclopentadienyl complexes with chelating bis(NHC) ligands (40)

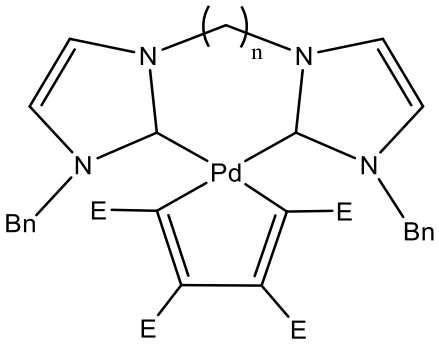

n=1 E=$COOCH_3$ **40a**
n=2 E=$COOCH_3$ **40b**

Synthesis of the complex 40a

0.0391 g (0.100 mmol) of the polymeric precursor $[PdC_4(COOCH_3)_4]_n$ was dissolved in 10 mL of anhydrous dichloromethane in a 50 mL two necked flask under inert atmosphere (Ar). To this solution was added a mixture constituted by 0.0705 g (0.100 mmol) of the silver complex **39a** dissolved in ca. 15 mL of anhydrous dichloromethane.

The mixture was stirred at R.T. for 1 h and subsequently the precipitated AgBr was removed by filtration on a millipore membrane filter.

Addition of diethylether to the concentrated solution yields the precipitation of the complex **40a** as a brownish solid which was filtered off on a gooch and washed with *n*-pentane.

0.0654 g of **40a** was obtained (yield 90%).

^{1}H-NMR (400 MHz, $CDCl_3$, T = 298K, ppm) δ: 3.44 (s, 6H, 2 OCH_3), 3.69 (s, 6H, 2 OCH_3), 4.98 and 5.60 (AB system, 4H, J = 15.0 Hz, 2 -$\underline{CH_2}$Ph), 6.00 and 6.49 (AB system, 2H, J = 13.6 Hz, N$\underline{CH_2}$N), 6.65 (d, 2H, J = 1.8 Hz, 2 CH_{Im}), 6.99 (d, 4H, J = 7.1 Hz, 4 Ph^{orto}), 7.16-7.26 (m, 6H, 4 Ph^{meta} + 2 Ph^{para}), 7.32 (d, 2H, J = 1.8 Hz, 2 CH_{Im}).

^{13}C{^{1}H}-NMR ($CDCl_3$, T = 298K, ppm) δ: 50.7 (CH_3, OCH_3), 51.3 (CH_3, OCH_3), 54.5 (CH_2, CH_2Ph), 65.5 (CH_2, NCH_2N), 119.4 (CH, CH_{Im}), 122.6 (CH, CH_{Im}), 127.8-136.4 (Ph), 145.7 (C, $\underline{C}$-$COOCH_3$), 166.5 (C, $\underline{C}OOCH_3$), 169.7 (C, $\underline{C}$-$COOCH_3$), 177.5 (C, $\underline{C}OOCH_3$), 179.7 (C, carbene).

IR (KBr): $\nu_{C=O}$ = 1733 cm^{-1}, 1686 cm^{-1}, ν_{C-O} = 1194 cm^{-1}, 1159 cm^{-1}

Synthesis of 40b

Complex **40b** was prepared in analogues manner as that described for **40a** starting from 0.0385 g of $[PdC_4(COOCH_3)_4]_n$ and 0.0707 g of **39b**.

0.0707 g of **40b** was obtained (yield 97%).

^{1}H-NMR (400 MHz, $CDCl_3$, T = 298K, ppm) δ: 3.32 (s, 6H, 2 OCH_3), 3.58 (s, 6H, 2 OCH_3), 4.35 (m, 2H, NCH_2CH_2N), 5.02 and 5.07 (AB system, 4H, J = 15.4 Hz, $2CH_2Ph$), 5.33 (m, 2H, NCH_2CH_2N), 6.56 (d, 2H, J = 1.9 Hz, 2 CH_{Im}), 6.86 (d, 4H, J = 8.1 Hz, 4 Ph^{orto}), 6.93 (d, 2H, J = 1.9 Hz, 2 CH_{Im}), 7.10-7.15 (m, 6H, 4 Ph^{meta} + 2 Ph^{para}).

^{13}C{^{1}H}-NMR ($CDCl_3$, T = 298K, ppm) δ: 48.2 (CH_2, NCH_2CH_2N), 50.7 (CH_3, OCH_3), 51.1 (CH_3, OCH_3), 54.4 (CH_2, CH_2Ph), 120.5 (CH, CH_{Im}), 121.9 (CH, CH_{Im}), 128.0-136.2 (Ph), 144.8 (C, C-$COOCH_3$), 165.9 (C, $COOCH_3$), 169.9 (C, C-$COOCH_3$), 177.4 (C, $COOCH_3$), 178.9 (C, carbene).

IR (KBr): $\nu_{C=O}$ = 1691 cm^{-1}, ν_{C-O} = 1202 cm^{-1}

9.7.11. Synthesis of bis(NHC) palladacyclopentadienyl complexes (41)

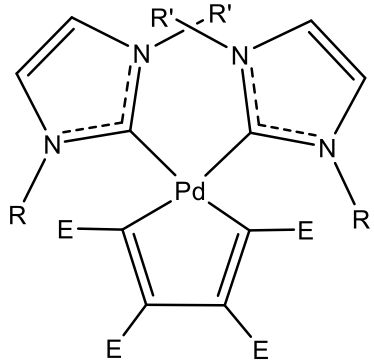

E= $COOCH_3$ R= CH_3 R'= CH_2Py **41a**

E= $COOCH_3$ R= CH_3 R'= CH_2SCH_3 **41b**

E= $COOCH_3$ R= CH_3 R'= Bn **41c**

Complexes **41a-c** were synthesized according to published procedures [38].

9.7.12. Synthesis of palladacyclopentadienyl complexes bearing hemi-labile NHCs (42-43)

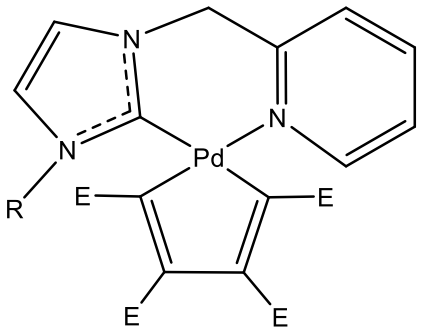

E=$COOCH_3$ R=CH_3 **42a**
E=$COOCH_3$ R=Mes **42b**

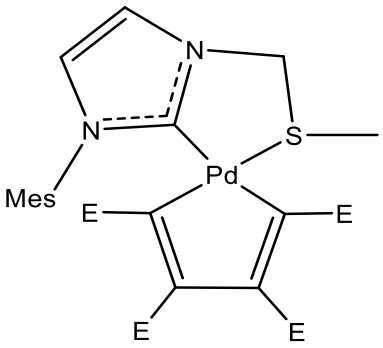

E=$COOCH_3$ **43**

Complexes **42a-b** and **43** were synthesized according to published procedures [38].

9.7.13. Synthesis of mixed NHC/PPh_3 and NHC/DIC palladacyclopentadienyl complexes (44-46)

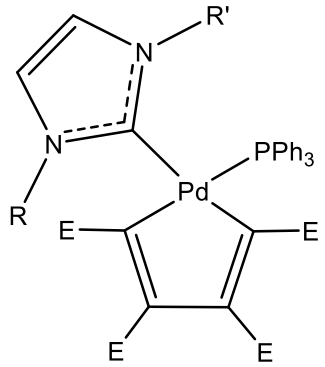

E=$COOCH_3$	R= CH_3	R'= CH_2Py	**44a**
E=$COOCH_3$	R= CH_3	R'= Bn	**44b**
E=$COOCH_3$	R= AcGluc	R'= *n*-Bu	**45a**
E=$COOCH_3$	R= AcGluc	R'= CH_3	**45b**
E=$COOCH_3$	R= AcGluc	R'= Mes	**45c**

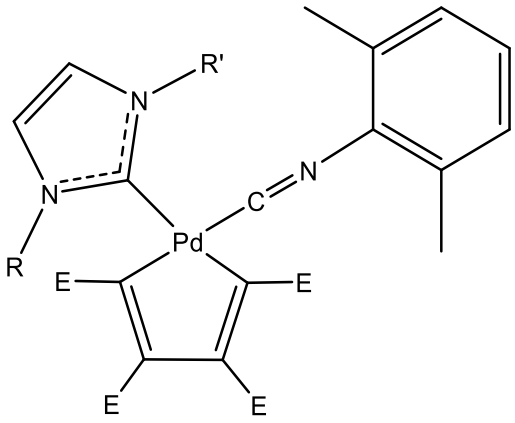

E=$COOCH_3$ R= CH_3 R'= CH_2Py **46a**
E=$COOCH_3$ R= CH_3 R'= CH_2Tol **46b**

Synthesis of complexes 44 and 46

Complexes **44** and **46** were synthesized according to published procedures [38].

Synthesis of the complex 45a

0.0308 g (0.0789 mmol) of the polymeric precursor $[PdC_4(COOCH_3)_4]_n$ was dissolved in 10 mL of anhydrous dichloromethane in a 50 mL two-necked flask under inert atmosphere (Ar). To this solution was added a mixture constituted by 0.0505 g (0.0789 mmol) of the silver complex **38a** and 0.0207 g (0.0789 mmol) of PPh_3 dissolved in ca. 15 mL of anhydrous dichloromethane.

The mixture was stirred at R.T. for 30 min and subsequently the precipitated AgBr was removed by

filtration on a millipore membrane filter.

Addition of *n*-hexane to the concentrated solution yields the precipitation of the complex **45a** as a yellow solid which was filtered off on a gooch.

0.0758 g of **45a** was obtained (yield 87%).

Anomer 1 (62%)

^{1}H-NMR (300 MHz, CD_2Cl_2, T = 298 K, ppm selected peaks) δ: 0.80-0.86 (m, 3H, $CH_3^{4'}$), 0.97-1.04 (m, 2H, $2CH_2^{3'}$), 1.10-1.31 (m, 2H, $2CH_2^{2'}$), 2.04 (s, 6H, 2 OCH_3), 2.07 (s, 3H, OCH_3), 2.09 (s, 3H, OCH_3), 2.58 (s, 3H, OCH_3), 3.18 (s, 3H, OCH_3), 3.57 (s, 3H, OCH_3), 3.58 (s, 3H, OCH_3), 6.15 (d, 2H, J= 8.8 Hz, H^1), 6.71 (d, 1H, J= 2.1 Hz, H^{Im}), 7.25 (d, 1H, J= 2.1 Hz, H^{Im}), 7.25-7.75 (m, 15H, 3Ph).

^{31}P{^{1}H}-NMR (CD_2Cl_2, T = 298 K, ppm) δ: 24.4.

^{13}C{^{1}H}-NMR ($CDCl_3$, T = 233 K, ppm selected peaks) δ: 14.0 (CH_3, $CH_3^{4'}$), 20.3 (CH_2, $CH_2^{3'}$), 20.9-21.4 (CH_3, OCH_3), 30.4 (CH_2, $CH_2^{2'}$), 50.7 (CH_2, $CH_2^{1'}$), 51.2-52.1 (CH_3, OCH_3), 85.8 (CH, CH^1), 169.5-171.4 (C, C=O), 174.2 (d, J_{C-P}= 19.5 Hz, C, carbene).

Anomer 2 (38%)

^{1}H-NMR (300 MHz, CD_2Cl_2, T = 298 K, ppm selected peaks) δ: 0.80-0.86 (m, 3H, $CH_3^{4'}$), 0.97-1.04 (m, 2H, $2CH_2^{3'}$), 1.10-1.31 (m, 2H, $2CH_2^{2'}$), 1.94 (s, 3H, OCH_3), 1.97 (s, 3H, OCH_3), 2.04 (s, 3H, OCH_3), 2.08 (s, 3H, OCH_3), 2.56 (s, 3H, OCH_3), 3.17 (s, 3H, OCH_3), 3.56 (s, 3H, OCH_3), 3.61 (s, 3H, OCH_3), 6.24 (d, 2H, J= 8.8 Hz, H^1), 6.76 (d, 1H, J= 2.1 Hz, H^{Im}), 7.17 (d, 1H, J= 2.1 Hz, H^{Im}), 7.25-7.75 (m, 15H, 3Ph).

^{31}P{^{1}H}-NMR (CD_2Cl_2, T = 298 K, ppm) δ: 25.2.

^{13}C{^{1}H}-NMR ($CDCl_3$, T = 233 K, ppm selected peaks) δ: 14.0 (CH_3, $CH_3^{4'}$), 20.4 (CH_2, $CH_2^{3'}$), 20.9-21.4 (CH_3, OCH_3), 30.4 (CH_2, $CH_2^{2'}$), 50.9 (CH_2, $CH_2^{1'}$), 51.2-52.1 (CH_3, OCH_3), 85.9 (CH, CH^1), 169.5-171.4 (C, C=O), 175.4 (d, J_{C-P}= 19.8 Hz, C, carbene).

IR(KBr): $\nu_{C=O}$ = 1753 cm^{-1}, 1714 cm^{-1} ν_{C-O} = 1229 cm^{-1}

Synthesis of the complex 45b

Complex **45b** was prepared in analogues manner as that described for **45a** starting from 0.0309 g of $[PdC_4(COOCH_3)_4]_n$, 0.0510 g of **38b** and 0.0207 g of PPh_3.

0.0707 g (yield 84%) of **45b** was obtained.

Anomer 1 (60%)

^{1}H-NMR (300 MHz, $CDCl_3$, T = 298 K, ppm selected peaks) δ: 1.98 (s, 3H, OCH_3), 2.04 (s, 3H, OCH_3), 2.08 (s, 3H, OCH_3), 2.13 (s, 3H, OCH_3), 2.61 (s, 3H, OCH_3), 3.03 (s, 3H, NCH_3), 3.17 (s,

3H, OCH_3), 3.62 (s, 3H, OCH_3), 3.63 (s, 3H, OCH_3), 6.12 (d, 2H, J= 8.9 Hz, H^1), 6.54 (d, 1H, J= 2.1 Hz, H^{Im}), 7.12 (d, 1H, J= 2.1 Hz, H^{Im}), 6.98-7.47 (m, 15H, 3Ph).

$^{31}P\{^1H\}$-NMR ($CDCl_3$, T = 298 K, ppm) δ: 24.4.

$^{13}C\{^1H\}$-NMR ($CDCl_3$, T = 233 K, ppm selected peaks) δ: 20.6-21.4 (CH_3, OCH_3), 37.1 (CH_3, NCH_3), 50.7 (CH_3, OCH_3), 51.2 (CH_3, OCH_3), 51.7 (CH_3, OCH_3), 51.8 (CH_3, OCH_3), 85.9 (CH, CH^1), 169.9-171.4 (C, C=O), 181.7 (d, J_{C-P}= 19.7 Hz, C, carbene).

Anomer 2 (40%)

^1H-NMR (300 MHz, $CDCl_3$, T = 298 K, ppm selected peaks) δ: 1.99 (s, 3H, OCH_3), 2.03 (s, 3H, OCH_3), 2.05 (s, 3H, OCH_3), 2.07 (s, 3H, OCH_3), 2.60 (s, 3H, OCH_3), 2.97 (s, 3H, NCH_3), 3.19 (s, 3H, OCH_3), 3.60 (s, 3H, OCH_3), 3.61 (s, 3H, OCH_3), 6.30 (d, 2H, J= 8.8 Hz, H^1), 6.60 (d, 1H, J= 2.1 Hz, H^{Im}), 7.08 (d, 1H, J= 2.1 Hz, H^{Im}), 6.98-7.47 (m, 15H, 3Ph).

$^{31}P\{^1H\}$-NMR ($CDCl_3$, T = 298 K, ppm) δ: 25.3.

$^{13}C\{^1H\}$-NMR ($CDCl_3$, T = 233 K, ppm selected peaks) δ: 20.6-21.4 (CH_3, OCH_3), 37.1 (CH_3, NCH_3), 51.0 (CH_3, OCH_3), 51.7 (CH_3, OCH_3), 51.8 (CH_3, OCH_3), 51.9 (CH_3, OCH_3), 85.9 (CH, CH^1), 169.9-171.4 (C, C=O), 185.1 (d, J_{C-P}= 19.7 Hz, C, carbene).

IR(KBr): $\nu_{C=O}$ = 1753 cm^{-1}, 1714 cm^{-1} ν_{C-O} = 1228 cm^{-1}.

Synthesis of the complex 45c

Complex **45c** was prepared in analogues manner as that described for **45a** starting from 0.0323 g of $[PdC_4(COOCH_3)_4]_n$, 0.0546 g of **38c** and 0.0217 g of PPh_3.

0.0894 g (yield 92%) of **45c** was obtained.

Anomer 1 (70%)

^1H-NMR (300 MHz, $CDCl_3$, T = 298 K, ppm selected peaks) δ: 1.61-2.42 (m, 21H, 4 OCH_3 + $3CH_3^{Mes}$), 2.86-3.73 (m, 12H, 4 OCH_3), 5.87 (d, 2H, J= 8.9 Hz, H^1), 6.81-7.78 (m, 17H, 3Ph+$2H^{Im}$).

$^{31}P\{^1H\}$-NMR ($CDCl_3$, T = 298 K, ppm) δ: 22.9.

$^{13}C\{^1H\}$-NMR ($CDCl_3$, T = 233 K, ppm selected peaks) δ: 20.8-21.4 (CH_3, OCH_3), 51.4-52.4 (CH_3, OCH_3), 169.3-171.3 (C, C=O), 182.1 (d, J_{C-P}= 17.0 Hz, C, carbene).

Anomer 2 (30%)

^1H-NMR (300 MHz, $CDCl_3$, T = 298 K, ppm selected peaks) δ: 1.61-2.42 (m, 21H, 4 OCH_3 + $3CH_3^{Mes}$), 2.86-3.73 (m, 12H, 4 OCH_3), 6.09 (d, 2H, J= 8.8 Hz, H^1), 6.81-7.78 (m, 17H, 3Ph+$2H^{Im}$).

$^{31}P\{^1H\}$-NMR ($CDCl_3$, T = 298 K, ppm) δ: 22.7.

$^{13}C\{^1H\}$-NMR ($CDCl_3$, T = 233 K, ppm selected peaks) δ: 20.8-21.4 (CH_3, OCH_3), 51.4-52.4 (CH_3, OCH_3), 169.3-171.3 (C, C=O), 183.6 (d, J_{C-P}= 16.2 Hz, C, carbene).

IR(KBr): $\nu_{C=O}$ = 1753 cm^{-1}, 1714 cm^{-1} ν_{C-O} = 1229 cm^{-1}.

9.7.14. Synthesis of the unexpected products of halogen addition (47)

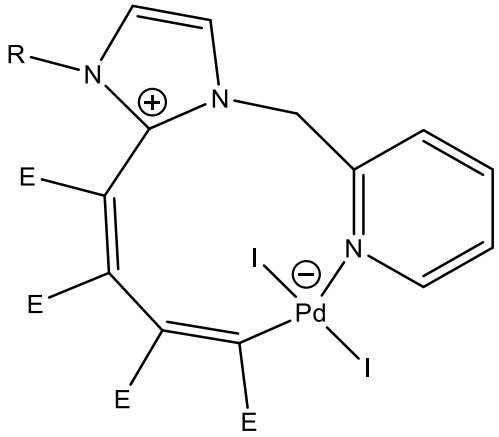

E= $COOCH_3$ R= CH_3 **47a**
E= $COOCH_3$ R= Mes **47b**

Synthesis of complex 47a

To 0.0958 g (0.170 mmol) of complex **42a** dissolved in ca. 20 ml of anhydrous CH_2Cl_2 in a two-necked 100 ml flask, 0.0517 g (0.204 mmol) of I_2 dissolved in a small quantity of anhydrous CH_2Cl_2 was added under inert atmosphere (Ar). The reaction mixture was stirred for 3 days at R.T. and evaporated to small volume under vacuum. Addition of diethyl ether induces the precipitation of the orange complex **47a** which was filtered off on a gooch, repeatedly washed with diethyl ether and finally dried under vacuum. 0.1274 g (yield 92%) of the complex **47a** was obtained.

^{1}H NMR ($CDCl_3$, T = 298 K, ppm), δ: 3.66 (s, 3H, OCH_3), 3.71 (s, 3H, NCH_3), 3.76 (s, 3H, OCH_3), 3.82 (s,3H, OCH_3), 3.93 (s, 3H, OCH_3), 5.06 (d, J = 14.4 Hz, 1H, NCH_2), 6.48 (d, J = 14.4 Hz, 1H, NCH_2), 6.76 (bs,1H, CH=CH Im), 7.38 (m, 1H, 5-Pyr), 7.42 (bs, 1H, CH=CH Im), 7.59 (d, J = 7.7 Hz, 1H, 3-Pyr), 7.83 (t, J =7.7, 1H, 4-Pyr), 8.84 (d, J = 4.9 Hz, 1H, 6-Pyr).

^{13}C{^{1}H} NMR ($CDCl_3$, T = 298 K, ppm), δ: 36.9 (CH_3, NCH_3), 51.8 (CH3, OCH_3), 52.4 (CH_3, OCH_3), 53.3 (CH_3, OCH_3), 54.1 (CH_3, OCH_3), 54.7 (CH_2, NCH_2), 118.1 (C, C=C), 122.3 (CH, CH=CH Im), 125.9 (CH,5-Pyr), 126.1 (CH, CH=CH Im), 126.8 (CH, 3-Pyr), 132.3 (C, C=C), 138.7 (CH, 4-Pyr), 139.8 (C, NCN),151.7 (C, 2-Pyr), 154.8 (CH, 6-Pyr), 156.5 (C, C=C), 162.4 (C, C=C), 162.7 (C, C=O), 165.4 (C, C=O),165.9 (C, C=O), 171.6 (C, C=O).

IR (KBr pellets): $\nu_{c=o}$: 1717 cm^{-1} , ν_{c-o} : 1241 cm^{-1}

Synthesis of complex 47b

Complex **47b** was obtained according to the above described protocols using the appropriate starting complex (**42b**) and I_2. The yield, color, reaction time and, where necessary, some supplementary information will be reported under the title.

Reaction time: 28 days. Temperature: R.T. Yield 93%. Color: orange.

^{1}H NMR ($CDCl_3$, T = 298 K, ppm), δ: 2.04 (s, 3H, *o*-mesytil-CH_3), 2.34 (s,3H, *o*-mesityl-CH_3), 2.39 (s, 3H, *p*-mesityl-CH_3), 3.25 (s, 3H, OCH_3), 3.68 (s, 3H, OCH_3), 3.73 (s, 3H, OCH_3), 3.93 (s, 3H, OCH_3), 5.13 (d, J = 14.4 Hz, 1H, NCH_2), 6.57 (d, J = 14.4 Hz, 1H, NCH_2), 6.92 (s, 1H, *m*-mesityl-H), 7.01 (s, 1H, *m*-mesityl-H), 7.23 (d, J = 2.1 Hz, 1H, CH=CH Im), 7.39 (d, J = 2.1 Hz, 1H, CH=CH Im), 7.45 (ddd, 1H, J = 7.7, 5.4, 1.6 Im, 5-Pyr), 7.63 (d, J = 7.7 Hz, 1H, 3-Pyr), 7.90 (td, J = 7.7, 1.6 Hz, 1H, 4-Pyr), 8.97 (ddd, J = 5.4, 1.6, 0.7 Hz, 1H, 6-Pyr).

^{13}C{^{1}H } NMR ($CDCl_3$, T = 298 K, ppm) δ: 17.8 (CH_3, *o*-mesityl-CH_3), 20.6 (CH_3, *o*-mesityl-CH_3), 21.8 (CH_3, *p*-mesityl-CH_3), 51.2 (CH_3, OCH_3), 51.2 (CH_3, OCH_3), 52.9 (CH_3, OCH_3), 53.5 (CH_3, OCH_3), 56.3 (CH_2, NCH_2), 116.2 (C, Pd-C-C, C=C), 123.6 (CH, CH=CH Im), 125.7 (CH,5-Pyr), 125.9 (CH, CH=CH Im), 127.3 (CH, 3-Pyr), 129.2 (CH, *m*-mesityl), 130.1 (CH, *m*-mesityl), 130.7 (C, *i*-mesityl), 131.4 (C, Pd-C-I), 135.3 (C, *o*-mesityl), 137.0 (C, *o*-mesityl), 140.4 (C, *p*-mesityl), 138.9 (CH, 4-Pyr), 142.2 (C, NCN), 150.7 (C, 2-Pyr), 155.1 (CH, 6-Pyr), 159.8 (C, C=O), 161.4 (C, C=C), 164.6 (C, C=O), 165.3 (C, C=O), 171.7 (C, C=O), 181.4 (C, C=C).

IR (KBr pellets):$\nu_{c=o}$: 1723 cm^{-1}, ν_{c-o}: 1225 cm^{-1}

9.7.15. Synthesis of palladium η^3-allyl complexes with chelating bis(NHC) ligands (48)

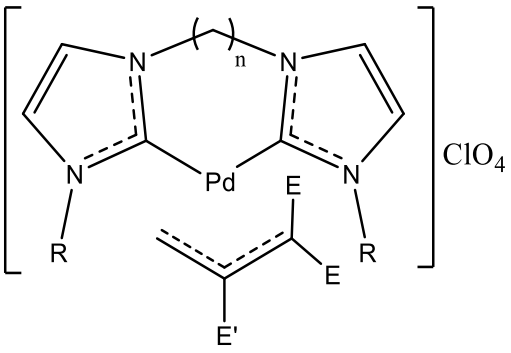

R= Bn	n=1	E=H	E'=H	**48a**
R= Bn	n=2	E=H	E'=H	**48b**
R= Mes	n=1	E=H	E'=H	**48c**
R= Mes	n=2	E=H	E'=H	**48d**
R= Mes	n=1	E=H	E'=CH_3	**48e**
R= Mes	n=1	E=CH_3	E'=H	**48f**
R= CH_3	n=1	E=H	E'=H	**48g**
R= CH_3	n=2	E=H	E'=H	**48h**

Synthesis of the complex 48a

0.0527 g (0.1137 mmol) of the precursor [Pd(Me-PyCH_2SPh)(η^3-C_3H_5)]ClO_4 was dissolved in 15 mL of anhydrous dichloromethane in a 50 mL two-necked flask under inert atmosphere (Ar). Subsequently was added 0.0802 g (0.181 mmol) of the silver complex **39a**, previously dissolved in ca. 5 mL of CH_2Cl_2. The mixture was stirred at R.T. for 15 min and the precipitated AgBr was

removed by filtration on a millipore membrane filter.

The solvent was reduced under vacuum and the white solid was precipitated by addition of diethylether and filtered off on a gooch.

0.0651 g of **48a** was obtained (brownish solid, yield 98%).

^{1}H NMR (300 MHz, $CDCl_3$, T=298 K, ppm) δ : 2.79 (d, J=13.3 Hz, 2H, 2 *anti* allyl-H), 4.05 (d, J = 7.6 Hz , (2H, 2 *syn* allyl-H), 5.26 (m, 1H, *central*-allyl-H), 5.29 (s, 2H, $2NCH_2$), 6.24-6.61 (AB system, J= 13.1 Hz, 2H, NCH_2N), 6.90 (d, J =1.9 Hz, 2H, $CH=CH^{Im}$), 7.11-7.38 (10H, Ar-H), 7.89 (d, J=1.9 Hz, 2H, $CH=CH^{Im}$).

^{13}C{^{1}H} NMR (CD_2Cl_2, T=298 K, ppm) δ : 55.1 (CH_2, NCH_2), 58.9 (CH_2, allyl- CH_2), 63.0 (CH_2, NCH_2N), 119.7 (CH, *central* allyl), 120.6 (CH, $CH=CH^{Im}$), 123.1 (CH, $CH=CH^{Im}$), 127.2-135.7 (Ar-C), 176.1 (C, carbene).

IR [KBr Pellet]: ν_{ClO} = 1088, δ_{ClO} = 620, cm^{-1}.

Synthesis of the complex 48b

Complex **48b** was prepared in analogues manner as that described for **48a** starting from 0.0512 g (0.1105 mmol) of [[Pd(Me-$PyCH_2SPh$)(η^3-C_3H_5)]ClO_4 and 0.0793 g (0.1105 mmol) of **39b**.

0.0641 g (yield 98%) of **48b** was obtained.

^{1}H NMR (300 MHz, $CDCl_3$, T=298 K, ppm) δ : 2.62 (d, J=15.8 Hz, 2H, 2 *anti* allyl-H), 3.81 (d, J = 7.3 Hz, 2H, 2 *syn* allyl-H), 4.84-5.27 (9H, $2NCH_2$, NCH_2CH_2N,*central* allyl-H), 6.94-7.42 (14H, Ar-H, $2CH=CH^{Im}$)

^{13}C{^{1}H} NMR ($CDCl_3$, T=298 K, ppm) δ : 48.6 (CH_2, NCH_2CH_2N), 55.0 (CH_2, NCH_2), 58.5 (CH_2, allyl CH_2), 122.1 (CH, *central* allyl), 124.2 (CH, $CH=CH^{Im}$), 126.9 (CH, $CH=CH^{Im}$), 128.4-135.9 (Ar-C), 174.7 (C, carbene).

IR [KBr Pellet]: ν_{ClO} = 1093, δ_{ClO} = 620, cm^{-1}.

Synthesis of the complex 48c

Complex **48c** was prepared in analogues manner as that described for **48a** starting from 0.0515 g (0.1112 mmol) of [[Pd(Me-$PyCH_2SPh$)(η^3-C_3H_5)]ClO_4 and 0.0845 g (0.1112 mmol) of **39c**.

0.0605 g (yield 86%) of **48c** was obtained.

<u>Most abundant isomer (ca. 60%):</u>

^{1}H NMR (300 MHz, $CDCl_3$, T=298 K, ppm) δ : 1.87 (d, J=13.8 Hz, 2H, 2 *anti* allyl-H), 1.91 (s, 6H, 2 o-aryl-CH_3), 1.96 (s, 6H, 2 o-aryl-CH_3), 2.35 (s, 6H, 2 p-aryl-CH_3), 2.94 (d, J=7.5 Hz, 2H, 2 *syn* allyl-H), 4.68 (m, 1H, *central* allyl-H), 6.33-6.84 (AB system, J= 13.2 Hz, 2H, NCH_2N), 6.85-8.16 (8H, Ar-H, $2CH=CH^{Im}$).

$^{13}C\{^1H\}$ NMR ($CDCl_3$, T=298 K, ppm) δ : 17.7 (CH_3, o-mesityl-CH_3), 21.1 (CH_3, p-mesityl-CH_3), 58.6 (CH_2, allyl CH_2), 62.9 (CH_2, NCH_2N), 118.8 (CH, *central* allyl), 121.7 (CH, $CH=CH^{Im}$), 123.3 (CH, $CH=CH^{Im}$), 129.0-139.6 (Ar-C), 176.1 (C, carbene).

Less abundant isomer (ca. 40%):

^1H NMR (300 MHz, $CDCl_3$, T=298 K, ppm) δ : 1.37 (s, 6H, 2 o-aryl-CH_3), 1.66 (s, 6H, 2 o-aryl-CH_3), 1.68 (d, J=13.6 Hz, 2H, 2 *anti* allyl-H), 2.36 (d, J=7.4 Hz, 2H, 2 *syn* allyl-H), 2.47 (s, 6H, 2 p-aryl-CH_3), 4.68 (m, 1H, *central* allyl-H) 6.33-6.84 (AB system, J= 13.7 Hz, 2H, NCH_2N), 6.85-8.16 (8H, Ar-H, $2CH=CH^{Im}$).

$^{13}C\{^1H\}$ NMR ($CDCl_3$, T=298 K, ppm) δ : 17.7 (CH_3, o-mesityl-CH_3), 21.1 (CH_3, p-mesityl-CH_3), 58.6 (CH_2, allyl CH_2), 62.9 (CH_2, NCH_2N), 118.8 (CH, *central* allyl), 121.7 (CH, $CH=CH^{Im}$), 123.3 (CH, $CH=CH^{Im}$), 129.0-139.6 (Ar-C), 176.1 (C, carbene).

IR [KBr Pellet]: ν_{ClO} = 1096, δ_{ClO} = 623, cm^{-1}.

Synthesis of the complex 48d

Complex **48d** was prepared in analogues manner as that described for **48a** starting from 0.0361 g (0.0779 mmol) of $[Pd(Me\text{-}PyCH_2SPh)(\eta^3\text{-}C_3H_5)]ClO_4$ and 0.0603 g (0.0779 mmol) of **39d**.

0.0465 g (yield 92%) of **49d** was obtained.

Most abundant isomer (ca. 70%):

^1H NMR (300 MHz, $CDCl_3$, T=298 K, ppm) δ : 1.65 (d, J=13.5 Hz, 2H, 2 *anti* allyl-H), 1.91 (s, 6H, 2 o-aryl-CH_3), 1.94 (s, 6H, 2 o-aryl-CH_3), 2.33 (s, 6H, 2 p-aryl-CH_3), 3.22 (d, J=7.5 Hz, 2H, 2 *syn* allyl-H), 4.66 (m, 1H, *central* allyl-H), 5.00 (m, 4H, NCH_2CH_2N), 6.91-6.93 (4H, Ar-H), 6.96 (d, J=1.9 Hz, 2H, $CH=CH^{Im}$), 7.59 (d, J=1.9 Hz, 2H, $CH=CH^{Im}$).

$^{13}C\{^1H\}$ NMR ($CDCl_3$, T=298 K, ppm) δ : 17.5 (CH_3, mesityl-CH_3), 18.0 (CH_3, mesityl-CH_3), 18.3 (CH_3, mesityl-CH_3), 21.0 (CH_3, mesityl-CH_3), 49.5 (CH_2, NCH_2CH_2N), 59.3 (CH_2, allyl CH_2), 118.4 (CH, *central* allyl), 123.5 (CH, $CH=CH^{Im}$), 123.6 (CH, $CH=CH^{Im}$), 128.9-139.3 (Ar-C), 174.7 (C, carbene).

Less abundant isomer (ca. 30%):

^1H NMR (300 MHz, $CDCl_3$, T=298 K, ppm) δ : 1.65 (d, J=13.5 Hz, 2H, 2 *anti* allyl-H), 1.69 (s, 12H, 2 o-aryl-CH_3), 2.43 (s, 6H, 2 p-aryl-CH_3), 3.22 (d, J=7.5 Hz, 2H, 2 *syn* allyl-H), 4.81 (s, 4H, NCH_2CH_2N), 5.02 (m, 1H, *central* allyl-H), 6.86 (d, J=1.9 Hz, 2H, $CH=CH^{Im}$), 6.91-6.93 (4H, Ar-H), 7.91 (d, J=1.9 Hz, 2H, $CH=CH^{Im}$).

$^{13}C\{^1H\}$ NMR ($CDCl_3$, T=298 K, ppm) δ : 17.5 (CH_3, mesityl-CH_3), 18.0 (CH_3, mesityl-CH_3), 18.3 (CH_3, mesityl-CH_3), 21.0 (CH_3, mesityl-CH_3), 49.5 (CH_2, NCH_2CH_2N), 59.3 (CH_2, allyl CH_2), 118.4 (CH, *central* allyl), 123.5 (CH, $CH=CH^{Im}$), 123.6 (CH, $CH=CH^{Im}$), 128.9-139.3 (Ar-C), 174.7 (C, carbene).

Synthesis of the complex 48e

Complex **48e** was prepared in analogues manner as that described for **48a** starting from 0.0436 g (0.0913 mmol) of [[Pd(Me-PyCH$_2$SPh)(η^3-2-MeC$_3$H$_4$)]ClO$_4$ and 0.0694 g (0.0913 mmol) of **39c**.

0.0491 g (yield 83%) of **48e** was obtained.

Most abundant isomer (ca. 52%):

^{1}H NMR (300 MHz, CDCl$_3$, T=298 K, ppm) δ : 1.18 (s, 3H, allyl-CH$_3$), 1.80 (s, 2H, 2 *anti* allyl-H), 1.86 (s, 6H, 2 o-aryl-CH$_3$), 1.97 (s, 6H, 2 o-aryl-CH$_3$), 2.37 (s, 6H, 2 p-aryl-CH$_3$), 2.52 (s, 2H, 2 *syn* allyl-H), 6.51-6.73 (AB system, J= 13.2 Hz, 2H, NCH$_2$N), 6.85-8.15 (8H, Ar-H, 2CH=CH^{Im}). ^{13}C{^{1}H} NMR (CDCl$_3$, T=298 K, ppm) δ : 17.7 (CH$_3$, o-Mesityl-CH$_3$), 17.8 (CH$_3$, o-Mesityl-CH$_3$), 21.1 (CH$_3$, p-Mesityl-CH$_3$), 23.7 (CH$_3$, allyl CH$_3$), 58.0 (CH$_2$, allyl CH$_2$), 63.1 (CH$_2$, NCH$_2$N), 121.7 (CH, CH=CH^{Im}), 123.3 (CH, CH=CH^{Im}), 128.9-139.6 (Ar-C), 132.7 (C, *central* allyl-C), 176.7 (C, carbene).

Less abundant isomer (ca. 48%):

^{1}H NMR (300 MHz, CDCl$_3$, T=298 K, ppm) δ : 1.37 (s, 6H, 2 o-aryl-CH$_3$), 1.51 (s, 3H, allyl-CH$_3$), 1.67 (s, 6H, 2 o-aryl-CH$_3$), 1.81 (s, 2H, 2 *anti* allyl-H), 2.39 (s, 2H, 2 *syn* allyl-H), 2.47 (s, 6H, 2 p-aryl-CH$_3$), 6.86-6.96 (AB system, J= 13.6 Hz, 2H, NCH$_2$N), 6.85-8.15 (8H, Ar-H, 2CH=CH^{Im}). ^{13}C{^{1}H} NMR (CDCl$_3$, T=298 K, ppm) δ : 17.0 (CH$_3$, o-Mesityl-CH$_3$), 17.3 (CH$_3$, o-Mesityl-CH$_3$), 21.3 (CH$_3$, p-Mesityl-CH$_3$), 23.7 (CH$_3$, allyl CH$_3$), 58.0 (CH$_2$, allyl CH$_2$), 63.1 (CH$_2$, NCH$_2$N), 121.7 (CH, CH=CH^{Im}), 123.3 (CH, CH=CH^{Im}), 128.9-139.6 (Ar-C), 132.7 (C, *central* allyl-C), 176.7 (C, carbene).

Synthesis of the complex 48f

Complex **48f** was prepared in analogues manner as that described for **48a** starting from 0.1603 g (0.3270 mmol) of [Pd(Me-PyCH$_2$SPh)(η^3-1,1-dimethylC$_3$H$_3$)]ClO$_4$ and 0.2485 g (0.3270 mmol) of **39c**.

The mixture of **48f** and the Pd(I) dimer **87** was dissolved in a CH$_2$Cl$_2$/Et$_2$O mixture (30 mL : 67 mL) and set at 5°C overnight. The Pd(I) dimer **87** was filtered in a gooch and, from the resulting solution, the solvent was reduced under vacuum and the brownish solid (compound **48f)** was precipitated by addition of diethylether.

0.1224 g of **48f** was obtained.

Equimolar mixture of the two atropoisomers

^{1}H NMR (300 MHz, CDCl$_3$, T=298 K, ppm) δ : 0.55 (s, 6H, 2 allyl-CH$_3$), 1.27 (s, 6H, 2 allyl-CH$_3$), 1.50 (d, J=12.0 Hz , 2H, 2 *anti* allyl-H), 1.96 (s, 6H, 2 o-aryl-CH$_3$), 1.99 (s, 12H, 4 o-aryl-CH$_3$), 2.04 (s, 6H, 2 o-aryl-CH$_3$), 2.36 (s, 12H, 4 p-aryl-CH$_3$), 2.63 (d, J=6.4 Hz , 2H, 2 *syn* allyl-H), 4.54 (m,

2H, 2 *central* allyl-H), 6.22-6.76 (AB system, J= 11.6 Hz, 4H, 2NCH_2N), 6.80-8.05 (16H, Ar-H, 4CH=CH^{Im}).

$^{13}C\{^1H\}$ NMR ($CDCl_3$, T=298 K, ppm) δ : 15.3 (CH_3, allyl CH_3), 17.8 (CH_3, o-Mesityl-CH_3), 18.0 (CH_3, o-Mesityl-CH_3), 18.2 (CH_3, o-Mesityl-CH_3), 18.3 (CH_3, o-Mesityl-CH_3), 19.7 (CH_3, allyl CH_3), 21.0 (CH_3, p-Mesityl-CH_3), 22.6 (CH_3, allyl CH_3), 26.2 (CH_3, p-Mesityl-CH_3), 31.6 (CH_3, allyl CH_3), 46.6 (CH_2, allyl CH_2), 62.9 (CH_2, NCH_2N), 111.7 (CH, *central* allyl-CH), 122.2-123.3 (CH, $CH=CH^{Im}$), 128.9-139.5 (Ar-C), 177.0 (C, carbene), 179.0 (C, carbene).

IR [KBr Pellet]: ν_{ClO} = 1085, δ_{ClO} = 620, cm^{-1}.

Synthesis of the complex 48g

Complex **48g** was prepared in analogues manner as that described for **48a** starting from 0.0361 g (0.0779 mmol) of [[Pd(Me-PyCH_2SPh)(η^3-C_3H_5)]ClO_4 and 0.0603 g (0.0779 mmol) of **39e**.

0.0480 g (yield 90%) of **48g** was obtained.

^1H NMR (300 MHz, CD_3CN, T=298 K, ppm) δ : 2.92 (d, J= 13.3 Hz,2H, 2 *anti* allyl-H), 3.79 (s, 6H, 2 NCH_3), 4.27 (d, J=7.4 Hz, 2H, 2 *syn* allyl-H), 5.36 (m, 1H, *central* allyl-H), 5.85-6.04 (m, 4H, NCH_2N), 7.18 (d, J= 1.9 Hz, 2H, $CH=CH^{Im}$), 7.39 (d, J= 1.9 Hz, 2H, $CH=CH^{Im}$).

$^{13}C\{^1H\}$ NMR (CD_3CN, T=298 K, ppm) δ : 38.2 (CH_3, NCH_3), 58.4 (CH_2, allyl-CH_2), 62.9 (CH_2, NCH_2N), 119.6 (CH, *central* allyl), 121.6 (CH, $CH=CH^{Im}$), 122.1 (CH, $CH=CH^{Im}$), 175.8 (C, carbene).

IR [KBr Pellet]: ν_{ClO} = 1081, δ_{ClO} = 623, cm^{-1}.

Synthesis of the complex 48h

Complex **48h** was prepared in analogues manner as that described for **48a** starting from 0.0720 g (0.156 mmol) of [[Pd(Me-PyCH_2SPh)(η^3-C_3H_5)]ClO_4 and 0.0880 g (0.156 mmol) of **39f**.

0.0655 g (yield 96%) of **48h** was obtained.

^1H NMR (300 MHz, CD_2Cl_2, T=298 K, ppm) δ : 2.77 (d, J= 13.4 Hz, 2H, 2 *anti* allyl-H), 3.69 (s, 6H, 2 NCH_3), 4.08 (d, J=7.4 Hz, 2H, 2 *syn* allyl-H), 4.69 (m, 4H, NCH_2N), 5.40 (m, 1H, *central* allyl-H), 7.08 (d, J= 1.9 Hz, 2H, $CH=CH^{Im}$), 7.24 (d, J= 1.9 Hz, 2H, $CH=CH^{Im}$).

$^{13}C\{^1H\}$ NMR (CD_2Cl_2, T=298 K, ppm) δ : 38.7 (CH_3, NCH_3), 48.3 (NCH_2CH_2N), 58.2 (CH_2, allyl-CH_2), 119.0 (CH, *central* allyl), 122.8 (CH, $CH=CH^{Im}$), 122.9 (CH, $CH=CH^{Im}$), 174.6 (C, carbene).

IR [KBr Pellet]: ν_{ClO} = 1090, δ_{ClO} = 623, cm^{-1}.

9.7.16. Synthesis of bis(NHC) palladium η^3-allyl complexes (49)

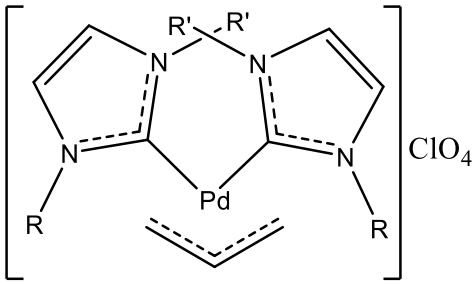

R= CH_2Tol	R'= CH_2Tol	**49a**
R= CH_3	R'= CH_2Tol	**49b**
R= CH_3	R'= CH_2Py	**49c**
R= CH_3	R'= CH_2SPh	**49d**

Synthesis of the complex 49a

0.0406 g (0.0904 mmol) of the precursor [Pd(Me-PyCH_2SPh)(η^3-C_3H_5)] was dissolved in 10 mL of anhydrous dichloromethane in a 50 mL two-necked flask under inert atmosphere (Ar). Subsequently was added 0.0839 g (0.181 mmol) of the silver complex **37a**, previously dissolved in ca. 5 mL of CH_2Cl_2. The mixture was stirred at R.T. for 15 min and the precipitated AgBr was removed by filtration on a millipore membrane filter.

The solvent was removed under reduced pressure and the white solid was washed with ca. 5 mL of diethylether and filtered off on a gooch.

0.0578 g of **49a** was obtained (yield 80%).

^{1}H NMR (400 MHz, $CDCl_3$, T=298 K, ppm) δ : 2.30 (s, 12H, 4CH_3^{Tol}), 2.51 (d, J = 13.3 Hz, 2H, 2 *anti* allyl-H), 3.73 (d, J = 7.3 Hz , 2H, 2 *syn* allyl-H), 5.12 (AB system, J = 15.5 Hz, J= 34.6 Hz, 8H, 4NCH_2), 5.13 (m, 1H, *central*-allyl-H), 6.86 (d, J = 7.9 Hz, 8H, m-Ph), 6.89 (s, 4H, 2CH=CH^{Im}), 7.10 (d, J = 7.9 Hz, 8H, o-Ph).

^{13}C{^{1}H} NMR ($CDCl_3$, T=298 K, ppm) δ : 21.1 (CH_3, CH_3^{Tol}), 54.3 (CH_2, NCH_2), 61.0 (CH_2, allyl-CH_2), 119.3 (CH, *central* allyl), 122.8 (CH, CH=CH^{Im}), 126.8-138.0 (Ar-C), 177.2 (C, carbene).

IR [KBr Pellet]: ν_{ClO} = 1090, δ_{ClO} = 620, cm^{-1}.

Synthesis of the complex 49b

Complex **49b** was prepared in analogues manner as that described for **49a** starting from 0.0362 g (0.0781 mmol) of [[Pd(Me-PyCH_2SPh)(η^3-C_3H_5)]ClO_4 and 0.0586 g (0.156 mmol) of **37d**.

0.0400 g (yield 83%) of **49b** was obtained.

^{1}H NMR (400 MHz, $CDCl_3$, T=298 K, ppm) δ : 2.32 (s, 6H, 2CH_3^{Tol}), 2.66 (d, J = 13.2 Hz, 2H, 2 *anti* allyl-H), 3.71 (s, 6H, 2NCH_3), 3.87 (d, J = 7.5 Hz , 2H, 2 *syn* allyl-H), 5.08 (s, 4H, 2NCH_2), 5.30

(m, 1H, *central*-allyl-H), 6.77-7.12 (10H, Ar-H), 6.87 (d, J = 1.9 Hz, 2H, CH=CH^{Im}), 7.10 (d, J = 1.9 Hz, 2H, CH=CH^{Im}).

$^{13}C\{^{1}H\}$ NMR ($CDCl_3$, T=298 K, ppm) δ : 21.1 (CH_3, CH_3^{Tol}), 38.3 (CH_3, NCH_3), 54.1 (CH_2, NCH_2), 60.2 (CH_2, allyl-CH_2), 119.3 (CH, *central* allyl), 122.1 (CH, CH=CH^{Im}), 123.9 (CH, CH=CH^{Im}), 126.7-138.0 (Ar-C), 176.8 (C, carbene).

IR [KBr Pellet]: ν_{ClO} = 1090, δ_{ClO} = 623, cm^{-1}.

Synthesis of the complexes 49c and 49d

Complexes **49c** and **49d** were synthesized according to published procedures [31c].

9.7.17. Synthesis of palladium η^3-allyl complexes bearing hemi-labile NHCs (50-55)

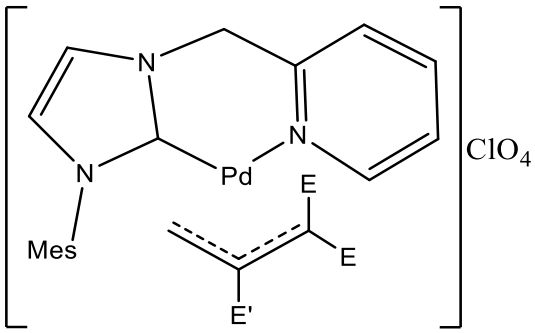

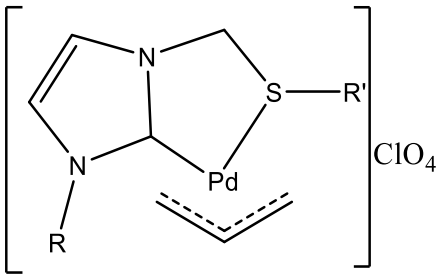

E= H	E'= H	**50**
E= H	E'=CH_3	**51**
E= CH_3	E'=H	**52**

R= Mes	R'= CH_3	**53**
R= Mes	R'= Ph	**54**
R= CH_3	R'= Ph	**55**

Synthesis of the complex 50

0.0501 g (0.137 mmol) of the dimer [Pd(μ-Cl)(η^3-C_3H_5)]$_2$ was dissolved in ca. 10 ml of anhydrous CH_2Cl_2 in a two-necked flask and 0.1274 g (0.2739 mmol) of the silver complex **35b** was added under inert atmosphere (Ar) and the mixture was stirred at RT for ca. 30 m. The precipitated AgBr was removed by filtration on a millipore membrane filter and 0.067 g (0.55 mmol) of $NaClO_4 \cdot H_2O$ dissolved in ca. 10 ml of methanol (CH_2Cl_2/MeOH≈ 3/1) was added to the clear solution. The mixture was stirred for ca. 15 min, dried under vacuum and treated with CH_2Cl_2 and activated carbon. The inorganic salts were filtered off on a Celite filter and repeatedly washed with CH_2Cl_2, whereas the resulting solution was concentrated under vacuum. Addition of diethylether to the concentrated solution yields the precipitation of the complex **50** as a white solid which was filtered off on a gooch and washed with *n*-pentane. 0.1313 g of **50** was obtained (yield 91%).

^{1}H NMR ($CDCl_3$, T=298 K, ppm) δ : 1.93 (d, J = 12.3 1H, *anti* allyl-H *trans*-N), 1.97 (s, 3H, *o*-aryl-CH_3), 1.99 (s, 3H, *o*-aryl-CH_3), 2.39 (s, 3H, *p*-aryl-CH_3), 2.91 (d, J = 6.9 Hz, 1H, *syn* allyl-H *trans*-N), 3.44 (d, J = 13.7 Hz , 1H, *anti* allyl-H *trans*-C), 4.29 (d, J = 7.7 Hz, 1H, *syn* allyl-H *trans*-C), 5.40

(m, 1H, *central*-allyl-H), 5.47, 5.82 (AB system, J = 15.2 Hz, 2H, CH_2N), 6.94 (d, J = 1.9 Hz, 1H, $CH=CH^{Im}$), 7.01 (bs, 2H, *m*-aryl-H),7.46 (ddd, J = 7.7, 5.4, 1.4 Hz, 1H , 5-Pyr); 7.92 (d, J = 1.9 Hz, 1H, $CH=CH^{Im}$), 8.02 (td, J = 7.7, 1.7 Hz, 1H, 4-Pyr), 8,19 (d, J = 7.7 Hz, 1H, 3-Pyr); 8.79 (d, J = 5.4 Hz, 1H, 6- Pyr).

$^{13}C\{1H\}$ NMR ($CDCl_3$, T=298 K, ppm) δ : 17.7 (CH3, *o*-mesityl-CH_3), 17.9 (CH_3, *o*-mesityl-CH_3), 21.1 (CH_3, *p*-mesityl-CH_3), 47.9 (CH_2, allyl *trans*-N), 54.7 (CH_2, CH_2-Pyr), 74.1 (CH2, allyl *trans*-C), 120.3 (CH, central allyl), 121.7 (CH, $CH=CH^{Im}$), 123.6 (CH, $CH=CH^{Im}$), 125.3 (CH, 5-Pyr), 127.4 (CH, 3-Pyr), 129.0 (CH, *m*-mesityl), 129.2 (CH, *m*-mesityl), 134.8 (C, *o*-mesityl), 135.2 (C, *o*-mesityl), 135.9 (C, *i*-mesityl), 139.7 (C, *p*-mesityl), 140.5 (CH, 4-Pyr), 153.8 (C, 2-Pyr), 155.6 (CH, 6-Pyr), 176.4 (C, carbene).

IR [KBr Pellet]: υClO = 1090, υClO = 620, cm^{-1}.

Synthesis of the complex 51

Complex **51** was prepared in analogues manner as that described for **50** starting from 0.0534 g of $[Pd(\mu\text{-}Cl)(\eta^3\text{-}2MeC_3H_4)]_2$, 0.1261 g of **35b** and 0.0759 g of $NaClO_4 \cdot H_2O$.

0.1299 g (yield 89%) of **51** was obtained.

^1H NMR ($CDCl_3$, T=298 K, ppm) δ : 1.83 (s, 3H, allyl-CH_3), 1.92 (d, J = 2.1 Hz, 1H, *anti* allyl-H *trans*-N), 1.96 (s, 3H, *o*-aryl-CH_3), 1.99 (s, 3H, *o*-aryl-CH_3), 2.39 (s, 3H, *p*-aryl-CH_3), 2.56 (t, J = 2.6 Hz, 1H, *syn* allyl-H *trans*-N), 3.29 (s, 1H, *anti* allyl-H *trans*-C), 4.01 (d, J = 3.0 Hz, 1H, *syn* allyl-H *trans*-C), 5.52, 5.80 (AB system, J = 15.3 Hz, 2H, CH_2N), 6.93 (d, J = 1.8 Hz, 1H, $CH=CH^{Im}$), 7.01 (bs, 2H, *m*-aryl-H), 7.44 (ddd, J = 7.7, 5.3, 1.5 Hz, 1H , 5-Pyr); 7.92 (d, J = 1.8 Hz, 1H, $CH=CH^{Im}$), 8.01 (td, J = 7.7, 1.7 Hz, 1H, 4-Pyr), 8,19 (d, J = 7.7 Hz, 1H, 3-Pyr); 8.76 (d, J = 5.3 Hz, 1H, 6- Pyr).

$^{13}C\{^1H\}$ NMR ($CDCl_3$, T=298 K, ppm) δ : 17.8 (CH_3, *o*-mesityl-CH_3), 17.8 (CH3, *o*-mesityl-CH_3), 23.9 (CH_3, allyl-CH_3), 21.1 (CH_3, *p*-mesityl-CH_3), 48.1 (CH_2, allyl *trans*-N), 54.8 (CH_2, CH_2-Pyr), 72.0 (CH_2, allyl *trans*-C), 121.6 (CH, $CH=CH^{Im}$), 123.7 (CH, $CH=CH^{Im}$), 125.2 (CH, 5-Pyr), 127.4 (CH, 3-Pyr), 129.0 (CH, *m*-mesityl), 129.1 (CH, m-mesityl), 134.9 (C, *o*-mesityl), 135.3 (C, *o*-mesityl), 135.3 (C, central allyl), 136.1 (C, *i*-mesityl), 139.6 (C, *p*-mesityl), 140.5 (CH, 4-Pyr), 153.9 (C, 2-Pyr), 155.6 (CH, 6-Pyr), 176.8 (C, NHC).

IR [KBr Pellet]: υClO = 1093, υClO = 620, cm^{-1}.

Synthesis of the complex 52

Complex **52** was prepared in analogues manner as that described for **50** starting from 0.0505 g of $[Pd(\mu\text{-}Cl)(\eta^3\text{-}1,1\text{-}dimethylC_3H_3)]_2$, 0.1113 g of **35b** and 0.0672 g of $NaClO_4 \cdot H_2O$.

0.1159 g (yield 88%) of **52** was obtained.

^1H NMR ($CDCl_3$, T=298 K, ppm) δ : 1.35 (s, 3H, *anti* allyl-CH_3), 1.75 (s, 3H, *syn* allyl-CH_3),1.93

(dd, J = 12.7, 3.3 Hz, 1H, *anti* allyl-H *trans*-N), 1.97 (s, 3H, *o*-aryl-CH_3), 1.98 (s, 3H, *o*-aryl-CH_3), 2.38 (s, 3H, *p*-aryl-CH3), 2.91 (dd, J = 7.5 , 3.3 Hz, 1H, *syn* allyl-H *trans*-N), 4.91 (dd, J = 12.7 , 7.5 Hz, 1H, *central*-allyl-H), 5.48, (d, J = 15.1 Hz, 1H, CH_2N), 5.78, (d, J = 15.1 Hz, 1H, CH_2N), 6.93 (d, J = 1.9 Hz, 1H, CH=CH Im), 7.02 (bs, 2H, *m*-aryl-H),7.57 (ddd, J = 7.7, 5.4, 1.6 Hz, 1H , 5-Pyr); 7.91 (d, J = 1.9 Hz, 1H, CH=CH Im), 8.03 8,18 (d, J = 7.7 Hz, 1H, 3-Pyr); 8.45 (d, J = 5.4 Hz, 1H, 6- Pyr).

$^{13}C\{^1H\}$ NMR ($CDCl_3$, T=298 K, ppm) δ : 17.7 (CH_3, *o*-mesityl-CH_3), 17.9 (*o*-mesityl-CH_3), 20.4 (CH_3, *anti* allyl-CH_3), 21.1 (CH_3, *p*-mesityl-CH_3), 25.5 (CH_3, *syn* allyl-CH_3), 40.7 (CH_2, allyl *trans*-N), 54.7 (CH_2, CH_2-Pyr), 104.1 (C, allyl *trans*-C), 109.9 (CH, central allyl), 121.9 (CH, CH=CH Im), 123.6 (CH, CH=CH Im), 125.7 (CH, 5-Pyr), 127.2 (CH, 3-Pyr), 128.9 (CH, *m*-mesityl), 129.0 (CH, *m*-mesityl), 134.9 (C, *o*-mesityl), 135.1 (C, *o*-mesityl), 136.0 (C, *i*-mesityl), 139.5 (C, *p*-mesityl), 140.4 (CH, 4-Pyr), 150.5 (C, 2-Pyr), 154.1 (CH, 6-Pyr), 177.2 (C, NHC).

Synthesis of the complex 53

Complex **53** was synthesized according to published procedures [31c].

Synthesis of the complex 54

Complex **54** was prepared in analogues manner as that described for **50** starting from 0.0500 g of $[Pd(\mu\text{-}Cl)(\eta^3\text{-}C_3H_5)]_2$, 0.1357 g of **36d** and 0.1040 g of $NaClO_4 \cdot H_2O$.

0.1407 g (yield 93%) of **54** was obtained.

^1H NMR ($CDCl_3$, T = 298 K, ppm) d: 1.94 (s, 3H, o-aryl-CH_3), 2.04 (s, 3H, o-aryl-CH_3), 2.40 (s, 3H, p-aryl-CH_3), 2.43 (d, J = 15.9 Hz, 1H, anti allyl-H trans-S), 3.00 (d, J = 6.9 Hz, 1H, syn allyl-H trans-S), 3.09 (d, J = 13.7 1H, anti allyl-H trans-C), 4.40 (d, J = 7.6 Hz, 1H, syn allyl-H trans-C), 5.40 (m, 1H, central-allyl-H), 5.73, 5.88 (AB system, J = 13.6 Hz, 2H, CH_2S), 7.03 (bs, 2H, m-aryl-H), 7.05 (d, J = 1.9 Hz, 1H, $CH=CH^{Im}$), 7.37–7.47 (m, 3H, Ph), 7.54–7.60 (m, 2H, Ph), 7.84 (d, J = 1.9 Hz, 1H, $CH=CH^{Im}$).

$^{13}C\{^1H\}$ NMR ($CDCl_3$, T = 298 K, ppm) d: 17.6 (CH_3, o-mesityl-CH_3), 17.8 (CH_3, o-mesityl-CH_3), 21.1 (CH_3, p-mesityl-CH_3), 59.0 (CH_2, CH_2-S), 59.2 (CH_2, allyl trans-S), 69.9 (CH_2, allyl trans-C), 118.4 (CH, central allyl), 121.6 (CH, $CH=CH^{Im}$), 123.5 (CH, $CH=CH^{Im}$), 129.0 (CH, m-mesityl), 129.2 (CH, m-mesityl), 130.1 (CH, o-Ph), 130.3 (C, i-Ph), 130.5 (CH, p-Ph), 132.1 (CH, m-Ph), 135.3 (C, o-mesityl), 135.7 (C, o-mesityl), 136.6 (C, i-Ph), 139.9 (C, p-mesityl), 180.7 (C, NHC).

IR [KBr Pellet]: υClO = 1085, υClO = 620, cm^{-1}.

Anal. Calc. for $C_{22}H_{25}N_2PdS$: C, 57.95; H, 5.53; N, 6.14. Found: C, 58.12; H, 5.44, N, 6.02%.

Synthesis of the complex 55

Complex **55** was prepared in analogues manner as that described for **50** starting from 0.0503 g of $[Pd(\mu\text{-}Cl)(\eta^3\text{-}C_3H_5)]_2$, 0.1081 g of **36b** and 0.0772 g of $NaClO_4 \cdot H_2O$.

0.0931 g (yield 96%) of **55** was obtained.

^1H NMR (CD_2Cl_2, T = 298 K, ppm) δ: 3.33 (d, J = 13.6 Hz, 1H, anti allyl-H trans-C), 3.43 (d, J = 12.5 Hz, 1H, anti allyl-H trans-S), 3.93 (s, 3H, NCH_3), 4.62 (dd, J = 7.6 , J = 2.2, 1H, syn allyl-H trans-S), 4.73 (dt, J = 7.0, 1.9 Hz, 1H, syn allyl-H trans-C), 5.33, 5.43 (AB system, J= 12.9 Hz, 2H, CH_2S), 5.62 (m, 1H, central-allyl -H), 7.23 (d, J = 1.9 Hz, 1H, CH=CH Im), 7.46 (d, J = 1.9 Hz, 1H, CH=CH Im), 7.43-751 (m, 3H, SPh-H), 7.57-7.61 (m, 2H, SPh-H).

9.7.18. Synthesis of mixed NHC/Cl palladium η^3-allyl complexes (56-58)

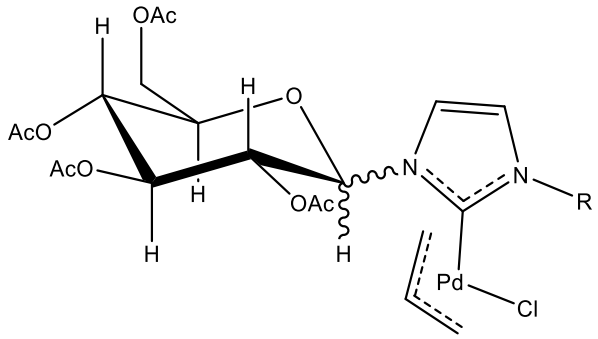

R= *n*-Bu **(56a)**
R= CH_3 **(56b)**
R= Mes **(56c)**

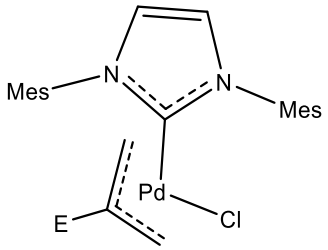

E= H **57**
E= CH_3 **58**

Synthesis of the complex 56a

0.0243 g (0.0664 mmol) of the dimer $[Pd(\mu\text{-}Cl)(\eta^3\text{-}C_3H_5)]_2$ was dissolved in ca. 25 mL of anhydrous dichloromethane in a 50 mL two necked flask under inert atmosphere (Ar). The resulting mixture was treated with 0.0853 g (0.133 mmol) of the silver complex **38a** and stirred at RT for ca. 30 min.

The precipitated AgBr was removed by filtration on a millipore membrane filter.

Addition of diethylether to the concentrated solution yields the precipitation of the complex **56a** as a brownish solid which was filtered off on a gooch and washed with *n*-pentane.

0.0703 g of **56a** was obtained (yield 76%).

(α Anomer + β Anomer) ^1H-NMR (300 MHz, CD_2Cl_2, T = 298 K, ppm) δ: 0.95-1.00 (m, 6H, $2CH_3^{4'}$), 1.33-1.42 (m, 4H, $2CH_2^{3'}$), 1.79-1.88 (m, 4H, $2CH_2^{2'}$), 1.95 (s, 3H, OCH_3), 1.97 (s, 3H, OCH_3), 2.03 (s, 3H, OCH_3), 2.04 (s, 3H, OCH_3), 2.07 (s, 3H, OCH_3), 2.08 (s, 3H, OCH_3), 2.09 (s, 3H, OCH_3), 2.10 (s, 3H, OCH_3), 2.45 (d, 2H, J= 12.1 Hz, 2*anti* allyl-H *trans*-Cl), 3.32 (d, 1H, J= 12.2 Hz, *anti* allyl-H *trans*-C), 3.36 (d, 1H, J= 12.2 Hz, *anti* allyl-H *trans*-C), 3.48 (d, 2H, J= 6.7 Hz, 2*syn* allyl-H *trans*-Cl), 4.02 (m, 2H, $2H^5$), 4.15-4.32 (m, 10H, 2*syn* allyl-H *trans*-C+$2CH_2^{1'}$+$2CH_2^6$), 5.22 (t, 2H,

J= 9.7 Hz, 2H^{3}), 5.38-5.48 (m, 6H, 2*central* allyl-H +2H^{2}+2H^{4}), 6.15 (d, 1H, J= 8.5 Hz, H^{1}), 6.20 (d, 1H, J= 8.5 Hz, H^{1}), 7.05 (d, 1H, J= 2.1 Hz, H^{Im}), 7.07 (d, 1H, J= 2.1 Hz, H^{Im}), 7.24 (d, 2H, J= 2.1 Hz, 2H^{Im}).

(α Anomer + β Anomer) $^{13}C\{^{1}H\}$-NMR (CD_2Cl_2, T = 298 K, ppm) δ: 13.4 (CH_3, $CH_3^{4'}$), 13.5 (CH_3, $CH_3^{4'}$), 19.6 (CH_2, $CH_2^{3'}$), 19.7 (CH_2, $CH_2^{3'}$), 20.2 (CH_3, OCH_3), 20.3 (CH_3, OCH_3), 20.4 (CH_3, OCH_3), 20.5 (CH_3, OCH_3), 32.7 (CH_2, $CH_2^{2'}$), 32.8 (CH_2, $CH_2^{2'}$), 48.9 (CH_2, allyl *trans*-Cl), 49.3 (CH_2, allyl *trans*-Cl), 51.0 (CH_2, $CH_2^{1'}$), 51.1 (CH_2, $CH_2^{1'}$), 61.8 (CH_2, CH_2^{6}), 61.9 (CH_2, CH_2^{6}), 67.9 (CH, CH^{4}), 68.0 (CH, CH^{4}), 70.0 (CH, CH^{2}), 70.1 (CH, CH^{2}), 72.0 (CH_2, allyl *trans*-C), 72.4 (CH_2, allyl *trans*-C), 72.8 (CH, CH^{3}), 72.9 (CH, CH^{3}), 74.6 (CH, CH^{5}), 74.7 (CH, CH^{5}), 86.7 (CH, CH^{1}), 86.8 (CH, CH^{1}), 115.1 (CH, *central* allyl), 118.0 (CH, CH^{Im}), 118.1 (CH, CH^{Im}), 122.0 (CH, CH^{Im}), 122.1 (CH, CH^{Im}), 169.2 (C, C=O), 169.5 (C, C=O), 169.6 (C, C=O), 170.3 (C, C=O), 182.7 (C, carbene), 183.0 (C, carbene).

IR(KBr): $\nu_{C=O}$ = 1754cm^{-1}, ν_{C-O} = 1231 cm^{-1}.

Synthesis of the complex 56b

Complex **56b** was prepared in analogues manner as that described for **56a** starting from 0.0243 g of [Pd(μ-Cl)(η^{3}-allyl)]$_2$ and 0.0860 g of **38b**.

0.0566 g (yield 72%) of **56b** was obtained.

(α Anomer + β Anomer) ^{1}H-NMR (300 MHz, $CDCl_3$, T = 298 K, ppm) δ: 1.97 (s, 3H, OCH_3), 1.98 (s, 3H, OCH_3), 2.03 (s, 3H, OCH_3), 2.04 (s, 3H, OCH_3), 2.07 (s, 3H, OCH_3), 2.08 (s, 3H, OCH_3), 2.09 (s, 3H, OCH_3), 2.11 (s, 3H, OCH_3), 2.45 (d, 2H, J= 13.2 Hz, *anti* allyl-H *trans*-Cl), 2.48 (d, 2H, J= 13.2 Hz, *anti* allyl-H *trans*-Cl), 3.38 (d, 1H, J= 13.4 Hz, *anti* allyl-H *trans*-C), 3.42 (d, 1H, J= 13.4 Hz, *anti* allyl-H *trans*-C), 3.48 (d, 2H, J= 5.4 Hz, 2*syn* allyl-H *trans*-Cl), 3.83 (s, 3H, NCH_3), 3.88 (s, 3H, NCH_3), 3.98 (m, 2H, 2H^{5}), 4.14-4.30 (m, 4H, 2CH_2^{6}), 4.38 (d, 1H, J= 5.3 Hz, *syn* allyl-H *trans*-C), 4.41 (d, 1H, J= 5.3 Hz, *syn* allyl-H *trans*-C), 5.20 (t, 2H, J= 9.7 Hz, 2H^{3}), 5.41-5.44 (m, 6H, 2*central* allyl-H +2H^{2}+2H^{4}), 6.18 (d, 1H, J= 8.6 Hz, H^{1}), 6.24 (d, 1H, J= 8.6 Hz, H^{1}), 6.96 (d, 1H, J= 2.1 Hz, H^{Im}), 6.98 (d, 1H, J= 2.1 Hz, H^{Im}), 7.20 (d, 2H, J= 2.1 Hz, 2H^{Im}).

(α Anomer + β Anomer) $^{13}C\{^{1}H\}$-NMR ($CDCl_3$, T = 298 K, ppm) δ: 20.4 (CH_3, OCH_3), 20.5 (CH_3, OCH_3), 20.6 (CH_3, OCH_3), 20.7 (CH_3, OCH_3), 38.5 (CH_3, NCH_3), 48.8 (CH_2, allyl *trans*-Cl), 49.1 (CH_2, allyl *trans*-Cl), 61.8 (CH_2, CH_2^{6}), 61.9 (CH_2, CH_2^{6}), 68.0 (CH, CH^{4}), 68.1 (CH, CH^{4}), 69.9 (CH, CH^{2}), 70.0 (CH, CH^{2}), 73.0 (CH, CH^{3}), 73.1 (CH, CH^{3}), 73.4 (CH_2, allyl *trans*-C), 73.8 (CH_2, allyl *trans*-C), 74.6 (CH, CH^{5}), 74.7 (CH, CH^{5}), 86.4 (CH, CH^{1}), 86.5 (CH, CH^{1}), 115.2 (CH, *central* allyl), 118.3 (CH, CH^{Im}), 118.4 (CH, CH^{Im}), 123.2 (CH, CH^{Im}), 123.4 (CH, CH^{Im}), 169.4 (C, C=O), 169.5 (C, C=O), 169.7 (C, C=O), 170.5 (C, C=O), 183.1 (C, carbene), 183.6 (C, carbene).

IR(KBr): $\nu_{C=O}$ = 1752 cm^{-1}, ν_{C-O} = 1230 cm^{-1}.

Synthesis of the complex 56c

Complex **56c** was prepared in analogues manner as that described for **56a** starting from 0.0112 g of $[Pd(\mu\text{-}Cl)(\eta^3\text{-allyl})]_2$ and 0.0400 g of **38c**.

0.0290 g (yield 68%) of **56c** was obtained.

β Anomer (60%):

^{1}H-NMR (300 MHz, $CDCl_3$, T = 298 K, ppm selected peaks) δ: 1.46 (d, 1H, J= 12.0 Hz, *anti* allyl-H *trans*-C), 1.89-2.84 (21H, $3CH_3^{Mes}$+$4OCH_3$), 2.95-3.10 (m, 2H, 3.32 (d, 3H, *anti* allyl-H *trans*-Cl + *syn* allyl-H *trans*-C + *anti* allyl-H *trans*-Cl), 4.26 (d, 1H, J= 3.2 Hz, *syn* allyl-H *trans*-C), 5.12 (m, 1H, *central* allyl-H), 6.94-6.99 (m, 3H, Ph+H^{Im}), 7.40 (d, 1H, J= 1.9 Hz, H^{Im}).

$^{13}C\{^1H\}$-NMR ($CDCl_3$, T = 298 K, ppm selected peaks) δ: 17.4 (CH_3, *p*-CH_3^{Mes}), 18.8 (CH_3, *m*-CH_3^{Mes}), 20.3-21.1 (CH_3, OCH_3), 49.5 (CH_2, allyl *trans*-Cl), 74.5 (CH_2, allyl *trans*-C), 86.1 (CH, CH^1), 114.8 (CH, *central* allyl), 128.6-139.3 (Ph), 168.9-170.5 (C, C=O), 183.0 (C, carbene).

α Anomer (40%):

^{1}H-NMR (300 MHz, $CDCl_3$, T = 298 K, ppm selected peaks) δ: 1.46 (d, 1H, J= 12.0 Hz, *anti* allyl-H *trans*-C), 1.89-2.84 (21H, $3CH_3^{Mes}$+$4OCH_3$), 2.95-3.10 (m, 2H, 3.32 (d, 3H, *anti* allyl-H *trans*-Cl + *syn* allyl-H *trans*-C + *anti* allyl-H *trans*-Cl), 4.22 (d, 1H, J= 3.0 Hz, *syn* allyl-H *trans*-C), 4.87 (m, 1H, *central* allyl-H), 6.94-6.99 (m, 3H, Ph+H^{Im}), 7.42 (d, 1H, J= 1.9 Hz, H^{Im}).

$^{13}C\{^1H\}$-NMR ($CDCl_3$, T = 298 K, ppm selected peaks) δ: 17.6 (CH_3, *p*-CH_3^{Mes}), 18.5 (CH_3, *m*-CH_3^{Mes}), 20.3-21.1 (CH_3, OCH_3), 49.5 (CH_2, allyl *trans*-Cl), 74.6 (CH_2, allyl *trans*-C), 86.4 (CH, CH^1), 114.8 (CH, *central* allyl), 128.6-139.3 (Ph), 168.9-170.5 (C, C=O), 183.1 (C, carbene).

IR(KBr): $\nu_{C=O}$ = 1752 cm^{-1}, ν_{C-O} = 1230 cm^{-1}.

Synthesis of complexes 57

0.0802 g (0.220 mmol) of the dimer $[Pd(\mu\text{-}Cl)(\eta^3\text{-}C_3H_5)]_2$ was dissolved in ca. 20 mL of anhydrous dichloromethane in a 50 mL two necked flask under inert atmosphere (Ar). The resulting mixture was treated with 0.1963 g (0.440 mmol) of the silver complex **37b** and stirred at RT for ca. 30 min.

The precipitated AgCl was removed by filtration on a millipore membrane filter.

Addition of a diethylether/n-pentane mixture (1:1) to the concentrated solution yields the precipitation of the complex **57** as a white solid which was filtered off on a gooch and washed with *n*-pentane.

0.1807 g of **57** was obtained (yield 85%).

^{1}H NMR ($CDCl_3$, T=298 K, ppm) δ: 1.82 (d, J= 12Hz, 1H, *anti* allyl-H *trans*-Cl), 2.21 (s, 6H, *o*-*m*-mesityl-CH_3), 2.24 (s, 6H, *o*-*m*-mesityl-CH_3), 2.34 (s, 6H, *p*- *m*-mesityl-CH_3), 2.83 (d, J = 13.4, 1H, *anti* allyl-H *trans*-C), 3.21 (d, J = 7.4 Hz,1H, *syn* allyl-H *trans*-Cl), 3.89 (dd, J = 7.5, 2.2 Hz,1H, *syn* allyl-H *trans*-C), 4.87 (m, 1H, CH central allyl), 6.99 (s, 4H, *m*-mesityl-H), 7.11 (s, 2H, CH=CH^{Im}).

Synthesis of complexes 58

Complex **58** was prepared in analogues manner as that described for **57** starting from 0.0803 g of $[Pd(\mu\text{-}Cl)(\eta^3\text{-}2\text{-}Me\text{-}C_3H_4)]_2$ and 0.1826 g of **37b**.

0.1877 g (yield 92%) of **58** was obtained.

^1H NMR ($CDCl_3$, T=298 K, ppm) δ: 1.36 (s, 3H, allyl-CH_3), 1.86 (s,1H, *anti* allyl-H *trans*-Cl), 2.21 (s, 6H, *o*- *m*-mesityl -CH_3), 2.26 (s, 6H, *o*- *m*-mesityl -CH_3), 2.34 (s, 6H, *p*- *m*-mesityl -CH3), 2.71 (s, 1H, *syn* allyl-H *trans*-Cl), 2.96 (dd, J = 3.0, 1.0 Hz, 1H, *anti* allyl-H *trans*-C), 2.96 (d, J = 3.0 Hz,1H, *syn* allyl-H *trans*-C), 6.98 (s, 2H, *m*-mesityl -H), 7.00 (s, 2H, *m*-mesityl-H), 7.11 (s, 2H, CH=CH Im).

9.7.19. Synthesis of mixed NHC/PPh_3 palladium η^3-allyl complexes (59-75)

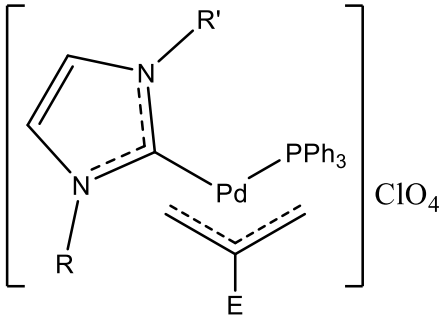

R= CH_2Tol	R'= CH_2Tol	E= H	**59**
R= CH_2Tol	R'= CH_2Tol	E=CH_3	**60**
R= Mes	R'= Mes	E= H	**61**
R= Mes	R'= Mes	E=CH_3	**62**
R= CH_3	R'= Bn	E=H	**63**
R= CH_3	R'= CH_2Py	E=H	**64**
R= Mes	R'= CH_2Py	E=H	**65**
R= CH_3	R'= CH_2SPh	E=H	**66**
R= Mes	R'= CH_2SPh	E=H	**67**
R= Mes	R'= CH_2SCH_3	E=H	**68**
R= AcGluc	R'= *n*-Bu	E=H	**69a**
R= AcGluc	R'= CH_3	E=H	**69b**
R= AcGluc	R'= Mes	E=H	**69c**

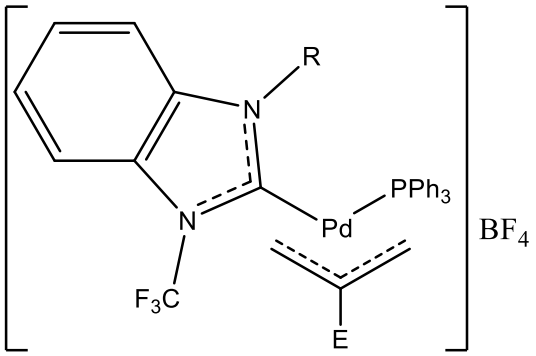

R= CH_3	E= H	**70**
R= CH_3	E= CH_3	**71**
R= i-Pr	E= H	**72**
R= i-Pr	E= CH_3	**73**
R= Ph	E= H	**74**
R= Ph	E=CH_3	**75**

Synthesis of complex 59

0.0502 g (0.137 mmol) of the dimer $[Pd(\mu\text{-}Cl)(\eta^3\text{-}C_3H_5)]_2$ was dissolved in ca. 10 ml of anhydrous CH_2Cl_2 and 0.1269 g (0.274 mmol) of the silver complex **37a** dissolved in ca. 7 ml of CH_2Cl_2 was added and the mixture was stirred at RT for ca. 30 min in a 50 mL two necked flask under inert atmosphere (Ar).

The precipitated AgBr was removed by filtration on a millipore membrane filter and 0.0718 g (0.274 mmol) of PPh_3 was added to the clear solution which was left aside for ca. 15 min. The resulting

mixture was treated with 0.0800 g (0.570 mmol) of $NaClO_4 \cdot H_2O$ dissolved in ca. 8 ml of methanol (CH_2Cl_2/MeOH≈ 2/1). and further stirred for ca. 15 min, dried under vacuum and treated with CH_2Cl_2 and activated carbon. The inorganic salts were filtered off on a Celite filter and repeatedly washed with CH_2Cl_2, whereas the resulting solution was concentrated under vacuum. Addition of diethylether to the concentrated solution yields the precipitation of the complex **59** as a white solid which was filtered off on a gooch and washed with *n*-pentane. 0.1865 g of **59** was obtained (yield 87%).

^{1}H NMR ($CDCl_3$, T = 298 K, ppm, selected peaks) δ: 2.30 (s, 6H, tol-CH_3), 2.61 (dd, J = 13.3, 10.5 Hz, 1H, anti allyl-H trans-P), 2.85 (d, J = 13.4 Hz, 1H, anti allyl-H trans-C), 3.99 (m, 2H, syn allyl-H trans-C, syn allyl-H trans-P), 4.59, 4.64 (AB system, J = 15.3 Hz, 2H, NCH_2), 4.68, 4.84 (AB system, J = 14.8 Hz, 2H, NCH_2), 5.37 (m, 1H, central-allyl-H), 6.80–6.85 (m, 4H, tol o-H), 7.02–7.17 (m, 12H, $CH{=}CH^{Im}$, PPh), 7.41–7.57 (m, 9H, tol m-H, PPh).

^{13}C{1H} NMR ($CDCl_3$, T = 298 K, ppm selected peaks) δ: 21.1 (CH_3, tol-CH_3), 54.4 (CH_3, NCH_2), 54.5 (CH_2, NCH_2), 67.9 (d, CH_2, J_{CP} = 29.5 Hz, CH_2 allyl trans-P), 68.8 (CH_2, allyl trans-C), 121.2 (d, CH, J_{CP} = 5.1 Hz, central allyl), 123.2 (CH, $CH{=}CH^{Im}$), 123.6 (CH, $CH{=}CH^{Im}$), 176.1 (d, C, J_{CP} = 19.0 Hz, carbene).

^{31}P{1H} NMR ($CDCl_3$, T = 298 K) δ: 25.8.

IR [KBr Pellet]: υClO = 1090, υClO = 618, cm^{-1}.

Anal. Calc. for $C_{40}H_{40}N_2PPd$: C, 70.02; H, 5.88; N, 4.08. Found: C, 69.97; H, 5.91; N, 3.87%.

Synthesis of the complex 60

Complex **60** was prepared in analogues manner as that described for **59** starting from 0.0538 g of $[Pd(\mu\text{-}Cl)(\eta^3\text{-}2\text{-}MeC_3H_4)]_2$, 0.1270 g of the silver complex **37a**, 0.0719 g of PPh_3 and 0.080 g of $NaClO_4 \cdot H_2O$.

0.1980 g (yield 91%) of **60** was obtained.

^{1}H NMR ($CDCl_3$, T=298 K, ppm, selected peaks) δ : 1.69 (s, 3H, allyl-CH_3), 2.28 (s, 3H, tol-CH_3), 2.30 (s, 3H, tol-CH_3), 2.65 (dd, J = 10.1, 1.4 Hz, 1H, *anti* allyl-H *trans*-P), 2.88 (s, 1H, *anti* allyl-H *trans*-C), 3.70 (s, 1H, *syn* allyl-H *trans*-C), 3.97 (bt, 1H, *syn* allyl-H *trans*-P), 4.49, 4.83 (AB system, J = 15.1 Hz, 2H, NCH_2), 4.78, 4.94 (AB system, J = 14.8 Hz, 2H, NCH_2), 6.74-6.90 (m, 4H, tol *o*-H), 7.00-7.15 (m, 12 H, CH=CH Im, PPh), 7.40-7.57 (m, 9H, tol *m*-H, PPh).

^{13}C{1H} NMR ($CDCl_3$, T=298 K, ppm selected peaks) δ : 21.0 (CH3, tol-CH_3), 21.1 (CH_3, tol-CH_3), 54.3 (CH_3, NCH_2), 54.5 (CH2, NCH_2), 66.8 (d, CH_2, J_{CP} = 31.2 Hz, CH2 allyl *trans*-P), 68.5 (CH_2, allyl *trans*-C), 123.1 (CH, CH=CH Im), 123.7 (CH, CH=CH Im), 135.8 (d, C, J_{CP} = 4.9 Hz, central allyl), 176.6 (d, C, J_{CP} = 18.5 Hz, carbene). ^{31}P{1H} NMR ($CDCl_3$, T = 298 K) δ : 27.5.

IR [KBr Pellet]: υClO = 1093, υClO = 620, cm^{-1}.

Synthesis of complex 61

Complex **61** was synthesized according to published procedures [39a].

Synthesis of complex 62

Complex **62** was prepared in analogues manner as that described for **59** starting from 0.0197 g of $[Pd(\mu\text{-}Cl)(\eta^3\text{-}2\text{-}MeC_3H_4)]_2$, 0.0457 g of the silver complex **37b**, 0.0262 g of PPh_3 and 0.0281 g of $NaClO_4 \cdot H_2O$.

0.0726 g (yield 88%) of **62** was obtained.

^{1}H NMR (CD_2Cl_2, T=233 K, ppm) δ : 1.12 (s, 3H, allyl-CH_3), 1.48 (s, 3H, *p*-mesityl -CH_3), 1.85 (s,1H, *anti* allyl-H *trans*-C), 1.88 (s, 3H, *p*-mesityl -CH_3), 2.11 (s, 3H, *o*-mesityl -CH_3), 2.16 (s, 3H, *o*-mesityl -CH_3), 2.40 (d, J_{HP} = 10.1 Hz, 1H, *anti* allyl-H *trans*-P), 2.40 (s, 3H, *o*-mesityl -CH_3), 2.43 (s, 3H, *o*-mesityl -CH_3), 3.02 (bt, 1H, *syn* allyl-H *trans*-C), 3.82 (bt, 1H, *anti* allyl-H *trans*-P), 6.83-7.50 (m, 19 H, *m*-mesityl, CH=CH Im, PPh_3).

^{31}P{^{1}H} NMR ($CDCl_3$, T = 298 K) δ : 28.8.

^{13}C{^{1}H} NMR (CD_2Cl_2, T=298 K, ppm) δ : 18.0 (bs, CH_3, *p*-mesityl-CH_3), 18.5 (bs,CH_3, *o*-mesityl-CH_3, *p*-mesityl-CH_3), 20.8 (CH_3, *o*-mesityl-CH_3), 21.4 (CH_3, allyl-CH_3), 68.0 (d, CH_2, J_{CP} = 31.6 Hz, allyl *trans*-P), 72.4 (CH_2, allyl *trans*-C), 125.1 (CH, *m*-mesityl), 128.8. (CH, CH=CH Im), 129.7 (CH, *m*-mesityl), 135.0 (C, *o*-mesityl), 135.5 (C, *i*-mesityl), 136.0 (d, J_{CP} = 4.6 Hz, C, central allyl), 139.9 (C, *p*-mesityl), 179.9 (d, C, J_{CP} = 14.4 Hz, NHC).

Synthesis of complex 63

Complex **63** was prepared in analogues manner as that described for 5**9** starting from 0.0502 g of $[Pd(\mu\text{-}Cl)(\eta^3\text{-}C_3H_5)]_2$, 0.0986 g of the silver complex **37c**, 0.0718 g of PPh_3 and 0.080 g of $NaClO_4 \cdot H_2O$.

0.1752 g (yield 94%) of **63** was obtained.

<u>Most abundant isomer (ca. 55%):</u>

^{1}H NMR ($CDCl_3$, T=298 K, ppm, selected peaks) δ : 3.08 (d, J = 13.4 Hz, 1H, *anti* allyl-H *trans*-C), 3.31 (dd, J = 13.2, 9.6 Hz, 1H, *anti* allyl-H *trans*-P), 3.32 (s, 3H, NCH_3), 3.95-4.00 (m, 2H, *syn* allyl-H *trans*-P, *syn* allyl-H *trans*-C, partially overlapped), 4.60 (bs, 5.84, 2H, NCH_2), 5.28 (m, 1H, *central*-allyl-H).

^{13}C{1H} NMR ($CDCl_3$, T=298 K, ppm selected peaks) δ : 38.1 (CH_3, NCH_3), 54.3 (CH_2, NCH_2), 67.4 (d, CH_2, J_{CP} = 30.0 Hz, CH_2 allyl *trans*-P), 69.1 (CH_2, allyl *trans*-C), 121.0 (d, CH, J_{CP} = 5.0 Hz, central allyl), 123.1 (CH, $CH{=}CH^{Im}$), 123.4 (CH, $CH{=}CH^{Im}$), 176.4 (d, C, J_{CP} = 19.5 Hz, carbene).

^{31}P{1H} NMR ($CDCl_3$, T = 298 K) δ: 26.1.

Less abundant isomer (ca. 45%):

^{1}H NMR ($CDCl_3$, T=298 K, ppm, selected peaks) δ : 2.51 (dd, J = 13.2, 10.2 Hz, 1H, *anti* allyl-H *trans*-P), 2.84 (d, J = 13.5 Hz, 1H, *anti* allyl-H *trans*-C), 3.95-4.00 (m, 1H, *syn* allyl-H *trans*-C, partially overlapped), 3.98 (dd, 6.9, 6.8 Hz, 1H, *syn* allyl-H *trans*-P), 4.68, 4.80 (AB system, J = 15.0 Hz, 2H, NCH_2), 5.82 (m, 1H, *central*-allyl-H).

^{13}C{1H} NMR ($CDCl_3$, T=298 K, ppm selected peaks) δ : 38.0 (CH_3, NCH_3), 54.3 (CH_2, NCH_2), 67.0 (d, CH_2, J_{CP} = 30.0 Hz, CH_2 allyl *trans*-P), 68.9 (CH_2, allyl *trans*-C), 121.7 (d, CH, J_{CP} = 5.2 Hz, central allyl), 124.0 (CH, $CH{=}CH^{Im}$), 124.2 (CH, $CH{=}CH^{Im}$), 176.1 (d, C, J_{CP} = 19.3 Hz, carbene).

^{31}P{1H} NMR ($CDCl_3$, T = 298 K) δ: 25.7.

IR [KBr Pellet]: υClO = 1090, υClO = 623, cm^{-1}.

Synthesis of the complex 64

0.0801 g (0.170 mmol) of the complex [Pd(Me-$PyCH_2SPh$)(η^3-C_3H_5)]ClO_4 was dissolved in ca. 30 ml of anhydrous CH_2Cl_2.

The resulting mixture was treated with 0.0624 g (0.170 mmol) of the silver complex **35a** and 0.0454 g (0.170 mmol) of PPh_3 dissolved in ca. 60 ml of anhydrous CH_2Cl_2, further stirred for ca. 30 min and the precipitated AgBr was removed by filtration on a millipore membrane filter.

Addition of diethylether to the concentrated solution yields the precipitation of the complex **64** as a white solid which was filtered off on a gooch and washed with *n*-pentane.

0.1141 g of **64** was obtained (yield 96%).

Most abundant isomer (ca. 52%):

^{1}H NMR (CD_2Cl_2, T=233 K, ppm, selected peaks) δ : 2.44 (dd, J_{HH} = 13.1 Hz, J_{HP} = 10.9 Hz, 1H, *anti* allyl-H *trans*-P), 2.86 (d,1H, J_{HH} = 13.1 Hz *anti* allyl-H *trans*-C), 3.25 (s, 3H, NCH_3), 4.01 (dd, J_{HH} = 7.9 Hz, J_{HP} = 7.9 Hz, 1H, *syn* allyl-H *trans*-P), 4.09 (d, 1H, J_{HH} = 7.9 Hz, *syn* allyl-H *trans*-C), 4.75, 4.81 (AB system, J = 15.5 Hz, 2H, NCH_2), 6.98 (d, J = 1.8 Hz, 1H, CH=CH Im), 7.18 (d, J = 1.8 Hz, 1H, CH=CH Im), 8.36 (d, J = 4.8 Hz, 1H, 6- Pyr).

^{13}C{^{1}H} NMR (CD_2Cl_2, T=233 K, ppm selected peaks) δ: 37.7 (CH_3, NCH_3), 55.6 (CH_2, NCH_2), 66.8 (d, CH_2, J_{CP} = 29.9 Hz, CH_2 allyl *trans*-P), 68.3 (CH_2, allyl *trans*-C), 123.6 (CH, CH=CH Im), 124.0 (CH, CH=CH Im), 121.2 (d, CH, J_{CP} = 4.9 Hz, central allyl), 137.1 (CH, 4-Pyr), 149.6 (C, 2-Pyr), 154.7 (CH, 6-Pyr), 176.2 (d, C, J_{CP} = 14.5 Hz, NHC).

^{31}P{1H} NMR ($CDCl_3$, T = 298 K) δ : 26.2.

Less abundant isomer (ca. 48%):

^{1}H NMR (CD_2Cl_2, T=233 K, ppm, selected peaks) δ : 2.86 (d,1H, J_{HH} = 13.1 Hz *anti* allyl-H *trans*-C), 3.09 (dd, J_{HH} = 13.1 Hz, J_{HP} = 10.9 Hz, 1H, *anti* allyl-H *trans*-P), 3.16 (s, 3H, NCH_3), 4.03 (d, 1H, J_{HH} = 7.9 Hz, *syn* allyl-H *trans*-C), 4.26 (dd, J_{HH} = 7.9 Hz, J_{HP} = 7.9 Hz, 1H, *syn* allyl-H *trans*-

P), 4.73 (s, 2H, NCH_2), 7.02 (d, J = 1.8 Hz, 1H, CH=CH Im), 7.13 (d, J = 1.8 Hz, 1H, CH=CH Im), 8.40 (d, J = 4.9 Hz, 1H, 6- Pyr).

$^{13}C\{^1H\}$ NMR (CD_2Cl_2, T=233 K, ppm selected peaks) δ: 37.8 (CH_3, NCH_3), 55.7 (CH_2, NCH_2), 66.5 (d, CH_2, J_{CP} = 30.3 Hz, CH_2 allyl *trans*-P), 68.4 (CH_2, allyl *trans*-C), 123.4 (CH, CH=CH Im), 123.7 (CH, CH=CH Im), 121.1 (d, CH, J_{CP} = 5.3 Hz, central allyl), 137.3 (CH, 4-Pyr), 149.4 (C, 2-Pyr), 155.0 (CH, 6-Pyr), 176.3 (d, C, J_{CP} = 14.5 Hz, NHC).

$^{31}P\{1H\}$ NMR (CD_2Cl_2, T = 233 K) δ : 25.7.

Synthesis of the complex 65

0.0639 g (0.122 mmol) of the complex **50** was dissolved in ca. 15 ml of anhydrous CH_2Cl_2 and the resulting mixture was treated with 0.0319 g (0.122 mmol) of PPh_3 and further stirred for ca. 10 min. Addition of diethylether to the concentrated solution yields the precipitation of the complex **65** as a white solid which was filtered off on a gooch and washed with *n*-pentane.

0.0936 g of **65** was obtained (yield 98%).

Most abundant isomer (ca. 61%):

^1H NMR (CD_2Cl_2, T=233 K, ppm, selected peaks) δ : 1.45 (s, 3H, *o*-aryl-CH_3), 1.90 (s, 3H, *o*-aryl-CH_3), 2.25 (dd, J_{HH} = 13.3 Hz, J_{HP} = 10.9 Hz, 1H, *anti* allyl-H *trans*-P), 2.33 (s, 3H, *p*-aryl-CH_3), 2.71 (d,1H, J_{HH} = 13.3 Hz *anti* allyl-H *trans*-C), 3.39 (d, 1H, J_{HH} = 7.2 Hz, *syn* allyl-H *trans*-C), 3.77 (dd, J_{HH} = 7.2 Hz, J_{HP} = 7.2 Hz, 1H, *syn* allyl-H *trans*-P), 4.41, 4.46 (AB system, J = 15.7 Hz, 2H, NCH_2), 4.92 (m, CH, central allyl), 7.76 (td, J = 7.7, 1.6 Hz, 4- Pyr),8.56 (d, J = 4.5 Hz, 1H, 6- Pyr).

$^{13}C\{^1H\}$ NMR (CD_2Cl_2, T=233 K, ppm selected peaks) δ : 17.8 (CH_3, *o*-mesityl-CH_3), 17.9 (*o*-mesityl-CH_3), 20.4 (CH_3, *anti* allyl-CH_3), 21.1 (CH_3, *p*-mesityl-CH_3), 55.6 (CH_2, NCH_2), 66.9 (d, CH_2, J_{CP} = 30.0 Hz, CH_2 allyl *trans*-P), 71.7 (CH_2, allyl *trans*-C), 120.7 (CH, central allyl), 121.9 (CH, CH=CH Im), 123.6 (CH, 3-Pyr), 124.5 (CH, 5-Pyr), 125.1 (CH, CH=CH Im), 137.4 (CH, 4-Pyr), 149.7 (C, 2-Pyr), 155.5 (CH, 6-Pyr), 178.9 (d, C, J_{CP} = 19.6 Hz, NHC).

$^{31}P\{^1H\}$ NMR (CD_2Cl_2, T = 233 K) δ : 23.4.

Less abundant isomer (ca. 39%):

^1H NMR (CD_2Cl_2, T=233 K, ppm, selected peaks) δ : 1.37 (s, 3H, *o*-aryl-CH_3), 1.90 (s, 3H, *o*-aryl-CH_3), 2.15 (d,1H, J_{HH} = 13.4 Hz *anti* allyl-H *trans*-C), 2.22 (dd, J_{HH} = 13.4 Hz, J_{HP} = 10.9 Hz, 1H, *anti* allyl-H *trans*-P), 2.32 (s, 3H, *p*-aryl-CH_3), 3.69 (d, 1H, J_{HH} = 7.3 Hz, *syn* allyl-H *trans*-C), 3.94 (dd, J_{HH} = 7.3 Hz, J_{HP} = 7.3 Hz, 1H, *syn* allyl-H *trans*-P), 4.59, 4.80 (AB system, J = 15.5 Hz, 2H, NCH_2), 4.92 (m, CH, central allyl), 7.76 (td, J = 7.7, 1.6 Hz, 4- Pyr), 8.55 (d, J = 4.5 Hz, 1H, 6- Pyr).

$^{13}C\{^1H\}$ NMR (CD_2Cl_2, T=233 K, ppm selected peaks) δ : 18.1 (CH_3, *o*-mesityl-CH_3), 18.1 (*o*-mesityl-CH_3), 20.4 (CH_3, *anti* allyl-CH_3), 21.1 (CH_3, *p*-mesityl-CH_3), 56.0 (CH_2, NCH_2), 68.0 (CH_2, allyl *trans*-C), 69.4 (d, CH_2, J_{CP} = 29.3 Hz, CH_2 allyl *trans*-P), 120.5 (CH, central allyl), 122.0 (CH,

CH=CH Im), 123.8 (CH, 3-Pyr), 124.1 (CH, 5-Pyr), 125.4 (CH, CH=CH Im), 137.7 (CH, 4-Pyr), 149.5 (C, 2-Pyr), 155.7 (CH, 6-Pyr), 178.9 (d, C, J_{CP} = 19.6 Hz, NHC).

$^{31}P\{^{1}H\}$ NMR (CD_2Cl_2, T = 233 K) δ : 24.0.

Synthesis of the complex 66

Complex **66** was prepared in analogues manner as that described for **65** starting from 0.0640 g of the complex **55** and 0.0373 g of PPh_3.

0.0947 g (yield 96%) of **66** was obtained.

Most abundant isomer (ca. 57%):

^{1}H NMR (CD_2Cl_2, T=233 K, ppm, selected peaks) δ : 2.93 (d,1H, J_{HH} = 13.6 Hz *anti* allyl-H *trans*-C), 3.06 (dd, J_{HH} = 13.6 Hz, J_{HP} = 9.7 Hz, 1H, *anti* allyl-H *trans*-P),3.27 (s,3H, NCH_3), 3.77 (dd, J_{HH} = 8,1 Hz, J_{HP} = 8.1 Hz, 1H, *syn* allyl-H *trans*-P), 4.05 (d, 1H, J_{HH} = 8.1 Hz, *syn* allyl-H *trans*-C), 4.32, (d, J = 14.1 Hz, 1H, NCH_2), 4.79, (d, J = 14.1 Hz, 1H, NCH_2), 5.46 (m, CH, central allyl), 6.96, 7.01 (AB system, J = 1.9 Hz, 2H, CH=CH Im).

$^{13}C\{^{1}H\}$ NMR (CD_2Cl_2, T=233 K, ppm selected peaks) δ : 38.0 (CH_3, NCH_3), 55.3 (CH_2, NCH_2), 67.1 (d, CH_2, J_{CP} = 29.1 Hz, CH_2 allyl *trans*-P), 68.6 (CH_2, allyl *trans*-C), 121.2 (d, J_{CP} = 4.9 Hz, CH, central allyl), 122.2 (CH, CH=CH Im), 124.1 (CH, CH=CH Im), 176.3 (d, C, J_{CP} = 18.8 Hz, NHC).

$^{31}P\{^{1}H\}$ NMR (CD_2Cl_2, T = 233 K) δ : 26.3.

Less abundant isomer (ca. 43%):

^{1}H NMR (CD_2Cl_2, T=233 K, ppm, selected peaks) δ : 2.57 (dd, J_{HH} = 13.6 Hz, J_{HP} = 10.7 Hz, 1H, *anti* allyl-H *trans*-P), 2.93 (d,1H, J_{HH} = 13.6 Hz *anti* allyl-H *trans*-C), 3.14 (s,3H, NCH_3), 4.02 (d, 1H, J_{HH} = 8.1 Hz, *syn* allyl-H *trans*-C), 4.18 (dd, J_{HH} = 8,1 Hz, J_{HP} = 8.1 Hz, 1H, *syn* allyl-H *trans*-P), 4.47, (d, J = 14.2 Hz, 1H, NCH_2), 4.86, (d, J = 14.2 Hz, 1H, NCH_2), 5.64 (m, CH, central allyl), 6.99, 7.00 (AB system, J = 1.9 Hz, 2H, CH=CH Im).

$^{13}C\{^{1}H\}$ NMR (CD_2Cl_2, T=233 K, ppm selected peaks) δ : 38.1 (CH_3, N-CH_3), 55.1 (CH_2, NCH_2), 67.0 (d, CH_2, J_{CP} = 29.6 Hz, CH_2 allyl *trans*-P), 68.1 (CH_2, allyl *trans*-C), 121.1 (d, J_{CP} = 5.0 Hz, CH, central allyl), 122.2 (CH, CH=CH Im), 124.3 (CH, CH=CH Im), 176.4 (d, C, J_{CP} = 17.3 Hz, NHC).

$^{31}P\{1H\}$ NMR (CD_2Cl_2, T = 233 K) δ : 26.0.

Synthesis of the complex 67

Complex **67** was prepared in analogues manner as that described for **65** starting from 0.0640 g of the complex **54** and 0.0302 g of PPh_3.

0.0765 g (yield 85%) of **67** was obtained.

Most abundant isomer (ca. 75%):

^{1}H NMR (CD_2Cl_2, T=233 K, ppm, selected peaks) δ : 1.42 (s, 3H, *o*-aryl-CH_3), 1.71 (s, 3H, *o*-aryl-CH_3), 1.84 (dd, J_{HH} = 13.3 Hz, J_{HP} = 10.1 Hz, 1H, *anti* allyl-H *trans*-P), 2.28 (s, 3H, *p*-aryl-CH_3), 2.76 (d,1H, J_{HH} = 13.3 Hz *anti* allyl-H *trans*-C), 3.16 (dd, J_{HH} = 7.2 Hz, J_{HP} = 7.2 Hz, 1H, *syn* allyl-H *trans*-P), 3.34 (d, J = 13.6 Hz, 1H, NCH_2), 3.45 (d, 1H, J_{HH} = 7.2 Hz, *syn* allyl-H *trans*-C), 4.67 (d, J = 13.6 Hz, 1H, NCH_2), 5.00 (m, CH, central allyl), 6.78 (d, J = 1.9 Hz, 1H, CH=CH Im), 6.92 (d, J = 1.9 Hz, 1H, CH=CH Im).

^{13}C{^{1}H} NMR (CD_2Cl_2, T=233 K, ppm selected peaks) δ : 17.8 (CH_3, *o*-mesityl-CH_3), 18.3 (*o*-mesityl-CH_3), 21.1 (CH_3, *p*-mesityl-CH_3), 56.1 (CH_2, NCH_2), 67.0 (d, CH_2, J_{CP} = 29.5 Hz, CH_2 allyl *trans*-P), 71.3 (CH_2, allyl *trans*-C), 120.4 (d, CH, J_{CP} = 4.8 Hz, central allyl), 121.9 (CH, CH=CH Im), 126.3 (CH, CH=CH Im), 177.4 (d, C, J_{CP} = 17.2 Hz, NHC).

^{31}P{^{1}H} NMR (CD_2Cl_2, T = 233 K) δ : 24.5.

Less abundant isomer (ca. 25%):

^{1}H NMR (CD_2Cl_2, T=233 K, ppm, selected peaks) δ : 1.42 (s, 3H, *o*-aryl-CH_3), 1.80 (s, 3H, *o*-aryl-CH_3), 1.94 (dd, J_{HH} = 13.8 Hz, J_{HP} = 9.6 Hz, 1H, *anti* allyl-H *trans*-P), 2.09 (d,1H, J_{HH} = 13.8 Hz *anti* allyl-H *trans*-C), 2.30 (s, 3H, *p*-aryl-CH_3), 3.55 (dd, J_{HH} = 6.7 Hz, J_{HP} = 6.7 Hz, 1H, *syn* allyl-H *trans*-P), 3.69 (d, J = 13.9 Hz, 1H, NCH_2), 3.80 (d, 1H, J_{HH} = 6.7 Hz, *syn* allyl-H *trans*-C), 4.74 (m, CH, central allyl), 4.94 (d, J = 13.9 Hz, 1H, NCH_2), 6.73 (d, J = 1.9 Hz, 1H, CH=CH Im), 6.97 (d, J = 1.9 Hz, 1H, CH=CH Im).

^{13}C{^{1}H} NMR (CD_2Cl_2, T=233 K, ppm selected peaks) δ : 17.9 (CH_3, *o*-mesityl-CH_3), 18.4 (*o*-mesityl-CH_3), 21.1 (CH_3, *p*-mesityl-CH_3), 56.4 (CH_2, NCH_2), 67.8 (CH_2, allyl *trans*-C), 69.6 (d, CH_2, J_{CP} = 28.7 Hz, CH_2 allyl *trans*-P), 120.6 (d, CH, J_{CP} = 4.6 Hz, central allyl), 122.0 (CH, CH=CH Im), 126.3 (CH, CH=CH Im), 177.4 (d, C, J_{CP} = 17.2 Hz, NHC).

^{31}P{^{1}H} NMR (CD_2Cl_2, T = 233 K) δ : 25.3.

Synthesis of the complex 68

Complex **68** was prepared in analogues manner as that described for **65** starting from 0.0858 g of the complex **53** and 0.0455 g of PPh_3.

0.1270 g (yield 97%) of **68** was obtained.

Most abundant isomer (ca. 67%):

^1H NMR (CD_2Cl_2, T=233 K, ppm, selected peaks) δ : 1.51 (s, 3H, *o*-aryl-CH_3), 1.94 (s, 6H, *o*-aryl-CH_3), 1.94. (s, 3H, SCH_3), 2.33 (s, 3H, *p*-aryl-CH_3), 2.38 (dd, J_{HH} = 13.4 Hz, J_{HP} = 9.5 Hz, 1H, *anti* allyl-H *trans*-P), 2.94 (d,1H, J_{HH} = 13.4 Hz, *anti* allyl-H *trans*-C), 3.43 (d, J = 13.8 Hz, 1H, NCH_2), 3.54 (d, 1H, J_{HH} = 6.9 Hz, *syn* allyl-H *trans*-C), 4.25 (dd, J_{HH} = 6.9 Hz, J_{HP} = 6.9 Hz, 1H, *syn* allyl-H *trans*-P), 4.32 (d, J = 13.8 Hz, 1H, NCH_2), 5.54 (m, CH, central allyl), 6.83 (d, J = 1.9 Hz, 1H, CH=CH Im), 7.00 (d, J = 1.9 Hz, 1H, CH=CH Im).

$^{13}C\{^1H\}$ NMR (CD_2Cl_2, T=233 K, ppm selected peaks) δ : 14.2 (CH_3, SCH_3), 17.8 (CH_3, *o*-mesityl-CH_3), 18.1 (*o*-mesityl-CH_3), 21.1 (CH_3, *p*-mesityl-CH_3), 53.2 (CH_2, NCH_2), 67.7 (d, CH_2, J_{CP} = 30.1 Hz, CH_2 allyl *trans*-P), 71.8 (CH_2, allyl *trans*-C), 120.7 (d, CH, J_{CP} = 4.7 Hz, central allyl), 122.6 (CH, CH=CH Im), 126.0 (CH, CH=CH Im), 178.0 (d, C, J_{CP} = 17.5 Hz, NHC).

$^{31}P\{1H\}$ NMR (CD_2Cl_2, T = 233 K) δ : 24.3

Less abundant isomer (ca. 33%):

^1H NMR (CD_2Cl_2, T=233 K, ppm, selected peaks) δ : 1.43 (s, 3H, *o*-aryl-CH_3), 1.94 (s, 3H, SCH_3), 2.00 (s, 3H, *o*-aryl-CH_3), 2.33 (s, 3H, *p*-aryl-CH_3) 2.36 (d,1H, J_{HH} = 13.4 Hz, *anti* allyl-H *trans*-C), 3.04 (dd, J_{HH} = 13.4 Hz, J_{HP} = 9.5 Hz, 1H, *anti* allyl-H *trans*-P), 4.03 (d, 1H, J_{HH} = 6.9 Hz, *syn* allyl-H *trans*-C), 4.12 (dd, J_{HH} = 6.9 Hz, J_{HP} = 6.9 Hz, 1H, *syn* allyl-H *trans*-P), 3.71 (d, J = 13.8 Hz, 1H, NCH_2), 4.45 (d, J = 13.8 Hz, 1H, NCH_2), 4.93 (m, CH, central allyl), 6.77 (d, J = 1.9 Hz, 1H, CH=CH Im), 7.03 (d, J = 1.9 Hz, 1H, CH=CH Im).

$^{13}C\{^1H\}$ NMR (CD_2Cl_2, T=233 K, ppm selected peaks) δ : 14.2 (CH_3, SCH_3), 18.1 (CH_3, *o*-mesityl-CH_3), 18.3 (*o*-mesityl-CH_3), 21.1 (CH_3, *p*-mesityl-CH_3), 53.4 (CH_2, NCH_2), 67.5 (CH_2, allyl *trans*-C), 67.4 (d, CH_2, J_{CP} = 29.2 Hz, CH_2 allyl *trans*-P), 120.4 (d, CH, J_{CP} = 4.6 Hz, central allyl), 122.8 (CH, CH=CH Im), 125.9 (CH, CH=CH Im), 178.6 (d, C, J_{CP} = 17.5 Hz, NHC).

$^{31}P\{1H\}$ NMR (CD_2Cl_2, T = 233 K) δ : 24.8.

Synthesis of the complex 69a

0.0365 g (0.0525 mmol) of the allyl complex **56a** and 0.0138 g (0.0525 mmol) of PPh_3 were dissolved in ca. 25 ml of anhydrous CH_2Cl_2 and stirred at RT for ca. 30 min in a 50 mL two necked flask under inert atmosphere (Ar).

The resulting mixture was treated with 0.0155 g (0.127 mmol) of $NaClO_4 \cdot H_2O$ dissolved in ca. 4 ml of methanol (CH_2Cl_2/MeOH≈ 3/1). and further stirred for ca. 20 min, dried under vacuum and treated with CH_2Cl_2 and activated carbon. The inorganic salts were filtered off on a Celite filter and repeatedly washed with CH_2Cl_2, whereas the resulting solution was concentrated under vacuum. Addition of diethylether to the concentrated solution yields the precipitation of the complex **69a** as a white solid which was filtered off on a gooch and washed with *n*-pentane.

0.0423 g of **69a** was obtained (yield 83%).

2 *Exo* isomers (α Anomer + β Anomer) (73%)

^{1}H-NMR (300 MHz, CD_2Cl_2, T = 298 K, ppm) δ: 0.79-0.89 (m, 6H, $2CH_3^{4'}$), 1.05-1.49 (m, 8H, $2CH_2^{3'}$+$2CH_2^{2'}$), 1.89 (s, 3H, OCH_3), 1.94 (s, 3H, OCH_3), 1.98 (s, 3H, OCH_3), 2.01 (s, 3H, OCH_3), 2.02 (s, 3H, OCH_3), 2.03 (s, 3H, OCH_3), 2.05 (s, 3H, OCH_3), 2.07 (s, 3H, OCH_3),), 3.65 (d, 2H, J= 12.7 Hz, 2*anti* allyl-H *trans*-C), 3.01-3.42 (m, 4H, 2*anti* allyl-H *trans*-P+$2H^5$), 3.82 (d, 1H, J= 3.9 Hz, *syn* allyl-H *trans*-C), 3.86 (d, 1H, J= 3.9 Hz, *syn* allyl-H *trans*-C), 4.30-4.41 (m, 2H, 2*syn* allyl-H *trans*-P), 5.03-5.77 (m, 12H, $2CH_2^6$ + $2H^3$ + $2H^2$ + $2H^4$ + $2H^1$), 5.93 (m, 2H, 2*central* allyl-H), 6.93 (d, 1H, J= 2.1 Hz, H^{Im}), 6.98 (d, 1H, J= 2.1 Hz, H^{Im}), 7.13-7.58 (m, 32H, 6Ph+$2H^{Im}$).

^{31}P{^{1}H}-NMR (CD_2Cl_2, T = 298 K, ppm) δ: 25.6, 25.5.

^{13}C{^{1}H}-NMR ($CDCl_3$, T = 298 K, ppm selected peaks) δ: 13.6 (CH_3, $CH_3^{4'}$), 13.7 (CH_3, $CH_3^{4'}$), 19.5 (CH_2, $CH_2^{3'}$), 19.6 (CH_2, $CH_2^{3'}$), 20.4-20.7 (CH_3, OCH_3), 31.4 (CH_2, $CH_2^{2'}$), 31.5 (CH_2, $CH_2^{2'}$), 50.5 (CH_2, $CH_2^{1'}$), 51.0 (CH_2, $CH_2^{1'}$), 60.4 (CH_2, CH_2^6), 60.7 (CH_2, CH_2^6), 67.2 (CH, CH^4), 67.3 (CH, CH^4), 68.3 (d, CH_2, $J_{C\text{-}P}$ = 29.6 Hz, allyl *trans*-P), 68.4 (d, CH_2, $J_{C\text{-}P}$ = 27.7 Hz, allyl *trans*-P), 69.3 (CH_2, allyl *trans*-C), 69.7 (CH_2, allyl *trans*-C), 86.4 (CH, CH^1), 86.5 (CH, CH^1), 119.3 (CH, CH^{Im}), 119.4 (CH, CH^{Im}), 122.0 (d, CH, $J_{C\text{-}P}$ = 5.3 Hz, *central* allyl), 122.4 (d, CH, $J_{C\text{-}P}$ = 4.8 Hz, *central* allyl), 123.0 (CH, CH^{Im}), 123.2 (CH, CH^{Im}), 129.2-133.4 (Ph), 169.1 (C, C=O), 169.2 (C, C=O), 169.4 (C, C=O), 169.5 (C, C=O), 169.6 (C, C=O), 169.7 (C, C=O), 170.1 (C, C=O), 170.2 (C, C=O), 179.7 (d, $J_{C\text{-}P}$ = 19.1 Hz, C, carbene), 179.9 (d, $J_{C\text{-}P}$= 15.1 Hz, C, carbene).

2 *Endo* isomers (α Anomer + β Anomer) (27%)

^{1}H-NMR (300 MHz, CD_2Cl_2, T = 298 K, ppm) δ: 0.79-0.89 (m, 6H, $2CH_3^{4'}$), 1.05-1.49 (m, 8H, $2CH_2^{3'}$+$2CH_2^{2'}$), 1.43 (s, 3H, OCH_3), 1.45 (s, 3H, OCH_3), 1.94 (s, 3H, OCH_3), 1.98 (s, 3H, OCH_3), 2.00 (s, 3H, OCH_3), 2.10 (s, 3H, OCH_3), 2.11 (s, 3H, OCH_3), 2.12 (s, 3H, OCH_3), 2.84 (d, 2H, J= 12.7 Hz, 2*anti* allyl-H *trans*-C), 3.01-3.42 (m, 4H, 2*anti* allyl-H *trans*-P+$2H^5$), 3.65 (d, 1H, J= 3.9

Hz, *syn* allyl-H *trans*-C), 3.73 (d, 1H, J= 3.9 Hz, *syn* allyl-H *trans*-C), 4.12-4.16 (m, 2H, 2*syn* allyl-H *trans*-P), 5.03-5.77 (m, 12H, $2CH_2^6$+ $2H^3$+ $2H^2$ +$2H^4$+ $2H^1$), 5.93 (m, 2H, 2*central* allyl-H), 7.03 (d, 1H, J= 2.1 Hz, H^{Im}), 7.08 (d, 1H, J= 2.1 Hz, H^{Im}), 7.13-7.58 (m, 32H, 6Ph+$2H^{Im}$).

$^{31}P\{^1H\}$-NMR (CD_2Cl_2, T = 298 K, ppm) δ: 25.2, 25.4.

$^{13}C\{^1H\}$-NMR ($CDCl_3$, T = 298 K, ppm selected peaks) δ: 13.5 (CH_3, $CH_3^{4'}$), 13.6 (CH_3, $CH_3^{4'}$), 19.6 (CH_2, $CH_2^{3'}$), 19.7 (CH_2, $CH_2^{3'}$), 20.1-20.9 (CH_3, OCH_3), 31.6 (CH_2, $CH_2^{2'}$), 31.7 (CH_2, $CH_2^{2'}$), 51.0 (CH_2, $CH_2^{1'}$), 51.1 (CH_2, $CH_2^{1'}$), 62.2 (CH_2, CH_2^6), 62.4 (CH_2, CH_2^6), 67.6 (CH, CH^4), 67.8 (CH, CH^4), 68.3 (d, CH_2, J_{C-P} = 29.6 Hz, allyl *trans*-P), 68.4 (d, CH_2, J_{C-P} = 27.7 Hz, allyl *trans*-P), 68.8 (CH_2, allyl *trans*-C), 69.0 (CH_2, allyl *trans*-C), 86.0 (CH, CH^1), 86.1 (CH, CH^1), 119.9 (CH, CH^{Im}), 119.9 (CH, CH^{Im}), 121.7 (d, CH, J_{C-P} = 5.8 Hz, *central* allyl), 122.6 (CH, CH^{Im}), 122.8 (CH, CH^{Im}), 129.2-133.4 (Ph), 169.2 (C, C=O), 169.2 (C, C=O), 169.3 (C, C=O), 169.3 (C, C=O), 169.9 (C, C=O), 170.0 (C, C=O), 170.3 (C, C=O), 170.4 (C, C=O), 180.1 (d, J_{C-P} = 18.0 Hz, C, carbene), 181.1 (d, J_{C-P} = 19.2 Hz, C, carbene).

IR(KBr): $\nu_{C=O}$ = 1754 cm^{-1}, ν_{C-O} = 1231 cm^{-1}.

Synthesis of the complex 69b

Complex **69b** was prepared in analogues manner as that described for **69a** starting from 0.0442 g of **56b**, 0.0196 g of PPh_3 and 0.0236 g of $NaClO_4$.

0.0519 g (yield 85%) of **69b** was obtained.

2 *Exo* isomers (α Anomer + β Anomer) (67%)

^1H-NMR (300 MHz, $CDCl_3$, T = 298 K, ppm) δ: 1.95 (s, 3H, OCH_3), 1.98 (s, 3H, OCH_3), 2.00 (s, 3H, OCH_3), 2.02 (s, 3H, OCH_3), 2.03 (s, 3H, OCH_3), 2.04 (s, 3H, OCH_3), 2.05 (s, 3H, OCH_3), 2.06 (s, 3H, OCH_3), 3.05 (s, 3H, NCH_3), 3.31 (s, 3H, NCH_3), 3.17 (d, 2H, J= 12.7 Hz, 2*anti* allyl-H *trans*-C), 3.39 (m, 2H, 2*anti* allyl-H *trans*-P), 3.59-3.92 (m, 4H, 2*syn* allyl-H *trans*-C+$2H^5$), 4.01-4.58 (m, 2H, 2*syn* allyl-H *trans*-P), 4.01-4.58 (m, 2H, 2*syn* allyl-H *trans*-P), 5.04-5.54 (m, 10H, $2CH_2^6$+$2H^3$+$2H^2$+$2H^4$), 5.74 (d, 2H, J= 8.6 Hz, H^1), 5.92 (m, 2H, 2*central* allyl-H), 6.82 (d, 1H, J= 2.1 Hz, H^{Im}), 6.85 (d, 1H, J= 2.1 Hz, H^{Im}), 7.20-7.53 (m, 32H, 6Ph+$2H^{Im}$).

$^{31}P\{^1H\}$-NMR ($CDCl_3$, T = 298 K, ppm) δ: 26.0, 25.6.

$^{13}C\{^1H\}$-NMR ($CDCl_3$, T = 298 K, ppm selected peaks) δ: 20.0 (CH_3, OCH_3), 20.4 (CH_3, OCH_3), 20.5 (CH_3, OCH_3), 20.7 (CH_3, OCH_3), 20.7 (CH_3, OCH_3), 20.8 (CH_3, OCH_3), 20.8 (CH_3, OCH_3), 20.9 (CH_3, OCH_3), 37.6 (CH_3, NCH_3), 38.0 (CH_3, NCH_3), 69.7 (d, CH_2, J_{C-P} = 38.8 Hz, allyl *trans*-P), 60.2 (CH_2, CH_2^6), 60.5 (CH_2, CH_2^6), 74.1 (CH_2, allyl *trans*-C), 86.5 (CH, CH^1), 86.6 (CH, CH^1), 118.9 (CH, CH^{Im}), 119.0 (CH, CH^{Im}), 122.2 (CH, *central* allyl), 124.9 (CH, CH^{Im}), 125.0 (CH, CH^{Im}), 129.2-133.4 (Ph), 169.1 (C, C=O), 169.2 (C, C=O), 169.4 (C, C=O), 169.5 (C, C=O), 169.8 (C, C=O),

169.9 (C, C=O), 170.1 (C, C=O), 170.2 (C, C=O), 180.4 (d, J_{C-P}= 19.5 Hz, C, carbene), 181.0 (d, J_{C-P}= 19.5 Hz, C, carbene).

2 *Endo* isomers (α Anomer + β Anomer) (33%)

^{1}H-NMR (300 MHz, $CDCl_3$, T = 298 K, ppm) δ: 1.98 (s, 3H, OCH_3), 1.99 (s, 3H, OCH_3), 2.07 (s, 3H, OCH_3), 2.09 (s, 3H, OCH_3), 2.10 (s, 3H, OCH_3), 2.11 (s, 3H, OCH_3), 2.12 (s, 3H, OCH_3), 2.19 (s, 3H, OCH_3), 2.95 (d, 2H, J= 12.7 Hz, 2*anti* allyl-H *trans*-C), 2.99 (s, 3H, NCH_3), 3.23 (s, 3H, NCH_3), 3.39 (m, 2H, 2*anti* allyl-H *trans*-P), 3.59-3.92 (m, 4H, 2*syn* allyl-H *trans*-C+2H^{5}), 4.01-4.58 (m, 2H, 2*syn* allyl-H *trans*-P), 5.04-5.54 (m, 10H, 2CH_2^{6}+2H^{3}+2H^{2}+2H^{4}), 5.76 (d, 2H, J= 8.6 Hz, H^{1}), 5.92 (m, 2H, 2*central* allyl-H), 6.95 (d, 1H, J= 2.1 Hz, H^{Im}), 6.98 (d, 1H, J= 2.1 Hz, H^{Im}), 7.20-7.53 (m, 32H, 6Ph+2H^{Im}).

^{31}P{^{1}H}-NMR ($CDCl_3$, T = 298 K, ppm) δ: 25.4, 25.1.

^{13}C{^{1}H}-NMR ($CDCl_3$, T = 298 K, ppm selected peaks) δ: 20.4 (CH_3, OCH_3), 20.5 (CH_3, OCH_3), 20.6 (CH_3, OCH_3), 20.7 (CH_3, OCH_3), 37.5 (CH_3, NCH_3), 37.8 (CH_3, NCH_3), 60.2 (CH_2, CH_2^{6}), 60.5 (CH_2, CH_2^{6}), 73.0 (CH, CH^{3}), 69.3 (d, CH_2, J_{C-P} = 27.4 Hz, allyl *trans*-P), 74.2 (CH_2, allyl *trans*-C), 86.0 (CH, CH^{1}), 86.2 (CH, CH^{1}), 121.8 (CH, CH^{Im}), 121.9 (CH, CH^{Im}), 122.1 (CH, *central* allyl), 122.6 (CH, CH^{Im}), 122.7 (CH, CH^{Im}), 129.2-133.4 (Ph), 169.0 (C, C=O), 169.3 (C, C=O), 169.4 (C, C=O), 169.7 (C, C=O), 169.8 (C, C=O), 169.9 (C, C=O), 170.3 (C, C=O), 170.4 (C, C=O), 180.2 (d, J_{C-P}= 19.5 Hz, C, carbene), 181.1 (d, J_{C-P}= 19.5 Hz, C, carbene).

IR(KBr): $\nu_{C=O}$ = 1752 cm^{-1}, ν_{C-O} = 1231 cm^{-1}.

Synthesis of the complex 69c

Complex **69c** was prepared in analogues manner as that described for **69a** starting from 0.0369 g of **56c**, 0.0143 g of PPh_3 and 0.0150 g of $NaClO_4$.

0.0488 g (yield 88%) of **69c** was obtained.

2 *Exo* isomers (α Anomer + β Anomer) (55%)

^{1}H-NMR (300 MHz, $CDCl_3$, T = 298 K, ppm selected peaks) δ: 1.28 (s, 3H, *p*-CH_3^{Mes}), 1.76 (s, 3H, OCH_3), 1.90 (s, 6H, 2 *o*-CH_3^{Mes}), 2.03 (s, 3H, OCH_3), 2.07 (s, 3H, OCH_3), 2.37 (s, 3H, OCH_3), 2.84 (d, 2H, J= 12.7 Hz, 2*anti* allyl-H *trans*-C), 3.32 (d, 2H, J= 7.4 Hz, 2*syn* allyl-H *trans*-C), 3.60 (m, 2H, 2*anti* allyl-H *trans*-P), 4.40 (m, 2H, 2 *syn* allyl-H *trans*-P), 5.11 (m, 2H, 2*central* allyl-H), 6.62-7.62 (m, 34H, 6Ph+4H^{Im}).

^{31}P{^{1}H}-NMR ($CDCl_3$, T = 298 K, ppm) δ: 23.0, 22.3.

^{13}C{^{1}H}-NMR ($CDCl_3$, T = 298 K, ppm selected peaks) δ: 16.6-17.6 (CH_3, CH_3^{Mes}), 20.5-21.1 (CH_3, OCH_3), 71.5 (d, CH_2, J_{C-P} = 28.4 Hz, allyl *trans*-P), 74.2 (CH_2, allyl *trans*-C), 86.4 (CH, CH^{1}), 119.7 (CH, CH^{Im}), 120.0 (CH, CH^{Im}), 122.8 (d, CH, J_{C-P} = 3.2 Hz, *central* allyl), 126.4 (CH, CH^{Im}), 126.6 (CH, CH^{Im}), 128.9-140.2 (Ph), 169.3-170.4 (C, C=O), 181.8 (d, J_{C-P}= 14.7 Hz, C, carbene).

2 *Endo* isomers (α Anomer + β Anomer) (45%)

^{1}H-NMR (300 MHz, $CDCl_3$, T = 298 K, ppm selected peaks) δ: 1.09 (s, 3H, *p*-CH_3^{Mes}), 1.77 (s, 3H, OCH_3), 1.90 (s, 6H, 2 *o*-CH_3^{Mes}), 2.06 (s, 3H, OCH_3), 2.09 (s, 3H, OCH_3), 2.34 (s, 3H, OCH_3), 2.84 (d, 2H, J= 12.7 Hz, 2*anti* allyl-H *trans*-C), 3.32 (d, 2H, J= 7.4 Hz, 2*syn* allyl-H *trans*-C), 3.60 (m, 2H, 2*anti* allyl-H *trans*-P), 4.32 (m, 2H, 2 *syn* allyl-H *trans*-P), 6.06 (m, 2H, 2*central* allyl-H), 6.62-7.62 (m, 34H, 6Ph+4H^{Im}).

^{31}P{^{1}H}-NMR ($CDCl_3$, T = 298 K, ppm) δ: 21.8, 21.8.

^{13}C{^{1}H}-NMR ($CDCl_3$, T = 298 K, ppm selected peaks) δ: 16.6-17.6 (CH_3, CH_3^{Mes}), 20.5-21.1 (CH_3, OCH_3), 71.5 (d, CH_2, J_{C-P} = 28.4 Hz, allyl *trans*-P), 74.1 (CH_2, allyl *trans*-C), 86.5 (CH, CH^{1}), 119.7 (CH, CH^{Im}), 120.0 (CH, CH^{Im}), 120.8 (d, CH, J_{C-P} = 5.3 Hz, *central* allyl), 126.4 (CH, CH^{Im}), 126.6 (CH, CH^{Im}), 128.9-140.2 (Ph), 169.3-170.4 (C, C=O), 181.8 (d, J_{C-P}= 14.7 Hz, C, carbene).

IR(KBr): $\nu_{C=O}$ = 1752 cm^{-1}, ν_{C-O} = 1230 cm^{-1}.

Synthesis of the complex 70

0.0394 g (0.137 mmol) of the imidazolium salt **32a** was dissolved in 15 mL of anhydrous CH_3CN in a 50 mL two-necked flask and 0.0174 g (0.075 mmol) of Ag_2O was added under inert atmosphere (Ar). The mixture was stirred for 7 h at R.T. in the dark. The resulting mixture was treated with 0.0358 g (0.137 mmol) of PPh_3 and 0.0250 g (0.068 mmol) of the precursor $[Pd(\mu\text{-}Cl)(\eta^3\text{-}C_3H_5)]_2$ and further stirred at R.T. for 1h. The precipitated AgCl was removed by filtration on a millipore membrane filter. The solution was dried under vacuum and the residue treated with 1 mL of CH_2Cl_2.

Addition of diethylether/*n*-hexane (1:1) to the concentrated solution yields the precipitation of the complex **70** as a white solid which was filtered off on a gooch, washed with *n*-pentane and dried under vacuum.

0.0702 g of **70** was obtained (yield 74%).

Most abundant isomer (ca. 52%):

^{1}H NMR ($CDCl_3$, T=298 K, ppm, selected peaks) δ : 3.38 (d, J = 13.4 Hz, 1H, *anti* allyl-H *trans*-C), 3.63 (s, CH_3, NCH_3), 3.86 (dd, J = 13.3, 9.6 Hz, 1H, *anti* allyl-H *trans*-P), 4.16 (d, J= 7.8 Hz, 1H, *syn* allyl-H *trans*-C), 4.54 (dd, J = 6.4, 6.4 Hz, 1H, *syn* allyl-H *trans*-P), 5.61 (m, 1H, *central*-allyl-H), 7.20-7.51 (m, 19H, ArH).

^{13}C{1H} NMR ($CDCl_3$, T=298 K, ppm selected peaks) δ : 36.6 (CH_3, NCH_3), 69.3 (d, CH_2, J_{CP} = 2.3 Hz, CH_2 allyl *trans*-C), 70.6 (d, CH_2, J_{CP} = 26.6 Hz, allyl *trans*-P), 111.6-134.8 (Ar-C), 125.4 (d, CH, J_{CP} = 4.9 Hz, central allyl), 192.9 (m, C, carbene).

^{31}P{1H} NMR ($CDCl_3$, T = 298 K) δ: 26.6

^{19}F{1H} NMR ($CDCl_3$, T = 298 K) δ: -54.6 (CF_3), -152.7 ($^{10}BF_4$), -152.8 ($^{11}BF_4$).

Less abundant isomer (ca. 48%):

^{1}H NMR ($CDCl_3$, T=298 K, ppm, selected peaks) δ : 3.04 (d, J = 13.2 Hz, 1H, *anti* allyl-H *trans*-C), 3.14 (dd, J = 13.2, 9.5 Hz, 1H, *anti* allyl-H *trans*-P), 3.79 (s, CH_3, NCH_3), 4.11 (d, J= 7.0 Hz, 1H, *syn* allyl-H *trans*-C), 4.85 (dd, J = 6.2, 6.2 Hz, 1H, *syn* allyl-H *trans*-P), 6.19 (m, 1H, *central*-allyl-H), 7.20-7.51 (m, 19H, ArH).

^{13}C{1H} NMR ($CDCl_3$, T=298 K, ppm selected peaks) δ : 36.7 (CH_3, NCH_3), 68.9 (d, CH_2, J_{CP} = 2.3 Hz, CH_2 allyl *trans*-C), 70.0 (d, CH_2, J_{CP} = 27.7 Hz, allyl *trans*-P), 111.6-134.8 (Ar-C), 121.3 (d, CH, J_{CP} = 5.2 Hz, central allyl), 192.2 (m, C, carbene).

^{31}P{1H} NMR ($CDCl_3$, T = 298 K) δ: 25.1 (q, J_{P-F} =3.1 Hz)

^{19}F{1H} NMR ($CDCl_3$, T = 298 K) δ: -55.2 (d, J_{F-P} =3.1 Hz, CF_3), -152.7 ($^{10}BF_4$), -152.8 ($^{11}BF_4$).

IR [neat]: 2980, 1437, 1366, 1093, 1051, 748, 698 cm^{-1}.

Anal. Calc. for $C_{30}H_{27}BF_7N_2PPd$: C, 51.72; H, 3.91; N, 4.02. Found: C, 51.84; H, 4.01; N, 3.76%.

Synthesis of the complex 71

Complex **71** was prepared in analogues manner as that described for **70** starting from 0.0414 g of **32a**, 0.0199 g of Ag_2O, 0.0377 g of PPh_3 and 0.0283 g of the precursor $[Pd(\mu\text{-}Cl)(\eta^3\text{-}2\text{-}MeC_3H_4)]_2$. 0.0715 g (yield 70%) of **71** was obtained (pale-yellow solid).

Most abundant isomer (ca. 60%):

^{1}H NMR ($CDCl_3$, T=298 K, ppm, selected peaks) δ : 2.02 (s, 3H, allyl-CH_3), 3.29 (s, 1H, *anti* allyl-H *trans*-C), 3.66 (d, J = 21.3 Hz, 1H, *anti* allyl-H *trans*-P), 3.82 (s, 3H, NCH_3), 3.89 (s, 1H, *syn* allyl-H *trans*-C), 4.32 (bs, 1H, *syn* allyl-H *trans*-P), 7.20-7.54 (m, 19H, ArH).

^{13}C{1H} NMR ($CDCl_3$, T=298 K, ppm selected peaks) δ : 23.4 (CH_3, allyl-CH_3), 36.8 (CH_3, NCH_3), 68.9 (CH_2, allyl *trans*-C), 69.3 (d, CH_2, J_{CP} = 28.3 Hz, CH_2 allyl *trans*-P), 111.2-134.6 (Ar-C), 136.5 (d, C, J_{CP} = 5.0 Hz, central allyl), 193.2 (m, C, carbene).

^{31}P{1H} NMR ($CDCl_3$, T = 298 K) δ: 27.4 (q, J_{P-F}=1.0 Hz)

^{19}F{1H} NMR ($CDCl_3$, T = 298 K) δ: -54.4 (d, J_{F-P}=1.0 Hz, CF_3), -152.8 ($^{10}BF_4$), -152.9 ($^{11}BF_4$).

Less abundant isomer (ca. 40%):

^{1}H NMR ($CDCl_3$, T=298 K, ppm, selected peaks) δ : 2.18 (s, 3H, allyl-CH_3), 3.04 (s, 1H, *anti* allyl-H *trans*-C), 3.05 (d, J = 12.3 Hz, 1H, *anti* allyl-H *trans*-P), 3.68 (s, 3H, NCH_3), 3.80 (s, 1H, *syn* allyl-H *trans*-C), 4.55 (bs, H, *syn* allyl-H *trans*-P), 7.20-7.54 (m, 19H, ArH).

^{13}C{1H} NMR ($CDCl_3$, T=298 K, ppm selected peaks) δ : 23.9 (CH_3, allyl-CH_3), 37.0 (CH_3, NCH_3), 68.2 (d, CH_2, J_{CP} = 26.9 Hz, CH_2 allyl *trans*-P), 68.4 (CH_2, allyl *trans*-C), 111.2-134.6 (Ar-C), 137.5 (d, C, J_{CP} = 5.0 Hz, central allyl), 193.0 (m, C, carbene).

^{31}P{1H} NMR ($CDCl_3$, T = 298 K) δ: 26.8 (q, J_{P-F}=2.4 Hz)

$^{19}F\{1H\}$ NMR ($CDCl_3$, T = 298 K) δ: -54.9 (d, J_{F-P}=2.4 Hz, CF_3), -152.8 ($^{10}BF_4$), -152.9 ($^{11}BF_4$).

IR [neat]: 2977, 1436, 1369, 1093, 1047, 742, 706 cm^{-1}.

Anal. Calc. for $C_{31}H_{29}BF_7N_2PPd$: C, 52.38; H, 4.11; N, 3.94. Found: C, 52.20; H, 4.02; N, 3.80%.

Synthesis of the complex 72

Complex **72** was prepared in analogues manner as that described for **70** starting from 0.0321 g of **32b**, 0.0129 g of Ag_2O, 0.0266 g of PPh_3 and 0.0186 g of the precursor $[Pd(\mu\text{-}Cl)(\eta^3\text{-}C_3H_5)]_2$.

0.0634 g (yield 86%) of **72** was obtained (white solid).

Most abundant isomer (ca. 60%):

^1H NMR ($CDCl_3$, T=298 K, ppm, selected peaks) δ : 1.14 (d, J= 7.0 Hz, 3H, $CH_3^{i\text{-}Pr}$), 1.73 (d, J= 7.0 Hz, 3H, $CH_3^{i\text{-}Pr}$), 3.69 (d, J = 13.4 Hz, 1H, *anti* allyl-H *trans*-C), 3.75 (dd, J = 13.4, 9.7 Hz, 1H, *anti* allyl-H *trans*-P), 3.97 (d, J= 7.3 Hz, 1H, *syn* allyl-H *trans*-C), 4.50 (dd, J = 6.5, 6.5 Hz, 1H, *syn* allyl-H *trans*-P), 5.48 (hept, J= 7.0 Hz, 1H, $\underline{CH}(CH_3)_2$), 5.64 (m, 1H, *central*-allyl-H), 7.15-7.71 (m, 19H, ArH).

$^{13}C\{1H\}$ NMR ($CDCl_3$, T=298 K, ppm selected peaks) δ : 19.4 (CH_3, $CH_3^{i\text{-}Pr}$), 19.4 (CH_3, $CH_3^{i\text{-}Pr}$), 58.7 (CH, $\underline{CH}(CH_3)_2$), 69.0 (d, CH_2, J_{CP} = 13.3 Hz, CH_2 allyl *trans*-P), 71.7 (d, CH_2, J_{CP} = 1.5 Hz, allyl *trans*-C), 112.5-133.3 (Ar-C), 119.0 (apt d, C, J_{CP} = 265.7 Hz, NCF_3), 121.1 (d, CH, J_{CP} = 5.4 Hz, central allyl), 190.5 (m, C, carbene).

$^{31}P\{1H\}$ NMR ($CDCl_3$, T = 298 K) δ: 24.4 (q, J_{P-F}=3.2 Hz)

$^{19}F\{1H\}$ NMR ($CDCl_3$, T = 298 K) δ: -55.1 (d, J_{F-P}=3.2 Hz, CF_3), -153.0 ($^{10}BF_4$), -153.1 ($^{11}BF_4$).

Less abundant isomer (ca. 40%):

^1H NMR ($CDCl_3$, T=298 K, ppm, selected peaks) δ : 1.09 (d, J= 7.0 Hz, 3H, $CH_3^{i\text{-}Pr}$), 1.68 (d, J= 7.0 Hz, 3H, $CH_3^{i\text{-}Pr}$), 2.91 (d, J = 13.2 Hz, 1H, *anti* allyl-H *trans*-C), 3.15 (dd, J = 13.4, 9.5 Hz, 1H, *anti* allyl-H *trans*-P), 4.11 (d, J= 7.3 Hz, 1H, *syn* allyl-H *trans*-C), 4.68 (dd, J = 6.2, 6.2 Hz, 1H, *syn* allyl-H *trans*-P), 5.13 (hept, J= 7.0 Hz, 1H, $\underline{CH}(CH_3)_2$), 6.31 (m, 1H, *central*-allyl-H), 7.15-7.71 (m, 19H, ArH).

$^{13}C\{1H\}$ NMR ($CDCl_3$, T=298 K, ppm selected peaks) δ : 21.0 (CH_3, $CH_3^{i\text{-}Pr}$), 21.4 (CH_3, $CH_3^{i\text{-}Pr}$), 58.3 (CH, $\underline{CH}(CH_3)_2$), 68.7 (d, CH_2, J_{CP} = 13.9 Hz, CH_2 allyl *trans*-P), 69.6 (d, CH_2, J_{CP} = 1.8 Hz, allyl *trans*-C), 112.5-133.3 (Ar-C), 119.1 (apt d, C, J_{CP} = 265.8 Hz, NCF_3), 123.4 (d, CH, J_{CP} = 5.3 Hz, central allyl), 191.5 (m, C, carbene).

$^{31}P\{1H\}$ NMR ($CDCl_3$, T = 298 K) δ: 24.2 (q, J_{P-F}=5.0 Hz)

$^{19}F\{1H\}$ NMR ($CDCl_3$, T = 298 K) δ: -55.6 (d, J_{F-P}=5.0 Hz, CF_3), -153.0 ($^{10}BF_4$), -153.1 ($^{11}BF_4$).

IR [neat]: 2972, 1434, 1356, 1100, 1056, 748, 694, 526 cm^{-1}.

Anal. Calc. for $C_{32}H_{31}BF_7N_2PPd$: C, 53.03; H, 4.31; N, 3.87. Found: C, 53.15; H, 4.22; N, 3.97%.

Synthesis of the complex 73

Complex **73** was prepared in analogues manner as that described for **70** starting from 0.0400 g of **32b**, 0.0162 g of Ag_2O, 0.0332 g of PPh_3 and 0.0249 g of the precursor $[Pd(\mu\text{-}Cl)(\eta^3\text{-}2\text{-}MeC_3H_4)]_2$. 0.0765 g (yield 82%) of **73** was obtained (brownish solid).

Most abundant isomer (ca. 65%):

^{1}H NMR ($CDCl_3$, T=298 K, ppm, selected peaks) δ : 1.15 (d, J= 6.9 Hz, 3H, $CH_3^{i\text{-}Pr}$), 1.71 (d, J= 6.8 Hz, 3H, $CH_3^{i\text{-}Pr}$), 1.97 (s, 3H, allyl-CH_3), 3.61 (s, 1H, *anti* allyl-H *trans*-C), 3.66 (s, 1H, *syn* allyl-H *trans*-C), 3.22 (d, J = 9.5, 1H, *anti* allyl-H *trans*-P), 4.24 (dd, J = 3.9, 3.9 Hz, 1H, *syn* allyl-H *trans*-P), 5.50 (hept, J= 6.8 Hz, 1H, $\underline{CH}(CH_3)_2$), 7.13-7.74 (m, 19H, ArH).

^{13}C{1H} NMR ($CDCl_3$, T=298 K, ppm selected peaks) δ : 19.4 (CH_3, $CH_3^{i\text{-}Pr}$), 21.3 (CH_3, $CH_3^{i\text{-}Pr}$), 23.5 (CH_3, allyl-CH_3), 58.7 (CH, $\underline{CH}(CH_3)_2$), 67.6 (d, CH_2, J_{CP} = 28.1 Hz, CH_2 allyl *trans*-P), 71.2 (CH_2, allyl *trans*-C), 112.5-133.6 (Ar-C), 136.4 (d, C, J_{CP} = 5.1 Hz, central allyl), 191.6 (m, C, carbene).

^{31}P{1H} NMR ($CDCl_3$, T = 298 K) δ: 26.0 (q, $J_{P\text{-}F}$=3.8 Hz)

^{19}F{1H} NMR ($CDCl_3$, T = 298 K) δ: -55.0 (d, $J_{F\text{-}P}$=3.8 Hz, CF_3), -153.2 ($^{10}BF_4$), -153.3 ($^{11}BF_4$).

Less abundant isomer (ca. 35%):

^{1}H NMR ($CDCl_3$, T=298 K, ppm, selected peaks) δ : 1.08 (d, J= 7.0 Hz, 3H, $CH_3^{i\text{-}Pr}$), 1.68 (d, J= 7.1 Hz, 3H, $CH_3^{i\text{-}Pr}$), 2.15 (s, 3H, allyl-CH_3), 2.99 (s, 1H, *anti* allyl-H *trans*-C), 3.07 (d, J = 9.6, 1H, *anti* allyl-H *trans*-P), 3.73 (s, 1H, *syn* allyl-H *trans*-C), 4.37 (dd, J = 4.0, 4.0 Hz, 1H, *syn* allyl-H *trans*-P), 4.98 (hept, J= 7.2 Hz, 1H, $\underline{CH}(CH_3)_2$), 7.13-7.74 (m, 19H, ArH).

^{13}C{1H} NMR ($CDCl_3$, T=298 K, ppm selected peaks) δ : 19.3 (CH_3, $CH_3^{i\text{-}Pr}$), 20.9 (CH_3, $CH_3^{i\text{-}Pr}$), 23.8 (CH_3, allyl-CH_3), 58.5 (CH, $\underline{CH}(CH_3)_2$), 67.9 (d, CH_2, J_{CP} = 25.7 Hz, CH_2 allyl *trans*-P), 68.9 (CH_2, allyl *trans*-C), 112.5-133.6 (Ar-C), 137.4 (d, C, J_{CP} = 5.0 Hz, central allyl), 191.8 (m, C, carbene).

^{31}P{1H} NMR ($CDCl_3$, T = 298 K) δ: 25.6 (q, $J_{P\text{-}F}$=4.5 Hz)

^{19}F{1H} NMR ($CDCl_3$, T = 298 K) δ: -55.3 (d, $J_{F\text{-}P}$=4.5 Hz, CF_3), -153.2 ($^{10}BF_4$), -153.3 ($^{11}BF_4$).

IR [neat]: 2986, 1436, 1099, 1055, 744, 696, 524 cm^{-1}.

Anal. Calc. for $C_{33}H_{33}BF_7N_2PPd$: C, 53.65; H, 4.50; N, 3.79. Found: C, 53.80; H, 4.32; N, 3.94%.

Synthesis of the complex 74

Complex **74** was prepared in analogues manner as that described for **70** starting from 0.0404 g of **32c**, 0.0154 g of Ag_2O, 0.0303 g of PPh_3 and 0.0211 g of the precursor $[Pd(\mu\text{-}Cl)(\eta^3\text{-}C_3H_5)]_2$.

0.0801 g (yield 91%) of **74** was obtained (white solid).

Most abundant isomer (ca. 58%):

^1H NMR ($CDCl_3$, T=298 K, ppm, selected peaks) δ : 3.00 (d, J = 13.1 Hz, 1H, *anti* allyl-H *trans*-C), 3.48 (m, 1H, *anti* allyl-H *trans*-P), 3.61 (d, J= 7.2 Hz, 1H, *syn* allyl-H *trans*-C), 5.10 (dd, J = 6.7, 6.7 Hz, 1H, *syn* allyl-H *trans*-P), 5.70 (m, 1H, *central*-allyl-H), 6.77-7.74 (m, 24H, ArH).

$^{13}C\{1H\}$ NMR ($CDCl_3$, T=298 K, ppm selected peaks) δ : 68.4 (d, CH_2, J_{CP} = 1.8 Hz, CH_2 allyl *trans*-C), 72.3 (d, CH_2, J_{CP} = 27.1 Hz, allyl *trans*-P), 112.2-135.9 (Ar-C), 126.4 (d, CH, J_{CP} = 5.8 Hz, central allyl), 192.8 (m, C, carbene).

$^{31}P\{1H\}$ NMR ($CDCl_3$, T = 298 K) δ: 24.4 (q, $J_{P\text{-}F}$ =2.5 Hz)

$^{19}F\{1H\}$ NMR ($CDCl_3$, T = 298 K) δ: -55.2 (d, $J_{F\text{-}P}$ =2.5 Hz, CF_3), -153.8 ($^{10}BF_4$), -153.9 ($^{11}BF_4$).

Less abundant isomer (ca. 42%):

^1H NMR ($CDCl_3$, T=298 K, ppm, selected peaks) δ : 2.55 (d, J = 13.4 Hz, 1H, *anti* allyl-H *trans*-C), 3.37 (m, 1H, *anti* allyl-H *trans*-P), 4.04 (d, J= 7.2 Hz, 1H, *syn* allyl-H *trans*-C), 4.86 (dd, J = 7.0, 7.0 Hz, 1H, *syn* allyl-H *trans*-P), 5.70 (m, 1H, *central*-allyl-H), 6.77-7.74 (m, 24H, ArH).

$^{13}C\{1H\}$ NMR ($CDCl_3$, T=298 K, ppm selected peaks) δ : 69.1 (d, CH_2, J_{CP} = 2.1 Hz, CH_2 allyl *trans*-C), 71.8 (d, CH_2, J_{CP} = 27.4 Hz, allyl *trans*-P), 112.2-135.9 (Ar-C), 126.2 (d, CH, J_{CP} = 5.5 Hz, central allyl), 192.6 (m, C, carbene).

$^{31}P\{1H\}$ NMR ($CDCl_3$, T = 298 K) δ: 24.8

$^{19}F\{1H\}$ NMR ($CDCl_3$, T = 298 K) δ: -54.5, -153.8 ($^{10}BF_4$), -153.9 ($^{11}BF_4$).

IR [neat]: 2970, 1436, 1362, 1095, 1048, 754, 711, 528 cm^{-1}.

Anal. Calc. for $C_{35}H_{29}BF_7N_2PPd$: C, 55.40; H, 3.85; N, 3.69. Found: C, 55.25; H, 4.02; N, 3.77%.

Synthesis of the complex 75

Complex **75** was prepared in analogues manner as that described for **70** starting from 0.0443 g of **32c**, 0.0169 g of Ag_2O, 0.0332 g of PPh_3 and 0.0249 g of the precursor $[Pd(\mu\text{-}Cl)(\eta^3\text{-}2\text{-}MeC_3H_4)]_2$.

0.0821 g (yield 84%) of **75** was obtained (white solid).

Most abundant isomer (ca. 65%):

^1H NMR ($CDCl_3$, T=298 K, ppm, selected peaks) δ : 1.66 (s, 3H, allyl-CH_3), 2.94 (s, 1H, *anti* allyl-H *trans*-C), 3.20 (d, J = 9.6 Hz, 1H, *anti* allyl-H *trans*-P), 3.37 (s, 1H, *syn* allyl-H *trans*-C), 4.65 (bs, 1H, *syn* allyl-H *trans*-P), 6.80-7.74 (m, 19H, ArH).

$^{13}C\{1H\}$ NMR ($CDCl_3$, T=298 K, ppm selected peaks) δ : 23.0 (CH_3, allyl-CH_3), 68.7 (CH_2, allyl *trans*-C), 70.1 (d, CH_2, J_{CP} = 28.5 Hz, CH_2 allyl *trans*-P), 112.2-136.0 (Ar-C), 137.6 (d, C, J_{CP} = 5.0 Hz, central allyl), 193.3 (m, C, carbene).

$^{31}P\{1H\}$ NMR ($CDCl_3$, T = 298 K) δ: 25.3 (q, J_{P-F}=3.1 Hz)

$^{19}F\{1H\}$ NMR ($CDCl_3$, T = 298 K) δ: -54.9 (d, J_{F-P}=3.1 Hz, CF_3), -153.9 ($^{10}BF_4$), -154.0 ($^{11}BF_4$).

Less abundant isomer (ca. 35%):

^{1}H NMR ($CDCl_3$, T=298 K, ppm, selected peaks) δ : 2.04 (s, 3H, allyl-CH_3), 2.47 (s, 1H, *anti* allyl-H *trans*-C), 3.28 (d, J = 9.6 Hz, 1H, *anti* allyl-H *trans*-P), 3.72 (s, 1H, *syn* allyl-H *trans*-C), 4.61 (bs, 1H, *syn* allyl-H *trans*-P), 6.80-7.74 (m, 19H, ArH).

$^{13}C\{1H\}$ NMR ($CDCl_3$, T=298 K, ppm selected peaks) δ : 23.1 (CH_3, allyl-CH_3), 68.7 (CH_2, allyl *trans*-C), 68.7 (d, CH_2, J_{CP} = 28.7 Hz, CH_2 allyl *trans*-P), 112.2-136.0 (Ar-C), 136.6 (d, C, J_{CP} = 5.0 Hz, central allyl), 193.1 (m, C, carbene).

$^{31}P\{1H\}$ NMR ($CDCl_3$, T = 298 K) δ: 26.6 (q, J_{P-F}=2.0 Hz)

$^{19}F\{1H\}$ NMR ($CDCl_3$, T = 298 K) δ: -54.3 (d, J_{F-P}=2.0 Hz, CF_3), -153.9 ($^{10}BF_4$), -154.0 ($^{11}BF_4$).

IR [neat]: 2973, 1436, 1364, 1098, 1056, 757, 698, 528 cm^{-1}.

Anal. Calc. for $C_{36}H_{31}BF_7N_2PPd$: C, 55.95; H, 4.04; N, 3.62. Found: C, 55.83; H, 4.14; N, 3.79%.

9.7.20. Synthesis of mixed NHC/PTA palladium η^3-allyl complexes (76-84)

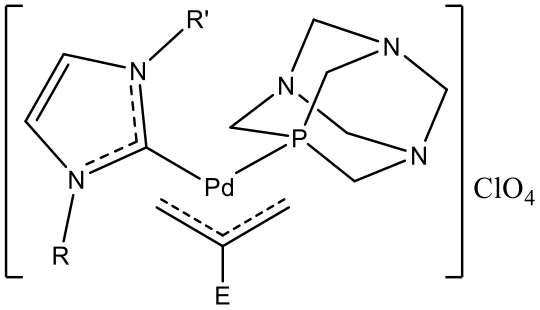

R= Mes	R'= Mes	E= H	**76**
R= Mes	R'= Mes	E= CH_3	**77**
R= CH_3	R'= CH_2Py	E= H	**78**

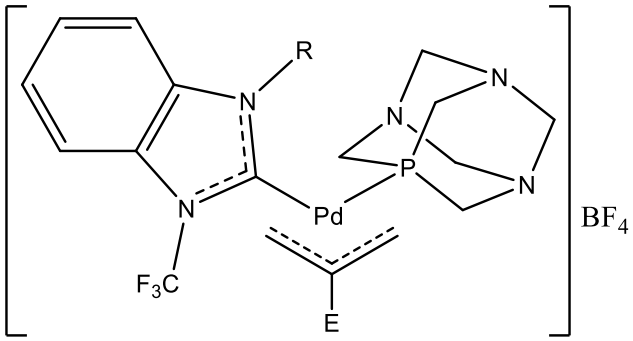

R= CH_3	E= H	**79**
R= CH_3	E= CH_3	**80**
R= i-Pr	E= H	**81**
R= i-Pr	E=CH_3	**82**
R= Ph	E= H	**83**
R= Ph	E=CH_3	**84**

Synthesis of the complex 76

0.0508 g (0.104 mmol) of the complex **57** was dissolved in ca. 6 mL of anhydrous CH_2Cl_2 and 0.0164 g (0.104 mmol) of PTA dissolved in ca. 6 ml of CH_2Cl_2 was added and the mixture was stirred at RT for ca. 10 min in a 50 mL two necked flask under inert atmosphere (Ar).

The resulting mixture was treated with 0.0282 g (0.208 mmol) of $NaClO_4 \cdot H_2O$ dissolved in ca. 4 ml of methanol (CH_2Cl_2/MeOH≈ 2/1). and further stirred for ca. 10 min, dried under vacuum and treated with CH_2Cl_2 and activated carbon. The inorganic salts were filtered off on a Celite filter and repeatedly washed with CH_2Cl_2, whereas the resulting solution was concentrated under vacuum. Addition of diethylether to the concentrated solution yields the precipitation of the complex **76** as a white solid which was filtered off on a gooch and washed with *n*-pentane. 0.0558 g of **76** was obtained (yield 75%).

^{1}H NMR (CD_2Cl_2, T=298 K, ppm) δ : 2.13 (s, 3H, *o*-mesityl -CH_3), 2.18 (dd, J_{HH} = 14.0 Hz, J_{HP} = 9.4 Hz, 1H, *anti* allyl-H *trans*-P), 2.17 (s, 3H, *o*-mesityl -CH_3), 2.37 (d,1H, J_{HH} = 14.0 Hz *anti* allyl-H *trans*-C), 2.40 (s, 3H, *p*-mesityl -CH_3), 3.64 (m, 1H, allyl-H *trans*-C), 3.76 (m, 6H, NCH_2N), 4.12 (m, 1H, *anti* allyl-H *trans*-P), 4.44 (m, 6H, PCH_2N), 7.11 (s, 2H, *m*-mesityl -H), 7.14 (s, 2H, *m*-mesityl-H), 7.39 (s, 2H, CH=CH Im).

^{13}C{^{1}H} NMR (CD_2Cl_2, T=298 K, ppm) δ : 18.6 (CH_3, *o*-mesityl-CH_3), 18.8 (CH_3, *o*-mesityl-CH_3), 20.7 (CH_3, *p*-mesityl-CH_3), 52.5 (d, CH_2, J_{CP} = 11.4 Hz, NCH_2N), 60.4 (CH_2, allyl *trans*-C), 70.9 (d, CH_2, J_{CP} = 27.5 Hz, allyl *trans*-P), 72.9 (d, CH_2, J_{CP} = 7.4 Hz, PCH_2N), 120.7 (d, CH, J_{CP} = 4.5 Hz, central allyl), 124.8. (CH, CH=CH Im), 129.8 (CH, *m*-mesityl), 130.0 (CH, *m*-mesityl), 134.2 (C, *o*-

mesityl), 134.7 (C, *o*-mesityl), 135.3 (C, *i*-mesityl), 140.1 (C, *p*-mesityl), 178.3 (d, C, J_{CP} = 16.4 Hz, NHC).

$^{31}P\{^{1}H\}$ NMR ($CDCl_3$, T = 298 K) δ : -59.7.

Synthesis of the complex 77

Complex **77** was prepared in analogues manner as that described for **76** starting from 0.0504 g of **58**, 0.0158 g of PTA and 0.0282 g of $NaClO_4 \cdot H_2O$.

0.0536 g (yield 75%) of **77** was obtained (white solid).

^{1}H NMR (CD_2Cl_2, T=298 K, ppm) δ : 1.25 (s, 3H, allyl-CH_3), 2.16 (s, 3H, *o*-mesityl -CH_3), 2.22 (s, 3H, *o*-mesityl -CH_3), 2.30 (d,1H, J_{HP} = 1.2 Hz *anti* allyl-H *trans*-C), 2.31 (d, J_{HP} = 9.7 Hz, 1H, *anti* allyl-H *trans*-P), 2.40 (s, 3H, *p*-mesityl -CH_3), 3.64 (ddt, 1H, J_{HP} = 3.2 Hz, J_{HH} = 3.2 Hz, J_{HH} = 1.2 Hz, *syn* allyl-H *trans*-C), 3.76 (m, 6H, NCH_2N), 3.85 (dd, 1H, J_{HP} = 5.1 Hz, J_{HH} = 3.2 Hz, *anti* allyl-H *trans*-P), 4.45 (m, 6H, PCH_2N), 7.13 (s, 2H, *m*-mesityl -H), 7.16 (s, 2H, *m*-mesityl-H), 7.37 (s, 2H, CH=CH Im).

$^{13}C\{^{1}H\}$ NMR (CD_2Cl_2, T=298 K, ppm) δ : 18.7 (CH_3, *o*-mesityl-CH_3), 20.7 (CH_3, *p*-mesityl-CH_3), 22.5 (CH_3, allyl-CH_3), 52.8 (CH_2, NCH_2N), 60.4 (CH_2, allyl *trans*-C), 70.9 (d, CH_2, J_{CP} = 29.2 Hz, allyl *trans*-P), 72.9 (d, CH_2, J_{CP} = 7.1 Hz, PCH_2N), 124.8. (CH, CH=CH Im), 129.9 (CH, *m*-mesityl), 130.0 (CH, *m*-mesityl), 134.3 (C, *o*-mesityl), 134.6 (C, *i*-mesityl), 135.5 (C, *o*-mesityl), 136.0 (d, C, J_{CP} = 4.5 Hz, central allyl), 140.1 (C, *p*-mesityl), 178.7 (d, C, J_{CP} = 15.7 Hz, NHC).

$^{31}P\{^{1}H\}$ NMR ($CDCl_3$, T = 298 K) δ: -59.5.

Synthesis of the complex 78

0.0714 g (0.170 mmol) of the complex [Pd(Me-Im-CH_2Pyr)(η^3-C_3H_5)]ClO_4, previously synthetized in analogues manner as that described for **50,** was dissolved in ca. 20 mL of anhydrous CH_2Cl_2.

The resulting mixture was treated with 0.0267 g (0.170 mmol) of PTA dissolved and further stirred for ca. 30 min.

Addition of diethylether to the concentrated solution yields the precipitation of the complex **78** as a white solid which was filtered off on a gooch and washed with *n*-pentane.

0.0952 g of **78** was obtained (yield 97%).

<u>Most abundant isomer (ca. 52%):</u>

^{1}H NMR (CD_2Cl_2, T=233 K, ppm, selected peaks) δ: 2.91 (dd, J_{HH} = 13.9 Hz, J_{HP} = 9.8 Hz, 1H, *anti* allyl-H *trans*-P), 2.64 (d,1H, J_{HH} = 13.9 Hz *anti* allyl-H *trans*-C), 3.71 (s, 3H, NCH_3), 3.9-4.17 (m, 8H, *syn* allyl-H *trans*-P, *syn* allyl-H *trans*-C, NCH_2N), 4.46- 4.58 (m, 6H, PCH_2N), 5.01, 5.10 (AB system, J = 15.4 Hz, 2H, NCH_2), 7.16-7.34 (m, 4H, CH=CH Im, 3-pyr, 5-pyr), 7.78 (td J = 7.7, 1.8 Hz, 1H, 4-pyr), 8. 57 (d, J = 4.8 Hz, 1H, 6- Pyr).

$^{31}P\{1H\}$ NMR ($CDCl_3$, T = 233 K) δ: -55.8.

Less abundant isomer (ca. 48%):

^{1}H NMR (CD_2Cl_2, T=233 K, ppm, selected peaks) δ: 2.58 (dd, J_{HH} = 13.9 Hz, J_{HP} = 9.8 Hz, 1H, *anti* allyl-H *trans*-P), 2.69 (d,1H, J_{HH} = 13.9 Hz *anti* allyl-H *trans*-C), 3.55 (s, 3H, NCH_3), 3.9-4.17 (m, 8H, *syn* allyl-H *trans*-P, *syn* allyl-H *trans*-C, NCH_2N), 4.46- 4.58 (m, 6H, PCH_2N), 5.21, 5.30 (AB system, J = 15.8 Hz, 2H, NCH_2), 7.16-7.34 (m, 4H, CH=CH Im, 3-pyr, 5-pyr), 7.79 (td J = 7.7, 1.8 Hz, 1H, 4-pyr), 8. 57 (d, J = 4.8 Hz, 1H, 6- Pyr).

$^{31}P\{1H\}$ NMR ($CDCl_3$, T = 233 K) δ: -55.9.

IR (KBr pellet, cm-1): 1095 (stretching ClO), 621 (bending ClO)

Synthesis of the complex 79

0.0432 g (0.150 mmol) of the imidazolium salt **32a** was dissolved in 20 mL of anhydrous CH_3CN in a 50 mL two-necked flask and 0.0191 g (0.082 mmol) of Ag_2O was added under inert atmosphere (Ar). The mixture was stirred for 7 h at R.T. in the dark.

The resulting mixture was treated with 0.0236 g (0.150 mmol) of PTA (1,3,5-triaza-7-phosphadamantane) and 0.0274 g (0.075 mmol) of the precursor $[Pd(\mu\text{-}Cl)(\eta^3\text{-}C_3H_5)]_2$ and further stirred at R.T. for 1h. The precipitated AgCl was removed by filtration on a millipore membrane filter. The solution was dried under vacuum and the residue treated with 1 mL of CH_2Cl_2.

Addition of diethylether to the concentrated solution yields the precipitation of the complex **79** as a brownish solid which was filtered off on a gooch, washed with *n*-pentane and dried under vacuum. 0.0785 g of **79** was obtained (yield 88%).

Equimolar mixture of the two isomers

^{1}H NMR (CD_3CN, T=298 K, ppm, selected peaks) δ : 2.85-3.27 (m, 4H, 2 *anti* allyl-H *trans*-C, 2 *anti* allyl-H *trans*-P), 3.84 (s, 3H, NCH_3), 4.03 (s, 3H, NCH_3), 4.22-4.69 (m, 28H, 2 *syn* allyl-H *trans*-C, 2 *syn* allyl-H *trans*-P, 6 NCH_2N, 6 NCH_2P), 5.45 (m, 2H, 2 *central*-allyl-H), 7.51-7.82 (m, 8H, ArH).

$^{13}C\{1H\}$ NMR (CD_3CN, T=298 K, ppm selected peaks) δ : 37.2 (CH_3, NCH_3), 37.5 (CH_3, NCH_3), 52.7 (d, CH_2, J= 12.6 Hz, NCH_2P), 52.7 (d, CH_2, J= 12.6 Hz, NCH_2P), 62.5 (CH_2, allyl *trans*-C), 62.6 (CH_2, allyl *trans*-C), 71.3 (d, CH_2, J_{CP} = 26.5 Hz, CH_2 allyl *trans*-P), 71.9 (d, CH_2, J_{CP} = 26.7 Hz, CH_2 allyl *trans*-P), 73.3 (d, CH_2, J= 7.0 Hz, NCH_2N), 73.3 (d, CH_2, J= 7.0 Hz, NCH_2N), 122.5 (d, C, J_{CP} = 4.9 Hz, central allyl), 122.5 (d, C, J_{CP} = 4.9 Hz, central allyl), 191.4 (m, C, carbene). 191.6 (m, C, carbene).

$^{31}P\{1H\}$ NMR (CD_3CN, T = 298 K) δ: -57.2, -57.2

$^{19}F\{1H\}$ NMR (CD_3CN, T = 298 K) δ: -55.8 (CF_3), -56.2 (CF_3), -151.8 ($^{10}BF_4$), -151.9 ($^{11}BF_4$).

IR [neat]: 2940.5, 1354.0, 1031.1, 1013.3, 968.9, 754.6, 582.8 cm^{-1}.

Anal. Calc. for $C_{18}H_{24}BF_7N_5PPd$: C, 36.54; H, 4.09; N, 11.84. Found: C, 36.73; H, 4.18; N, 11.61%.

Synthesis of the complex 80

Complex **80** was prepared in analogues manner as that described for **79** starting from 0.0401 g of **32a**, 0.0194 g of Ag_2O, 0.0219 g of PTA (1,3,5-triaza-7-phosphadamantane) and 0.0275 g of the precursor $[Pd(\mu\text{-}Cl)(\eta^3\text{-}2\text{-}MeC_3H_4)]_2$.

0.0791 g (yield 94%) of **80** was obtained (white solid).

Equimolar mixture of the two isomers

^1H NMR (CD_3CN, T=298 K, ppm, selected peaks) δ : 1.80 (s, 3H, allyl-CH_3), 1.86 (s, 3H, allyl-CH_3), 2.72-3.06 (m, 4H, 2 *anti* allyl-H *trans*-C, 2 *anti* allyl-H *trans*-P), 3.82 (s, 3H, NCH_3), 3.89 (s, 3H, NCH_3), 4.08-4.67 (m, 28H, 2 *syn* allyl-H *trans*-C, 2 *syn* allyl-H *trans*-P, 6 NCH_2N, 6 NCH_2P), 7.52-7.79 (m, 8H, ArH).

$^{13}C\{1H\}$ NMR (CD_3CN, T=298 K, ppm selected peaks) δ : 23.6 (CH_3, allyl-CH_3), 24.1 (CH_3, allyl-CH_3), 37.5 (CH_3, NCH_3), 37.6 (CH_3, NCH_3), 52.8 (d, CH_2, J= 12.7 Hz, NCH_2P), 52.8 (d, CH_2, J= 12.7 Hz, NCH_2P), 61.9 (CH_2, allyl *trans*-C), 62.1 (CH_2, allyl *trans*-C), 70.1 (d, CH_2, J_{CP} = 26.5 Hz, CH_2 allyl *trans*-P), 71.0 (d, CH_2, J_{CP} = 27.2 Hz, CH_2 allyl *trans*-P), 73.4 (d, CH_2, J= 8.7 Hz, NCH_2N), 73.4 (d, CH_2, J= 8.7 Hz, NCH_2N), 137.2 (d, C, J_{CP} = 5.0 Hz, central allyl), 137.4 (d, C, J_{CP} = 4.8 Hz, central allyl), 191.6 (m, C, carbene), 191.7 (m, C, carbene).

$^{31}P\{1H\}$ NMR (CD_3CN, T = 298 K) δ: -56.8 (q, $J_{P\text{-}F}$ = 4.1 Hz), -56.9 (q, $J_{P\text{-}F}$ = 4.4 Hz),

$^{19}F\{1H\}$ NMR (CD_3CN, T = 298 K) δ: -55.5 (d, $J_{F\text{-}P}$ = 3.0 Hz, CF_3), -56.1 (d, $J_{F\text{-}P}$ = 3.4 Hz, CF_3), -151.7 ($^{10}BF_4$), -151.8 ($^{11}BF_4$).

IR [neat]: 2926.3, 1666.2, 1354.7, 1049.6, 968.9, 752.9, 572.5 cm^{-1}.

Anal. Calc. for $C_{19}H_{26}BF_7N_5PPd$: C, 37.68; H, 4.33; N, 11.56. Found: C, 37.53; H, 4.28; N, 11.80%.

Synthesis of the complex 81

Complex **81** was prepared in analogues manner as that described for **79** starting from 0.0400 g of **32b**, 0.0161 g of Ag_2O, 0.0199 g of PTA (1,3,5-triaza-7-phosphadamantane) and 0.0231 g of the precursor $[Pd(\mu\text{-}Cl)(\eta^3\text{-}C_3H_5)]_2$. 0.0552 g (yield 71%) of **81** was obtained (brownish solid).

Equimolar mixture of the two isomers

^1H NMR (CD_3CN, T=298 K, ppm, selected peaks) δ : 1.57 (d, J= 7.0 Hz, 3H, $CH_3^{i\text{-}Pr}$), 1.64 (d, J= 7.0 Hz, 3H, $CH_3^{i\text{-}Pr}$), 1.71 (d, J= 7.0 Hz, 3H, $CH_3^{i\text{-}Pr}$), 1.83 (d, J= 7.0 Hz, 3H, $CH_3^{i\text{-}Pr}$), 2.86-3.12 (m, 4H, 2 *anti* allyl-H *trans*-C, 2 *anti* allyl-H *trans*-P), 4.25-4.70 (m, 28H, 2 *syn* allyl-H *trans*-C, 2 *syn* allyl-H *trans*-P, 6 NCH_2N, 6 NCH_2P), 4.84 (hept, J= 7.0 Hz, 1H, $\underline{CH}(CH_3)_2$), 5.08 (hept, J= 7.0 Hz, 1H, $\underline{CH}(CH_3)_2$), 5.46 (m, 1H, *central*-allyl-H), 5.48 (m, 1H, *central*-allyl-H), 7.55-7.97 (m, 8H, ArH).

$^{13}C\{1H\}$ NMR (CD_3CN, T=298 K, ppm selected peaks) δ : 21.0 (CH_3, $CH_3^{i\text{-}Pr}$), 21.2 (CH_3, $CH_3^{i\text{-}Pr}$), 52.9 (d, CH_2, J= 12.7 Hz, NCH_2P), 57.7 (CH, $\underline{CH}(CH_3)_2$), 58.3 (CH, $\underline{CH}(CH_3)_2$), 62.0 (CH_2, allyl *trans*-C), 62.6 (CH_2, allyl *trans*-C), 71.1 (d, CH_2, J_{CP} = 24.9 Hz, CH_2 allyl *trans*-P), 72.0 (d, CH_2, J_{CP}

= 25.7 Hz, CH_2 allyl *trans*-P), 73.3 (d, CH_2, J= 7.3 Hz, NCH_2N), 122.2 (d, CH, J_{CP} = 5.3 Hz, central allyl), 122.3 (d, CH, J_{CP} = 4.6 Hz, central allyl), 190.9 (m, C, carbene), 191.0 (m, C, carbene).

$^{31}P\{1H\}$ NMR (CD_3CN, T = 298 K) δ: -57.4 (m)

$^{19}F\{1H\}$ NMR (CD_3CN, T = 298 K) δ: -55.8 (d, J_{F-P}=5.0 Hz, CF_3), -56.3 (d, J_{F-P}=5.8 Hz, CF_3), -151.7 ($^{10}BF_4$), -151.8 ($^{11}BF_4$).

IR [neat]: 2933.8, 1665.1, 1354.4, 1048.7, 968.6, 752.0, 572.2 cm^{-1}.

Anal. Calc. for $C_{20}H_{28}BF_7N_5PPd$: C, 38.77; H, 4.55; N, 11.30. Found: C, 38.93; H, 4.38; N, 11.14%.

Synthesis of the complex 82

Complex **82** was prepared in analogues manner as that described for **79** starting from 0.0408 g of **32b**, 0.0165 g of Ag_2O, 0.0202 g of PTA (1,3,5-triaza-7-phosphadamantane) and 0.0254 g of the precursor $[Pd(\mu\text{-}Cl)(\eta^3\text{-}2\text{-}MeC_3H_4)]_2$.

0.0752 g (yield 92%) of **82** was obtained (pale-yellow solid).

Equimolar mixture of the two isomers

^1H NMR (CD_3CN, T=298 K, ppm, selected peaks) δ : 1.57 (d, J= 7.4 Hz, 3H, $CH_3^{i\text{-}Pr}$), 1.60 (d, J= 7.4 Hz, 3H, $CH_3^{i\text{-}Pr}$), 1.73 (d, J= 7.1 Hz, 3H, $CH_3^{i\text{-}Pr}$), 1.79 (d, J= 7.1 Hz, 3H, $CH_3^{i\text{-}Pr}$), 1.79 (s, 3H, allyl-CH_3), 1.85 (s, 3H, allyl-CH_3), 2.75-3.09 (m, 4H, 2 *anti* allyl-H *trans*-C, 2 *anti* allyl-H *trans*-P), 4.07-4.69 (m, 28H, 2 *syn* allyl-H *trans*-C, 2 *syn* allyl-H *trans*-P, 6 NCH_2N, 6 NCH_2P), 4.77 (hept, J= 7.1 Hz, 1H, $\underline{CH}(CH_3)_2$), 5.09 (hept, J= 7.4 Hz, 1H, $\underline{CH}(CH_3)_2$), 7.54-7.95 (m, 8H, ArH).

$^{13}C\{1H\}$ NMR (CD_3CN, T=298 K, ppm selected peaks) δ : 20.9 (CH_3, $CH_3^{i\text{-}Pr}$), 21.0 (CH_3, $CH_3^{i\text{-}Pr}$), 21.1 (CH_3, $CH_3^{i\text{-}Pr}$), 21.2 (CH_3, $CH_3^{i\text{-}Pr}$), 23.6 (CH_3, allyl-CH_3), 23.8 (CH_3, allyl-CH_3), 53.0 (d, CH_2, J= 12.7 Hz, NCH_2P), 53.0 (d, CH_2, J= 12.7 Hz, NCH_2P), 58.2 (CH, $\underline{CH}(CH_3)_2$), 58.4 (CH, $\underline{CH}(CH_3)_2$), 61.7 (CH_2, allyl *trans*-C), 62.1 (CH_2, allyl *trans*-C), 70.2 (d, CH_2, J_{CP} = 26.6 Hz, CH_2 allyl *trans*-P), 71.1 (d, CH_2, J_{CP} = 27.4 Hz, CH_2 allyl *trans*-P), 73.4 (d, CH_2, J= 7.1 Hz, NCH_2N), 73.4 (d, CH_2, J= 7.1 Hz, NCH_2N), 137.0 (d, C, J_{CP} = 4.7 Hz, central allyl), 137.3 (d, C, J_{CP} = 4.6 Hz, central allyl), 190.9 (m, C, carbene). 191.0 (m, C, carbene).

$^{31}P\{1H\}$ NMR (CD_3CN, T = 298 K) δ: -57.6 (q, J_{P-F} = 4.1 Hz), -57.7 (q, J_{P-F} = 4.4 Hz),

$^{19}F\{1H\}$ NMR (CD_3CN, T = 298 K) δ: -55.6 (d, J_{F-P} = 4.1 Hz, CF_3), -56.2 (d, J_{F-P} =4.4 Hz, CF_3), -151.7 ($^{10}BF_4$), -151.8 ($^{11}BF_4$).

IR [neat]: 2935.8, 1664.0, 1354.4, 1053.2, 971.9, 752.6, 572.3 cm^{-1}.

Anal. Calc. for $C_{21}H_{30}BF_7N_5PPd$: C, 39.80; H, 4.77; N, 11.05. Found: C, 39.91; H, 4.93; N, 10.89%.

Synthesis of the complex 83

Complex **83** was prepared in analogues manner as that described for **79** starting from 0.0404 g of **32c**, 0.0160 g of Ag_2O, 0.0181 g of PTA (1,3,5-triaza-7-phosphadamantane) and 0.0211 g of the precursor $[Pd(\mu\text{-}Cl)(\eta^3\text{-}C_3H_5)]_2$.

0.0542 g (yield 75%) of **83** was obtained (white solid).

Most abundant isomer (ca. 60%):

^1H NMR (CD_3CN, T=298 K, ppm, selected peaks) δ : 2.73 (d, J= 13.2 Hz, 1H, *anti* allyl-H *trans*-C), 3.12 (m, 1H, *anti* allyl-H *trans*-P), 3.81-4.71 (m, 14H, *syn* allyl-H *trans*-C, *syn* allyl-H *trans*-P, 3 NCH_2N, 3 NCH_2P), 5.21 (m, 2H, 2 *central*-allyl-H), 7.43-7.91 (m, 9H, ArH).

$^{13}C\{1H\}$ NMR (CD_3CN, T=298 K, ppm selected peaks) δ : 52.7 (d, CH_2, J= 12.4 Hz, NCH_2P), 61.4 (CH_2, CH_2 allyl *trans*-C), 73.1 (d, CH_2, J= 7.4 Hz, NCH_2N), 73.5 (CH_2, allyl *trans*-P), 122.3 (d, CH, J_{CP} = 5.0 Hz, central allyl), 192.0 (m, C, carbene).

$^{31}P\{1H\}$ NMR (CD_3CN, T = 298 K) δ: -57.2 (q, $J_{P\text{-}F}$= 2.9 Hz)

$^{19}F\{^1H\}$ NMR (CD_3CN, T = 298 K) δ: -56.4 (d, $J_{F\text{-}P}$= 2.9 Hz, CF_3), -151.9 ($^{10}BF_4$), -152.0 ($^{11}BF_4$).

Less abundant isomer (ca. 40%):

^1H NMR (CD_3CN, T=298 K, ppm, selected peaks) δ : 2.56 (d, J= 13.6 Hz, 1H, *anti* allyl-H *trans*-C), 2.93 (m, 1H, *anti* allyl-H *trans*-P), 3.81-4.71 (m, 14H, *syn* allyl-H *trans*-C, *syn* allyl-H *trans*-P, 3 NCH_2N, 3 NCH_2P), 5.40 (m, 2H, 2 *central*-allyl-H), 7.43-7.91 (m, 9H, ArH).

$^{13}C\{1H\}$ NMR (CD_3CN, T=298 K, ppm selected peaks) δ : 52.8 (d, CH_2, J= 11.4 Hz, NCH_2P), 61.8 (CH_2, CH_2 allyl *trans*-C), 73.8 (CH_2, allyl *trans*-P), 73.1 (d, CH_2, J= 7.4 Hz, NCH_2N), 122.1 (d, CH, J_{CP} = 4.8 Hz, central allyl), 192.3 (m, C, carbene).

$^{31}P\{1H\}$ NMR (CD_3CN, T = 298 K) δ: -57.4

$^{19}F\{^1H\}$ NMR (CD_3CN, T = 298 K) δ: -56.0 (CF_3), -151.9 ($^{10}BF_4$), -152.0 ($^{11}BF_4$).

IR [neat]: 2934.6, 1362.9, 1052.0, 1013.0, 970.3, 763.4, 573.2 cm^{-1}.

Anal. Calc. for $C_{23}H_{26}BF_7N_5PPd$: C, 42.26; H, 4.01; N, 10.71. Found: C, 42.35; H, 3.93; N, 10.59%.

Synthesis of the complex 84

Complex **84** was prepared in analogues manner as that described for **79** starting from 0.0185 g of **32c**, 0.0071 g of Ag_2O, 0.0083 g of PTA (1,3,5-triaza-7-phosphadamantane) and 0.0104 g of the precursor $[Pd(\mu\text{-}Cl)(\eta^3\text{-}2\text{-}MeC_3H_4)]_2$.

0.0282 g (yield 80%) of **84** was obtained (white solid).

Most abundant isomer (ca. 58%):

^{1}H NMR (CD_3CN, T=298 K, ppm, selected peaks) δ : 1.48 (s, 3H, allyl-CH_3), 2.59 (s, 1H, allyl-H *trans*-C), 2.96 (d, J= 8.8 Hz, 1H, allyl-H *trans*-P), 3.83-4.65 (m, 14H, *syn* allyl-H *trans*-C, *syn* allyl-H *trans*-P, 3 NCH_2N, 3 NCH_2P), 7.38-7.88 (m, 9H, ArH).

^{13}C{1H} NMR (CD_3CN, T=298 K, ppm selected peaks) δ : 23.3 (CH_3, allyl-CH_3), 52.9 (d, CH_2, J= 12.8 Hz, NCH_2P), 61.4 (CH_2, allyl *trans*-C), 72.0 (d, CH_2, J_{CP} = 25.9 Hz, CH_2 allyl *trans*-P), 73.2 (d, CH_2, J= 7.5 Hz, NCH_2N), 137.3 (d, C, J_{CP} = 4.6 Hz, central allyl), 192.9 (m, C, carbene).

^{31}P{1H} NMR (CD_3CN, T = 298 K) δ: -57.5 (q, $J_{P\text{-}F}$ = 3.9 Hz).

^{19}F{1H} NMR (CD_3CN, T = 298 K) δ: -56.2 (d, $J_{F\text{-}P}$ = 3.9 Hz, CF_3), -151.8 ($^{10}BF_4$), -151.9 ($^{11}BF_4$).

Less abundant isomer (ca. 42%):

^{1}H NMR (CD_3CN, T=298 K, ppm, selected peaks) δ : 1.79 (s, 3H, allyl-CH_3), 2.42 (s, 1H, allyl-H *trans*-C), 2.79 (d, J= 8.4 Hz, 1H, allyl-H *trans*-P), 3.83-4.65 (m, 14H, *syn* allyl-H *trans*-C, *syn* allyl-H *trans*-P, 3 NCH_2N, 3 NCH_2P), 7.38-7.88 (m, 9H, ArH).

^{13}C{1H} NMR (CD_3CN, T=298 K, ppm selected peaks) δ : 23.4 (CH_3, allyl-CH_3), 52.9 (d, CH_2, J= 12.6 Hz, NCH_2P), 61.3 (CH_2, allyl *trans*-C), 72.1 (d, CH_2, J_{CP} = 27.0 Hz, CH_2 allyl *trans*-P), 73.2 (d, CH_2, J= 7.5 Hz, NCH_2N), 137.0 (d, C, J_{CP} = 4.8 Hz, central allyl), 193.2 (m, C, carbene).

^{31}P{1H} NMR (CD_3CN, T = 298 K) δ: -57.1 (q, $J_{P\text{-}F}$ = 2.9 Hz).

^{19}F{1H} NMR (CD_3CN, T = 298 K) δ: -55.7 (d, $J_{F\text{-}P}$ = 2.9 Hz, CF_3), -151.8 ($^{10}BF_4$), -151.9 ($^{11}BF_4$).

IR [neat]: 2914.3, 1665.6, 1352.9, 1029.0, 1012.7, 968.6, 740.8, 582.0 cm^{-1}.

Anal. Calc. for $C_{24}H_{28}BF_7N_5PPd$: C, 43.17; H, 4.23; N, 10.49. Found: C, 43.25; H, 4.03; N, 10.20%.

9.7.21. Synthesis of mixed NHC/DIC and DIC/PPh_3 palladium η^3-allyl complexes (85-86)

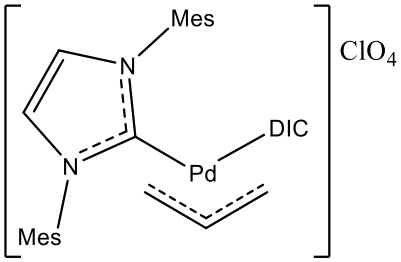

85

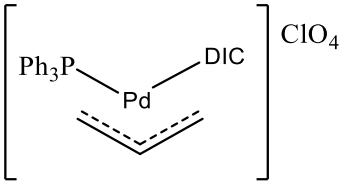

86

The mixed NHC/DIC (**85**) and DIC/PPh_3 (**86**) complexes were synthesized according to published procedures [39].

9.7.22. Synthesis of the Pd(I) dimer (87)

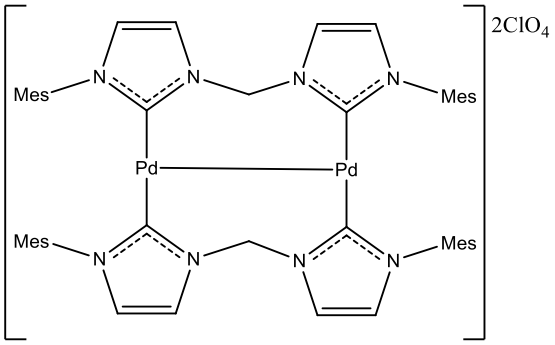

Compound **87** was synthesized according to the procedure described for compound **48f** (see section 6.7.15). 0.0354 g of **87** was obtained.

^{1}H NMR (300 MHz, d^6-DMSO, T=298 K, ppm) δ : 1.26 (s, 12H, 4 o-aryl-CH_3), 1.59 (s, 12H, 4 o-aryl-CH_3), 2.43 (s, 12H, 4 p-aryl-CH_3), 6.51 and 7.23 (AB system, J= 13.6 Hz, 4H, 2NCH_2N), 6.95-7.07 (8H, Ar-H), 7.45-8.03 (8H, CH^{Im}).

^{13}C{^{1}H} NMR (d^6-DMSO, T=298 K, ppm) δ : 16.8 (CH_3, o-Mesityl-CH_3), 17.2 (CH_3, o-Mesityl-CH_3), 21.2 (CH_3, p-Mesityl-CH_3), 64.0 (CH_2, NCH_2N), 122.6-125.1 (CH, $CH=CH^{Im}$), 129.6-139.3 (Ar-C), 182.8 (C, carbene).

Anal. Calc. for $C_{50}H_{56}Cl_2N_8O_8Pd_2$: C, 50.86; H, 4.78; N, 9.49. Found: C, 51.02; H, 4.70; N, 9.57%.

9.8. References

[1] L. Canovese, F. Visentin, G. Chessa, P. Uguagliati, C. Levi, A. Dolmella, *Organometallics*, 2005, **24**, 5537.

[2] (a) L. Canovese, F. Visentin, G. Chessa, P. Uguagliati, A. Dolmella, *J. Organomet. Chem*, 2000, **601**, 1; (b) L. Canovese, F. Visentin, P. Uguagliati, B. Crociani, *J. Chem. Soc. Dalton Trans.*, 1996, 1921; (c) L. Canovese, C. Santo, F. Visentin, *Organometallics*, 2008, **27**, 3577; (d) L. Canovese, F. Visentin, C. Biz, T. Scattolin, C. Santo, V. Bertolasi, *Polyhedron*, 2015, **102**, 94.

[3] L. Canovese, F. Visentin, P. Uguagliati, G. Chessa, A. Pesce, *J. Organomet. Chem*., 1998, **566**, 61.

[4] Y. Zhao and D. G. Truhlar, *Acc. Chem. Res*., 2008, **41**, 157.

[5] Y. Zhao and D. G. Truhlar, *Theor. Chem. Acc*., 2008, **120**, 215.

[6] P. J. Hay and W. R. Wadt, *J. Chem. Phys.*, 1985, **82**, 270.

[7] L. E. Roy, P. J. Hay and R. L. Martin, *J. Chem. Theory Comput.*, 2008, **4**, 1029.

[8] C. E. Check, T. O. Faust, J. M. Bailey, B. J. Wright, T. M. Gilbert and L. S. Sunderlin, *J. Phys. Chem. A*, 2001, **105**, 8111.

[9] V. Barone, M. Cossi and J. Tomasi, *J. Chem. Phys.*, 1997, **107**, 3210.

[10] V. Barone and M. Cossi, *J. Phys. Chem. A*, 1998, **102**, 1995.

[11] (a) C. J. Cramer, in *Essentials of Computational Chemistry*, John Wiley and Sons, Chichester, 2nd edn, 2004; (b) F. Jensen, in *Introduction to Computational Chemistry*, John Wiley and Sons, Chichester, 2nd edn, 2007.

[12] M. J. Frisch, G. W. Trucks, H. B. Schlegel, G. E. Scuseria, M. A. Robb, J. R. Cheeseman, G. Scalmani, V. Barone, B. Mennucci, G. A. Petersson, H. Nakatsuji, M. Caricato, X. Li, H. P. Hratchian, A. F. Izmaylov, J. Bloino, G. Zheng, J. L. Sonnenberg, M. Hada, M. Ehara, K. Toyota, R. Fukuda, J. Hasegawa, M. Ishida, T. Nakajima, Y. Honda, O. Kitao, H. Nakai, T. Vreven, J. A. Montgomery Jr., J. E. Peralta, F. Ogliaro, M. Bearpark, J. J. Heyd, E. Brothers, K. N. Kudin, V. N. Staroverov, R. Kobayashi, J. Normand, K. Raghavachari, A. Rendell, J. C. Burant, S. S. Iyengar, J. Tomasi, M. Cossi, N. Rega, J. M. Millam, M. Klene, J. E. Knox, J. B. Cross, V. Bakken, C. Adamo, J. Jaramillo, R. Gomperts, R. E. Stratmann, O. Yazyev, A. J. Austin, R. Cammi, C. Pomelli, J. W. Ochterski, R. L. Martin, K. Morokuma, V. G. Zakrzewski, G. A. Voth, P. Salvador, J. J. Dannenberg, S. Dapprich, A. D. Daniels, Ö. Farkas, J. B. Foresman, J. V. Ortiz, J. Cioslowski, D. J. Fox, *Gaussian 09, Revision D.01, Gaussian 09, Gaussian, Inc.*, Wallingford,CT, 2009.

[13] M.T. Khan, M. Borgatti, N. Bianchi, R. Gambari, *Evid. Based Complement Alternat. Med.*, 2008, **5**, 303.

[14] P. Bergamini, L. Marvelli, V. Ferretti, C. Gemmo, R. Gambari, Y. Hushcha, I. Lampronti, *Dalton Trans.*, 2016, **45**, 10752.

[15] R. Milani, A. Marcellini, G. Montagner, A. Baldisserotto; S. Manfredini, R. Gambari; I. Lampronti, *Eur. J. Pharm. Sci.*, 2015, **78**, 225.

[16] Z. Otwinowski, W.Minor, *Methods in Enzymology*, C.W. Carter, R.M. Sweet Editors, Vol. 276, Part A, Academic Press, London, 1997, 307.

[17] R.H. Blessing, *Acta Crystallogr. Sect A* 1995, **51**, 33.

[18] A. Altomare, M.C. Burla, M. Camalli, G.L. Cascarano, C. Giacovazzo, A. Guagliardi, A.G. Moliterni, G. Polidori R. Spagna, *J. Appl. Crystallogr*. 1999, **32**, 115.

[19] A.L. Spek, *Acta Crystallogr. Sect. D* 2009, **65**, 148.

[20] G.M. Sheldrick, SHELX-97, *Program for Crystal Structure Refinement*, University of Gottingen, Germany, 1997.

[21] M. Nardelli, *J. Appl. Crystallogr*. 1995, **28**, 659.

[22] L.J. Farrugia, *J. Appl. Crystallogr*. 1999, **32**, 837.

[23] [23] A. Lausi, M. Polentarutti, S. Onesti, J. R. Plaisier, E. Busetto, G. Bais, L. Barba, A. Cassetta, G. Campi, D. Lamba, A. Pifferi, S. C. Mande, D. D. Sarma, S. M. Sharma, G. Paolucci, *Eur Phys. J. Plus*, 2015, **130,** 1.

[24] W. Kabsch, *Acta Cryst. D*, 2010, **66**, 125.

[25] (a) M. D. Winn, C. C. Ballard, K. D. Cowtan, E. J. Dodson, P. Emsley, P. R. Evans, R. M. Keegan, E. B. Krissinel, A. G. W. Leslie, A. McCoy, S. J. McNicholas, G. N. Murshudov, N. S. Pannu, E. A. Potterton, H. R. Powell, R. J. Read, A. Vagin, K. S. Wilson, *Acta Cryst. D*, 2011, **67**, 235; (b) P. R. Evans, G. N. Murshudov, *Acta Cryst. D*, 2013, **69**, 1204.

[26] G. M. Sheldrick, *Acta Cryst. A*, 2015, **71**, 3.

[27] G. M. Sheldrick, *Acta Cryst. C*, 2015, **71**, 3.

[28] P. Emsley, B. Lohkamp, W. Scott, K. Cowtan, *Acta Cryst. D*, 2010, **66**, 486.

[29] L. Farrugia, *J. of App. Cryst.*, 2012, **45**, 849.

[30] J. Liu, J. Chen, J. Zaho, Y. Zhao, H. Zhang, *Synthesis*, 2003, 2661.

[31] (a) S.-T. Liu, C.-I. Lee, C.-F. Fu, C.-H. Chen, Y.-H. Liu, C.J. Elsevier, S.-M. Peng, J.-T. Chen, *Organometallics*, 2009, **28**, 6597; (b) L. Canovese, F. Visentin, C. Levi, C. Santo, V. Bertolasi, *Inorg. Chim. Acta*, 2012, **390**, 105; (c) L. Canovese, F. Visentin, C. Levi, C. Santo, V. Bertolasi, *J. Organomet. Chem.*, 2013, **732**, 27 and refs. therein.

[32] A.A.D. Tulloch, A.A. Danoupolos, S. Winston, S. Khleinhenz, G. Eastham, *J. Chem. Soc., Dalton Trans.*, 2000, 4499.

[33] P.S. Engl, R. Senn, E. Otth, A. Togni, *Organometallics*, 2015, **34**, 1384.

[34] Z. Zhou, J. Qiu, L. Xie, F. Du, G. Xu, Y. Xie, Q. Ling, *Catal. Lett.*, 2014, **144**, 1911.

[35] F. Tewes, A. Schlecker, K. Harms, F. Glorius, *J. Organomet. Chem.*, 2007, **692**, 4593.

[36] (a) H. M. Lee, C. Y. Lu, C. Y. Chen, W. L. Chen, H. C. Lin, P. L. Chiu and P. Y. Cheng, *Tetrahedron*, 2004, **27**, 5807; (b) D. J. Williams, D. Vanderveer, R. L. Jones, D. S. Menaldino, *Inorg. Chim. Acta*, 1989, **165**, 173; (c) D. Pugh, N. J. Wells, D. J. Evans, A. A. Danopoulos, *Dalton Trans.*, 2009, **35**, 7189.

[37] (a) Y. A. Wanniarachchi, M. A. Khan and L. M. Slaughter, *Organometallics*, 2004, **23**, 5881–5884; (b) Y. Cheng, X. Y. Lu, H. J. Xu, Y. Z. Li, X.-T. Chen, Z. L. Xue, *Inorg. Chim. Acta*, 2010, **363**, 430.

[38] L. Canovese, C. Santo, T. Scattolin, F. Visentin, V. Bertolasi, J. *Organomet. Chem.*, 2015, **794**, 288.

[39] (a) L. Canovese, F. Visentin, C. Levi, A. Dolmella, *Dalton Trans.*, 2011, **40**, 966; (b) L. Canovese, F. Visentin, C. Levi, C. Santo, V. Bertolasi, *Inorganica Chimica Acta*, 2011, **378**, 239.

10

Supplementary Materials

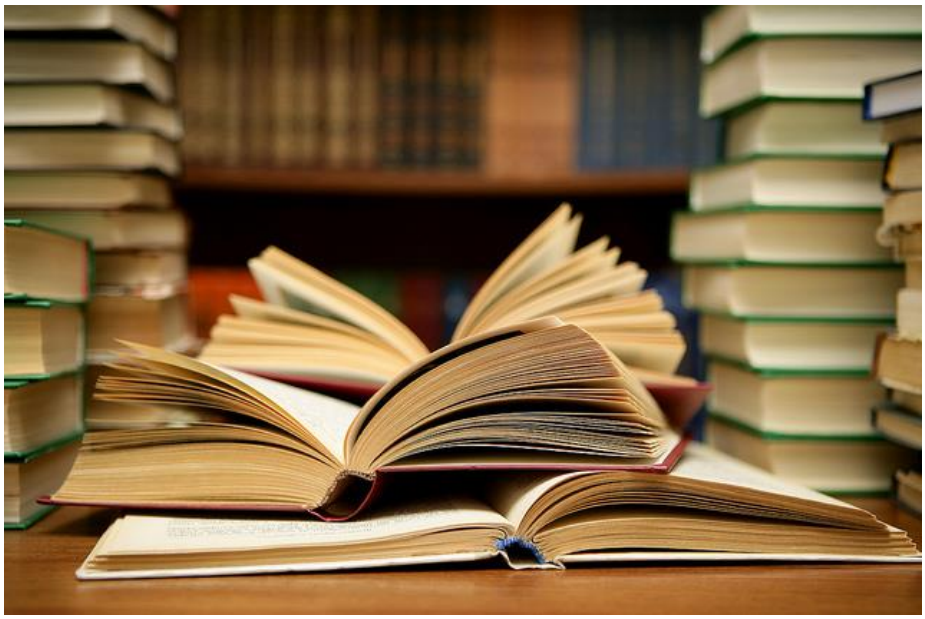

Table of contents

1. Crystallographic data and Selected bond distances/angles for **4b** (**Tables S1-S2**)
2. Crystallographic data and Selected bond distances/angles for **6a** and **10d** (**Tables S3-S4**)
3. Crystallographic data and Selected bond distances/angles for **11b** (**Tables S5-S6**)
4. Crystallographic data and Selected bond distances/angles for **47b** (**Tables S7-S8**)
5. Crystallographic data and Selected bond distances/angles for **48e, 74, 87** (**Tables S9-S10**)
6. Crystallographic data and Selected bond distances/angles for **42a** (**Tables S11-S12**).
7. Crystallographic data and Selected bond distances/angles for **60** (**Tables S13-S14**).

The figure proposed at the beginning of the chapter is related to this source: https://www.fb.is/boksalan-opin/

1. Crystallographic data and Selected bond distances/angles for **4b** (**Tables S1**-**S2**)

Table S1. Crystallographic data for **4b**

Compound	**4b**
Formula	$[Ag(C_{15}H_{16}N_4O_2)_2]^+ \cdot BF_4^-$
M	763.31
Space group	*C2/c*
Crystal system	Monoclinic
a/Å	24.619(5)
b/Å	8.689(2)
c/Å	14.402(3)
β/°	101.07(3)
V/Å^3	3023.5(11)
Z	4
T/K	100(2)
D_c/g cm^{-3}	1.677
F(000)	1552
μ(0.7Å)/cm^{-1}	7.05
Measured Reflections	26696
Unique Reflections	4161
R_{int}	0.0345
Obs. Refl.ns [I≥2σ(I)]	3881
θ_{min}- θ_{max}/°	1.66 – 29.08
hkl ranges	-34,34; -12,12; -19,19
R(F^2) (Obs.Refl.ns)	0.0342
wR(F^2) (All Refl.ns)	0.0366
No. Variables	245
Goodness of fit	1.094
$\Delta\rho_{max}$; $\Delta\rho_{min}$ /e Å^{-3}	0.56; -2.18
CCDC Deposition N.	1551527

Table S2. Selected bond distances and angles (Å and degrees) for **4b**.

Distances	(Å)	**Angles**	**(°)**
Ag-C8	2.0975(23)	C8-Ag-C8_$1	176.69(10)

$1 = -x+1, y, -z+3/2

2. Crystallographic data and Selected bond distances/angles for **6a** and **10d** (**Tables S3-S4**)

Table S3. Crystallographic data for **6a** and **10d.**

Compound	**10d**	**6a**
Formula	$PdC_{33}H_{37}N_8O_4 \cdot BF_4$	$PdC_{30}H_{32}N_4O_2P \cdot BF_4 \cdot 0.5CH_2Cl_2$
M	802.91	747.24
Space group	$P2_1/c$	$P2_1/n$
Crystal system	Monoclinic	Monoclinic
a/Å	8.200(2)	8.818(2)
b/Å	13.605(3)	15.614(3)
c/Å	30.666(6)	23.329(5)
β/°	96.85(3)	94.90(3)
V/Å^3	3396.7(12)	3200.3(11)
T/K	100	100
D_c/g cm^{-3}	1.570	1.551
F(000)	1640	1516
μ(0.7Å)/cm^{-1}	5.88	7.31
Measured Reflections	77120	38281
Unique Reflections	6783	8782
R_{int}	0.0311	0.0304
Obs. Refl.ns [I≥2σ(I)]	6042	8453
θ_{min}- θ_{max}/°	1.32 – 25.77	1.55 – 29.08
hkl ranges	-10,10; -16,16; -14,38	-11,11; -21,21; -32,32
R(F^2) (Obs.Refl.ns)	0.1325	0.0276
wR(F^2) (All Refl.ns)	0.3219	0.0714
No. Variables	407	449
Goodness of fit	1.139	1.000
$\Delta\rho_{max}$; $\Delta\rho_{min}$ /e Å^{-3}	3.95; -4.43	1.20; -0.90
CCDC Deposition N.	1825947	1825948

Table S4. Selected bond distances and angles (Å and degrees) for **6a** and **10d.**

8d				**4a**			
Distances	(Å)	**Angles**	**(°)**	**Distances**	(Å)	**Angles**	**(°)**
Pd_1-C19_2	2.1653(184)	C19_2-Pd_1-C20_2	68.64(58)	Pd_1-C19_2	2.1776(20)	C19_2-Pd_1-C20_2	67.50(8)
Pd_1-C20_2	2.1467(125)	C8_3-Pd_1-C8_4	98.14(51)	Pd_1-C20_2	2.1543(16)	P_4-Pd_1-C8_3	95.17(4)
Pd_1-C8_3	2. 0298(123)	C8_3-Pd_1-C20_2	98.97(47)	Pd_1-C8_3	2.0354(15)	C8_3-Pd_1-C20_2	94.62(7)
Pd_1-C8_4	2. 0294(120)	C8_4-Pd_1-C19_2	94.38(58)	Pd_1-P_4	2.3041(6)	P_4-Pd_1-C19_2	102.80(6)

3. Crystallographic data and Selected bond distances/angles for **11b** (**Tables S5-S6**)

Table S5. Crystallographic data for **11b.**

Compound	**1**
Formula	$PdC_{45}H_{43}N_4O_{10}P \cdot 0.65H_2O$
M	948.91
Space group	*C2/c*
Crystal system	Monoclinic
a/Å	24.468(5)
b/Å	13.682(3)
c/Å	26.059(5)
β/°	90.05(3)
V/Å^3	8724(3)
Z	8
T/K	100
D_c/g cm^{-3}	1.445
F(000)	3908
μ(0.7Å)/cm^{-1}	0.50
Measured Reflections	78925
Unique Reflections	12211
R_{int}	0.0406
Obs. Refl.ns [I≥2σ(I)]	10282
θ_{min}- θ_{max}/°	1.54 – 29.08
hkl ranges	-33,33; -18,18; -36,36
R(F^2) (Obs.Refl.ns)	0.0373
wR(F^2) (All Refl.ns)	0.1029
No. Variables	577
Goodness of fit	1.035
$\Delta\rho_{max}$; $\Delta\rho_{min}$ /e Å^{-3}	0.75; -2.47

Table S6. Selected bond distances and angles (Å and degrees) for **11b**.

11b			
Distances	(Å)	**Angles**	**(°)**
Pd_1-C1_3	2.0757(17)	C1_3-Pd_1-C4_3	80.08(7)
Pd_1-C4_3	2.0647(18)	C1_3-Pd_1-P_2	95.81(5)
Pd_1-P_2	2.3367(8)	P_2-Pd_1-C8_4	92.83(5)
Pd_1-C8_4	2.0379(17)	C8_4-Pd_1-C4_3	91.21(7)

4. Crystallographic data and Selected bond distances/angles for **47b** (**Tables S7-S8**)

Table S7. Crystallographic data for **47b** and **47bsolv.**

	Orthorhombic 47b $[PdC_{30}H_{31}I_2N_3O_8]$	**Monoclinic 47b·¾CH_2Cl_2** $[PdC_{30}H_{31}I_2N_3O_8 \cdot 0.75CH_2Cl_2]$
Chemical Formula	$PdC_{30}H_{31}I_2N_3O_8$	$PdC_{30.75}H_{32.5}Cl_{1.5}I_2N_3O_8$
Formula weight	921.78 g/mol	985.47 g/mol
Temperature	100(2) K	100(2) K
Wavelength	0.700 Å	0.700 Å
Crystal system	Orthorhombic	Monoclinic
Space Group	*P bca*	*P* $2_1/c$
Unit cell dimensions	*a* = 19.777(4) Å *b* = 15.975(3) Å *c* = 20.563(4) Å α = 90° β = 90° γ = 90°	*a* = 10.929(2) Å *b* = 15.041(3) Å *c* = 21.431(4) Å α = 90° β = 94.00(3)° γ = 90°
Volume	6497(2) $Å^3$	3514.3(12) $Å^3$
Z	8	4
Density (calculated)	1.885 $g \cdot cm^{-3}$	1.863 $g \cdot cm^{-3}$
Absorption coefficient	2.392 mm^{-1}	2.322 mm^{-1}
F(000)	3584	1918
Crystal size	0.08 x 0.02 x 0.02 mm^3	0.08 x 0.02 x 0.02 mm^3
Crystal habit	Dark yellow thin rods	Dark yellow thin rods
Theta range for data collection	1.89° to 27.04°	1.63° to 27.42°
Index ranges	$-25 \le h \le 25$, $-19 \le k \le 19$, $-26 \le l \le 26$	$-14 \le h \le 14$, $-19 \le k \le 19$, $-28 \le l \le 28$
Reflections collected	82101	52503
Independent reflections	7229, 6011 data with $I>2\sigma(I)$	8252, 7003 data with $I>2\sigma(I)$
Data multiplicity (max resltn)	10.54 (10.42)	2.57 (2.49)
$I/\sigma(I)$ (max resltn)	25.88 (15.89)	10.89 (6.67)
R_{merge} (max resltn)	0.047 (0.104)	0.053 (0.101)
Data completeness (max resltn)	97% (95%)	99% (99%)
Refinement method	Full-matrix least-squares on F^2	Full-matrix least-squares on F^2
Data / restraints / parameters	7229/36/456	8252/6/443
Goodness-of-fit on F^2	1.047	1.045
Δ/σ_{max}	0.001	0.003
Final R indices [$I>2\sigma(I)$]	R_1 = 0.0426, wR_2 = 0.1080	R_1 = 0.0623, wR_2 = 0.1666
R indices (all data)	R_1 = 0.0525, wR_2 = 0.1157	R_1 = 0.0715, wR_2 = 0.1755
Largest diff. peak and hole	2.487 and -1.424 $eÅ^{-3}$	2.352 and -1.955 $eÅ^{-3}$
R.M.S. deviation from mean	0.157 $eÅ^{-3}$	0.217 $eÅ^{-3}$

Table S8. Selected bond distances and angles (Å and degrees) for **47b** and **47bsolv.**

47b				**47bsolv**			
Distances	(Å)	**Angles**	**(°)**	**Distances**	(Å)	**Angles**	**(°)**
Pd-I1	2.614(1)	I1-Pd-I2	165.75(2)	Pd-I1	2.628(1)	I1-Pd-I2	163.65(3)
Pd-I2	2.601(1)	I1-Pd-N1	86.03(10)	Pd-I2	2.610(1)	I1-Pd-N1	86.15(17)
Pd-N1	2.113(4)	I2-Pd-N1	88.54(10)	Pd-N1	2.131(6)	I2-Pd-N1	90.49(16)
Pd-C13	1.988(4)	C13-Pd-N1	174.52(15)	Pd-C13	1.993(7)	C13-Pd-N1	172.92(25)

5. Crystallographic data and Selected bond distances/angles for **48e, 74, 87** (**Tables S9-S10**)

Table S9. Crystallographic data for for **48e, 74** and **87.**

Compound	**48e**	**87**	**74**
Formula	$PdC_{29}H_{35}N_4 \cdot ClO_4 \cdot CHCl_3$	$Pd_2C_{50}H_{56}N_8 \cdot 2ClO_4 \cdot 3CHCl_3$	$PdC_{35}H_{29}N_2F_3P \cdot BF_4$
M	764.83	1538.83	758.78
Space group	$P2_1/c$	$P2_1/n$	Cc
Crystal system	Monoclinic	Monoclinic	Monoclinic
a/Å	16.774(3)	12.180(2)	10.329(2)
b/Å	14.074(3)	15.906(3)	19.223(4)
c/Å	15.262(3)	33.211(7)	16.587(3)
β/°	113.44(3)	93.15(3)	105.00(3)
V/Å^3	3305.8(13)	6424(2)	3181.2(12)
Z	4	4	4
T/K	100	100	100
D_c/g cm^{-3}	1.537	1.591	1.584
F(000)	1560	3104	1528
μ(0.7Å)/cm^{-1}	6.31	7.29	4.85
Measured Reflections	23773	126769	31018
Unique Reflections	9846	26232	12600
R_{int}	0.0358	0.0477	0.0198
Obs. Refl.ns [I≥2σ(I)]	8856	20246	12447
θ_{min}- θ_{max}/°	1.71 – 21.85	1.24 – 21.85	1.85 – 30.01
hkl ranges	-23,23; -20,20; -21,21	-19,19; -25,25; -53,53	-16,16; -30,30; -26,26
R(F^2) (Obs.Refl.ns)	0.0590	0.0532	0.0211
wR(F^2) (All Refl.ns)	0.1482	0.1558	0.0563
No. Variables	395	826	461
Goodness of fit	1.049	1.042	1.064
$\Delta\rho_{max}$; $\Delta\rho_{min}$ /e Å^{-3}	6.81; -3.09	1.31; -1.69	0.64; -1.08

Table S10. Selected bond distances and angles (Å and degrees) for **48e, 74** and **87.**

48e

Distances	(Å)	**Angles**	**(°)**
Pd_1-C19_3	2.1710(36)	C19_3-Pd_1-C20_3	67.40(14)
Pd_1-C20_3	2.1703(34)	C2_2-Pd_1-C12_2	86.89(12)
Pd_1-C2_2	2.0387(31)	C2_2-Pd_1-C20_3	103.05(13)
Pd_1-C12_2	2.0422(30)	C12_2-Pd_1-C19_3	102.11(13)

87

Distances	(Å)	**Angles**	**(°)**
Pd_1-C2_3	2.0831(26)	C2_3-Pd_1-C12_4	170.41(10)
Pd_1-C12_4	2.0783(25)	C2_3-Pd_1-Pd_2	103.08(8)
Pd_2-C2_4	2.0894(26)	C12_4-Pd_1-Pd_2	86.14(7)
Pd_2-C12_3	2.0909(25)	C2_4-Pd_2-C12_3	171.66(10)
Pd_1-Pd_2	3.1624(5)	C2_4-Pd_2-Pd_1	101.73(8)
		C12_3-Pd_2-Pd_1	86.45(7)

74

Distances	(Å)	**Angles**	**(°)**
Pd_1-C19_2	2.1694(21)	C19_2-Pd_1-C20_2	68.03(9)
Pd_1-C20_2	2.1812(20)	P_4-Pd_1-C8_3	100.36(5)
Pd_1-C8_3	2.0350(20)	C8_3-Pd_1-C20_2	96.44(8)
Pd_1-P_4	2.3044(6)	P_4-Pd_1-C19_2	95.26(6)

6. Crystallographic data and Selected bond distances/angles for **42a** (**Tables S11-S12**).

Table S11. Crystallographic data for for **42a.**

Formula	$C_{22}H_{23}N_3O_8Pd$
M	563.83
Space group	$P2_1/n$
Crystal system	Monoclinic
a/Å	12.2088(2)
b/Å	10.1565(2)
c/Å	18.8943(4)
β/°	97.2508(8)
U/Å^3	2324.13(8)
T/K	295
D_c/g cm^{-3}	1.611
F(000)	1144
μ(Mo-Kα)/cm^{-1}	8.51
Measured Reflections	21222
Unique Reflections	6763
R_{int}	0.0369
Obs. Refl.ns [I≥2σ(I)]	5020
θ_{min}- θ_{max}/°	3.54 – 30.00
hkl ranges	-17,17;-14,14;-19,26
R(F^2) (Obs.Refl.ns)	0.0352
wR(F^2) (All Refl.ns)	0.0953
No. Variables	312
Goodness of fit	1.021
$\Delta\rho_{max}$; $\Delta\rho_{min}$ /e Å^{-3}	0.68; -0.84
CCDC Deposition N.	1059980

Table S12. Selected bond distances and angles (Å and degrees) for **42a.**

Distances	**42a**
Pd1–C1	2.027(2)
Pd1–N3	2.140(2)
Pd1–C11	2.013(2)
Pd1–C14	2.072(2)
C11–C12	1.338(3)
C12–C13	1.475(3)
C13–C14	1.349(3)
Angles	
C1–Pd1–N3	83.94(8)
C1–Pd1–C11	95.01(9)
C1–Pd1–C14	173.91(9)
N3–Pd1–C11	175.40(8)

Distances	42a
N3–Pd1–C14	101.88(8)
C11–Pd1–C14	79.32(9)

7. Crystallographic data and Selected bond distances/angles for **60** (**Tables S13-S14**).

Table S13. Crystallographic data for for **60.**

Formula	$(C_{41}H_{42}N_2PPd)^+ \bullet (ClO_4)^-$
Space group	P-1
Crystal system	Triclinic
a/Å	10.8829(2)
b/Å	11.2739(4)
c/Å	17.4886(6)
α/°	74.597(2)
β/°	85.914(2)
γ/°	67.153(2)
U/Å^3	1905.1(1)
T/K	295
D_c/g cm^{-3}	1.394
F(000)	824
μ(Mo-Kα)/mm^{-1}	0.642
Measured Reflections	22736
Unique Reflections	10937
R_{int}	0.0490
Obs. Refl.ns [I≥2σ(I)]	8272
θ_{min}- θ_{max}/°	2.72 – 30.00
hkl ranges	-15,15;-14,15; -24,22
R(F^2) (Obs.Refl.ns)	0.0462
wR(F^2) (All Refl.ns)	0.1278
No. Variables	478
Goodness of fit	1.036
$\Delta\rho_{max}$; $\Delta\rho_{min}$ /e Å^{-3}	1.174; -0.740

Table S14. Selected bond distances and angles (Å and degrees) for **60.**

Distances		**Angles**	
Pd1-C1	2.047(3)	C1-Pd1-P1	94.42(7)
Pd1-P1	2.3042(6)	C1-Pd1-C20	166.93(12)
Pd1-C20	2.157(3)	C1-Pd1-C21	131.07(12)
Pd1-C21	2.173(3)	C1-Pd1-C22	100.05(14)
Pd1-C22	2.179(3)	P1-Pd1-C20	98.60(10)
C1-N1	1.342(4)	P1-Pd1-C21	130.63(9)
C1-N2	1.350(4)	P1-Pd1-C22	165.23(12)
C20-C21	1.391(5)	C20-Pd1-C21	37.48(14)
C21-C22	1.400(5)	C20-Pd1-C22	66.89(15)
C21-C23	1.514(6)	C21-Pd1-C22	37.52(14)
		N1-C1-N2	104.2(2)
		C20-C21-C22	117.8(4)